13 March 2008 | www.nature.com/nature | $10

THE INTERNATIONAL WEEKLY JOURNAL OF SCIENCE

# nature

nature 452, 127-252 13 March 2008

www.nature.com/nature

**GIANT TELESCOPES**
The race to a 30-metre mirror

**RADICAL BIOCHEMISTRY**
*C. difficile*'s surprising enzyme

**SUPRAMOLECULAR SELF-ASSEMBLY**
DNA bricks make complexity simple

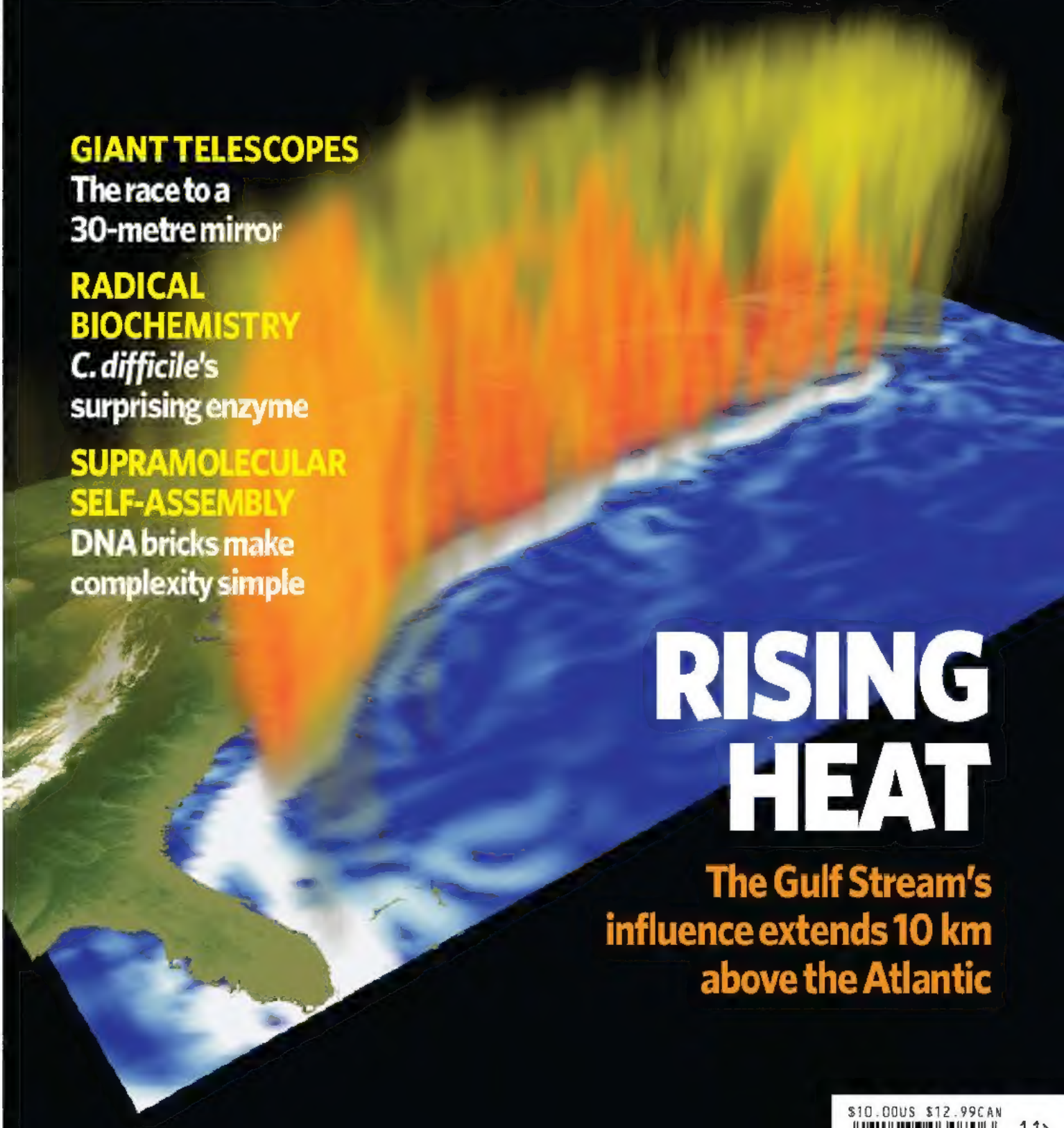

## RISING HEAT

The Gulf Stream's influence extends 10 km above the Atlantic

**NATUREJOBS**
Florida targets biotech

$10.00US $12.99CAN
11>
0 71486 03070 6

no.7184 npg

# Isolate!

SIGMA Life Science

*Better Isolation,*
*Better Performance*

## Sigma's mirPremier™ microRNA Isolation Kit —

### Higher purity miRNA, 50% faster with no detectable large RNA

mirPremier microRNA Isolation Kit provides a rapid and efficient method for purifying and enriching miRNAs and other small RNAs directly from cells or tissues as rapidly and simply as a total RNA preparation.

- Optimized for purification of miRNAs and other small RNAs directly from diverse biological sources
- Rapidly purify and enrich miRNA in 30 minutes for downstream applications
- Higher purity miRNA with no detectable large RNA
- No hazardous organic extractions

**More rapid, more pure, less hands-on.** To learn more, *visit sigma.com/mirpremier*

Our Innovation, Your Research — Shaping the Future of Life Science

# Make Illumina part of your DNA.

## The most comprehensive set of DNA analysis tools available.

Illumina's portfolio of DNA analysis products delivers industry-leading data quality at the lowest cost per study. Accelerate discovery by looking at DNA from every angle.

- **SNP genotyping** — Achieve significance with the industry's best genomic coverage and data quality.
- **CNV analysis** — Obtain the most comprehensive access to known and novel CNV regions.
- **DNA sequencing** — Sequence virtually anything at a fraction of the cost and time.
- **DNA methylation** — Get single CpG site resolution with high-multiplex standard or custom methylation panels.
- **ChIP-Seq** — Obtain genome-wide maps of DNA-protein interactions with unprecedented resolution, quality and cost.

Make us part of your DNA. Join the growing Illumina Community.

Find out how to make
Illumina part of your DNA:

www.illumina.com/DNA

illumina®

Now you have the freedom to perform real-time PCR the way you want—with the dyes and chemistries you want—and get the high-quality results your research demands.

# Experience the freedom of Stratagene real-time PCR.

Stratagene real-time PCR combines the Mx3005P® system, with Brilliant® reagents, Absolutely RNA® purification products, and the Agilent 2100 bioanalyzer to create a powerful, truly flexible, and easy-to-use solution that is ideal for multi-user environments.

**All at a cost that frees up more of your research dollars.**

## Unlock more possibilities

With its 5-color detection and user-selectable filters, the Mx3005P[a] system accommodates virtually all fluorescent dyes and chemistries. Precision optics and uniform thermal response ensure maximum sensitivity and linear performance over a broad wavelength range. So, all the users in your lab have the freedom to run their applications of choice, including gene expression analysis, SNP genotyping, pathogen detection, and microarray validation.

Unlock the potential of real-time PCR by downloading the Stratagene Intro to QPCR Guide—go to **www.stratagene.com/freedom**

*a. This is a Licensed Real-Time Thermal Cycler(s) or Licensed Real-Time Temperature Cycling Instrument(s) under ABI's United States Patent No. 6,814,934 and corresponding claims in non-U.S. counterparts thereof, for use in research and for all other applied fields except human in vitro diagnostics. No right is conveyed expressly, by implication or by estoppel under any other patent claim.*

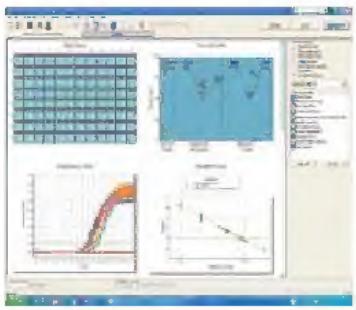

## Freedom from tedium

MxPro™ QPCR software is easy to learn and use. Yet it provides powerful, automated system set-up, analysis and reporting, and data exporting capabilities that save valuable time. New users will be up and running in no time. Expert users will appreciate the power and convenience of multi-tasking accelerators that speed them through their work—without repetitive and time consuming procedures.

## Freedom of choice

Brilliant kits offer a selection of high-performance reagents for sensitive, reproducible results on the Mx3005P and other platforms. Choose from a variety of formats, including SYBR or probe-based, multiplexing, and 1-step or 2-step RT-PCR. All Brilliant reagents are validated and quality controlled on our Mx systems to ensure the highest level of performance and the most affordable price.

## Freedom from DNA contamination

Our Absolutely RNA Purification kits isolate highly pure, DNA-free RNA from cells, fresh or frozen tissue, FFPE tissue and laser micro-dissected cells. RNA purified using this method is free of genomic DNA and other impurities. Available in miniprep, microprep, nanoprep, and 96-well versions, Absolutely RNA kits help you get absolutely the best results.

## Freedom from electrophoresis

The Agilent 2100 bioanalyzer is the industry standard for RNA sample QC and has replaced gel electrophoresis for this application. The advantages are that the Agilent 2100 gives you improved data precision and reproducibility, short analysis times, minimal sample consumption, improved automation, and integration of complex workflows. Plus, you can use the same instrument for DNA fragment analysis, flow cytometry, and protein sizing and quantitation.

## The freedom to focus

Our knowledgeable and responsive customer support experts are here to ensure you get the best possible results sample after sample, day after day. So you can focus on your research, not on instrument maintenance, and watch your productivity soar.

Take a closer look at Stratagene RNA Purification kits. Request a new selection guide at **www.stratagene.com/kitselection**

## Bring the freedom of Stratagene real-time PCR to your lab

Visit **www.stratagene.com/mylab** for your freedom card redeemable at the Stratagene booth at FASEB #1443 and AACR #1541.

**STRATAGENE**

An **Agilent Technologies** Company

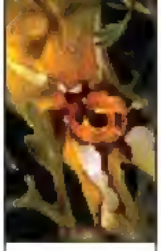

Innovative Discovery Tools for Signal Transduction Research

# PathScan® Sandwich ELISA Kits

## ...from Cell Signaling Technology

**PathScan® Cell Growth Multi-Target Sandwich ELISA Kit #7239**

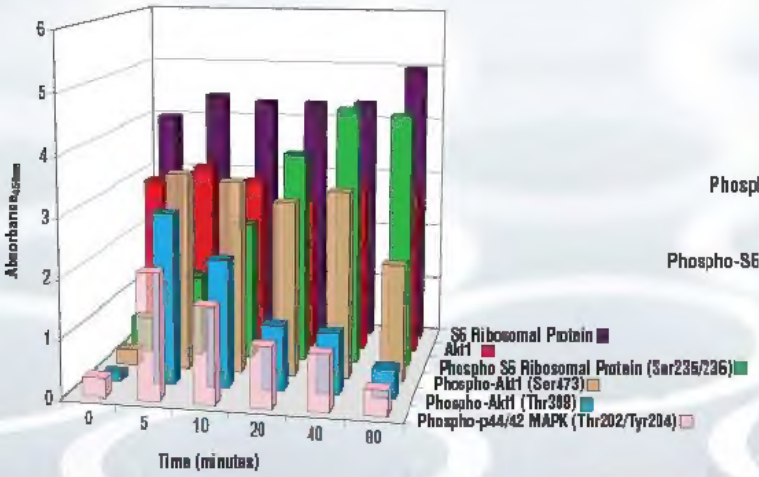


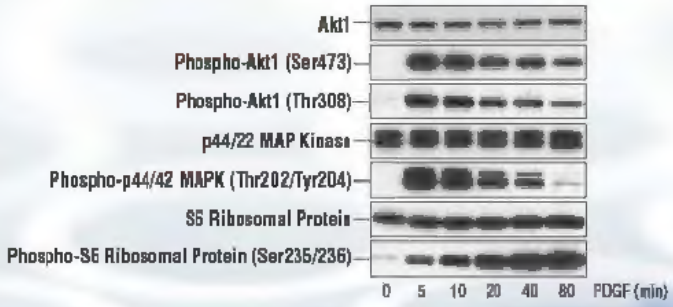


*Treatment of NIH/3T3 cells with PDGF induces phosphorylation of Akt1 at Thr308 and Ser473, S6 Ribosomal Protein at Ser235/236 and p44/42 MAPK at Thr202/Tyr204 as detected by the PathScan® Cell Growth Multi-Target Sandwich ELISA Kit #7239.*

Cell Signaling Technology (CST) has applied its antibody expertise to identify antibody pairs with optimal activity in sandwich ELISAs. These assays enable the detection of low amounts of target protein from cell lysates.

:: In-house development, production and validation ensures the highest kit quality

:: Technical support provided by the same scientists that develop and produce the kits

:: Matched modification state and total ELISA kits available

:: Custom 96- and 384-well formatting available upon request

:: Select antibody pairs available separately

:: New multitarget kits available for parallel analysis of several signaling molecules

### New PathScan® Multi Target ELISA Kits Available

| | |
|---|---|
| PathScan® Inflammation Multi-Target Sandwich ELISA Kit #7276 | new |
| PathScan® Cell Growth Multi-Target Sandwich ELISA Kit #7239 | new |
| PathScan® MAP Kinase Multi-Target Sandwich ELISA Kit #7274 | new |
| PathScan® Signaling Nodes Multi-Target Sandwich ELISA Kit #7272 | new |

### Over 80 PathScan® Sandwich ELISA Kits available, including...

| Target | | PathScan® Sandwich ELISA Kits | PathScan® ELISA Antibody Pair |
|---|---|---|---|
| Phospho-4E-BP1 (Thr37/Thr46) | | #7216 | |
| Total 4E-BP1 Sandwich ELISA Kit | new | #7179 | |
| Phospho-Akt (Thr308) | | #7252 | #7144 |
| Phospho-Akt1 (Ser473) | | #7160 | #7143 |
| Akt1 | | #7170 | #7142 |
| β-Catenin | | #7308 | |
| Phospho-EGF Receptor (Tyr1068) | | #7240 | |
| Acetylated Histone H3 | | #7232 | #7209 |
| Phospho-Histone H3 (Ser10) | | #7155 | #7207 |
| Phospho-IκB-α (Ser32) | | #7355 | |
| Phospho-IRS-1 (panTyr) | new | #7133 | #7347 |
| Phospho-IRS-1 (Ser302) | | #7283 | #7284 |
| Phospho-c-Kit (Tyr719) | new | #7296 | #7299 |
| Phospho-MEK1 (Ser217/221) | | #7175 | #7211 |
| MEK1 | | #7165 | #7215 |
| Phospho-p38α MAPK (Thr180/Tyr182) | | #7140 | #7221 |
| Phospho-p44/42 MAPK (Thr202/Tyr204) | new | #7177 | #7246 |
| Phospho-S6 Ribosomal Protein (Ser235/236) | | #7205 | #7201 |
| S6 Ribosomal Protein | | #7225 | #7203 |
| Phospho-Stat3 (Tyr705) | | #7300 | #7146 |
| Phospho-TrkA (Tyr490) | | #7210 | |

For a complete product listing visit...

www.cellsignal.com

Cell Signaling TECHNOLOGY®

Orders (toll-free) 1-877-616-CELL (2355) orders@cellsignal.com Fax ordering 1-978-867-2488 Technical support (toll-free) 1-877-678-TECH (8324) support@cellsignal.com Inquiries info@cellsignal.com

Nature Publishing Group
The Macmillan Building,
4 Crinan St, London N1 9XW, UK
e-mail: nature@nature.com


*NATURE'S MISSION, 1869:*
*'The objective which it is proposed to attain by this periodical may be broadly stated as follows. It is intended, first, to place before the general public the grand results of scientific work and scientific discovery; and to urge the claims of science to move to a more general recognition in education and in daily life... Secondly, to aid scientific men [sic] themselves, by giving early information of all advances made in any branch of natural knowledge throughout the world, and by affording them an opportunity of discussing the various scientific questions which arise from time to time.'*

**Nature's mission statement was updated in 2000:**
**www.nature.com/nature/about**
**Submissions and Guide to Authors:**
**www.nature.com/nature/authors**

**Author and referee policies and services:**
**www.nature.com/authors**

*Nature*® (ISSN 0028-0836) is published by Nature Publishing Group, a division of Macmillan Publishers Ltd (The Macmillan Building, 4 Crinan Street, London N1 9XW). Registered as a newspaper at the British Post Office.
North and South American orders to Nature, Subscription Dept, 342 Broadway PMB 301, New York NY 10013-3910, USA.
Other orders to Nature, Brunel Road, Basingstoke, Hants RG21 2XS, UK.

Identification code for Nature: 0028-0836/03
CPC PUB AGREEMENT #40032744.
In the US Nature (ISSN 0028-0836) is published weekly on Thursday, except the last week in December by Nature Publishing Group, 75 Varick St, 9th Fl, New York NY 10013-1917, USA. US Periodicals postage paid at New York NY, and additional mailing post offices.
US POSTMASTER: send address changes to Nature, Subscription Dept, 342 Broadway PMB 301, New York NY 10013-3910, USA.
Published in Japan by NPG Nature Asia-Pacific, Chiyoda Building, 2-37 Ichigayatamachi, Shinjuku-ku, Tokyo 162-0843, Japan.



nature publishing group

# nature




DAVID HALL USDA-ARS

Citrus greening disease is a threat to US fruit growers, p. **148**.


P MAARLER

In your own words: animal language controversies, p. **154**.


## FastStart Taq DNA Polymerase

# Set Your Sights on The New Standard for Everyday PCR

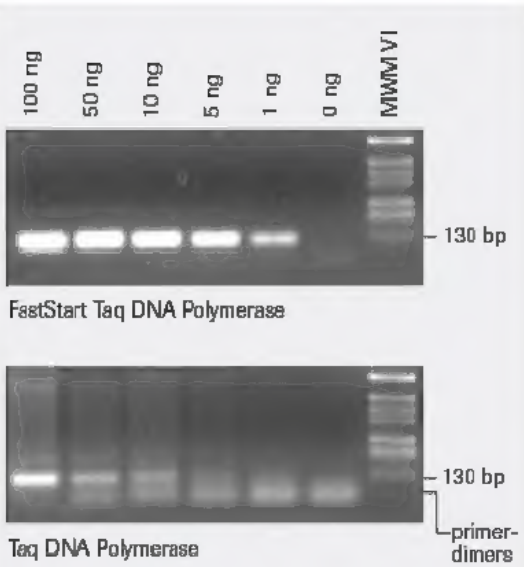


**Detect products from 100-fold less template DNA, without the primer-dimers common to standard Taq DNA Polymerase.**

Still using standard Taq DNA Polymerase for everyday PCR applications? Upgrade to hot start PCR with FastStart Taq DNA Polymerase:

- **Achieve 100-fold higher sensitivity, and easily detect low-abundance genes.**
- **Obtain results that are easy to interpret** by minimizing nonspecific amplification products and primer-dimers.
- **Save time, effort, and money** by utilizing the same robust, economical enzyme in all your applications; use the supplied buffers and additives to optimize for virtually any template up to 3 kb.
- **Select the best product for your lab's needs:** Choose from the convenient master mix, or economical dNTPacks combining the enzyme, all buffers, and Roche's unmatched PCR-Grade Nucleotides.

**Upgrade from basic Taq for a lot less than you would expect.**
Raise your standards for everyday PCR – without significantly raising your expenses!

For more information, visit *www.roche-applied-science.com/pcr*

To place your order, visit
*www.roche-applied-science.com*
or call **800 262 1640** today.

Roche Diagnostics
Roche Applied Science
Indianapolis, Indiana

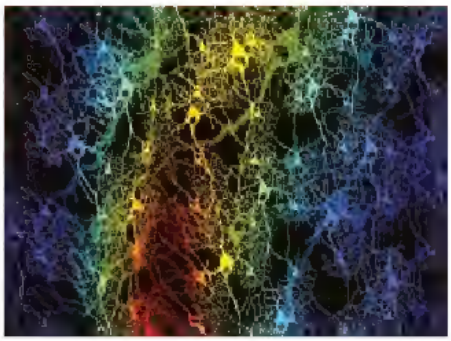

Scene building: coding neurons in the visual cortex, p. **220**.

## REVIEW



## ARTICLES



## LETTERS



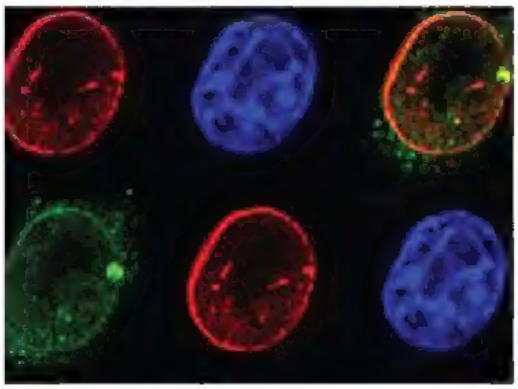

Quiet there: gene silencing by cellular location, p. **243**.

# NATURE ONLINE

## ADVANCE ONLINE PUBLICATION

PUBLISHED ON 9 MARCH 2008

**Following translation by single ribosomes one codon at a time**
J-D Wen *et al.* doi:10.1038/nature06716

PUBLISHED ON 12 MARCH 2008

**Sophisticated particle-feeding in a large Early Cambrian crustacean**
T H P Harvey & N J Butterfield doi:10.1038/nature06724

**Opposing effects of polyglutamine expansion on native protein complexes contribute to SCA1**
J Lim *et al.* doi:10.1038/nature06731

**SIRT6 is a histone H3 lysine 9 deacetylase that modulates telomeric chromatin**
E Michishita *et al.* doi:10.1038/nature06736

**Impaired $T_H17$ cell differentiation in subjects with autosomal dominant hyper-IgE syndrome**
J D Milner *et al.* doi:10.1038/nature06764

**SAR11 marine bacteria require exogenous reduced sulphur for growth**
H J Tripp *et al.* doi:10.1038/nature06776

**Functional metagenomic profiling of nine biomes**
E A Dinsdale *et al.* doi:10.1038/nature06810

## BRIEF COMMUNICATIONS ARISING

PUBLISHED ON 13 MARCH 2008

Arising from 'Genetic evidence for complex speciation of humans and chimpanzees' by N Patterson *et al. Nature* **441,** 1103–1108 (2006).

**Complex speciation of humans and chimpanzees**
J Wakeley doi:10.1038/nature06805

**Reply:** N Patterson *et al.* doi:10.1038/nature06806

## ON THE PODCAST

Each week the podcast contains background interviews on the week's *Nature* papers and on other science topics in the news. Subscribe — for free — to the weekly programme or download single copies from iTunes or from:
www.nature.com/podcast

For the podcast archive in mp3 format, visit:
http://tinyurl.com/k62cvt

# Replace cumbersome BrdU assays with one simple click

## Accurate cell proliferation with Click-iT™ EdU

Measuring cell proliferation is a fundamental way to assess cell health, determine genotoxicity, and evaluate anti-cancer drugs. Bromodeoxyuridine (BrdU) cell labeling, followed by antibody detection, is the standard method to detect actively proliferating cells or cells in S-phase. Antibody detection of BrdU requires harsh treatments or nuclease digestion to facilitate epitope access. However, a new method from Invitrogen can detect proliferating cells with the nucleoside analog EdU (5-ethynyl-2'-deoxyuridine) without the need for antibodies or radioactivity.

Both the Invitrogen Click-iT™ EdU and BrdU assays follow similar workflows: cells or animals are given with the nucleoside analog, and the incorporated nucleoside is detected following fixation and permeabilization.

Where EdU and BrdU methods differ is in their simplicity of detection (Figure 1); detection of EdU is based on a click reaction—a copper-catalyzed covalent reaction between an azide and an alkyne. The dye azide's small size allows efficient detection of incorporated EdU under mild conditions. Standard aldehyde-based fixation and detergent permeabilization are sufficient for the Click-iT™ detection reagent to gain access to the DNA. This is in contrast to BrdU assays, which require DNA denaturation (using HCl, heat, or DNase) to expose the BrdU so that it may be detected with an anti-BrdU antibody.

By eliminating DNA denaturation, additional targets can be easily and reliably investigated. BrdU assay's DNA denaturation protocols using HCl and methanol can damage cell morphology and antigen recognition sites. And although milder than HCl, DNase denaturation can destroy your ability to perform cell cycle analysis. Finding the right balance between sufficiently denatured DNA and adequate amounts of dsDNA for the cell cycle dye to bind is difficult. With Click-iT™ EdU, however, content-rich results are now truly easy to obtain. You not only accurately measure proliferation of individual cells by flow cytometry, microscopy, or high-throughput imaging, but also simultaneously detect cell cycle, intracellular, and extracellular targets (Figure 2) in significantly less time than with the BrdU method.

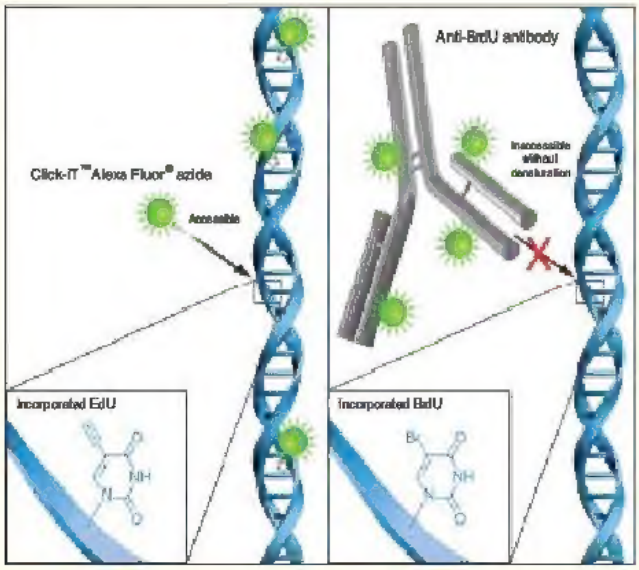


**Figure 1—Detection of the incorporated EdU with the Alexa Fluor® azide versus incorporated BrdU with an anti-BrdU antibody.** The small size of the Alexa Fluor® azide eliminates the need to denature the DNA in order for the detection reagent to gain access to the nucleoside.

### Click chemistry makes biodiscovery a snap

To EdU-cate yourself further about this innovative new technology, visit www.invitrogen.com/edu.

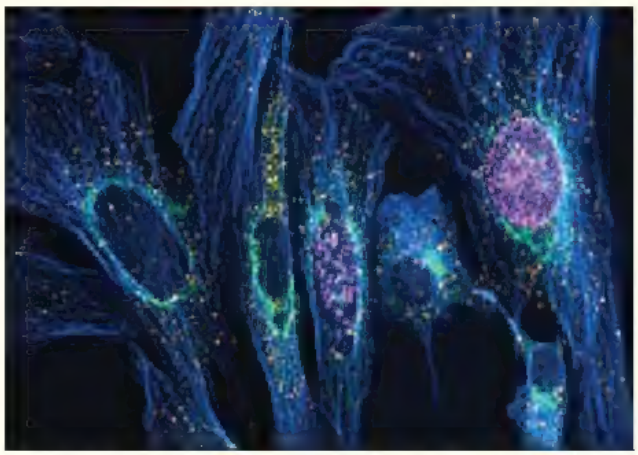

**Figure 2—Multicolor imaging is a snap with Click-iT™ EdU.** Muntjac cells were treated with 10 µM EdU for 45 minutes. EdU incorporated into newly synthesized DNA was detected with the far red–fluorescent Click-iT™ EdU Alexa Fluor® 647 Imaging Assay Kit (C10085). Tubulin was labeled with an anti-tubulin antibody (A11126) and visualized with an Alexa Fluor® 350 goat anti–mouse IgG antibody (A21049). The Golgi complex was stained with the green–fluorescent Alexa Fluor® 488 conjugate of lectin HPA from *Helix pomatia* (edible snail) (L11271), and peroxisomes were labeled with an anti-peroxisome antibody and visualized with an orange–fluorescent Alexa Fluor® 555 donkey anti–rabbit IgG antibody (A31572).

invitrogen™

www.invitrogen.com

# THIS ISSUE

**THINK BIG** The Hubble Space Telescope has been a remarkable success yet the advent of high-powered orbiting telescopes did not spell the end of their terrestrial counterparts. Adaptive optics and other advanced observational tools have enabled terrestrial telescopes to compete and in one area — the sheer light-gathering power that comes with size — to outdo orbiting observatories. Now the race is on to build the next generation of telescopes, dramatically bigger than the current crop. [News Feature p. 142]

**NORTH AND SOUTH** The habit of the Earth's magnetic field to 'flip' every now and again remains somewhat mysterious. But palaeomagnetic and geomagnetic data, together with sophisticated modelling

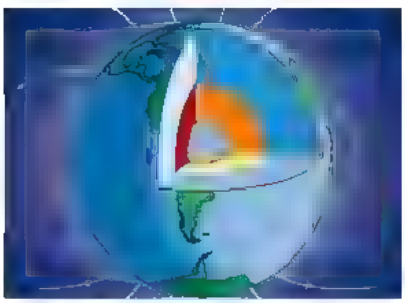

Core business, the roots of Earth's magnetic field.

studies, are beginning to explain what's going on beneath our feet. David Gubbins conducts a question and answer session on this and other mysteries of Earth's magnetic field. [News & Views Q&A p. 165]

**CANCER TARGET** A study of normal and cancerous breast epithelial cell lines shows that the chromatin organizer protein SATB1 is expressed in aggressive breast cancer cells but not in normal cells. It is often overexpressed in breast tumours, correlating with poor prognosis, and it alters the expression of many genes that contribute enhanced tumorigenesis and metastasis. Thus SATB1 seems to act as a genome organizer promoting breast tumour growth and metastasis, and it may be a useful therapeutic target. [Article p. 187]

**FOLLOW THE MONEY** Since 1980, US patent law has allowed universities to register patents for inventions made from federally funded research, and to exploit them either through a spin-off company or via licensing deals. But the academic sector has not prospered as much as was hoped. Some patents escape the clutches of the university in which the work was done and find their way to third-party companies. A new report suggests that this phenomenon of 'patent diversion' is more common than was thought. [Business Feature p. 146]


The Gulf Stream is a warm Atlantic current that transports heat northward, keeping Western Europe significantly warmer than North America in winter. It is known to influence short-term weather phenomena such as surface winds and cyclone formation, but its effects on longer-term climate and at higher levels in the atmosphere are poorly understood. Now a combination of weather analyses, satellite data and an atmospheric general circulation model reveals that the Gulf Stream's influence is felt well above the near-surface portion of the atmosphere. The current anchors a tall wall of atmospheric upward motion that penetrates into the upper troposphere and supports deep raining clouds. This provides a pathway by which the Gulf Stream can affect local climate, and possibly climate in remote regions via an effect on planetary wave propagation. The cover graphic represents surface current speeds in blue-white colours (white is the fastest) and upward wind velocities in yellow-red colours (red for stronger winds), along with land-surface topography in eastern North America. [Letter p. 206]

F. ARAGAKI AND S. KAWAHARA, ESC. JAMSTEC

## *C. difficile*'s radical solution

In the human gut the bacterium *Clostridium difficile*, a common cause of hospital acquired infection worldwide, utilizes L-leucine as both oxidant and reductant. The fermentation involves a chemically demanding dehydration, catalysed by an iron–sulphur cluster-containing dehydratase, and thought to involve ketyl radicals. This suspicion has been confirmed with the identification of a product-related allylic ketyl radical bound to the dehydratase. The radical enzymes described previously require radical generators such as coenzyme $B_{12}$, *S*-adenosylmethionine or oxygen. Such assistance is not necessary for the *C. difficile* 2-hydroxyacyl-CoA dehydratase, making this enzyme unprecedented in biochemistry. Similar enzymes might be found in other bacteria growing anaerobically. [Letter p. 239; News & Views p. 163]

## Supramolecular structures

A variety of patterned materials and nanostructures have been made from DNA, by exploiting its programmability to control molecular interactions. But making larger, more complex three-dimensional structures with current fabrication methods would require hundreds of unique DNA strands, an impractical proposition. Help is at hand. A team from Purdue University has developed a modular approach that can be likened to a DNA equivalent of Lego bricks. A few DNA molecules are programmed to fold into a basic structural unit, with four, twenty or sixty copies of that unit then assembling according to reaction conditions into tetrahedra, dodecahedra or buckyballs, respectively. Other complex structures should also be accessible using this strategy. [Letter p. 198]

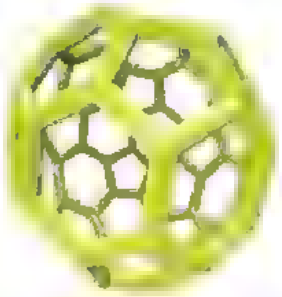

DNA components can shape a buckyball structure

## Survival fit for a genome

In their Review Article on the genetic basis of fitness, Hans Ellegren and Ben Sheldon argue that the fields of population biology and genomics are converging to a point where it will soon be possible to make major advances in our understanding of evolution in natural populations. Concentrating on animals — though similar work is being done with plants — they explain how genomic approaches can establish genotype–phenotype relationships in natural populations, giving insight into the genetic architecture of quantitative variation and the genetic substrate of natural selection. [Review Article, p. 169]

## A new class of anthelmintic

The use of drugs to control pathogenic roundworms in farm animals, an important tool of modern livestock management, is being undermined by the spread of multidrug resistance against all three types of anthelmintic

Microsoft®
HealthVault™
Be Well Fund

# It's time to bring healthcare into the Internet Age.

## Let's do it *together*.

Microsoft is calling on research and academic health institutions to join us in the search for new, innovative health applications that accelerate connections between consumers and physicians and the information they need to make informed and personalized decisions.

Working together, we can empower physicians and patients with the solutions they need to make a difference.

Building on the Microsoft® HealthVault™ consumer health platform, you have the potential to enable fundamentally new and innovative scenarios.

Submit your ideas to the HealthVault Be Well Fund and join our goal of identifying and developing new, yet-to-be-imagined Web applications that will help people live longer, healthier lives.

For more information on how your institution can submit a proposal to the HealthVault Be Well Fund, visit **www.healthvault.com/fund**

Microsoft

currently available. No new anthelmintic class has reached the market in the past 25 years save the cyclodepsipeptides, indicated for use in cats but not in livestock. Kaminsky *et al.* now report the discovery of a new class of anthelmintics — amino-acetonitrile derivatives — that appear to act via acetylcholine receptors specific to nematodes. They are effective against various livestock pathogens, and if successful in animals, may also provide alternative drugs for use in humans, where drug resistance is also increasing. [Article p. 176; News & Views p. 157; www.nature.com/podcast]

## The Warburg effect

Metabolic regulation in rapidly growing tissues such as fetal tissue and tumours tends to differ from that in most normal adult tissues, and many tumour cells are known to express the M2 (fetal) form of the glycolysis pathway enzyme pyruvate kinase (PKM2) rather than the adult M1 isoform. Two linked papers in this issue focus on role of PKM2 in tumour cells. In the first, PKM2 was identified in a proteomic screen as a phosphotyrosine binding protein. Replacement of endogenous PKM2 with a point mutant that cannot bind phosphotyrosine slows the growth of cancer cells in culture, indicating that regulation of PKM2 via phosphotyrosine binding is essential for cancer cell proliferation. [Article p. 181] In the second paper, PKM2 is shown to promote tumorigenesis and to switch cellular metabolism to increased lactate production and reduced oxygen consumption. This pattern resembles aspects of the Warburg effect, Otto Warburg's observation, made in the 1930s, that many cancer cells produce energy by glycolysis followed by lactic acid fermentation in the cytosol, rather than by mitochondrial oxidation of pyruvate. [Letter p. 230]

## Early signs of new planets

The formation of Earth-like planets is thought to start with the coagulation of interstellar grains that are only about 1 μm in diameter to form millimetre (sand), centimetre (pebble) and metre-sized (boulder) objects relatively rapidly. The prospect of observing such small objects in a protoplanetary disk seems pretty remote, but the combination of reflectance spectroscopy and the fortuitous geometry of the dust disk in the KH 15D eclipsing binary system has provided an indirect view of the process. The spectra of the light reflected from the disk are consistent with the presence of sand grains that have grown to about a millimetre in size or larger in the terrestrial zone of the host star. [Letter p. 194, Author page]

## Evolution of diversity

A number of studies have demonstrated a positive relationship between species diversity and ecosystem productivity over short

Biodiversity, evolving on Biolog microplates.

periods, but little is known about how they relate over evolutionary time. The use of bacteria as a model is one way of cracking the timescale problem. In an experiment in *Pseudomonas fluorescens* microcosms evolving for around 500 generations, adaptive radiation driven by environmental heterogeneity and dispersal resulted in the *de novo* evolution of a positive relationship between functional diversity and productivity, which both peak at intermediate dispersal rates. This suggests that evolutionary diversification plays a central role in generating community and ecosystem properties related to those observed in nature. [Letter p. 210]

## Mapping the methylome

A newly developed method of characterizing an organism's 'methylome', that is the pattern of DNA methylation in the genome, has been used to generate a map of methylated cytosines in *Arabidopsis* to single base-pair resolution. The procedure, termed BS-Seq, combines bisulphite treatment of genomic DNA with ultra-high throughput DNA sequencing to achieve a more precise and comprehensive result than previously possible. DNA methylation is an important factor in regulating gene expression, and this method, which can be applied to larger genomes like the mouse as well as to *Arabidopsis*, could prove a significant advance in the study of this form of gene regulation. [Letter p. 215]

## An RNA to block 'stemness'

Epithelial tissues such as the skin are able to self renew, thanks to the stem cells located in a basal layer. Cells originating from these stem cells differentiate — losing the ability to proliferate — as they grow towards the tissue surface. Now a microRNA has been linked to this process of stratification and differentiation. miR-203 is not expressed in epidermal stem cells, but it is made as cells commit to differentiate. It represses the cell's 'stemness' and enforces differentiation by suppressing the production of p63, a protein that is known to regulate stem cell maintenance in skin. [Letter p. 225, Author page]

# Abstractions

**FIRST AUTHOR**

Many stars are surrounded by a swirling mass of interstellar dust, known as a protoplanetary disk. Over millennia, the dust coagulates to form pebbles, then boulders and, eventually, planets. Thousands of such disks exist, but most are too far away for us to study the details and timing of planet formation. On page 194, William Herbst at Wesleyan University in Middletown, Connecticut, and his colleagues use the unique geometry of the system surrounding a star called KH 15D to observe the growth of grain-sized particles from interstellar dust — the first step in the evolution of protoplanetary material. Herbst talks to *Nature* about the project.

**How did this star's discovery change your research?**

Wesleyan students discovered the KH 15D star in 1995, using a small telescope, as part of a training project I started almost 30 years ago. Originally, we were looking for stars with odd behaviours. KH 15D was known as the winking star because it goes from normal brightness to almost undetectable during the course of a single day. The winking occurs because the KH 15D system contains not one but two stars that orbit one another in a 48-day cycle. The geometry of these stars' orbits caused the disk to be illuminated in a way that allowed us to see the particles in the disk.

**Will this system continue to be productive?**

Definitely. So far, we have only scratched the surface by analysing light that is reflected by the particles in the disk. We still have high-resolution spectroscopy data to explore that include light transmitted from the stars through the disk. Our work is complicated by the fact that the disk's orientation is changing at the moment, and will block the stars in future observations.

**Will this compromise your work?**

We won't be able to replicate this work. We don't have any way to see around the blockage, and we don't know how long we'll have to wait for conditions to change — it could be 30 years, or just until tomorrow. In the meantime, we hope to use different techniques to get further clues from the stars' reflections as the system shifts.

**What was the biggest challenge?**

It is very difficult for researchers, especially those at small institutions, to get time on the top telescopes around the world. With collaborators in Germany and Uzbekistan, we were able to continuously monitor the stars and gather preliminary data. This, in turn, allowed us to successfully compete for limited telescope time at the W. M. Keck Observatory in Hawaii and at the Chile-based Very Large and Magellan telescopes. ■

# MAKING THE PAPER

## Elaine Fuchs

**RNA fragments in skin provide a fine degree of control.**

As a young researcher, Elaine Fuchs was drawn to skin because of all that this most accessible of organs could reveal about cellular development. It is, she says, "a wonderful experimental system" — one that led her and her colleagues to discover a molecule responsible for fine-tuning the switch that causes a stem cell to produce a specialized cell.

Our skin's surface, or epidermis, comprises several layers of cells, all of which begin life as stem cells in the innermost 'basal' layer. From there, they stop dividing and move towards the outer layer, developing into specialized protective cells through a process known as differentiation as they go. For years, Fuchs, now a Howard Hughes Medical Institute cell biologist based at the Rockefeller University in New York, and others used cultured cells and animal studies to tease out the details of how cells migrate through the epidermis. By 2004, much had been learned about the mechanisms that demarcate the switch from proliferation to differentiation.

Then microRNAs appeared on the scene. These short, single-stranded RNA molecules turn down the production of certain proteins by binding to the mRNAs that normally serve as 'recipes' for those proteins' synthesis. "We started to wonder whether microRNAs might also be involved in the switch," says Fuchs.

Working with mice, Fuchs' postdoc Rui Yi found a wealth of microRNAs in skin at various stages of the animals' development. One in particular, named miR-203, stood out. Early in embryonic development, when the epidermis comprises just one layer, Yi found no miR-203 expression. But by the time these stem cells began to generate differentiating epidermal layers, miR-203 levels were high. This suggests that the microRNA might be involved in the switch to stratification and differentiation.

So Fuchs and her collaborators began investigating miR-203's function — work that involved many late nights in the lab. "I received plenty of emails from Rui at 2 and 3 a.m.," Fuchs acknowledges. But the results were worth the hard work. The team discovered that miR-203 interacts with the mRNA for a protein that is known to help epithelial stem cells maintain their proliferative abilities or 'stemness' (see page 225). The prevalence of this protein, called p63, was reduced whenever miR-203 was expressed.

Knockout of p63 in mice leads to stem-cell depletion and severe developmental abnormalities. Fuchs and her team found that precocious expression of miR-203 in mouse basal layer cells causes lethal flaws that resemble those of p63-knockout mice. Conversely, miR-203 knockdown resulted in p63 levels being boosted, and sustained cell proliferation in epidermal layers beyond the basal layer.

Fuchs suggests that, in skin, miR-203 may function as a fine-tuning system for the switch from stem-cell proliferation to differentiation. "When a cell commits to differentiate, the first step is to induce changes in gene expression and generate different mRNAs," she says. "But simultaneously reducing protein expression makes for a cleaner, swifter change in the transition."

MicroRNAs may have roles in many developmental processes and some cancers. MiR-203 might be a therapeutic target for a type of cancer known as squamous cell carcinoma, Fuchs suggests. She adds that "if microRNAs turn out to be broadly important in controlling the balance between stem cells and differentiation, their therapeutic potential could be even greater". ■

# FROM THE BLOGOSPHERE

Posters are an important tool for communicating research findings to a large audience, but their value can be hit-and-miss, according to Martin Fenner's Nature Network blog Gobbledygook (http://tinyurl.com/2d8tob). The research presented in many posters will never be peer-reviewed or published. And although at some meetings the poster presentation leads to stimulating discussions, at others, Fenner says, it is mainly "a trick to increase conference attendance".

The authors of a paper in *Deutsches Ärzteblatt* interviewed poster authors and attendees at a conference and found that although poster-session attendance was very low, the event was valued by younger scientists and by the meeting's moderators. Almost one-third of the posters had already been presented elsewhere.

Fenner concludes that poster presentations should be taken more seriously. Meeting organizers should select abstracts through a competitive peer-review process, rejecting those that have already been presented or published, and should allow space and time for viewing posters during a meeting. ■

**Visit Nautilus for regular news relevant to *Nature* authors ▸ http://blogs.nature.com/nautilus and see Peer-to-Peer for news for peer reviewers and about peer review ▸ http://blogs.nature.com/peer-to-peer.**

nature

www.nature.com/nature

Vol 452 | Issue no. 7184 | 13 March 2008

## EDITORIAL

**LONDON** nature@nature.com
The Macmillan Building, 4 Crinan Street, London N1 9XW
Tel: +44 (0)20 7833 4000 Fax: +44 (0)20 7843 4596/7
**EDITOR-IN-CHIEF:** Philip Campbell
**PUBLISHING EXECUTIVE EDITOR:** Maxine Clarke
**EDITORIALS:** Philip Campbell, M Mitchell Waldrop
**NEWS/FEATURES/ONLINE NEWS:** Oliver Morton, Geoff Brumfiel, Daniel Cressey, Michael Hopkin, Nicola Jones, Anna Petherick, Katharine Sanderson, Sarah Tomlin, Gaia Vince
**BOOKS & ARTS/CORRESPONDENCE & ESSAYS/COMMENTARIES:** Sara Abdulla, Joanne Baker, Lucy Odling-Smee, Sarah Tomlin
**NATURE PODCAST:** Sara Abdulla, Adam Rutherford, Kerri Smith, Charlotte Stoddart
**NEWS AND VIEWS:** Tim Lincoln, Andrew Mitchinson, Sadaf Shadan, Richard Webb
**PHYSICAL, CHEMICAL AND EARTH SCIENCES:** Karl Ziemelis, Rosamund Daw, Joshua Finkelstein, Magdalena Helmer, Juliane Mössinger, Karen Southwell, John VanDecar, Liesbeth Venema
**BIOLOGICAL SCIENCES:** Ritu Dhand, Lesley Anson, Tanguy Chouard, Henry Gee, Marie-Thérèse Heemels, Rory Howlett, Claudia Lupp, Barbara Marte, Deepa Nath, Ursula Weiss **INSIGHTS/REVIEWS/PROGRESS:** Lesley Anson
**SUBEDITORS:** Colin Sullivan, Sarah Archibald, Anne Blewett, Catherine Cassidy Davina Dadley-Moore, Isobel Flanagan, Paul Fletcher, Jenny Gillion, Dinah Loon, David Price, Chris Simms, Anna York
**EDITORIAL PRODUCTION:** James McQuat, Alison Hopkins, Marta Rusin, Charles Wenz, Lauren Wehmar
**MANUFACTURING PRODUCTION:** Jenny Henderson, Stewart Fraser, Susan Gray, Jocelyn Hilton, Yvonne Strong
**ART AND DESIGN:** Martin Harrison, Wesley Fernandes, Madeline Hutchinson, Barbara Izdebska, Paul Jackman, Fern McNulty, Nik Spencer
**ADMINISTRATION:** Karen Jones, Helen Anthony, Jayne Henderson, Diane Kempinski, Aimee Knight, Alison McGill, Jenny Meyer, Nichola O'Brien, Naomi Thornhill, Holly Welham
**PRESS OFFICE:** Ruth Francis, Katherine Anderson, Jen Middleton, Rachel Twinn

**WASHINGTON DC** nature@naturedc.com
968 National Press Building, 529 14th St NW, Washington DC 20045-1938
Tel: +1 202 737 2355 Fax: +1 202 628 1609
**EDITORIAL:** Eric Hand, Gene Russo, Leslie Sage, Jeff Tollefson, M Mitchell Waldrop, Alexandra Witze **ADMINISTRATION:** Katie McGoldrick, Kenneth Simpson

**NEW YORK** nature@natureny.com
75 Varick St, 9th Floor, New York, NY 10013-1917
Tel: +1 212 726 9200 Fax: +1 212 696 9006
**EXECUTIVE EDITOR:** Linda Miller
**EDITORIAL:** I-han Chou, Chris Gunter, Kalyani Narasimhan, Helen Pearson

**BOSTON** nature@boston.nature.com
25 First Street, Suite 104, Cambridge, MA 02141
Tel +1 617 475 9275 Fax: +1 617 494 4960
**EDITORIAL:** Angela Eggleston, Joshua Finkelstein, Heidi Ledford **ADMINISTRATION:** Eric Schwartz

**SAN FRANCISCO** nature@naturesf.com
225 Bush Street, Suite 1453, San Francisco, CA 94104
Tel +1 415 403 9027 Fax: +1 415 781 3805
**EDITORIAL:** Erika Check Hayden, Natalie DeWitt, Alex Eccleston
**ADMINISTRATION:** Jessica Kolman

**SAN DIEGO** n.dalton@naturesf.com
3525 Del Mar Heights Road, PMB No. 462, San Diego, CA 92130
Tel +1 858 755 6670 Fax: +1 858 755 8779
**EDITORIAL:** Rex Dalton

**MUNICH** a.abbott@nature.com
Josephspitalstrasse 15, D-80331 München
Tel. +49 89 549057-13 Fax. +49 89 549057-20
**EDITORIAL:** Alison Abbott, Quirin Schiermeier

**PARIS** d.butler@nature.com
2 rue Moreau Vincent, 37270 Véretz Tel +33 2 47 35 72 15
**EDITORIAL:** Declan Butler

**TOKYO** editnature@natureasia.com
Chiyoda Building 5-6th Floor, 2-37 Ichigaya Tamachi, Shinjuku-ku, Tokyo 162-0843
Tel +81 3 3267 8751 Fax: +813 3267 8754
**EDITORIAL:** David Cyranoski, Mika Nakano, Akemi Tanaka

**CONTRIBUTING CORRESPONDENTS**
**AUSTRALASIA:** Carina Dennis Tel: +61 2 9404 8255
**INDIA:** K. S. Jayaraman Tel: +91 80 2696 6579
**ISRAEL:** Haim Watzman Tel: +972 2 671 4077
**SOUTH AFRICA:** Michael Cherry Tel: +27 21 886 4194
**WASHINGTON DC:** Meredith Wadman Tel +1 202 626 2514
**MISSOURI:** Emma Marris Tel: +1 573 256 0611

## NATURE ONLINE

www.nature.com/nature

**CHIEF TECHNOLOGY OFFICER:** Howard Ratner **PUBLISHING DIRECTOR, NATURE.COM:** Timo Hannay
**WEB PRODUCTION/DESIGN:** Jeremy Macdonald, Glennis McGregor, Alexander Thurrell
**WEB PRODUCTION TECHNOLOGIES:** Heather Rankin **APPLICATION DEVELOPMENT:** Peter Hausel

## PUBLISHING

**LONDON** feedback@nature.com
The Macmillan Building, 4 Crinan Street, London N1 9XW
Tel: +44 (0)20 7833 4000 Fax: +44 (0)20 7843 4596/7
**MANAGING DIRECTOR:** Steven Inchcoombe
**PUBLISHER:** Steven Inchcoombe
**ASSISTANT PUBLISHER:** Samia Mantoura
**PUBLISHING ASSISTANT:** Claudia Banks

**TOKYO** feedback@natureasia.com
Chiyoda Building 5-6th Floor, 2-37 Ichigaya Tamach , Shinjuku-ku, Tokyo, 162-0843
Tel: +81 3 3267 8751 Fax. +81 3 3267 8754
**PUBLISHING DIRECTOR — ASIA-PACIFIC:** David Swinbanks
**ASSOCIATE DIRECTOR — ASIA-PACIFIC:** Antoine E Bocquet

## DISPLAY ADVERTISING

**MANAGEMENT:** John Michael

**NORTH AMERICA** display@natureny.com
**NEW ENGLAND:** Sheila Reardon Tel: +1 617 494 4900 Fax +1 617 494 4960
**NEW YORK/MID-ATLANTIC/SOUTHEAST:** Jim Breault Tel: +1 212 726 9334 Fax: +1 212 696 9481
**MIDWEST:** Mike Rossi Tel: +1 212 726 9255 Fax: +1 212 696 9481
**WEST COAST SOUTH:** George Lui Tel: +1 415 781 3804 Fax: +1 415 781 3805
**WEST COAST NORTH:** Bruce Shaver Tel +1 415 781 6422 Fax +1 415 781 3805

**EUROPE/REST OF WORLD** display@nature.com
**GERMANY/SWITZERLAND/AUSTRIA/OTHER EUROPE:** Sabine Hugi-Fürst
Tel: +41 52 761 3386 Fax: +41 52 761 3419
**UK/IRELAND/FRANCE/BELGIUM:** Jeremy Betts
Tel: +44 (0)20 7843 4959 Fax +44 (0)20 7843 4749
**SCANDINAVIA/THE NETHERLANDS/ITALY/SPAIN/PORTUGAL/ISRAEL/ICELAND:** Graham Combe
Tel: +44 (0)20 7843 4914 Fax, +44 (0)20 7843 4749

**ASIA-PACIFIC** display@natureasia.com
**JAPAN:** Kate Yoneyama, Ken Mikami
Tel: +813 3267 8765 Fax +813 3267 8746
**GREATER CHINA/SINGAPORE:** Gloria To
Tel: +852 2811 7191 Fax: +852 2811 0743

## SPONSORSHIP

**EUROPE/NORTH AMERICA** e.green@nature.com
**NATURE BUSINESS DEVELOPMENT EXECUTIVE:** Emma Green
Tel: +44 (0)20 7833 4000 Fax: +44 (0)20 7843 4749

## NATUREJOBS

naturejobs@nature.com

Please refer to panel at the start of the *NatureJobs* section at the back of the issue

## MARKETING & SUBSCRIPTIONS

**USA/CANADA/LATIN AMERICA** subscriptions@natureny.com
Nature Publishing Group, 75 Varick St, 9th Floor, New York, NY 10013-1917
Tel: (USA/Canada) +1 866 363 7860; (outside USA/Canada) +1 212 726 9365
**MARKETING:** Sara Girard **FULFILMENT:** Karen Marshall

**JAPAN/CHINA/KOREA** subscriptions@natureasia.com
Chiyoda Building 5-6th Floor, 2-37 Ichigaya Tamachi, Shinjuku-ku, Tokyo, 162-0843
Tel: +81 3 3267 8751 Fax: +81 3 3267 8746
**MARKETING/PRODUCTION:** Keiko Ikeda, Takesh Murakami

**EUROPE/REST OF WORLD** subscriptions@nature.com
Nature Publishing Group, Subscriptions, Brunel Road, Basingstoke, Hants RG21 6XS, UK
Tel: +44 (0)1256 329242 Fax +44 (0)1256 812358
**MARKETING:** Katy Dunningham, Elena Woodstock

**INDIA** npgindia@nature.com
Nature Publishing Group, 3A, 4th Floor, DLF Corporate Park, Gurgaon 122002
Tel: +91 124 2881053/54 Fax: +91 124 2881052
**HEAD OF BUSINESS DEVELOPMENT, INDIA:** Jaishree Srinivasan **MARKETING:** Harpal Singh Gill

**Annual subscriptions (including post and packing)**

| | |
|---|---|
| **INSTITUTIONAL/CORPORATE RATE:** | $2,730 |
| **PERSONAL RATE:** | $199 |
| **STUDENT RATE:** | $99 |
| **POSTDOC RATE:** | $119 |

Printed in USA. Individual rates available only to subscribers paying by personal check or credit card. Orders for student/postdoc subscriptions must be accompanied by a copy of student ID. Rates apply to USA, Canada, Mexico/Central & South America.
Add 7% GST tax in Canada (Canadian GST number 140911595).
**BACK ISSUES:** US$20.00

## SITE LICENSES FULFILMENT & CUSTOMER SERVICES

feedback@nature.com

**SITE LICENSES:** npg.nature.com/libraries
**FULFILMENT:** Dominic Pettit
**CUSTOMER SERVICE:** Gerald Coppin

**ELECTROCOMPETENT STRAINS NOW AVAILABLE**

NEW ENGLAND BIOLABS


# Competent Cells from New England Biolabs

## COMPLETING YOUR CLONING NEEDS

Make the switch to competent cells from New England Biolabs to help bring success to your research. Our expanded line of competent cells includes a variety of strains for cloning and expression, as well as strains with unique properties (see chart). For added convenience we offer a choice of efficiencies, formats and customized packaging. Now you can digest, ligate and transform with reagents from the name you trust.

**Advantages**

- Extremely high transformation efficiencies
- Phage T1 resistance (*fhuA2*) preserves clone integrity
- Choice of protocols: high efficiency or 5 minute transformation
- Nonspecific endonuclease activity eliminated, resulting in highest quality plasmid preparations
- Express difficult or toxic proteins with T7 Express strains containing $lacI^q$ and/or a novel lysY variant
- Obtain colonies faster than any other commercial strain with NEB Turbo
- SOC Outgrowth Media and pUC19 Control Plasmid included
- Free of animal products

| Cloning strain characteristics | Strain | NEB # |
|---|---|---|
| Obtain colonies faster than any other commercial strain (6.5 hours) | | C2984H/I |
| Versatile cloning strain | | C2987H/I |
| Cloning of toxic genes | | C2992H/I |
| Cloning of large plasmids and BACs | | C3019H/I |
| Growth of unmethylated | | |

| Expression strain characteristics | Strain | NEB # |
|---|---|---|
| Most popular non-T7 protein expression strain | NEB Express Competent *E. coli* | C2523H/I |
| Added control of IPTG induced expression with non-T7 plasmids | | C3037H/I |
| Most popular T7 protein expression strain | | C2566H/I |
| | T7 Express Competent *E. coli* | |
| Tight control of protein expression by inhibition of T7 RNA Polymerase | | C3010H/I |
| Highest level of protein expression control | | C3013H/I |
| For crystallography experiments/SeMet labeling | | C3022H/I |

† *Available as subcloning efficiency* * *Available as electrocompetent cells*

For more information and our international distribution network, please visit www.neb.com
For a copy of our new Competent Cell Brochure, please visit www.neb.com/literaturerequest

**New England Biolabs Inc.** 240 County Road, Ipswich, MA 01938 USA 1-800-NEB-LABS Tel. (978) 927-5054 Fax (978) 921-1350 info@neb.com
**Canada** Tel. (800) 387-1095 info@ca.neb.com • **China** Tel. 010-82378266 beijing@neb-china.com • **Germany** Tel. 0800/246 5227 info@de.neb.com
**Japan** Tel. +81 (0)3 5669 6191 info@neb-japan.com • **UK** Tel. (0800) 318486 info@uk.neb.com

NEW ENGLAND BioLabs® Inc.
*the leader in enzyme technology*

nature

www.nature.com/nature

Vol 452 | Issue no. 7184 | 13 March 2008

# Growing pains

The fight against agricultural diseases in the United States has been boosted by fresh funds and a national monitoring network. But these advances are being undermined by inflexible bureaucracy.

The US government's restrictions on research into 'select agents' — organisms that could potentially be used as bioweapons — have rarely been popular among scientists, largely because of the monitoring and bureaucracy involved. But after the terrorist attacks of 11 September 2001 and the anthrax mailings that followed, researchers have accepted the restrictions as a fact of life. And the consequences have sometimes proved to be positive for science.

This is especially true for research into agriculturally important plant diseases; pathogens that were first included on the select-agent list in 2002. The concern was that 'agroterrorists' might use these diseases to devastate crops across whole regions or countries. The result has been a much-needed boost in funding for the field — especially for detecting outbreaks of plant disease, whether the origins are natural, accidental or intentional. Before 2002, each state ran its own plant-pathology lab, creating a patchwork monitoring infrastructure with disparate practices and little communication. Now the US Department of Agriculture (USDA) operates an integrated network of plant-disease labs that spans the nation.

Nevertheless, the regulations can be inflexible. Take the case of huanglongbing, or citrus greening (see page 148), a disease from Asia that was first seen in the United States in 2005 near Miami, Florida, and has now spread to nearly half of the state's 67 counties. Scientists there can find the bacterium that causes huanglongbing right outside their windows. But because it is listed as a select agent, they cannot study infected plants in their labs for more than a week without violating the law. So in this instance the listing has become not only irrelevant, but downright harmful because it prevents or delays research that might stop the scourge.

To its credit, the law on select agents allows for situations such as this to be remedied through a biennial re-evaluation of the list. The USDA is undertaking such a review at the moment, and may remove one species of huanglongbing bacterium from the list this year. But the process is far too slow — not least because the USDA casts such a wide net in soliciting feedback for its re-evaluations. When pathogens can explode out of nowhere within months or even weeks, such well-intentioned mechanisms can do more harm than good.

**"When pathogens can explode out of nowhere within months, the slow review process can do more harm than good."**

To prevent this from happening again, the USDA needs to streamline its re-evaluation process to allow it quickly to de-list a plant disease once it becomes widespread in US soil. Waiting for an arbitrary deadline or excessive amounts of outside input before making such decisions undoes what good the select-agent rule has done.

Last October, the House Committee on Energy and Commerce held a hearing in which some members called for greater oversight of biosecurity research. The focus was the proliferation of laboratories studying human and animal pathogens that could be used as agents of terror. But Congress should also reconsider what oversight and coordination can do to protect people and plants. And it should pay heed to the Catch-22 of regulating research that needs to be nimble and creative to effect such protection. ■

# Markets can save forests

With the right infrastructure, the forces threatening to destroy the world's trees could be their salvation.

Trees are worth more dead than alive on the international market — a stark economic fact that has undermined countless programmes to protect rainforests over the years. It is a lesson that should not be forgotten as the international community explores ways to reduce global-warming emissions from deforestation. Conventional programmes involving incentives, laws and enforcement may prove useful, or even necessary — as highlighted by Brazil's approach to the issue (see page 134) — but to solve the problem completely, the international community will need to design a better market that recognizes the value of standing trees, forests and the less tangible services they provide. Integrating deforestation into international carbon markets, the most notable of which is the European emission-trading scheme, is a good place to start.

In this context, the European Commission's recent proposal to bar deforestation credits from the next phase of trading is a disappointment. The commission's fear is that cheap deforestation credits will suddenly soak up all of the money for reducing emissions (see *Nature* 452, 8–9; 2008). If ending deforestation quickly is indeed the cheapest way of reducing emissions, it is not clear why this should be a problem. But in truth, a great deal has to be accomplished before any market scheme will be viable.

In recent years, for example, scientists have greatly improved their models for estimating the most critical number for deforestation: the amount of carbon released into the atmosphere when a given plot of land is razed. This information can now be extracted fairly accurately from satellite images. But to do that consistently, on a global scale, rainforest nations will need to train people and develop a standing infrastructure for monitoring. This will not be cheap — and is another area in which conventional government-run programmes might be needed. The scientific community can play a direct role as well, by helping to get these programmes up and running.

Access to information will be critical. A few satellites can cover the

entire globe, but there needs to be a system in place to ensure their images are readily available to everyone who needs them. Brazil has set an important precedent by making its Earth-observation data available, and the rest of the world should follow suit. This is more than a matter of common courtesy. It will foster the kinds of checks and balances and independent analysis that must necessarily underpin a viable carbon market.

And the international community needs to start thinking about the next step: how to encourage good forest stewardship. As it stands, nations such as India and Costa Rica are in the odd position of receiving little or no benefit from a market in carbon credits precisely because they have been able to control deforestation. And if illegal deforestation were to come to a halt, then those nations benefiting from the carbon market would see that source of income dry up, creating the same pressures that caused the problem in the first place.

True, dealing with standing forests will be tricky; no one wants to create a permanent welfare programme for the tropics. Nevertheless it is vital that the issue is tackled. This is essentially what the delegates agreed to do last December at the United Nations climate-change conference in Bali, and their decision was a wise one. As long as the international community is playing with the architecture of a carbon economy, it should explore new and creative ways to build in 'ecosystem services' such as biodiversity and coastal protection. Bear in mind that the alternative to putting an economic value on these intangibles is implicitly to set their value at zero.

**"Global warming has given the world the opportunity to build a more comprehensive and inclusive economic model."**

One of the oddly positive effects of global warming is that it has given the world the opportunity to build a more comprehensive and inclusive economic model by forcing all of us to grapple with our impact on the natural environment. We are entering a phase in which new ideas can be developed, tested, refined and rejected as necessary. If we find just one that can beat the conventional economic measure of gross domestic product, and can quantify some of the basic services provided by rainforests and other natural ecosystems, it will more than pay for itself. ■

# On message, off target

## Official advice on vaccination is too often poorly transmitted.

The cause of science-based policy was not helped late last month when the presumptive Republican candidate for the US presidency, John McCain, promoted the discredited notion that a preservative in vaccines causes autism. Such statements have power, as Anna Pearce and her colleagues remind us in the online edition of the *British Medical Journal* (A. Pearce *et al. Br. Med. J.* doi:10.1136/bmj.39489.590671.25; 2008). They find that, following the 1998 scare in Britain, when autism was baselessly linked to the triple vaccination for measles, mumps and rubella, uptake by parents, having bottomed out at 79%, has now climbed to 89% — but still falls below the 95% level required for herd immunity.

The paper, valuable in its analysis of parents' decision-making, emphasizes the need to provide "evidence based information … tailored to respond to particular concerns, questions, and beliefs of different groups". Unfortunately, it seems that official sources are not following that advice.

Consider, for example, a separate study of the cognitive frameworks that US parents use to absorb information about vaccination, carried out by Baruch Fischhoff, an authority on risk perception, and his colleagues at Carnegie Mellon University in Pittsburgh, Pennsylvania (J. S. Downs *et al. Vaccine* doi:10.1016/j.vaccine.2008.01.011; 2008). The researchers conducted phone interviews with parents in three US cities — Kansas City, Philadelphia and Eugene — and did in-depth interviews with parents selected by a market-research company for diversity in race, background and vaccination attitudes. The number was small — 30 — and the authors rightly emphasize that the study is preliminary rather than conclusive. But the results are suggestive, and consistent enough to make any sensible policy-maker think.

Working with officials at the Centers for Disease Control and Prevention (CDC) in Atlanta, Georgia, the team identified 24 possible conceptual variables that might feature explicitly or implicitly in parents' decisions whether or not to have their child vaccinated. These include 'public-health credibility', 'benefit of vaccinating', 'herd immunity', 'information', 'personal values', 'vaccine safety research' and 'risk of vaccinating'.

The parents, all with children aged between 18 and 23 months, were interviewed individually in a way that explored their 'mental model' of vaccination — that is, their beliefs about these concepts and the relationships between them. The parents were also presented with official pro-vaccination communications from the CDC and unofficial anti-vaccination communications, along with questions that explored their trust in both. By analysing the parents' responses for each communication, the authors were able to map how it influenced their mental models, and ultimately their decision whether to vaccinate.

The authors' conclusion is that anti-vaccination communications play on a much richer field of considerations in parents' heads than the official communications. The latter rely on science-based reassurance — and, indeed, were received by the parents with a relatively high degree of trust. But they tell a much less comprehensive and connected story than the anti-vaccination communications, which in some cases ended up having a correspondingly higher degree of influence.

Not surprisingly, many parents spoke of the Internet as a key source of advice. The authors explored how the parents were using the Internet and then conducted similar searches to see what they would find. They concluded that more than 90% of the parents would encounter anti-vaccination advice among the top 10 returns from search engines, with such results often ranking higher than official websites.

John McCain's comments won't have helped US public health — but neither, it seems, do most official communications. The CDC and others sources of health advice need to be much more sophisticated in how they communicate if vaccination myths are to be successfully countered. ■

# RESEARCH HIGHLIGHTS

## Nosing around

*J. Exp. Biol.* 211, 921-934 (2008)

The elephant nose fish uses its eponymous if misnamed adaptation — actually a protuberant chin appendage — as an electrical 'flashlight', and Jacob Engelmann at the University of Bonn in Germany and his colleagues have shown how *Gnathonemus petersii* senses objects through the distortions they cause in an electric field that it creates.

The researchers confirm that elephant noses have two different high-acuity sensory regions, known as foveae. One is the actual nasal region, and the other is in its characteristic chin, called a Schnauzenorgan. The highest density of electrical receptors is at the tip of this appendage.

PIXONNET.COM/A_AMY

EVOLUTION

## Streetwise weeds

*Proc. Natl Acad. Sci. USA* 105, 3796-3799 (2008)

City weeds are adapting to their urban environment at a staggering rate, suggests a research team in France.

Pierre-Olivier Cheptou and his colleagues at the CNRS, France's basic-research agency, in Montpellier analysed the dispersal of the weed *Crepis sancta*, which produces two types of seed — a light, feathery, wind-dispersed one and a heavy one. The researchers found that feathery seeds dispersed along Montpellier's city streets have a 55% lower chance of successfully settling in their parent's local patch than heavy seeds. In patchy, pavement-dense habitats, weeds release a significantly higher proportion of heavy seeds than do their country counterparts.

Genetic evaluations suggest that short-term evolution has taken place during a mere 5–12 generations.

ASTRONOMY

## Magnetic flux

*Mon. Not. R. Astron. Soc.* doi:10.1111/j.1365-2966.2008.12946.x (2008)

The Sun's magnetic poles are known to reverse their polarity every 11 years, but it is not alone — another 'flip-flopper' has been identified. Recent mapping of the magnetic field around nearby star Tau Bootis shows that its polarity has reversed since the last observation in 2006.

Measurements of the polarization of the light emitted by Tau Bootis allow its complicated magnetic structure to be calculated. Astronomers expect that many stars periodically reverse their magnetic polarity, but so far only about 20 stars have had magnetic polarization measurements taken more than once.

Jean-François Donati of France's CNRS and his colleagues, who made the discovery, estimate that Tau Bootis's poles flip every year or so.

CHEMISTRY

## A ring-side seat for chloride

*Angew. Chem. Int. Edn* doi:10.1002/anie.200704717 (2008)

Normally, opposites attract, but chemists at Indiana University in Bloomington have designed an uncharged organic molecule that can nevertheless attract and hold negatively charged ions.

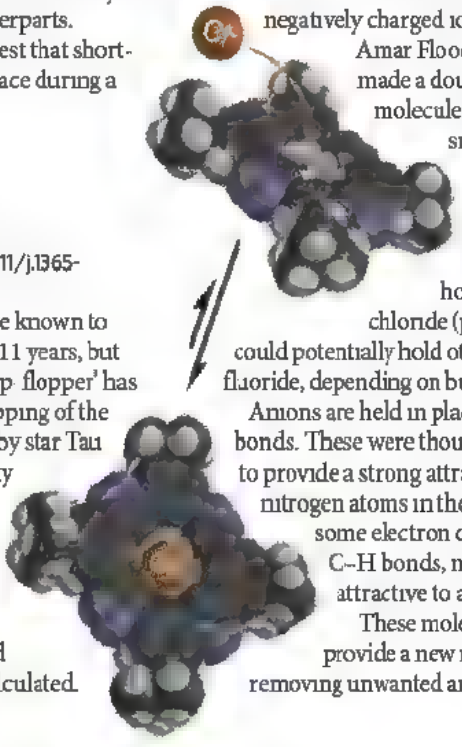

Amar Flood and Yongjun Li made a doughnut-shaped molecule from a number of small building-block molecules, using a technique called 'click chemistry'. The doughnut's hole snugly fits a chloride (pictured left), and could potentially hold other anions such as fluoride, depending on building-block size.

Anions are held in place by hydrogen bonds. These were thought to be too weak to provide a strong attractive pull, but nitrogen atoms in the doughnut draw some electron density out of the C–H bonds, making it more attractive to a negative ion.

These molecules could provide a new regime for removing unwanted anions from solution.

THEORETICAL PHYSICS

## Holographic memory

*Phys. Rev. A* 77, 020302 (2008)

A special type of hologram may provide a way to store light's quantum information.

Regular holograms store three-dimensional information in an interference pattern, often etched on a glass surface. But such a system won't work for quantum information, which includes fundamental uncertainties that cannot be held in a classical medium.

Eugene Polzik of the Danish Research Center for Quantum Optics in Copenhagen and his colleagues at St Petersburg University in Russia determined a way to store light's quantum properties in a cloud of atoms. By entangling the light with atoms at a temperature close to absolute zero, it should be possible to store the quantum features of the light in the atoms' collective spins. The information can then be read from the atoms by reversing the process.

CHEMICAL BIOLOGY

## Fixing fragile flies

*Nature Chem. Biol.* doi:10.1038/nchembio.78 (2008)

A fruitfly model of fragile X syndrome, a common cause of mental retardation in humans, has unveiled possible therapeutic targets to combat the condition.

Flies lacking a gene called *Fmr1* exhibit some physical and behavioural features of fragile X syndrome. Stephen Warren at Emory University School of Medicine in Atlanta, Georgia, and his colleagues found that food enriched with glutamate, which functions as an excitatory neurotransmitter, kills mutant embryos.

The researchers screened a library of 2,000 compounds and characterized nine that

allowed *Fmr1* mutants to survive a high glutamate diet. Three of the compounds affect the inhibitory neurotransmitter, GABA. Treating mutants with GABA relieved glutamate toxicity, and restored several features, including normal courtship behaviour and some brain morphology

FOOD SCIENCE

## The origins of *la louche*

*Langmuir* 24, 1701-1706 (2008)

Part of the allure of aniseed-flavoured spirits such as absinthe (pictured below), ouzo and pastis is the mysterious 'louche' — their transformation from clear to cloudy and opalescent with the addition of water. The effect comes from the formation of insoluble, milky droplets of anise-flavoured oil

Details of the process are murky, however. Erik van der Linden of Wageningen University in the Netherlands and his colleagues made the first direct measurement of the oil droplets' interfacial tension, which determines how fast they grow. These rates, and their dependence on ethanol concentration, differ from those predicted by conventional theory.

Because this 'spontaneous emulsification' is being explored for various purposes, including the production of drug-loaded nanoparticles and microcapsules, the discrepancy is more than just a puzzle for barflies.

PIXONNET.COM/A.AMY


GEOLOGY

## Glacier slimming

*Geology* 36, 223-226 (2008)

Satellites have documented the rapid decline of the West Antarctic ice sheet during the past two decades, with thinning of more than a metre per year. But pre-satellite — let alone prehistoric — data are harder to come by.

Joanne Johnson from the British Antarctic Survey in Cambridge, UK, and her colleagues used rocks to gain insight into the history of glaciers by the Amundsen Sea Embayment. They suggest that, for most of the past 10,000 years, these glaciers have been thinning at rates of just a few centimetres per year

The team took samples from nunataks — rocky peaks that poke through the ice and sometimes, like dipsticks, contain evidence of historical glacier heights. The thinning rates, which the researchers established by isotopic dating of quartz grains from within seven rock samples, suggest a lower boundary for long-term ice loss. In this context, contemporary loss rates are catastrophic.

STRUCTURAL BIOLOGY

## Into the groove

*Mol. Cell* 29, 525-531 (2008)

Genes are often marked for silencing by the addition of methyl groups to DNA. This type of modification is recognized by transcriptional regulators such as the repressor MeCP2, but not in the way generally predicted, according to research by Adrian Bird and Malcolm Walkinshaw at the University of Edinburgh, UK, and their collaborators.

Previous studies predicted that a hydrophobic patch in the MeCP2 protein made contact with methylated DNA. However, structural analysis of how the two molecules bind together suggests that hydrogen bonding of MeCP2 with the water-containing groove in the DNA double helix is crucial.

The research also reveals how a mutation common in Rett syndrome, an autism spectrum disorder, might disrupt this binding.

OPTICS

## How to make a black hole

*Science* 319, 1367-1370 (2008)

Researchers have created an analogue of a black hole in a lab, using light trapped in an optical fibre. This optical black hole affects light in ways equivalent to the intense gravity at a black hole's 'event horizon', beyond which no light can escape.

Pulses of light travelling down the fibre affect the fibre's light-carrying properties in a manner analogous to the bending of space-time by gravity. The leading edge of a pulse then acts like an event horizon when it catches up with slower light up ahead. Meanwhile, the pulse's trailing edge becomes equivalent to a white-hole event horizon, where no light can enter. Here, a faster-moving stream of light behind the pulse is reflected back, and shifted in frequency, just as is predicted for a real white hole.

## JOURNAL CLUB

**John Church**
**Centre for Australian Weather and Climate Research, Tasmania, Australia**

**An oceanographer ponders the difficulty of accurately estimating abyssal-ocean warming.**

Estimating how much oceans are warming and where within them heat is stored is a fascinating challenge for me and my fellow oceanographers. So far, most studies comparing observations and models of changing ocean temperatures have focused on the upper 1 kilometre of water. But what about the abyssal depths, from about 3,000 metres to the bottom? Are changes in those waters really so slow as to be essentially irrelevant to atmospheric warming?

The most comprehensive surface-to-bottom measurements of ocean temperature were collected by research ships over many months during the World Ocean Circulation Experiment in the 1990s. By comparing these observations with more recent ones from the World Climate Research Programme's CLIVAR Project, Greg Johnson and his colleagues have shown that the Pacific Ocean's abyssal waters have warmed during the past two decades (G. C. Johnson *et al. J. Clim.* 20, 5365–5375; 2007).

Although the temperature increase is small — up to about 0.01 °C — compared with the much larger changes in the upper 1,000 metres of the ocean, it has occurred over a thickness of several kilometres, implying a huge quantity of heat storage. The deep warming is strongest in the south-west Pacific, where newly ventilated abyssal waters enter from the south.

The Pacific warming, and abyssal warming elsewhere, means that we should start considering abyssal waters when estimating sea-level rise and the climate's sensitivity to increasing greenhouse-gas concentrations. There is plenty to find out: how does the heat reach abyssal waters? Is the warming human-induced? Designing and implementing an adequate abyssal-water-observing system is a high priority.

Discuss this paper at **http://blogs.nature.com/nature/journalclub**

NEWS

# Stem-cell claim gets cold reception

A Californian biotech company claims that it has used carbon nanotubes to 'reprogramme' adult human cells to an embryonic-like state — a breakthrough that removes the elevated risk of cancer that blights other techniques. But uncertainties about the cells, which have yet to be reported in a peer-reviewed journal, have left many sceptical.

Last year, researchers led by Shinya Yamanaka of Kyoto University demonstrated that by using just four genes it was possible to reprogramme adult human skin cells to a stem-cell like pluripotent state — meaning that they could develop into any of the body's cell types. These 'induced pluripotent stem' (iPS) cells hold tremendous therapeutic potential. But to insert the genes into the cells, researchers have had to use viral vectors, which can turn the cells cancerous.

PrimeGen, based in Irvine, claims to have got around this problem by using single-walled carbon nanotubes — cylinders of carbon molecules only a few nanometers in diameter — to introduce a complex of around a dozen proteins, including the ones coded for by the four genes used by Yamanaka, plus a fifth called Nanog. The researchers used the nanotube delivery system to introduce genes into human testicular and retinal cells, and PrimeGen reports that they were quickly taken up by an impressive 80% of the cells.

The method is based on work by Hongjie Dai of Stanford University in Palo Alto, California. Dai's group has demonstrated that nanotubes can deliver cancer-targeting drugs[1], proteins and DNA[2] into cells. According to Dai, the nanotubes with their cargo are absorbed by the cells through endocytosis, a process by which the cell membrane envelopes molecules outside the cell, but there is uncertainty over how this happens.

PrimeGen has now announced an alliance with Unidym, based in Menlo Park, California, which makes the nanotubes. Robert Bismuth, vice president of marketing at Unidym, says that the researchers used nanotubes because they "are quite good at getting through a cell membrane" and because their long tubular structure enables each to carry several molecules.

But on the bigger claim that they can reprogramme cells, PrimeGen president John Sundsmo admits a few problems. He says that from around day three the cells start acting like embryonic stem cells and expressing proteins characterizing pluripotency. But after day 14 "they almost all stop". "It's like a switch is turned on and then turned off," Sundsmo says. True embryonic stem cells and iPS cells exhibit pluripotent markers and proliferate quickly and endlessly.

Konrad Hochedlinger, a stem-cell researcher at Harvard University who has done some of the most rigorous tests on iPS cells, suggests that the introduced factors produced a momentary blip of activity before being diluted. "These findings are less interesting as they may only reflect transient transcriptional changes but not stable cellular changes," he says.

"They look really good. But what I'd really like to see is the paper published."

However, Sundsmo says that the cells show a stable "intermediate" stage of reprogramming that will be useful for therapy and basic research. He admits however the word "intermediate" is "loose and somewhat arbitrary". "There is a disconnect between pluripotency and proliferation," he says. "We haven't figured it out yet." Sundsmo says that they await results of a teratoma test — where cells are allowed to develop *in vivo* — that could prove whether the cells actually are pluripotent.

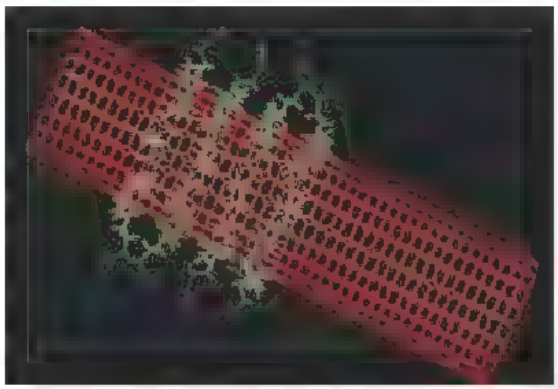

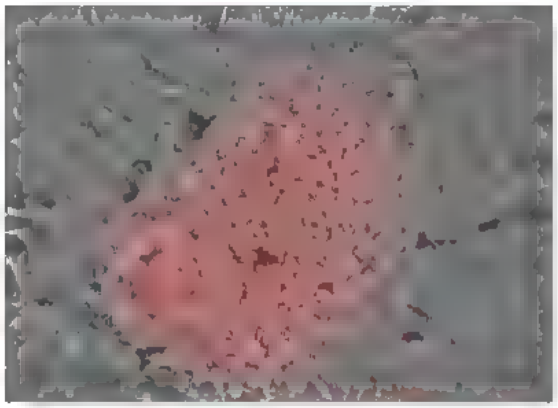

Nanotubes (above) were used to introduce a complex of proteins into testicular cells (stained, below).

JUNDYM

PRIMEGEN

Frank Edenhofer, a stem-cell expert at University of Bonn in Germany, calls the technique "attractive and promising" But his own experiments have shown nanoparticles to be "toxic and display low efficiency". Other groups have also found that nanotubes can kill cells and have difficulty releasing their cargo. Matt Becker of the National Institute of Standards and Technology in Gaithersburg, Maryland, says that the ability of nanotubes to transfect cells without doing harm "depends critically on how the materials were prepared, dispersed in solution, and specific mechanism of entry into the cell interior".

Few scientists have seen PrimeGen's cells. One, Peter Donovan, a stem-cell expert at the University of California in Irvine and a member of PrimeGen's advisory board, says: "They look really good. But what Id really like to see is the paper published."

Most scientists contacted by *Nature* have expressed scepticism because PrimeGen announced its findings on 26 February at an investors meeting rather than in a scientific publication. Another PrimeGen scientific advisory board member, stem-cell pioneer Rudolf Jaenisch of the Massachusetts Institute of Technology in Cambridge, told *Nature*, without giving a reason, that he quit the board the following day. PrimeGen seemed unaware of Jaenisch's move when contacted by *Nature*.

Sundsmo says that they decided to announce the results ahead of publication because the company has already filed patent applications. He says: "This is conceptually a very simple observation that is easily repeated."

Two years ago, PrimeGen similarly publicized experimental results describing the derivation of pluripotent stem cells from sperm precursor cells (see *Nature* **440**, 586–587; 2006). At the time PrimeGen told *Nature* they would publish a paper, but haven't. Sundsmo says that the science behind that paper, which has been at the core of the company's technology, had to be reformulated because of internal disagreement over what the experiment showed. Sundsmo says that half the company was let go and that the paper has been accepted for publication. ■

**David Cyranoski and Monya Baker**

1. Feazel, R. *et al. J. Am Chem. Soc* **129**, 8438–8439 (1997)
2. Kam, N. W. S. *et al. Angew. Chem. Int. Edn* **44**, 4782–4785 (2005)

**BLACK HOLE' MADE FROM LIGHT**
Pulses in an optical fibre can mimic the space-bending physics of collapsed stars.
www.nature.com/news

GETTY

# Pacific 'dwarf' bones cause controversy

**KOROR, PALAU**

An anthropologist claims to have identified a number of bones belonging to a new type of small-bodied human in island caves in the South Pacific.

Lee Berger of the University of Witwatersrand in South Africa asserts that the skulls and bones, belonging to 26 individuals that lived between 1,000 and 3,000 years ago, provide new insight into how humans can dwarf in island settings. If so, the find fuels the debate on the 'hobbit' — a small early human skeleton found in Flores, Indonesia, about 2,000 kilometres south of Palau[1]. Some researchers claim the hobbit is a separate species, *Homo floresiensis*, which survived on Flores until 13,000 years ago; others say the bones are of dwarfed or otherwise malformed *Homo sapiens*.

Berger is not calling the Palau bones a new species: unlike in the Flores hobbit, the Palau skulls show no evidence of a particularly small brain. Berger says the small pelvis, dental formations and long-bone measurements belong to true dwarfs — people who got smaller, perhaps owing to the islands' limited resources or a genetic disorder. "I felt right away this was a minute human being," he says. Berger and his colleagues report their findings this week in the journal *PLoS One*[2].

D. PERRINE/NATUREPL.COM

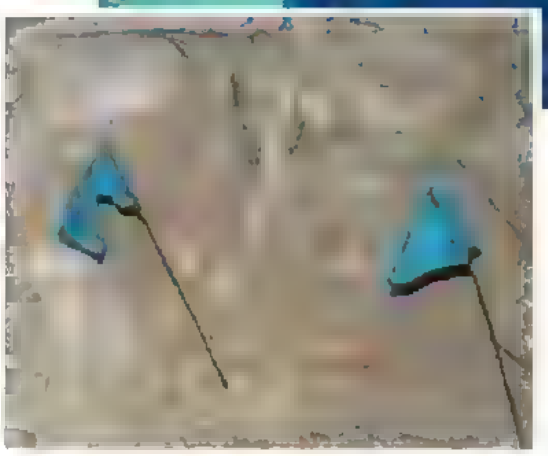

R. DALTON

**Bones found on Palau will fuel the debate over whether islands harboured small humans.**

But other researchers are sceptical of the dwarf theory. "On a scientific level, it is almost unbelievable," says Scott Fitzpatrick, an anthropologist at North Carolina State University in Raleigh who has studied the region for a decade. "This will really take independent confirmation."

The Palau bones could simply belong to children. Fitzpatrick found a number of juvenile bones at the burial site he studied on Orrak Island, four kilometres north of one of Berger's sites. It may have been local custom to bury children together, he notes.

Fitzpatrick questions why this group would dwarf when people of normal stature lived around them at the same time. "This seems very weird to me," he says. Fitzpatrick has reported on the western Pacific's oldest burials, dated to 3,000 years ago, on a Palau island just north of Berger's sites[3].

The new claim was first disclosed in a commercial movie produced by the National Geographic Society, which partially funded Berger's work. Although the movie is not scheduled for broadcast in the United States until 17 March, it was shown in Asia on 1 March, before the journal publication, drawing criticism.

In Palau, some officials and traditional leaders are concerned that sacred burial sites were exploited for movie-making rather than scientific purposes. Adalbert Eledui, the state resource manager who oversees the region, describes the movie as "unscientific" and says he should have had notice before it was broadcast to protect the sites from an expected influx of visitors. Now, he says, resource managers may need to build cages to restrict access to the caves.

> "On a scientific level it is almost unbelievable. This will take independent confirmation."

The bones Berger describes come from two burial sites 15 kilometres apart, long known to scientists, tourists and looters. One site, Uchelungs, is called 'Tarzan cave' locally, because people swing from its vines. The other, Omedokel — known as 'bone cave' — is in the heart of diving waters and once contained piles of bones, skulls, pottery and other artefacts that have mostly been looted.

Most of the island's chiefs had never visited the caves before last week, because Palauans typically avoid burial sites. Palau's paramount chief Yutaka Gibbons told *Nature* that he had heard about the bones from people talking in a restaurant about the movie. "This shows disrespect to our people, country and laws," he says. "Before they did anything, they should have sat with us." Berger says he believed that traditional leaders had been briefed on his work in the caves.

"This looks like a classic example of what can go wrong when science and the review process are driven by popular media," says Tim White, a palaeoanthropologist at the University of California, Berkeley.

Berger says he didn't know the movie was scheduled to premiere before the journal report came out. "That is just stupid," he says. ■

**Rex Dalton**


1. Brown, P. *et al. Nature* **431**, 1055–1061 (2004)
2. Berger, L. R., Church[ill], S. E., De Klerk, B. & Quinn, R. L. *PLoS One* **3**, e1780 (2008)
3. Fitzpatrick, S. M. *Antiquity* **77**, 719–731 (2003)

SPECIAL REPORT

# Brazil goes to war against logging

It represents half of the world's rainforest and is home to one-third of Earth's species, yet the Amazon has one of the highest rates of deforestation. **Jeff Tollefson** looks at efforts to curb the problem.

Brazilian President Luiz Inácio Lula da Silva (Lula) mounted a military-style crackdown on deforestation in the Amazon in January — just a month after the government proclaimed that deforestation rates had dropped 59% over the previous three years. The action was prompted by alarming new satellite data from the National Institute for Space Research (INPE) in São José dos Campos, indicating that clear-cutting is once again on the rise.

Brazilian police forces, hundreds strong, are blockading roads, conducting aerial surveys and inspecting agricultural and logging operations. And the nation has singled out about three dozen communities for inspections of land registrations as part of a broader effort to endorse legal development and punish illicit operations by confiscating the land.

The international community is watching closely. More than half of the Amazon lies within Brazil's borders, and the vast majority of deforestation there takes place in just three states — Mato Grosso, Para and Rondonia — on the southern and eastern parts of the rainforest. This area has one of the highest rates of deforestation in the world — deforestation accounts for upward of 20% of the world's greenhouse-gas emissions.

"Brazil is probably the exception to the rule."

In many ways, Brazil is better equipped to deal with the problem than other rainforest nations. Scientists at the INPE have pioneered methods and technologies for tracking deforestation in the Amazon, giving the nation unparalleled ability to monitor its forests from space. "We do not have the atom bomb," says INPE director Gilberto Câmara. "Our space programme is based on the assumption that Brazil is an environmental power." To that end, Câmara says that Brazil is looking for partners to create a centre that would extend Brazil's model of satellite-based monitoring to other nations.

The country is now in a unique position to benefit from a global-warming treaty that rewards nations for avoiding deforestation, a goal that was outlined in December during a United Nations summit in Bali, Indonesia. "A lot of countries are not yet ready for this. They don't yet have the data that would allow you to really start attaching firm numbers to what is happening on the ground," says Hans Verolme, director of global climate change for the conservation group the WWF in Washington DC. "Brazil is probably the exception to the rule."

Brazilian officials know this, just as they are acutely aware of the international community's interest in the Amazon, its biodiversity and, increasingly, the carbon it stores in plants and soils. Brazil is using its substantial influence to oppose the market-based approach to addressing deforestation that is endorsed by many other rainforest nations, opting instead for a more traditional programme involving government aid. In either case, nations would be required to set a baseline on deforestation rates. The market-based approach would involve selling credits for avoided deforestation into a carbon trading market, but Brazil's proposal is that the funds should be distributed directly — and perhaps more quickly — to governments that succeed in reducing deforestation.

It has the capability and commitment, Brazil says, but lacks the resources, to monitor and eventually halt deforestation before it becomes impossible to undo the damage (see 'Beyond redemption?').

Matthew Perl, who handles an Amazon conservation programme for the WWF in Washington DC, credits Lula's administration with going beyond a simple police raid — a tactic that has failed many times in the past — and actually conducting a legal review of land holdings. This might seem easy and obvious, but simple questions about land ownership, zoning and management facilitate illegal activities across the board — precisely because much of the public land has not been through any kind of formal planning process.

Perl offers some rough figures: 20% of the Amazon is in some sort of federal or state protected area; 21% is administered as indigenous territories, occupied by a quarter of a million people; and 24% is nominally private, keeping in mind that many holdings may be illegal.

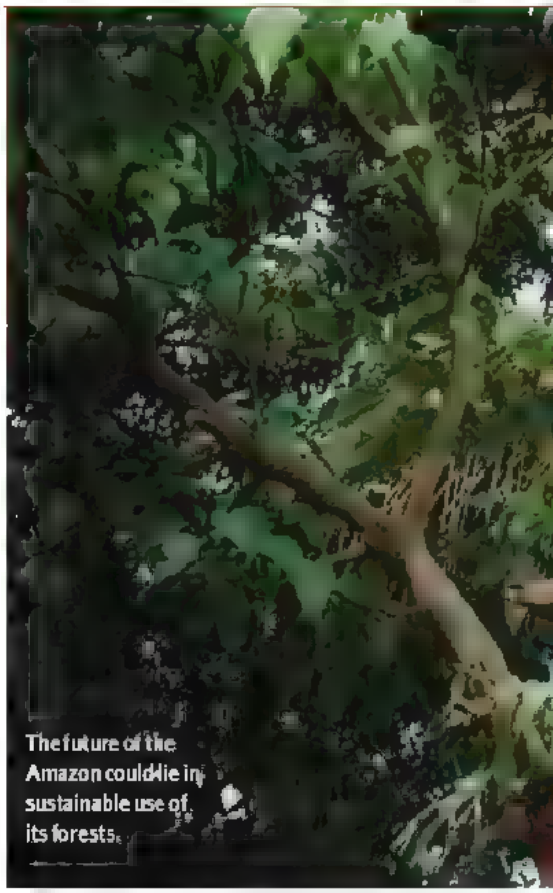

The future of the Amazon could lie in sustainable use of its forests.

© MCPHERSON/CORBIS

The remaining 35% — roughly 38.5 million hectares, an area larger than Germany — is in an 'open-access' category that has no formal zoning plan. Going through existing land registrations, as the government has proposed, is different from designating the remaining land. Tackling that would be difficult, as Brazil would need to address the most contentious questions regarding future development of the Amazon, and to a certain extent Brazil.

## Open claim

In the meantime, these open-access areas of virgin forest fall prey to squatters who claim title to the unregistered land. The logging follows in waves, starting with specialty hard woods such as mahogany and teak and ending with construction-quality timber. Eventually the land is burned and cleared and grazed with cattle, or sown with soya beans. By this time, the squatters have moved deeper into the forest. By some estimates, this process has devoured some 18% of the Amazon.

The Amazon Protected Areas Programme (ARPA), a partnership between the WWF, the Brazilian government, the Global Environment Facility — an organization that funds projects in developing countries — and others, was designed to expand legal protection and ultimately administration of public lands in the Amazon. In many cases, says Gustavo Fonseca, who handles the programme for the

**A RECIPE FOR FOOD EVOLUTION**
Researchers apply statistics to cookery books in different cultures.
www.nature.com/news

Global Environment Facility, a simple registration process has been sufficient to prevent deforestation. Some timber activities or mining operations might take place on the fringes, but nobody wants to invest time and money in a major agricultural operation only to have the government confiscate the land a few years later, he says. "It would be too big a risk."

ARPA was established in 2002 and so far it has registered 14.5 million hectares under strict protections and another 9 million hectares under sustainable-use rules that allow for certain commercial activities such as fishing and rubber extraction and the collection of oils and seeds. Once these communities have a vested interest — sometimes with some training — they can help to enforce their own protections.

This is the ultimate goal of those pushing to create markets for avoiding deforestation. If communities can make money without chopping down trees, they will be more inclined to protect the forest. Unfortunately, that hasn't always happened. As they accumulated a little wealth, some of the communities began investing in something more profitable: cattle. "Not good," says Perl. "Not good at all."

Many experts agree that cattle ranches, driven in part by booming exports, are responsible for most of Amazon deforestation, with some estimates as high as 80% of the total. But researchers are now probing the correlation between increased deforestation and rising commodity prices for crops such as soya beans, which have been linked to demand for corn-based ethanol in the United States. To analyse this relationship, experts need to know what type of land use will follow the current deforestation, and even that might not tell the whole story. There have been reports of soya-bean farmers acquiring land on the fringe of cattle country, thereby driving cattle ranchers farther into the forest.

Ruth DeFries of the University of Maryland in College Park says that soya-bean prices might have an effect but probably aren't the main driver. She was part of a team that used satellite imagery and ground validation to study the crop's impact in Mato Grosso, where soya-bean farming is common. The team found that in the period 2001–04, direct conversion from forest to cropland peaked at 23% of the annual deforestation in 2003.

If the international community is serious about tackling deforestation, it will probably need to use a hybrid approach: helping national governments such as Brazil to fund traditional policies for enforcement and monitoring and enabling communities to experiment with a market-based approach. The Brazilian state of Amazonas, where deforestation is less of a problem, is already talking about offering some kind of forestry credit on the international market.

Describing the shifting dynamic as a "tug-of-war on the agricultural frontier", Fonseca says that agile market-based projects will be needed to ensure that communities can earn more while pursuing benign uses, such as the extraction of brazil nuts, essential oils and resins, than they would otherwise make by investing in soya beans or cattle. "I believe, at the end of the day, there will be a need for all of these systems," he says. ■

**See Editorial, page 127, and Q&A, page 137.**

## Beyond redemption?

While policy-makers work on a way to reduce deforestation, scientists are scrambling to understand whether humans are pushing the forest towards a threshold beyond which it will become impossible to reverse course.

Some climate models suggest that droughts will become more frequent as the globe warms. Assuming that trends remain the same over the next two decades, some 55% of the Amazon could be wiped out or degraded by logging, agriculture, fires and droughts, according to a study led by Daniel Nepstad at the Woods Hole Research Center in Massachusetts (D. C. Nepstad *et al. Phil. Trans. R. Soc. B*; doi:10.1098/rstb.2007.0036, 2008).

The Amazon has so many trees pumping water into the atmosphere that it generates its own weather, but this also makes it fragile. As the forest shrinks, so too does its ability to provide for itself. Beyond a certain point, scientists say, the resultant loss of rainfall could mean that vast swaths of the southeastern Amazon become savannahs. And global warming itself might well come back to haunt Brazil even if deforestation issues are resolved. Many climate models project broad declines in rainfall, which could produce the same type of 'savannization'.

Nepstad's study acknowledges that shifting agricultural trends and practices and protecting forested land could reduce deforestation. "In the long term, the avoidance of an Amazon forest dieback may depend on worldwide reductions of greenhouse-gas emissions that are large enough to prevent global temperatures from rising more than a degree or two," the study concludes. **J.T.**

**Introducing**

# Neuropsychopharmacology REVIEWS

**A special issue of *Neuropsychopharmacology***

# A new era in neuroscience

Considered the 13th issue of *Neuropsychopharmacology* and previously published as the *Generations* of *Progress* series, this reviews collection has been redesigned for 2008. The inaugural issue of *Neuropsychopharmacology Reviews*, available in print January 2008, will cover **neuroplasticity** with more than 12 in-depth articles, complete with NPG-quality Illustrations that can be downloaded into power point slides, in more than 200 pages. **Complimentary with any *Neuropsychopharmacology* subscription, *Neuropsychopharmacology Reviews* is also available for single issue purchase.**

**First issue contents include:**

- Synaptic Plasticity: Multiple Forms Functions, and Mechanisms
  *Ami Citri and Robert C Malenka*
- Neuroplasticity Mediated by Altered Gene Expression
  *Colleen A McClung and Eric J Nestler*
- Drug Addiction as a Pathology of Staged Neuroplasticity
  *Peter W Kalivas and Charles O'Brien*
- Neuroplasticity of Neocortical Circuits in Schizophrenia
  *David A Lewis and Guillermo González-Burgos*

Visit **www.nature.com/nppr** to view the full selection of first issue contents.

Order your single issue today!

**www.neuropsychopharmacologyreviews.org**

nature publishing group npg

Q&A

# All eyes on the Amazon

Meteorologist and biosphere scientist **Carlos Nobre** of Brazil's National Institute for Space Research in São Paulo has modelled the effects of deforestation and global warming on the Amazon. *Nature* talks to him about the future of the unique rainforest.

**Some people link deforestation with commodity prices for cattle and soya beans. Is it that simple?**
The recent decline in deforestation was driven by a very complex blend of factors. Of course, the Brazilian government may prefer to say it was law enforcement. At the same time, commodity prices in the international market for soya beans, and in the domestic market for beef, were low. In fact, all of these factors played a role, and with the reversal of this downward trend, these factors are there again. Commodity prices have gone up. But it's premature to say what is driving deforestation now, and what the impact of law enforcement will be.

**Which is a bigger threat: deforestation or global warming?**
That depends on the timescale. For the next 30 years, the combination of deforestation, degradation and fire is the greatest threat, but it's likely that will slow down. For the second half of the twenty first century, global warming becomes the big, big menace. It would be too risky to gamble the future of the Amazon on the expectation that one of the models that projects a 20% increase in rainfall is correct.

**Is it useful to talk about 'tipping points'?**
Complex systems present this behaviour: nonlinearities, abrupt transitions, thresholds, critical points, attractors — to use the language of mathematics. So intellectually it's nice to frame the problem like that, because as soon as you talk to other communities that deal with complex systems, they understand you. I've seen criticism that the use of tipping points can be a scare tactic because the public understands tipping points in a different way from scientists, but I still like the concept to explain the likelihood of an abrupt change.

**Does the Amazon have a tipping point?**
Tropical forests exist only when there is plenty of soil moisture to transpire into the air throughout the year — less water vapour flux into the atmosphere, so less local rainfall. In our calculations, when you clear a very large chunk of forest, the climate will change and rainfall will diminish during the dry season. If the total deforested area is larger than 40–50%, there is a risk of rapid savannization in the eastern to southeastern Amazon as the regional climate changes. This preliminary estimate is conservative — it does not consider fire and other forest degradation.

Another tipping point occurs with global warming. If the temperature warms more than 4 °C, there is also a risk of savannization in the east to southeast. This is mostly due to the way models handle regional differences in sea surface temperatures, which also affect the climate.

**What's the next big question scientists need to address in the Amazon?**
There are so many important scientific questions, but I think it's the role of human-caused fire. Fire is such a radical transformation in a tropical forest ecosystem that biodiversity loss is accelerated tremendously — by orders of magnitude. If you just do selective logging and let the area recover naturally, perhaps in 20–30 years only a botanist will be able to tell that a forest has been logged. If you have a sequence of vegetation fires going through that area, forget it. It won't recover any more.


INSTITUTO NACIONAL DE PESQUISAS ESPACIAIS

**Are you optimistic about the Amazon's future?**
If I were a politician, of course, I would have to answer 'yes'. As a scientist, I have to say no, I'm pessimistic in the short term. Everything is working against the Amazon right now. But I'm optimistic in the long run. Agriculture will become more effective. Regrowing forests and avoiding deforestation will probably be an effective answer to global warming. There is a big surge of interest in changing the economic model in the tropics, to decouple deforestation from development.

Fifty years of deforestation did not bring wealth. Selling carbon credits on the international market is not going to bring the type of money into tropical countries that would make them completely independent, wealthy countries. This is not oil. But it's a sizeable amount of money that can be used to leverage a new model of development. The fact that there will be a market will instil a sense of responsibility into tropical countries. ■

**Interview by Jeff Tollefson**


R. FUNARI/FSP/FOLHAPRESS

Fire is one of the biggest threats to Brazil's tropical rainforest.

## ON THE RECORD

**"When we eliminate the need to launch off Mars, we remove the mission's most daunting obstacle."**

Former NASA engineer James McLane on how Mars missions could be easier if we don't bother making provision for astronauts coming back.

## SCORECARD

**Galileo Galilei**
The Vatican is finally set to recognize Galileo's contribution to science by erecting his statue, four centuries after accusing him of heresy.

**American PhDs**
Seven US-educated scientists working at the Max Planck Society's institutes are facing criminal charges for impersonating a doctor — under German law, a US PhD does not qualify them to use the title.

## 3 GOOD REASONS

J. W. PORTER/CORBIS

**... to celebrate Pi Day on 14 March**

1. You can be as accurate as you like — for example, 'pi second' will occur on 3/14 at 1:59:26 p.m.

2. You can engage in pi-related activities, such as, erm, eating pie (circular pies only, please ...).

3. It's more accurate than 'Pi approximation day', celebrated on 22 July (or 22/7 to Europeans).

## NUMBER CRUNCH

**5,000** cows are the newest contributors to California's energy grid, after the opening of a new biogas facility aiming to capitalize on bovine bodily emissions

**1,200** homes per day could be powered by the scheme, which captures natural gas from manure.

**16 million** citizens of Karachi, Pakistan, wish they were so fortunate — the city has been plunged into blackouts after the energy company that supplies it was cut off over unpaid bills.

*Sources: The Times, ABCnews.com, piday.org, Chem. Eng. News*

SIDELINES

M. YORK/AP

## SNAPSHOT
# Flooding the canyon

Gushing through the bypass gates of the Glen Canyon Dam in northern Arizona, the turbid, ruddy waters that once gave the Colorado River its name poured into the Grand Canyon last week at more than twice the usual rate.

The flush was intended to mimic floods that carried large quantities of sediment into the canyon before the dam's construction 45 years ago, which cut the mud flow to 6% of its natural level. The floods built sandbars and maintained the river's copper colour, enabling the vulnerable native fish, called humpback chub, to hide from predators.

Although the river level temporarily rose by up to 5 metres in the canyon, it is unclear whether the torrent successfully dirtied the water, as the models had predicted. ■

**Anna Petherick**

# Libya progresses on HIV

Scientists and physicians meeting in Tripoli last month reported substantial improvement in the treatment of hundreds of Libyan children who had been accidentally infected with HIV in the late 1990s.

Cooperation between the European Union and Libya has also led to a new multidisciplinary, integrated approach towards HIV/AIDS treatment in Libya that could be a model for North Africa and the Middle East, according to a draft report from the meeting, which was organized by the Gaddafi International Charity and Development Foundation, headed by Seif al Islam al-Gaddafi.

Senior Libyan, US and European health officials were joined at the workshop by scientists, such as Nobel laureate Richard Roberts and HIV researcher Vittorio Colizzi, who had agitated prominently for the liberation of six foreign medical workers jailed in Libya. The Palestinian doctor and five Bulgarian nurses were convicted of deliberately infecting more than 400 children with HIV and sentenced to death. The six were freed last July following an international outcry.

The meeting was held to examine ways of preventing future tragedies similar to the infection acquired at the al-Fateh Children's Hospital in Benghazi, and to look generally at improving the treatment of HIV/AIDS in the country.

"Out of the disaster of Benghazi is emerging progress," says Rafeek Hosny, a UK based coordinator of the European Union's €2.5-million (US$3.9-million) HIV Action Plan for Benghazi, a humanitarian package agreed in 2004. Libya's openness in dealing with its HIV problem — including introducing condoms and needle-exchange programmes in prisons — is now far better than any other Middle Eastern country, Hosny claims. This month, Libya is to issue national guidelines, drafted in collaboration with the European Union, for managing HIV.

But scientists at the meeting criticized lack of progress on Libya's proposal to build an African centre for infectious disease control and research. Such a centre, they say, could potentially be of immense benefit to Libyans as well as a major resource for the whole of Africa. ■

**Declan Butler**

# Probe readies for dip into geyser on Enceladus

J. KAUFMANN

NASA's Cassini spacecraft is set to plunge into an intriguing plume of gas spouting from Enceladus, one of Saturn's moons.

Cassini stumbled upon the astonishing discovery — a geyser of ice and water vapour spewing out of cracks in the tiny satellite's south pole — during a fly-by in 2005. But the spacecraft's probe barely touched the plume. This week, Cassini's instruments will get their first true taste of the tantalizing plume, when they try to measure the size and speed of the gas and ice particles, and their chemical composition.

"Last time, we just skimmed the edge," says Cassini scientist John Spencer at the Southwest Research Institute in Boulder, Colorado. At its closest point in the fly-by, the probe will come within 200 kilometres of the plume's source (see graphic).

A key question is, will it find ammonia? The gas is an antifreeze, allowing water to remain liquid at lower temperatures. But during the last fly by, ammonia was strangely absent. If it remains undetected, this would suggest that the moon's interior is hot enough to host liquid water.

Just how hot it is inside and how much liquid water exists are much debated. The mechanism for how the plume is produced is also poorly understood, but is known to be driven by Saturn's gravity, which kneads the moon and causes internal shearing and heating. Some scientists maintain that the water comes from large oceans deep under the surface that erupt like volcanoes, whereas others argue that it exists in cracks closer to the surface. Either way, astrobiologists are excited, says Spencer. "Any kind of ocean is going to be hot by Saturn standards, and that's plenty warm enough for astrobiology."

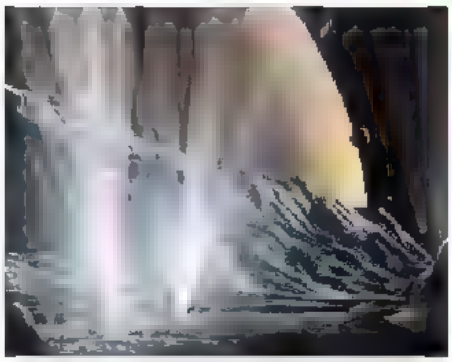

Artist's impression of the plumes.

Susan Kieffer, a geologist at the University of Illinois at Urbana–Champaign, proposes a third model that doesn't require liquid water. Mixed in with the plume's water vapour are other gases, including nitrogen, carbon dioxide and methane — far too much, Kieffer argues, to be dissolved in liquid water in Enceladus' weak-pressure environment. Those gases, she says, exist more comfortably if trapped in ice-cage structures called clathrates, which could erupt into the plume and immediately form water vapour.

Enceladus is only 500 kilometres in diameter, so the fly-by will be over in minutes. But as Cassini departs, it will turn its thermal imager back for a glance. At that time, Saturn will be casting a shadow onto the moon, presenting a ripe opportunity for accurate, high resolution readings of the surface temperature.

The thermal imager has so far detected temperatures only as high as 145 K from the south pole of the moon. But Spencer hopes it will record much higher values as the imager zeroes in on the 'tiger stripes' — the four long, thin cracks on the moon's surface from which the gas plume emanates.

Cassini will return to Enceladus in August, for the second of eight further fly-bys in its extended mission. Each time, it will inch closer to the plume's centre. Scientists want to test the waters slowly — any encounters with particles bigger than one millimetre could damage the spacecraft. ■

**Eric Hand**

J. SPENCER, SWRI, NASA/JPL/SSI

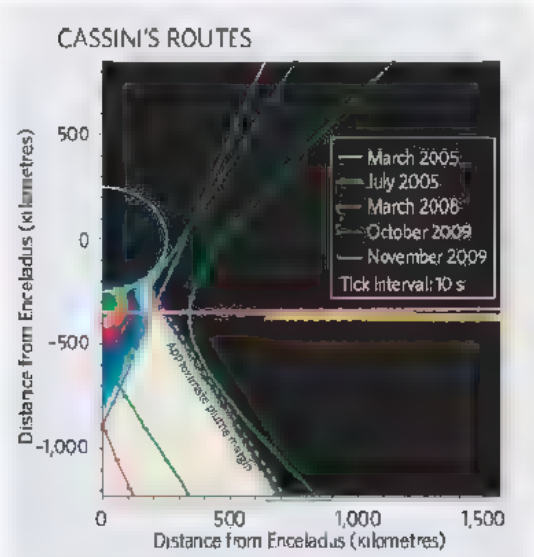

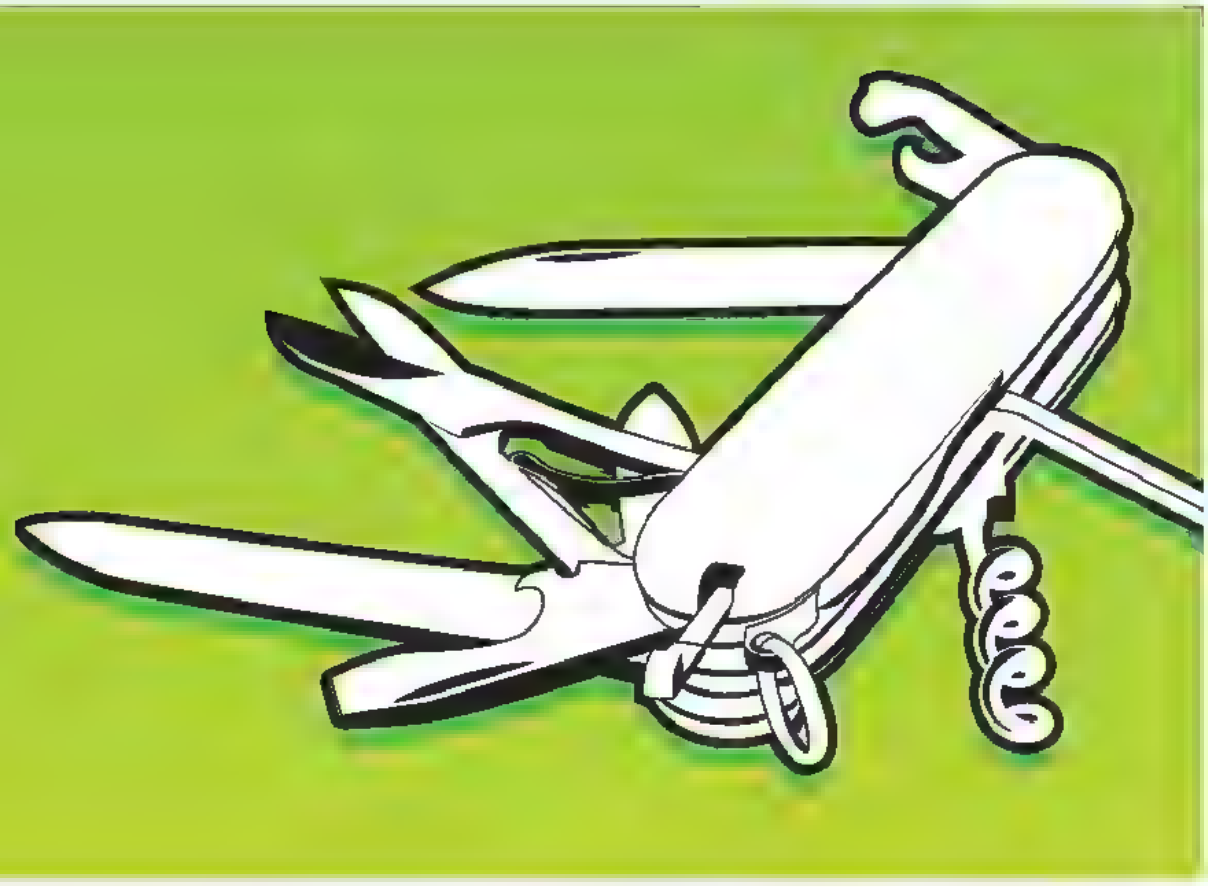

# *My Tetra Is...Versatile.*

*Transform the Mini-PROTEAN® Tetra cell to a Mini Trans-Blot® cell by simply swapping modules.*

The Mini-PROTEAN Tetra system for one-dimensional vertical gel electrophoresis comprises a modular design to easily convert the electrophoresis cell into a blotting apparatus. The Mini-PROTEAN Tetra system can run as many as four SDS-PAGE gels simultaneously and is compatible with the Mini Trans-Blot module for gel transfer (one module can transfer two gels), eliminating the need for an extra blotting tank. Supported by Bio-Rad's 20 years of experience in gel electrophoresis and blotting, the Mini-PROTEAN Tetra system increases throughput, simplicity, and versatility in your experiments.

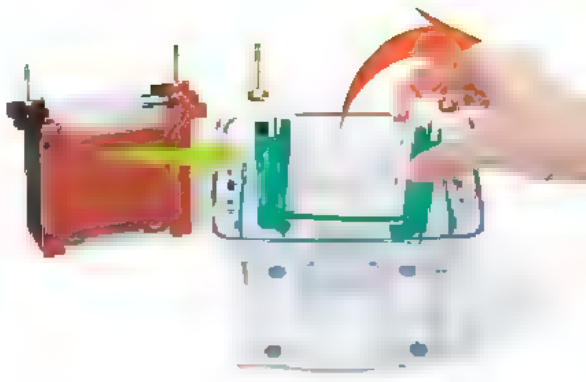

Interchangeable module system

**With the Mini-PROTEAN Tetra system, you can:**

- Convert the electrophoresis cell to a blotting apparatus
- Run up to 4 mini SDS-PAGE gels
- Use handcast or precast gels
- Be confident that the error-proof design ensures correct polarity and orientation

Explore, share, and connect at **myTetraCell.com**.

## Seattle laboratory arsonist faces prison stretch

An environmental extremist has been convicted on two counts of arson for her role in a fire at a university laboratory.

On 6 March, a federal jury found Briana Waters guilty of aiding the torching on 21 May 2001 of the University of Washington's Center for Urban Horticulture in Seattle, where activists wrongly believed that trees were being genetically engineered. The jury could not agree on three other counts of conspiracy, possession and use of a destructive device in a crime of violence.

Waters, who acted as lookout, was one of more than a dozen people indicted in 2006 for a series of arsons with environmental motives (see *Nature* 443, 498; 2006). She faces a minimum of five years in prison.

## Giant telescope gets double vision

The Large Binocular Telescope, situated atop Mount Graham in Arizona, has opened both its eyes.

With two primary mirrors, each of which has a diameter of 8.4 metres, the Large Binocular Telescope is now the world's largest telescope on a single mount. It has a light-collecting area that is equivalent to 11.8 metres. Each mirror can gather light from a different part of the spectrum, or the mirrors can work together to produce sharp images.

The first light pictures gathered by both mirrors, released on 6 March, show a nearby spiral galaxy. The US$120-million telescope is a joint effort by three Arizona universities; Ohio State University in Columbus; Research Corporation, a private foundation based in Tucson, Arizona; and Italian and German partners. Astronomers are now planning even bigger telescopes (see page 142).

LARGE BINOCULAR CAMERA TEAM, ROME OBSERV.

Nearby galaxy NGC 2770, as seen by the Large Binocular Telescope.

## Chinese scientists lead panda genome project

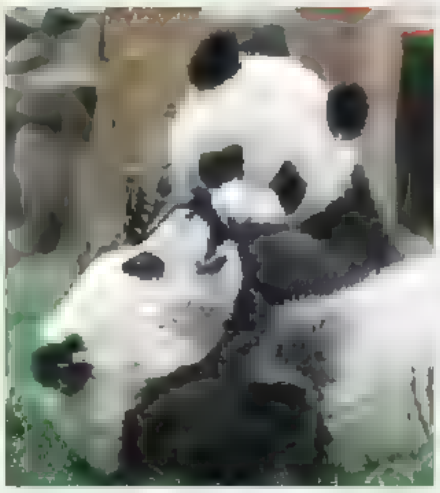

Z. ZHANG

Conservation biologists and geneticists from five countries are planning to sequence the genome of the giant panda.

There are only 1,600 giant pandas in the wild and another 270 in captivity. Loss of habitat, finicky eating habits and disease have taken their toll on the wild population, and breeding efforts have largely failed because of a disinterest in mating. Scientists hope that the sequencing project, announced on 6 March, will yield information that can help both groups.

The genome contains some 3 billion base pairs, and scientists suspect that it holds about the same number of genes as the human genome. The team, led by the Beijing Genomics Institute's Shenzhen branch, hopes to finish a draft within six months.

## Officials downplay vaccine's link with autism

In the wake of a court ruling disclosed last week, US officials have conceded that vaccines may have exacerbated an autism-like disorder in a young girl. The Centers for Disease Control and Prevention (CDC) in Atlanta, Georgia, emphasized that the decision to award damages to the victim's family does not prove a link between autism and vaccines.

The girl has a rare disorder that produces symptoms similar to autism. Her parents argued before a special 'vaccine court' that the disorder surfaced after she received five vaccine shots as an infant. CDC director Julie Gerberding downplayed the link, calling the case "very special".

The ruling was hailed as a victory by activists who believe there is a connection between the vaccines' preservative, thimerosal, and the disorder. About 5,000 other families are also seeking compensation in court.

## British government to demand clinical trial data

The British government is promising to toughen laws to prevent drug companies from withholding data from clinical trials.

Dawn Primarolo, the UK minister of public health, says that both European and British law should be amended to force the timely disclosure of any information relevant to assessing drug risk. She also says that the government will seek clearly defined penalties for non-compliance.

Last week, regulators ended a four-year investigation into the British pharmaceutical firm GlaxoSmithKline without bringing prosecution. The company allegedly failed to provide data related to suicide risk for children taking its anti-depressant drug Seroxat (sold in the United States as Paxil). But it did not violate laws in place at the time, investigators say.

## Jules Verne sets off for space station

After years of delay, the European Space Agency has launched what it describes as its most sophisticated spacecraft to date.

An Ariane 5 rocket carried the craft, named Jules Verne, into orbit on 9 March. The spacecraft is the first of a series of Automated Transfer Vehicles (ATVs) that will take supplies to the International Space Station. Unlike current supply vessels, the ATV will dock with the station using lasers rather than being guided by astronauts.

The Jules Verne is scheduled to rendezvous with the station in early April. At least four more ATVs will follow, one every 18 months.

## Charity to focus scientists' skills on the needy

A new charity will direct British scientific talent towards problems in the developing world. Science for Humanity is funded by the London-based National Endowment for Science, Technology and the Arts and the Sloane Robinson Foundation, which supports educational and research charities.

Launched in London on 4 March, the organization is asking researchers to help tackle issues such as sanitation, energy, agriculture and shelter. It will begin by recruiting members from the United Kingdom, but hopes to extend its reach to scientists in other nations.

"We understand that the problems in developing countries are complex," says Susan Greenfield, director of the Royal Institution of Great Britain and one of the agency's founders. "That is challenging. But scientists love a challenge." ■

NATURE|Vol 452|13 March 2008

T. MASON/GMT/CARNEGIE OBSERVATORIES

# EYES AS BIG AS THE SKY

Three teams are racing each other to build the next generation of telescopes that would dramatically dwarf the largest on Earth today. **Eric Hand** checks out the competition.

Buddy Martin gets nervous before setting foot on the glass. He reaches into his pockets and sets aside a mobile phone, coins and fingernail clippers. He checks the soles of his shoes for grit. Then he gingerly steps out onto the 8.4-metre-wide disc, parked underneath the University of Arizona football stadium in the hangar-like cavern of the Steward Observatory mirror laboratory in Tucson.

Still unpolished and milky white, the disc sits like a record on a turntable — except that this record is borosilicate glass instead of vinyl, spins at 1 revolution per minute instead of 45, and weighs as much as 3 buses. Martin, a polishing scientist, is the disc jockey. He needs to shape the surface like a saddle and get it right to within 20 nanometres. Proportionately, it is like bulldozing all of Brazil to a smoothness of less than a centimetre. Thus Martin's anxiety over errant scrapes: "We have rules such as 'no tools above the glass'," he says. "A wrench falling would wreck it."

When Martin can confirm that the glass is polished correctly, it will be ready to become a mirror. Technicians will seal a giant bell jar over the glass and vaporize a soda can's worth of aluminium over the surface. The result will be as large or larger than all but two of the telescope mirrors currently in use around the world. But that is only the beginning. The Giant Magellan Telescope (GMT), pictured above, which is under development by a consortium led by the Carnegie Observatories in Pasadena, California, and the University of Arizona, will require six more mirrors just as big. If the first mirror is Brazil, there is still the rest of the Americas, all of Europe and a good chunk of Africa to go.

With its seven mirrors the GMT will be 25 metres across, dwarfing the biggest telescope mirrors in the world today — those in the twin 10-metre Keck scopes in Mauna Kea, Hawaii. Yet even the GMT will be the smallest of the bigs in a game of one upmanship that has emerged among astronomers. A second group, led by the University of California and the California Institute of Technology (Caltech) in Pasadena, is planning a giant named the Thirty-Meter Telescope (TMT). And the European Southern Observatory (ESO), headquartered in Garching, Germany, aims to build the biggest 'light bucket' of all: a 42-metre design called the European Extremely Large Telescope (E-ELT). All told, these three competing behemoths could cost more than US$3 billion (see Table, overleaf).

The giant size of these scopes leads exponentially to big science. A telescope's ability to gather light increases with the area of the primary mirror, and its ability to resolve details increases with the diameter. All told, tripling in diameter from the Kecks, this new generation of telescopes will be roughly nine times better at grasping the light from distant stars, and nine times better at distinguishing them from darkness.

Telescopes this big could tackle fundamental and currently unanswered problems, such as the direct imaging of light from an extrasolar planet or measurement of the mysterious repulsive force that's accelerating the expansion of the Universe. "It's not just pushing for bigger toys," says Matt Mountain, director of the Space Telescope Science Institute in Baltimore, Maryland. "They open up a new parameter space that we don't have access to."

The giant telescopes would rival, even in some ways surpass, the James Webb Space Telescope (JWST), the 6.5-metre replacement to the Hubble Space Telescope that is supposed to launch into orbit in 2013. By getting above Earth's atmosphere, the space telescope will be able to see deeper into the infrared portion of the spectrum. But the ground-based telescopes, with their larger mirrors, would be able to spot smaller and fainter objects. Both the JWST and the ground-based telescopes are aiming to spot 'first light', the time 400 million years after the Big Bang when stars first began their fusion fire. "We want to observe photons from the first stars in the Universe," says TMT observatory scientist David Silva. "Are we crazy or what?"

> "We want to observe photons from the first stars in the Universe. Are we crazy or what?" — David Silva

The three groups are lining up partner nations and some are competing for private donors. The Canadians have committed to the TMT, and the Japanese are likely partners too. The Australian National University in Canberra, joined eight American institutions* in the GMT project's growing list of partners, and now South Korea is working to find the money to become the tenth partner. Private funding is also playing a large role; in December, Intel founder Gordon Moore, a Caltech graduate, gave the TMT project $200 million, making it the team to beat. It's far from clear if all three scopes will be built, but each is pressing ahead, hoping to commence construction within the next two years.

Part of the competitiveness stems from the importance of finishing first. The Keck telescopes beat other telescopes in their class to operation by a few years and skimmed the creamiest science off the top. And so the TMT's competitors want to keep it from drinking everyone's milkshake before they have their own straws ready. But the tension also derives from a historical discord between the three rival groups, groups that have generally got what they wanted even as they pursued telescopes of different sizes and shapes. "The worst job in the world would be to get these three teams in a room and say, 'How do we collaborate?'" says Mountain.

## The acrimonious divorce

To understand two-thirds of the competition, one needs to go to Pasadena, home to the small, privileged institutions of Carnegie and Caltech. For astronomers through much of the twentieth century, this Los Angeles suburb was the sociological centre of the Universe. Initially united, Carnegie and Caltech worked together to finish in 1948 the 200-inch (5-metre) Hale Telescope at Palomar Observatory in the southern California mountains. For decades it was the biggest eye on the Universe, one that discovered the incredible redshift of quasars in distant galaxies.

But in 1979 the two institutions divorced. The director at the time, Maarten Schmidt, orchestrated the dissolution of the telescope's joint operation, frustrated by managing a place that had two bodies to approve every decision. Carnegie, the scorned spouse, left to establish the two 6.5-metre Magellan telescopes in Chile, while Caltech pursued the twin Kecks with the University of California system (and, later on, NASA). The two institutions are separated by only a few miles, but today they are divided by more than just fault-lines and freeways. Bitterness lingers.

On one side is the TMT headquarters, a renovated Catholic hospital on Caltech's satellite campus, where staff scientists work in the former dormitories of nuns. These blue-ribbon scientists work as if for a blue-chip business, jetting around the world to nail down partners, vendors and site licences. Recently they gathered in a glass-walled conference room to debate the finer points of five possible sites for the telescope — even though many acknowledge that a site on Hawaii's Mauna Kea would do the most to seduce the Japanese, who are also flirting with the ESO. While one astronomer lectures on the emerging problem of light pollution at a potential Baja California site, the remaining scientists peck away on laptops, multitasking. Silva, who has also worked for the ESO programme and the US National Optical Astronomy Observatory in Tucson, finds the TMT culture different from that of his former workplaces. "It's a confidence, it's an arrogance, it's a sense of not being afraid to be leaders," he says. "It's a sense of 'We are the best and we're not going to be humble about that.'" It's Caltech to a T.

Caltech's rivals work just a few miles away, at the shady Santa Barbara Street headquarters for Carnegie. The GMT programme is the smaller operation, with 20 full-time employees to the TMT's 100. For the moment they also have much less money — although that could change at any moment with partners such as Harvard University, with its $34-billion endowment, and two Texas universities that have recently benefited from Houston billionaire George Mitchell and his new-found interest in cosmology. Carnegie director Wendy Freedman says she's expecting several major donations in the coming months that could collectively rival Moore's to the TMT.

## Grand design

But the biggest difference between the two projects is in the technological ambition of the GMT design. The TMT mirror is designed on the same basis as the Kecks, just on a grander scale: 492 hexagonal mirrors 1.44 metres across instead of 36 mirrors 1.8 metres across. The seven mirrors of the GMT, however, represent a huge step up — some say a leap of faith — from the Carnegie's single-mirrored Magellan telescopes. The organization has never before dealt with the difficulties of focusing light from multiple primary mirrors. To remind his colleagues of the challenge, staff astronomer Steve Shectman got the building crew to paint the outline of the GMT's 8.4-metre mirrors in the car park at Carnegie. The circles dwarf the parked sport utility vehicles. The intent, he says, was to scare Freedman into a more cautious approach. "But it didn't scare her. It just got her all excited."

The two groups have been jockeying for years, ever since a Keck follow-on called the California Extremely Large Telescope was reborn

R. BERTRAM/STEWARD OBSERVATORY MIRROR LABORATORY

Big glass. Buddy Martin on one of the Giant Magellan Telescope's mirrors. Three proposed telescopes would together provide a greater mirror area than all previous astronomical telescopes combined.




*Carnegie Observatories, University of Arizona, Harvard University, University of Texas at Austin, Texas A&M University, Smithsonian Astrophysical Observatory, University of Michigan, Massachusetts Institute of Technology

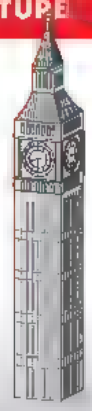

Big Ben clocktower (96.6 metres) for scale

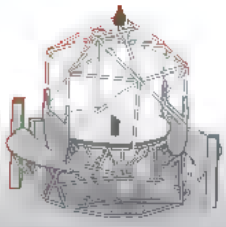

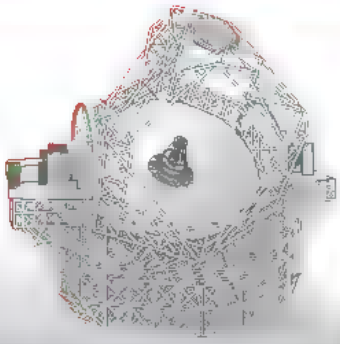

GMT/TMT/ESO

| | Giant Magellan Telescope | Thirty-Meter Telescope | European Extremely Large Telescope |
|---|---|---|---|
| **Telescope diameter** | 25.2 metres | 30 metres | 42 metres |
| **Component mirror segments** | 7 (8.4-metre segments) | 492 (1.44-metre segments) | 984 (1.45-metre segments) |
| **Cost** | US$600 million | US$754 million | €900 million (US$1.37 billion) |
| **Planned location** | Chile | Candidates: Hawaii; Mexico; three sites in Chile | Candidates: Canary Islands; Morocco; Argentina; two sites in Chile |
| **Planned construction period** | 2010–2017 (First mirror already cast) | 2009–2016 | 2010–2017 |
| **Technical advantages** | Adaptive optics integrated within secondary mirror<br>Shortest focal length means it has the smallest and cheapest structure | Mirror segments are comparatively cheap and more easily replaced<br>Similar scaled-up version of the existing Keck telescopes | Five-mirror design results in a flat focal plane and better images<br>Similar mirror-segment size to the TMT, so greater vendor choice |
| **Financial advantages** | Potential support from $34-billion Harvard endowment or Texas billionaire George Mitchell | $200-million gift from Intel founder Gordon Moore | Steady European funding stream |
| **Disadvantages** | Only one place can make the mirrors<br>Gaps in mirror limit the effective aperture to 21.5 metres | Adaptive optics performed after the light leaves the telescope, so the 'natural seeing' mode cannot benefit from adaptive corrections to wind effects | Biggest and most expensive design<br>No similar design experience<br>Reflections through five mirrors reduce light levels |

as the TMT in 2002. Caltech's leadership had realized just how expensive the TMT would be, and that they would need as many partners as possible, not just Californians. But by that time Carnegie had gone off to start its own designs, says Richard Ellis, a lead TMT astronomer and former Palomar director. "Great opportunities were lost to get everyone on board."

Led by Freedman, the GMT board worked quickly to level the playing field, which they felt favoured its competition, particularly given the involvement of the Association of Universities for Research in Astronomy (AURA). AURA operates US public telescopes with taxpayers' money, and was a partner on the TMT but not the GMT project. In late 2005, the GMT board sent a letter to AURA president William Smith, complaining that the association had already "picked the winner" and noting that no federal support had gone to early GMT work. The National Science Foundation (NSF) then told AURA to back out of the TMT project and shepherd both designs along. The GMT group has since lobbied the NSF to split whatever support it offers the two projects. Many scientists at the TMT, predictably, given its lead in money and design progress, would prefer a winner-take-all competition.

Some astronomers suggest that it would have been difficult for the groups to work together anyway. Too much time, money and prestige, they say, has been invested in two rival technologies: the segmented-mirror approach pioneered by Jerry Nelson at the University of California, Santa Cruz, now being applied by Caltech, and the honeycombed, spun-cast mirrors developed by Roger Angel at the University of Arizona, used by Carnegie. "There are almost religious issues tied up in these designs," says Mountain.

## Vanity mirrors

Nelson has been pushing fly-eyed telescopes for nearly three decades. The inspiration for using segments as opposed to a complete mirror, he says, wasn't hard to find. the Romans used small tiles to create larger mosaic wholes. The real challenge was in finding a way to shape the segments. Most telescope mirrors are parabolic — a curved surface that reflects incoming parallel light waves towards a central focus. These mirrors are relatively easy to polish to high precision. But in a segmented telescope, each off-axis mirror occupies just a portion of the parabola and needs a custom shape — a much more difficult polishing task. In the late 1970s at Lawrence Berkeley National Laboratory in California, Nelson discovered that he could warp the mirror precisely by hanging lead weights in buckets from the edges of a mirror segment. He polished the mirror as if it were a symmetric parabola, then released the weights. The mirror popped back into the precise asymmetric shape he needed. "Working with the edges was all we needed to do," he says.

At one level, the GMT is also a segmented mirror, but one with only seven giant segments — each one of which relies on the method long advocated by Angel. Nearly 30 years ago, using a backyard kiln constructed from bricks and heating coils bought from Kmart, Angel and his former graduate student John Hill began experimenting with Pyrex glass, fusing together glass bowls from Angel's kitchen cupboard. Eventually, Angel worked towards two innovations: honeycomb moulds, to create a stiff, lightweight mirror that was mostly hollow, and spin-casting. Spin-casting involves spinning the glass as it cools so that centripetal forces guide the glass naturally into a parabolic shape, granting the grinders and polishers a head start. And the honeycomb technique gives the glass a thinness and lightness that keeps it from deforming because of its own weight and thermal expansion.

But like Nelson, Angel faces the problem of asymmetry. The earlier 8.4-metre mirrors made in Tucson were polished as parabolas; the six off-axis mirrors for the GMT have to be saddles. And that means Martin, the polishing scientist, thinks very hard about what they call "The Test". The test is a problem of metrology — how to measure mirror curvature to a strict standard. Measuring incorrectly means failure, such as when the main mirror for the Hubble Space Telescope was ground ever-so-slightly wrong, resulting in blurry pictures. "We all stay awake at night trying to figure out how not to make that mistake," says Martin.

So he and other opticians have constructed an elaborate Rube Goldberg-like system in a 28 metre tower above the GMT mirror, which will bounce light through two more mirrors and a hologram before an interferometer measures the patterns that signify perfection or not. One of the test mirrors alone is 3.75 metres across, nearly as big as the Hale Telescope atop Palomar. All sides acknowledge that the test of the first saddle-shaped mirror, scheduled for July, will be the GMT's crucial juncture. The GMT has received good publicity by being the first group to cast a mirror. But what the GMT team is really trying to do, in casting a mirror early and moving quickly to the test, says TMT scientist Chuck Steidel, is "retire risk"

## The other side

Meanwhile, the Europeans have remained out of the fray, quietly corralling a consensus among the ESO's 13 member states and working towards a design that borrows from both the TMT and the GMT. The E-ELT will be segmented like the TMT, but bigger, with nearly 1,000 mirror segments. These are similar in size to the TMT segments, which will allow the two projects to pit vendors against each other. The European design borrows from the GMT in that the adaptive optics will be integrated into the telescope's mirrors (whereas the TMT corrects for atmospheric effects with extra mirrors farther down the optical path). Proponents of the former approach say that it yields a cleaner image and a wider corrected field of view.

The Europeans have had to set their sights a bit lower than originally planned, abandoning the preciously named OWL, or OverWhelmingly Large Telescope, after its 100-metre primary mirror proved preposterous. But by developing designs for the 42-metre E-ELT, a mirror that can be made now rather than in 20 years, the Europeans are playing to their strong suit: the dependable ESO budget. "On a year by year basis, I don't have to go and ask for money," says Jason Spyromilio, director of the E-ELT project office.

With its €900 million (US$1.37 billion) price tag, the European project is by far the most expensive of the three, roughly twice as expensive as the Very Large Telescope — a four-telescope array in Chile that the ESO finished in 2000 after more than a decade. But the Europeans still think they can build the E-ELT without private money. "Yes, it's a big step, a larger project, a much more complex project," says E-ELT principal investigator Roberto Gilmozzi. "It breaks every assumption we've made about the art of building telescopes so far But we're restricting our worries to the technical side. Finding the funds is something we can do."

"The E-ELT breaks every assumption we've made about the art of building telescopes so far."
— Roberto Gilmozzi

Others say that Spyromilio and Gilmozzi are optimists — that they will either have to ask the ESO's member states for more money or find more partners (the two American projects are united in their fear that Japan or the NSF will partner with the ESO instead of with them). A third option, Spyromilio says, is that the ESO programme takes out a loan against its future funding streams — mortgaging the ESO's future to pay for the E ELT now.

All eyes are now on the NSF to see what it will do next. All three projects need more money just to begin building their telescopes. Yet the NSF will have none to disburse until it finishes the Atacama Large Millimeter Array (ALMA) radio telescope in Chile, in the next five years. NSF astronomy director Wayne van Citters told astronomers in November that after ALMA's completion, the agency could provide a similar contribution — about $500 million — towards the construction of a giant telescope.

Dave Hilyard, Jerry Nelson and Eric Williams (left to right) work on the Thirty-Meter Telescope.

Also on the minds of the Americans is the question of who will pay for operational costs, which typically amount to 10% of construction costs annually. At that rate it would cost more than $100 million each just to operate the GMT and the TMT each year, and the NSF would be likely to have to abandon its long-term support of telescopes in the 2-, 4- and 8-metre classes. The astronomy community seems unlikely to want to make that sacrifice; a 2006 'senior review' from the US astronomical community found that these smaller telescopes provided valuable training and employment for the majority of astronomers. Small telescopes, the report noted, also provide excellent science: the first extrasolar planet around a Sun-like star, for instance, was discovered by a modest 2-metre telescope in France. And the discovery of dark energy — a huge discovery that surely will be afforded a Nobel prize some day — was achieved with a hodgepodge of telescopes, most of them 4 metres or smaller.

For now, the TMT seems to be holding on to its lead, although members of all projects know how tenuous such an advantage can be. The TMT programme is managed by Gary Sanders, who has shepherded through other massive science projects such as the Laser Interferometer Gravitational-Wave Observatory sites in Livingston, Louisiana and Hanford, Washington state. But he also worked on the Superconducting Super Collider in Waxahachie, Texas, a project that Congress killed in 1993 after construction had already started. "If the astronomy community spoke with unanimity and rallied around one telescope," Sanders says with the voice of experience, "the case would be clearer."

But the deep historical competition between American astronomers may end up working to everyone's benefit. The number of Gordon Moores in the world — billionaires with an eye to the heavens — is clearly finite. But Sanders remembers a time in the 1980s when astronomers thought that there was only enough money for a single 8-metre-class telescope in the world. In the end, astronomers found enough money to build a dozen.

And so if history is any guide, the future of astronomy may end up looking like its past. In 1996, Schmidt, the former Palomar director, gave an interview to a historian, and marvelled at how the Carnegie–Caltech divorce seemed to lead directly to the Keck and the Magellan telescopes, record setters in their time. "And I cannot believe that if we'd stayed together we would have had four of the largest telescopes in the world together." ■

**Eric Hand covers physics and astronomy from *Nature*'s Washington DC office.**

# Stepping out

**A surprisingly large number of university-inspired patents may be going to industry instead. Rex Dalton reports.**


B. RYDER

As patent battles go, it seemed one never to be repeated. In 1999, the Californian biotechnology company Genentech resolved a long-running law suit with the University of California. For US$200 million, the firm agreed to settle over claims that a researcher had slipped human growth hormone DNA out of the university's lab on a midnight run down to the firm — which promptly turned the material into its blockbuster drug Protropin (somatrem).

But such patent diversions may be more common than was thought, a study now suggests. A management researcher at the University of Georgia in Athens and his colleagues say that US universities are losing many of their researchers' inventions to industry. One-third of the patented discoveries made at universities were redirected to belong to private firms instead — and those taken away were the ones most highly cited in future patents, suggesting that they were the most valuable.

"This is largely a system failure — professors [are] systematically engaging in invention diversion into a black market, where industries patent them," says Gideon Markman, who led the team that published the findings (G. D. Markman, P. T. Gianiodis and P. H. Phan *J. IEEE Trans. Eng. Manage.* 55, 29–36; 2008).

## Royal top-up

For universities, the financial stakes can be substantial. For instance, the 10-campus University of California system received $193.5 million in fiscal year 2006 from patent royalties and fees. The absolute numbers may be small compared with overall institutional budgets — the state budget for the University of California that year was around $3.5 billion — but the flow from patents is, in essence, free money for the universities at a time when funds are getting tight.

Markman is one of just a few scholars looking at how universities are faring in the wake of revolutionary changes in patenting academic research. In 1980, a law called the Bayh–Dole Act allowed US universities to start patenting inventions stemming from federally funded research. For a particular invention, a university could either forgo a patent right or claim it and then encourage development under a licensing agreement with a firm. The firm would then pay royalties to the university and inventing professor. Technology-transfer offices sprang up to facilitate this new law.

But as researchers, their business partners and even universities can make fortunes off publicly funded discoveries, temptations to use the system for personal benefit have grown immensely. University executives, government officials and leaders of watchdog organizations often chatter about subversions: a lab animal making valuable protein might quietly disappear, or an engineering tool might shift from a professor's academic computer to his or her consulting business.

Markman and his team have been tracking what happens to this lost information. Their study focuses on 7,650 patented discoveries in biomedicine, information science and engineering made between 1989 and 2003 at 54 US universities. It shows that the more valuable the patent is, the more likely it is to be diverted to industry.

> "The technology-transfer concept is still in its infancy."
> — Michael Crow

"I'm not surprised — that's consistent with my own thinking," says Michael Crow, president of Arizona State University in Tempe, which is itself trying to spin off an industrial cluster. "The technology-transfer concept is still in its infancy, and universities are still figuring out how to do things."

Administrators at technology-transfer offices are more sceptical. "I really question if one-third of the best inventions are leaking out the backdoor," says Jon Soderstrom, director of Yale University's technology-transfer office. "It seems awfully high to me — but it may be."

Data confirming Markman's results are expected in the near future from David Audretsch, a researcher from Indiana University in Bloomington who is on leave at the Max Planck Institute of Economics in Jena, Germany. Audretsch's earlier work found that 30% of researchers funded by the US National Cancer Institute do not assign their patents to their universities.

## Deal makers

Others aren't so sure. A team from the Georgia Institute of Technology in Atlanta has published a study online in the National Bureau of Economic Research (J. Thursby, A. Fuller and M. Thursby www.nber.org/papers/w13256, 2007). The results showed that many discoveries that could be interpreted as being 'lost' in fact occurred when professors were doing outside consulting with industry that had been previously approved. The team found that 26% of 5,800 patents went solely to outside firms — a similar proportion to what Markman found — but say that follow-up interviews suggest these numbers are due to acceptable outside consulting.

For his part, Markman says that professors who do the most consulting also divert the most technology. Once an academic has started working with an outside firm, he or she is in a better position to divert technology, Markman argues.

Markman plans to examine the diverted patents in case studies to determine exactly what happened to each. "It should be fascinating to see what we find," he says.

In the meantime, experts suggest simple ways to keep patents at the universities at which they were made. Step one is to break down all barriers between technology-transfer offices and faculty members, to ensure proper working relations. Step two is to maintain constant relationships with industry, intellectual-property attorneys and venture-capital firms.

Given the history of patent diversion, though, both steps may be harder than they seem. ■

**Rex Dalton is a US west coast correspondent for *Nature*.**

To Find Extraordinary SNP Selection,
Accuracy, and Reliability...

Look Where the Data Points

## Industry Leading SNP Genotyping Solutions

With TaqMan® SNP Genotyping Assays, TaqMan® SNP Genotyping Systems leading to the Applied Biosystems 7900HT Fast Real-Time PCR System, Applied Biosystems delivers the best quality and most effective solutions available today for high performance SNP genotyping. Whether you are studying SNPs in [illegible] genetic variation, or validating SNPs for [illegible] you can count on Applied Biosystems for [illegible] results.

All SNP data points to www.allsnps.com

Applied Biosystems

NATURE|Vol 452|13 March 2008

# The green menace

Huanglongbing, a disease that could devastate the US citrus industry, pits national security against plant pathologists looking to battle natural outbreaks, **Ewen Callaway** reports.

In California's San Joaquin valley, it is citrus season. An open-air warehouse on the outskirts of Dennis Johnston's 600-hectare citrus grove brims with huge crates of oranges, mandarins and grapefruits. This year, his farm will ship around US$8-million to $10-million worth of citrus around the United States and the Pacific Rim.

Cruising through the labyrinthine dirt roads that criss-cross his farm, Johnston surveys the winter crop, passing tree after tree, each a mop of dark green dotted with baseball-size fruits.

The trees are productive and the fruit healthy, but in the back of Johnston's mind is the possibility that trees could fall sick from insect-spread infections. Tristeza virus, for instance, felts a tree every few years, he says. Johnston is vigilant. He serves on his county's pest-control board and educates other growers about plant diseases that range from minor nuisances to epidemics that could ruin the San Joaquin valley's billion-dollar citrus industry. "We have a hard time getting growers to understand the severity of these bacterial and viral infections," says the easy-going third-generation grower.

> "Huanglongbing is a disease that can wipe out citrus as we know it."
> — Larry Bezark

## Green alert

Mention huanglongbing, and Johnston cringes. "We were being warned by the scientists and the people in the know that this is a serious, serious thing and we've got to, at all costs, keep it out of the valley and keep it out of California," he says.

Named for the colour of the infected leaves, huanglongbing is Chinese for yellow dragon disease. It is a bacterial infection that spreads from tree to tree via citrus psyllids, draining nutrients from the plant and resulting in diminutive green fruits, thinning branches and eventually death of the tree. It has devastated the citrus industry in many Asian countries, killed hundreds of thousands of trees in Brazil, and swept through 26 Florida counties since it first arrived on US soil in 2005. It is considered the most dangerous citrus pathogen in the world.

The US government agrees. The bacterium that causes the disease, '*Candidatus* Liberibacter', comes under the same regulations that restrict research on Ebola, anthrax and other microbes that have been deemed potential agents of terror. An attack on the food supply with a plant pathogen such as '*Ca.* Liberibacter', some say, could have disastrous effects on the nation's economy. Researchers who study these 'select agents' must submit to background checks by the Federal Bureau of Investigation (FBI), install extra security outside their labs, and file mounds of paperwork.

These measures are necessary, the government says, to keep the pathogens from falling into the wrong hands. A terrorist spread epidemic of huanglongbing, for instance, could kill millions of trees and rattle consumer confidence, says Jacqueline Fletcher, director of the National Institute for Microbial Forensics and Food and Agricultural Biosecurity in Stillwater, Oklahoma.

Other scientists, though, say that treating '*Ca.* Liberibacter' and other emerging plant pathogens as potential agents of terror leaves growers such as Johnston worse off. Slapping the select agent status on plant pathogens inevitably means that fewer researchers can study the organisms, slowing the development of countermeasures. Compliance with the strict regulations is costly and time-consuming, researchers say. And officials in Florida contend that the bacterium's select-agent status sapped their response to the 2005 outbreak of huanglongbing, which continues to rage. Diagnostic tests have been slow to develop and researchers still haven't figured out how to grow the bacterium in the lab.

"There's no question that select-agent type regulations are necessary for Ebola virus and 1918 influenza," says Caitlyn Allen, a microbiologist at the University of Wisconsin–Madison. "The question that needs to be considered seriously is whether these plant pathogens pose a similar risk." Indeed, the US government is now deliberating changes to the select-agent list to reflect the growing prominence of huanglongbing in Florida.

T. GOTTWALD

## The war on agroterror

In 1996, the US government created its first list of select agents, after Larry Wayne Harris, a microbiologist and white supremacist, tried to purchase vials of the bacterium that causes bubonic plague. The initial list included pathogens in humans and animals, but not plants.

But biosecurity soon became an important issue for plant pathologists too. In 1999, the American Phytopathological Society in St Paul, Minnesota, hosted a well-attended symposium on the potential for plant pathogens to be used as weapons. That same year, the organization issued a statement recommending better surveillance of plant-disease outbreaks, eyeing the possibility of agroterror.

J. M. BOVÉ

Those flirtations with biosecurity turned serious after letters laced with anthrax started appearing in the US mail system shortly after the terrorist attacks of 11 September 2001. Fletcher was then president-elect of the American Phytopathological Society. In February 2002, she and several other scientists briefed Congress on the potential for plant pathogens to be used by terrorists. "While there is no evidence that agriculture might be a current target of terrorism, September 11 has made us all more aware of the need to be prepared for any possibility,"

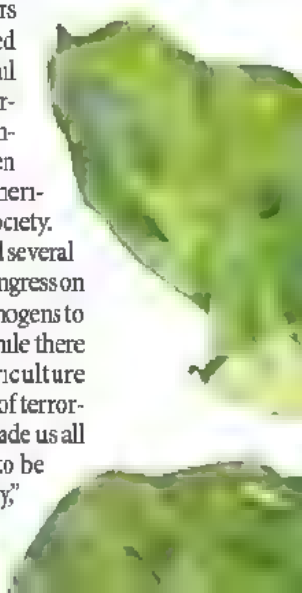

D. HALL, J. M. BOVÉ

The psyllid bug (left) carries the bacterium that causes huanglongbing in citrus.

Fletcher said at the time.

Congress and President Bush listened. On 12 June that year, Bush signed the Agricultural Bioterrorism Protection Act, ordering the US Department of Agriculture (USDA) to include plant pathogens on the select-agent list. Two months later, the agency began enforcing the law, listing nine plant pathogens, including two species of '*Ca.* Liberibacter' (see 'The select few')

To ensure flexibility, the USDA included only exotic pathogens — those usually found outside the United States — as select agents and mandated that they be removed from the list once they took hold in the country. The law would be updated every two years to accommodate such changes, although not until extensive consultation has been done.

Some researchers view this elevation of status as a boon. "Having the select-agent list helps us to prioritize," says Fletcher. "It also targets special funds for working on those things if they should come in." Indeed, the USDA's biodefence budget bloomed from $200 million in 2003, the first year that numbers were made available, to $340 million in the 2008 budget, according to the Center for Biosecurity at the University of Pittsburgh Medical Center in Baltimore, Maryland.

> "Few, if any, plant pathogens should be considered bioterror agents."
> — Tim Gottwald

Heightened awareness of plant pathogens also spurred the USDA to establish a national network of laboratories to diagnose plant diseases. Before 9/11, every state ran its own plant-pathology lab, each of which had different procedures for testing diseased plants. But funding was scarce and "all these labs were languishing", Fletcher says. Although agroterrorism was the motivation behind the long-overdue network, improved diagnostics and communication between state labs will speed the response to any outbreak, she says.

On 23 August 2005, plant pathologists had their worst fears realized: huanglongbing was found in the pomelo trees of two homeowners near Miami. Ten days later, the USDA confirmed the diagnosis. In the months that followed, officials found the disease in thousands of trees in most of Florida's citrus-growing counties.

Where it came from no one knows, but historical records suggest that the disease originated in the Guangdong province in southern China or in central India in the late 1800s. It quickly sped through Asia, where one species, '*Ca.* L. asiaticus', is now endemic from Japan to Pakistan. A second species, '*Ca.* L. africanus' is found throughout eastern, central and southern Africa, and a third species, '*Ca.* L. americanus' has been discovered in Brazil.

## Yellow dragon

Citrus trees infected with huanglongbing show few symptoms for several years. Eventually, their leaves develop characteristic yellow splotches, and trees produce puny, discoloured fruit. Production drops rapidly, until the trees eventually die. Worse, infected trees churn out bacteria for the psyllid to cart elsewhere.

Given the havoc the disease has wreaked around the world, there is good reason to worry that huanglongbing will spread throughout the United States, says Phil Berger, acting director of the USDA's Center for Plant Health Science and Technology in Raleigh, North Carolina. A survey in the late 1990s estimated that 53 million trees in Asia were infected with huanglongbing, and 10 million in Africa. A systematic survey of the Reunion Islands in the 1980s found that huanglongbing had killed 65% of their citrus trees within seven years of planting. And in parts of northern Thailand, the bacterium kills at least one-tenth of tangerine trees every year. In the state of São Paulo in Brazil, an estimated 800,000 trees have been lost since an outbreak hit in 2004.

As the citrus psyllid moves west from Florida — it has turned up in Texas and Mexico — officials and growers are preparing for the worst. "The threat is enormous," says Larry Bezark, of the California Department of Food and Agriculture in Sacramento. Bezark spearheads the state's response to huanglongbing — scouring farms, nurseries and even ports for psyllids and infected plants. "This is a disease that can wipe out citrus as we know it," he says.



M. A. AVREZ/AP

THE SELECT FEW

| Microbe | Disease | Select agent status |
|---|---|---|
| *'Candidatus* Liberibacter africanus | Huanglongbing | Current |
| *'Ca.* L. asiaticus' | Huanglongbing | Current |
| *Peronosclerospora philippinesis* | Philippine downy mildew of corn | Current |
| *Ralstonia solonacearum*, race 3, biovar. 2 | Brown rot of potato | Current |
| *Sclerophthora rayssiae* var. *zeae* | Brown stripe downy mildew of corn | Current |
| *Synchytrium endobioticum* | Potato wart disease | Current |
| *Xanthomonas oryzae* pathovar *oryzicola* | Rice leaf streak | Current |
| *Xylella fastidiosa* (citrus variegated chlorosis strain) | Citrus variegated chlorosis | Current |
| *Phakospora pachyrhizi* | Asian soya bean rust | Removed 2005 |
| Plum Pox potyvirus | Plum pox | Removed 2005 |
| *'Ca.* L. americanus' | Huanglongbing | Proposed 2007 |
| *X. oryzae* pathovar. *oryzae* | Rice leaf streak | Proposed 2007 |
| *Phoma glycinicola* | Ref leaf blotch of soya bean | Proposed 2007 |
| *Phytophthora kernoviae* | Related to sudden oak death | Proposed 2007 |
| *Rathayibacter toxicus* | Gumming disease in ryegrass | Proposed 2007 |

But while California prepares for an outbreak, researchers and officials in Florida feel handcuffed by the pathogen's continued status as a select agent, even though it is now widespread in Florida. "We had our hands tied," says Wayne Dixon, chief of plant pathology at the Florida Department of Agriculture and Commerce in Gainesville. Whenever a sample from a tree turns up positive, the select-agent law mandates that the lab notify the USDA and destroy the sample within a week. This complicates efforts to perform additional diagnostics, says Dixon, who supports listing some exotic plant pathogens as select agents but not '*Ca.* Liberibacter asiaticus'

To comply with the select-agent listing, researchers must register with the federal government, install added security to their labs such as video monitors and fingerprint-accessed doors, and submit to background checks. Foreign researchers have an especially hard time getting approved to work on select agents. The penalties for violating the law are harsh — up to $250,000 and five years in jail.

## Species swap

In August 2007, the USDA proposed updating the select-agent list to remove the asiaticus species found in Florida, while adding the Brazilian americanus species to the list. It is now reviewing the comments it received on its proposals, which are overwhelmingly in favour of lifting the select-agent status of the asiaticus species — and hopes to issue a final rule later this year, says Michael Firko, a USDA official who is leading the agency's efforts.

While the proposal to remove the asiaticus strain from the select-agent list seems to be headed for approval, several other plant pathogens may be added, including diseases of soya, rye, woody trees and shrubs, and rice.

The proposed addition of a strain of the rice pathogen *Xanthomonas oryzae* has left some microbiologists scratching their heads. The cause of leaf streak in rice, *X. oryzae* has done significant damage to crops in Asia and Africa. Yet the pathogen is unlikely to take hold in the United States because of different farming practices and a hostile climate, says Leach, who studies the bacterium.

> "It doesn't make sense to have such enormous restrictions when it's already outside our window."
> — Eric Triplett

The added cost of complying with the select agent rule may force some researchers to abandon their work on *X. oryzyae*. "I stay up late at night worrying about this stuff," says Pam Ronald, a geneticist at the University of California in Davis who studies the rice pathogen

Firko contends that the select-agent status of '*Ca.* Liberibacter asiaticus' hasn't hampered research. "We have not refused registration to anybody for this agent, and I don't think we have refused any experiment that people want to do."

Classifying '*Ca.* L. asiaticus' as a potential agent of bioterror is paradoxical, says Eric Triplett, a microbiologist at the University of Florida in Gainesville. "It doesn't make sense to have such enormous restrictions on laboratories and confine it to strict BSL-3 conditions when it's already outside our window." To study the disease, Triplett and his lab members must travel to a facility 225 kilometres away that has been approved specifically for work on select agents. The microbiologist would like a lab of his own to work on huanglongbing, but the government has yet to approve it.

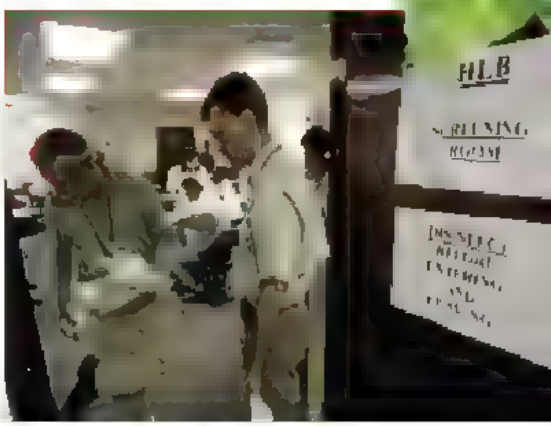


T. GOTTWALD, W. LEE/APS

**Are the complex rules and regulations governing select agents stymying work to study and monitor the spread of huanglongbing (HLB)?**

"Few, if any, plant pathogens should be considered bioterror agents," says Tim Gottwald, a plant pathologist at the research wing of the USDA in Fort Pierce, Florida, who studies huanglongbing. Gottwald estimates that he spent $50,000 upgrading his lab to comply with the select agent rules. More troubling, he says, are delays in getting scientists approved to work on the disease. "I have 12 to 14 people somewhere in the FBI black hole," he says.

The pathogen's select-agent status may also scare away promising young scientists because the restrictions slow down the progress of research, says Triplett. "It's very hard to persuade a post-doc or grad student to work on a project when it's going to hamper [his] career," he says.

More than 3,000 kilometres away, Johnston has his own worries as he scans his grove at the end of a long day. He stops at a navel tree and plucks a shoulder-high fruit, then slices the orange open with a couple of quick motions of a pocket knife. Its juice squirts out and the tangy perfume fills the air for a second. Huanglongbing would reduce the sweet fruit to a withered, bitter gall.

Meanwhile, Johnston says that he hasn't even heard of the select-agent rule. "I am much more concerned that the US government, through inaction, will allow this stuff to move from Florida to Texas to California." When asked about agroterror, he laughs and points out that those wishing to do harm could pick a better weapon than huanglongbing. "Are they going to try to kill orange trees rather than people? I doubt it." ■

**Ewen Callaway is a science journalist in Washington DC.**

**See Editorial, page 127.**

## Poor countries left behind in rush to claim sea floor

SIR — The News Feature 'The next land rush' (*Nature* **451**, 12–15; 2008) highlights the challenges faced by states attempting to claim areas of the sea floor under United Nations rules. Although some countries can finance well-resourced expeditions to confront these challenges, the developing world risks being left behind.

Unfortunately, it was not until developing states recently became aware of the extent of potentially eligible seabed territory that their national governments woke up. With the May 2009 submission deadline given by the UN Convention on the Law of the Sea affecting most of them, a different rush has ensued — to ensure they are not overlooked in this historical process.

The United Nations is helping many states in Africa, the South Pacific and Latin America to make submissions, but many problems are unresolved as the deadline draws closer.

There are various avenues whereby the world's richer countries could provide much-needed support to developing states to ensure a fair, strong and complete Article 76 process and guarantee that the poorest states secure their access to deep-marine resources. We call on these countries to increase sharing of marine data and transfer of scientific and technical knowledge. This would be the spark for larger bi- and multilateral cooperation.

**Morten Sørensen**
UNEP Shelf Programme, Bratteklev,
4818 Færvik, Norway

## Directive will unleash new generation of coal polluters

SIR — We find that the European Union's proposed directive on carbon-capture 'readiness', as reported in your News story 'Europe to capture carbon', is unacceptable (*Nature* **451**, 232; 2008). It clears the way for a new generation of coal-fired power stations to be built in Europe without any abatement of emissions when they start operating, and without any certainty about when, or if, such technology will be available and affordable.

Already, proposals for new coal plants that will emit tens of millions of tonnes of carbon dioxide are working their way through the planning systems of several European countries. In Britain, for instance, plans for the energy company E.ON's proposed coal power station at Kingsnorth in the Medway estuary, Kent, are with the business secretary, John Hutton, and there's no certainty that he will call a public inquiry to examine the national and international implications.

If allowed, Kingsnorth would start generating in 2012, even before the UK carbon-capture demonstration projects are up and running. With every year that passes without such technology being retrofitted, it would emit more than seven million tonnes of carbon dioxide — ten times more than the entire annual emissions of Rwanda.

If Europe's member states are serious about climate change and meeting the targets they have set themselves for reducing harmful emissions, they will impose strict standards of greenhouse-gas efficiency on all new power stations. New coal-fired power plants of the kind proposed at Kingsnorth should be reconsidered only if carbon capture and sequestration are proved safe, effective and commercially available for fitting from the moment they begin to burn fuel.

**Mark Avery*, John Sauven†, Keith Allot‡, Benedict Southworth§, Andrew Pendleton‖**
*Royal Society for the Protection of Birds, The Lodge, Sandy, Bedfordshire SG19 2DL, UK
†Greenpeace, Canonbury Villas, London N1 2PN, UK
‡World Development Movement, 66 Offley Road, London SW9 0LS, UK
§WWF, Panda House, Weyside Park, Godalming, Surrey GU7 1XR, UK
‖Christian Aid, 35 Lower Marsh, London SE1 7RL, UK

## How academic corporatism can lead to dictatorship

SIR — Michael Crow's Book Review of Daniel Greenberg's *Science for Sale* (*Nature* **449**, 405; 2007) calls for a response because it reflects a worsening philosophical divide in US academia between those who regard universities as analogous to corporations and think they should be run that way (mostly career administrators) and those who see universities as primarily intellectual enterprises governed by academic core values (mostly line faculty). Asserting that the university is an idea — not an ideal or an ideology — Crow, who is president of Arizona State University, plays down or ignores most of the dangerous consequences of campus capitalism.

Faculty members would generally hold that universities represent ideals as well as ideas. These are manifest in a value system that is among the first casualties of academic corporatism. Derived from political corporatism, academic corporatism is an administrative strategy that is antithetical to the spirit that academics hold dear — including openness, transparency, collegiality, meritocracy, rule-governed procedures, balanced curriculum, a level playing field for probationary faculty and participation by faculty in governance.

Like its political counterpart, academic corporatism often results in dictatorships, with ideas originating only from the top and nothing going the other way. Academic assemblies, unions and senates are eviscerated, neutralized or eliminated altogether. Faculty members are disenfranchised. There is a chilling effect on free speech and the notion of an open marketplace for ideas.

This can wreak havoc with a university's curriculum, jeopardize its intellectual and educational missions and compromise its future. As former Harvard president Derek Bok said: "The end to which this process could lead is not a pleasant prospect to behold."

**G. A. Clark**
Department of Anthropology, School of Human Evolution and Social Change, Arizona State University, Tempe, Arizona 85287-2402, USA

## Results of rush to sequence genomes may be nonsense

SIR — In the Commentary 'Common sense for our genomes' (*Nature* **449**, 783–784, 2007), Steven Brenner welcomes the sequencing of the genomes of James Watson and Craig Venter. Although the generally hypothesis-free collection of large amounts of sequence information may indeed turn out to be important, caution is warranted.

First, it is not the static genome but rather the dynamic proteome that regulates the enormous changes occurring in an organism between conception and death. Second, only the most radical reductionist would argue that a person's essence can be captured by his or her proteome, let alone his or her genome.

Our lives are unrepeatable experiments lacking a control. Myriad external factors interact with genetic and epigenetic factors and with chance to determine whether we are well or ill, smart or dull, successes or failures. A study on some 44,000 twin pairs concluded that environmental and not inherited genetic factors were the main determinants of sporadic cancer (P. Lichtenstein *et al. N. Engl. J. Med.* **343**, 78–85; 2000). Brute-force genome sequencing and Brenner's proposed Genome Commons could yield nonsense if environmental factors are overlooked.

This is not just an academic issue. Membership of the 'diploid genome club' is set to rise rapidly (see *Nature* **447**, 358–359; 2007). The X Prize Foundation is offering the Archon genomics prize of US$10 million to the first team able to sequence 100 human genomes accurately within ten days. But whether the winners will understand the results is a different question entirely.

**Thomas C. Erren*, Paul Cullen†, Michael Erren‡**
*Institute and Polyclinic for Occupational and Social Medicine, University of Cologne, D-50937 Köln, Lindentha , Germany
†Medizinisches Versorgungszentrum für Laboratoriumsmedizin Dr Löer, Dr Treder, Hafenweg 11, 49155 Münster, Germany
‡Institute of Clinical Chemistry and Laboratory Medicine, Westphalian Wilhelms-University of Münster, Münster, Germany

# CHEMBRIDGE CORPORATION

## Setting the Gold Standard in Discovery Chemistry

### EXPERIENCE:

- 15 years of excellence in chemistry
- Client exclusive library production
- Top tier chemists: lead discovery libraries & med chem support

### PORTFOLIO:

- 700,000 screening compounds: targeted & diverse
- Discovery chemistry research services
- Novel scaffolds & building blocks
- Hit2Lead.com online chemical store

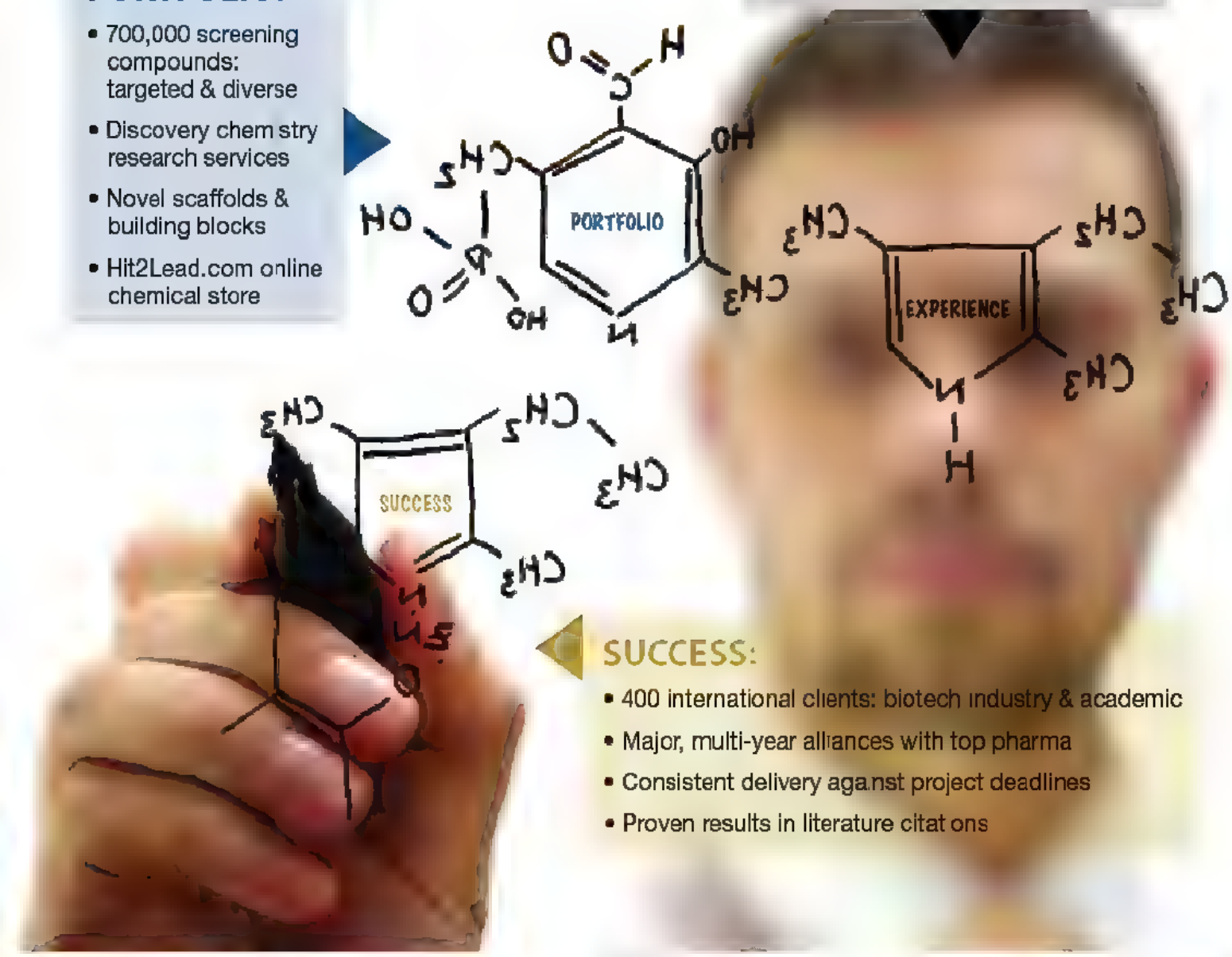


### SUCCESS:

- 400 international clients: biotech industry & academic
- Major, multi-year alliances with top pharma
- Consistent delivery against project deadlines
- Proven results in literature citations

San Diego, California | 1-800-964-6143 | sales@chembridge.com

BOOKS & ARTS

# One long argument

**Revisiting ancient Greek debates about the natural world should broaden biologists' horizons.**

**Creationism and its Critics in Antiquity**
by David Sedley
University of California Press: 2008
296 pp £17.95

**Armand M. Leroi**

Evolutionary biologists are — as modern scientists go — a historically minded lot. All of us acknowledge the greatness of Charles Darwin and some have even read *On the Origin of Species*. A few speak of Geoffroy Saint Hilaire, Lamarck or Goethe. Yet our historical horizon is actually very near. The pre-1859 theoretical landscape is shrouded in a Judeo-Christian gloom that reaches without interruption to the dawn of recorded time, where it dissolves into the Stygian darkness of pagan creation myth.

David Sedley's book will change that view. He argues that, for the philosophers of ancient Greece, the central cosmological question was this: is the world, and all that it contains, the handiwork of an intelligent designer? Between 500 and 300 BC, about a dozen major thinkers essayed answers that are bewildering in their variety and ingenuity. Some were as creationist as a Christian. Others appealed to more remote forces such as love. Others again were ardent materialists and thought the world just self-assembled. From the presocratics to Galen, the Creator advances, retreats or sometimes just curls up and contemplates himself. At times — although it's hard to tell when — God becomes a metaphor.

The pivotal figure in Sedley's story is Socrates. It seems an odd choice. The issue is the origin of the world, about which Socrates had little to say because he thought science was a waste of time. For him, knowledge came from debating questions such as 'what is good?' Yet Sedley credits him with one of the most potent arguments in the history of cosmology: the argument from design. That argument became the centrepiece of the cosmology that Socrates' pupil, Plato, sketched in the *Timaeus* and thence, by descent, the source of the extraordinary teleological account that Aristotle, Platos pupil, gave of the natural world.

Sedley's argument is subtle and expert; he is the Laurence Professor of Ancient Philosophy at the University of Cambridge, UK. But it won't wash. To elevate Socrates he diminishes Aristotle to the position of Plato's epigone. But how different the thinkers are. Plato's god is a cosmic craftsman; Aristotle's god just thinks. Plato's world has a beginning, Aristotle's is eternal. Plato's animals get their form from the mind of god, Aristotle's are formed from information in the seminal fluid of their parents.

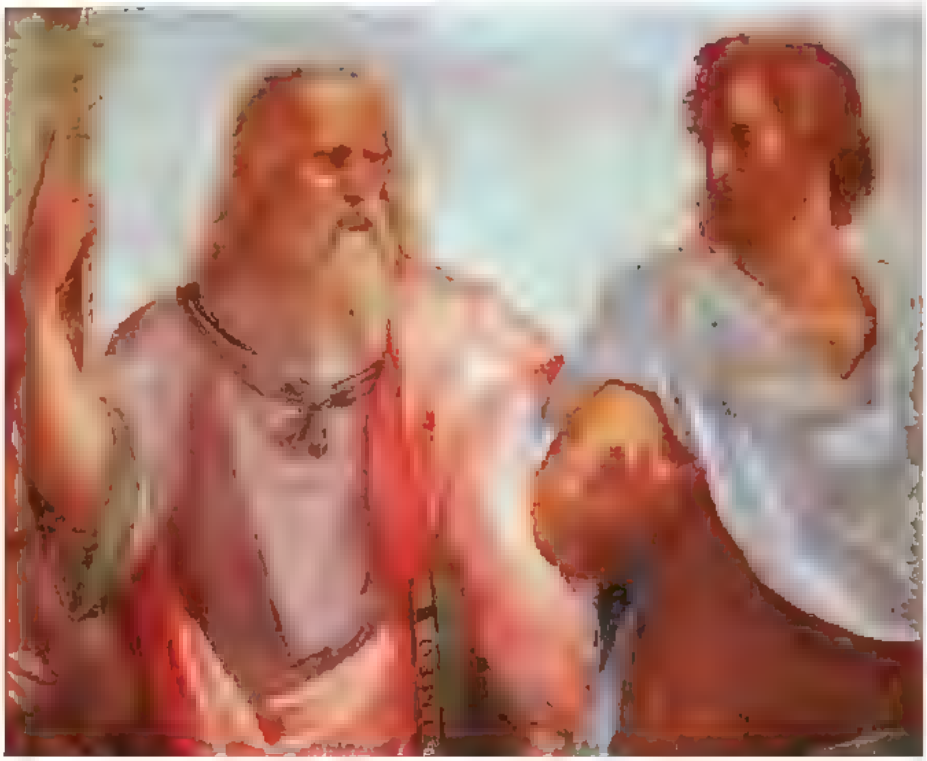

A. DAGLI ORTI/THE ART ARCHIVE

In Plato (left) one hears a poet; in Aristotle (right), a colleague — albeit one with some cranky views.

It's not just the ideas that differ, it's also the style. The *Timaeus* is a drawing-room monologue in the form of a myth: one rich in zoological weirdness but devoid of scholarly citation, empirical evidence or even much reasoned argument. Aristotle's works are a relentless, reasoned assault on reality that, in modern print, run to thousands of pages. They are an exhaustive and exhausting analysis of what his predecessors thought about the causes and structure of the natural world, why they are (more often than not) wrong, and the empirical evidence for thinking so.

For a modern scientist, if not for a philosopher, the difference could not be greater. Listen to Plato and one hears a poet or, at best, a moralist; listen to Aristotle and one hears a colleague — albeit one with some cranky views. In a piquant preface, Sedley tells us that the dining room of his Cambridge college displays the portraits of two of its alumni, the Christian philosopher William Paley and Darwin. The parallel with fourth century Athens is exact. As a student, Darwin read and enjoyed Paley's *Natural Theology*, and may have even acquired from it his keen sense of the exquisite design displayed by living things. Yet who would call Darwin a paleyite? It would be the equivalent of calling Aristotle a platonist.

And that's absurd. Or is it? The brilliance of this book is that Sedley lets the Greeks talk to us and, surprisingly, we can understand what they're saying. Listen to Empedocles describing a time when the world was filled with a diversity of creatures with improbable combinations of features, most of which were then winnowed out, and you hear the late Stephen Jay Gould illuminating the body plans of the Burgess Shale fossils. Listen to Aristotle heaping scorn on Democritus for supposing that living things self assemble from accidental combinations of atoms, and you hear Fred Hoyle's gambit that "a tornado sweeping through a junkyard might assemble a Boeing 747 from the materials therein". Truly it has been, as Darwin said, just "one long argument". ■

Armand Leroi is Reader in Evolutionary Developmental Biology at Imperial College London, UK. He is author of *Mutants: On the Forms, Varieties and Errors of the Human Body*.

# Storming the language barrier

**The Simian Tongue: The Long Debate about Animal Language**
by Gregory Radick
University of Chicago Press. 2008
544 pp. $45

**Frans B. M. de Waal**

People sometimes view the scientific community through rose-coloured glasses. I recall a presentation by a management trainer who was seeking to contrast the world of science with that of business. He showed a table with a 'business' column with characteristics, such as 'competitive', 'seeking money' and 'back-stabbing'. Next to it was a 'science' column, which included 'cooperative', 'seeking the truth' and 'open communication'.

*The Simian Tongue* is a good corrective to such naivety. A key theme in the quest for the animal origins of language is the lengths to which scientists will go to disagree with and discredit each other. Gregory Radick, a British science historian and philosopher, leaves no quarrel unexplored in the saga that began around 150 years ago when German-born philologist Friedrich Max Müller declared: "No process of natural selection will ever distill significant words out of the notes of birds or the cries of beasts."

Language requires thought and thought requires language, argued Müller. Given that animals obviously lack thought, he said, what would be the point of debating the animal origins of language? This position still reverberates with modern followers of Noam Chomsky's theory of universal human grammar, who rarely bother to mention animal communication. Radick contrasts this assumption of abrupt 'saltationist' evolutionary change with a darwinian view of continuity.

The hero of Radick's tale is the American Richard Lynch Garner (1848–1920) — probably the only investigator to have conducted a captive study in the wild. This former schoolteacher objected to the received wisdom that language is what separates us from the beasts. But he was so afraid of the tropical animals that he wanted to investigate, such as gorillas, that he locked himself into a metal cage in the French Congo with two guns and 2,000 rounds of ammunition to watch them from safety. His exploits read like a Jules Verne tale (indeed, Verne put a Garner-like explorer in his novel *The Aerial Village*).

Garner's recordings of primate calls with Thomas Edison's new phonograph, and Edison's financial support, made him famous. Things took an ugly turn when a duplicitous missionary, who didn't care for Garner's darwinism, tried to lose him or cause him to catch a deadly fever in the jungle, and when a British tabloid newspaper spread false rumours that

P. MARLER

**Peter Marler recorded primate calls and showed that they alter depending on who is listening.**

Garner had spent hardly any time in his cage. By the end of his life, the misunderstood scientist complained: "No one but myself can take a monkey seriously."

Of course, it is a rather anthropocentric enterprise to scrutinize animals to understand human language. Current scholars of primate vocalization follow the dictum of ethology (the biological study of animal behaviour) — that animals should be studied for their own sake. One such ethologist, Peter Marler, figures as Garner's modern counterpart. Like Garner, Marler believes that the answer to the language question will come from recording primate calls in the field and playing them back to gauge reactions. He and his students have made a persuasive case that vocalizations provide listeners with detailed information about social relationships and the environment, such as in the predator-specific calls of vervet monkeys on the plains of Kenya.

But *The Simian Tongue* is not the book for those wanting to learn what primate communication is all about. Its focus is the human primate: the personalities behind the research, the ideas they develop and the battles they fight. These lively stories contain enough context to illustrate the larger shifts in theoretical perspective. And as such, it is an instructive read for anyone interested in the language barrier, or absence thereof, between humans and other animals.

My only complaint about *The Simian Tongue* concerns a general flaw of contemporary English science writing; it invariably locates the epicentre of science at British and North American universities. The debate about the evolution of language would have taken a completely different turn were it not for the following: the rise of ethology in continental Europe; the nineteenth century discoveries of brain areas by Broca and Wernicke (a Frenchman and a German, respectively); and the development of modern primatology, which owes much to Kinji Imanishi's school in Japan. Of these contributions, Radick makes scant mention.

Imanishi's student, Jun'ichiro Itani, suggested that the evolution of speech would have required a decoupling of vocal production from the emotions. He thus highlighted a concern that many experts have with the simian tongue as a forerunner of human language. Primate vocalizations are somewhat modifiable (Marler himself was one of the first to show audience effects), but seem to be under limited voluntary control. The abject failure to teach articulate speech to apes illustrates their limited vocal control, in contrast to the ease with which apes learn gestures, such as American Sign Language. Our primate relatives have excellent control over their hands and gesture with remarkable flexibility in their natural communication. This gestural modality ought to be part of any debate about language origins.

It is nonetheless fascinating to follow the shifts in questions and approaches throughout the time that Radick chronicles. Garner, for example, looked for animals with human like language and humans with animal-like language because he lived in an era when human languages were still ranked from primitive to advanced. In those days, language hypotheses went by bizarre names such as the 'bow-wow', 'pooh pooh' or 'ding-dong' theory, depending on the role they assigned to sounds, emotions or concepts. Modern scientists, by contrast, deem all human languages to be equally complex. They focus instead on the 'design features' of language, believing that some or all of these features are present in other species, although it is also evident that language as we know it is limited to just one species.

Many see the future of this field as a closer integration between naturalistic approaches to animal communication and cognitive neuroscience. It would be unrealistic, however, to expect this to lower the temperature of the debates. If the recent exchange between Patricia Churchland and Steven Pinker in this journal's pages (see *Nature* 450, 788; 2007) about the connection between language and thought is any indication, adding the brain to the mix will only introduce another fertile layer of potential discord. ■

Frans B. M. de Waal is director of the Living Links Center at the Yerkes National Primate Research Center, Emory University, Atlanta, Georgia 30322, USA. He is author of *Our Inner Ape*.

EXHIBITION

# A protein ghost etched in glass

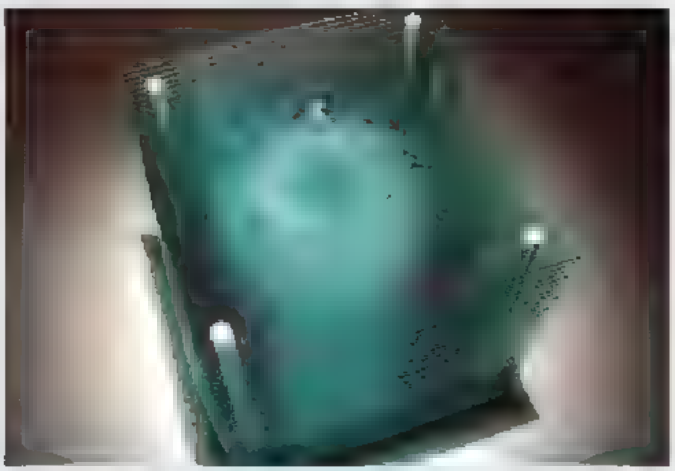

DESIGN4SCIENCE

**Marta Paterlini**

The starting point of the touring exhibition *Design4Science*, now running at the Nobel Museum in Stockholm, was the pioneering Laboratory of Molecular Biology in Cambridge, UK — the birthplace of protein crystallography. Max Perutz, who was chairman of the lab when it was founded in 1962, encouraged photographers and designers to be part of the scientific team from the start.

Wandering around the well-known protein and virus models that resulted, one much more recent piece stands out, a dizzying ghost of a protein molecule mounted in a block of glass. Colin Rennie, a young artist from Sunderland, UK, took inspiration from ATP synthase, the molecule that rotates to produce adenosine triphosphate, the universal currency of biological energy. Rennie used a powerful water-jet cutter to recreate the three-dimensional structure of the molecule in a 780-kilogram cube of 30 glass layers measuring 1 metre across.

Rennie's vibrant artwork captures the spatial and temporal fixity of protein crystallography and the sense of motion of this particular molecule. The transparent glass embodies the tension between the seen and the unseen that is intrinsic to our perception of the molecular world. At the same time, it mimics the protein crystals that give scientists their atomic models.

As the renowned scientific artist Irving Geis once said: "We can only say 'it's something like that' — and only create a visual metaphor." ■

Marta Paterlini is a writer based in Stockholm, Sweden

***Design4Science* runs until 31 August at the Nobel Museum, Stockholm (www.nobelmuseum.se).**

# Census of cyberspace censoring

**Access Denied**
edited by Ronald Deibert, John Palfrey, Rafal Rohozinski and Jonathan Zittrain
MIT Press: 2008. 320 pp. $20.00, £12.95

**Bruce Schneier**

In 1993, Internet pioneer John Gilmore said "the net interprets censorship as damage and routes around it", and we believed him. In 1996, cyberlibertarian John Perry Barlow issued his 'Declaration of the Independence of Cyberspace' at the World Economic Forum at Davos, Switzerland, and online. He told governments: "You have no moral right to rule us, nor do you possess any methods of enforcement that we have true reason to fear."

At the time, many shared Barlow's sentiments. The Internet empowered people. It gave them access to information and couldn't be stopped, blocked or filtered. Give someone access to the Internet, and they have access to everything. Governments that relied on censorship to control their citizens were doomed.

Today, things are very different. Internet censorship is flourishing. Organizations selectively block employees' access to the Internet. At least 26 countries — mainly in the Middle East, North Africa, Asia, the Pacific and the former Soviet Union — selectively block their citizens' Internet access. Even more countries legislate to control what can and cannot be said, downloaded or linked to. "You have no sovereignty where we gather," said Barlow. Oh yes we do, the governments of the world have replied.

*Access Denied* is a survey of the practice of Internet filtering, and a sourcebook of details about the countries that engage in the practice. It is written by researchers of the OpenNet Initiative (ONI; www.opennet.net), an organization that is dedicated to documenting global Internet filtering around the world.

The first half of the book comprises essays written by ONI researchers on the politics, practice, technology, legality and social effects of Internet filtering. There are three basic rationales for Internet censorship: politics and power; social norms, morals and religion; and security concerns.

Some countries, such as India, filter only a few sites, others, such as Iran, extensively filter the Internet. Saudi Arabia tries to block all pornography (social norms and morals). Syria blocks everything from the Israeli domain '.il' (politics and power). Some countries filter only at certain times. During the 2006 elections in Belarus, for example, the website of the main opposition candidate disappeared from the Internet.


TEH ENG KOON/AFP/GETTY IMAGES

China restricts Internet access by keyword.

The effectiveness of Internet filtering is mixed; it depends on the tools used and the granularity of filtering. It is much easier to block particular URLs or entire domains than it is to block information on a particular topic. Some countries block specific sites or URLs based on some predefined list but new URLs with similar content appear all the time. Other countries — notably China — try to filter on the basis of keywords in the actual web pages. A halfway measure is to filter on the basis of URL keywords: names of dissidents or political parties, or sexual words.

Much of the technology has other applications. Software for filtering is a legitimate product category, purchased by schools to limit access by children to objectionable material and by corporations trying to prevent their employees from being distracted at work. One chapter discusses the ethical implications of companies selling products, services and technologies that enable Internet censorship.

Some censorship is legal, not technical. Countries have laws against publishing certain content, registration requirements that prevent anonymous Internet use, liability laws that force Internet service providers to filter themselves, or surveillance. Egypt does not engage in technical Internet filtering; instead, its laws discourage the publishing and reading of certain content — it has even jailed people for their online activities.

EXHIBITION

# Beauty meets utility at MoMA

Josie Glausiusz

A pudgy, pink, pig-like creature, lacking a head but sprouting a tuft of unruly hair, sits in a corner of the Museum of Modern Art (MoMA) in New York. *Epidermits*, a stubby-legged quadruped, was purportedly spawned from a skin-and-hair-cell culture grown from a human cheek swab, and is fed on a 'sustain solution' infused through its tail. If carefully nurtured, it could be expected to live as long as "a large dog or a donated kidney".

So says designer Stuart Karten, who claims that his ten-centimetre-long, yet-to-be-realized organism could be a pet of the future. Our ability to incorporate such fantastic ideas into everyday life is the subject of MoMA's new exhibition, *Design and the Elastic Mind*, which explores the myriad ways in which our minds rapidly adapt to technological changes. This marvellous hodge-podge of exhibits comprises 200 creations that range in size from nano-scale smiley-faces stitched together from viral DNA, to an imposing five-metre-tall sculpture by Chuck Hoberman called *Emergent Surface* — a screen of twisting and unfolding slatted steel panels that move in response to changes in light. Practical gadgets sit beside whimsical pieces such as the 'smell augmentation' plugs that artist Susana Soares invites us to stuff up our nostrils.

At their best, these devices marry beauty and utility. Martin and Erik Demaine, a father-and-son team from the Massachusetts Institute of Technology (MIT), created *Computational Origami* — delicately folded, interlocking paper loops that demonstrate the use of computer-aided design to squeeze large objects into small spaces. A similar concept underlies Robert Lang's origami models of the Fresnel lens for the Eyeglass Space Telescope (a mothballed project of the Lawrence Livermore National Laboratory in California). The lens, if realized, could have been scrunched up, launched and then expanded in space to a diameter of 100 metres — roughly the length of an American football field. Elegance and expediency also underlie the *Sonumbra* sculpture created by Rachel Wingfield and Mathias Gmachl, a tree-like 'sonic shade of light' that transforms peoples' movements via software into serene sounds that are reminiscent of those produced with a Tibetan singing bowl. Solar cells embedded in the green, umbrella-like shade of *Sonumbra* harvest energy during the day to power the lights at night.

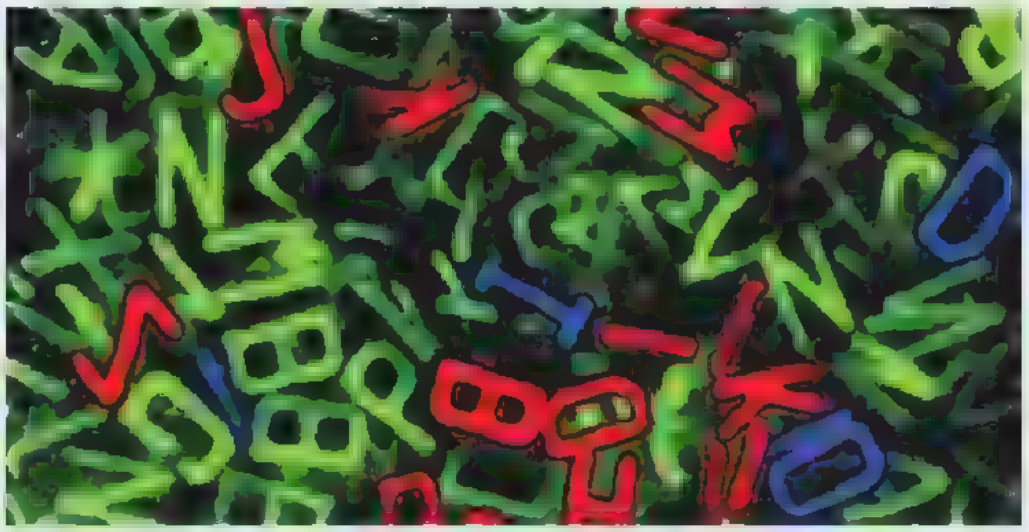

JK_A/KOLODIA, IMAGE BY T G MASON/K. J. HERNANDEZ

'Colloidal Alphabet Soup': these 7-micrometre-long polymer letters could be used to label individual cells.

Some of the most compelling items in *Design and the Elastic Mind* are simple, yet could prove essential to populations that lack basic equipment. Bernhard Weigl's credit-card-sized 'Lab on a Card' can diagnose an intestinal infection from a small faecal sample in 20 minutes. Emili Padrós's 'Non-Stop Shoes' use the energy generated from walking and stair-climbing to run lamps and radios. Similarly, the green-keyed XO laptop computer designed by MIT's Media Lab is "lighter than a lunchbox" and has a battery that can be recharged by pulling a cord wrapped like a yo-yo. It is being distributed to schools in Uruguay, Afghanistan, Cambodia and Mexico, among others, as part of the 'One Laptop Per Child' project, a non-profit programme to deliver laptops to the world's poorest children in remote areas.

What makes the exhibition so electrifying is the imagination that drives these innovations. A charming example is a series of drawings inspired by artist Alan Outten, who challenged British primary-school children to design the future. Their inventions included 'Super-Human Mermaid', a genetically engineered human with the genes, gills and tails of a fish "in case the world floods due to pollution", and 'The Apple Phone', a tree with man-made seeds that "use nature as their energy source" to grow apple-like telephones, "so if you are having a private conversation, you just eat the apple". To quote Outten, I left the exhibition "with a sense that creativity and design are safe in the hands of the next generation". ■

Josie Glausiusz is a journalist based in New York.

***Design and the Elastic Mind*** **runs at the Museum of Modern Art, New York, until 12 May (www.moma.org).**

The second half of *Access Denied* consists of detailed descriptions of Internet use, regulations and censorship in eight regions of the world, and in each of 40 different countries. The ONI found evidence of censorship in 26 of those 40. For the other 14 countries, it summarizes the legal and regulatory framework surrounding Internet use, and tests the results that indicated no censorsh.p. This leads to 200 pages of rather dry reading, but it is vitally important to have this information well-documented and easily accessible. The book's data are from 2006, but the authors promise frequent updates on the ONI website.

No set of Internet censorship measures is perfect. It is often easy to find the same information on uncensored URLs, and relatively easy to get around the filtering mechanisms and to view prohibited web pages if you know what you're doing. But most people don't have the computer skills to bypass controls, and in a country where doing so is punishable by jail — or worse — few take the risk. So even porous and ineffective attempts at censorship can become very effective socially and politically.

In 1996, Barlow said. "You are trying to ward off the virus of liberty by erecting guard posts at the frontiers of cyberspace. These may keep out the contagion for some time, but they will not work in a world that will soon be blanketed in bit-bearing media."

Brave words, but premature. Certainly, there is much more information available to many more people today than there was in 1996. But the Internet is made up of physical computers and connections that exist within national boundaries. Today's Internet still has borders and, increasingly, countries want to control what passes through them. In documenting this control, the ONI has performed an invaluable service. ■

Bruce Schneier is chief security technology officer for BT Counterpane, Santa Clara, California. He is author of *Beyond Fear: Thinking Sensibly About Security in an Uncertain World*.

**Correction**

Ken Arnold's review of *The Anatomist* by Bill Hayes (*Nature* 451, 247; 2008) incorrectly said that the mother's blood enters the fetal heart through a hole. In fact, this hole lets blood move from the right to the left atrium *in utero* and is sealed after birth

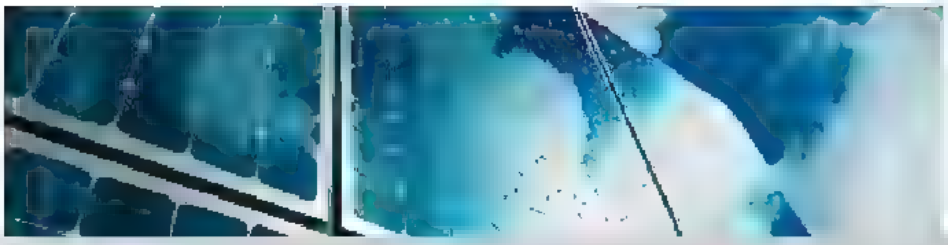

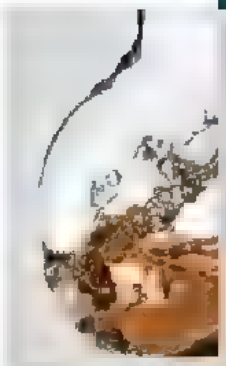

# Eni Award 2008

Eni announces the winners of the 2008 Eni Award, aimed to promote Research and Technology Innovation in the field of energy and its conversion, with particular focus on renewable sources.

## Arthur J. Nozik AND Stefan W. Glunz
FOR THE SCIENCE AND TECHNOLOGY PRIZE

## J. Craig Venter
FOR THE RESEARCH AND ENVIRONMENT PRIZE

## Silvia Cereda AND Gian Luca Chiarello
FOR THE DEBUT IN RESEARCH PRIZES

Eni w shes to thank all the scientists and researchers who took part in the initiative, and announces that registration for the

**2009 Eni Award**

is now open. Enrolment deadline: 10 October 2008

For more information concerning the Eni Award and enrolment method, please visit www.eni.it or contact the Eni Award scientific office:

Fondazione Eni Enrico Mattei
Corso Magenta, 63
20123 Milano
Tel: +39 02 52036934 / +39 02 52036964
Fax: +39 02 52036946
E-mail: eniaward@feem.it

Eni strategies in the energy field focus on technological innovation and cutting edge research. The Eni Award fosters, supports and rewards these efforts. Eni has been included in the leading sustainability indexes, namely the Dow Jones Sustainability Index, the FTSE4Good Index and the CDP5 Climate Disclosure Leadership Index.

Eni

www.eni.it

NEWS & VIEWS

DRUG DISCOVERY

# Fresh hope to can the worms

Roger K. Prichard and Timothy G. Geary

**Parasitic worms kill many livestock, and the drugs used against them are becoming less effective. The discovery of a class of compounds that kills worms resistant to existing drugs is thus a welcome development.**

The scourge of parasitic nematodes in farm animals is rising[1], as these worms increasingly develop resistance to the drugs — known as anthelmintics — that are used against them. For example, drug-resistant strains of *Haemonchus contortus* (Fig. 1), also known as the barber's pole worm, have become common. Sheep and goats infected with this worm develop severe anaemia that is often lethal without effective treatment. No new class of anthelmintics has reached the market in the past 25 years (with the exception of the cyclodepsipeptides, which are currently restricted to use in cats[2]). As a result, drug resistance is now so widespread that there is an urgent need for new drugs to control nematode parasites in livestock. A similar problem faces humans, as medical programmes for combating parasitic diseases in the developing world are threatened by a combination of emerging anthelmintic resistance and a severe lack of investment in new drugs[3].

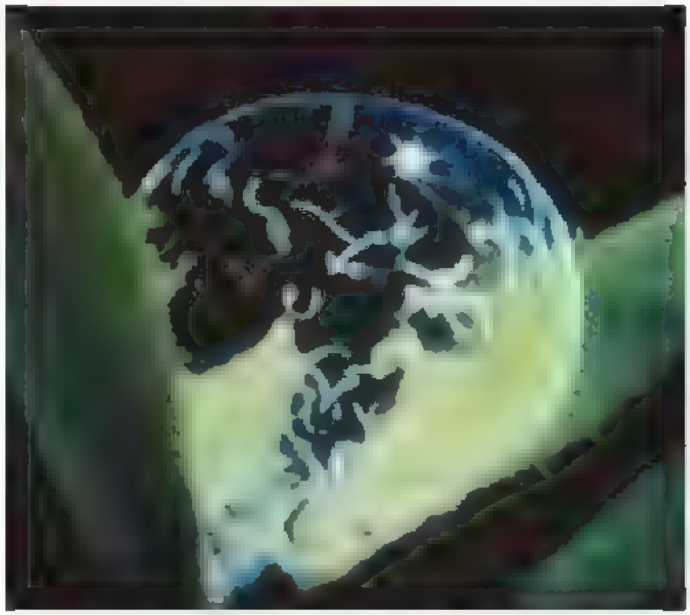

**Figure 1 Infective larvae in a water droplet in pasture.** Sheep and goats infected with *Haemonchus contortus* parasitic worms become anaemic and often die. Adult female worms lay eggs in the host's digestive tract. The eggs are excreted in the host's faeces, where they develop into larvae that move into the surrounding environment. The larvae can then be ingested by other grazing hosts, where they turn into adults, mate and continue the life cycle.

In this issue (page 176), Kaminsky *et al.*[4] report the discovery of a new class of anthelmintics, known as amino-acetonitrile derivatives (AADs), which have potent activity against parasitic nematodes in animals. These drug candidates seem to have a mode of action that overcomes resistance to currently available anthelmintics. To determine the likely mechanism of action of AADs, the authors have exploited the powerful tools that became available upon the completion of the first animal genome — that of the nematode *Caenorhabditis elegans*, which is commonly used as a simple model of a multicellular organism by biologists.

Most anthelmintics were discovered in the 1960s and 1970s. They include the benzimidazole class of drugs, which dissolves the subcellular structure of nematode cells, levamisole and pyrantel, which paralyse worms by targeting acetylcholine receptors; and the macrocyclic lactones, which paralyse parasites by making their nerve cells permeable to chloride ions. But with the inevitable spread of drug resistance after decades of use, these mainstay anthelmintics are becoming less effective. Kaminsky and colleagues' compounds[4] will therefore be a cause of great excitement, especially because they are active against a broad range of nematode pathogens, including resistant strains of *H. contortus*.

Kaminsky and colleagues' report reads like a textbook case of modern anthelmintic discovery. Beginning with an *in vitro* screen of hundreds of AADs against larval stages of nematodes, the authors identified active compounds and determined which chiral form of each compound was the more effective. They then validated the best drug candidates in rodents, and finally tested them in sheep and cattle, where they were effective against many different parasite nematode species that infect livestock. Anthelmintic activity in animals was correlated with a compound's half life — a measure of how stable its molecules are to metabolic inactivation and elimination. Furthermore, the most active AADs showed no overt toxic effects in mammals at doses much higher than those that were lethal to parasites.

So far, so good, but what biological system do AADs target? Fortunately for the authors, they found that not only are AADs active against parasitic nematodes, but they also exert similar effects on the movement, growth and survival of the non-parasitic *C. elegans*. This provided them with a perfect model organism in which to conduct mechanistic investigations. No other class of anthelmintics produced the same effects as AADs, suggesting that the new compounds have a different mechanism from that of existing drugs.

The authors observed that when *C. elegans* are exposed to a compound[5] that acts at nicotinic acetylcholine receptors (nAChRs, which are involved in neurotransmission), they display the same symptoms as worms treated with AADs. Crucially, *C. elegans* did not show these symptoms when exposed to the anthelmintic levamisole, which acts at a specific subtype of nAChR[6]. This suggests that another kind of nAChR is the target for AADs.

With this clue in hand, Kaminsky *et al.*[4] went on to work out how AADs affect parasitic nematodes (Fig. 2, overleaf). They selectively bred mutant *C. elegans* that had resistance to AADs, and then performed a screen of the worms' DNA to find the gene responsible for resistance, using information obtained from the *C. elegans* genome to aid their search. The culprit was a gene known as *acr-23*. The authors compared the sequence of *acr-23* with genes that have known protein products, and so predicted that this resistance-associated gene encodes a nAChR. Tellingly, the ACR-23 protein seems to be nematode-specific, and certainly is not

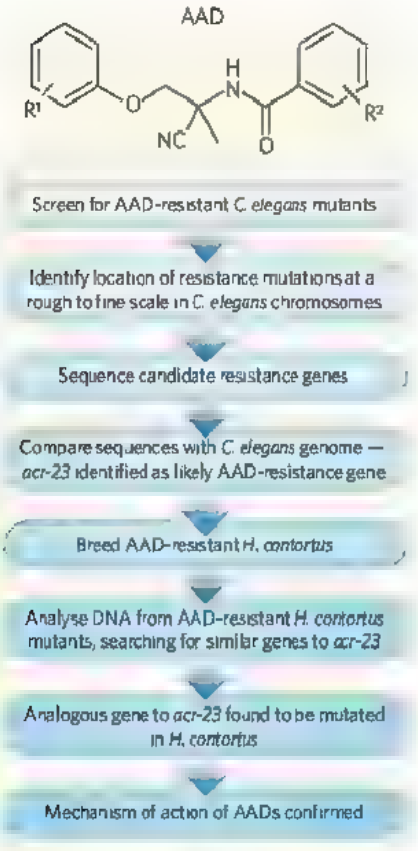


**Figure 2 | Determining the biological target of antiparasitic drugs.** Kaminsky *et al.*[4] report a class of compounds known as amino-acetonitrile derivatives (AADs) that kill parasitic worms such as *H. contortus* in livestock. $R^1$ and $R^2$ represent general chemical groups, and may be attached to the aromatic rings at any vacant position. AADs also kill the non-parasitic worm *C. elegans*, the genome of which has been sequenced. The authors were therefore able to determine the biological target of AADs by studying AAD resistant *C. elegans*, as shown in the flow chart. The gene responsible for AAD resistance must produce the protein targeted by the compounds.

found in mammals. The mutant worms were susceptible to other classes of anthelmintics, providing further credence to the idea that AADs have a new biological target.

The authors then looked to see whether AADs attack the same target in parasitic nematodes. They selected for AAD-resistant *H. contortus* larvae *in vitro*, and for adult worms *in vivo*, by giving sheep doses of the new anthelmintic that were too low to get rid of the parasite completely. They then used nAChR-specific DNA probes on both AAD-resistant and AAD-susceptible parasites to find nAChR genes likely to be responsible for the resistance. They found that part of a nematode-specific nAChR gene (named *Hcdes-2H* by the authors) was missing in the AAD-resistant worms, and that this gene was closely related to *acr-23*. This suggests that the mode of action of AADs is similar in both *C. elegans* and *H. contortus*. It also suggests that the presence of evolutionarily related nAChRs in other species of parasitic nematode can be used to predict the effectiveness of AADs against those species, which could be useful when deciding on a course of treatment for worm-infected animals.

Kaminsky and colleagues' compounds[4] show considerable promise as a new class of anthelmintics, although further development will be necessary before a drug reaches the market. Of course, as with any class of drugs against infective pathogens, there is a risk that resistance to AADs may develop; indeed, the authors have already shown that this is possible. But knowing the likely mode of action of AADs will help in devising strategies to slow the development of resistance, and will also enable sensitive molecular tools to be made for detecting AAD resistance if and when it appears. ■

Roger K. Prichard and Timothy G. Geary are at the Institute of Parasitology, McGill University, Sainte Anne-de-Bellevue, Quebec H9X3V9, Canada.
e-mail: roger.prichard@mcgill.ca, timothy.g.geary@mcgill.ca

1. Wolstenholme, A. J. *et al. Trends Parasitol.* **20**, 469–476 (2004)
2. Jeschke, P. *et al. Bioorg. Med. Chem. Lett.* **16**, 4410–4415 (2006)
3. Osei-Atweneboana, M. Y. *et al. Lancet* **369**, 2021–2029 (2007)
4. Kaminsky, R. *et al. Nature* **452**, 176–180 (2008)
5. Ruaud, A.-F. & Bessereau, J.-L. *Development* **133**, 2211–2222 (2006)
6. Martin, R. J. & Robertson, A. P. *Parasitology* **134**, 1093–1104 (2007)

COSMOLOGY

# Patchy solutions

George Ellis

**The Universe seems to be expanding ever faster — a phenomenon generally ascribed to the influence of 'dark energy'. But might the observed acceleration be a trick of the light in an inhomogeneous Universe?**

Ten years ago, observations of distant supernovae brought a startling realization: the Universe's expansion is apparently accelerating. This observation required a quick patch-up of the dynamics of cosmologists' standard 'concordance' model of the Universe. The sticking plaster was dark energy — a mysterious substance contrived to counteract the attractive tendencies of cosmology's dominant force, gravity.

Unfortunately, the physical origin of dark energy is almost as problematic as the problem it solves. A favoured explanation is a 'cosmological constant' with a small positive value that arises from a non-zero energy density of the cosmic vacuum. But when particle theory is used to tot up the energy of the quantum vacuum, the answer greatly exceeds the size of cosmological constant required to explain acceleration. So might dark energy instead be some kind of anti-gravity field — a 'quintessence'? But even less is known of the essence of quintessence than of the cosmological constant. Given this situation, a quite different explanation for the acceleration observations — one that does not invoke any new physics — would be welcome. A clutch of recent papers[1–8] rehearses and refines one such idea: that the observed cosmic acceleration might be caused by an inhomogeneous Universe.

The fundamental dynamics of the Universe are embodied in Albert Einstein's general-relativistic field equations, which describe how gravity arises through the distortion of space-time by mass and energy. The simplest class of solution to those equations, that on which the concordance model is based, assumes that matter is distributed both homogeneously (everything is similar in all regions of space) and isotropically (everything looks the same in all directions). That assumption is consistent with observations, but it is not a direct consequence of them. It is the favoured solution both because it is the simplest and because it rests on a cherished cosmological assumption. This is the 'copernican principle': that the characteristics of the Universe in our neighbourhood are not special in any way, but are typical of the whole.

A cherished assumption this might be, but it is also fundamentally untested. It is consistent with the supernova observations, but only provided that some form of dark energy is present. The central plank of the new research is the claim that, by jettisoning the copernican principle and our assumptions about the distribution of matter in the Universe, we can also abandon the troublesome chimaera of dark energy.

The first type of inhomogeneity considered is local inhomogeneity[1–5]. Local inhomogeneities in the Universe's matter distribution certainly exist — we live in one, a galaxy — but there is always an averaging scale implicit in the representation of any physical variable (Fig. 1), which might hide such inhomogeneities. The essential question[9] is in what way the dynamics of the Universe is altered when the bumpy local representation is averaged out to the homogeneous, isotropic global model assumed by standard cosmology. In a recent status review, Thomas Buchert shows[4] how averaging Einstein's equations on a small scale leads to a repulsive 'back-reaction' term in the equations representing the large-scale, smoothed-out Universe that mimics the effect of dark energy.

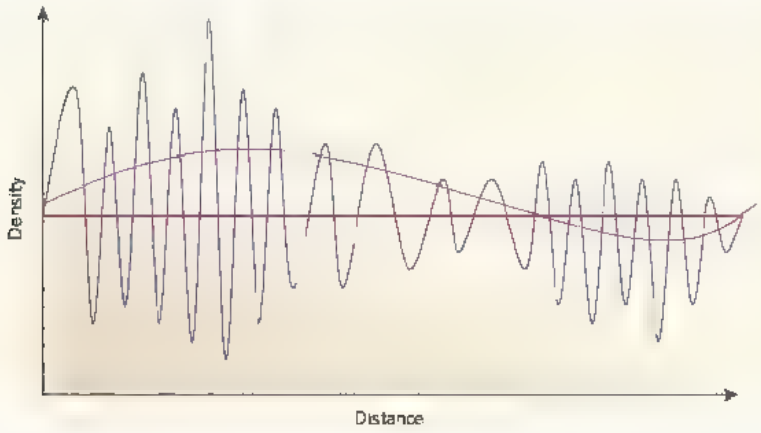


**Figure 1 | Averaging the Universe.** These three curves represent the same distribution of matter on three different averaging scales. The blue curve shows considerable detail, the pink one is averaged on a medium scale to show the overall inhomogeneity; and the red one is averaged on a very large scale to show the uniform cosmological average. The effective general relativistic field equations describing the behaviour of the Universe will be different at each of these scales; the essential question in assessing the role of inhomogeneities is how the averaging of the small-scale terms adds up to affect the dynamics of the large-scale averaged depiction.

But local inhomogeneities also affect cosmological observations of distant sources, which are sensitive to focusing effects on the emitted light caused by changes to the local gravitational field[9]. Averaged over all sources, the focusing of null geodesics — the paths followed through space-time by massless particles such as photons — agrees when a lumpy, small-scale model is averaged to attain a smooth, large-scale model. But for individual sources, a correction will be required depending on whether the light rays from the observed object traverse mainly voids or matter before reaching us. The observational effects of lumps should be determined using an averaging process based on the paths taken by light[11], rather than just by averaging over space. This might significantly change the apparent luminosity of distant objects, but the result will depend on the details of how matter is distributed — which is not well enough known to give a definite answer.

A new dimension to this discussion comes from David Wiltshire and others[2,3], and from Teppo Mattsson[4], who argue that in analysing the observations one should take into account the dominance of large-scale voids in the Universe and the way that local pockets of higher density are tied into the expanding Universe. By going back to the roots of general relativity, Wiltshire considers how measurements of space-time in a smoothed model and in a small-scale model that takes voids into account are related. It seems that our interpretation of observations is crucially affected by the differences between the two. The magnitude of the effect may be sufficient to significantly affect the acceleration that the supernova observations seemingly demand; indeed, some claim it can explain it away fully[3,4]. But this point of view is disputed[5], and needs to be evaluated carefully in light of a realistic view of the nature of local inhomogeneities in the real Universe.

An alternative to locally inhomogeneous models that might provide an explanation of the acceleration observations is large-scale inhomogeneity — a breakdown of the copernican assumption on the Hubble scale (the scale of the visible Universe)[6]. The observed acceleration and data from NASA's WMAP satellite, which is probing anisotropies in the cosmic microwave background (the radiation left over from the Big Bang), can be explained by assuming that we are near the centre of a Hubble-scale inhomogeneity of anomalously low density in a Universe that is spherically symmetrical[7]. Testing the existence of the requisite spatial inhomogeneity is difficult with observations of galaxies or other sources, because their evolution over time is unknown, but is in principle possible[12] using the anisotropies or the spectrum of the cosmic microwave background. But such tests are dependent on models of matter–radiation interactions.

Spatial homogeneity is one of the foundations of standard cosmology, so any chance to check those foundations observationally should be welcomed with open arms. Further tests are being proposed[13], but they depend on models of gravity or matter. A potentially substantial step forward is provided by Clarkson *et al.*[8]. They show that a simple observation of the copernican principle that is independent of any theory of gravity or model for dark energy is possible through redshift and area–distance observations of distant galaxies.

As the supernova observations are analysed further, a pivotal question is what physical properties are acceptable for any proposed dark-energy solution. Despite what some adventurous workers propose, we perhaps need to query any violation of energy conditions that implies the existence of negative kinetic energy terms, as indicated by some analyses[14]. It may be that such observations are trying to tell us that there is something fundamentally wrong in our assumptions; and that the acceleration

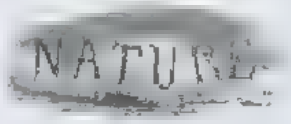


## 50 YEARS AGO

In these days when the output of scientific literature challenges the ability of the worker in even the most specialized fields to keep himself informed about current research, news of the publication of yet another scientific journal must sometimes be received with mixed feelings. This will not, however, prevent geologists from wishing success to the Geological Society of Egypt, which in 1957 published the first number of the *Egyptian Journal of Geology*, which is to be produced in the future twice-yearly

From *Nature* 15 March 1958.

## 100 YEARS AGO

*The Diseases of Animals*. By Nelson S. Mayo — This work, which purports to be one of popular advice on the care and common ailments of farm animals, is written entirely from the American point of view, and deals with American methods principally. In most distinctly American orthography it cannot be doubted that its usefulness to the British rural public not less than the pleasure of reading it, are considerably lessened thereby. It is decidedly irritating to readers on this side of the Atlantic to see such abominations as "sulfur," "esophagus," "sulfate," "mold," and others of a similar kind. There is, nevertheless, a good deal of useful and practical information on the care of animals and farm stock which the farmer would do well to know, no matter in what part of the world he carries on his occupation ... So far as this country is concerned, there is still room for a good up-to-date popular scientific work which will give the farmer such simple knowledge of the breeding, accidents, and diseases of his animals as will show him the occasion and the wisdom of consulting the skilled veterinarian.

From *Nature* 12 March 1908.

50 & 100 YEARS AGO

BioMark
GENETIC ANALYSIS BY FLUIDIGM

THE NEW STANDARD IN HIGH THROUGHPUT REAL TIME PCR

# You can learn from the past.

96-WELL MICROPLATES
- 24x more plates
- 48x more tips
- 125x more reagents
- 18x more time

# You can improve on it.

384 WELL MICROPLATES
- 6x more plates
- 12x more tips
- 50x more reagents
- 5x more time

# Or you can leave it behind.

**The BioMark 48.48 Dynamic Array**
- 1 simple, powerful, fast solution.

A single BioMark™ 48.48 Dynamic Array generates as much real-time PCR data as 24 96-well microplates. Surprisingly, this radically higher throughput requires 50-fold fewer pipetting steps and far less hands-on processing time. And you can switch to dynamic arrays and continue using the licensed PCR reagents already in your lab.

It's no wonder the BioMark system is emerging as the new standard for high-throughput gene expression profiling. Are you thinking about leaving the past behind? Contact Fluidigm to learn how the Biomark system can help your organization achieve a higher throughput future.

Heat Map View provides a macro-to-micro view of $C_t$ values within the entire array.

Fluidigm

Toll-free: 1.866.FLUIDLINE (866.358.4354) | Fax: 650.871.7152 | www.fluidigm.com

Sales: North America: 1 650.266 6170 | biomark@fluidigm.com
Europe/EMEA: +31 20 578 8853 | biomarkeurope@fluidigm.com
Asia: +81 3 3555 2351 biomarkasia@fluidigm.com

conundrum could have a geometric, rather than a dynamic, solution. ■

George Ellis is in the Department of Mathematics and Applied Mathematics, University of Cape Town, Rondebosch 7701, South Africa
e-mail george.ellis@uct.ac.za

1. Buchert, T. *Gen. Rel. Grav.* **40**, 467–527 (2008)
2. Whitshire, D. L. *New J. Phys.* **9**, 377 (2007)
3. Leith, B. M., Ng, S. C. C. & Whitshire, D. L. *Astrophys. J.* **672**, L91–L94 (2008)
4. Mattsson, T. preprint at http://arxiv.org/abs/0711.4264 (2007)
5. Rasanen, S. preprint at http://arxiv.org/abs/0801.2692 (2008)
6. Célérier, M.-N. preprint at http://arxiv.org/abs/astro-ph/0702416 (2007)
7. Alexander, S., Biswas, T., Notari, A. & Vaid, D. preprint at http://arxiv.org/abs/0712.0370 (2007)
8. Clarkson, C., Bassett, B. A. & Lu, T. H.-C. preprint at http://arxiv.org/abs/0712.3457 (2007)
9. Ellis, G. F. R. in *General Relativity and Gravitation* (eds Bertotti, B., de Felice, F. & Pascolini, A.) 215–288 (Reidel, Dordrecht, 1984).
10. Bertotti, B. *Proc. R. Soc. Lond. A* **294**, 195–207 (1966)
11. Marra, V., Kolb, E. W. & Matarrese, S. *Phys. Rev. D* **77**, 023003 (2008)
12. Goodman, J. *Phys. Rev. D* **52**, 1821–1827 (1995)
13. Uzan, J.-P., Clarkson, C. & Ellis, G. F. R. preprint at http://arxiv.org/abs/0801.0068 (2008)
14. Lima, M. P., Vitenti, S. & Reboucas, M. J. preprint at http://arxiv.org/abs/0802.0706 (2008)

PHYSICAL CHEMISTRY

# Did life grind to a start?

J. Michael McBride and John C. Tully

**Many solids can adopt two mirror-image crystal forms, and often grow as mixtures of both. A curious mechanism of crystal growth might explain why some mixtures convert into one form when subjected to grinding.**

If Alice had been a biochemist, she would have found an even more unfamiliar world on the far side of the looking-glass. In principle, the molecules of life can adopt two mirror-image forms (often described as left- and right-handed), which from a chemical perspective are equally likely to exist. Yet all biological molecules on Earth adopt a single handedness, even though their reflections in Alice's looking-glass world should function just as well (Fig. 1). Did the machinery of early life impose the observed bias, or was the development of life favoured by a pre-existing pool of single-handed molecules? And if the latter is true, how could this pool have formed?

One explanation could be that a fundamental physical bias exists that generates an excess of a particular molecular handedness. Proposed theories invoke the weak nuclear force, or the action of 'circularly' polarized light somewhere in the Universe. But these influences would be far too weak to explain the existence of a single molecular form. So, if a pool of single-handed molecules existed on prebiotic Earth, it must have developed from a mixture containing almost equal numbers of mirror-image forms where the excess of the major form was amplified dramatically. Reporting in the *Journal of the American Chemical Society*[1], and at a meeting at the Nordic Institute for Theoretical Physics in Stockholm[2], Noorduin *et al.* describe a remarkably simple system for the spontaneous amplification of molecular handedness — stirring a slurry of crystals in the presence of glass beads.

More than 50 years ago, the theoretical physicist Charles Frank addressed the existence of single-handed biomolecules in what became a much-cited paper[3]. He commented: "I have long supposed that this was no problem on the basis of a supposition that the initial production of life is a rare event." He went on to prove mathematically that, in a system containing entities that both copy themselves and destroy their mirror images, an initial random event that provides a tiny excess of one hand would necessarily lead to the exclusive occurrence of that form, even if mirror-image versions could also form randomly. He concluded: "A laboratory demonstration may not be impossible." This seminal paper was Frank's sole contribution to biology — he is better known for his insights concerning the mechanisms of crystal growth. He might have been gratified to learn that his own field is supplying increasingly convincing laboratory demonstrations to support his biological model.

The first such demonstration came in 1990 with the report[4] that a highly concentrated solution of sodium chlorate (whose dissolved molecules have no handedness) deposits crystals of a single mirror-image form on cooling, if stirred. This phenomenon was soon understood to involve the random formation of a single crystal of arbitrary handedness, from which seed crystals of the same handedness were broken off by the stirrer[5,6]. A feature of this 'secondary nucleation' mechanism is that only crystals larger than a certain critical size will grow; smaller crystals dissolve, because a higher proportion of their molecules occupy unstable positions at the crystal surface. The critical size is inversely related to the concentration of the solution. Because the initial fortuitous growth of crystals of one handedness reduces the concentration of the surrounding solution, the formation of mirror-image crystals that are large enough to grow becomes impossible.

THE ART ARCHIVE

**Figure 1 | Molecules through the looking-glass.** The molecules of life in Alice's looking-glass world would be mirror images of those in ours, and should work just as well. So why don't they exist?

To obtain single-handed crystals of sodium chlorate by secondary nucleation, a single seed crystal is required, and the solution must begin in a so-called supersaturated state, which is far from equilibrium. But in 2005, it was discovered that single-handed crystals of sodium chlorate could be obtained from a slurry of mixed mirror-image crystals in a saturated solution[7] (a system near to equilibrium). If there was an excess of one crystal form in the solid material, simply stirring the slurry resulted in complete conversion of the crystals to the dominant form, even if the initial excess was only a few per cent. The secret of this success was to add glass beads, which continually grind the crystals during stirring. As the starting conditions in this system are so different from those required for secondary nucleation, the mechanism must be different.

Noorduin *et al.*' now show that the grinding method works for a different compound — an amino-acid derivative. This may not seem like big news, but there is a crucial distinction from the previous work. Unlike sodium chlorate, the amino-acid derivative

retains its handedness in solution, although the mirror-image molecules do interconvert slowly when the solution is basic. For this reason, a base was required, as well as glass beads, to obtain single-handed crystals in the new system. But for the conversion to work, a seemingly unlikely condition must prevail: the concentration of the dissolved molecules from the minor population of crystals must be higher than that of the dissolved molecules from the major population of crystals.

The mechanism underlying this remarkable behaviour is unknown. Noorduin *et al.*[1] propose that 'Ostwald ripening' — the growth of large crystals at the expense of smaller ones — might be a crucial factor. Alternatively, a theory[8] proposed to explain the conversion of sodium chlorate crystals to a single-handed form might also apply here. This theory concerns tiny crystal fragments chipped from the larger, growing crystals — fragments that are small enough to be subcritical (and thus expected to dissolve), but large enough to retain their handedness. Chipping off such fragments artificially accelerates the dissolution of the larger crystals. But the acceleration is reduced if the fragments are rescued from dissolving by merging with larger crystals of the same hand.

If this explanation is correct, then subcritical fragments that can be incorporated into the dominant population of crystals have more chance of being saved from dissolving than their mirror images (for which fewer rescuing crystals exist). For the dominant crystals, this selective reincorporation is particularly effective at reducing the portion of their dissolution that is induced by grinding. Abrasion therefore speeds up the net dissolution of the minor population of crystals; once dissolved, their molecules convert into their mirror-image form, thereby feeding the growth of the major population of crystals. This process also satisfies the curious requirement for the concentration of molecules dissolved from the smaller component of the solid to be greater than that of molecules from the larger component.

Crystals from the smaller population eventually convert completely into the same form as the larger population, in a process that actually accelerates as the conversion proceeds (unlike most spontaneous transformations). The conversion is entropically unfavourable, but grinding supplies the energy needed to overcome this obstacle.

Were Frank alive today, he would be delighted by these observations, because the crystallization fits his model for amplification of a single-handed entity: the major crystals catalyse their own production by capturing fragments destined for dissolution; and they catalyse the destruction of their mirror image by capturing more molecules from solution than they contribute to it.

It is impossible to say whether grinding of crystals in a prebiotic world, perhaps by wave-tossed sand, might have supplied single-handed molecules to support early life. Nevertheless, Noorduin and colleagues[1] might have provided dramatic evidence to support the idea that substantial clusters of molecules can be incorporated intact into existing crystals. Their report suggests new opportunities for manufacturers of pigments or pharmaceuticals who must prepare solids in only one of several possible crystal forms. Furthermore, grinding is arguably the first original method for isolating single-handed crystals from a mixture of mirror-image forms since Pasteur used tweezers to effect such a separation in 1848. ■

J. Michael McBride and John C. Tully are in the Department of Chemistry, Yale University, Box 208107, New Haven, Connecticut 06520, USA.
e-mails: j.mcbride@yale.edu, john.tully@yale.edu

1. Noorduin, W. L. *et al. J. Am. Chem. Soc.* **130**, 1158–1159 (2008)
2. http://nordita.org/programs/homochirality
3. Frank, F. C. *Biochim. Biophys. Acta* **11**, 459–463 (1953)
4. Kondepudi, D. K., Kaufman, R. J. & Singh, N. *Science* **250**, 975–976 (1990)
5. McBride, J. M. & Carter, R. L. *Angew. Chem. Int. Edn* **30**, 293–295 (1991)
6. Holden, A. & Singer, P. *Crystals and Crystal Growing* 291 (Anchor/Doubleday, Garden City, NY, 1960)
7. Viedma, C. *Phys. Rev. Lett.* **94**, 065504 (2005)
8. Uwaha, M. J. *Phys. Soc. Jpn* **73**, 2601–2603 (2004)

NITROGEN CYCLE

# Out of reach

Sybil Seitzinger

**Denitrifying bacteria and hungry plants do sterling work in disposing of the nitrates that we pump into rivers and streams. But as the excess influx goes up and up, the efficiency of removal goes down and down.**

Thanks to human contributions — from fossil fuel combustion, the growth of agricultural crops, and above all the fertilizers that help to keep the more than six billion humans worldwide in food[1] — nitrogen is entering Earth's soils at more than twice its natural rate. Much of the nitrogen from these sources goes on to enter streams, primarily as nitrates, and is transported downriver to coastal marine systems. There, it fuels excessive rates of plant growth and decay in the process known as eutrophication. This can result in hypoxia (shortage of oxygen) or, in extreme cases, anoxia (total loss of oxygen), creating the 'dead zones' seen in places such as Chesapeake Bay, the Gulf of Mexico and the Baltic Sea.

"As we use land ever more intensively, the pressure on policy-makers to limit anthropogenic nitrogen entering rivers will grow."

Fortunately, as Mulholland and colleagues detail on page 202 of this issue[2], not all the extra nitrates that we pile into streams make it to coastal systems; instead, some is removed and retained by biological processes. In the short term, aquatic plants and microbes take up and store nitrogen as a nutrient. But by far the greatest part in long-term nitrogen removal is played by the denitrifying bacteria that live in anoxic sediments in a stream's bed and banks. These microbes transform the nitrogen in nitrates to gaseous forms such as molecular nitrogen ($N_2$) and nitrous oxide ($N_2O$), which diffuse out of river water into the air. Such denitrification is not without environmental consequences: whereas $N_2$ is harmless (and makes up almost 80% of the atmosphere), $N_2O$, although only a small portion of the total gaseous nitrogen produced, is a potent greenhouse gas that has also been implicated in stratospheric ozone destruction.

Because many different methods have been used to measure rates of denitrification, comparison of the many measurements that have been made is difficult. In addition, the physical and chemical characteristics of rivers that might affect nitrogen removal are extremely diverse, depending in part on the type and extent of human disturbance in the surrounding landscape. Developing predictive, widely applicable relationships linking river and watershed characteristics to nitrogen removal and retention rates is quite a challenge[3].

Mulholland *et al.*[2] attacked these shortcomings with a study of unparalleled scale. They used a consistent method to quantify the fate of nitrate ($NO_3^-$) in 72 small streams in pristine, urban and agricultural watersheds throughout the United States and Puerto Rico, adding trace amounts of nitrates labelled with the nitrogen isotope $^{15}N$ to stream waters over periods of around 24 hours during spring or summer. The stable (non-radioactive) isotope $^{15}N$ is rare in nature, occurring at less than 0.4% of the abundance of $^{14}N$. Using mass spectrometry, it was relatively easy to detect small decreases in $^{15}NO_3^-$, and increases in $^{15}N_2$ and $^{15}N_2O$ from denitrification. Decreases in labelled nitrates not accounted for by an increase in labelled $N_2$ and $N_2O$ were attributed to uptake by plants and microbes within each stream segment, or reach. This approach maintained existing conditions in the stream, and not only permitted

the authors to distinguish denitrification from the temporary storage of nitrogen in biomass, but also allowed the rates of denitrification and biotic uptake to be assessed for the entire reach.

The authors found that measurable rates of nitrate removal occurred through biotic uptake and denitrification in most streams, and that absolute rates of removal generally increased as nitrate concentrations increased. But the efficiency of nitrate removal — the proportion of nitrate removed relative to the total amount present — decreased exponentially as nitrate concentrations increased. This pattern held across nitrate concentrations that differed by six orders of magnitude in eight different biomes. As we use land ever more intensively, the effectiveness of the receiving streams in removing the additional nitrate pollution is likely to continue to diminish. Thus, looking at the results of this study, the pressure on policy-makers to reduce the load of anthropogenic nitrogen entering rivers from terrestrial systems will grow.

Of course, small streams are only one component of the filigree of flowing waters that drain a landscape. Small streams connect to middling channels, which connect to larger rivers, all of which propel water and its dissolved and particulate constituents towards coastal systems. The length of all the channels in a river system is often extensive — those within the 30,000 $km^2$ watershed of the Potomac River in the eastern United States amount to a length of some 25,000 km, equivalent to about five times the distance across the United States from coast to coast. Unsurprisingly, therefore, there are ample opportunities for nitrates to be removed on their journey from a river's headwaters to the coast that are not covered by Mulholland and colleagues' study.

To address this point, the researchers use a model to scale up their results to an entire river network. The outcome underscores the importance of river channels of all sizes, as well as the distribution of nitrate loading within the river network, in controlling the amount of nitrates reaching coastal waters. Nitrates not removed within a particular stream reach may be removed in the next, and so on down to the coast; but the relative importance of small, medium and large channels depends in part on where the nitrate concentration in a particular stream reach is on the curve of nitrate removal efficiency. A small stream might remove most of the nitrates quite effectively if the concentration is low, but if the local nitrate concentration increases such that nitrate removal efficiency decreases, the capacity of downstream reaches to remove excess nitrates becomes relatively more important. And if the nitrate concentration throughout a river network continues to increase, the network's overall capacity to remove nitrates decreases. The importance of nitrogen removal across all channel sizes in a river network underlines the need for comprehensive studies such as that of Mulholland *et al.*[2] across a range of stream sizes and throughout the annual cycle.

Denitrification occurs not only in rivers, but in almost all environments at some time and place: nearly 80% of all reactive nitrogen is disposed of before it reaches coastal waters. Soils are generally the first receptor of the large amounts of nitrogen that we add to terrestrial systems, and the amount of denitrification in soils can substantially exceed that removed in the stream network[4]. Groundwater, lakes and coastal systems are also important sites of denitrification. For all these environments we urgently need advances in methods and models[5] that will increase our understanding of how large amounts of nitrogen move and are removed as they journey from soils to the sea. ■

Sybil Seitzinger is at the Institute of Marine and Coastal Sciences, Rutgers, The State University of New Jersey, Rutgers/NOAA CMER Program, 71 Dudley Road, New Brunswick, New Jersey 08901-8521, USA.
e-mail: sybil@marine.rutgers.edu

1. Galloway, J. N. *et al. Biogeochemistry* **70**, 153–226 (2004).
2. Mulholland, P. J. *et al. Nature* **452**, 202–205 (2008).
3. Alexander, R. B., Smith, R. A. & Schwarz, G. E. *Nature* **403**, 758–761 (2000).
4. Seitzinger, S. *et al. Ecol. Appl.* **16**, 2064–2090 (2006).
5. Groffman, P. M. *et al. Ecol. Appl.* **16**, 2091–2122 (2006).

BIOCHEMISTRY

# Radicals by reduction

Joseph T. Jarrett

**Many enzymes convert their substrates into organic radicals to allow challenging reactions to occur. A microbial enzyme does so by simple electron transfer, casting fresh light on enzyme evolution.**

The harmful effects of free radicals have been widely publicized over the past two decades. As a result, pharmacists are now well stocked with vitamins and nutritional supplements purported to combat the damage caused by these chemical bogeymen. Less attention has been given to the many beneficial uses of radicals in biology, where they are often generated by enzymes to overcome chemically difficult problems. On page 239, Kim *et al.*[1] report a remarkable example of this in certain anaerobic bacteria found in the human gut. These bacteria generate energy by breaking down the amino acid leucine; this is a particularly tough chemical process in the absence of oxygen. The authors show that a key enzyme for this process overcomes the reaction barriers by sequentially converting leucine into two different radicals. This previously unknown mechanism might also be used by many other enzymes.

Most stable covalent molecules, with rare exceptions, require electrons with opposite spin to be paired within each atomic and molecular orbital. But in an organic radical, one electron remains unpaired — an unstable configuration that is highly reactive. When radicals are generated within an organism and allowed to roam free, they can react rapidly with DNA, proteins and lipids, causing chemical modifications collectively known as oxidative damage. In contrast, when organic radicals are generated within an enzyme active site, their reactivity can be harnessed to promote a variety of essential biochemical transformations.

The role of organic radicals in several enzyme-catalysed reactions has been recognized only relatively recently[2]. The first suggestion that enzymes might use transient radicals as intermediates came with the discovery of vitamin $B_{12}$. The active cofactor form of this vitamin contains a weak carbon–cobalt bond that is broken to generate a carbon radical[3]; this radical transiently oxidizes other molecules by removing a hydrogen atom, a process that can often promote difficult chemical reactions (Fig. 1a, overleaf).

Around the same time as the discovery of vitamin $B_{12}$, organic radicals were shown to be essential for the activity of ribonucleotide reductase, an enzyme that controls the cellular concentrations of deoxyribonucleotides (the building-blocks of DNA)[4]. The active form of ribonucleotide reductase has a radical on the side chain of a tyrosine amino acid (Fig. 1b). This radical forms when the tyrosine side chain is oxidized, in a process that requires oxygen and two iron ions (which make the oxygen more reactive and provide a source of electrons for the reaction). Perhaps surprisingly, given that radicals usually have a fleeting existence, the tyrosyl radical is so stable that it can be observed for days.

Many more enzymes are now known to exploit radical reactions using vitamin $B_{12}$, *S*-adenosylmethionine (a common coenzyme) or various metal cofactors to turn organic compounds into radicals, usually by removing a hydrogen atom directly from the substrate. Organic radicals have thus gained acceptance as plausible reaction intermediates for biochemical reactions, with both direct and indirect evidence from dozens of enzymatic processes supporting this idea. Many of these enzymes are found in anaerobic bacteria, where they take part in the catabolic pathways

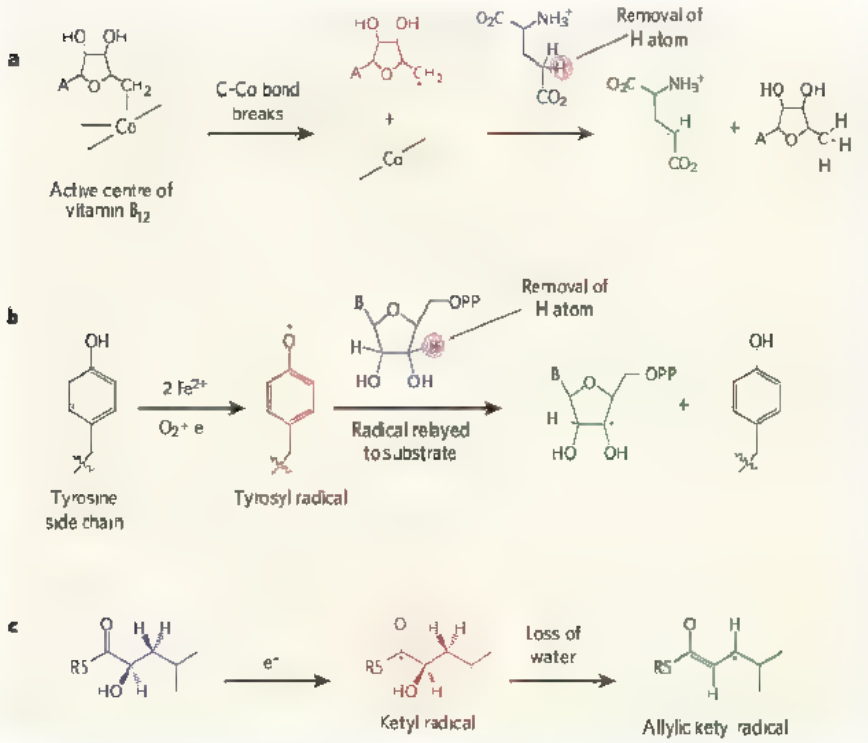


**Figure 1 | Enzymatic conversion of organic molecules into radicals.** Enzyme mechanisms that involve radicals are relatively rare. **a**, Some enzymes require vitamin $B_{12}$ as a cofactor. Vitamin $B_{12}$ contains a weak carbon–cobalt bond that breaks apart to form an organic radical (red). This in turn converts the enzyme substrate (blue) into a radical (green) by removing a hydrogen atom, as in this example. Co represents a cobalt atom; A is the DNA base adenine. **b**, In the enzyme ribonucleotide reductase, the side chain of a tyrosine amino acid is converted into a tyrosyl radical (red) in a reaction involving oxygen and electrons (e⁻) from two iron ions ($Fe^{2+}$). The radical is relayed to the substrate, which is oxidized to another radical (green) by the removal of a hydrogen atom. B represents an RNA base, OPP is a diphosphate group. **c**, Kim *et al.*[1] report a previously undiscovered radical mechanism in the enzyme 2-hydroxyisocaproyl-CoA dehydratase. The enzyme adds an electron directly to the substrate (blue) in a reduction process, forming a ketyl radical (red). The ketyl radical then loses hydrogen and oxygen atoms as a water molecule, forming an allylic ketyl radical (green). This is the first example of a radical enzyme mechanism in which the substrate is reduced, rather than oxidized. R represents coenzyme A, a common cofactor.

used by the organisms to generate energy.

One such bacterium is *Clostridium difficile*, which lives in the human gut. This bacterium fuels its growth by breaking down leucine using the Stickland reaction, in which amino acids are both oxidized and reduced in parallel biochemical pathways. But the reduction of leucine is difficult: the pathway gets stuck halfway through, because an intermediate (a 2-hydroxyacid) forms that cannot be reduced further until it eliminates a water molecule. Most enzymes use biological acids and bases as catalysts to bring about water-elimination reactions (known as dehydration reactions), but 2-hydroxyacids are impervious to such treatment — they hold onto their hydrogen atoms too strongly for biological bases to remove them in dehydration reactions. So how does the 2-hydroxyacid dehydratase enzyme in anaerobic bacteria overcome this chemical bottleneck?

One hypothesis is that the enzyme uses a principle known as reactivity 'umpolung', in which the electrostatic charge of a chemical group is reversed[2]. 2-Hydroxyacids contain a carbonyl group, in which a carbon atom forms a double bond to an oxygen atom. The C–O bond is polarized, so that the carbon atom harbours a small amount of positive charge. But if the carbonyl group is first coupled to coenzyme (a common metabolic cofactor), it can then be reduced by accepting a single electron, generating a ketyl radical in which the carbon atom has partial negative charge. This charge inversion makes the other atoms near the ketyl radical much more reactive towards acids and bases, and the molecule can easily undergo dehydration to form a second intermediate known as an allylic ketyl radical (Fig. 1c).

To investigate this theory, Kim *et al.*[1] used a technique known as electron paramagnetic resonance (EPR) spectroscopy to directly observe the formation of an allylic ketyl radical in the dehydratase reaction. EPR spectroscopy uses a strong magnet and microwaves to detect the spin of unpaired electrons. With this technique, the authors were able to pinpoint the location of the unpaired electron in the radical, confirming conclusively that an allylic radical had formed. Furthermore, they identified exactly which hydrogen atoms are eliminated from the substrate during dehydration. This is crucial information, because different atoms are predicted to be eliminated depending on the reaction mechanism. The pattern of elimination observed by Kim *et al.* supports the proposed radical mechanism. The authors also performed kinetic experiments to prove that the allylic radical forms rapidly enough to be part of the catalytic mechanism.

Kim and colleagues' results[1] provide exciting confirmation of the proposed radical mechanism, suggesting that many other enzymes could also work in this way. The mechanism is noteworthy because the dehydratase enzyme generates radicals by transferring electrons to the substrate, whereas most enzymes that are known to generate radicals do so by removing a hydrogen atom from the substrate. Only one other well-characterized enzyme is known to generate radicals by electron transfer — pyruvate ferredoxin oxidoreductase[6], a bacterial enzyme involved in energy production from simple sugars. In this case, the organic radical forms within a specialized cofactor derived from the vitamin thiamine. But 2-hydroxyacid dehydratases are the first enzymes shown to generate a substrate radical by reduction (rather than oxidation), and in which the radical is quenched at the end of the reaction by oxidation (not reduction).

The source of electrons for the *C. difficile* dehydratase reaction is a cluster of iron and sulphur atoms. This will ring bells for biochemists, because many other dehydratases also use iron–sulphur clusters, not as sources of single electrons but as Lewis acids (acceptors of electron pairs) that promote the elimination of water from substrates. Such dehydratases have a central role in sugar and amino-acid catabolism in almost all known organisms, including those that breathe air.

The choice of an air-sensitive iron–sulphur cluster is therefore curious: many other metal ions that aren't air sensitive could be used as Lewis-acid catalysts instead. The anaerobic degradation of amino acids by a redox active iron–sulphur cluster, as seen in *C. difficile*, is probably a primitive reaction that predated the evolution of oxygen-breathing organisms. When the enzymes in anaerobic organisms evolved into their modern counterparts, the air-sensitive iron-sulphur clusters may simply have been co-opted for a different enzyme mechanism, despite their practical drawbacks in an oxygen-rich world.

Time will tell whether this newly discovered radical mechanism is widely used by other enzymes. But Kim *et al.* have shown that, even in the relatively mature field of enzymology, there is still much to learn. ■

Joseph T. Jarrett is in the Department of Chemistry, University of Hawai'i at Manoa, 2545 McCarthy Mall, Honolulu, Hawai'i 96822, USA.
e-mail: jtj@hawaii.edu

1. Kim, J., Darley, D. J., Buckel, W. & Pierik, A. J. *Nature* **452**, 239–242 (2008)
2. Stubbe, J. & van der Donk, W. A. *Chem. Rev.* **98**, 705–762 (1998)
3. Babior, B. M. *Acc. Chem. Res.* **8**, 376–384 (1975)
4. Ehrenberg, A. & Reichard, P. *J. Biol. Chem.* **247**, 3485–3488 (1972)
5. Buckel, W. & Keese, R. *Angew. Chem. Int. Edn Engl.* **34**, 1502–1506 (1995)
6. Ragsdale, S. W. *Chem. Rev.* **103**, 2333–2346 (2003)

Q&A

EARTH SCIENCE

# Geomagnetic reversals

David Gubbins

**Earth's magnetic field is unstable. Not only does it vary in intensity, but from time to time it flips, with the poles reversing sign. Much of this behaviour remains a mystery, but a combination of geomagnetic observations with theoretical studies has been providing enlightenment.**

### Has Earth always had a magnetic field?

Yes — or at least for a very long time. There are magnetized rocks of all geological ages, going back some 3 billion years. It also seems that the field has always been dipolar, with a north and a south pole (Fig. 1), except during reversal of the poles.

### How is the field generated?

It is continually maintained by a dynamo acting in the liquid-iron outer core. It works in the same way as a car alternator. The liquid iron moves at speeds of about one millimetre per second, and when it cuts magnetic field lines it generates a voltage that reinforces the original magnetic field. The fluid motion is driven by buoyancy forces arising from density gradients caused by slow cooling of the whole Earth. The core solidifies from the centre outwards, with the lighter elements in the liquid separating and rising to help thermal currents drive convection. The solid inner core has grown to its present size over the past billion years or so. Earth's rotation affects the style of fluid motion, for example by aligning structures along the spin axis, but does not actually drive it.

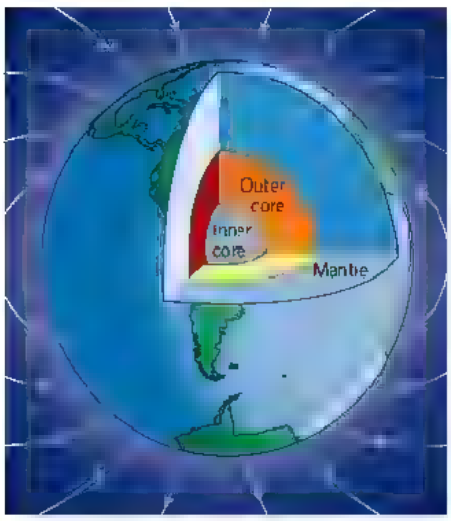


**Figure 1 | Earth's magnetic field.** The field looks like that of a bar magnet aligned with Earth's geographical axis, a so-called dipole structure. The non-dipole part of the field is significant, however, and accounts for why the compass rarely points exactly to true north. The field is generated in Earth's liquid outer core, some 3,000 kilometres below us; the rocky solid mantle is a fairly good electrical insulator and most of it is too hot to be magnetized, so it does not affect the field much.

### What forms does the field take?

At Earth's surface the magnetic field closely resembles that of a bar magnet placed at Earth's centre and aligned approximately with the geographical axis. The geomagnetic poles are where the axis of this hypothetical bar magnet cuts Earth's surface (at present, the north magnetic pole is in the Canadian Arctic). When a measurement is available only from a single site, as is usually the case with palaeomagnetic data, a virtual geomagnetic pole (VGP) is determined by assuming a dipole form. The VGP can be a good approximation to the geomagnetic pole if the non-dipole field is small, but not during a polarity reversal. When surface observations are projected down to the core surface a more complicated structure appears (Fig. 2): the field still has the same average dipole structure and the geomagnetic poles are in the same place, but the non-dipole parts are now so strong that there are many places where the magnetic field is vertical ('dip poles'). The vertical field is strongest, not at the geomagnetic poles, but in two areas some 20° away from the geographical pole, the deep blue patches in Figure 2.

### How do we know that Earth's polarity has flipped?

Rocks are magnetized and retain the direction of the magnetic field at the time of their formation. A good lava-flow sequence or sediment column can preserve the record of many reversals over a long period of time. There is also the evidence from magnetic stripes on the ocean floor

### How were these magnetic stripes produced?

Oceanic crust forms at ridges where two tectonic plates move apart. As the crust forms, it becomes magnetized by the magnetic field, leaving linear segments of new crust on each side of the ridge. When the magnetic field reverses, the new strip of crust is formed magnetized in the opposite direction, and this can be detected by a magnetometer towed behind a ship. When the magnetic anomalies are plotted they form a pattern of stripes; the rocks in any one stripe have the same mean age, which is how we know the age of the ocean floors so

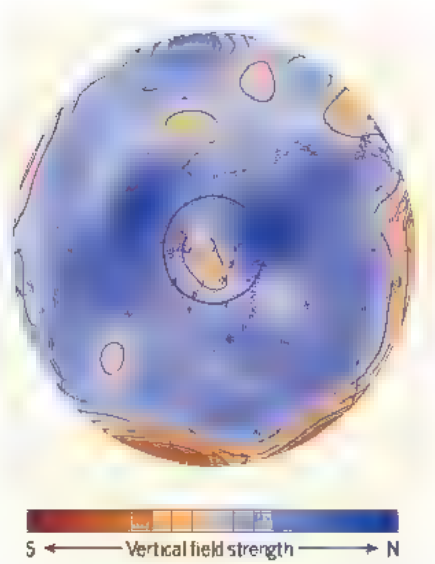


**Figure 2 Magnetic field at the surface of Earth's core.** Only the Northern Hemisphere is shown in this projection of the surface of the outer core. The central circle denotes the position of the solid inner core. The magnetic field is stronger at this depth, 3,000 km below the surface, and the non-dipole part is more evident. Most surprisingly, the magnetic field is strongest (deepest blue) not over the North Pole, as one would expect from a dipole field, but in two blobs outside the central circle. The field within the circle is nearly zero (blue/orange boundary). This is the effect of the tangent cylinder, an imaginary cylinder around the inner core aligned with the geographical axis, that creates different dynamics in the polar regions. Mapping the field at the core surface was made possible by satellite data, and the discovery of a weak field over the poles marked the first real connection between observation and the dynamo theory.

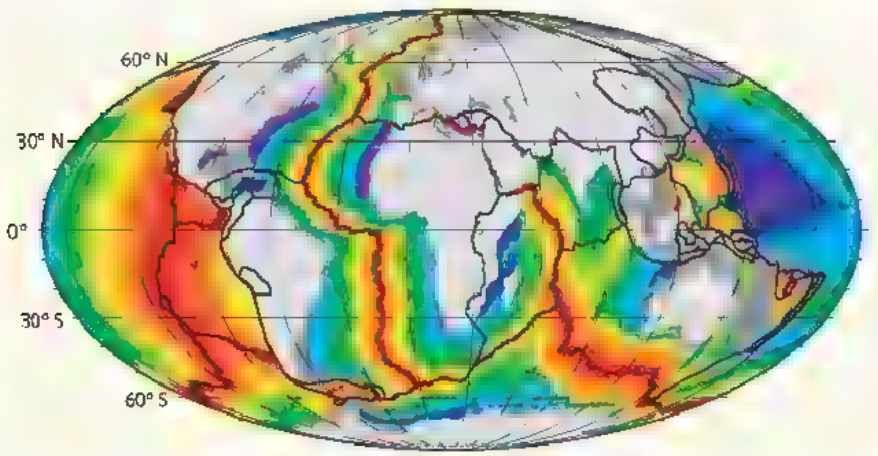


**Figure 3 | Magnetic stripes on the ocean floor.** The identification of these stripes meant that the corresponding rocks on the ocean floor could be dated rather precisely against the reversal timescale (see Fig. 4). The youngest floor (red) is close to the mid-ocean ridges where oceanic crust is formed, and the oldest (blue) is at the Atlantic coast and in the southwest Pacific. (Courtesy of R. D. Müller See R. D. Müller *et al. Geochem. Geophys. Geosyst.* doi.10.1029/2007GC001743; 2008.)

well (Fig. 3). There are no stripes in the older parts of the Pacific Ocean, or at the edges of the Atlantic, because this crust was extruded at a time when there were no reversals.

### Why does the magnetic field reverse?

Because it can: the forces involved and magnetic induction are the same regardless of the sign of the magnetic field. As the magnetic field varies all the time, it is a matter of chance whether a fall in the field ends up with it regrowing with the same or the opposite polarity. This suggests that a reversal is not just a flipping of the poles: on average, even the non-dipole parts must reverse.

### And how does it reverse?

The basic dipole is not preserved during the reversal. Many observations suggest that the VGPs move around the rim of the Pacific, following one of two preferred longitudes, depending on the measurement site. If correct, this would imply that a magnetic field remains concentrated around the Pacific rim during the reversal (see below).

### How long does the reversal take?

The magnetic field becomes progressively weaker, typically for several thousand years, before the direction changes, usually in a much shorter time. The reversed field then grows in strength over another few thousand years.

### How frequent are reversals?

Recently (in geological terms), once every 300,000 years, on average (Fig. 4). The last time was 780,000 years ago, however, so we are somewhat overdue for another one. Since then, the polarity has started to change but flipped back straight away, in what is called an excursion, or aborted reversal. The field has done this at least ten times since the last full reversal.

### Is there any pattern to the reversal timescale?

Much work has been done on the statistics of this timescale, with no convincing conclusion other than that it is random.

### Has the magnetic field always reversed irregularly like this?

No, there are very long intervals of time, called superchrons, when there were no reversals. The last one, the Cretaceous normal superchron, was from about 124 million to 80 million years ago. There was probably an earlier one, the Kiaman, around 300 million years ago, which is much less well documented because there is no ocean floor of that age.

### Why did reversals stop during superchrons?

Everyone is agreed that the timescale is too long for superchrons to be the consequence of a natural core process — the outer core turns over every 1,000 years and it is very unlikely to have changed of its own accord in the past 100 million years. It is probably an effect of the changing solid mantle. The dynamo is driven by cooling from the top of the outer core, and this cooling is controlled by plate tectonics and mantle convection, so a change in the cooling regime could spark a change in the behaviour of the dynamo. Either some dramatic event occurred that changed the rate at which the core lost heat, with the assumption that a dynamo will reverse only if driven hard, or the pattern of cooling on the core surface altered to change the nature of the fluid flow. The second option is more appealing to me, if less dramatic, because it is an inevitable consequence of mantle evolution.

### Are the reversed and normal magnetic fields exactly the same?

Probably. This has been the subject of extensive studies of the data, and there are some claims of a difference. But it is most likely that the entire field reverses each time. Complete reversal is the only type allowed by theory; any normal–reversed differences are because the reversal is incomplete. How long complete reversal takes is again a subject of research, but theory suggests no longer than a few tens of thousands of years.

### Why do some reversals go through and others do not?

If the geomagnetic field is greatly disrupted it will grow again in either direction with equal probability. The field can reverse in the outer core by fluid motion moving the electric currents around, which takes only about 500 years. In the solid inner core things are different. In a solid the electric currents, and therefore the magnetic fields, can only change because of electrical resistance — a process that takes much longer, about 5,000 years, than induction by a moving conductor as in the liquid part of the core. The inner core may therefore impart some stability, or longer memory of the previous state. The field could remain reversed in the outer core for 5,000 years and still have a persistent normal direction in the inner core, encouraging the field to return to normal. This may be why there are many excursions between full reversals: nine times out of ten, the persistent inner-core field could

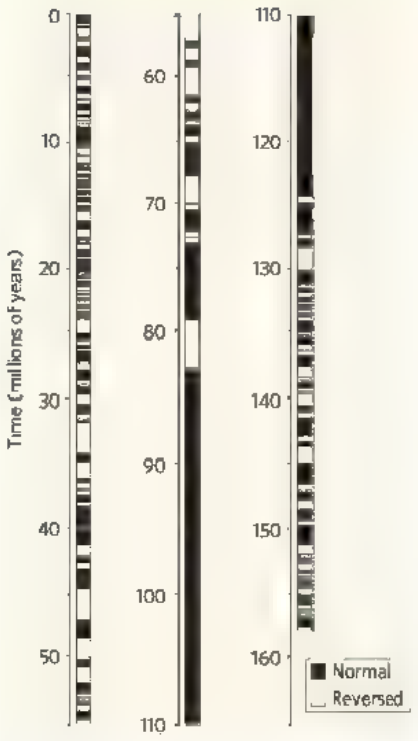


**Figure 4 | Reversal timescale.** Note the long black interval when the polarity was normal and there were no reversals, the so-called Cretaceous normal superchron (CNS). It may also be possible to discern an increase in the frequency of reversals since 80 million years ago, when the CNS ceased. (Revised from W. Lowrie *Fundamentals of Geophysics*; Cambridge Univ. Press, 1997.)

force the dynamo field back to its original polarity (Fig. 5).

### Is there a connection between reversal behaviour and plate tectonics?

Possibly. Cooling drives the dynamo, and mantle convection means the heat lost from the core will vary from place to place. In particular, it seems that persistent subduction of tectonic plates around the Pacific for the past 150 million years has cooled off the whole of the lower mantle in a ring beneath the rim of the Pacific, and far more heat is drawn from the core in this location than elsewhere. When we use seismological data to set a boundary condition in numerical simulations of the geodynamo, we get downwelling of fluid in the outer core and concentration of magnetic flux beneath the cold regions. The magnetic-field concentrations coincide with those of the present-day field, as shown in Figure 6. This concentration of magnetic field can also explain why in some reversals the poles tend to follow the Pacific rim.

### Are computer simulations of the dynamo informative?

Early attempts to understand the dynamo action of a liquid conductor were largely unsuccessful because only complicated fluid flows can produce the required regeneration of the magnetic field. It is now possible to model the magnetic-induction effects by supercomputer, but not the turbulence of flow in Earth's outer core nor Earth's rapid spin rate. Perhaps surprisingly, computer models using greatly simplified assumptions do reproduce aspects of the geomagnetic field such as the dipole, somewhat unrealistic reversals, and parts of the present non-dipole field (Fig. 6). Some theoreticians think the next generation of supercomputers will be powerful enough to answer some of the remaining questions.

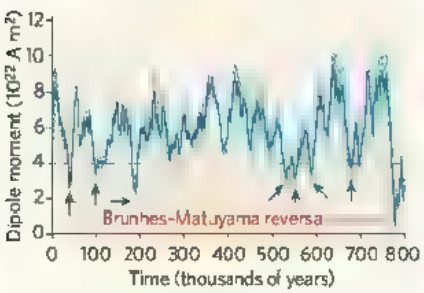


**Figure 5 | Excursions.** Compilation of records of magnetic intensity (dipole moment) for the past 800,000 years, the present value is about 8 on this scale. The last reversal, between the present Brunhes chron and previous reversed Matuyama chron, is marked by a dramatic low in intensity 780,000 years ago. Excursions, indicated with arrows and as measured by quite different data indicating the wayward direction of the magnetic field, occur when the field strength falls below about 4 (dotted line). These data showed, for the first time, the highly erratic behaviour of Earth's magnetic field even during times of stable polarity. (Redrawn from Y. Guyodo and J. P. Valet *Nature* 399, 249–252, 1999.)

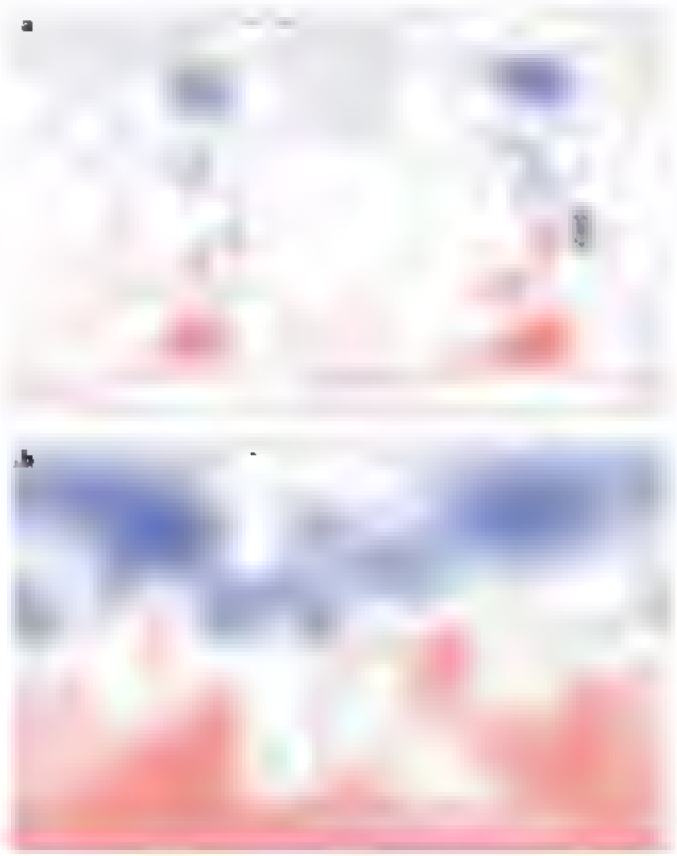


**Figure 6 | Computer models of Earth's dynamo.** **a**, The magnetic field generated by a dynamo model in which heat flow from the core surface matches that estimated from temperature in the solid mantle immediately above it. The four locations of strongest field lie very close to the corresponding locations in the modern Earth's magnetic field, shown in **b**. Cold mantle around the Pacific rim induces downwelling in the core, and this concentrates magnetic field lines. Generation is strongest around the tangent cylinder (Fig. 2), which explains the displacement of these lobes away from the geographical poles. (Reproduced from D. Gubbins *et al.*, 2007 see further reading.)

### And laboratory experiments?

There are ambitious attempts to study dynamo action in the lab using large containers of liquid metal — sodium, gallium and mercury have all been used. Experiments can reach higher spin rates than computers, but the problem is the great size required to produce a large enough induction to regenerate a magnetic field. the inductive effect depends on the product of the electrical conductivity, size and fluid flow speed. Reducing the size from the radius of Earth's core to lab scale means the fluid must flow fast to compensate. We are likely to learn a great deal about the nature of fluid flow and turbulence from experiments, but not so much about the dynamo action.

### Is it true that we're heading for another reversal?

It could be. The dipole has been weakening by about 5% per century since at least 1850, and archaeological artefacts show it to have been much stronger in Rome 2,000 years ago. The present fall is associated with activity in Earth's core beneath the South Atlantic and Indian oceans, where the field is reversing locally in a process similar to that in sunspots during the Sun's 11-year cycle of magnetic reversal. This could be the start of a reversal, but we have not yet reached the point of no return. If the dipole does fail, it is more likely to be an excursion than a full reversal, because many such dramatic falls have occurred in the past without a full reversal (Fig. 5).

### Should we be worried about a reversal?

A weaker magnetic field means more cosmic radiation reaching Earth's surface because of the lessened shielding effect of the magnetosphere — the local region of space dominated by the field. We can also expect more auroral activity. In the past, species that use the magnetic field for navigation have become extinct during reversals (but mostly single-cell organisms that presumably use the magnetic field to tell up from down). Increased atmospheric geomagnetic activity means more disruption to electronic communication and power distribution, but we know little about the way in which the magnetosphere would react to a different geomagnetic field. Whether a reversal would present a health risk to humans is less clear, even a weak field may have a shielding effect. The human race has survived many excursions and a few reversals already, so we are likely to come through the next one unscathed. ■

David Gubbins is in the School of Earth Sciences, University of Leeds, Leeds LS2 9JT, UK.
e-mail: gubbins@earth.leeds.ac.uk

FURTHER READING
Jacobs, J. A. *Reversals of the Earth's Magnetic Field* (Cambridge Univ. Press, 1994)
Merrill, R. T., McElhinny, M. W. & McFadden, P. L. *The Magnetic Field of the Earth* (Academic, New York, 1996)
Gubbins, D., Willis, A. P. & Sreenivasan, B. *Phys. Earth Planet. Inter.* **162**, 256–260 (2007).
Laj, C., Mazaud, A., Weeks, R., Fuller, M. & Herrero-Bervera, E. *Nature* **351**, 447 (1991).
Gurnis, M., Wysession, M. E., Knittle, E. & Buffett, B. A. (eds) *The Core–Mantle Boundary Region* (Am. Geophys. Un., Washington DC, 1998)

# nature podcast

Sponsored by

BIO-RAD

[illegible] www.nature.com/nature/podcast

Subscribe via iTunes http://tinyurl.com/2rszua

REVIEWS

# Genetic basis of fitness differences in natural populations

Hans Ellegren[1] & Ben C. Sheldon[2]

**Genomics profoundly influences current biology. One of many exciting consequences of this revolution is the potential for identifying and studying the genetic basis of those traits affecting fitness that are key to natural selection. Recent studies using a multitude of genomic approaches have established such genotype–phenotype relationships in natural populations, giving new insight into the genetic architecture of quantitative variation. In parallel, an emerging understanding of the quantitative genetics of fitness variation in the wild means that we are poised to see a synthesis of ecological and molecular approaches in evolutionary biology.**

The darwinian evolutionary process can be summarized into three components: struggle for existence, variation in characters that influence success in that struggle, and transmission of that variation from parents to offspring. Understanding the causes of variation among individuals in their contribution to future generations—variation in fitness—and the way in which that variation is inherited—its genetic basis—thus lies at the heart of our understanding of evolution. In this review we discuss the genetic architecture of fitness traits in wild populations and how new genomic approaches to non-model organisms can pinpoint the genetic 'locus' of evolution. We argue that we are approaching a synthesis of population biology and genomics, with the potential greatly to advance our understanding of evolution in wild populations. We focus on animal populations, because these are easier to study in the wild; for related work on plants see ref. 1.

## Fitness variation in the wild

For most biological problems, studying laboratory model organisms offers tremendous advantages in terms of control, replication and convenience. However, it is precisely those advantages that undermine the utility of these models for studying fitness variation (see Box 1), and its basis. In this case, field studies are of most relevance, because laboratory studies provide novel, stable, uniform, benign environments, where selection is unlikely to operate as it would in wild populations. In some cases (such as *Drosophila* populations used by biologists for experimental evolution studies[2]), laboratory populations have been maintained for long enough (hundreds of generations), and with sufficient competition, that adaptation to this novel environment has presumably occurred. Even in these cases, the relative invariance of the environment (or the arbitrariness of any imposed variation) suggests that they may be poor models of natural populations. On the other hand, laboratory models offer very clear advantages for testing the plausibility of evolutionary hypotheses, and for fine-scale dissection of their operation, and are often able to suggest novel hypotheses that can be further tested in field populations[3–5]. In addition to the environment influencing the relevance of fitness measures, the expression of genetic variance depends strongly on the environment in which it is measured. Comparisons across environments both in the laboratory and in the field indicate strong interactions between the expression of genetic variance and environmental axes[6]. Hence, studies of fitness, and the genetic factors influencing it, must be carried out in matching environments, ideally those to which organisms are adapted. This was appreciated by early ecological geneticists such as Ford and Dobzhansky; indeed, there are interesting parallels between their work and current interest in moving genomics into the field.

Measuring fitness in natural populations requires dedicated field effort, sometimes for decades, and the scale of these studies makes them particularly valuable for studying genetics of fitness in the wild. Studies over tens of generations result in long-term pedigrees of animals of known relatedness, inhabiting a wide range of environmental conditions. Currently, reliance on physical marking methods (banding or tagging), and the need for some observational information to frame inferences about parentage, has restricted such studies to vertebrates that undergo limited dispersal, particularly birds and mammals. This may change, and genetic-marker-based approaches may soon be used to reconstruct pedigrees in population types such as free-ranging invertebrates, or organisms with external fertilization. There are now numerous studies of selection on morphological, behavioural and life-history characters, replicated over many years within populations[7–9]. These studies confirm that natural selection often acts strongly and consistently within populations; the strength of selection is comparable to, or stronger than, that obtained from shorter-term studies of selection[10].

## Quantitative genetics of fitness in the wild

The maturation of long-term population studies, and the opportunities they offer for measuring selection, has been accompanied by a surge of interest in applying quantitative genetic models, particularly the 'animal model' approach[11] to wild populations. This has confirmed the empirical generalization from laboratory studies that additive genetic variance varies with respect to trait type: characters under strong selection have low heritabilities, high additive genetic variance, and even higher environmental variance[12]. Estimates of the heritability of fitness itself have generally been unable to exclude zero in their range when using traditional measures of fitness; those that have taken account of demography, and which are measured at a per-generation scale (for example, Box 1) have found small, but significant, heritability of lifetime fitness[5,13]. Simultaneous estimation of environmental and genetic influences on characters, and their separation in individuals, which animal models allow, is vital to gain unbiased estimates of the force of selection on characters. Both

[1]Department of Evolutionary Biology, Evolutionary Biology Centre, Uppsala University, Norbyvägen 18D, SE-752 36 Uppsala, Sweden. [2]Edward Grey Institute, Department of Zoology, University of Oxford, South Parks Road, Oxford OX1 3PS, UK.

**Box 1 | Fitness variation and natural selection in the wild**

A mathematical model for the relationship between natural selection and evolution was developed in the 1960s and 1970s by Robertson, ... and particularly Price, encapsulated by the Price equation, which specifies the relationship between evolutionary change and selection, conditional on the transmission of variation[65]. The link between genetics and selection was further developed in multivariate form by Lande and co-workers[66,67], who proposed an intuitive multiple-regression-based approach for the quantification of selection in natural populations. The essence of this approach is that selection gradients are derived that describe associations between fitness and trait variation. Its appeal is that, in principle, in combination with information about genetic variances and covariances, inferences about the evolutionary forces acting on populations, and potential evolutionary trajectories, may be derived. A central challenge for studies in the wild is to understand the importance of environmental covariance between traits (Box 1 figure). In this hypothetical example, selection $\beta$ is assessed by measuring the covariance $\phi$ between phenotype (subscript 'p') and fitness w, but the true relationship between the genetic component of a character and fitness (that is, the degree to which the trait will respond to selection) may be masked by environmentally induced covariances (where subscript 'e' refers to the environment) between the trait and fitness, which will be determined by the product of $\phi_{e,p}$ and $\phi_{e,w}$; when this covariance is positive, selection will be overestimated. To understand selection and fitness variation requires that fitness be measured. While fitness can be defined simply as the number of offspring contributed to future generations, either for individuals or for populations, this definition may not be reliable in non-stable populations, for which a measure of the intrinsic rate of increase at either population or individual levels that takes into account the timing during life that offspring are produced, is preferred. The appropriate definiton of fitness may also depend on the context: theoretical approaches typically focus on population fitness measures, whereas empirically oriented studies tend to focus on individual fitness[68]. A recently developed fitness measure that combines individual and population aspects of fitness designed to deal with unstable population dynamics and to take account of the continuous nature of evolution, has been termed 'delifing', because it assesses the effect on population growth of removing each individual's contribution to the population[69]. Application of this and other methods to take account of population demography may yield insights about the operation of selection and evolution in natural populations[70,71].

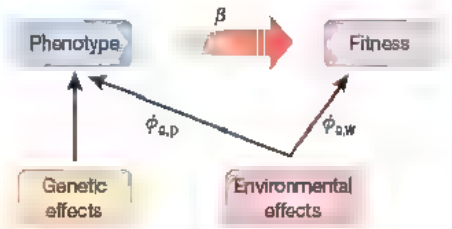


**Box 1 Figure | Genetic and environmental effects on fitness.**

Darwin and Fisher discussed cases of what we would now term environmental covariance between phenotype and fitness, where selection on a character is apparent, rather than real, because both are correlated with a third unmeasured character (Box 1). Such effects can be very important, with the result that selection is much weaker than would be apparent. For example, Kruuk and colleagues showed[7] in red deer stags that while the males with the largest antlers enjoyed highest reproductive success, most of this effect was due to correlated effects of the environment: the true force of selection on antler size was much weaker.

An emerging theme from recent studies of wild populations is the conditional nature of much of the expressed genetic variation, both with respect to the environment, but also to the life-stage of the focal individual[1-4], and its sex[5]. This has important consequences for our understanding of the evolutionary dynamics of characters in the wild. For example, Wilson and colleagues[6] showed that additive genetic

**Box 2 | Evolutionary change while the environment changes**

Whether populations are usually at evolutionary equilibria, evolving only in response to shifts in the adaptive landscape, or whether evolution is continually occurring, is fundamental to our understanding of the evolutionary process. Recent studies of wild populations suggest that observations of phenotypes alone offer little chance of resolving this question, because evolutionary responses may be hidden by environmental deterioration (for example, due to density-dependent competition for resources). Indeed, Fisher[70] and Price[71] showed that this can be expected to be the case when a change in gene frequencies itself causes a form of environmental deterioration, which will be true when fitness depends to a large extent on success in competition with conspecifics. If generally true, this implies that much evolutionary change, and differentiation in wild populations, may not be apparent at the level of the phenotype (Box 2 figure), detecting these differences becomes increasingly challenging using quantitative genetics alone, because the models and traits become ever more complex, and removed from raw phenotypes. Understanding the molecular genetic basis of the traits can make this problem far more tractable.

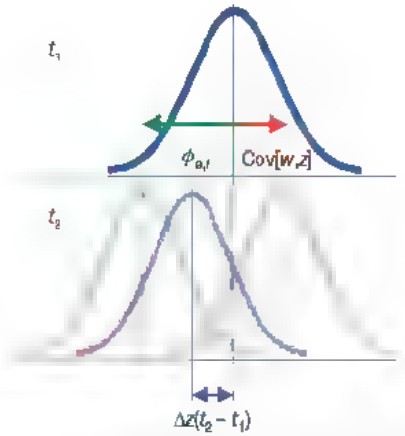


**Box 2 Figure Simplified representation of opposing effects of the environment and selection on the phenotypic evolution of a quantitative character.** If a trait is under directional selection, the mean phenotype is expected to change as a function of the genetic variance and the strength of selection on that character (Cov[$w$, $z$]), as shown in the top panel, the red curve at time $t_2$ (bottom panel) indicates a hypothetical change in the distribution of phenotypes due to selection. However, a simultaneous change in the environment ($\phi_{e,t}$ and the green curve) can act to mask any change due to selection. The resultant phenotype (blue curve), and the extent to which any evolutionary response over time $\Delta z(t_2 - t_1)$ is observed, depends on the balance between these two effects.

variance in birth weight in wild sheep, a trait under strong selection, was higher in years in which survival was high; conversely, selection was weakest in such environments. This had the effect of producing a negative covariance between the selection on this character, and the variance available for selection, a process that would act to constrain the evolutionary response to selection. A second recently emergent theme is that analysis at the level of phenotypes may give a very incomplete picture of the degree of genetic change occurring over time. Ecological geneticists have long been aware of the phenomenon of counter-gradient variation, where an ecological or environmental gradient acts to hide genetic differentiation along the same axis[15]. For example, selection may favour faster developmental rates at higher latitudes, but in ectotherms, lower ambient temperatures may reduce the effective rate of development[16]; 'common garden' experiments are used to separate such effects. Several recent long-term studies have demonstrated a form of temporal counter-gradient variation, where responses to selection on morphology (body mass in two bird species[17,18] and in wild sheep[19]) at the level of the breeding value were much larger than was apparent at the phenotypic level, because of simultaneous changes in the environment. Such a pattern of 'cryptic evolution' may be quite general (Box 2).

## What is the 'locus' of evolution?

The application of quantitative genetics should, ideally, be done bearing in mind the assumptions of this method of analysis: for example, that very large numbers of loci of small effect underlie traits. It will not be until the union of ecological and molecular genetics that we have an understanding of how realistic these assumptions are. Before we discuss the potential for unravelling the molecular basis of fitness differences in natural populations using genomic approaches, we must consider in which type of DNA sequence we expect to find adaptive mutations affecting fitness. What is, as Hoekstra and Coyne[20] put it, "the locus of evolution"? More than 30 years ago, King and Wilson[21], inspired by the similarity of human and chimpanzee proteins, suggested that it may be changes in regulation of gene expression, rather than changes in their structure, that mainly drive phenotypic evolution. Whether this is actually the case has been a contentious issue, perhaps more now (paradoxically, given the availability of sequence data) than ever before. One school of thought, whose advocates are mainly concerned with morphological evolution ('evo-devo'), holds that *cis*-regulatory elements are indeed the primary targets for genetic changes underlying new phenotypes[22]. Another school of thought maintains that changes in amino-acid-coding regions of genes, leading to new protein structures, are the key to functional evolution[20]. There is no reason to expect one or other of these mechanisms to the sole explanation, so the debate concerns their relative importance.

Work on model organisms rarely focuses on population data so there is little information available on naturally occurring variants that affect fitness that is relevant to this debate. Comparisons of closely related species in *Drosophila* and *Saccharomyces* show that regulatory mutations underlie several key fixed differences in phenotype[23–25]. However, there are also examples of structural changes in genes affecting phenotypes of central importance[26]. More generally, much recent work has demonstrated the role of positive selection in adaptive protein evolution across many different organisms[27]. As genomics is taken into natural populations, it seems prudent to expect that the loci of evolution will be both regulatory and structural in origin. We now review the resources and approaches (Fig. 1) that are currently available to find these loci.

## Genomic resources

Linking genes or other DNA sequences to fitness ultimately requires genome sequence information. Until recently, obtaining such data has been a limiting step for progress on non-experimental models. With the first gigabase-pair-sized genomes targeted, it was foreseen that genomic research would move rapidly into post-genomic approaches focusing on functional aspects rather than on gathering more sequence data. However, while functional genomics has indeed flourished, DNA sequence data continues to accumulate exponentially. New high-throughput technologies have hugely decreased the unit time and cost of obtaining sequence data and open up immense possibilities for large-scale sequencing initiatives in ecologically important species. One of the first such examples is the sequencing of a large fraction of the coding part of genome of the Glanville fritillary butterfly *Melitaea cinxia*, a key model species in studies of metapopulation ecology[28]. Moreover, it is increasingly recognized that comparative genomics, where sequences from two or more species are aligned and compared, is a powerful tool for detecting regions that evolve under negative or positive selection, indicative of functionality. Adaptive evolution can be inferred from, for example, gene sequences showing sites of repeated non-synonymous substitutions in multiple species alignments, an increased rate of non-synonymous substitutions in divergence compared to diversity data, or a high frequency of derived alleles[29].

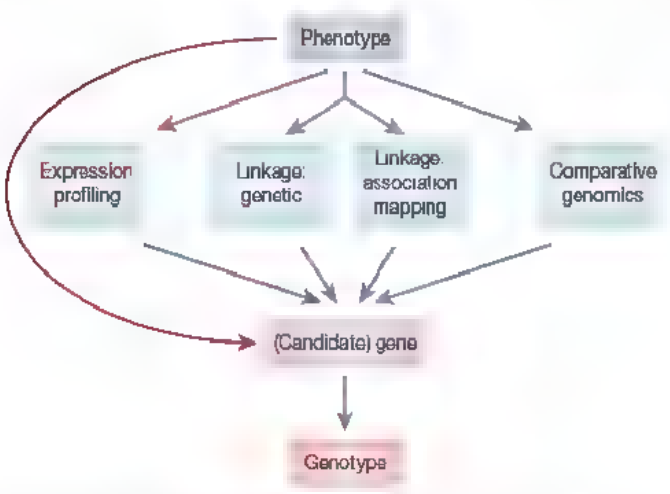


**Figure 1 | Linking phenotypes to genotypes.** Routes towards linking variation in phenotypes to variation in genotypes.

## Genetic mapping in natural populations

Linkage analysis is the traditional way of identifying chromosomal regions containing trait loci in model organisms. It relies on following the inheritance of segregating traits in pedigrees and seeks to find co-inheritance of traits and genetic markers; if this can be established, trait loci are inferred to map in the vicinity of marker loci. As the power of linkage analysis increases with number of meioses that can be studied, linkage maps have so far mainly been constructed for species that can be bred in captivity, including fishes, insects and mammals. However, linkage maps from wild populations are starting to accumulate, including some of model species for ecological research.

Decades of work on human disease genetics and trait mapping in model organisms has revealed that finding the causal genetic basis of segregating phenotypes can be extremely demanding. In general, the lower the heritability and the more loci involved, the more difficult it is to dissect genotype–phenotype relationships[30]. Added complexity results from the fact that genetic variation at different loci may contribute to similar phenotypes in different populations, notably due to gene–environment interactions. Given this, will quantitative trait locus (QTL) mapping be a useful method for unravelling genetic architecture of traits of modest heritability that demonstrate continuous variation in natural populations[31]? The answer is likely to depend on the character of the study system. The use of inbred line crosses is the most powerful method of QTL analysis, because it maximizes linkage disequilibrium between markers and trait loci[32]. Accordingly, if organisms from natural populations can be bred and selected for divergent phenotypes under controlled conditions, mapping is quite feasible, although, as stated above, laboratory conditions do not replicate the full range of environments experienced by organisms in the wild. Another caveat is that the use of inbred lines fails to mirror epistasis based on standing genetic variation shown by organisms in outbred populations.

For QTL mapping to become widely used for studies of outbred natural populations will require that large pedigrees, or extensive series of sibling-pairs, can be sampled and components of fitness measured in these individuals[33,34]. If this proves impractical, for instance because of long generation times or because fitness can be measured for few individuals in the pedigree, alternative approaches may be more promising, as discussed below. Moreover, it must be recognized that mapping chromosomal regions that co-segregate with traits of interest represents just the first step towards identification of causative genetic variants. Numerous genes usually reside within a targeted chromosomal region and the eventual identification of such variants may require positional cloning, refined mapping and nomination of candidate genes. Only a few studies of natural populations have yet gone all this way, notably the mapping[35] and subsequent identification of ectodysplasin[36] underlying armour plate patterning in different populations of threespine sticklebacks. Mutations at this locus have led freshwater forms of sticklebacks to evolve a loss of pelvic structure, possibly an adaptation to a change in the risk of predation.

An alternative method is to search for linkage between markers and trait loci by genome scans of population samples, rather than by pedigree analysis. Known as association mapping or linkage disequilibrium mapping, the approach relies on a statistical association between marker and trait loci that are in linkage disequilibrium, typically with much higher resolution than in conventional pedigree analysis. The efficiency of association mapping depends, among other things, on the number and distribution of markers used to scan the genome, and the extent of linkage disequilibrium. Extensive linkage disequilibrium facilitates detecting disequilibrium between trait loci and markers but comes with the price of reduced resolution; short-range linkage disequilibrium requires more markers but simplifies the subsequent process of identification of causative sequence variants. Data on linkage disequilibrium in natural populations are now accumulating and, not surprisingly, indicate that it varies among species and is at least in part dependent on population history[37,38]. It is important to note that population structure may result in artefactual associations[39].

If genetic markers spread across the genome are available, other approaches can be used for the identification of regions subject to adaptive evolution, using population samples. Selective sweep mapping[40] takes advantage of the fact that strong positive selection is expected to leave a local footprint in form of reduced genetic diversity around the selected locus; when a selected allele goes to fixation, linked neutral variants will also increase in frequency. However, it can be demanding to achieve sufficient statistical power in genome-wide scans, in part relating to dominance and whether selection has been acting on standing variation or a new mutation[41,42]. Finally, it has recently been argued that, by studying the distribution of inbreeding coefficients across the genome, regions that show apparent adaptive divergence among populations can be identified[43,44]. Often referred to as population genomics[45], this approach is particularly suited for identifying loci under disruptive selection, such as in recently derived species or in diverging populations. It has been applied to a variety of species in which genomic regions with a high distribution of inbreeding coefficients, suggestive of strong assortative mating, or even reproductive isolation, contrast with a genomic background of almost free gene flow[46]. Local adaptation often occurs along environmental gradients associated with continuously varying phenotypic characters, so it is sensible to search for outlier loci in consecutive pairwise comparisons along such gradients. For example, in the common frog (*Rana temporaria*), a number of candidate loci for adaptation to altitude have been found, identified through showing a significantly higher degree of differentiation than under neutral expectation[47].

In combination, genome scans are important in confirming that QTLs identified in contemporary populations have played a part in adaptive phenotypic differentiation, driven by directional selection. If signs of selection as revealed by scans for reduced within-population variability or increased between-population divergence coincide with the chromosomal location of QTLs, this highlights the significance of genes within these regions in adaptive evolution[48].

## Candidate gene approaches

A major advantage of studies of the genetic basis of fitness differences in natural populations is that candidates for trait loci can be nominated on the basis of knowledge of similar phenotypes in model species, circumventing the tedious process of unprejudiced genome-wide approaches. A successful example of this approach is the analysis of adaptive variation in vertebrate pelage and plumage traits. Coat-colour mutations in laboratory mice provide a detailed catalogue of proteins involved in pigmentation with associated information on how these proteins interact with each other. The melanin-based pigmentation pathway leading to melanocyte development and migration is highly conserved in vertebrates, so the wealth of information provided by mouse genetics is broadly applicable. The melanocortin-1 receptor (Mc1r), a G-protein-coupled receptor that induces cAMP production needed in the synthesis of eumelanin, is known to be a major determinant of pigmentation phenotypes[49]. A candidate gene approach focusing on allelic variation in *Mc1r* has successfully linked this gene to colour morphs of adaptive significance in several natural populations, including pigmentation variation relating to crypsis in pocket mice[50], little striped whiptail and lesser earless lizards[51], and to mate choice in arctic skuas and lesser snow geese[52]. Other genes involved in this pathway, like *Tyrp1*, *Agouti*[53] and *Kitlg*[54], have also been shown to be associated with pigmentation polymorphisms in natural populations. In the case of *Mc1r*, there is compelling evidence that the causative genetic background to phenotypic variation is coding sequence polymorphism. As such, fitness-related coat-colour polymorphism mediated by *Mc1r* exemplifies a mendelian trait governed by variation in gene structure rather than gene expression.

An excellent example of how the power of the candidate gene approach can be strengthened by parallel genetic mapping is the case of albinism in Mexican tetra fish (*Astyanax fasciatus/mexicanus*). Several cave populations of these fish have independently evolved reduced pigmentation and regressed eyes compared with surface or river-dwelling sister populations. By constructing a microsatellite-based genetic map, Protas *et al.*[55] obtained a very strong signal of linkage between albinism and a single chromosomal region. When testing the segregation of a number of candidate genes known to have profound effect on pigmentation in model species, the gene ocular and cutaneous albinism-2 (*Oca2*) was found to map to the same region and thus co-segregate with albinism. Subsequent sequence analysis showed that amino-acid substitutions and coding sequence deletions occur in *Oca2* of albinistic cave fish. This study is of particular importance because, as is now commonplace in studies of, for example, human disease mutations, the identification of a causative locus was supported by functional studies in a mouse model. Although technologically demanding, such dual strategies (genetic and functional) will be very important in future studies of natural populations.

Another category of genes that are good candidates for those influencing fitness in natural populations is those encoding proteins involved with glucose metabolism ('energy production'). For example, the enzyme phosphoglucose isomerase (Pgi) catalyses the conversion of glucose-6-phosphate to fructose-6-phosphate in the first phase of glycolysis. *Pgi* polymorphism has major fitness effects in a diverse range of species[56]. In the Glanville fritillary butterfly, allelic variation at *Pgi* correlates with flight metabolic rate and is related to dispersal rate and the ability to establish new and isolated populations[57]. As such, this system constitutes one of the best examples of how genetic variation at a fitness-related locus affects metapopulation dynamics and population growth. The effect of *Pgi* polymorphism was found to be dependent on the size and isolation of populations; hence the genetic effect was strongly dependent on the environmental context, underlining the importance of combining ecological and genetic approaches. A caveat is that it remains to be formally demonstrated that *Pgi* is the causally responsible locus; in theory, a closely linked locus may be involved.

## Transcriptome analysis

Improvement in array technology has had a significant impact on large-scale studies of gene expression—transcriptome profiling—with increasing application to natural populations[58]. A case study of the genetic background to adaptive variation in beak morphology among Darwin's finches is described in Box 3. A microarray experiment uses representative probes corresponding to known genes from a genome, or of most of the sequence from a genomic region (tiling paths or tiling arrays), to which tissue messenger RNA is hybridized and quantified on the basis of hybridization intensity. The experimental rationale is usually straightforward: hybridization data from two or more groups of samples (treatments) are compared to seek evidence of differentially expressed genes. The access to

**Box 3 | The genetic basis of beak morphology in Darwin's finches**

Adaptive radiation among Darwin's finches has resulted in more than ten different finch species exploiting a variety of ecological niches on the Galápagos islands, reflected in distinct beak morphology. Species feeding on cactus flowers have long, pointed beaks, species eating seeds on the ground have deep, wide beaks, while insect eaters have slender, pointed beaks. Differences in external beak morphology are consistent with corresponding differences in craniofacial skeletons and it has been shown experimentally in other bird species that the cellular origin of beak development is in the neural crest-derived mesenchyme[72]. Studying the expression pattern of growth factors implicated in avian craniofacial development, Abzhanov *et al.*[73] found a strong correlation between beak morphology and the level of expression of bone morphogenetic protein 4 (*Bmp4*) in the mesenchyme of the upper beak. This suggests that regulation of *Bmp4* expression is a key variable determining quantitative variation in beak morphology of Darwin's finches, although it cannot distinguish between a role of *cis*-regulatory elements or of variation in the induction/transduction of upstream factors. Subsequently, the same group used microarray hybridization to identify differentially expressed genes among finches with different beak morphology[74]. This led to the identification of calmodulin (CaM), a key component of a $Ca^{2+}$-dependent signal transduction pathway essential for the control of bone differentiation and growth, being expressed at much higher levels in cactus-feeding finches than in other species. These studies not only provide new insight into this textbook example of evolution by natural selection. They also show both the power and feasibility of combining several genomic approaches to non-model species, in this case including the construction of a species-specific expression array. In addition, they constitute an unusual example of experimental confirmation of the functional significance of the proposed genetic mechanism by experimental manipulation in a model system: misexpression of *Bmp4* and *CaM* in developing chicken embryos has an effect on beak morphology similar to that seen in finches[74].

species-specific arrays, typically limited to organisms in focus for genome projects, has somewhat impeded widespread use of microarrays. However, cross-species application of arrays developed for related species is a useful alternative.

Transcriptome profiling has in several cases shown distinct differences in gene expression between divergent natural populations, particularly for fish species[58]. For example, differences in the expression of genes involved with swimming activity were found between the dwarf and lake ecotypes of whitefish, consistent with differences in feeding behaviour and niche exploitation[59]. However, just as the relative importance of natural selection and genetic drift has been a long-standing issue in molecular evolution, there is ongoing debate concerning how much variation in gene expression results from neutral processes and selection, respectively. Similarly, the relative influence of directional selection and stabilizing selection is debated[60]. Many microarray studies use pooled rather than individual samples for analysis, but there is increasing evidence for significant inter-individual variation in patterns of gene expression, perhaps for the majority of genes[58]. Moreover, there is an emerging understanding that much of the expression variation seen under controlled environmental conditions is heritable[61]. Hence, in principle, there is raw material for evolution by natural selection. Also, as genes are typically part of networks, it is easy to see that many, if not most, of the differences in gene expression seen between two phenotypes do not necessarily represent genetic differences underlying phenotypic difference. As an illustrative example, thousands of transcripts can be found differentially expressed between males and females of many species[62], yet the great majority of these genes are not directly involved with sex determination.

With new, ultrahigh-throughput sequencing technology, the way gene expression is studied is likely to change soon. Rather than relying on measuring gene transcript abundance from hybridization intensity to microarrays, the number of times transcripts are called in deep-coverage sequencing affords direct quantification of expression levels. An attractive feature of this approach for studies of non-model organisms is that there is no need for the construction of species-specific microarrays.

## Future directions

As outlined above, the past few years have seen remarkable growth in the range and scope of applications of genetic tools to evolutionary problems. Many conceptual, technological and analytical innovations, driven by work on the major genomic models, have hugely increased the applicability of these methods to non-model organisms. As sequence and genome structure data continue to accumulate, the possibilities for using these data for comparative purposes, and for leaping between species, will become ever richer. Given the rate of development, predicting where the limits of technology will lie in five years' time is very difficult.

Coupled with the huge increase in the applicability of genomic resources has been an improved understanding of the operation of natural selection from a quantitative genetic perspective in wild populations. This has been driven by the increased availability of high quality, long-term data sets from natural population studies, as well as the application of analytical techniques from other fields. These new studies have, in some cases, studied selection, phenotypic changes, and inheritance over tens of generations, providing richly detailed insights into the importance of spatial and temporal variation and their interaction with selection and inheritance.

The merging of these two research traditions offers the possibility for important insights into major problems in the evolutionary biology of wild populations; we outline three candidates here. First, the ability to identify specific genetic loci influencing phenotypes will enable a much more precise understanding of what constitutes a trait that can be the target of selection. For example, there is considerable interest at present in the evolutionary ecology of plasticity, partly owing to its relevance to adaptation to human-induced environmental change, and a reaction norm approach is often taken, where the expression of phenotypes across environment is analysed as a trait[63]. Knowledge of the molecular genetic basis of characters, coupled with expression studies, will enable the determination of whether phenotypes in different environments are really the same traits, and also potentially of the loci ('plasticity genes') which control the expression of these phenotypes across environments. In general, field biologists have tended to ignore the problem of the relationship between traits and underlying genetic causes (the 'phenotypic gambit'), but there is no longer any excuse to do so.

Second, with an increased focus on the loci underlying traits, several related issues are brought closer to solution. For example, recent interest in the role of sexually antagonistic genetic variation is based on classical quantitative genetics[4,5] or laboratory-based *Drosophila* breeding experiments[3]. A genomic perspective allows the possibility—for example through whole-genome scans or the analysis of sex-by-linkage-disequilibrium interactions—of identifying and characterizing any sex-antagonistic genes, and testing evolutionary theories about their genomic location.

Genomic approaches can also be used to determine the molecular genetic basis of genetic correlations, whether resulting from linkage disequilibrium or pleiotropy, and hence are of considerable importance in determining their role in directing evolutionary trajectories. A much-debated question in evolutionary biology concerns the stability of the genetic variance–covariance matrix. While assessing the temporal component of this problem may still be beyond reach, it might be approached at least from a spatial or environmental perspective. The genetic structure of traits is also of great importance for debates about the forces driving sexual selection, and the evolution of costly mate choice. The application of genomics has the potential to resolve questions such as the importance of additive and non-additive genetic variance in sexual display characters, and hence to

determine the extent to which female choice predicated solely on characteristics that can be transmitted to offspring is plausible[64].

Third, a general problem concerns the extent to which environmental and temporal variation act to maintain genetic variation for characters under fluctuating selection. There are many candidate processes that can maintain genetic variation in natural populations[29]; some of these processes can be studied by linking genes and fitness variation in ecological studies. For example, testing for the presence and importance of QTL and gene–environment interactions will shed light on this problem from a within-population perspective, whereas comparisons of selection on allelic variants in populations in different selective environments can place this question in a spatial context. Extending this question to a temporal framework offers the possibility of addressing (for example by applying a re-sequencing approach involving archived specimens or samples, and contemporary populations) the extent to which populations are continually undergoing adaptive evolution, or are relatively static.

## Challenge and conclusion

A challenge must be accepted for this synthesis to occur. Each field has been based around the choice of different attributes for model organisms. It is inevitable that our understanding of evolutionary genomics is best developed in those organisms that have longest served as models for laboratory genetics (*Drosophila*, rodents), or that have most relevance to biomedical science (for example, primates). The most effective choice for studies of fitness in wild populations is diurnally active vertebrates that live at high densities (ungulate mammals, passerine birds, squamate reptiles). This has affected the kinds of problems that are tackled, more overlap between these questions should develop as more genomic information becomes available. For example, bird genomes appear to show high degrees of conservation in terms of organization, suggesting that with the impending addition of the zebra finch to the completed genome sequences of birds, much more work on wild birds that is genomic in focus will become possible. Equally, the increased ease of obtaining genomic information may reduce the need for observations of matings or parentage that motivates the choice of ecological models. Nevertheless, it would be naive to suggest that purely field-based models are soon likely to offer the opportunities that laboratory models do: there is a continuum between experimental model and ecological realism, and the most productive ground may lie with species that occupy an intermediate position on this continuum, such as sticklebacks or mice. Some field biologists may need to reassess their choice of model species, or be prepared to wait some time before they can apply the full range of genomic approaches. Equally, some laboratory-based scientists may need to consider whether placing their studies within an ecologically relevant context may offer, in the long run, more insight into contemporary evolution.


1 Mitchell-Olds, T. & Schmitt, J. Genetic mechanisms and evolutionary significance of natural variation in *Arabidopsis*. *Nature* 441, 947–952 (2006)
2 Rice, W. R. Sexually antagonistic male adaptation triggered by experimental arrest of female evolution. *Nature* 381, 232–234 (1996)
3 Chippindale, A. K., Gibson, J. R. & Rice, W. R. Negative genetic correlation for adult fitness between sexes reveals ontogenetic conflict in *Drosophila*. *Proc. Natl Acad. Sci. USA* 98, 1671–1675 (2001).
4 Fedorka, K. M. & Mousseau, T. A. Female mating bias results in conflicting sex-specific offspring fitness. *Nature* 429, 65–67 (2004).
5 Foerster, K. *et al.* Sexually antagonistic genetic variation for fitness in red deer *Nature* 447, 1107–1110 (2007)
6 Wilson, A. J. *et al.* Environmental coupling of selection and heritability limits evolution. *PLoS Biol.* 4, e216 (2006).
7 Kruuk, L. E. B. *et al.* Antler size in red deer: heritability and selection but no evolution. *Evol. Int. J. Org. Evol.* 56, 1683–1695 (2002)
8 Grant, P. R. & Grant, B. R. Unpredictable evolution in a 30-year study of Darwin's finches. *Science* 296, 707–711 (2002)
9 Garant, D., Kruuk, L. E. B., McCleery, R. H. & Sheldon, B. C. Evolution in a changing environment: a case study with great tit fledging mass. *Am. Nat.* 164, 115–129 (2004)
10 Knapczyk, F. N. & Conner, J. K. Estimates of the average strength of selection are not inflated by sampling error or publication bias. *Am. Nat.* 170, 501–508 (2007)
11 Kruuk, L. E. B. Estimating genetic parameters in natural populations using the 'animal model'. *Phil. Trans. R. Soc. Lond. B* 359, 873–890 (2004)
12 Kruuk, L. E. B. *et al.* Heritability of fitness in a wild mammal population. *Proc. Natl Acad. Sci. USA* 97, 698–703 (2000).
13 Pelletier, F., Clutton-Brock, T. H., Pemberton, J. M., Tuljapurkar, S. & Coulson, T. The evolutionary demography of ecological change: linking trait variation and population growth. *Science* 315, 1571–1574 (2007)
14 Charmantier, A., Perrins, C., McCleery, R. H. & Sheldon, B. C. Quantitative genetics of age at reproduction in wild swans: support for antagonistic pleiotropy models of senescence. *Proc. Natl Acad. Sci. USA* 103, 6587–6592 (2006).
15 Conover, D. O. & Schultz, E. T. Phenotypic similarity and the evolutionary significance of counter-gradient variation. *Trends Ecol. Evol.* 10, 248–252 (1995)
16 Laugen, A. T. *et al.* Latitudinal countergradient variation in the common frog (*Rana temporaria*) development rates—evidence for local adaptation. *J. Evol. Biol.* 16, 996–1005 (2003).
17 Merilä, J., Kruuk, L. E. B. & Sheldon, B. C. Cryptic evolution in a wild bird population. *Nature* 412, 76–79 (2001)
18 Garant, D., Kruuk, L. E. B., Wilkin, T. A., McCleery, R. H. & Sheldon, B. C. Evolution driven by differential dispersal within a wild bird population. *Nature* 433, 60–65 (2005)
19 Wilson, A. J. *et al.* Quantitative genetics of growth and cryptic evolution of body size in an island population. *Evol. Ecol.* 21, 337–356 (2007)
20 Hoekstra, H. E. & Coyne, J. A. The locus of evolution: evo devo and the genetics of adaptation. *Evol. Int. J. Org. Evol.* 61, 995–1016 (2007)
21 King, M. C. & Wilson, A. C. Evolution at two levels in humans and chimpanzees. *Science* 188, 107–116 (1975)
22 Carroll, S. B. *Endless Forms Most Beautiful: the New Science of Evo-Devo* (W. W. Norton & Co., New York, 2005)
23 Prud'homme, B. *et al.* Repeated morphological evolution through *cis*-regulatory changes in a pleiotropic gene. *Nature* 440, 1050–1053 (2006).
24 Borneman, A. R. *et al.* Divergence of transcription factor binding sites across related yeast species. *Science* 317, 815–819 (2007)
25 McGregor, A. P. *et al.* Morphological evolution through multiple *cis*-regulatory mutations at a single gene. *Nature* 448, 587–590 (2007).
26 ffrench-Constant, R. H., Rocheleau, T. A., Steichen, J. C. & Chalmers, A. E. A point mutation in a *Drosophila* GABA receptor confers insecticide resistance. *Nature* 363, 448–451 (1993)
27 Bustamante, C. D. *et al.* Natural selection on protein-coding genes in the human genome. *Nature* 437, 1153–1157 (2005)
28 Vera, J. C. *et al.* Rapid transcriptome characterization for a nonmodel organism using 454 pyrosequencing. *Mol. Ecol.* advance online publication, doi:10.1111/j.1365-294x.2008.03666.x (5 February 2008)
29 Mitchell-Olds, T., Willis, J. H. & Goldstein, D. B. Which evolutionary processes influence natural genetic variation for phenotypic traits? *Nature Rev. Genet.* 8, 845–856 (2007).
30 Williams, J. T. & Blangero, J. Power of variance component linkage analysis to detect quantitative trait loci. *Ann. Hum. Genet.* 63, 545–563 (1999).
31 Barton, N. H. & Keightly, P. D. Understanding quantitative genetic variation *Nature Rev. Genet.* 3, 11–21 (2002)
32 Lynch, M. & Walsh, B. *Genetics and Analysis of Quantitative Traits* (Sinauer Associates, Sunderland, Massachusetts, 1998)
33 Slate, J. *et al.* A genome scan for quantitative trait loci in a wild populations of red deer (*Cervus elaphus*). *Genetics* 162, 1863–1873 (2002)
34 Beraldi, D. *et al.* Mapping quantitative trait loci underlying fitness-related traits in a free-living sheep population. *Evol. Int. J. Org. Evol.* 61, 1403–1416 (2007)
35 Colosimo, P. F. *et al.* The genetic architecture of parallel armor plate reduction in threespine sticklebacks. *PLoS Biol.* 2, e109 (2004)
36 Colosimo, P. F. *et al.* Widespread parallel evolution in sticklebacks by repeated fixation of ectodysplasin alleles. *Science* 307, 1928–1933 (2005)
37 Backström, N., Qvarnstrom, A., Gustafsson, L. & Ellegren, H. Levels of linkage disequilibrium in a wild bird population. *Biol. Lett.* 2, 435–438 (2006)
38 Slate, J. & Pemberton, J. M. Admixture and patterns of linkage disequilibrium in a free-living vertebrate population. *J. Evol. Biol.* 20, 1415–1427 (2007).
39 Yu, J. *et al.* A unified mixed-model method for association mapping that accounts for multiple levels of relatedness. *Nature Genet.* 38, 203–208 (2006).
40 Williamson, S. *et al.* Localizing recent adaptive evolution in the human genome. *PloS Genet.* 3, e90 (2007)
41 Pennings, P. S. & Hermisson, J. Soft sweeps III: The signature of positive selection from recurrent mutation. *PloS Genet.* 2, e186 (2006)
42 Teshima, K. M., Coop, G. & Preworski, M. How reliable are empirical genomic scans for selective sweeps? *Genome Res.* 16, 702–712 (2006)
43 Beaumont, M. A. Adaptation and speciation: what can $F_{ST}$ tell us? *Trends Ecol. Evol.* 20, 435–440 (2005)
44 Storz, J. F. Using genome scans of DNA polymorphism to infer adaptive population divergence. *Mol. Ecol.* 14, 671–688 (2005)
45 Luikart, G., England, P. R., Tallman, D., Jordan, S. & Taberlet, P. The power and promise of population genomics: from genotyping to genome typing. *Nature Rev. Genet.* 4, 981–993 (2003).
46 Campbell, D. & Bernatchez, L. Generic scan using AFLP markers as a means to assess the role of directional selection in the divergence of sympatric whitefish ecotypes. *Mol. Biol. Evol.* 21, 945–956 (2004)

47 Bonin, A. Explorative genome scan to detect candidate loci for adaptation along a gradient of altitude in the common frog (*Rana temporaria*). *Mol. Ecol.* 23, 773–783 (2006)
48. Rogers, S. M. & Bernatchez, L. Integrating QTL mapping and genome scans towards the characterization of candidate loci under parallel selection in the lake whitefish (*Coregonus clupeaformis*). *Mol. Ecol.* 14, 351–361 (2005).
49 Lin, J. Y. & Fisher, D. E. Melanocyte biology and skin pigmentation. *Nature* 445, 843–850 (2007)
50 Hoekstra, H. E., Hirschmann, R. J., Bundey, R. A., Insel, P. A. & Crossland, J. P. A single amino acid mutation contributes to adaptive beach mouse color pattern. *Science* 313, 101–104 (2006)
51. Rosenblum, E. B., Hoekstra, H. E. & Nachman, M. W. Adaptive reptile color variation and the evolution of the *MC1R* gene. *Evolution Int. J. Org. Evolution* 58, 1794–1808 (2004)
52 Mundy, N. I. *et al.* Conserved genetics basis of a quantitative plumage trait involved in mate choice. *Science* 303, 1870–1873 (2004)
53. Steiner, C. C., Weber, J. N. & Hoekstra, H. E. Adaptive variation in beach mice produced by two interacting pigmentation genes. *PLoS Biol.* 5, e239 (2007).
54. Miller, C. T. *et al. cis*-regulatory changes in Kit ligand expression and parallel evolution of pigmentation in sticklebacks and humans. *Cell* 131, 1179–1189 (2007)
55 Protas, M. E. *et al.* Genetic analysis of cavefish reveals molecular convergence in the evolution of albinism. *Nature Genet.* 38, 107–111 (2006).
56. Dahlhoff, E. P. & Rank, N. E. Functional and physiological consequences of genetic variation at phosphoglucose isomerase: Heat shock protein expression is related to enzyme genotype in a montane beetle. *Proc. Natl Acad. Sci. USA* 97, 10056–10061 (2000)
57 Haag, C. R., Saastamoinen, M., Marden, J. H. & Hanski, I. A candidate locus for variation in dispersal rate in a butterfly metapopulation. *Proc. Biol. Sci.* 272, 2449–2456 (2005)
58. Whitehead, A. & Crawford, D. L. Variation within and among species in gene expression: raw material for evolution. *Mol. Ecol.* 15, 1197–1211 (2006)
59 Derome, N. & Bernatchez, L. The transcriptomics of ecological convergence between two limnetic coregonine fishes (Salmonidae). *Mol. Biol. Evol.* 23, 2370–2378 (2006)
60. Gilad, Y., Oshlack, A. & Rifkin, S. A. Natural selection on gene expression. *Trends Genet.* 22, 456–461 (2006)
61. Gibson, G. & Weir, B. The quantitative genetics of transcription. *Trends Genet.* 21, 616–623 (2005)
62. Ellegren, H. & Parsch, J. The evolution of sex-biased genes and sex-biased gene expression. *Nature Rev. Genet.* 8, 689–698 (2007)
63. Nussey, D. H., Postma, E., Gienapp, P. & Visser, M. E. Selection on heritable phenotypic plasticity in a wild bird population. *Science* 310, 304–306 (2005)
64. Charmantier, A. & Sheldon, B. C. Testing genetic models of mate choice evolution in the wild. *Trends Ecol. Evol.* 21, 417–419 (2006)
65. Frank, S. A. George Price's contributions to evolutionary genetics. *J. Theor. Biol.* 175, 373–388 (1995)
66. Lande, R. A quantitative genetic theory of life history evolution. *Ecology* 63, 607–615 (1982).
67. Lande, R. & Arnold, S. J. The measurement of selection on correlated characters. *Evolution Int. J. Org. Evolution* 37, 1210–1226 (1983)
68. Metcalf, C. J. E. & Pavard, S. Why evolutionary biologists should be demographers. *Trends Ecol. Evol.* 22, 205–212 (2007).
69. Coulson, T. *et al.* Estimating individual contributions to population growth: evolutionary fitness in ecological time. *Proc. R. Soc. Lond. Ser. B* 273, 547–555 (2006).
70 Fisher, R. A. *The Genetical Theory of Natural Selection* (Clarendon Press, Oxford, 1930)
71. Price, G. R. Fisher's 'fundamental theorem' made clear. *Ann. Hum. Genet.* 36, 129–140 (1972)
72. Schneider, R. A. & Helms, J. A. The cellular and molecular origins of beak morphology. *Science* 299, 565–568 (2003).
73. Abzhanov, A. *et al. Bmp4* and morphological variation of beaks in Darwin's finches. *Science* 305, 1462–1465 (2004)
74. Abzhanov, A. *et al.* The calmodulin pathway and evolution of elongated beak morphology in Darwins finches. *Nature* 442, 563–567 (2006).

**Acknowledgements** This work was supported by grants from the Swedish Research Council (H.E.) and by a Roya Society University Research Fellowship and an Erskine Fellowship (B.C.S).

**Author Contributions** H.E. and B.C.S. wrote the paper together.

**Author Information** Reprints and permissions information is available at www.nature.com/reprints. Correspondence and requests for materials should be addressed to H.E. (hans.ellegren@ebc.uu.se) or B.C.S. (ben.sheldon@zoo.ox.ac.uk)

ARTICLES

# A new class of anthelmintics effective against drug-resistant nematodes

Ronald Kaminsky[1], Pierre Ducray[2], Martin Jung[1], Ralph Clover[3], Lucien Rufener[1,4], Jacques Bouvier[1], Sandra Schorderet Weber[1], Andre Wenger[1], Susanne Wieland-Berghausen[2], Thomas Goebel[2], Noelle Gauvry[2], François Pautrat[2], Thomas Skripsky[2], Olivier Froelich[1], Clarisse Komoin-Oka[5], Bethany Westlund[3], Ann Sluder[3] & Pascal Mäser[4]

**Anthelmintic resistance in human and animal pathogenic helminths has been spreading in prevalence and severity to a point where multidrug resistance against the three major classes of anthelmintics—the benzimidazoles, imidazothiazoles and macrocyclic lactones—has become a global phenomenon in gastrointestinal nematodes of farm animals. Hence, there is an urgent need for an anthelmintic with a new mode of action. Here we report the discovery of the amino-acetonitrile derivatives (AADs) as a new chemical class of synthetic anthelmintics and describe the development of drug candidates that are efficacious against various species of livestock-pathogenic nematodes. These drug candidates seem to have a novel mode of action involving a unique, nematode-specific clade of acetylcholine receptor subunits. The AADs are well tolerated and of low toxicity to mammals, and overcome existing resistances to the currently available anthelmintics.**

The nematodes, or roundworms, comprise a large number of pathogens of man and domestic animals. Gastrointestinal nematodes, such as the blood-sucking *Haemonchus contortus*, are major parasites of ruminants that cause substantial economic losses to livestock production worldwide. In the absence of vaccines for gastrointestinal nematodes, control of infections relies mainly on chemotherapy. Anthelmintic chemotherapy is limited to three major chemical classes, and, inevitably, drug resistance has emerged in human[1–4] and animal[5,6] pathogenic helminths against each class. The appearance of multidrug-resistant nematodes that withstand all available classes of anthelmintics[7,8] further underscores the need for new drugs[9]. No new anthelmintic class has reached the market during the past 25 yr with the exception of the cyclodepsipeptides represented by emodepside, which is indicated for use in cats but not in livestock. We have pursued extensive *ex vivo* screening followed by lead optimization in rodent models and evaluation in farm animals, and identified AADs as resistance-breaking drug development candidates. Their mode of action was investigated using drug-resistant mutants of *Caenorhabditis elegans* and *H. contortus*.

## Synthesis and anthelmintic potential of AADs

The AADs are a class of low molecular mass compounds that are easily accessible by alkylation of phenols with chloroacetone, Strecker reaction and acylation of the amine with aroyl chlorides (Fig. 1a). Over 600 compounds bearing different aryloxy and aroyl moieties on an amino-acetonitrile core have been synthesized and evaluated for anthelmintic activity. Some exhibited high activity against *H. contortus* and *Trichostrongylus colubriformis*, with $EC_{100}$ (the minimum effective concentration that eliminates 100% of nematodes) values for the best molecules in the range of 0.01–0.032 parts per million (p.p.m.) in an *in vitro* larval development assay (LDA). After chiral resolution (Fig. 1b) a significant difference in the potency of each enantiomer was observed (see Supplementary Information). Promising AADs were validated in a rodent model using *Meriones unguiculatus* infected with *H. contortus* and *T. colubriformis*. Although the original lead compound, AAD 450, was fully active against *H. contortus* at 10 mg racemate $kg^{-1}$ (not shown; where racemate is an equimolar mixture of a pair of enantiomers) but not at 3.2 mg racemate $kg^{-1}$ after oral application, the compounds obtained at the end of the optimization process (AADs 1336 and 1470; Fig. 2) cured infected rodents at 3.2 mg racemate $kg^{-1}$ (Fig. 2). These compounds were also effective against both species when applied subcutaneously, indicating systemic anthelmintic activity (Fig. 2). At doses up to 32 mg racemate $kg^{-1}$ the AADs 1336 and 1470 did not show insecticidal (*Ctenocephalides felis*) nor acaricidal (*Rhipicephalus sanguineus*) activity (data not shown).

## Efficacy of the AADs in ruminants

When tested in ruminants, all AADs were able to eliminate fourth larval (L4) stages of *H. contortus* in sheep and *Cooperia oncophora* in cattle at a single oral dose of 20 mg racemate $kg^{-1}$ (corresponding to 10 mg active enantiomer per kg). In addition, the optimized AADs 1336 and 1470 were able to eliminate L4 stages of *T. colubriformis* in sheep and *Ostertagia ostertagi* in cattle (Fig. 2). Compound AAD 1470 administered orally at a dose of 10 mg racemate $kg^{-1}$ to sheep ($n = 6$), infected simultaneously with L4 stages of five major nematode species, was 100% effective based on faecal nematode egg counts (EPG, eggs per gram faeces) and 90–100% effective based on nematode counts for *Nematodirus spathiger*, *H. contortus*, *Teladorsagia circumcincta* and *T. colubriformis*. Furthermore, compound 1470 was more than 98% effective at a dose of 10 mg racemate $kg^{-1}$ against adult stages of *H. contortus*, *Trichostrongylus axei*, *T. circumcincta*, *T. colubriformis*, *Cooperia curticei*, *N. spathiger* and *Chabertia ovina* in sheep.

The anthelmintic efficacy of AAD 1470 was also tested in naturally parasitized sheep. Ten diseased sheep were used in a trial in the Ivory Coast with the study inclusion criteria of EPG above 500 (to ensure a high infection with gastrointestinal nematodes) plus the presence of *Moniezia expansa* (sheep tapeworm) proglottids. Eight sheep were treated orally at 40 mg racemate $kg^{-1}$ body weight. Two untreated control sheep were necropsied and found to be positive for

[1]Novartis Centre de Recherche Santé Animale, CH-1566 St Aubin (FR) Switzerland [2]Novartis Animal Health Inc., CH-4002 Basel, Switzerland. [3]Cambria Biosciences, Woburn, Massachusetts 01801, USA. [4]Institute of Cell Biology, University of Bern, CH-3012 Bern, Switzerland. [5]Laboratoire Central Vétérinaire de Bingerville, BP 206, Lanada, Côte d'Ivoire.

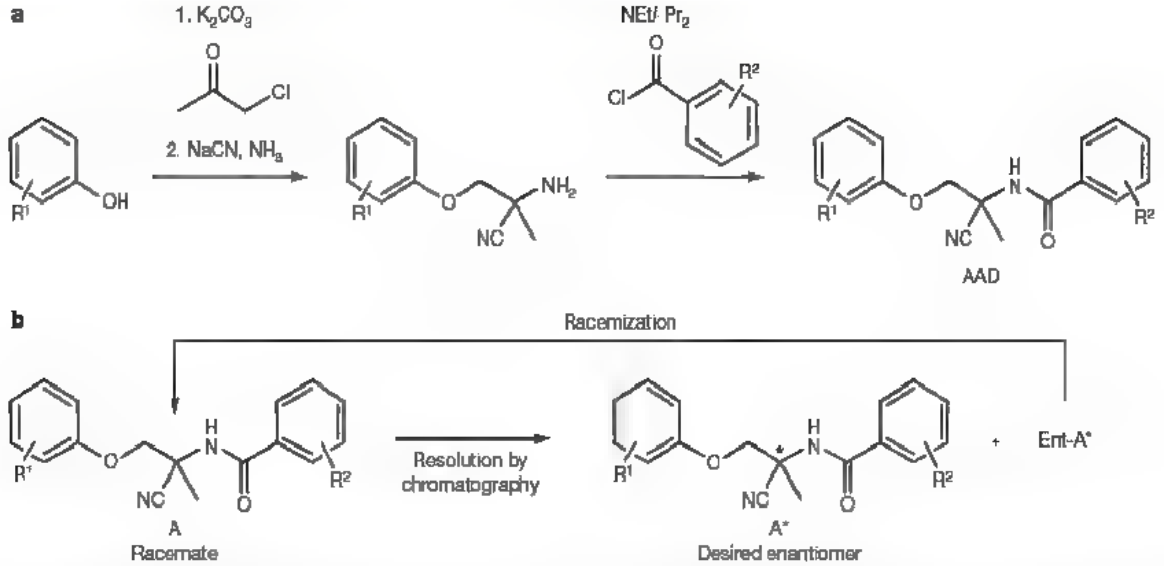


**Figure 1 | Amino-acetonitrile derivatives (AADs).** **a**, Chemical synthesis (for details see Supplementary Methods and Supplementary Fig. 1). $R^1$ and $R^2$ represent different possible chemical substituents on the phenyl rings, as detailed in figure 2. **b**, Enantiomerically pure AADs are obtained by chiral chromatography of the racemic mixtures followed by recycling of the undesired isomers via base-catalysed racemization. This route was used on a 100-g scale for AAD 1470

*H. contortus*, *T. colubriformis*, *Trichostrongylus* sp., *Oesophagostomum columbianum* and *M. expansa*. AAD 1470 eliminated all gastrointestinal nematodes (on the basis of EPGs and nematode counts at necropsy), but was ineffective against *M. expansa* and coccidia (on the basis of faecal examination). The nematicidal efficacy of AAD 1470 was further demonstrated in cattle. When treated orally at 20 mg racemate $kg^{-1}$ ($n = 3$) or topically at 40 mg racemate $kg^{-1}$ ($n = 7$), all cattle were cured from infections with adult *O. ostertagi* and *C. oncophora*.

## Pharmacokinetics and tolerability

Comparison of the pharmacokinetics in sheep showed that AADs 1336 and 1470 are eliminated more slowly than the other AADs (Fig. 3a). Unlike the situation with other molecules of the class, the pharmacokinetic disposition of AAD 1470 is not enantioselective in sheep. Therefore, the blood profiles displayed in Fig. 3b as well as the calculated pharmacokinetic parameters are valid for either enantiomer. The kinetic profile of AAD 1470 is characterized by a rather slow clearance of 0.111 $kg^{-1}$ $h^{-1}$, a very high volume of distribution ($V_{D\ area}$ of 33 l $kg^{-1}$; $V_{ss}$ of 27 l $kg^{-1}$; where $V_{D\ area}$ is the apparent volume of distribution during the terminal phase and $V_{ss}$ is the apparent volume of distribution at steady state), a rapid decline of the blood levels below 20 ng $ml^{-1}$ within 2 days owing to distribution into peripheral compartments (mainly fat) followed by a slow elimination (terminal half life of 215 h), and a good oral bioavailability of 57%.

All AADs tested were well tolerated and of low toxicity to rodents and ruminants. The micronucleus test (*in vitro*, using L5178Y mouse lymphoma cells) and Ames test screens for the racemate of AAD 450

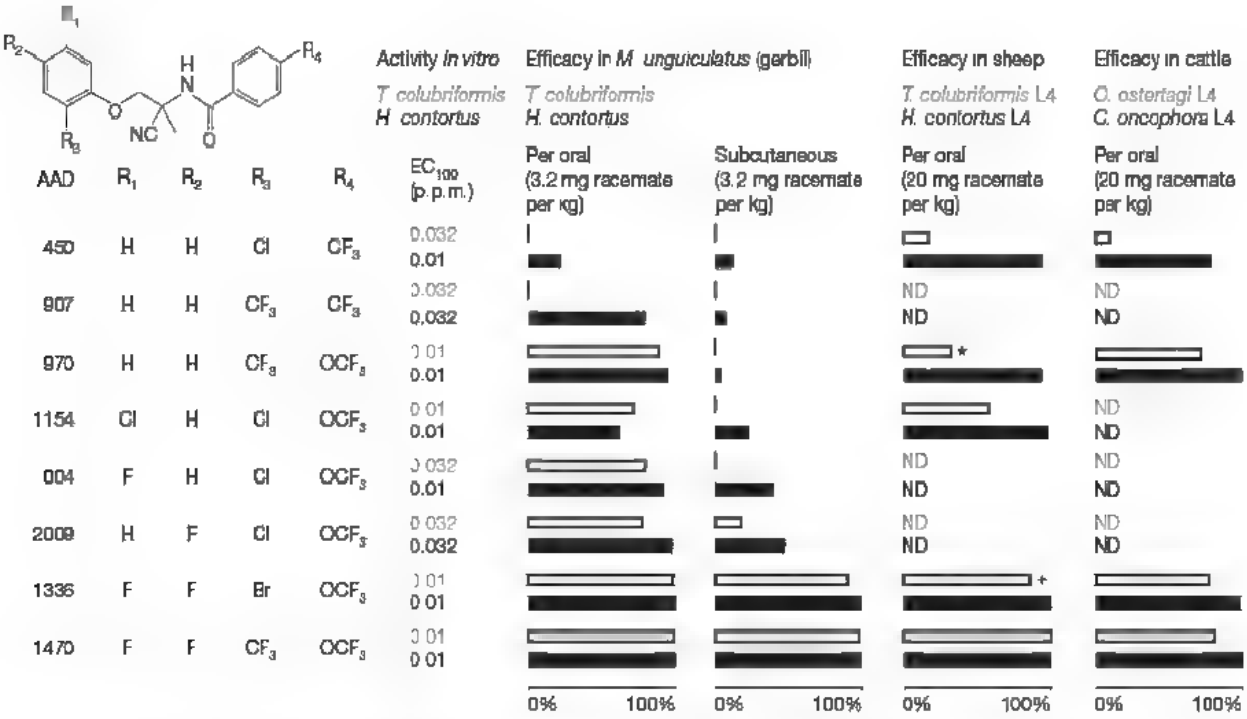


**Figure 2 | Selected AADs, their structures and the corresponding anthelmintic efficacies *in vitro* and *in vivo*.** Efficacy is given as percentage based on nematode count reduction. Asterisk, 40 mg racemate $kg^{-1}$, plus symbol, 10 mg racemate $kg^{-1}$. All compounds were fully effective in sheep against adult stages of *H. contortus* (not shown). ND, not determined.

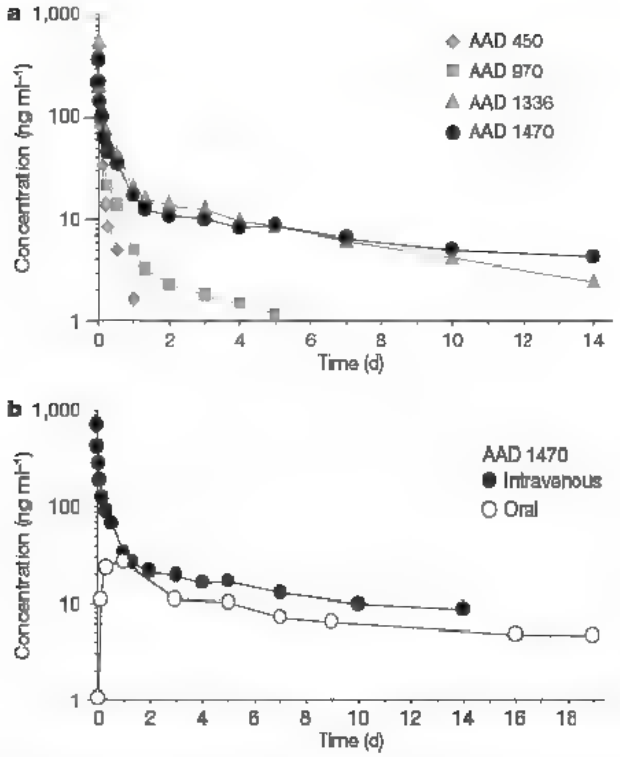


**Figure 3 | Pharmacokinetics of AADs.** **a**, Group mean blood profiles ($n = 3$) of AADs after intravenous administration as a cocktail at 0.5 mg racemate kg$^{-1}$ in sheep. **b**, Group mean ($n = 2$) blood profiles of AAD 1470 after oral application at 20 mg racemate kg$^{-1}$ and intravenous application at 0.5 mg racemate kg$^{-1}$ in sheep (both profiles normalized to 1 mg kg$^{-1}$). For the chemical structures, see Fig. 2.

and for both enantiomers of AAD 1470 revealed no clastogenic, aneugenic, or mutagenic potentials (data not shown). The oral lethal doses in rats of these compounds were above 2 g kg$^{-1}$, indicating low acute toxicity to rodents. The AADs 450, 970, 1336 and 1470 were tested in sheep up to an oral dose of 200 mg kg$^{-1}$ without any adverse clinical effects. Overall, the toxicity and tolerability studies showed that AADs are well tolerated and of low toxicity to mammals.

### Activity against drug-resistant nematodes

AADs active against parasitic nematodes also exerted marked effects on the movement, growth and viability of the free-living nematode *C. elegans*, inducing a pleiotropic combination of phenotypes distinct from the effects of any single known anthelmintic. The AADs cause hypercontraction of the body wall muscles leading to paralysis, spasmodic contractions of the anterior portion of the pharynx and ultimately death (phenotypic effects are observed at AAD 1336 or AAD 1470 concentrations of ≥50–100 ng ml$^{-1}$, with full lethality occurring above 1 μg ml$^{-1}$). Similar effects were observed for *H. contortus* (adults). AAD-exposed *C. elegans* also exhibited moulting defects and growth-arrested nematodes frequently developed large vacuoles characteristic of necrosis. Similar phenotypes were also observed after exposure of *C. elegans* to the general nicotinic agonist 1,1-dimethyl-4-phenylpiperazinium (DMPP)[10] but not to the anthelmintic levamisole, which agonizes a specific subtype of nicotinic acetylcholine receptor (nAChR)[11]. AAD 1470 showed similar activity against ivermectin-, benzimidazole- and levamisole-resistant *C. elegans* strains as against the wild-type strain (Supplementary Table 1). Notably, resistance to the AADs was not conferred by loss of any of the three required nAChR subunits of the levamisole receptor (UNC-29, UNC-38 and UNC-63; refs 12, 13).

AADs 450 and 1470 cured sheep infected with drug-resistant field isolates of *H. contortus*, *T. circumcincta* and *T. colubriformis* (Table 1), completely inhibiting egg shedding within 2 days after treatment, whereas the recommended doses of the three major classes of anthelmintics failed. AAD 1470 was effective against levamisole-, benzimidazole-, macrocyclic-lactone- and multidrug-resistant pathogenic nematodes at 10 mg racemate kg$^{-1}$ (Table 1). The resistance-breaking activities of the AADs and the unique suite of phenotypes induced in *C. elegans* suggest that these compounds act by a novel mode of action, different from those of the currently used anthelmintics.

### A unique nAChR is required for anthelmintic action

To explore further the AAD mode of action, we performed a forward genetic screen for AAD-resistant *C. elegans* mutants. Of 44 AAD-resistance alleles isolated, 36 fell into a single genetic complementation group that was mapped by genetic recombination to a ~5-map-unit interval on chromosome V. Two genes in this interval, *acr-17* and *acr-23*, encode predicted nAChR subunits. DNA sequencing of the corresponding regions from individual mutants revealed 27 independent mutations in *acr-23* (Fig. 4a and Supplementary Table 2), identifying *acr-23* as a major contributor to the AAD response in *C. elegans*. The ACR-23 protein belongs to the DEG-3 group of nAChRs, a nematode-specific subfamily that is not present in mammals[14]. Its role in AAD sensitivity is the first biological function to be described for ACR-23. The *acr-23* mutants did not exhibit any overt phenotypes other than AAD resistance and were fully susceptible to levamisole, ivermectin, benomyl, aldicarb and DMPP (Supplementary Table 3). Eleven AAD-resistance mutations result in truncation of the predicted ACR-23 protein (Fig. 4a and Supplementary Table 2) and are probably null alleles that do not produce any functional protein. The finding that high-level (>1,000-fold) AAD resistance is the major phenotype resulting from loss of functional ACR-23 protein is most simply explained by hypothesizing that AADs are direct agonists of ACR-23-containing ion channels. However, it remains possible that pathway activation results from compound interaction at another point, for example, through inhibition of a negative regulator of ACR-23.

To investigate whether related nAChRs may function in the AAD response in pathogenic nematodes, we probed for nAChR genes in *H. contortus* mutants selected for AAD resistance. Starting from the *H. contortus* isolates CRA and Howick, respectively, two independent lines were obtained by *in vitro* selection that were resistant to a full dose of AAD 1470 (2.5 mg active enantiomer per kg) in sheep. A third line, selected *in vivo* from *H. contortus* Courtion, was resistant to a one-quarter dose. Candidate nAChR genes were identified by polymerase chain reaction (PCR) with primers corresponding to conserved regions of the proteins and from the *H. contortus* genome

**Table 1 | Efficacy of AADs against adult stages of drug-resistant *H. contortus*, *T. circumcincta* and *T. colubriformis* in sheep**

| Species and isolate | Drug | Dose (oral drench) | Number of animals cured/number of animals treated |
|---|---|---|---|
| *H. contortus* | Levamisole | 7.5 mg kg$^{-1}$ | 0/2 |
| Baton Rouge | Levamisole | 15 mg kg$^{-1}$ | 0/2 |
| | AAD 450 | 10 mg racemate kg$^{-1}$ | 2/2 |
| *H. contortus* | Ivermectin | 0.2 mg kg$^{-1}$ | 1/4 |
| Howick | Levamisole | 7.5 mg kg$^{-1}$ | 1/2 |
| | AAD 1470 | 5 mg racemate kg$^{-1}$ | 6/6 |
| | AAD 1470 | 10 mg racemate kg$^{-1}$ | 2/2 |
| | Combination of: | | |
| | Ivermectin | 0.2 mg kg$^{-1}$ | 1/2 |
| | + albendazole | 3.8 mg kg$^{-1}$ | |
| | + levamisole | 7.5 mg kg$^{-1}$ | |
| *H. contortus* | Albendazole | 3.8 mg kg$^{-1}$ | 0/3 |
| Courtion | AAD 1470 | 10 mg racemate kg$^{-1}$ | 6/6 |
| *T. colubriformis* | Albendazole | 3.8 mg kg$^{-1}$ | 0/3 |
| Villarey | Levamisole | 7.5 mg kg$^{-1}$ | 0/3 |
| | AAD 1470 | 10 mg kg$^{-1}$ | 6/6 |
| *T. circumcincta* | Albendazole | 3.8 mg kg$^{-1}$ | 0/3 |
| Villarey | AAD 1470 | 10 mg kg$^{-1}$ | 6/6 |

Sheep were treated orally with commercial compounds at the recommended dose. Efficacy of all compounds was tested in parallel against a susceptible *H. contortus* isolate (data not shown). An animal was considered as cured when the EPG became negative and efficacy was >98% based on nematode count reduction at necropsy.

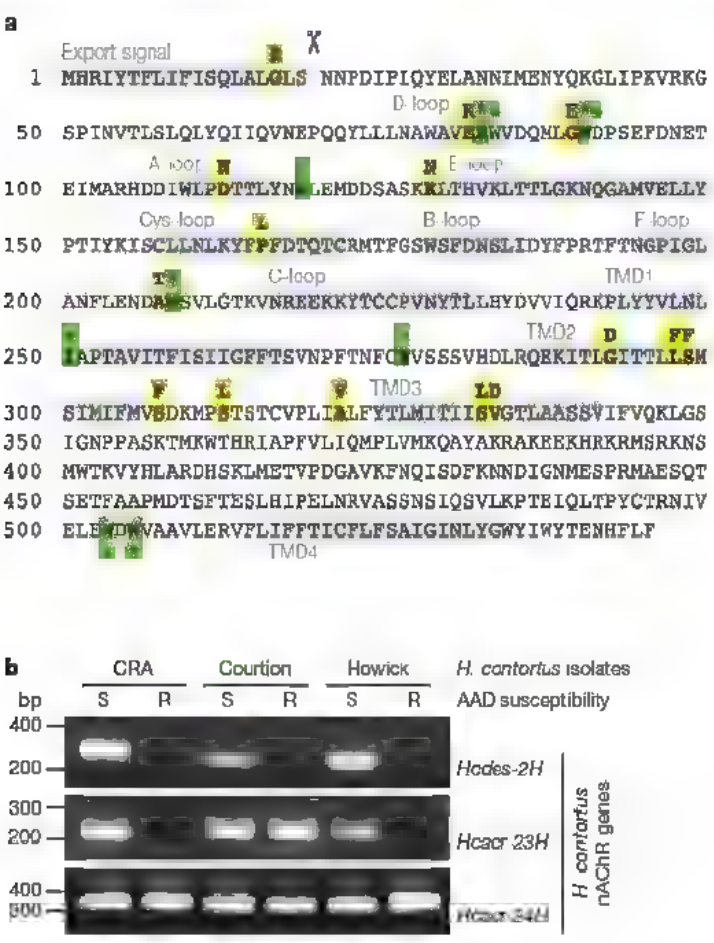


**Figure 4 | Involvement of nAChRs in AAD resistance. a**, *C. elegans* ACR-23 and mutations conferring AAD resistance (yellow, non-synonymous point mutations; green, nonsense mutations; asterisk, stop codon; hyphen, loss of splice acceptor). Conserved motifs in the extracellular ligand-binding domain[14] and transmembrane domains (TMD) are in grey. The cleavage site of the export signal is as predicted by SignalP[21]. **b**, nAChR-specific PCR products from AAD-sensitive parental *H. contortus* isolates (S) and their AAD-resistant progeny (R). bp, base pairs. **c**, Dendrogram[22] of nAChR α-subunits. The DEG-3 subfamily is highlighted in orange and members involved in AAD resistance are boxed (blue, *H. sapiens*; green, *Drosophila melanogaster*. Hc, *H. contortus*; grey bars, nomenclature of the *C. elegans* nAChR subfamilies[23]). Bootstrapping values are in per cent positives of 1,000 rounds. See Supplementary Fig. 2 for a multiple alignment of DEG-3 subfamily nAChRs from *C. elegans* and *H. contortus*.

project (http://www.sanger.ac.uk/Projects/H_contortus). All three AAD-resistant *H. contortus* mutants appeared to have lost at least part of a gene that we term *H. contortus des-2* homologue (*Hcdes-2H*; Fig. 4b) owing to its high degree of similarity (Fig. 4c) to *C. elegans des-2* (ref. 15). Like ACR-23, DES-2 belongs to the nematode-specific DEG-3 group of nAChRs. A *C. elegans* mutant lacking functional DES-2 did not exhibit AAD resistance (Supplementary Table 1). The two fully AAD-resistant mutants derived from *H. contortus* CRA and Howick had also lost at least part of the *H. contortus* homologue of *acr-23* (*Hcacr-23H*; Fig. 4b, c). No mutations were observed in the *H. contortus* homologue of *acr-24* (*Hcacr-24H*; Fig. 4b, c). The correlation of mutations in two nAChR genes of the *deg-3* subfamily with AAD resistance suggests that the hypothesized mode of action, activation of a nAChR signalling pathway, may be conserved between *C. elegans* and *H. contortus*.

## Conclusions

The optimized AAD compounds described here meet the following requirements for an urgently needed new anthelmintic for livestock: low toxicity, favourable pharmacokinetic properties and broad-spectrum efficacy against sheep and cattle nematodes. Moreover, this efficacy includes multidrug-resistant parasites owing to a presumed activation of signalling via nematode-specific DEG-3 subtype nAChRs. However, nematodes will ultimately develop resistance to any new drug, including the AADs. To secure the maximum lifespan of the AADs as well as the current anthelmintic drugs, monitoring of drug resistance and rational exploration of combinations with current or future drugs will be necessary. If the excellent tolerability of the AADs in ruminants can be proven for humans, the class may offer an alternative anthelmintic for human medical practice.

## METHODS SUMMARY

Anthelmintic efficacy tests in sheep and cattle were performed according to the guidelines of the World Association for the Advancement of Veterinary Parasitology[16]. Anthelmintic efficacy in *M. unguiculatus* was determined by nematode-count reduction after necropsy 3 days after treatment. *In vitro* activity on parasitic nematodes was assessed according to ref. 17 with minor modifications. For *C. elegans* bioassays, synchronously staged L1 hermaphrodite larvae were seeded on agar medium plus test compounds and incubated for 3 days, monitoring movement and viability. Endpoints were nematode growth and development.

Forty-three AAD-resistant *C. elegans* mutants were obtained after ethane methyl sulphonate (EMS) mutagenesis[18], one (*cb27*) was recovered spontaneously. The *cb27* mutation is semi-dominant and mapped[19] to a genetic interval between −12 and −7 on chromosome V. Candidate genes therein were amplified by PCR and sequenced, revealing a deletion in *acr-23*. The *acr-23* genomic sequence was determined for all EMS-induced AAD-resistant mutants, and all the mutations were tested for complementation of *cb27*.

*H. contortus* isolates CRA (drug-sensitive reference strain from South Africa), Courtion (field isolate from Switzerland) and Howick (multidrug resistant isolate from South Africa[20]) were maintained in sheep. *In vitro* selection for AAD resistance was performed by allowing eggs to develop to L3 larvae under drug pressure. Surviving larvae were used to re-infect sheep. AAD resistance was obtained after eight such cycles. *H. contortus* nAChR homologues were amplified by PCR from genomic DNA isolated from L3 larvae.

**Full Methods** and any associated references are available in the online version of the paper at www.nature.com/nature.

**Received 8 June 2007; accepted 15 January 2008.**


1. De Clercq, D. *et al.* Failure of mebendazole in treatment of human hookworm infections in the southern region of Mali. *Am. J. Trop. Med. Hyg.* 57, 25–30 (1997)
2. Geerts, S. & Gryseels, B. Drug resistance in human helminths: current situation and lessons from livestock. *Clin. Microbiol. Rev.* 13, 207–222 (2000)
3. Awadzi, K. *et al.* An investigation of persistent microfilarmias despite multiple treatments with ivermectin, in two onchocerciasis-endemic foci in Ghana. *Ann. Trop. Med. Parasitol.* 98, 231–249 (2004)
4. Osei-Atweneboana, M. Y., Eng, J. K., Boakye, D. A., Gyapong, J. O. & Prichard, R. K. Prevalence and intensity of *Onchocerca volvulus* infection and efficacy of ivermectin in endemic communities in Ghana: a two-phase epidemiological study. *Lancet* 369, 2021–2029 (2007)
5. Waller, P. J. Anthelmintic resistance. *Vet. Parasitol.* 72, 391–412 (1997).
6. Jackson, F. & Coop, R. L. The development of anthelmintic resistance in sheep nematodes. *Parasitology* 120 (suppl.), S95–S107 (2000)
7. Kaplan, R. M. Drug resistance in nematodes of veterinary importance: a status report. *Trends Parasitol.* 20, 477–481 (2004)
8. Besier, B. New anthelmintics for livestock: the time is right. *Trends Parasitol.* 23, 21–24 (2007)
9. Wolstenholme, A. J., Fairweather, I., Prichard, R., von Samson-Himmelstjerna, G. & Sangster, N. C. Drug resistance in veterinary helminths. *Trends Parasitol.* 20, 469–476 (2004)
10. Ruaud, A. F. & Bessereau, J. L. Activation of nicotinic receptors uncouples a developmental timer from the molting timer in *Caenorhabditis elegans*. *Development* 133, 2211–2222 (2006)
11. Rand, J. B. Acetylcholine. In *WormBook* (ed. The *C. elegans* Research Community) doi/10.1895/wormbook.1.131.1 (http://www.wormbook.org) (30 January 2007).
12. Fleming, J. T. *et al.* *Caenorhabditis elegans* levamisole resistance genes *lev-1*, *unc-29*, and *unc-38* encode functional nicotinic acetylcholine receptor subunits. *J. Neurosci.* 17, 5843–5857 (1997)
13. Culetto, E. *et al.* The *Caenorhabditis elegans unc-63* gene encodes a levamisole-sensitive nicotinic acetylcholine receptor α subunit. *J. Biol. Chem.* 279, 42476–42483 (2004)
14. Mongan, N. P., Jones, A. K., Smith, G. R., Sansom, M. S. & Sattelle, D. B. Novel α7-like nicotinic acetylcholine receptor subunits in the nematode *Caenorhabditis elegans*. *Protein Sci.* 11, 1162–1171 (2002).
15. Treinin, M., Gillo, B., Liebman, L. & Chalfie, M. Two functionally dependent acetylcholine subunits are encoded in a single *Caenorhabditis elegans* operon. *Proc. Natl Acad. Sci. USA* 95, 15492–15495 (1998)
16. Wood, I. B. *et al.* World Association for the Advancement of Veterinary Parasitology (W.A.A.V.P.) second edition of guidelines for evaluating the efficacy of anthelmintics in ruminants (bovine, ovine, caprine). *Vet. Parasitol.* 58, 181–213 (1995)
17. Boisvenue, R. J., Brandt, M. C., Galloway, R. B. & Hendrix, J. C. *In vitro* activity of various anthelmintic compounds against *Haemonchus contortus* larvae. *Vet. Parasitol.* 13, 341–347 (1983)
18. Anderson, P. Mutagenesis. *Methods Cell Biol.* 48, 31–58 (1995).
19. Wicks, S. R., Yeh, R. T., Gish, W. R., Waterston, R. H. & Plasterk, R. H. Rapid gene mapping in *Caenorhabditis elegans* using a high density polymorphism map. *Nature Genet.* 28, 160–164 (2001)
20. van Wyk, J. A. & Malan, F. S. Resistance of field strains of *Haemonchus contortus* to ivermectin, closantel, rafoxanide and the benzimidazoles in South Africa. *Vet. Rec.* 123, 226–228 (1988)
21. Bendtsen, J. D., Nielsen, H., von Heijne, G. & Brunak, S. Improved prediction of signal peptides: SignalP 3.0. *J. Mol. Biol.* 340, 783–795 (2004)
22. Thompson, J. D., Higgins, D. G. & Gibson, T. J. CLUSTAL W: improving the sensitivity of progressive multiple sequence alignment through sequence weighting, position-specific gap penalties and weight matrix choice. *Nucleic Acids Res.* 22, 4673–4680 (1994)
23. Jones, A. K., Davis, P., Hodgkin, J. & Sattelle, D. B. The nicotinic acetylcholine receptor gene family of the nematode *Caenorhabditis elegans*: an update on nomenclature. *Invert. Neurosci.* 7, 129–131 (2007)


**Supplementary Information** is linked to the online version of the paper at www.nature.com/nature.

**Acknowledgements** We thank F. Schroeder, E. Pradervand, S. Mulhauser, J. Lambert, D. Mosimann and A. Kazimi for technical assistance, C. Johnson for providing an ivermectin-resistant *C. elegans* strain, and C. Kempter for support on chemical characterization of AADs. We also thank S. Nanchen, B. Hosking, A. Redpath and R. Steiger for thorough review of and comments on the manuscript. P.M. is supported by the Swiss National Science Foundation.

**Author Information** *Hcdes-2H* sequences have been deposited in GenBank under accession numbers EF659746–EF659760. Reprints and permissions information is available at www.nature.com/reprints. The authors declare competing financial interests; details accompany the full-text HTML version of the paper at www.nature.com/nature. Correspondence and requests for materials should be addressed to R.K. (ronald.kaminsky@novartis.com).

ARTICLES

# Pyruvate kinase M2 is a phosphotyrosine-binding protein

Heather R. Christofk[1], Matthew G. Vander Heiden[1,3], Ning Wu[1], John M. Asara[2,4] & Lewis C. Cantley[1,4]

**Growth factors stimulate cells to take up excess nutrients and to use them for anabolic processes. The biochemical mechanism by which this is accomplished is not fully understood but it is initiated by phosphorylation of signalling proteins on tyrosine residues. Using a novel proteomic screen for phosphotyrosine-binding proteins, we have made the observation that an enzyme involved in glycolysis, the human M2 (fetal) isoform of pyruvate kinase (PKM2), binds directly and selectively to tyrosine-phosphorylated peptides. We show that binding of phosphotyrosine peptides to PKM2 results in release of the allosteric activator fructose-1,6-bisphosphate, leading to inhibition of PKM2 enzymatic activity. We also provide evidence that this regulation of PKM2 by phosphotyrosine signalling diverts glucose metabolites from energy production to anabolic processes when cells are stimulated by certain growth factors. Collectively, our results indicate that expression of this phosphotyrosine-binding form of pyruvate kinase is critical for rapid growth in cancer cells.**

Metabolic regulation in rapidly growing tissues such as fetal tissues and tumours is different from that in most adult tissues. Rapidly growing cells must take up nutrients at a high rate and maintain a balance between utilization of nutrients for energy production (for example, ATP synthesis) and for anabolic processes (for example, protein, lipid and nucleic acid synthesis). In contrast, most adult tissues require less nutrient uptake and use a greater fraction of available nutrients for energy production rather than macromolecule synthesis. This difference between metabolism of cancer cells and normal adult tissues was first pointed out by Warburg in 1929[1], who observed that cancer cells take up glucose at higher rates than normal tissue but use a smaller fraction of this glucose for oxidative phosphorylation, even when oxygen is not limiting. This effect, called aerobic glycolysis or the Warburg effect, is thought to be due to the reprogramming of metabolic genes to allow cancer cells to function more like fetal cells and to enable a greater fraction of glucose metabolites to be incorporated into macromolecule synthesis rather than burned to $CO_2$.

More recent studies have shown that growth factor signalling pathways have a major role in programming metabolic pathways in cells by mediating long-term[2,3] as well as acute[4] changes in cell metabolism. Paradoxically, there are reports that activation of protein-tyrosine kinases results in a decrease in the specific activity of pyruvate kinase, the enzyme that catalyses the penultimate step in glycolysis; that is, conversion of phosphoenolpyruvate to pyruvate[5,6]. The mechanism by which protein-tyrosine kinases affect the activity of pyruvate kinase has been controversial. Pyruvate kinase as well as several other enzymes involved in glycolysis (including enolase and lactate dehydrogenase) are phosphorylated on tyrosine residues in cancer cells[7,8], and it has been argued that the inhibition of pyruvate kinase observed in cells with activated protein-tyrosine kinases could be explained by direct tyrosine phosphorylation[9,10]. However, others have argued that the stoichiometry of tyrosine phosphorylation of pyruvate kinase (and of other glycolytic enzymes) is too low to affect catalytic activity. Here we present a novel mechanism to explain how protein-tyrosine kinases acutely regulate the activity of pyruvate kinase.

## Screen identifies PKM2 as a pTyr binding protein

We used a proteomic screening approach to identify novel phosphotyrosine (pTyr)-binding proteins from cell lysates (Fig. 1a). Using SILAC, stable isotope labelling of amino acids in cell culture[11], we prepared lysates from HeLa cells grown in either heavy isotopic $^{13}C$-arginine and $^{13}C$-lysine or normal isotopic $^{12}C$-arginine and $^{12}C$-lysine. 'Heavy' lysates were flowed over a phosphotyrosine peptide library affinity matrix, and 'light' lysates were flowed over a corresponding unphosphorylated peptide library affinity matrix. Bound proteins were eluted with sodium phenylphosphate, digested with trypsin, and the peptides were analysed by microcapillary liquid chromatography tandem mass spectrometry (LC-MS/MS). As shown in Fig. 1b, most of the proteins identified had peptides that yielded ~1:1 SILAC heavy to light ratios, thus indicating equal binding to the phosphotyrosine and tyrosine peptide matrices. As a validation of the approach, several proteins that contain well-characterized phosphotyrosine-binding domains were identified as showing >3:1 SILAC ratios, consistent with preferential binding to the phosphotyrosine peptide library affinity matrix. Surprisingly, despite the absence of a known phosphotyrosine-binding domain, pyruvate kinase exhibited a ≥15:1 SILAC heavy:light ratio, identifying it as a candidate novel phosphotyrosine-binding protein.

As validation of the phosphotyrosine-binding property of pyruvate kinase, lysates from HeLa cells were passed over the phosphotyrosine and tyrosine peptide library affinity matrices, and eluates were analysed by SDS–polyacrylamide gel electrophoresis (PAGE). LC-MS/MS analysis of those proteins visible by silver stain that selectively bound to the phosphotyrosine peptide library matrix also identified known phosphotyrosine-binding proteins as well as pyruvate kinase (Fig. 1c). To confirm the preferential binding of pyruvate kinase to the phosphotyrosine peptide affinity matrix, eluates from the phosphotyrosine and tyrosine peptide library columns were analysed by western blot using a pyruvate kinase antibody (Fig. 1d). p85, the SH2-domain-containing regulatory subunit of phosphatidylinositol-3 kinase, is used as a positive control, and GAPDH is used as a negative control. As shown in Fig. 1d, immunoblotting for both p85 and pyruvate kinase shows selective binding to the phosphotyrosine

[1]Department of Systems Biology, [2]Department of Pathology, Harvard Medical School, Boston, Massachusetts 02115, USA. [3]Dana Farber Cancer Institute, Boston, Massachusetts 02115, USA. [4]Division of Signal Transduction, Beth Israel Deaconess Medical Center, Boston, Massachusetts 02115, USA.

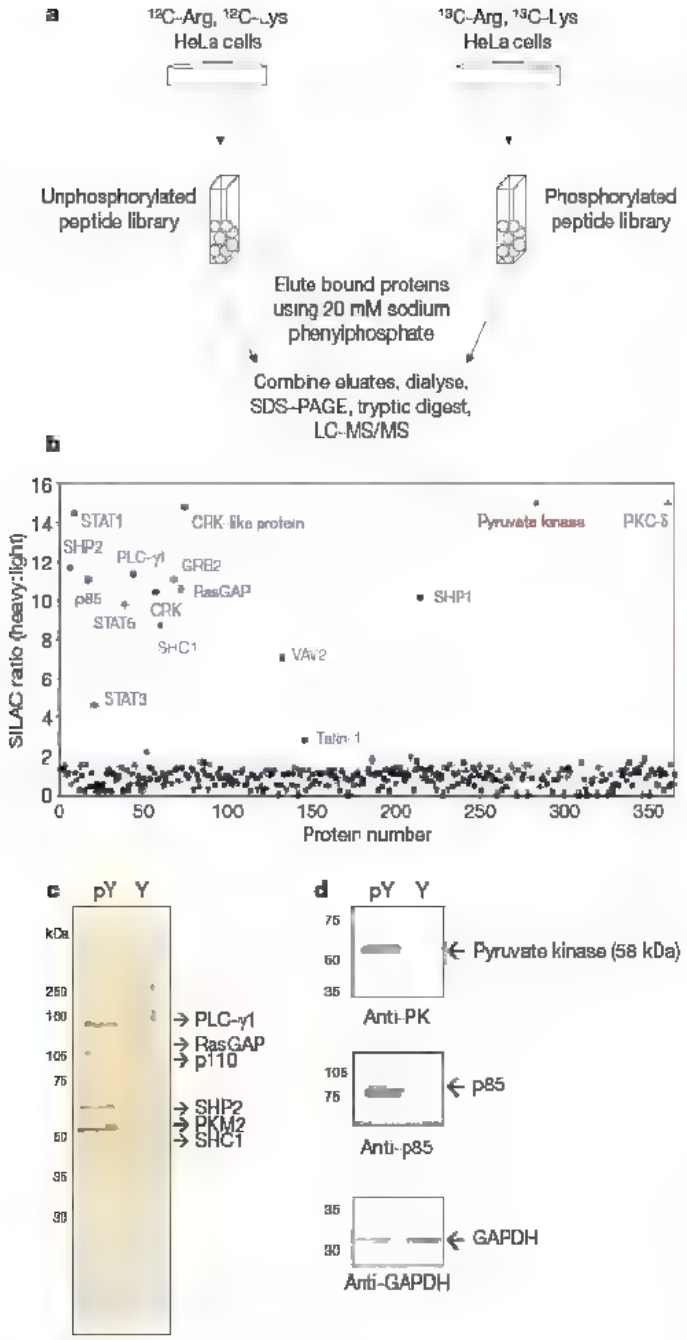


**Figure 1 | Proteomic screen identifies pyruvate kinase as a novel phosphotyrosine-binding protein. a**, A schematic diagram of the proteomic screen for phosphotyrosine binding proteins using SILAC and peptide library affinity matrices. The peptide libraries were designed as follows: phosphorylated peptide library (pY), biotin-Z-Z-Gly-Gly-Gly-X-X-X-X-X-pTyr-X-X-X-X-X-Gly-Gly; unphosphorylated peptide library (Y), biotin-Z-Z-Gly-Gly-Gly-X-X-X-X-X-Tyr-X-X-X-X-X-Gly-Gly, where Z indicates aminohexanoic acid and X denotes any amino acid except cysteine. Peptide libraries were incubated with streptavidin beads and packed onto columns to form the phosphotyrosine and tyrosine peptide library affinity matrices. Heavy lysates were flowed over the phosphotyrosine column, and light lysates were flowed over the tyrosine column. Bound proteins were eluted with 20 mM sodium phenylphosphate, digested with trypsin, and then analysed by microcapillary reversed-phase tandem mass spectrometry (LC-MS/MS). **b**, Screen results using commercially available software showing the SILAC ratios (heavy:light) for the proteins identified by LC-MS/MS. Background proteins yielded ~1:1 SILAC ratios. Known phosphotyrosine-binding proteins (blue) yielded >3:1 SILAC ratios. Pyruvate kinase (red) yielded a ≥15:1 SILAC ratio, identifying it as a candidate novel phosphotyrosine binder. **c**, A silver stain of proteins from HeLa cell lysates that bound to the phosphotyrosine compared with tyrosine peptide library columns. Differentially stained proteins identified by LC-MS/MS are indicated. **d**, Immunoblotting of proteins from HeLa cell lysates that bound to the phosphotyrosine versus tyrosine peptide library columns. Eluates from the columns were immunoblotted with antibodies for pyruvate kinase, p85 as a positive control, and GAPDH as a negative control.

peptide library matrix. Notably, whereas pyruvate kinase exhibited selective binding to the immobilized phosphotyrosine peptide library, it did not show selective binding to immobilized phosphoserine or phosphothreonine peptide libraries (Supplementary Fig. 1).

### pTyr binding is specific to pyruvate kinase isoform M2

Four pyruvate kinase isoforms exist in mammals: L, liver; R, red blood cell; M1, adult; and M2, embryonic/tumour[12] (Fig. 2a). The M1, M2 and L isoforms were transiently expressed as Flag-tagged proteins in 293 cells, and lysates were flowed over the phosphotyrosine and tyrosine peptide affinity columns to assess binding. Eluates from the columns were analysed by western blot using a Flag antibody (Fig. 2b). The M2 isoform is the only pyruvate kinase isoform that binds phosphotyrosine peptides. Given that PKM1, the splice variant of PKM2, does not bind to phosphotyrosine peptides, we looked to the crystal structures of these isoforms for a potential phosphotyrosine-binding site on PKM2. PKM1 and PKM2 are identical proteins with the exception of a 56-amino-acid stretch encoded by the alternatively spliced region. Previous studies have shown that this stretch of amino acids comprises the only structural difference between the M1 and M2 isoforms and forms an allosteric pocket unique to PKM2 that allows for binding of its activator, FBP[13].

To determine whether the FBP-binding pocket on PKM2 coordinates phosphotyrosine peptide binding, we assessed whether FBP could compete for binding of PKM2 to a phosphotyrosine peptide library column. Recombinant PKM2 was incubated with increasing amounts of FBP and then flowed over the phosphotyrosine peptide affinity matrix. A concentration of 20 μM FBP was able to compete for binding of recombinant PKM2 to phosphotyrosine peptides (Fig. 2c). To examine further how this region of PKM2 interacts with phosphotyrosine, point mutants of various residues in and around

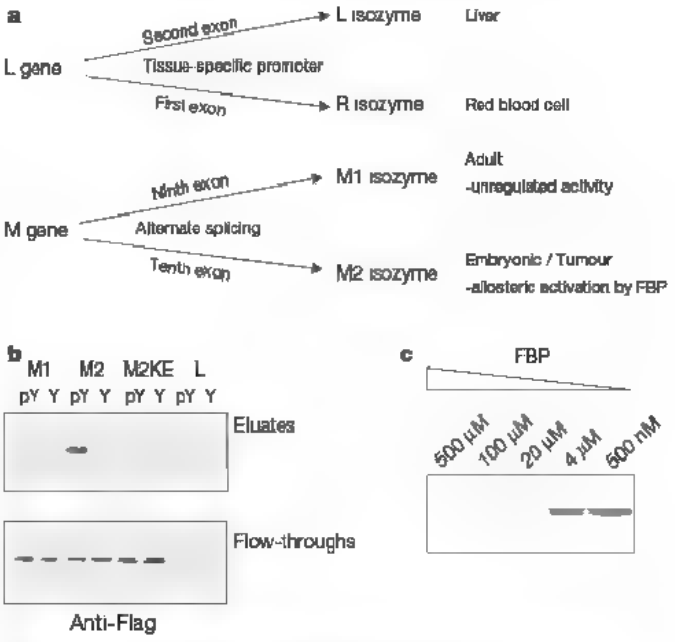


**Figure 2 | Phosphopeptide binding is specific to the M2 isoform of pyruvate kinase and involves lysine 433 near the FBP binding pocket. a**, A schematic diagram of the four mammalian pyruvate kinase isoforms. **b**, Immunoblotting showing the pyruvate kinase isoform specificity of phosphotyrosine binding. The M1, M2, M2KE and L Flag-tagged pyruvate kinase isoforms were transiently expressed in 293 cells, and lysates were flowed over the phosphotyrosine (pY) and tyrosine peptide library columns. The flow-throughs and eluates from the columns were immunoblotted with Flag antibody. Note that M2KE stands for the K433E point mutant of PKM2. **c**, A Coomassie stain of PKM2 bound to the phosphotyrosine peptide library column after incubation with increasing amounts of FBP. Recombinant PKM2 was incubated with increasing concentrations of FBP as indicated, before being flowed over and eluted from the phosphotyrosine peptide library affinity matrix with sodium phenylphosphate.

the FBP-binding pocket of PKM2 were constructed. Whereas mutation of residues within the FBP-binding pocket of PKM2 did not affect phosphotyrosine peptide binding (data not shown), mutation of lysine 433—located within the unique region of PKM2, which lies at the lip of the pocket—to glutamate abolished phosphotyrosine peptide binding (Fig. 2b). Note that the K433E (KE) point mutant of PKM2 that lacks phosphotyrosine peptide binding ability still gets activated by FBP to a similar degree as the wild-type protein (Supplementary Fig. 2). These data suggest that phosphotyrosine peptides are binding to PKM2 near the FBP-binding pocket of the enzyme and that lysine 433 is important for this interaction.

To examine the allosteric FBP-binding pocket of PKM2 more closely, we used X-ray crystallography to re-solve the structures of both the *apo*-form (2.5 Å) as well as the FBP-bound form (2 Å) of PKM2. Both forms crystallized as tetramers in the asymmetric units under physiological pH, with $Mg^{2+}$ and oxalate in the active sites (Supplementary Table 1). In the *apo* crystal, the residues around the FBP-binding pocket are not well ordered. In particular, loop W515–G520 has no visible electron density. In comparison, FBP is found in all four allosteric sites in the complex crystal (Fig. 3a), and its presence stabilizes many residue side chains including the W515–G520 loop, K433 and W482 (Fig. 3b). In the FBP-bound form of PKM2, the W515–G520 loop and other side chains are closed down on the FBP molecule, and only the P1 phosphate group of FBP is solvent accessible (Fig. 3c). These differences between the two structures are not unexpected, however, it was surprising to find FBP bound in any of the crystals as no FBP was added during any stage of protein purification. The fact that ~50% of PKM2 still retained FBP after affinity purification, dialysis and size exclusion column chromatography suggests that the release of FBP from the protein is very slow.

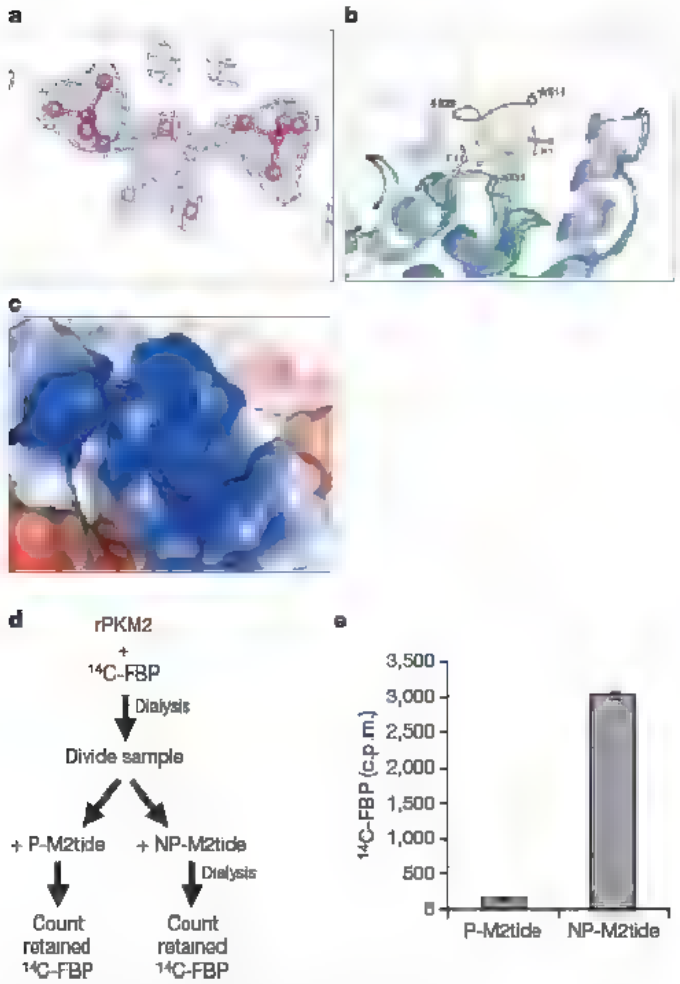


**Figure 3 | Phosphotyrosine peptide catalyses the release of FBP from PKM2.** **a**, Representative composite omit $2F_o - F_c$ electron density for FBP contoured at the 1.2 σ level. **b**, A close up of the allosteric pocket of PKM2 showing an overlay of the FBP-bound form (blue) and the *apo*-bound form (green). The flexible FBP activation loop including residues W515–G520 is structured in the FBP-bound form of PKM2, but not in the *apo* form of PKM2. **c**, Surface electrostatic potential of the FBP binding pocket in the same orientation as in **b**. The bound FBP is completely enclosed by the protein except for the P1 phosphate group. Basic moieties on the protein surface are shown in blue; acidic moieties are shown in red. **d**, A schematic diagram of the experiment to test the effect of phosphotyrosine peptide binding on FBP release from PKM2. First, recombinant PKM2 was soaked in $^{14}$C-FBP, and unbound FBP was removed by dialysis. Then the FBP-loaded PKM2 was incubated with P-M2tide or NP-M2tide, and the unbound FBP was removed by dialysis. $^{14}$C-FBP retained on PKM2 was measured using a scintillation counter. **e**, $^{14}$C scintillation counts retained on the recombinant PKM2 after exposure to P-M2tide versus NP-M2tide. Error bars denote s.e.m. ($n = 3$)

Published $K_d$ (dissociation constant) values for FBP binding to PKM2 are in the micromolar range[14]; however, FBP concentrations after protein purification would be orders of magnitude lower than this value. Our attempts to measure the dissociation constant based on Michaelis–Menten kinetics have suggested that FBP binding to PKM2 is nonlinear. To test the hypothesis suggested by the above structural studies that FBP binds tightly to PKM2, we soaked recombinant PKM1 and PKM2 in $^{14}$C-FBP, removed unbound FBP by dialysis, and measured the $^{14}$C-FBP retained on the proteins by scintillation counting. After dialysis overnight, the PKM1 sample had the same amount of $^{14}$C-FBP as the no-protein control sample. In contrast, the PKM2 sample exhibited 52 ± 5% more $^{14}$C counts than both the PKM1 sample and the no-protein control. On further analysis we have estimated that $^{14}$C-FBP is retained at roughly half a mole per mole on the PKM2 protein. Because 50% of the recombinant protein already had bacterial FBP bound, these results are consistent with the retained $^{14}$C-FBP being tightly bound to the protein.

### pTyr peptide catalyses the release of FBP from PKM2

To examine the effect of phosphotyrosine peptide binding on FBP-bound PKM2, we obtained a peptide binding motif for PKM2 using traditional peptide library screening, and synthesized both the phosphorylated and unphosphorylated versions of the optimal peptide: P-M2tide (GGAVDDDpYAQFANGG) and NP-M2tide (GGAVDDDYAQFANGG), respectively (Supplementary Fig. 3). We then incubated our $^{14}$C-FBP-loaded recombinant PKM2 with P-M2tide or NP-M2tide, dialysed away unbound FBP and peptide, and measured the counts retained on PKM2 (Fig. 3d). Exposure of PKM2 to the control NP-M2tide resulted in a significant amount of FBP remaining bound to PKM2. In contrast, exposure of PKM2 to the P-M2tide resulted in release of the majority of the FBP (Fig. 3e). These results indicate that phosphotyrosine peptide binding catalyses the release of FBP from PKM2.

Next we tested whether phosphotyrosine protein binding can catalyse the release of FBP from PKM2 in cells. To address this, we cultured cells overnight with $^{3}$H-glucose that can be metabolized to $^{3}$H-FBP. We then immunoprecipitated Flag-tagged PKM2, and determined the amount of $^{3}$H bound to PKM2 with and without pervanadate treatment by scintillation counting. Increasing the levels of phosphotyrosine proteins by a 15-min treatment with pervanadate resulted in a 30 ± 13% reduction in $^{3}$H that immunoprecipitated with PKM2. These results support the hypothesis that phosphotyrosine protein binding can catalyse the release of FBP from PKM2 *in vivo*.

### pTyr binding results in inhibition of PKM2 activity

To examine the effect that phosphotyrosine peptide binding has on PKM2 activity, we incubated increasing amounts of P-M2tide and NP-M2tide with recombinant PKM2 and measured the enzyme activity. As shown in Fig. 4a, P-M2tide exposure causes a 20–30% inhibition of PKM2 activity in a dose-dependent manner. Multiple phosphotyrosine peptides comprising *in vivo* phosphorylation sites previously identified on metabolic proteins[15] were synthesized

(Supplementary Table 2). Several of these phosphotyrosine peptides, as well as multiple phosphotyrosine peptides designed after known tyrosine kinase motifs, were also shown to inhibit PKM2 activity (Fig. 4b). Notably, the Src kinase motif, along with the *in vivo* Src kinase sites on enolase and lactate dehydrogenase, were able to inhibit PKM2 activity *in vitro*. Consistent with a catalytic FBP-release mechanism of P-M2tide enzyme inhibition, longer exposures of P-M2tide to recombinant PKM2 consistently result in greater decreases in PKM2 activity (data not shown). In addition, as little as 1 μM phosphotyrosine peptide can inhibit PKM2 activity, suggesting that a meaningful interaction between PKM2 and tyrosine-phosphorylated proteins can occur at the concentrations present in cells (Fig. 4a)

To address further whether PKM2 activity can be regulated by tyrosine phosphorylation levels in cells, we elevated phosphotyrosine levels in various cell lines by pervanadate stimulation, and measured pyruvate kinase activity. As shown in Fig. 4c, pervanadate stimulation in three different cancer cell lines resulted in a 20–30% decrease in total pyruvate kinase activity. To assess whether tyrosine kinase intracellular signalling could regulate PKM2 activity in cells, we tested the effects of overexpressing a tyrosine kinase and stimulating an RTK signalling pathway. Transient overexpression of constitutively active Src kinase in 293 cells resulted in inhibition of PKM2 activity (Fig. 4d). Additionally, acute stimulation of tyrosine kinase signalling by insulin-like growth factor (IGF) stimulation in A549 cells resulted in inhibition of PKM2 activity (Fig. 4e). Consistent with earlier studies from Eigenbrodt and co-workers[5], our data show that conditions that activate protein-tyrosine kinases in cells in culture result in an acute ~15% to 30% reduction in the activity of pyruvate kinase.

Cancer cell lines exclusively express the M2 isoform of pyruvate kinase[5]. However, to confirm that the decrease in pyruvate kinase activity on increasing phosphotyrosine levels was specific to the M2 isoform of pyruvate kinase and that it depended on the ability of PKM2 to bind to phosphotyrosine peptides, we constructed cell lines that express the M1, M2, L, or M2KE (phosphotyrosine-binding mutant) forms of pyruvate kinase (Fig. 4f). We made stable H1299 cells that express Flag-tagged mouse M1, M2, M2KE, or L, and then stably knocked down the endogenous (human) PKM2 using short hairpin (sh)RNA expression. As shown in Fig. 4f, we obtained efficient knockdown of the endogenous PKM2, and the Flag-tagged rescue proteins were expressed to similar, near endogenous, levels. Increased phosphotyrosine levels observed on pervanadate stimulation of the M1-, M2-, M2KE- and L-expressing knockdown cells resulted in specific inhibition of pyruvate kinase activity only in the wild-type M2-expressing cells (Supplementary Fig. 4 and Fig. 4g). Together, these data suggest that the regulation of pyruvate kinase activity by phosphotyrosine levels in cells is specific to the M2 isoform and requires the phosphotyrosine peptide binding capability. Similar results were also obtained in A549 cells (data not shown).

### Cell growth requires the pTyr-binding function of PKM2

To determine whether regulation of PKM2 activity by phosphotyrosine peptide binding has a biological role in the cell, we assessed the ability of the phosphotyrosine-binding mutant, M2KE, to rescue M2 knockdown in cancer cell lines. Knockdown of PKM2 expression in H1299 lung cancer cells results in reduced glycolysis and decreased cell proliferation (Fig. 5a, b). Both the wild-type mouse M2 and mouse M2KE rescue pyruvate kinase activity (data not shown) and

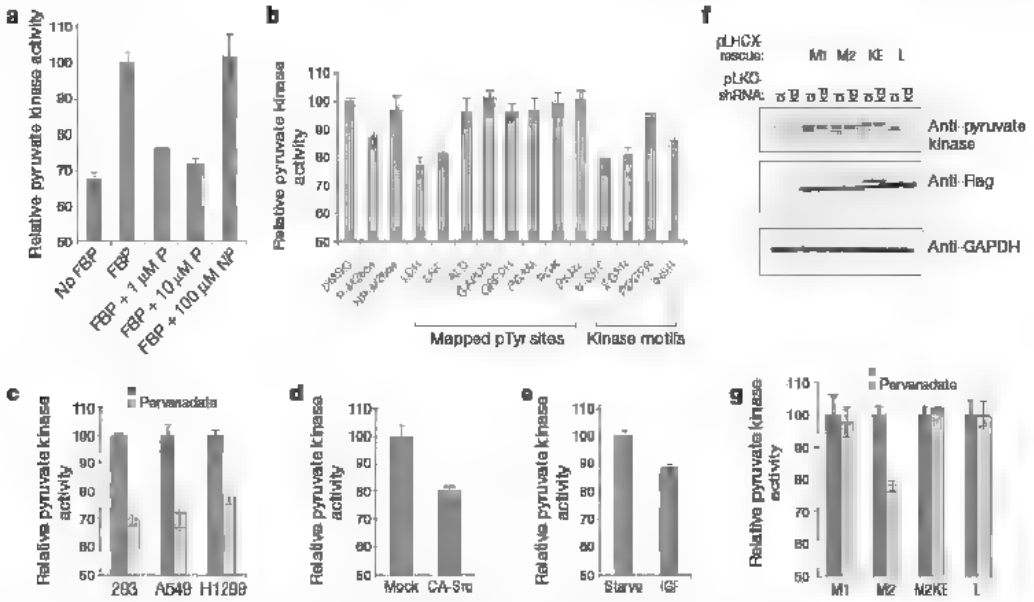


**Figure 4 | Phosphopeptide binding results in inhibition of PKM2 activity.** **a**, Comparison of pyruvate kinase activity in the presence of FBP, P-M2tide (P) and NP-M2tide (NP). Recombinant PKM2 was soaked in FBP, unbound FBP was removed by dialysis, and then 1 μM P-M2tide, 10 μM P-M2tide, or 100 μM NP-M2tide was added to the enzyme. After a 30-min incubation at room temperature, unbound FBP and peptide were removed by dialysis, and pyruvate kinase activity was assessed. **b**, Comparison of pyruvate kinase activity in the presence of various phosphotyrosine peptides. FBP-soaked recombinant PKM2 was incubated with 10 μM peptide for 10 min at room temperature and pyruvate kinase activity was assessed. Eight of the phosphopeptides tested comprised previously mapped phosphotyrosine sites on the metabolic proteins indicated. Four of the phosphopeptides tested were designed after known tyrosine kinase motifs. Because all of the peptides were dissolved in DMSO, DMSO was used as a negative control. **c**, Comparison of pyruvate kinase activity in lysates from 293, A549 and H1299 cells with and without ( ) pervanadate stimulation. **d**, Comparison of pyruvate kinase activity in lysates from 293 cells that were mock-transfected (mock) or transiently transfected with constitutively active Src kinase (CA-Src). **e**, Comparison of pyruvate kinase activity in lysates from A549 cells serum-starved overnight without (starve) or with 15 min of 20 nM IGF stimulation (IGF). **f**, Immunoblotting of lysates from H1299 cells stably expressing shRNA constructs and rescue constructs. Cells were infected with retrovirus containing the empty vector (pLHCX), or pLHCX with Flag-tagged mouse PKM1 (M1), mouse PKM2 (M2), mouse PKM2 KE point mutant (KE), or PKL (L). After 2 weeks selection in hygromycin, the cells were infected with lentivirus containing the pLKO vector with control shRNA (cl) or shRNA that knocks down PKM2 expression (kd). The cells were then selected in puromycin for 1 week. Total cell extracts were immunoblotted with antibodies for pyruvate kinase (recognizes both M1 and M2), Flag and GAPDH. Note that PKL is not recognized by the pyruvate kinase antibody. **g**, Comparison of pyruvate kinase activity in lysates from H1299 cells expressing knockdown shRNA and Flag–PKM1, PKM2, PKM2 KE and PKL with and without pervanadate stimulation. All scale bars denote s.e.m. ($n = 3$). In all cases, the changes in pyruvate kinase activity were significant as assessed by Student's *t*-test ($P < 0.01$).

glycolysis in PKM2 knockdown cells (Fig. 5a). Flow cytometry analysis indicates similar cell death, cell size and cell cycle profiles in the M2- and M2KE-expressing knockdown cells (data not shown). However, unlike the wild-type mouse M2, the mouse M2KE mutant is unable to rescue the decreased cell proliferation observed in the knockdown cells. These data suggest that the phosphotyrosine-binding ability of PKM2, although dispensable for the role of PKM2 in glycolysis under cell culture conditions, is important for its role in cell proliferation. Similar results were also obtained in A549 cells (data not shown).

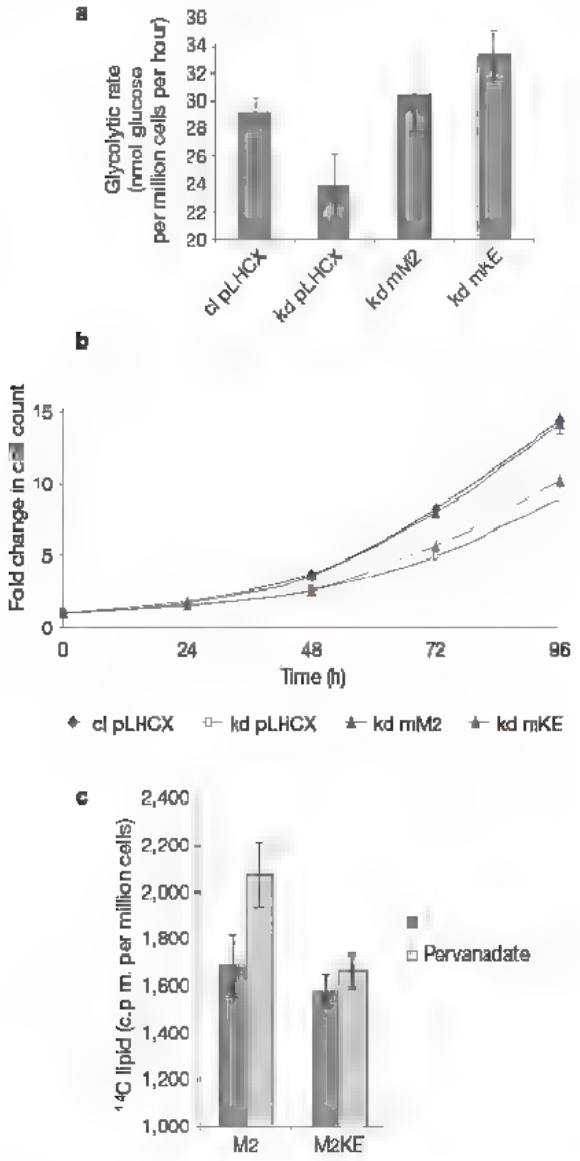


**Figure 5 | The phosphopeptide binding ability of PKM2 is important for cell proliferation.** cl pLHCX, cells with empty rescue vector and control shRNA, kd pLHCX, cells with empty rescue vector and knockdown shRNA, kd mM2, cells with Flag-tagged mouse PKM2 rescue and knockdown shRNA; kd mKE, cells with Flag-tagged mouse PKM2 KE point mutant rescue and knockdown shRNA. **a**, Glucose metabolism rates of the knockdown and rescue H1299 cells. **b**, Proliferation curves of the knockdown and rescue H1299 cells. Error bars in **a** and **b** denote s.e.m. ($n = 3$) At 96 h, the decreased proliferation of the mKE cells as compared with the mM2 cells was statistically significant, as assessed by Student's *t*-test ($P < 0.01$). **c**, $^{14}C$ incorporation into lipid in $^{14}C$-glucose-pulsed cells treated or untreated ( ) with pervanadate. M2 indicates cells expressing Flag-tagged mouse PKM2 and knockdown shRNA, and M2KE indicates cells expressing Flag-tagged mouse PKM2 KE point mutant and knockdown shRNA. Cells were pulsed with 2 μCi ml$^{-1}$ of $^{14}C$-glucose for 5 min before treatment with pervanadate for 10 min and then lipid extraction. $^{14}C$ counts in the lipid fractions were measured by scintillation counting. Error bars denote s.e.m. ($n = 6$). The increased incorporation of $^{14}C$ into lipid observed in the M2 cells after pervanadate stimulation was statistically significant as assessed by Student's *t*-test ($P < 0.05$).

### Inhibition of PKM2 by pTyr affects cellular metabolism

Our recent studies have shown that PKM2 is necessary for aerobic glycolysis in tumour cells[16]. Replacement of PKM2 with its more active splice variant, PKM1, was shown to result in reversal of the Warburg effect as judged by reduced lactate production and increased oxygen consumption. Because disruption of phosphotyrosine binding observed in the M2KE mutant is predicted to result in a more active PKM2 enzyme, we assessed whether the phosphotyrosine-binding ability of PKM2 is important for its role in aerobic glycolysis by measuring lactate production and oxygen consumption in cells expressing the M2KE point mutant. Notably, similarly to the changes that were observed when PKM2 was replaced by PKM1 (ref. 16), we observed a 36 ± 3% reduction in lactate production and 24 ± 4% increase in oxygen consumption in the M2KE-expressing cells when compared with the M2-expressing cells. These results suggest that tyrosine kinase regulation of PKM2 activity is involved in mediating the Warburg effect in tumour cells.

No changes in adenine nucleotide levels or the ATP/ADP ratios were observed in M2- versus M2KE-expressing cells, suggesting that this cannot account for the defect in cell proliferation observed in the M2KE-expressing cells. However, acute inhibition of PKM2 activity in proliferating cells by tyrosine kinase signalling may result in a temporary build-up of upstream glycolytic intermediates that can be used by the cell as precursors for fatty acid and nucleic acid synthesis, which could provide an advantage to PKM2-expressing cells for proliferation. Consistent with this model, we observed a 25% increase in the incorporation of metabolites from $^{14}C$-glucose into lipids on pervanadate treatment of PKM2-expressing cells. Notably, no significant increase in $^{14}C$ incorporation into lipids is seen in pervanadate-treated cells expressing the KE point mutant of PKM2 deficient in phosphotyrosine binding (Fig. 5c). A similar increase in the incorporation of $^{14}C$-glucose metabolites into lipids was observed on pervanadate stimulation of 293 cells (data not shown). In addition, acute pervanadate stimulation resulted in a 36 ± 1% decrease in oxygen consumption in PKM2-expressing cells with only a 15 ± 4% decrease in oxygen consumption in M2KE-expressing cells. These results demonstrate that phosphotyrosine-based regulation of PKM2 activity has consequences for metabolism in tumour cells and support the idea that regulation of PKM2 activity by tyrosine kinase signalling may enable glucose metabolites to be used for anabolic processes.

### Conclusions

We have shown that the activity of the glycolytic protein PKM2 can be regulated by tyrosine kinase signalling pathways via a novel phosphotyrosine-binding ability. Binding of phosphotyrosine peptides to PKM2 catalyses the release of FBP and subsequent inhibition of enzymatic activity. We propose that phosphotyrosine protein binding is a transient event that results in a conformational change in PKM2 structure that releases an otherwise tightly bound FBP molecule. Once released the ambient concentration of FBP at the time of the collision determines whether PKM2 goes into a low activity state or rebinds FBP and is reactivated. In this model, PKM2 only has the ability to undergo dynamic regulation by FBP (as occurs with bacterial, yeast and liver forms of pyruvate kinase) if a tyrosine kinase pathway is activated. We suspect that this mechanism evolved to ensure that fetal tissues only use glucose for growth when they are activated by appropriate growth factor receptor protein-tyrosine kinases. Cancer cells, by re-expressing PKM2, acquire the ability to use glucose for anabolic processes.

Because proliferating cells require *de novo* fatty acid synthesis as well as DNA replication, one possible model is that regulation of PKM2 activity allows for a balance between ATP production and fatty acid/nucleic acid production. Alternatively, phosphotyrosine-based regulation of PKM2 enzymatic activity may provide a direct link between cell growth signals using tyrosine kinases and control of glycolytic metabolism. Regardless, these data demonstrate a novel

mechanism for phosphotyrosine-based regulation of a metabolic protein that is important for cell proliferation.

## METHODS SUMMARY

Biotinylated peptide libraries were incubated with streptavidin beads and placed onto columns to construct peptide library affinity matrices. Five milligrams of SILAC lysates, made from HeLa cells as described[11], were flowed over affinity matrices, and bound proteins were digested with trypsin and analysed by microcapillary LC-MS/MS. SILAC ratios were determined using the Paragon algorithm in ProteinPilot software. Human PKM2 was cloned into pET-28a, expressed in bacteria, and purified as an amino-terminally tagged 6×His fusion protein. PKM2 crystals were grown by the hanging-drop method, and the structure was solved by molecular replacement. The binding motif for PKM2 was determined by flowing a phosphotyrosine-oriented degenerate peptide library over 6×His–PKM2-conjugated nickel beads. Bound peptides were sequenced by Edman degradation. For FBP-release analysis, recombinant pyruvate kinase was incubated with ~10 μM $^{14}$C-FBP for 30 min, dialysed for >7 h, then incubated with 1 mM peptide for 30 min, and dialysed again for >7 h before sample recovery and scintillation counting. Pyruvate kinase activity was assessed using a continuous assay coupled to lactate dehydrogenase. For cell line construction, Flag-tagged mouse pyruvate kinase isoforms were cloned into pLHCX and used to make retrovirus to infect H1299 and A549 cells. After 2 weeks of selection in 150 μg ml$^{-1}$ hygromycin, the stable cells expressing Flag-tagged mouse pyruvate kinase were infected with lentivirus containing knockdown or control shRNA towards human *PKM2*. These cells were selected for 1 week in 2 μg ml$^{-1}$ puromycin before experimentation. Cellular glucose metabolism rates were measured by following the conversion of 5-$^{3}$H-glucose to $^{3}H_2O$ as described previously[4]. Cellular proliferation rates were determined by seeding $5 \times 10^4$ cells in triplicate in 6-well plates and taking cell counts every 24 h using a Coulter particle analyser for a 3–5-day period. Oxygen consumption and lactate production were measured as described previously[16]. $^{14}$C-containing lipids were measured as described previously[17].

**Full Methods** and any associated references are available in the online version of the paper at www.nature.com/nature.

**Received 8 November 2007; accepted 3 January 2008.**

1. Warburg, O. On the origin of cancer cells. *Science* 123, 309–314 (1956).
2. Lum, J. J. *et al.* The transcription factor HIF-1α plays a critical role in the growth factor-dependent regulation of both aerobic and anaerobic glycolysis. *Genes Dev.* 21, 1037–1049 (2007).
3. Majumder, P. K. *et al.* mTOR inhibition reverses Akt-dependent prostate intraepithelial neoplasia through regulation of apoptotic and HIF-1-dependent pathways. *Nature Med.* 10, 594–601 (2004).
4. Vander Heiden, M. G. *et al.* Growth factors can influence cell growth and survival through effects on glucose metabolism. *Mol. Cell. Biol.* 21, 5899–5912 (2001).
5. Eigenbrodt, E., Reinacher, M., Scheefers-Borchel, U., Scheefers, H. & Friis, R. Double role for pyruvate kinase type M2 in the expansion of phosphometabolite pools found in tumor cells. *Crit. Rev. Oncog.* 3, 91–115 (1992).
6. Zwerschke, W. *et al.* Modulation of type M2 pyruvate kinase activity by the human papillomavirus type 16 E7 oncoprotein. *Proc. Natl Acad. Sci. USA* 96, 1291–1296 (1999).
7. Reiss, N., Kanety, H. & Schlessinger, J. Five enzymes of the glycolytic pathway serve as substrates for purified epidermal-growth-factor-receptor kinase. *Biochem. J.* 239, 691–697 (1986).
8. Sale, E. M., White, M. F. & Kahn, C. R. Phosphorylation of glycolytic and gluconeogenic enzymes by the insulin receptor kinase. *J. Cell. Biochem.* 33, 15–26 (1987).
9. Presek, P., Reinacher, M. & Eigenbrodt, E. Pyruvate kinase type M2 is phosphorylated at tyrosine residues in cells transformed by Rous sarcoma virus. *FEBS Lett.* 242, 194–198 (1988).
10. Mazurek, S., Grimm, H., Boschek, C. B., Vaupel, P. & Eigenbrodt, E. Pyruvate kinase type M2: a crossroad in the tumor metabolome. *Br. J. Nutr.* 87 (suppl 1), S23–S29 (2002).
11. Ong, S. E. & Mann, M. A practical recipe for stable isotope labeling by amino acids in cell culture (SILAC). *Nature Protocols* 1, 2650–2660 (2006).
12. Jurica, M. S. *et al.* The allosteric regulation of pyruvate kinase by fructose-1,6-bisphosphate. *Structure* 6, 195–210 (1998).
13. Dombrauckas, J. D., Santarsiero, B. D. & Mesecar, A. D. Structural basis for tumor pyruvate kinase M2 allosteric regulation and catalysis. *Biochemistry* 44, 9417–9429 (2005).
14. Yamada, K. & Noguchi, T. Nutrient and hormonal regulation of pyruvate kinase gene expression. *Biochem. J.* 337, 1–11 (1999).
15. Villen, J., Beausoleil, S. A., Gerber, S. A. & Gygi, S. P. Large-scale phosphorylation analysis of mouse liver. *Proc. Natl Acad. Sci. USA* 104, 1488–1493 (2007).
16. Christofk, H. R. *et al.* The M2 splice isoform of pyruvate kinase is important for cancer metabolism and tumour growth. *Nature* doi:10.1038/nature06734 (this issue).
17. Hatzivassiliou, G. *et al.* ATP citrate lyase inhibition can suppress tumor cell growth. *Cancer Cell* 8, 311–321 (2005).

**Supplementary Information** is linked to the online version of the paper at www.nature.com/nature.

**Acknowledgements** We thank W. Hahn for providing the lentiviral shRNA. We thank M. Liu for technical assistance. We thank J. Lee for help in developing the affinity purification techniques. M.G.V.H. is a Damon Runyon Fellow supported by the Damon Runyon Cancer Research Foundation. This research was supported by funding to L.C.C. from the National Institutes of Health.

**Author Information** PKM2 structure files are deposited in the Protein Data Bank under accession codes 3BJT (*apo* form) and 3BJF (FBP-bound form). Reprints and permissions information is available at www.nature.com/reprints. Correspondence and requests for materials should be addressed to L.C.C. (lcantley@hms.harvard.edu).

ARTICLES

# SATB1 reprogrammes gene expression to promote breast tumour growth and metastasis

Hye-Jung Han[1], Jose Russo[2], Yoshinori Kohwi[1]* & Terumi Kohwi-Shigematsu[1]*

**Mechanisms underlying global changes in gene expression during tumour progression are poorly understood. SATB1 is a genome organizer that tethers multiple genomic loci and recruits chromatin-remodelling enzymes to regulate chromatin structure and gene expression. Here we show that SATB1 is expressed by aggressive breast cancer cells and its expression level has high prognostic significance ($P < 0.0001$), independent of lymph-node status. RNA-interference-mediated knockdown of SATB1 in highly aggressive (MDA-MB-231) cancer cells altered the expression of >1,000 genes, reversing tumorigenesis by restoring breast-like acinar polarity and inhibiting tumour growth and metastasis *in vivo*. Conversely, ectopic SATB1 expression in non-aggressive (SKBR3) cells led to gene expression patterns consistent with aggressive-tumour phenotypes, acquiring metastatic activity *in vivo*. SATB1 delineates specific epigenetic modifications at target gene loci, directly upregulating metastasis-associated genes while downregulating tumour-suppressor genes. SATB1 reprogrammes chromatin organization and the transcription profiles of breast tumours to promote growth and metastasis; this is a new mechanism of tumour progression.**

Metastasis is the final step in solid tumour progression and is the most common cause of death in cancer patients[1]. Metastasis is a multi-step process: invasion of tumour cells into the adjacent tissues, entry of tumour cells in the systemic circulation (intravasation), survival in circulation, extravasation to distant organs, and finally growth of cancer cells to produce secondary tumours[2,3]. How tumour cells become metastatic is largely unknown. It was widely believed that metastatic cells are rare and evolve during late stages of tumour progression from a series of genetic changes that enable the cells to progress through the sequential steps that finally result in growth in distant organ microenvironments. Recently, however, gene expression analysis of human breast carcinomas with known clinical outcomes has revealed profiles that are associated with disease progression and has identified groups of genes whose characteristic expression pattern can predict the risk of metastatic recurrence[4–9]. The detection in some primary tumours of such poor-prognosis gene 'signatures' indicates that a large number of cells in the primary tumours already have such a gene expression pattern. Therefore, in addition to the traditional view of metastasis as an evolving process of rare variant clones, the poor-prognosis signatures suggest that cells in some primary tumours are predisposed to metastasis[10]. In fact, there might be an active molecular mechanism underlying such events. How gene expression profiles are established in these tumour cells such that they acquire metastatic properties is unknown.

Here we show that the protein SATB1 is necessary for breast cancer cells to become metastatic, and when ectopically expressed in non-metastatic cells, can induce invasive activity *in vivo*. We also show that SATB1 expression in breast cancer cells establishes gene expression profiles consistent with invasive tumours. SATB1 is a nuclear protein that functions as a 'genome organizer' essential for proper T-cell development[11]. SATB1 constitutes a functional nuclear architecture that has a 'cage-like' protein distribution surrounding heterochromatin. This architecture is referred to as 'the SATB1 regulatory network', as SATB1 regulates gene expression[11–14] by recruiting chromatin remodelling/modifying enzymes and transcription factors[13,14] to genomic DNA, which it tethers via specialized DNA sequences highly potentiated for unpairing (base unpairing regions, or BURs)[15–17]. On T-helper 2 cell activation, SATB1 becomes expressed and folds the cytokine-gene locus into dense loops for rapid induction of multiple cytokine genes[18]. In breast cancer cells, we find that once SATB1 is expressed, it coordinates expression of a large number of genes to induce metastasis. Removal of SATB1 from aggressive breast cancer cells not only reverses metastatic phenotypes but also inhibits tumour growth, indicating its key role in breast cancer progression.

## SATB1 expression correlates with poor prognosis

We examined SATB1 expression in 24 breast epithelial cell lines, including normal human mammary epithelial cells (HMECs), 5 immortalized derivatives, 13 non-metastatic cancer cell lines and 5 metastatic cancer cell lines. Both SATB1 messenger RNA and protein were detected only in metastatic cancer cell lines, correlating SATB1 expression with aggressive tumour phenotypes (results from representative cell lines shown in Fig. 1a). SATB2, a close homologue of SATB1, was expressed in both malignant and non-malignant cell lines (Supplementary Fig. 1a).

Among 28 human primary breast tumours, SATB1 protein was detected in all 16 poorly differentiated infiltrating ductal carcinomas ($P < 0.0001$). Low-level SATB1 expression was found in some moderately differentiated tumour samples (7 out of 12), and no SATB1 was detected in control samples taken from adjacent non-malignant tissues (representative data shown in Fig. 1b and Supplementary Table

[1]Life Sciences Division, Lawrence Berkeley National Laboratory, University of California, Berkeley, California 94720, USA. [2]Breast Cancer Research Laboratory, Fox Chase Cancer Center, Philadelphia, Pennsylvania 19111, USA
*These authors contributed equally to this work

1). Representative immunostaining images of SATB1 and epithelial cell markers in invasive ductal carcinomas are shown in Fig. 1c.

The prognostic significance of SATB1 was determined by assessing its nuclear staining using tissue microarrays containing 2,197 cases with known clinical follow-up records, from which 1,318 breast cancer specimens were analysable (Supplementary Table 2 shows tumour composition and SATB1 association with clinico-pathological parameters). Tissues were scored on the basis of the intensity of SATB1 nuclear labelling and percentage of SATB1-positive tumour cells (see Methods). Among these specimens, Kaplan–Meier survival analysis of 985 ductal carcinoma specimens revealed a correlation between higher SATB1 expression levels and shorter overall survival times ($P < 0.001$) (Fig. 1d). This correlation was also observed with all breast cancer types (1,318 specimens) (Supplementary Fig. 1b), except medullary cancer, which is rare and often has a relatively favourable prognosis despite its poorly differentiated nuclear grade.

To exclude the possibility that the prognostic effect of nuclear SATB1 expression was dependent on other established prognostic factors for breast cancer, including tumour stage, the histological grade (Bloom, Richardson, Elston-Ellis grading, BRE) and nodal stage, we performed a multivariate analysis. This analysis confirmed that SATB1 is an independent prognostic factor for breast cancer (Fig. 1e).

### SATB1 promotes aggressive cancer phenotypes *in vitro*

We investigated whether SATB1 is required for the invasive phenotypes of breast cancer cells *in vitro* by expressing short hairpin RNAs (shRNA) to knock down SATB1 expression. We expressed shRNA from two different *SATB1* sequences (shRNA1 or shRNA2) in the

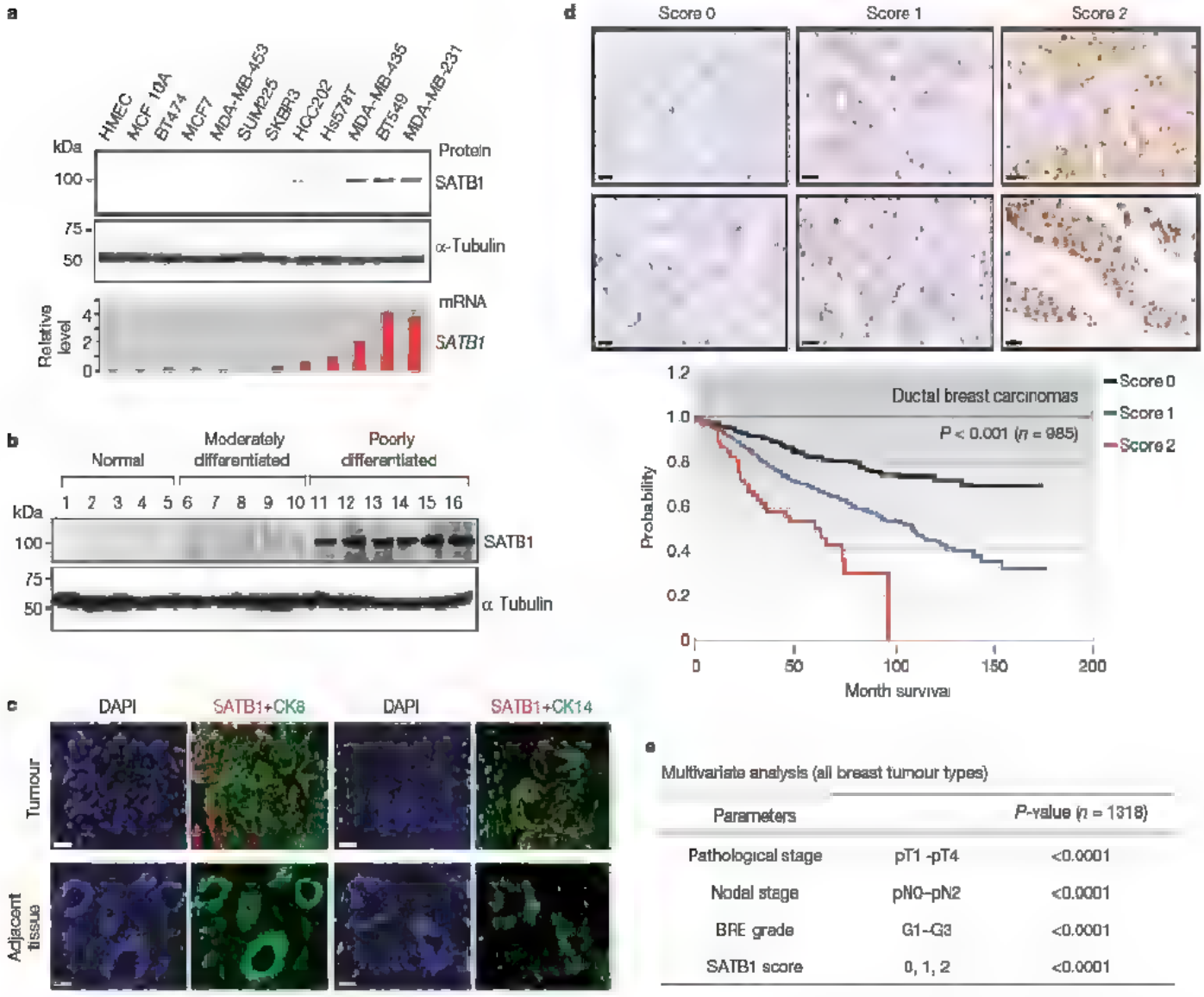


e

Multivariate analysis (all breast tumour types)

| Parameters | | *P*-value ($n = 1318$) |
|---|---|---|
| Pathological stage | pT1 -pT4 | <0.0001 |
| Nodal stage | pN0–pN2 | <0.0001 |
| BRE grade | G1–G3 | <0.0001 |
| SATB1 score | 0, 1, 2 | <0.0001 |

**Figure 1 | SATB1 expression in breast cancer is associated with poor prognosis. a**, Immunoblot analysis of SATB1 levels (top panel) in normal mammary epithelial cells (HMEC), immortalized mammary epithelial cells (MCF-10A), non-aggressive breast cancer cell lines (BT474, MCF7 MDA-MB-435, SUM225 and SKBR3) and aggressive breast cancer cell lines (HCC202, Hs578T, MDA-MB-435, BT549, MDA-MB-231); α-tubulin loading control is shown in the middle panel. The bottom panels shows transcript levels of *SATB1*, relative to *GAPDH*, determined by qRT–PCR and compared to Hs578T cells; error bars indicate s.e.m., $n = 3$ experiments. **b**, Immunoblot analysis of SATB1 in representative human primary breast tumour specimen (top panel); α-tubulin loading control is also shown (bottom panel). **c**, Immunofluorescence images of poorly differentiated ductal carcinomas (top row) and adjacent normal tissues (bottom row) stained with anti-SATB1 (red) and anti-cytokeratin 8 (CK8) or anti-cytokeratin 14 (CK14) (green) antibodies, counterstained with 4,6-diamidino-2-phenylindole (DAPI, to stain DNA, blue). Scale bars, 30 μm. **d**, SATB1 levels in representative tumour tissues (top; scale bar, 20 μm) and Kaplan–Meier plot (below) of overall survival of 985 patients with ductal breast carcinomas stratified by SATB1 expression level. Tissues scored as 0 (negative SATB1 nuclear staining for all tumour cells), 1 (positive SATB1 nuclear staining other than score 2) or 2 (moderate SATB1 nuclear staining for >50% tumour cells or strong staining for >5% tumour cells). A log-rank test showed significant differences between groups ($P < 0.001$). **e**, Relative multivariate significance of potential prognostic variables. Cox proportional hazards regression was used to test the independent prognostic contribution of SATB1 after accounting for other potentially important covariates.

highly metastatic MDA-MB-231 cell line. Expression of SATB1 protein became hardly detectable by immunoblotting and its mRNA levels were substantially reduced by 70% and 90% in both *SATB1*-shRNA1 and *SATB1*-shRNA2 expressing cells, respectively (Fig. 2a). SATB1 expression remained unaltered in MDA-MB-231 cells expressing a control shRNA whose sequence did not match any known human gene.

SATB1 knockdown decreased proliferation of *SATB1* shRNA1 and *SATB1* shRNA2 cells on Matrigel compared with the parental cell line and control shRNA cells (Fig. 2b). Furthermore, the invasive capacity *in vitro* of *SATB1* shRNA cells was reduced by 80–85% (Fig. 2c). Consistently, depletion of SATB1 prevented colony formation of these cell lines in soft agar, indicating that anchorage-dependent growth was restored (Fig. 2d).

Tissue organization and polarity are typically disrupted in mammary epithelial tumours *in vivo*. Therefore, we examined cell morphology of SATB1-depleted MDA-MB-231 cells. We observed major differences in cell morphology between control shRNA and *SATB1* shRNA1 cells grown on Matrigel. Where control cells exhibited a spindle-like fibroblastic morphology, *SATB1* shRNA cells had a cobble-stone-like morphology (Fig. 2e, left panel). We also observed similar cell morphology and reduction in invasive activity when SATB1 was depleted from the highly invasive BT549 breast tumour cell line (Supplementary Fig. 2a–d). When non-transformed mammary epithelial cells (MCF-10A cells) were cultured on Matrigel and analysed using markers of acinar formation—such as filamentous actin (F-actin), β-catenin, the basal extracellular matrix (ECM) receptor, and integrin α6—glandular-like structures (acini) formed, with a hollow lumen surrounded by polarized epithelial cells[19–21] (Fig. 2e, right panel). Control shRNA cells, however, formed disorganized structures lacking basal polarity (Fig. 2e, right panel). In contrast, *SATB1* shRNA1 cells cultured on Matrigel displayed normal acinar structures, showing uniform and polarized nuclei, cortically organized F-actin, basally distributed integrin α6, and β-catenin that localized to the lateral cell–cell junctions, as exhibited by MCF-10A cells. Similar results were confirmed with *SATB1* shRNA2 cells. Therefore, SATB1 knockdown in MDA-MB-231 breast cancer cells restores polarized cellular structures found in normal mammary epithelial cells.

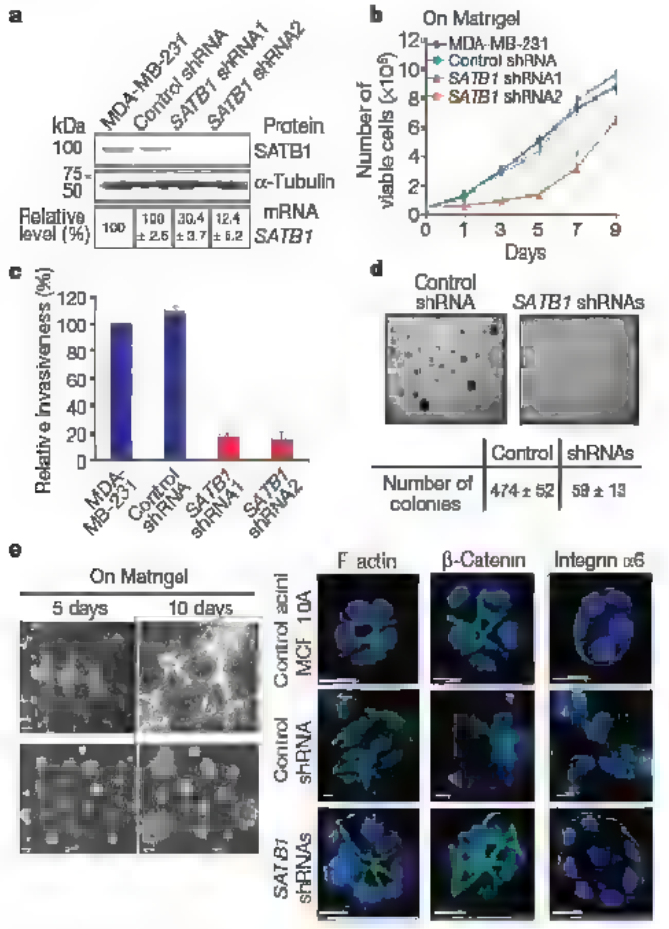


**Figure 2 | SATB1 depletion restores cell polarity and reduces aggressive phenotypes of MDA-MB-231 cells *in vitro*.** **a**, Reduced SATB1 expression, determined by immunoblot and quantitative RT–PCR analyses, in *SATB1* shRNA (1 and 2) cells, compared with controls (parental cell line MDA-MB-231 and contro. shRNA cells; α-tubulin levels as loading control). **b**, Reduced proliferation of *SATB1* shRNA (1 and 2) cells grown on Matrigel compared with controls. **c**, Chemoinvasion assay of *SATB1* shRNA (1 and 2) cells, compared with controls (error bars indicate s.e.m., $n = 3$ experiments). **d**, Representative photographs of soft agar colony formation 20 days after culture of control shRNA and *SATB1* shRNA (1 and 2) cells, with mean colony counts from three dishes. **e**, Left panel. Phase contrast micrographs of control shRNA (top row) or *SATB1* shRNA1 cells (bottom row) cultured on Matrigel. Scale bar, 40 μm. Right panel: morphologies of *SATB1* shRNA1 cells (acinar structure) and controls grown on Matrigel and stained for F-action, β-catenin or integrin α6 (green) and DAPI (blue). MCF-10A cells show the typical acinar structure. Scale bars, 15 μm. SATB1 nuclear distribution in MDA-MB-231 cells is shown in Supplementary Fig. 2e.

## SATB1 depletion reverses cancer metastasis

We next evaluated the *in vivo* effects of SATB1 depletion on metastasis. We used an assay called experimental metastasis, in which we injected *SATB1* shRNA1, *SATB1* shRNA2, or control shRNA cells ($1 \times 10^6$ cells) into the lateral tail vein of 6-week-old athymic mice

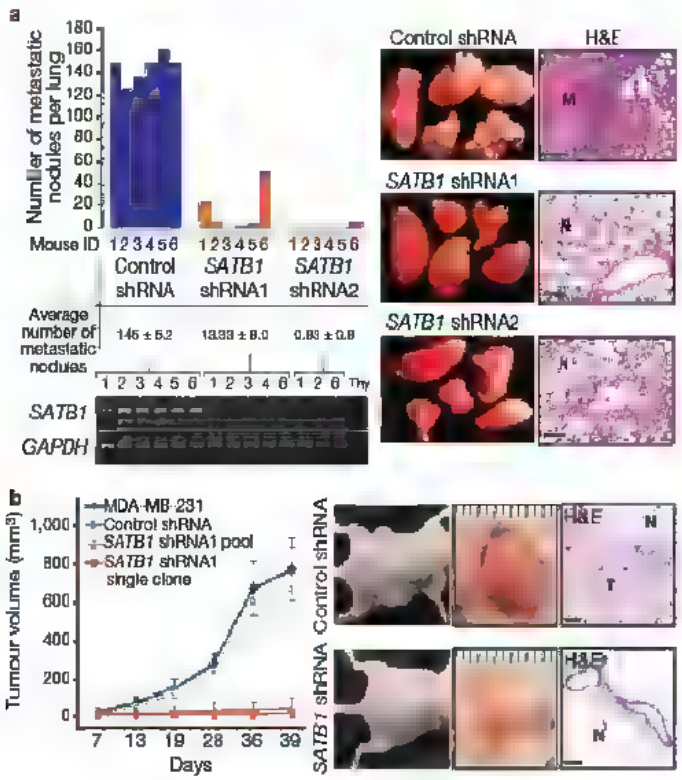


**Figure 3 | SATB1 is necessary for lung colonization and tumour growth.** **a**, Number of metastases in lungs of mice ($n = 6$ per group) 9 weeks after tail-vein injection of control shRNA, *SATB1* shRNA1 or *SATB1* shRNA2 cells (left), with mean nodule per lung values shown below. Expression levels of human *SATB1* in lungs was analysed by RT–PCR, with human *GAPDH* as a loading control and mouse thymocytes (Thy) as a negative control. Representative lungs and haematoxylin and eosin (H&E) staining of metastatic tumour (M) and normal (N) lung tissues are shown (right). **b**, Reduced tumour volumes in fat pads of nude mice injected with *SATB1* shRNA1 cells (single clones or pools), compared to controls (parental cell line MDA-MB-231 or control shRNA cells). Each data point is the mean value (±s.e.m.) of five–six primary tumours. Photographs of representative mice and tumours are shown, along with haematoxylin and eosin staining of tumour (T) and normal (N) breast tissue. Scale bar, 50 μm.

and evaluated their survival in circulation and extravasation to and growth in the lung.

After 9 weeks, injected control tumour cells formed 125 to 160 metastatic nodules per lung in all 6 mice analysed, detected under a dissection microscope (Fig. 3a). In contrast, mice injected with *SATB1* shRNA1 cells formed 0 to 50 nodules per lung and mice injected with *SATB1* shRNA2 cells formed 0 to 5 nodules ($n = 6$ mice each). Histological analyses confirmed that the number of micrometastatic lesions was markedly reduced in the lungs of mice injected with *SATB1* shRNA1 or *SATB1* shRNA2 cells (Fig. 3a). The presence of human cancer cells in each lung was verified by polymerase chain reaction with reverse transcription (RT–PCR). Our data indicate that SATB1 is necessary for the aggressive, highly metastatic phenotype of MDA-MB-231 cells.

We next tested whether SATB1 depletion from MDA-MB-231 cells also inhibits tumour growth. We injected control shRNA and *SATB1* shRNA1 cells into the fourth mammary fat pads of athymic nude mice and monitored tumour growth. In contrast to both parental MDA-MB-231 and control shRNA cells, which formed large tumours within 39 days (6 out of 6 mice), all six mice injected with an *SATB1* shRNA1 clone or a pool of *SATB1* shRNA1 cells resulted in either no tumours or greatly reduced tumour growth, respectively (Fig. 3b). These results indicate that SATB1 expression in MDA-MB-231 cells is necessary for the tumour growth of these cells in mammary fat pads of mice.

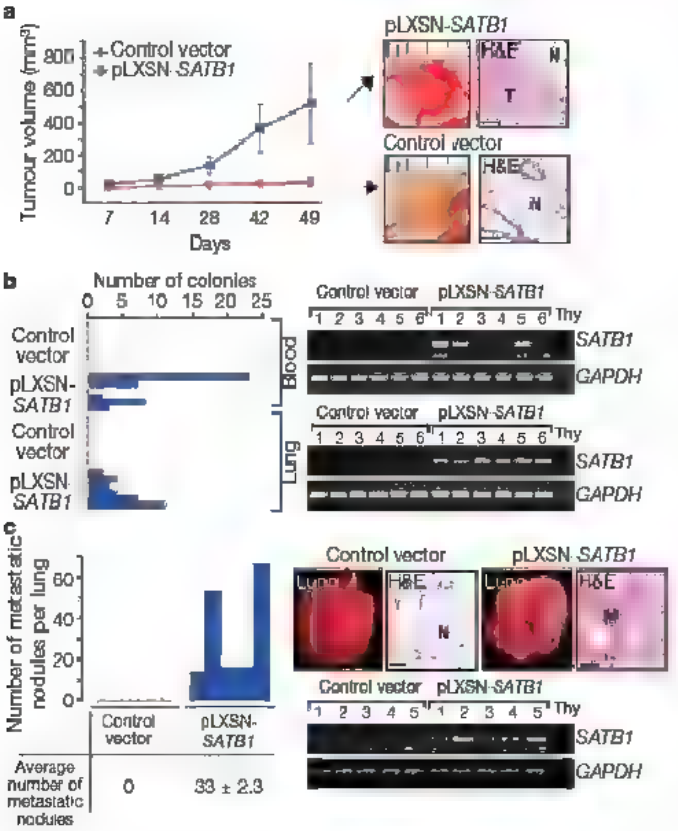


**Figure 4 | Ectopic expression of SATB1 in SKBR3 cells induced tumour growth, intravasation and lung colonization.** **a**, Left panel, mean volumes ($n = 6$ per group) of tumours formed in fat pads of mice injected with SATB1-overexpressing SKBR3 cells (pLXSN-*SATB1*) or controls (error bar indicates s.e.m.). Right panels: gross anatomy and haematoxylin-and-eosin-stained sections of tumours (pLXSN-*SATB1* cells) and normal breast tissues (control cells). T, tumour; N, normal breast tissue. Scale bar, 80 μm. **b**, Left panel, intravasation of tumour cells was determined from the numbers of colonies formed by pLXSN-*SATB1* or control cells grown in G418-containing media after isolation from blood or lung samples of tumour-bearing mice from experiments described in **a**. Right panel, RT–PCR analysis was used to detect human *SATB1* expression in cell colonies grown from blood and lung samples. *GAPDH* was the loading control and mouse thymocytes were the negative control (Thy). **c**, Left panel, the number of metastases that formed in the lungs of each nude mouse ($n = 5$) 10 weeks after the injection of pLXSN-*SATB1* or control cells, and mean values for each group. Right panel, representative photos of the lungs and haematoxylin and eosin staining sections show normal lung from mice injected with control vector cells and metastatic nodules from pLXSN-*SATB1* cells. N, normal lung tissue; M, metastatic nodule. Lung nodules were shown to express human *SATB1* by RT–PCR. Scale bar, 80 μm.

### Promotion of growth and metastasis by SATB1

We examined whether ectopic expression of SATB1 is sufficient to induce invasive activity in non-metastatic cancer cells. Control SKBR3 cells (a non-metastatic cell line, transfected with control vector) injected into the mammary glands of mice did not form tumours in mice after 7 weeks. In contrast, all six mice similarly injected with SKBR3 cells ectopically expressing SATB1 (pLXSN-*SATB1*) grew large, undifferentiated, highly vascularized tumours (Fig. 4a). To examine intravasation, cells isolated from blood and lung tissue from mice injected with SKBR3 cells (control or pLXSN-*SATB1*) were cultured for 4 weeks in the presence of G418, to select for transfected cells. In 5 out of the 6 mice injected with pLXSN-*SATB1* cells, 2 to 23 colonies formed from each blood sample, and in all these mice 2–11 colonies formed from each lung sample. No colonies grew from samples from mice injected with control cells (Fig. 4b). These data show that expression of SATB1 is sufficient to induce SKBR3 cells to form large tumours in mammary fat pads, to acquire the ability to invade blood vessels, and to survive in the circulation.

By 7 weeks after injection, we did not observe macroscopically visible metastases in the lungs of mice injected with SATB1-expressing cells in the mammary fat pads; longer monitoring times would be needed to observe such secondary tumours. However, we had to kill mice bearing large tumours after 7 weeks. Therefore, we intravenously injected SKBR3 cells (control vector or pLXSN-*SATB1*) into mice and found that at 10 weeks after injection, SATB1-expressing SKBR3 cells, but not control SKBR3 cells, formed many large metastatic nodules, indicating extravasation and tumour growth in lung (Fig. 4c).

We then analysed the invasive activity of breast cancer cells with differing levels of SATB1 expression using Hs578T cells, a breast cancer cell line that endogenously expresses lower levels of SATB1 than MDB-MB-231 cells. Compared to control Hs578T cells, Hs578T cells that overexpress SATB1 (pLXSN-*SATB1* transfection; HS25) showed increased invasive activity *in vitro*, promoted tumour growth in mammary fat pads and displayed experimental metastasis to lung *in vivo* (Supplementary Fig. 3). These results indicate that high-level expression of SATB1 is necessary and sufficient to promote metastasis of Hs578T cells to lung.

### Reprogramming of global expression profile

We performed gene expression profiling on MDA-MB-231 cells expressing either control shRNA or *SATB1* shRNA1 grown in culture. Unsupervised clustering analysis of 2,678 genes from two different microarray platforms (Affymetrix and Codelink) identified two groups of genes (tree 1 and tree 2) that significantly changed expression levels (by >1.5-fold) after SATB1 depletion under both plastic and Matrigel culture conditions. Tree 1 included 409 down-regulated genes, and tree 2 contained 456 upregulated genes on SATB1 depletion (Fig. 5a). Functional profiling of these genes revealed that the greatest proportion of the genes was associated with cell adhesion, followed by phosphatidylinositol signalling and cell cycle regulation. Individual SATB1-dependent genes and subgroups of different molecular pathways are shown in Supplementary Tables 3 and 4 and Supplementary Fig. 4. Among the 231 Rossetta poor-prognosis-associated genes[6], 174 were compared by our microarray to the SATB1-dependent gene set (shown in trees 1 and 2). Sixty-three of these genes (36%) whose expression was up- or downregulated in breast tumours with poor prognoses were correspondingly altered by SATB1 expression ($P = 0.02$) (Supplementary Fig. 5a).

Genes known to promote either bone[22] or lung metastasis[23] were also enriched among the SATB1-dependent genes in MDA-MB-231 cells ($P = 0.0002$ and $P = 0.021$, respectively; Supplementary Fig. 5b, c).

We used quantitative RT–PCR (qRT–PCR) and semi-qRT–PCR to confirm SATB1-dependent expression of over 40 genes identified in the microarray analysis (Fig. 5b and Supplementary Fig. 6). The expression of many genes known to have important functions in promoting metastasis was found to be upregulated by SATB1, including metastasin (*S100A4*)[24] and *VEGFB*[25], which have roles in metastasis and angiogenesis; matrix metalloproteases (MMPs) 2, 3 and 9, which degrade ECM and promote tumour invasion[26,27]; transforming growth factor-β1 (*TGFB1*), which stimulates invasion[28]; and connective tissue growth factor (*CTGF*), which mediates angiogenesis[29] and bone metastasis[22]. Many tumour cells exhibit increased invasiveness in response to TGF-β1 and increased levels of TGF-β1 have been reported in most tumour types[28]. Notably, SATB1 upregulates genes involved in epidermal growth factor (EGF) signalling[30], such as the EGF receptor subfamily members *ERBB1*, *ERBB2* (*HER-2* or *NEU*), *ERBB3*, *ERBB4* and the ligands *NRG* and *AREG*. ERBB2, the most oncogenic member of the ERBB family, is an important regulator of breast cancer progression[30], and drugs that intercept ERBB2 signalling are in routine clinical application[31]. SATB1 also represses the metastasis suppressor genes *BRMS1*, *KAI1* (also called CD82) *KISS1* and *NME1* (*NM23*)[32]. SATB1 expression induces a marked change in the gene expression pattern in cancer cells and promotes their acquisition of aggressive phenotypes.

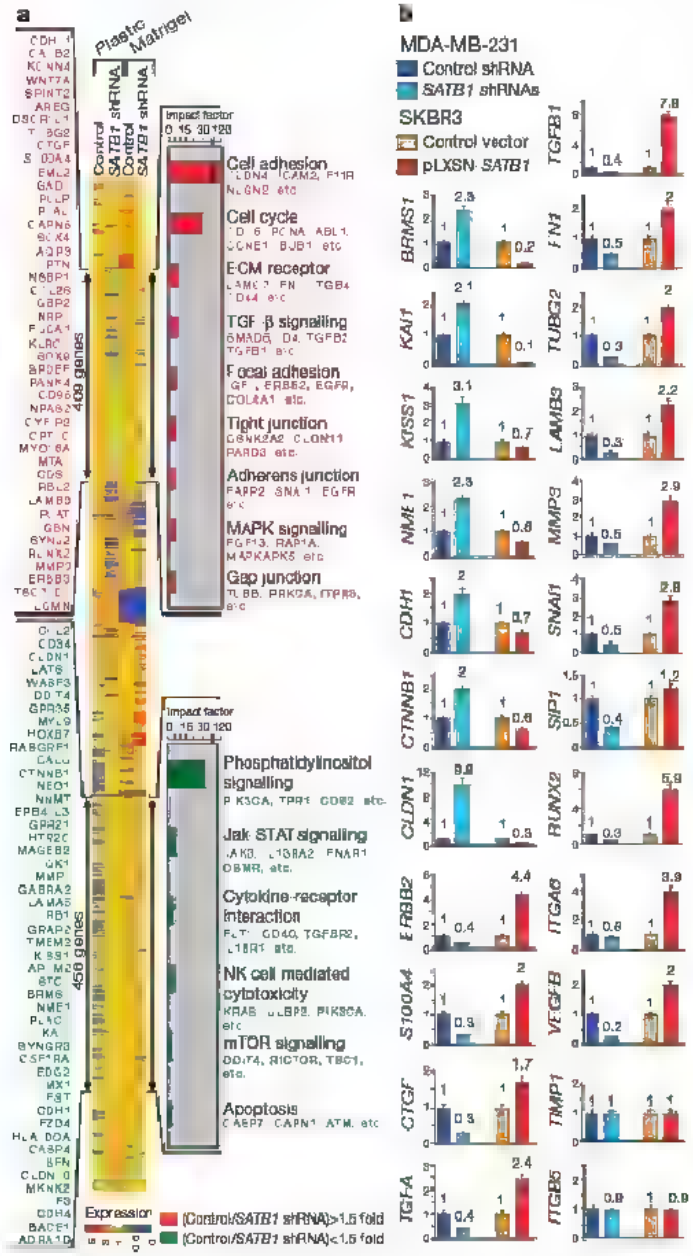


**Figure 5 | Global changes in expression profiles on SATB1 expression.** **a**, Unsupervised clustering (GeneSprung software) of genes differentially expressed between control shRNA and *SATB1* shRNA1 cells from both plastic and Matrigel culture conditions; 409 SATB1-activated genes and 456 SATB1-repressed genes are marked by double-headed arrows. Representative SATB1-activated (red) and SATB1-repressed genes (green) are either listed vertically or under each molecular pathway. Impact factor strength of SATB1-activated (red bars) and -repressed (green bars) genes is shown. **b**, Expression levels of multiple genes in the microarray, including cancer-related genes, confirmed with quantitative RT–PCR: control shRNA (dark blue) versus a mixture of *SATB1* shRNA1- and shRNA2-expressing clones grown on Matrigel (light blue); pooled SKBR3 control cells (orange) versus primary tumours from nude mice injected with SATB1-expressing cells (pLXSN-*SATB1*) (red). Genes analysed are shown on the *y* axis; numbers represent fold differences relative to *GAPDH*. Error bars indicate s.e.m. ($n = 3$ experiments).

Our observations that SATB1 depletion from MDA-MB-231 cells restores normal cell morphology. Such cell structure genes include the ECM protein fibronectin (*FN*), the intermediate filament protein vimentin (*VIM*)[33] and the cell–ECM interacting protein β4 integrin (*ITGB4*)[34]. Dysregulated expression of cadherin and catenins, which mediate cell-to-cell adhesion, has been associated with breast cancer[35,36]. OB-cadherin (*CDH11*), VE-cadherin (*CDH5*) and N-cadherin (*CDH2*), often upregulated in invasive breast cancer, were all upregulated by SATB1. In contrast, genes downregulated by SATB1 included claudin 1 (*CLDN1*), a tight junction protein that is commonly lost or mislocalized in invasive tumours[37]; β-catenin (*CTNNB1*), a critical member of the canonical Wnt pathway[38]; and E-cadherin (*CDH1*), an adherens junction protein and tumour suppressor[35,39]. Loss of E-cadherin is a hallmark for epithelial to mesenchymal transition, a process whereby epithelial cells lose polarity, cell-to-cell contacts, and cytoskeletal integrity contributing to the dissemination of carcinoma cells from epithelial tumours[40]. On SATB1 depletion, the observed upregulation of E-cadherin and downregulation of fibronectin and repressors of E-cadherin such as *SNAIL* and *SIP1* indicate that the epithelial to mesenchymal transition process is reversed, resulting in the restoration of acinar-like morphology.

### SATB1 regulates gene activity and epigenetics

To identify genes directly regulated by SATB1, we determined the *in vivo* binding status of SATB1 within genomic loci of nine SATB1-dependent genes: *ERBB2*, *S100A4*, *ABL1*, *TGFB1*, *MMP3* and *LMNA* (laminA/C), which are all upregulated by SATB1, and *BRMS1*, *CLDN1* and *CTNNB1*, which are all downregulated by SATB1. *GAPDH*, *ITBG5* and *TIMP1* were selected as non-SATB1-dependent controls (Fig. 5b and Supplementary Fig. 6). For each of these 12 genes, we analysed a ~20-kb region upstream and downstream of the gene's first exon for potential SATB1 binding *in vivo*, looking for all potential SATB1 target sequences (BURs) (indicated by red number), promoter sequences (if known: blue box), regions containing CpG islands (green box), and other regulatory sequences (light blue box) (Fig. 6a–c and Supplementary Fig. 7a, b). Potential BURs were identified by the genomic sequences characterized by the ATC sequence context and confirmed for *in vitro* SATB1 binding by electrophoresis-mobility shift assay (EMSA, data not shown). To assess SATB1 binding to these loci *in vivo*, we used the urea-chromatin immunoprecipitation (urea-ChIP) method[16]. All genes analysed contained several BURs. Most BURs of SATB1-dependent genes were bound to SATB1, whereas none or only a few BURs in SATB1-independent genes were bound (Supplementary Fig. 7a and data not shown). The SATB1-binding status of SATB1-dependent or -independent genes indicates that SATB1 directly regulates expression of *ERBB2*, *S100A4*, *BRMS1*, *CLDN1*, *ABL1*, *TGFB1*, *LMNA*, *MMP3* and *CTNNB1*.

We addressed the mechanism by which SATB1 regulates the expression of its target genes. Using the urea-ChIP assay followed by qPCR (urea-ChIP-qPCR), we determined whether the histone acetylation status and the *in vivo* binding status of histone acetyltransferase (p300) and histone deacetylase 1 (HDAC1) were dependent on SATB1. We focused our analyses on *ERBB2*, *S100A4*, *BRMS1*, *CLDN1*, *ITGB5* and *TIMP1* (Fig. 6). In control cells (blue bars), the *in vivo* SATB1-binding sites in *ERBB2* and *S100A4* (*ERBB2*, positions 10, 12 and 13; *S100A4*, positions 2, 6, 7, 10, 12, 13 and 14) corresponded to the main acetylation peaks for histone H3 at lysines 9/14 (Fig. 6a). These positions coincide with p300 binding peaks *in vivo*. On SATB1 depletion (red bars), histone acetylation levels and p300 binding were markedly reduced. Instead, HDAC1 binding at these specific positions was increased. These epigenetic changes are consistent with SATB1 promoting their gene expression. Opposite effects were observed for *BRMS1* and *CLDN1*, two genes repressed by SATB1 (Fig. 6b). On SATB1 depletion, histone H3 became more acetylated at SATB1-bound positions (*BRMS1*, positions 10 and 14; *CLDN1*, positions 9, 10 and 12), accompanied by increased p300 binding and reduced recruitment of HDAC1, leading to upregulation of these genes. Histone modifications and p300 binding status of non-target gene loci, transcriptionally active *ITGB5* and *TIMP1*, did not differ when SATB1 knockdown cells were compared with control MDA-MB-231 cells (Fig. 6c). Thus, SATB1 binds to its target gene loci at multiple positions and assembles the loci with histone-modifying factors to establish the epigenetic status.

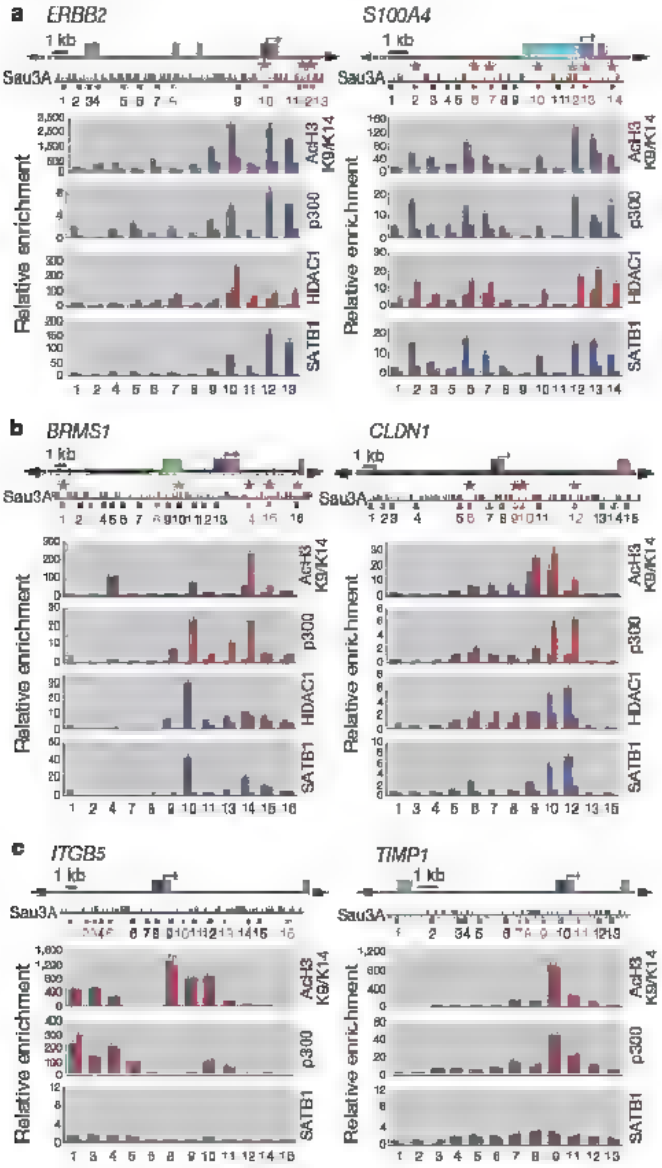


**Figure 6 | SATB1 defines the epigenetic status of target genes.** **a–c**, Urea-ChIP-qPCR was performed for MDA-MB-231 control shRNA (blue bar) and *SATB1* shRNA (red bar) cells using antibodies against acetylated histone H3 at K9/14, p300, HDAC1 and SATB1. SATB1-upregulated genes *ERBB2* and *S100A4* (metastasin) (**a**), SATB1-downregulated genes *BRMS1* and *CLDN1* (**b**) and SATB1-independent genes *ITGB5* and *TIMP1* (**c**) were selected for the analysis. Gene structures are based on the data from USCS (http://genome.ucsc.edu/). Numbers indicate positions of DNA fragments where primers were designed (black, non-SATB1-recognizing sequences; red, SATB1-binding sequences shown by EMSA *in vitro*). Red stars indicate *in vivo* SATB1-bound DNA fragments. Dark blue box, promoter regions; light blue box, transcription binding sites; green box, CpG island; arrows, transcriptional start sites; pink box, exon. Error bars indicate s.e.m. ($n = 3$ experiments).

## Discussion

We present a new model of gene regulation during tumour progression, in which the genome organizer SATB1 becomes expressed during malignancy, markedly altering the gene expression profile of breast cancer cells to induce an aggressive phenotype that promotes both tumour growth and metastasis.

The expression of over one-thousand genes is altered on SATB1 expression in breast cancer cells. We found that SATB1 directly bound to and established the epigenetic status of all SATB1-dependent genes randomly chosen for analysis. There are likely to be a large number of additional genes regulated in a similar manner. An attractive mechanism by which SATB1 globally reprogrammes gene expression during metastasis is by tethering hundreds of gene loci onto its regulatory network, assembling them with chromatin modifying and transcription factors. Our findings support the emerging links between chromatin remodelling enzymes, epigenetics and cancer[41–43]. We have shown that a variety of genes involved in many aspects of tumorigenesis are regulated by SATB1, indicating that a large group of SATB1-targeted genes collectively induce tumour growth and metastasis. Similar to the cytokine genes in activated T cells[18], it is likely that SATB1-target genes in breast cancer are brought together from intra- or even inter-chromosomal loci to form chromatin loops and are co-regulated by SATB1. These findings raise important questions regarding how tissue specificity of genes regulated by SATB1 is achieved (activated T cells versus breast cancer) and the mechanisms by which specific genes are either upregulated or repressed. Our results indicate that the SATB1-dependent gene expression pattern does not overlap completely between cancer cells cultured on plastic or on Matrigel, indicating crosstalk between the cellular environment and SATB1 nuclear architecture. It is possible that specific SATB1-regulated genes vary based on host organs to which cells metastasize. Other proteins that bind BURs[44], such as HMGI(Y), which also has an important role in breast cancer progression[45], may interact with SATB1 to promote cell growth in different cellular environments.

SATB1 expression is not restricted to late clinical stages of disease, but is observed in a subset of primary breast tumours at early clinical stages before lymph node metastasis. The SATB1 level in the nuclei of cancer cells has high prognostic significance, independent of the lymph node status ($P < 0.0001$), indicating its utility in predicting the likelihood of disease progression in patients with early-stage breast cancer.

Although it is still essential to confirm the fate of SATB1-expressing cells in human primary breast tumours, our findings suggest a new paradigm in tumour progression, in which SATB1 functions as a genome organizer during tumorigenesis to reprogramme expression and promote metastasis. Future studies will address how applicable this concept is to other tissues. SATB1 may be useful as a therapeutic target for metastatic breast disease.

## METHODS SUMMARY

SATB1 expression levels were quantified by qPCR and immunoblot analyses with human breast cancer and non-malignant cell lines and with human tissue specimens from primary tumours and adjacent tissues. Prognostic values of

SATB1 were evaluated by anti-SATB1 immunostaining of breast tissue microarrays containing >2,000 cases with clinical follow-up records. SATB1 expression in breast cancer cells was either knocked down by stable expression of shRNA against *SATB1* or induced by SATB1 expression from a retroviral expression construct, pLXSN-*SATB1*. Tumour growth and intravasation were studied by injecting *neo*-expressing human cancer cells proximal to the mammary glands in mice. Tumour growth was monitored for 6–7 weeks and the presence of human cells in blood and lung were determined by G418 selection. Tumour cells were intravenously injected in to mice and metastasis to lung was determined by quantifying lung colonization after 9–10 weeks. Colonized lung and mammary tumours were confirmed by pathological analyses. All animal work was done following Institutional Animal Care and Use Committee guidelines. Urea-ChIP-qPCR was performed to determine histone modification and binding status of modifying factors and SATB1 at selected gene loci. The expression and functional profiles of genes were compared between MDA-MB 231 cells expressing control shRNA and *SATB1* shRNA using Codelink Uniset Human 20K and Affymetrix HT-HG-U133A microarray chips (dataset on the GEO website; accession number GSE5417). Expression of ~40 genes was verified by qRT–PCR and semi-qRT–PCR.

**Full Methods** and any associated references are available in the online version of the paper at www.nature.com/nature.

**Received 11 September 2007; accepted 22 January 2008.**


1. Parker, B. & Sukumar, S. Distant metastasis in breast cancer: molecular mechanisms and therapeutic targets. *Cancer Biol. Ther.* 2, 14–21 (2003).
2. Chambers, A. F., Groom, A. C. & MacDonald, I. C. Dissemination and growth of cancer cells in metastatic sites. *Nature Rev. Cancer* 2, 563–572 (2002)
3. Fidler, I. J. The pathogenesis of cancer metastasis: the 'seed and soil' hypothesis revisited. *Nature Rev. Cancer* 3, 453–458 (2003)
4. Perou, C. M. *et al.* Molecular portraits of human breast tumours. *Nature* 406, 747–752 (2000)
5. van de Vijver, M. J. *et al.* A gene-expression signature as a predictor of survival in breast cancer. *N. Engl. J. Med.* 347, 1999–2009 (2002).
6. van't Veer, L. J. *et al.* Gene expression profiling predicts clinical outcome of breast cancer. *Nature* 415, 530–536 (2002)
7. Ince, T. A. & Weinberg, R. A. Functional genomics and the breast cancer problem. *Cancer Cell* 1, 15–17 (2002)
8. Sorlie, T. *et al.* Gene expression patterns of breast carcinomas distinguish tumor subclasses with clinical implications. *Proc. Natl Acad. Sci. USA* 98, 10869–10874 (2001).
9. Ramaswamy, S., Ross, K. N., Lander, E. S. & Golub, T. R. A molecular signature of metastasis in primary solid tumors. *Nature Genet.* 33, 49–54 (2003).
10. Nguyen, D. X. & Massague, J. Genetic determinants of cancer metastasis. *Nature Rev. Genet.* 8, 341–352 (2007)
11. Alvarez, J. D. *et al.* The MAR-binding protein SATB1 orchestrates temporal and spatial expression of multiple genes during T-cell development. *Genes Dev.* 14, 521–535 (2000)
12. Dickinson, L. A., Joh, T., Kohwi, Y. & Kohwi-Shigematsu, T. A tissue-specific MAR/SAR DNA-binding protein with unusual binding site recognition. *Cell* 70, 631–645 (1992).
13. Yasui, D., Miyano, M., Cai, S., Varga-Weisz, P. & Kohwi-Shigematsu, T. SATB1 targets chromatin remodelling to regulate genes over long distances. *Nature* 419, 641–645 (2002)
14. Cai, S., Han, H. J. & Kohwi-Shigematsu, T. Tissue-specific nuclear architecture and gene expression regulated by SATB1. *Nature Genet.* 34, 42–51 (2003)
15. Kohwi-Shigematsu, T. & Kohwi, Y. Torsional stress stabilizes extended base unpairing in suppressor sites flanking immunoglobulin heavy chain enhancer. *Biochemistry* 29, 9551–9560 (1990)
16. Kohwi-Shigematsu, T., deBelle, I., Dickinson, L. A., Galande, S. & Kohwi, Y. Identification of base-unpairing region-binding proteins and characterization of their *in vivo* binding sequences. *Methods Cell Biol.* 53, 323–354 (1998).
17. Bode, J. *et al.* Biological significance of unwinding capability of nuclear matrix-associating DNAs. *Science* 255, 195–197 (1992)
18. Cai, S., Lee, C. C. & Kohwi-Shigematsu, T. SATB1 packages densely looped, transcriptionally active chromatin for coordinated expression of cytokine genes. *Nature Genet.* 38, 1278–1288 (2006)
19. Debnath, J. *et al.* The role of apoptosis in creating and maintaining luminal space within normal and oncogene-expressing mammary acini. *Cell* 111, 29–40 (2002).
20. Weaver, V. M. *et al.* β4 integrin-dependent formation of polarized three-dimensional architecture confers resistance to apoptosis in normal and malignant mammary epithelium. *Cancer Cell* 2, 205–216 (2002)
21. Underwood, J. M. *et al.* The ultrastructure of MCF-10A acini. *J. Cell. Physiol.* 208, 141–148 (2006)
22. Kang, Y. *et al.* A multigenic program mediating breast cancer metastasis to bone. *Cancer Cell* 3, 537–549 (2003).
23. Minn, A. J. *et al.* Genes that mediate breast cancer metastasis to lung. *Nature* 436, 518–524 (2005)
24. Hellman, D. M., Kim, E. J., Lukanidin, E. & Grigorian, M. The metastasis associated protein S100A4: role in tumour progression and metastasis. *Br. J. Cancer* 92, 1955–1958 (2005)
25. Salven, P. *et al.* Vascular endothelial growth factors VEGF-B and VEGF-C are expressed in human tumors. *Am. J. Pathol.* 153, 103–108 (1998)
26. Chang, C. & Werb, Z. The many faces of metalloproteases: cell growth, invasion, angiogenesis and metastasis. *Trends Cell Biol.* 11, S37–S43 (2001)
27. Duffy, M. J., Maguire, T. M., Hill, A., McDermott, E. & O'Higgins, N. Metalloproteinases: role in breast carcinogenesis, invasion and metastasis. *Breast Cancer Res.* 2, 252–257 (2000).
28. Dumont, N. & Arteaga, C. L. Targeting the TGFβ signaling network in human neoplasia. *Cancer Cell* 3, 531–536 (2003).
29. Moussad, E. E. & Brigstock, D. R. Connective tissue growth factor: what's in a name? *Mol. Genet. Metab.* 71, 276–292 (2000).
30. Mosesson, Y. & Yarden, Y. Oncogenic growth factor receptors: implications for signal transduction therapy. *Semin. Cancer Biol.* 14, 262–270 (2004)
31. de Bono, J. S. & Rowinsky, E. K. The ErbB receptor family: a therapeutic target for cancer. *Trends Mol. Med.* 8, 519–526 (2002)
32. Steeg, P. S. Metastasis suppressors alter the signal transduction of cancer cells. *Nature Rev. Cancer* 3, 55–63 (2003).
33. Kang, Y. & Massague, J. Epithelial-mesenchyma transitions: twist in development and metastasis. *Cell* 118, 277–279 (2004)
34. Vidal, F. *et al.* Integrin β4 mutations associated with junctional epidermolysis bullosa with pyloric atresia. *Nature Genet.* 10, 229–234 (1995).
35. Takeichi, M. Cadherins in cancer: implications for invasion and metastasis. *Curr. Opin. Cell Biol.* 5, 806–811 (1993)
36. Cowin, P., Rowlands, T. M. & Hatsell, S. J. Cadherins and catenins in breast cancer. *Curr. Opin. Cell Biol.* 17, 499–508 (2005)
37. Tokes, A. M. *et al.* Claudin-1, -3 and -4 proteins and mRNA expression in benign and malignant breast lesions: a research study. *Breast Cancer Res.* 7, R296–R305 (2005)
38. Brembeck, F. H., Rosario, M. & Birchmeier, W. Balancing cell adhesion and Wnt signaling, the key role of β-catenin. *Curr. Opin. Genet. Dev.* 16, 51–59 (2006)
39. Berx, G. & Van Roy, F. The E-cadherin/catenin complex: an important gatekeeper in breast cancer tumorigenesis and malignant progression. *Breast Cancer Res.* 3, 289–293 (2001)
40. Thiery, J. P. Epithelial-mesenchymal transitions in tumour progression. *Nature Rev. Cancer* 2, 442–454 (2002)
41. Roberts, C. W. & Orkin, S. H. The SWI/SNF complex-chromatin and cancer. *Nature Rev. Cancer* 4, 133–142 (2004)
42. Bayin, S. B. & Ohm, J. E. Epigenetic gene silencing in cancer—a mechanism for early oncogenic pathway addiction? *Nature Rev. Cancer* 6, 107–116 (2006)
43. Drobic, B., Dunn, K. L., Espino, P. S. & Davie, J. R. Abnormalities of chromatin in tumor cells. *EXS* 96, 25–47 (2006).
44. Galande, S. & Kohwi-Shigematsu, T. Linking chromatin architecture to cellular phenotype: BUR-binding proteins in cancer. *J. Cell. Biochem., Suppl.* 35, 36–45 (2000)
45. Reeves, R., Edberg, D. D. & Li, Y. Architectural transcription factor HMGI(Y) promotes tumor progression and mesenchyma transition of human epithelial cells. *Mol. Cell. Biol.* 21, 575–594 (2001)
46. Neve, R. M. *et al.* A collection of breast cancer cell lines for the study of functionally distinct cancer subtypes. *Cancer Cell* 10, 515–527 (2006)
47. Holst, F. *et al.* Estrogen receptor α (ESR1) gene amplification is frequent in breast cancer. *Nature Genet.* 39, 655–660 (2007).
48. Severgnini, M. *et al.* Strategies for comparing gene expression profiles from different microarray platforms: application to a case-control experiment. *Anal. Biochem.* 353, 43–56 (2006).
49. Draghici, S., Khatri, P., Martins, R. P., Ostermeier, G. C. & Krawetz, S. A. Global functional profiling of gene expression. *Genomics* 81, 98–104 (2003)
50. Carter, D., Chakalova, L., Osborne, C. S., Dai, Y. F. & Fraser, P. Long-range chromatin regulatory interactions *in vivo*. *Nature Genet.* 32, 623–626 (2002).


**Supplementary Information** is linked to the online version of the paper at www.nature.com/nature.

**Acknowledgements** We thank J. W. Gray and M. Stampfer for providing some of the cell lines, M. J. Bissell, C. W. Roberts, J. A. Nickerson and S. A. Krauss for critical reading of the manuscript and useful suggestions, K. Novak and M. Kohwi for help in manuscript preparation, and R. Simon and M. Falduto for assisting expression microarray data analysis. This work was supported by a National Institute of Health grant to T.K.-S. and also by University of California Breast Cancer Research Program at its initial stage.

**Author Information** The expression data set is on the GEO website under accession number GSE5417. Reprints and permissions information is available at www.nature.com/reprints. Correspondence and requests for materials should be addressed to T.K.-S. (Terumiks@lbl.gov) or Y.K. (YKohwi@lbl.gov).

LETTERS

# Reflected light from sand grains in the terrestrial zone of a protoplanetary disk

William Herbst[1], Catrina M. Hamilton[2], Katherine LeDuc[1], Joshua N. Winn[3], Christopher M. Johns-Krull[4], Reinhard Mundt[5] & Mansur Ibrahimov[6]

**In the standard model of terrestrial planet formation, the first step in the process is for interstellar dust to coagulate within a protoplanetary disk surrounding a young star, forming large grains that settle towards the disk plane[1]. Interstellar grains of typical size ~0.1 μm are expected to grow to millimetre- (sand), centimetre- (pebble) or even metre-sized (boulder) objects rather quickly[2]. Unfortunately, such evolved disks are hard to observe because the ratio of surface area to volume of their constituents is small. We readily detect dust around young objects known as 'classical' T Tauri stars, but there is little or no evidence of it in the slightly more evolved 'weak-line' systems[3]. Here we report observations of a 3-Myr-old star, which show that grains have grown to about millimetre size or larger in the terrestrial zone (within ~3 AU) of this star. The fortuitous geometry of the KH 15D binary star system allows us to infer that, when both stars are occulted by the surrounding disk, it appears as a nearly edge-on ring illuminated by one of the central binary components. This work complements the study of terrestrial zones of younger disks that have been recently resolved by interferometry[4–6].**

Figure 1 shows two views of the geometry of the KH 15D system according to our present interpretation. We adopt an updated version of model 3 of ref. 7 for all quantitative discussion. KH 15D is known to be a pre-main-sequence binary system with an age of ~3 Myr and a distance of 760 pc (refs 8–10). It consists of $0.6M_{\odot}$ and $0.7M_{\odot}$ stars (designated A and B, respectively[7]; $M_{\odot}$ is the solar mass) in an eccentric orbit ($e = 0.6$) with a period of 48.37 days. Its orbit is inclined to a circumstellar disk that extends to ~5 AU (ref. 11); precession of the disk is causing an occulting edge to advance across the orbit of the binary, as shown in Fig. 1b[11,12]. The precession timescale for the disk is ~1,000 yr, and it must either be warped[11] or flared (or both) to cause both the foreground occultation and the background reflection. It is not known where, within this ring, the occulting edge is actually located—it could be at the inner or outer edge or at the high point of a warp somewhere in between. See Fig. 6 of the model paper[7] for a sketch of the possibilities.

For the past decade, only one star (A) has appeared above the disk edge, undergoing a dramatic 'sunrise' and 'sunset' every orbital cycle. During this time interval, the brightness of the system as measured at Earth has depended primarily on only one variable, namely the elevation ($\Delta$) of star A above (or below) the 'horizon' defined by the edge of the occulting screen as projected on the plane of the sky. We

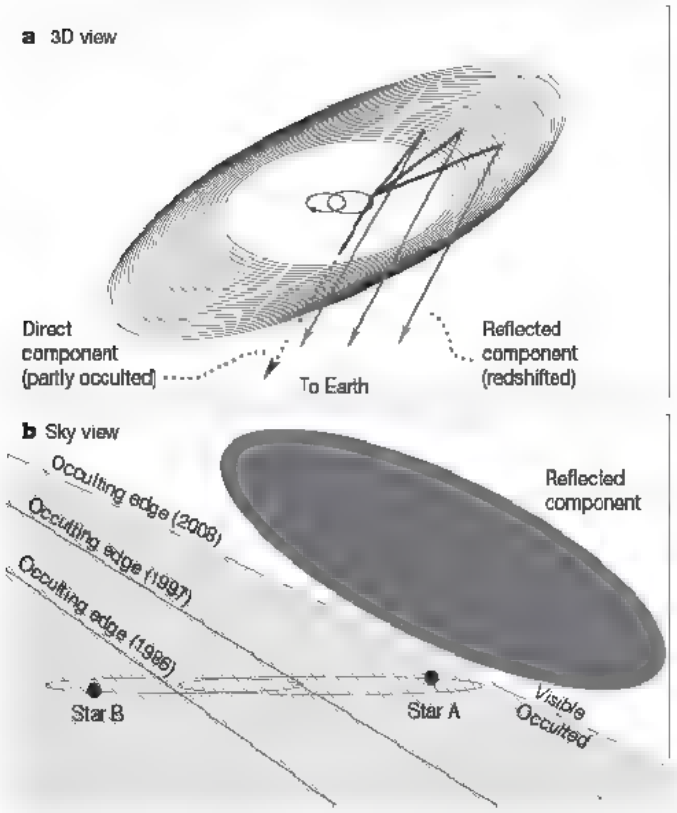


**Figure 1 | Schematic drawings showing our interpretation of the geometry of the KH 15D system. a, b,** Drawings showing a three-dimensional (3D) view (**a**) and a sky view (**b**). Only the part of the system to the right of the solid line in **b** is visible, owing to the opaque screen. The elliptical orbits of stars A and B are shown, as is the occulting edge, which advances from left to right. At present, the screen is just intercepting the outer edge of the orbit of star A, so that for a while, neither star will be seen above the occulting screen. The inner disk radius is located at 0.6 AU, which is approximately the location of the 3:1 orbital resonance that defines it according to dynamical models[16]. The outer disk is located at 5 AU, based on the precession timescale of ~1,000 yr (refs 7, 11). The important difference between this model and others is that the reflected light is now recognized to come from evolved solids, probably of millimetre size, that have condensed in the terrestrial planet formation zone of this pre-planetary disk. Disks like this have long been hypothesized to exist as an intermediate step between the gas-rich, dust-laden disks seen around classical T Tauri stars and the so-called 'debris' disks seen around older stars such as β Pictoris[17] that contain dust due to fragmenting collisions between metre- or kilometre-sized planetesimals. The KH 15D disk is remarkably dust-free, and represents an intermediate stage between a classical T Tauri star disk and a debris disk. Although not depicted here, there is still some gas in the disk, as evidenced by weak accretion signatures, including forbidden lines of sulphur and oxygen and extended emission wings to hydrogen lines[18,19].

[1]Astronomy Department, Wesleyan University, Middletown, Connecticut 06459, USA. [2]Physics and Astronomy Department, Dickinson College, Carlisle, Pennsylvania 17013, USA. [3]Department of Physics, Massachusetts Institute of Technology, 77 Massachusetts Avenue, Cambridge, Massachusetts 02139, USA. [4]Department of Physics and Astronomy, Rice University, Houston, Texas 77005, USA. [5]Max-Planck-Institut für Astronomie, Königstuhl 17, D-69117 Heidelberg, Germany. [6]Ulugh Beg Astronomical Institute of the Uzbek Academy of Sciences, Astronomicheskaya 33, 700052 Tashkent, Uzbekistan

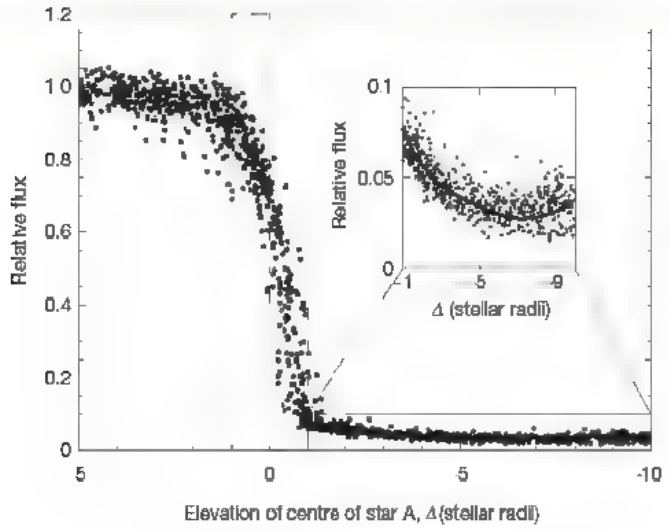


measure $\Delta$ in units of the radius of star A ($1.3R_\odot \approx 10^9$ m; $R_\odot$ is the solar radius). Figure 2 shows the system brightness at 0.80 μm wavelength, as a function of $\Delta$, during the last four years (ref. 13; K.I., *et al.*, manuscript in preparation). For $\Delta > 1$, the full disk of star A is

**Figure 2 | Brightness variation of KH 15D with elevation of star A.** Abscissa units are radii of star A ($1.3R_\odot \approx 10^9$ m). Dashed lines show the points where the screen first contacts the limb of the star ($\Delta = 1$), where the star is half obscured ($\Delta = 0$) and where it is just fully obscured ($\Delta = -1$). Inset, behaviour after occultation on a modified scale for clarity. The rise in brightness that occurs for elevations below −6 is due to the influence of star B, which is closer to the screen edge than star A at those orbital phases. The solid line is a 'proof-of-concept' model of the light curve discussed in more detail in Supplementary Information. It represents a fifth-order polynomial fit to the predicted flux of the system based on the expression.

$$\mathrm{Flux}(\Delta) = \exp[-\tau(\mathrm{A})] + 1.37\exp[-\tau(\mathrm{B})] + C_1 f_{\mathrm{refl}}(\Delta) + C_2$$

where $f_{\mathrm{refl}}(\Delta) = \Omega_{\mathrm{ring}}(\mathrm{A}) + 1.37\Omega_{\mathrm{ring}}(\mathrm{B})$, and $\Omega_{\mathrm{ring}}$ is the solid angle subtended by the top of the disk (as a fraction of $4\pi$ sr) as seen from the relevant star. The luminosity of star B is 1.37 times that of star A[7,20,21]. The disk is modelled as a flat ring of inner radius 0.5 AU and outer radius 5 AU (refs 11, 16). The exponential factors account for transmitted light, where $\tau = 1.46 - 1.46\Delta$. The parameters $C_1$ and $C_2$ were chosen to roughly fit the data by eye and have the values $C_1 = 2.0$ and $C_2 = 0.02$ for this 'proof-of-concept' model. Physically, $C_1$ controls the relative amount of phase-dependent scattered light and depends on the geometry, albedo and phase function of the particles. $C_2$ allows for a small amount of invariable scattered light. The maximum solid angle subtended by the top of the disk in our model is 0.43 sr for star A and 0.10 sr for star B.

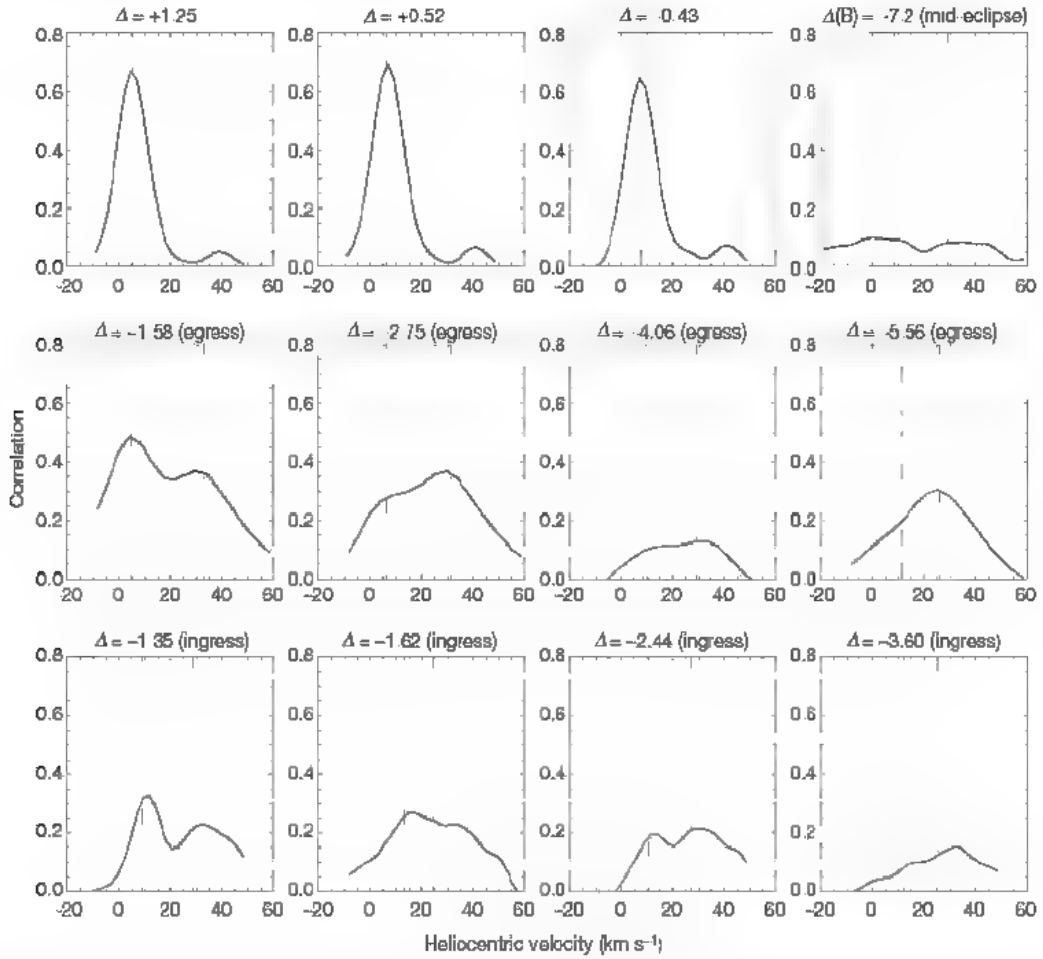


**Figure 3 | Spectral variation of KH 15D with elevation of star A.** Shown are cross-correlation functions of KH 15D spectra with a K7 V synthetic spectrum over the spectral range 0.644–0.645 μm. The telescopes and instruments used were the 10 m Keck I telescope and HIRES echelle spectrometer, the UV–visual echelle spectrograph on the European Southern Observatory's 8.2 m Very Large Telescope, and the 6.5 m Magellan II telescope and the MIKE echelle spectrometer. The spectral region includes several photospheric lines, primarily due to Ba I, and is not affected by emission lines or terrestrial features. The vertical dashed lines indicate the radial velocity of star A (or B, for the mid-eclipse spectrum) based on our model[7,22]. The dashed-dotted lines show the expected velocity of the reflected component if the mirroring particles had the systemic velocity of 18.65 km s$^{-1}$ and were located directly behind the star from our vantage point. When $\Delta > -1$, the light from KH 15D is dominated by star A (upper row, left three panels). When star A is fully occulted from our vantage point (middle and bottom rows), but still visible to the reflecting particles on the top side of the back of the disk ($-6 < \Delta < -1$), it is the reflected light from star A that contributes to the system's light and produces the red-shifted radial velocity component. The spectrum in the upper-right panel was obtained near mid-eclipse in 2004, at a time when $\Delta \equiv \Delta(\mathrm{A}) = -7.6$ and $\Delta(\mathrm{B}) = -7.2$. Hence, star B, which is also brighter, would be the expected source of most of the system's light in our model, and its velocity and predicted reflection component are shown.

visible and the system's flux is determined by its brightness; for $+1 > \Delta > -1$, the star is partly occulted; and for $\Delta < -1$, it is fully occulted. As Fig. 2 inset shows, while the total light from the KH 15D system plummets precipitously in the interval $+1 > \Delta > -1$, it also continues to depend on $\Delta$ even after full occultation ($\Delta < -1$).

In earlier studies, the system's visibility after full occultation has been attributed to haloes of scattered light around each component or around the system as a whole[7,14]. Analysis of high-resolution spectra of the system when faint now paints a different picture. Figure 3 displays the cross-correlation functions of a number of high-resolution spectra with a K7 V synthetic spectrum. The spectra show a single strong peak at the radial velocity of star A for $\Delta > -1$, but become double-peaked after full occultation, with one peak corresponding to star A and the other to a red-shifted component. The radial velocity of the second component does not match star B, which is also far below the horizon at these times (see Fig. 1) and heavily obscured. We propose that the second peak is reflected light from the part of KH 15D's disk that is behind the stars from our vantage point. Star A is moving towards the Earth (relative to the systemic velocity of $+18.65\,\mathrm{km\,s^{-1}}$) during both ingress and egress, so its reflection from a mirror behind the star would appear to be moving away from us (red-shifted). During mid-eclipse, it is star B that is more elevated with respect to the obscuring edge and we may see its direct light (very dimly) and its reflection, as the upper-right panel in Fig. 3 shows. We find good agreement, especially during ingress, between the predicted radial velocities according to this interpretation and the observed velocities of the red-shifted components.

Our reflection model also accounts well for the shape of the light variations during full occultation, as we now discuss (see Supplementary Information for additional details). The inclination of the orbit to the ring means that, viewed from a point on the 'top surface' (that is, the surface visible from Earth) of the back side of the ring, only one star is fully visible at any time and its height above the local horizon depends on the orbital phase. We assume that the brightness of the system is proportional to the solid angle subtended by the top of the ring as seen from the illuminating star. We also allow for a transmission component to the light, as required by the spectra. From simultaneous photometry obtained on three nights when we could separate the direct and reflected light, we can estimate the optical depth ($\tau$) of the occulting screen as a function of $\Delta$. These data show that $\tau = 2.9$ at $\Delta = -1$ and that it increases roughly linearly with $\Delta$, as one would expect. The reflection is assumed to come from a flat ring with inner and outer radii of 0.5 AU and 5 AU, respectively; a representative model light curve is shown as the solid line in Fig. 2 inset. It reproduces the shape of the observed light curve quite well, in particular the brightening that occurs for $\Delta < -6$ owing to the fact that star B has risen to become the illuminating star.

The data and our interpretation also permit us to derive constraints on the size of the grains that constitute the obscuring/reflecting disk. Figure 4 shows how the colour of the system changes during full occultation in the optical and near-infrared (Fig. 4a and b, respectively). Importantly, there is no evidence for reddening, which implies that the ring particles are significantly larger (by at least a factor of 20) than those in the interstellar medium[14]. Immediately after star A 'sets' ($\Delta < -1$), some light from that star is still visible through the occulting part of the disk, allowing a measurement of the optical depth along that path length, which provides a further size constraint on the grains. In our model, the screen optical depth ($\tau$) can be expressed as $\tau = 64MR^{-2}r^{-1}\rho^{-1}(L/T)$, where $M$ is the total mass of obscuring particles (in Earth masses), $R$ is the disk radius (in AU), $r$ is the grain radius (in mm), $\rho$ is the density of a grain (in $\mathrm{g\,cm^{-3}}$), $L$ is the path length of the radiation through the obscuring medium, and $T$ is the disk thickness. Our data show that $\tau = 2.9$ at $\Delta = -1$, so for representative choices of $\rho = 3$ and $L/T = 0.05$, we obtain $r \approx \Sigma$, where $\Sigma$ is the mass surface density of the disk in Earth masses per square AU. Using our own Solar System as a guide, we may

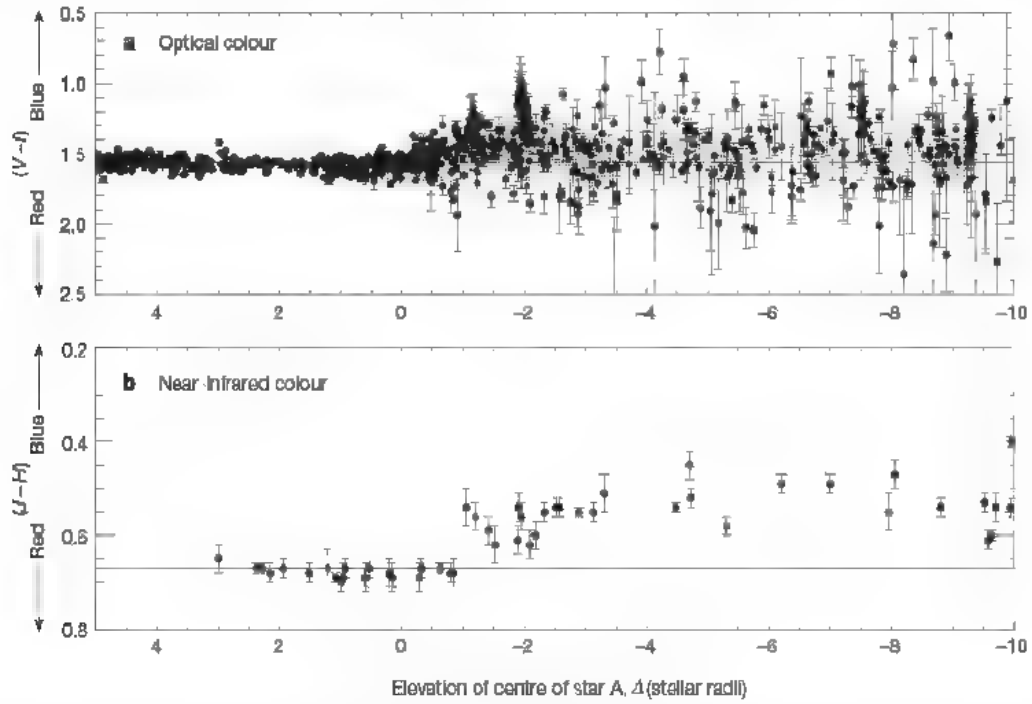


**Figure 4 | Colour variation of KH 15D with elevation of star A.** **a**, The $V$ $I$ colour of the Cousins system (ref. 13; K.L. *et al.*, manuscript in preparation), with effective wavelengths at 0.55 μm and 0.80 μm, respectively; **b**, comparison of brightness in $J$ (1.26 μm) and $H$ (1.66 μm)[23]. Error bars, ±1 s.d. In the optical range, KH 15D has a stable colour before the beginning of the eclipse ($\Delta > 1$), becomes steadily bluer during eclipse ($1 > \Delta >$ 1) and maintains the bluer colour during the phases when reflected light dominates ($\Delta <$ −1). In the near-infrared, there is also a transition to a bluer light during the reflection phases. The solid line shows the average colours out of eclipse. The blueness is consistent with what one might expect from unweathered silicates having particle sizes significantly larger than in the interstellar medium[24]. Relatively blue spectral response is characteristic of some asteroidal material found in the Solar System, such as eucrites (pyroxene plus plagioclase feldspar). We further note that the shape of the albedo function is not consistent with scattering from grains of interstellar-medium size nor is the fact that most of the scattered light clearly arrives by back-scattering, not forward scattering. Finally, note that there is no evidence of reddening of the direct light of either star at any phase; the occulting screen shows no evidence of submicrometre-sized dust.

infer a grain size for this path length through the disk of roughly 1 mm. Interestingly, this is characteristic of chondrules, the glassy spherules that are a primary component of the most primitive meteorites found in our own Solar System[15].

The most uncertain parameter in our expression for $\tau$ is $(L/T)$, and this could be larger than the value of 0.05 we adopt, which would increase the inferred size of the grains. Our derivation (see Supplementary Information) assumes that the grains are uniformly distributed through a cylindrical volume of thickness $T$, where $T$ is determined from the projected extent of the obscuring material on the plane of the sky. A more realistic picture may be that the grains are concentrated into a thinner structure, which is tilted, warped, corrugated and/or flared in such a way that its footprint of obscuration on the sky is much larger than its physical thickness. In this case $L/T > 0.05$, and one might have a disk composed of pebbles. Furthermore, if there were a vertical gradient of grain size within the disk, we would expect to be measuring the smallest grains present, as they would have the largest scale height. For both of these reasons, we consider our estimate of ~1 mm to be characteristic of the smallest grains that could be present in the disk; the bulk of the disk might consist of even larger grains.

**Received 11 September 2007; accepted 2 January 2008.**


1. Dominik, C., Blum, J., Cuzzi, J. N. & Wurm, G. in *Protostars and Planets V* (eds Reipurth, B., Jewitt, D. & Keil, K.) 783–800 (Univ. Arizona Press, Tucson, 2007).
2. Natta, A. *et al.* in *Protostars and Planets V* (eds Reipurth, B., Jewitt, D. & Keil, K.) 767–781 (Univ. Arizona Press, Tucson, 2007).
3. Wolk, S. J. & Walter, F. M. A search for protoplanetary disks around naked T Tauri stars. *Astron. J.* 111, 2066–2076 (1996).
4. van Boekel, R. *et al.* The building blocks of planets within the 'terrestrial' region of protoplanetary disks. *Nature* 432, 479–482 (2004).
5. Isella, A., Testi, L. & Natta, A. Large dust grains in the inner region of circumstellar disks. *Astron. Astrophys.* 451, 951–959 (2006).
6. Eisner, J. Water vapour and hydrogen in the terrestrial-planet-forming region of a protoplanetary disk. *Nature* 447, 562–564 (2007).
7. Winn, J. N. *et al.* The orbit and occultations of KH 15D. *Astrophys. J.* 644, 510–524 (2006).
8. Kearns, K. E. & Herbst, W. Additional periodic variables in NGC 2264. *Astron. J.* 116, 261–265 (1997).
9. Hamilton, C. M., Herbst, W., Shih, C. & Ferro, A. J. Eclipses by a circumstellar dust feature in the pre-main sequence star KH 15D. *Astrophys. J.* 554, L201–L204 (2001).
10. Herbst, W. *et al.* Fine structure in the circumstellar environment of a young, solar-like star: The unique eclipses of KH 15D. *Publ. Astron. Soc. Pacif.* 114, 1167–1172 (2002).
11. Chiang, E. I. & Murray-Clay, R. A. The circumbinary ring of KH 15D. *Astrophys. J.* 607, 913–920 (2004).
12. Winn, J. N., Holman, M. J., Johnson, J. A., Stanek, K. Z. & Garnavich, P. M. KH 15D: Gradual occultation of a pre-main sequence binary. *Astrophys. J.* 603, L45–L48 (2004).
13. Hamilton, C. M. *et al.* The disappearing act of KH 15D: Photometric results from 1995 to 2004. *Astron. J.* 130, 1896–1915 (2005).
14. Agol, E., Barth, A. J., Wolf, S. & Charbonneau, D. Spectropolarimetry and modeling of the eclipsing T Tauri star KH 15D. *Astrophys. J.* 600, 781–788 (2004).
15. Boss, A. P. in *Chondrules and the Protoplanetary Disk* (eds Hewins, R. H., Jones, R. H. & Scott, E. R. D.) 257–263 (Cambridge Univ. Press, New York, 1996).
16. Artymowicz, P. & Lubow, S. H. Dynamics of binary-disk interaction. 1. Resonances and disk gap sizes. *Astrophys. J.* 421, 651–667 (1994).
17. Golimowski, D. A. *et al.* HST/ACS multiband coronagraphic imaging of the debris disk around Beta Pictoris. *Astron. J.* 131, 3109–3130 (2006).
18. Hamilton, C. M., Herbst, W., Mundt, R., Baller-Jones, C. A. L. & Johns-Krull, C. M. Natural coronagraphic observations of the eclipsing T Tauri system KH 15D: Evidence of accretion and bipolar outflow in a weak-line T Tauri star. *Astrophys. J.* 591, L45–L48 (2004).
19. Tokunaga, A. T. *et al.* $H_2$ emission nebulosity associated with KH 15D. *Astrophys. J.* 601, L91–L94 (2004).
20. Johnson, J. A. & Winn, J. N. The history of the mysterious eclipses of KH 15D: Asiago Observatory, 1967–1982. *Astron. J.* 127, 2344–2351 (2004).
21. Johnson, J. A. *et al.* The history of the mysterious eclipses of KH 15D. II. Asiago, Kiso, Kitt Peak, Mount Wilson, Palomar, Tautenburg, and Rozhen Observatories, 1954–1997. *Astron. J.* 129, 1978–1984 (2005).
22. Johnson, J. A., Marcy, G. W., Hamilton, C. M., Herbst, W. & Johns-Krull, C. M. KH 15D: A spectroscopic binary. *Astron. J.* 128, 1265–1272 (2004).
23. Kusakabe, N. *et al.* Near-infrared photometric monitoring of the pre-main sequence object KH 15D. *Astrophys. J.* 632, L139–L142 (2005).
24. Burbine, T. H. & Binzel, R. P. in *Asteroids, Comets, Meteors 1993* (eds Milani, A., Di Martino, M. & Cellino, A.) 255–270 (Proc. IAU Symp. 160, Kluwer, Dordrecht, 1994).


**Supplementary Information** is linked to the online version of the paper at www.nature.com/nature.

**Acknowledgements** This material is based on work supported by the US National Aeronautics and Space Administration (NASA) through the Origins of Solar Systems programme. Some of the data presented here were obtained at the W. M. Keck Observatory from telescope time allocated to NASA through the agency's scientific partnership with the California Institute of Technology and the University of California. The Observatory was made possible by the financial support of the W. M. Keck Foundation. We appreciate comments from E. Chiang, M. Gilmore, J. Greenwood and E. Jensen.

**Author Information** Reprints and permissions information is available at www.nature.com/reprints. Correspondence and requests for materials should be addressed to W.H. (wherbst@wesleyan.edu).

LETTERS

# Hierarchical self-assembly of DNA into symmetric supramolecular polyhedra

Yu He[1], Tao Ye[1], Min Su[2], Chuan Zhang[1], Alexander E. Ribbe[1], Wen Jiang[2] & Chengde Mao[1]

**DNA is renowned for its double helix structure and the base pairing that enables the recognition and highly selective binding of complementary DNA strands. These features, and the ability to create DNA strands with any desired sequence of bases, have led to the use of DNA rationally to design various nanostructures and even execute molecular computations[1–4]. Of the wide range of self-assembled DNA nanostructures reported, most are one- or two-dimensional[5–9]. Examples of three-dimensional DNA structures include cubes[10], truncated octahedra[11], octohedra[12] and tetrahedra[13,14], which are all comprised of many different DNA strands with unique sequences. When aiming for large structures, the need to synthesize large numbers (hundreds) of unique DNA strands poses a challenging design problem[9,15]. Here, we demonstrate a simple solution to this problem: the design of basic DNA building units in such a way that many copies of identical units assemble into larger three-dimensional structures. We test this hierarchical self-assembly concept with DNA molecules that form three-point-star motifs, or tiles. By controlling the flexibility and concentration of the tiles, the one-pot assembly yields tetrahedra, dodecahedra or buckyballs that are tens of nanometres in size and comprised of four, twenty or sixty individual tiles, respectively. We expect that our assembly strategy can be adapted to allow the fabrication of a range of relatively complex three-dimensional structures.**

Our approach to forming DNA polyhedra is a one-pot self-assembly process illustrated in Fig. 1: individual single strands of DNA first assemble into sticky-ended, three-point-star motifs (tiles), which then further assemble into polyhedra through sticky-end association between the tiles. The three-point-star motif contains a threefold rotational symmetry and consists of seven strands: a long repetitive central strand (blue-red; strand L or L′), three identical medium strands (green; strand M), and three identical short peripheral strands (black; strand S). At the centre of the motif are three single-stranded loops (coloured red). The flexibility of the motif can be easily adjusted by varying the loop length, with increased loop length increasing tile flexibility. The termini of each branch of the tile carry two complementary, four-base-long, single-stranded overhangs, or sticky ends. Association between the sticky-ends allows the tiles to further assemble into larger structures such as the polyhedra described here.

The three-point-star motif has been used for the assembly of flat two-dimensional (2D) crystals[16,17], where neighbouring units face in opposite directions of the crystal plane to cancel the intrinsic curvature of the DNA tiles. Because polyhedra are closed three-dimensional (3D) objects containing a finite number of component tiles, we reasoned that three factors would promote polyhedron formation. (1) If all component DNA tiles face in the same direction, their curvatures would add up and promote the formation of closed structures. For example, some closed DNA tubular structures have been observed when all DNA tiles face the same side of the crystal plane[7]. This requirement can be easily satisfied by choosing the length of each pseudo-continuous DNA duplex in the final structures to be four turns (42 bases). (2) Self-assembly is an inter-unit process. This means that higher (micromolar) DNA concentrations favour large assemblies such as flat 2D crystals, whereas lower DNA concentrations favour small assemblies such as polyhedra. This concentration-dependent kinetic effect should also provide some control over polyhedral size. (3) 2D crystal formation was found to require loops that are two to three bases long[17]. Elongating the loops increases tile flexibility; this should prevent the assembly of DNA stars into large 2D crystals and instead promote the formation of smaller structures.

We first tested this hypothesis by assembling a DNA tetrahedron from four three-point-star tiles. Each tile sits at a vertex, and its branches each associate with a branch from another tile to form the edges of the tetrahedron. The assembled tiles at the four vertices retain the threefold rotational symmetry of the free, individual star tiles, but are no longer planar. In fact, they are significantly bent and thus need to be quite flexible. To provide this flexibility, the loop length is designed to be five bases long. This ensures that the DNA stars will associate with each other under hybridization conditions to form highly flexible assemblies, which allows the free sticky-ends in the assemblies to meet and associate with each other to yield closed

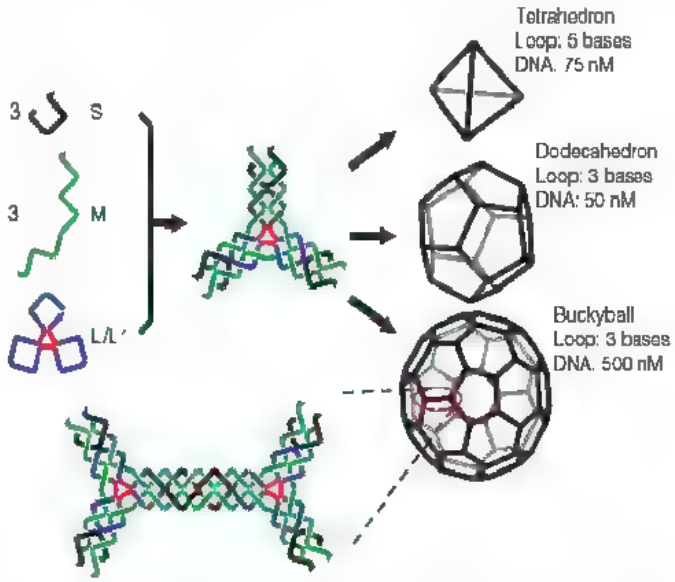


**Figure 1 | Self-assembly of DNA polyhedra.** Three different types of DNA single strands stepwise assemble into symmetric three-point-star motifs (tiles) and then into polyhedra in a one-pot process. There are three single-stranded loops (coloured red) in the centre of the complex. The final structures (polyhedra) are determined by the loop length (3 or 5 bases long) and the DNA concentration.

[1]Department of Chemistry, [2]Markey Center for Structural Biology and Department of Biological Sciences, Purdue University, West Lafayette, Indiana 47907, USA

structures (without any free sticky-ends). The size of the closed structures is concentration-dependent. At sufficiently low DNA concentration, we expect the formation of tetrahedra because they are the smallest closed structures that can form without deformation of the pseudo-continuous DNA duplexes.

The DNA tetrahedra form when solutions containing the DNA strands are mixed and slowly cooled from 95 °C to room temperature (22 °C). Non-denaturing polyacrylamide gel electrophoresis (PAGE) of the resultant solution shows that for DNA concentrations of <100 nM, the dominant DNA complex contains four star tiles (Supplementary Fig. 1). Dynamic light scattering (DLS) provides a direct measurement of the physical sizes of the dissolved DNA complexes (Fig. 2a), yielding an apparent hydrodynamic radius of ~10.3 ± 0.6 nm (s.d.). This value agrees with the radius of the circumscribed sphere of the DNA tetrahedron model (10.9 nm), assuming 0.33 nm per base pair for the pitch and 2 nm for the diameter of a DNA duplex, respectively.

To provide direct evidence for the self-assembly of DNA into tetrahedra, we imaged the samples using atomic force microscopy (AFM) and cryogenic transmission electronic microscopy (cryo-EM). DNA species appear as uniform-sized, triangular particles when imaged by AFM in air (Fig. 2b). Strong electrostatic interactions with the substrate and dehydration cause the 3D DNA tetrahedron to collapse into a 2D object with a triangle shape, which is consistent with the features observed by AFM. The most convincing experimental support for tetrahedron formation comes from cryo-EM analysis (Fig. 2c, d), with the images showing that most particles have tetrahedral shapes of the expected size. The yield of correctly assembled DNA tetrahedra is ~90%, as estimated from the number of particles observed by cryo-EM and by gel electrophoretic analysis (Supplementary Fig. 2). We reconstructed from the experimentally observed particles a 3D structure for the DNA tetrahedron at 2.6 nm resolution, using single-particle 3D reconstruction[18]. The computed projections from this 3D reconstruction match well to the individual particle images (Fig. 2d) and the class averages of raw particle images with similar views (Supplementary Fig. 4). In the reconstructed 3D tetrahedron structure (Fig. 2e), the observed edges are 16 nm long, nicely matching the designed model (16.2 nm). The thickness and width of the edge is also consistent with two DNA duplexes arranged side by side in the design. At the threefold vertices, a depression is visible, which is consistent with the central cavity in star motif.

To demonstrate the versatility of the hierarchical self-assembly approach, we produced a DNA dodecahedron consisting of 20 three-point-star tiles, 12 faces (pentagons), and 30 edges. Compared to a tetrahedron, dodecahedra are less curved and the star tiles need not be nearly as flexible. Thus, the length of the central single-stranded loop is reduced to three bases long to make the star tiles much stiffer.

At a low DNA concentration (50 nM), DNA star tiles readily assemble into dodecahedra (Fig. 3). DLS measurements (Fig. 3a) reveal an apparent hydrodynamic radius for the assembled objects of ~24.0 ± 1.8 nm (s.d.), which agrees with the value (23.6 nm) estimated from the designed structural model. AFM imaging in air reveals circular features with uniform sizes (Fig. 3b) and apparent diameters of ~70 nm. This appearance of the assembled objects can be explained by DNA dehydration and strong electrostatic interactions between the DNA and mica substrate surface, which collapses the DNA dodecahedra into two layers. A close-up view (Fig. 3b inset) shows a component pentagon located at the centre of the top layer, which is in reasonable agreement with a collapsed 2D projection of a dodecahedron.

The strongest experimental evidence for dodecahedron formation is provided by cryo-EM analysis (Fig. 3c–e), which reveals dodecahedron-shaped objects of the expected size (in the boxed areas in Fig. 3c and Supplementary Fig. 6). Single-particle reconstruction using experimentally observed particles yields a 3D map of the DNA dodecahedron. An icosahedral symmetry, which shares the same symmetry as a dodecahedron, was imposed during the reconstruction, resulting in a well-defined dodecahedron structure (with a resolution of 2.8 nm). The computed projections from this 3D reconstruction match well to the individual particle images (Fig. 3d) and the class averages of raw particle images with similar views (Supplementary Fig. 7). The radius of the circumscribed sphere of the reconstructed dodecahedron model is 23.5 nm, consistent with both the design and the DLS data. Each edge is 4 nm wide and 2 nm thick,

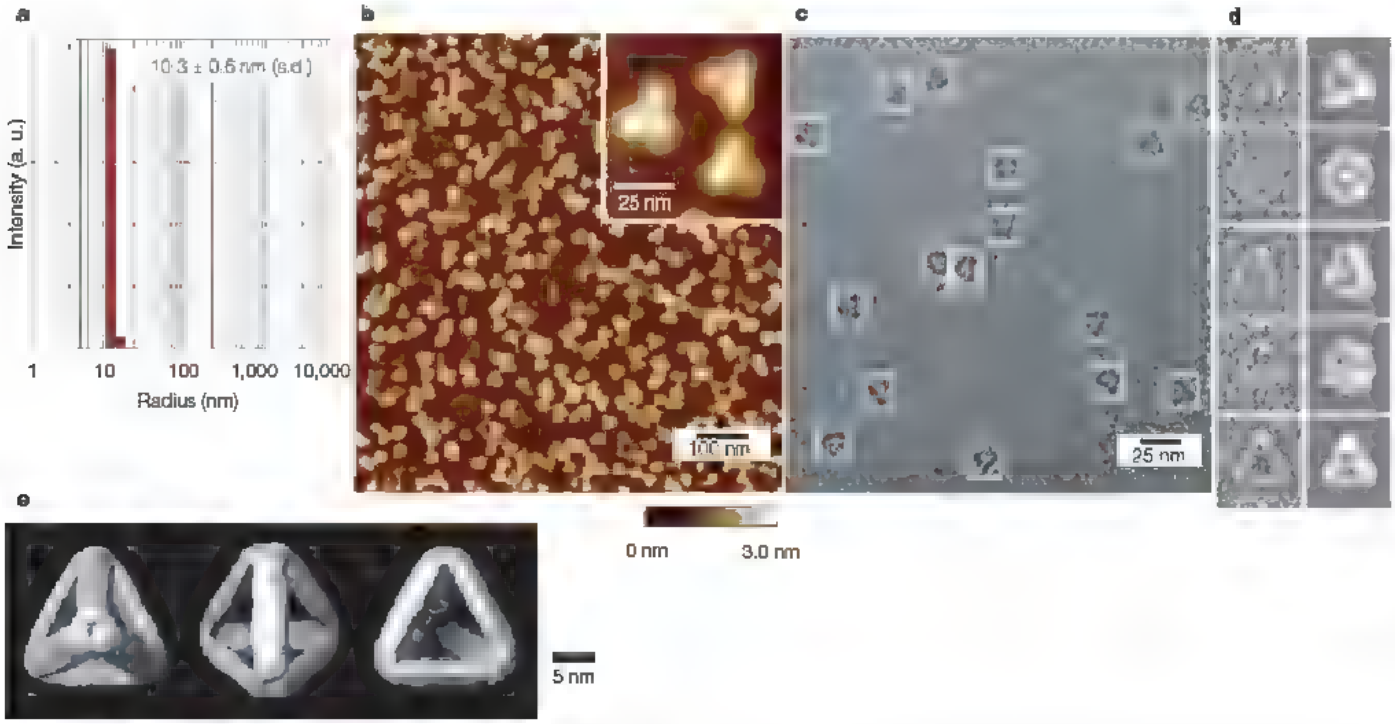


**Figure 2 | Characterization of the DNA tetrahedron by DLS, AFM and Cryo-EM.** **a**, DLS shows the size histogram of DNA tetrahedron. **b**, An AFM image of DNA tetrahedra and a close-up view (inset). A height scale bar is shown at the bottom. **c**, A representative cryo-EM image. White boxes indicate the DNA particles. For a magnified large view field, see Supplementary Fig. 3. **d**, Raw cryo-EM images of individual particles and the corresponding projections of the DNA tetrahedron 3D structure reconstructed from the cryo-EM images. These particles are selected from different image frames to represent views at different orientations. **e**, Three views of the reconstructed DNA tetrahedron structure

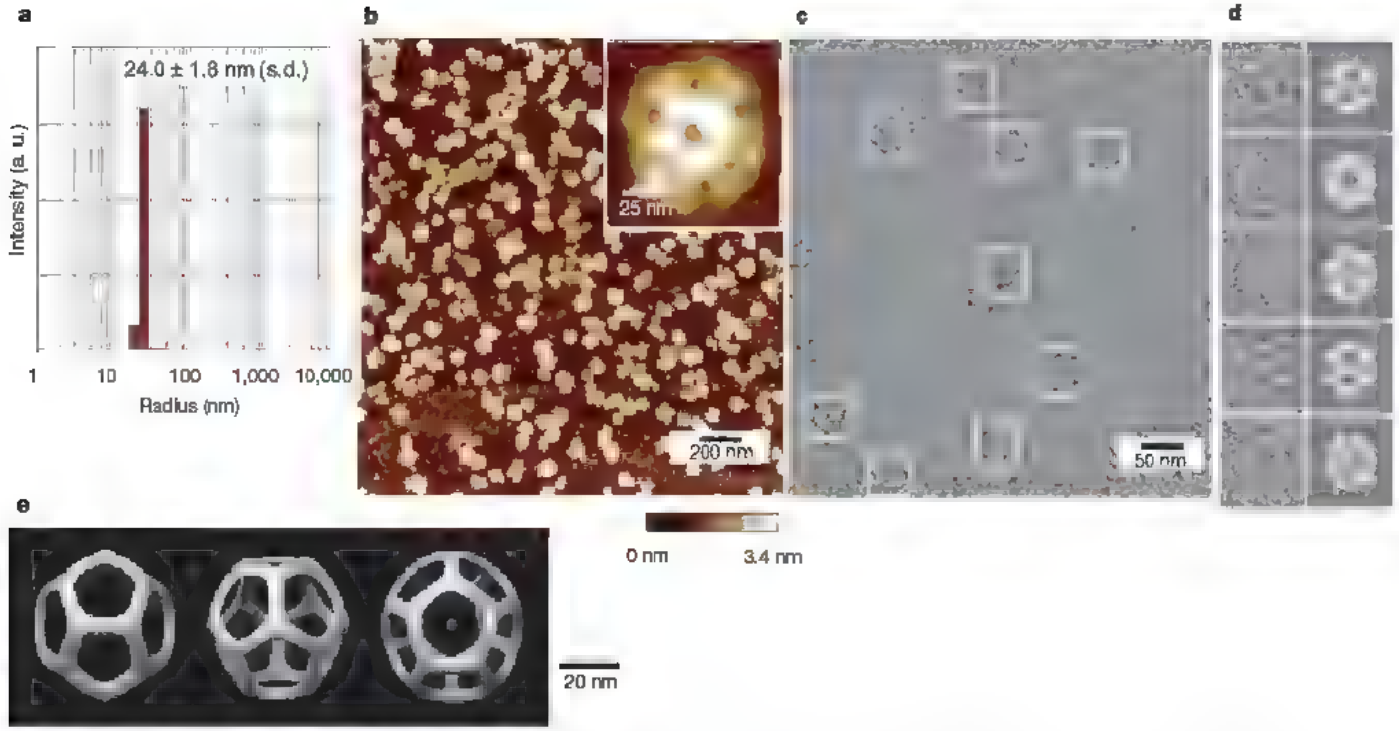


**Figure 3 | A DNA dodecahedron.** **a**, Size histogram of the DNA dodecahedron measured by DLS. **b**, **c**, An AFM image (**b**) and a cryo-EM image (**c**) of the DNA assemblies. For a magnified large view field, see Supplementary Fig. 6. **d**, Individual raw cryo-EM images and the corresponding projections of the DNA dodecahedron 3D structure reconstructed from cryo-EM images. These particles are selected from different image frames to represent views at different orientations. **e**, Three views of the DNA dodecahedron 3D structure.

which are reasonable dimensions for two associated branches from two neighbouring star tiles.

A truncated icosahedron structure is another type of highly symmetric polyhedron. It contains 60 vertexes, 90 edges and 32 faces (12 pentagons and 20 hexagons). Two well-known examples of such a structure are soccer balls and Buckminsterfullerene molecules (or buckyballs, $C_{60}$). It remains challenging to rationally design a molecular system that can self-assemble into such a complex structure. However, at a high DNA concentration (500 nM), the star tiles (with three-base-long, single-stranded loops at the centre) readily assemble into the buckyball structure—as suggested by DLS analysis, AFM imaging and cryo-EM analysis (Fig. 4). The DLS measurement indicates that the DNA assemblies have an apparent hydrodynamic radius of 42.2 ± 4.0 nm (s.d.), close to the calculated radius of the

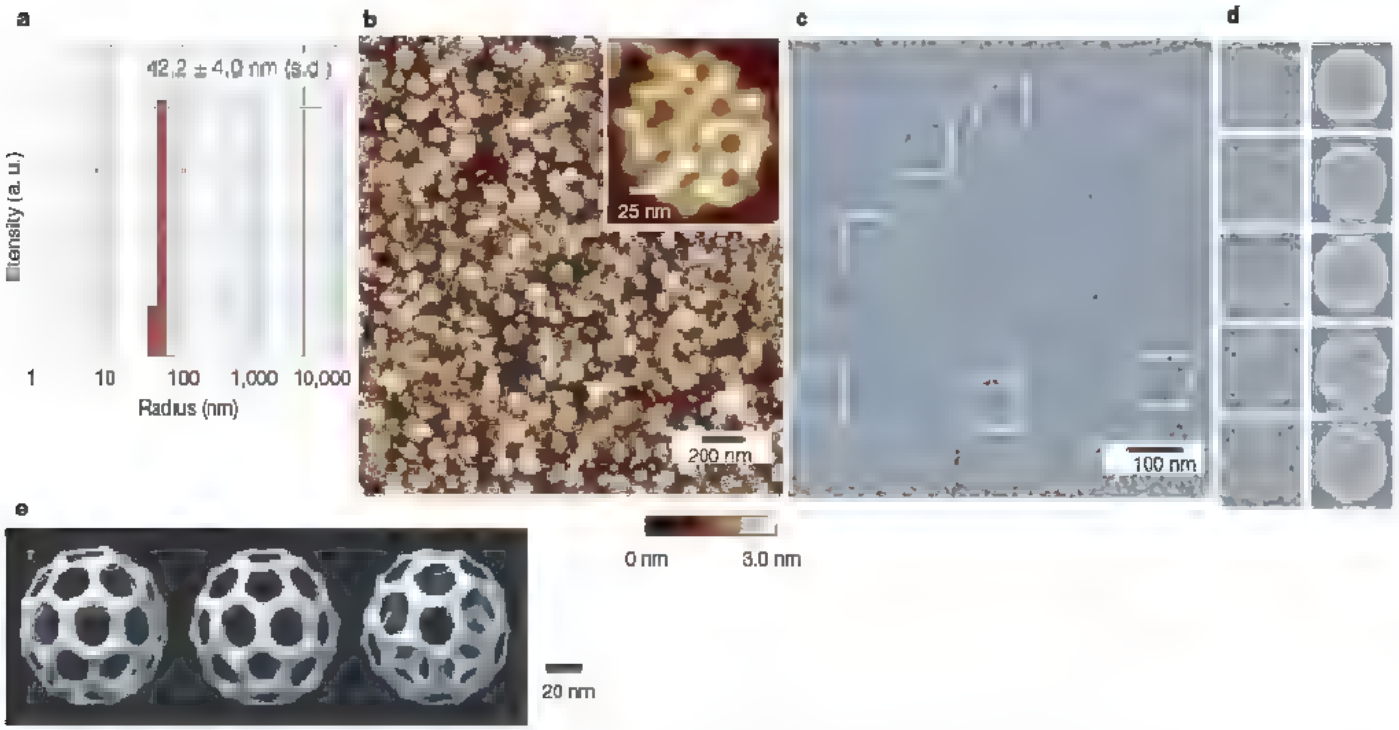


**Figure 4 | A DNA buckyball.** **a**, Size histogram of the DNA buckyball measured by DLS. **b**, **c**, An AFM image (**b**) and a cryo-EM image (**c**) of the DNA assemblies. For a magnified large view field, see Supplementary Fig. 9. **d**, Individual raw cryo-EM images and the corresponding projections of the DNA buckybal. 3D structure reconstructed from cryo-EM images. These particles are selected from different image frames to represent views at different orientations. **e**, Three views of the DNA buckybal. structure reconstructed from cryo-EM images

structural model (41.0 nm). However, the polydispersity of these assemblies is higher than that of the tetrahedron and dodecahedron assemblies. AFM imaging shows the DNA assemblies as uniform-sized, round, collapsed nanostructures with a diameter of ~110 nm. Once again, the most direct evidence for buckyball formation comes from cryo-EM imaging (Fig. 4c and Supplementary Fig. 9). Using hand-picked particles, a buckyball 3D structure can be obtained from reconstruction. However, the size distribution and the distortion of the particles in cryo-EM images look much worse than that from the AFM images. Many smaller particles and some networks are visible. These undesired particles introduce some uncertainties to the reconstruction process and lower the quality of the reconstructed structures. The 3D reconstruction merely represents the average structure of these distorted particles. Nevertheless, the resulting structure resembles a buckyball.

We note that the assembly yield decreases as the size of the target structure increases: the assembly yield for the tetrahedron is ~ 90%, but only 76% for the larger dodecahedron and 69% for the even larger buckyball (as analysed by agarose gel electrophoresis; see Supplementary Figure S2). This trend might be rationalized by the fact that larger structures require more star tiles and are thus more difficult to assemble. However, we also note that in the cryo-EM images of the DNA buckyballs, smaller objects and networks are abundant; this highlights that large structures such as buckyballs are easier to deform and break into open networks or smaller aggregates due to external disturbance (as will occur during sample preparation for imaging). The more demanding assembly and the increased lability are both likely to contribute to the apparently decreasing assembly yield for larger structures. However, the current data are not sufficient to evaluate the specific contribution of each of these factors.

We have shown that DNA can be programmed to assemble into well-defined, regular polyhedra that might find use as synthetic nanocontainers or 3D structural scaffolds. The current study used only DNA three-point-star motifs as primary building blocks, but we are currently investigating whether our hierarchical assembly strategy can be applied to other DNA motifs to prepare an even wider range of 3D objects.

## METHODS SUMMARY

**Oligonucleotides.** DNA sequences were adapted from previous works, which were originally designed by the SEQUIN[19] computer program. central long-strand L (blue-red): aggcaccatcgtaggtttcttgccaggcaccatcgtaggtttcttgccaggcaccatcgtaggtttcttgcc, central long strand L′ (blue-red) aggcaccatcgtaggtttaacttgccaggcaccatcgtaggtttaacttgccaggcaccatcgtaggtttaacttgcc; medium strand M (green): tagcaacctgccttggcaagcctacgatggacacggtaacgcc, short peripheral strand S (black): ttaccgtgtggttgctaggcg.

**Formation of DNA complexes.** DNA strands were combined according to the correct molecular ratios in a tris-acetic-EDTA-$Mg^{2+}$ (TAE/$Mg^{2+}$) buffer. Tetrahedron formation used strands L′, M and S, dodecahedron and buckyball formation used strands L, M and S. DNA assembly involved cooling solutions from 95 °C to room temperature over 48 h, using concentrations as indicated in Fig. 1 unless specifically stated otherwise. DNA samples were then directly used for characterization, without further fractionation or purification.

**Non-denaturing PAGE and AFM imaging and DLS.** Gels containing 4% polyacrylamide were run at 4 °C. For AFM, DNA samples were imaged in tapping-mode on a Multimode AFM with a Nanoscope IIIa controller (Veeco) using oxide-sharpened silicon probes in air at 22 °C. For DLS, 12 μl DNA sample solutions were measured by DynaPro 99 (Protein Solutions/Wyatt) with laser wavelength of 824 nm at 22 °C.

**Cryo-EM imaging.** DNA sample solutions were concentrated to ~3 μM, spread onto Quantifoil grids, then plunge-frozen. Data were recorded using a Gatan 4,080 × 4,080 pixel charge-coupled device (CCD) camera in a Philips CM200 transmission electron microscope with field-emission gun operating at 200 kV accelerating voltage.

**Single-particle reconstruction.** 3D reconstructions of the DNA polyhedra used the single-particle image processing software EMAN[18]. Correct symmetry for each of the polyhedra was established by processing the images, assuming different symmetries and finding the symmetry that yields a 3D reconstruction consistent with the particle images (Supplementary Figs 5 and 8). Final 3D maps were visualized using UCSF Chimera software[20].

**Full Methods** and any associated references are available in the online version of the paper at www.nature.com/nature.

**Received 10 July; accepted 18 December 2007.**

1. Seeman, N. C. DNA in a material world. *Nature* 421, 427–431 (2003).
2. Seeman, N. C. DNA enables nanoscale control of the structure of matter. *Q. Rev. Biophys.* 38, 363–371 (2005).
3. Feldkamp, U. & Niemeyer, C. M. Rational design of DNA nanoarchitectures. *Angew. Chem. Int. Edn Engl.* 45, 1856–1876 (2006).
4. Adleman, L. M. Molecular computation of solutions to combinatorial problems. *Science* 266, 1021–1024 (1994).
5. Winfree, E., Liu, F. R., Wenzler, L. A. & Seeman, N. C. Design and self-assembly of two-dimensional DNA crystals. *Nature* 394, 539–544 (1998).
6. Rothemund, P. W. K., Papadakis, N. & Winfree, E. Algorithmic self-assembly of DNA Sierpinski triangles. *PLoS Biol.* 2, 2041–2053 (2004).
7. Yan, H., Park, S. H., Finkelstein, G., Reif, J. H. & LaBean, T. H. DNA-templated self-assembly of protein arrays and highly conductive nanowires. *Science* 301, 1882–1884 (2003).
8. Scheffler, M., Dorenbeck, A., Jordan, S., Wustefeld, M. & von Kiedrowski, G. Self-assembly of trisoligo-nucleotidyls: the case for nano-acetylene and nano-cyclobutadiene. *Angew. Chem. Int. Edn Engl.* 38, 3312–3315 (1999).
9. Rothemund, P. W. K. Folding DNA to create nanoscale shapes and patterns. *Nature* 440, 297–302 (2006).
10. Chen, J. H. & Seeman, N. C. Synthesis from DNA of a molecule with the connectivity of a cube. *Nature* 350, 631–633 (1991).
11. Zhang, Y. W. & Seeman, N. C. Construction of a DNA-truncated octahedron. *J. Am. Chem. Soc.* 116, 1661–1669 (1994).
12. Shih, W. M., Quispe, J. D. & Joyce, G. F. A 1.7-kilobase single-stranded DNA that folds into a nanoscale octahedron. *Nature* 427, 618–621 (2004).
13. Goodman, R. P. *et al.* Rapid chiral assembly of rigid DNA building blocks for molecular nanofabrication. *Science* 310, 1661–1665 (2005).
14. Goodman, R. P., Berry, R. M. & Turberfield, A. J. The single-step synthesis of a DNA tetrahedron. *Chem. Commun.* 1372–1373 (2004).
15. Douglas, S. M., Chou, J. J. & Shih, W. M. DNA-nanotube-induced alignment of membrane proteins for NMR structure determination. *Proc. Natl Acad. Sci. USA* 104, 6644–6648 (2007).
16. He, Y., Chen, Y., Liu, H. P., Ribbe, A. E. & Mao, C. D. Self-assembly of hexagonal DNA two-dimensional (2D) arrays. *J. Am. Chem. Soc.* 127, 12202–12203 (2005).
17. He, Y. & Mao, C. D. Balancing flexibility and stress in DNA nanostructures. *Chem. Commun.* 968–969 (2006).
18. Ludtke, S. J., Baldwin, P. R. & Chiu, W. EMAN: Semiautomated software for high-resolution single-particle reconstructions. *J. Struct. Biol.* 128, 82–97 (1999).
19. Seeman, N. C. De novo design of sequences for nucleic-acid structural engineering. *J. Biomol. Struct. Dyn.* 8, 573–581 (1990).
20. Goddard, T. D., Huang, C. C. & Ferrin, T. E. Visualizing density maps with UCSF chimera. *J. Struct. Biol.* 157, 281–287 (2007).

**Supplementary Information** is linked to the online version of the paper at www.nature.com/nature.

**Acknowledgements.** We thank H. Liu for help with the initial DLS experiment. This work was supported by the National Science Foundation. AFM and DLS studies were carried out in the Purdue Laboratory for Chemical Nanotechnology (PLCN). The cryo-EM images were taken in the Purdue Biological Electron Microscopy Facility and the Purdue Rosen Center for Advanced Computing (RCAC) provided the computational resource for the 3D reconstructions.

**Author Information** Reprints and permissions information is available at www.nature.com/reprints. Correspondence and requests for materials should be addressed to C.M. (mao@purdue.edu).

LETTERS

# Stream denitrification across biomes and its response to anthropogenic nitrate loading

Patrick J. Mulholland[1,2], Ashley M. Helton[3], Geoffrey C. Poole[3,4], Robert O. Hall Jr[5], Stephen K. Hamilton[6], Bruce J. Peterson[7], Jennifer L. Tank[8], Linda R. Ashkenas[9], Lee W. Cooper[2], Clifford N. Dahm[10], Walter K. Dodds[11], Stuart E. G. Findlay[12], Stanley V. Gregory[9], Nancy B. Grimm[13], Sherri L. Johnson[14], William H. McDowell[15], Judy L. Meyer[3], H. Maurice Valett[16], Jackson R. Webster[16], Clay P. Arango[8], Jake J. Beaulieu[8]†, Melody J. Bernot[17], Amy J. Burgin[6], Chelsea L. Crenshaw[10], Laura T. Johnson[8], B. R. Niederlehner[16], Jonathan M. O'Brien[6], Jody D. Potter[15], Richard W. Sheibley[13]†, Daniel J. Sobota[9]† & Suzanne M. Thomas[7]

**Anthropogenic addition of bioavailable nitrogen to the biosphere is increasing[1,2] and terrestrial ecosystems are becoming increasingly nitrogen-saturated[3], causing more bioavailable nitrogen to enter groundwater and surface waters[4–6]. Large-scale nitrogen budgets show that an average of about 20–25 per cent of the nitrogen added to the biosphere is exported from rivers to the ocean or inland basins[7,8], indicating that substantial sinks for nitrogen must exist in the landscape[9]. Streams and rivers may themselves be important sinks for bioavailable nitrogen owing to their hydrological connections with terrestrial systems, high rates of biological activity, and streambed sediment environments that favour microbial denitrification[6,10,11]. Here we present data from nitrogen stable isotope tracer experiments across 72 streams and 8 regions representing several biomes. We show that total biotic uptake and denitrification of nitrate increase with stream nitrate concentration, but that the efficiency of biotic uptake and denitrification declines as concentration increases, reducing the proportion of in-stream nitrate that is removed from transport. Our data suggest that the total uptake of nitrate is related to ecosystem photosynthesis and that denitrification is related to ecosystem respiration. In addition, we use a stream network model to demonstrate that excess nitrate in streams elicits a disproportionate increase in the fraction of nitrate that is exported to receiving waters and reduces the relative role of small versus large streams as nitrate sinks.**

Biotic nitrogen uptake and denitrification account for nitrogen removal in streams, but a broad synthesis of their relative importance is lacking, in part because of the difficulty of measuring denitrification *in situ* and the lack of comparable data for streams across biomes and land-use conditions. The second Lotic Intersite Nitrogen Experiment (LINX II), a series of $^{15}N$ tracer additions to 72 streams across multiple biomes and land uses in the conterminous United States and Puerto Rico, provides replicated, *in situ* measurements of total nitrate ($NO_3^-$) uptake and denitrification. This new data set expands more than tenfold the number and type of streams for which we have reach-scale measurements of denitrification, the primary mechanism by which bioavailable nitrogen is permanently removed from ecosystems.

Streams were small (discharge: 0.2 to 268 l s$^{-1}$; median: 18.5 l s$^{-1}$) but spanned a wide range of $NO_3^-$ concentration (0.0001 to 21.2 mg N l$^{-1}$; median: 0.10 mg N l$^{-1}$) and other environmental conditions such as water velocity, depth and temperature (Supplementary Table 1). Concentrations of $NO_3^-$ were significantly greater in 'agricultural' and 'urban' streams than in 'reference' streams (Fig. 1a), despite substantial variation in the adjacent land use and in-stream conditions within each of these land-use categories.

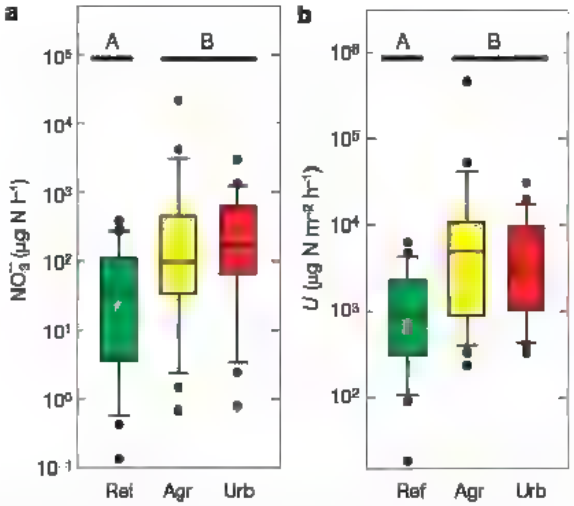


**Figure 1 | Observed stream $NO_3^-$ metrics by adjacent land use.** **a**, Streamwater $NO_3^-$ concentration. **b**, Total biotic $NO_3^-$ uptake rate per unit area of streambed ($U$). Box plots display 10th, 25th, 50th, 75th and 90th percentiles, and individual data points outside the 10th and 90th percentiles. Land use had a significant effect on $NO_3^-$ concentration ($P = 0.0055$) and $U$ ($P = 0.0013$) (Kruskal–Wallis test), horizontal bars above plots denote significant differences determined by pairwise comparisons among land-use categories with Bonferroni correction ($\alpha = 0.05$).

[1]Environmental Sciences Division, Oak Ridge National Laboratory, Oak Ridge, Tennessee 37831, USA. [2]Department of Ecology and Evolutionary Biology, University of Tennessee, Knoxville, Tennessee 37996, USA. [3]Odum School of Ecology, University of Georgia, Athens, Georgia 30602, USA. [4]Eco-metrics, Inc., Tucker, Georgia 30084, USA. [5]Department of Zoology and Physiology, University of Wyoming, Laramie, Wyoming 82071, USA. [6]Kellogg Biological Station, Michigan State University, Hickory Corners, Michigan 49060, USA. [7]Ecosystems Center, Marine Biological Laboratory, Woods Hole, Massachusetts 02543, USA. [8]Department of Biological Sciences, University of Notre Dame, Notre Dame, Indiana 46556, USA. [9]Department of Fisheries and Wildlife, Oregon State University, Corvallis, Oregon 97331, USA. [10]Department of Biology, University of New Mexico, Albuquerque, New Mexico 87131, USA. [11]Division of Biology, Kansas State University, Manhattan, Kansas 66506, USA. [12]Institute of Ecosystem Studies, Millbrook, New York 12545, USA. [13]School of Life Sciences, Arizona State University, Tempe, Arizona 85287, USA. [14]Pacific Northwest Research Station, US Forest Service, Corvallis, Oregon 97331, USA. [15]Department of Natural Resources, University of New Hampshire, Durham, New Hampshire 03824, USA. [16]Department of Biological Sciences, Virginia Tech, Blacksburg, Virginia 24061, USA. [17]Department of Biology, Ball State University, Muncie, Indiana 47306, USA. †Present addresses: US Environmental Protection Agency, Cincinnati, Ohio 45268, USA (J.J.B.); US Geological Survey, Tacoma, Washington 98402, USA (R.W.S.), School of Earth and Environmental Sciences, Washington State University Vancouver Campus, Vancouver, Washington 98686, USA (D.J.S.).

Areal rate of total $NO_3^-$ uptake ($U$, mass of $NO_3^-$ removed from water per unit area of streambed per unit time) also was greater in agricultural and urban streams (Fig. 1b), suggesting that higher $NO_3^-$ concentration stimulates uptake in these streams. Total uptake velocity of $NO_3^-$ ($v_f$, analogous to the average downward velocity at which $NO_3^-$ ions are removed from water, and a measure of uptake efficiency relative to availability[12]) was unrelated to land-use category but declined exponentially with increasing $NO_3^-$ concentration (Fig. 2a). Thus, although excess $NO_3^-$ increased uptake rate per area of streambed, streams became less efficient at removing $NO_3^-$, indicating that uptake does not increase in parallel with $NO_3^-$ concentration. The value of $v_f$ also increased with increasing gross primary production rate ($r^2 = 0.204$, $P < 0.0001$), revealing the importance of stream photoautotrophs in $NO_3^-$ removal. Although other research has documented the separate influence of $NO_3^-$ concentration[13,14] and gross primary production rate[15,16] on $v_f$ within a particular biome, our data reveal their combined influence on $NO_3^-$ removal efficiency, and demonstrate that the loss of efficiency holds across nearly six orders of magnitude in $NO_3^-$ concentration and eight different regions representing several different biomes.

A portion of total $NO_3^-$ uptake in streams can be attributed to denitrification, a microbial process occurring mostly in anoxic zones in the streambed that converts $NO_3^-$ to gaseous forms of nitrogen that are lost to the atmosphere. Our $^{15}N$-tracer approach allowed us to directly quantify uptake velocity resulting from denitrification of streamwater $NO_3^-$ ($v_{fden}$). The remainder of total $NO_3^-$ uptake represents biotic assimilation and storage in organic (usually particulate) form on the streambed. Some portion of stored nitrogen may be subsequently denitrified via tight spatial coupling of mineralization, nitrification and denitrification in sediments ('coupled denitrification'), which can be important in aquatic systems with $NO_3^-$ concentrations below ~300 μg N $l^{-1}$ (ref. 10). Thus, $v_f$ describes the upper limit and $v_{fden}$ the lower limit on rates of biotic $NO_3^-$ removal from stream water

Like $v_f$, $v_{fden}$ declined exponentially as $NO_3^-$ concentration increased (Fig. 2b), indicating reduced $NO_3^-$ removal efficiency via denitrification with increasing $NO_3^-$ concentration. It also increased with increasing ecosystem respiration rate ($r^2 = 0.318$, $P < 0.0001$), probably because aerobic respiration (that is, ecosystem respiration rate) lowers dissolved oxygen concentration and increases metabolic demand for alternative electron acceptors such as $NO_3^-$. In addition, ecosystem respiration is likely to be a good surrogate for the availability of labile organic carbon to fuel denitrification. The denitrification fraction of total $NO_3^-$ uptake (ratio of $v_{fden}$ to $v_f$) was highly variable across streams and was unrelated to land use (Fig. 3a), but was positively correlated with ecosystem respiration rate ($r = 0.40$, $P = 0.005$), further supporting the hypothesis that heterotrophic metabolism promotes denitrification[17].

Denitrification accounted for a median of 16% of total $NO_3^-$ uptake across all streams, and exceeded 43% of total uptake in a quarter of our streams. These values are conservative, however, because our measurement method does not account for delayed, coupled denitrification that may occur after $NO_3^-$ is assimilated by biota and remineralized in sediments[10].

Areal denitrification rate ($U_{den}$), a measure commonly reported in denitrification studies, was greatest in urban streams (Fig. 3b), probably because of high $NO_3^-$ concentration (Fig. 1a). Although our measurements of $U_{den}$ fall within the range observed for other aquatic systems[18], they are lower than other published values for rivers (Fig. 3b), possibly because they do not include coupled denitrification in sediments. However, our measurements of *in situ*, reach-scale denitrification may be more representative of stream ecosystem denitrification than the more commonly used acetylene-block technique in sediment cores[18].

In stream networks, any $NO_3^-$ not removed within a reach passes to the next reach downstream, where it may be subsequently removed. Stream size influences this serial processing in several ways. Small streams can remove $NO_3^-$ efficiently (because of their high ratios of streambed area to water volume) and have a cumulative influence on whole-network removal because they account for most of the stream length within a network[19,20]. By contrast, larger streams are effective $NO_3^-$ sinks owing to longer transport distances and therefore longer water residence times combined with higher nitrogen availability[21,22].

We developed a stream network model of $NO_3^-$ removal, incorporating downstream $NO_3^-$ transport through streams of increasing size and using removal rates that varied with $NO_3^-$ concentration

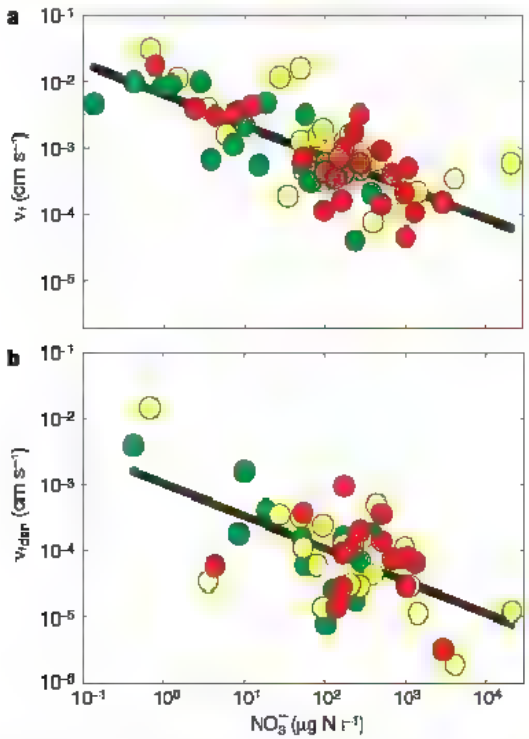


**Figure 2 | Relationships between $NO_3^-$ uptake velocity and concentration.** **a**, Regression of total $NO_3^-$ uptake velocity ($v_f$) on $NO_3^-$ concentration (log $v_f = -0.462 \times \log[NO_3^-] - 2.206$, $r^2 = 0.532$, $P < 0.0001$). **b**, Regression of denitrification uptake velocity ($v_{fden}$) on $NO_3^-$ concentration (log $v_{fden} = -0.493 \times \log[NO_3^-] - 2.975$, $r^2 = 0.355$, $P < 0.0001$)

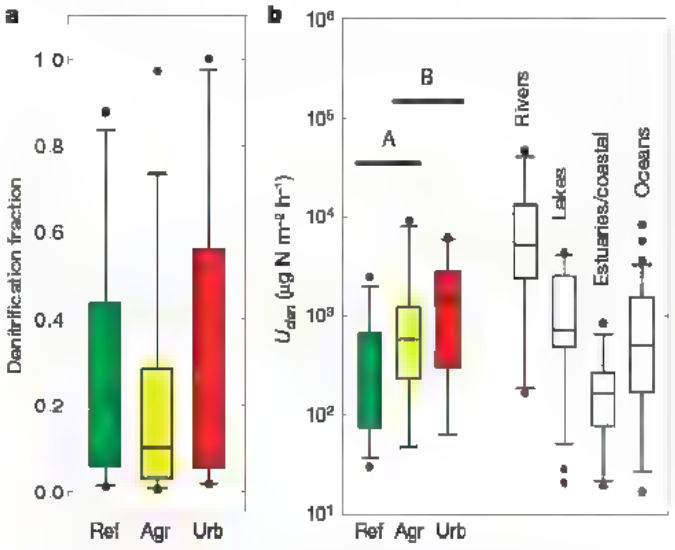


**Figure 3 | Observed stream denitrification rates by adjacent land use.** **a**, Denitrification as a fraction of total $NO_3^-$ uptake. **b**, Denitrification rate per unit area of streambed ($U_{den}$), including denitrification rates in other aquatic ecosystems (uncoloured box plots) from a recent compilation[18]. Land use had a significant effect on $U_{den}$ ($P = 0.049$) (Kruskal–Wallis test); horizontal bars above plots denote significant differences determined by pairwise comparisons among land-use categories with Bonferroni correction ($\alpha = 0.05$)

(Fig. 2). We used $v_f$ and $v_{fden}$, respectively, to model the upper and lower limits on $NO_3^-$ removal. Because our empirically derived rates of denitrification are apt to be conservative (for example, Fig. 3b), so too are the magnitudes of whole-network denitrification predicted by our model. Regardless, the model shows that $NO_3^-$ loading rates may markedly influence the importance of streams as landscape nitrogen sinks. For instance, higher loading rates stimulate $NO_3^-$ uptake and denitrification, but yield an associated disproportionate increase in downstream $NO_3^-$ export to receiving waters (Fig. 4a) as

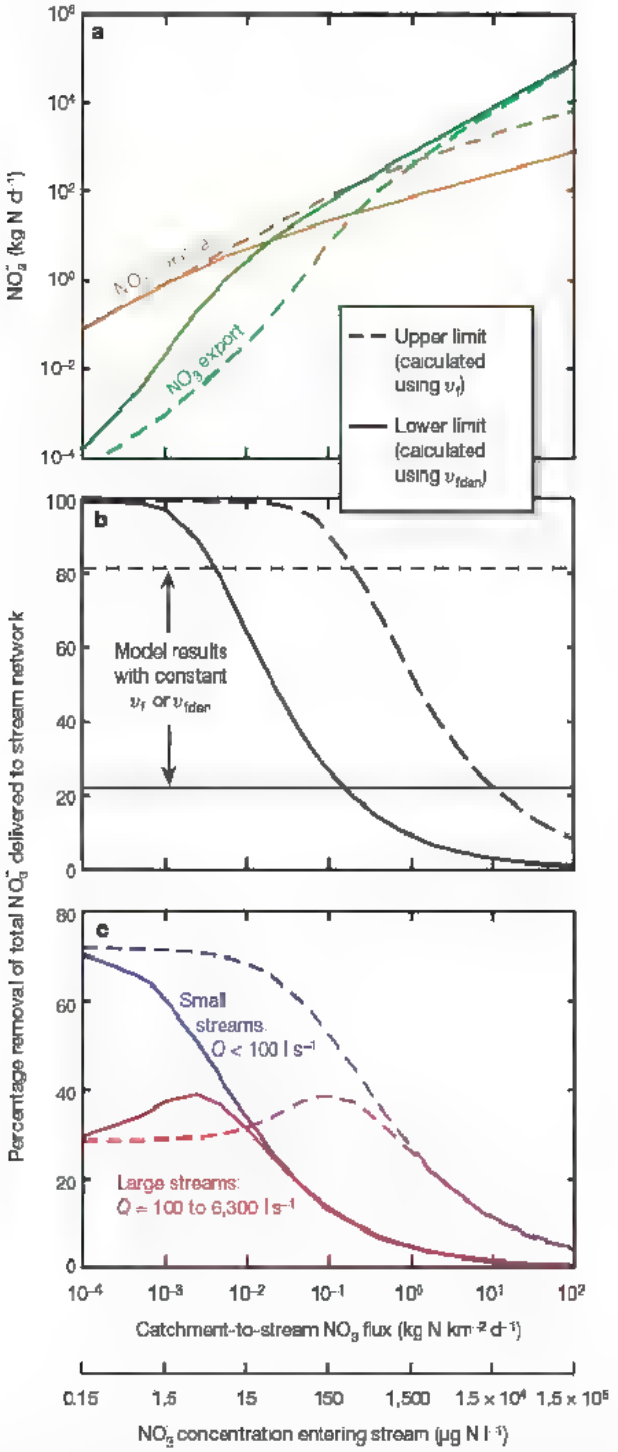


**Figure 4 | Simulated upper and lower limits on biotic removal of $NO_3^-$ from stream water within a fifth-order network.** **a**, Removal and export of $NO_3$ to receiving water bodies versus $NO_3$ loading rate (and equivalent concentration in catchment water entering the stream). **b**, Biotic removal expressed as a percentage of total $NO_3$ loading to the stream network versus $NO_3$ loading rate; curves represent model results when $v_f$ or $v_{fden}$ varies with $NO_3$ concentration (according to relationships in Fig. 2), horizontal lines show results using a constant $v_f$ or $v_{fden}$. **c**, Same as curves in **b**, but divided among 'small' and 'large' streams.

$NO_3^-$ removal efficiency declines (Fig. 4b). The loss of removal efficiency is not addressed by models where $v_f$ is independent of $NO_3^-$ concentration[22], which may yield overly optimistic projections of stream network $NO_3^-$ removal under increasing loading rates (Fig. 4b).

Small and large streams responded differently to simulated increases in $NO_3^-$ loading. The simulated percentage of network $NO_3^-$ load removed in small streams declined as loading increased (Fig. 4c). Unexpectedly, in large streams, simulated percentage removal peaked after $NO_3^-$ loading began to rise, owing to the interaction of two dynamics. Left of the peak, high removal efficiency in small streams yields little downstream $NO_3^-$ transport from small to large streams (Fig. 4a), and therefore, little $NO_3^-$ available for removal in large streams. Thus, percentage removal in large streams increases with $NO_3^-$ loading as downstream transport of $NO_3^-$ increases and large streams are released from $NO_3^-$ limitation. Right of the peak, $NO_3^-$ concentrations in large streams increase to the point where removal efficiency in large streams is lost, and the percentage removal in large streams decreases.

Our modelling results suggest three phases of nitrogen dynamics in stream networks as land-use intensity increases. First, at low nitrogen loading rates, biotic nitrogen removal is high and occurs primarily in smaller streams; removal in larger streams is limited by nitrogen availability. Second, at moderate loading rates, removal efficiency in smaller streams decreases; however, removal in larger streams responds, limiting nitrogen export. Third, at high loading rates, removal becomes ineffective across all stream sizes and the stream network exports virtually all catchment-derived nitrogen. Interestingly, direct anthropogenic $NO_3^-$ loading to large streams (for example, municipal wastewater plants) circumvents the stream network, and therefore may increase the relative role of large versus small streams in network $NO_3^-$ removal. Thus, both small and large streams can be important locations for nitrogen removal, although their relative roles are influenced by uptake efficiency in small streams (which determines downstream transport to large streams) and by the spatial pattern of $NO_3^-$ loading to the stream network.

Across biomes, our empirical data show that $NO_3^-$ removal efficiency decreases and downstream export to receiving water bodies increases as $NO_3^-$ concentration increases. Our modelling expands this finding to explain the response of stream networks as land-use intensity increases. Although our replicated inter-biome experiments add substantial insight to $NO_3^-$ dynamics in streams, we do not address some important considerations (see 'Study Limitations' in Supplementary Information) such as the ultimate fate of nitrogen removed from stream water but not immediately denitrified, variation in removal rates with season and stream discharge, the influence of off-channel and subsurface hydrology associated with floodplains and hyporheic flow paths, and the need for *in situ* empirical observations of nitrogen removal in large streams. These uncertainties prevent comparison of results from short-term, *in situ* experiments with annual stream network nitrogen budgets[7,9,19] and therefore represent critical research needs.

Our findings underscore the management imperative of controlling nitrogen loading to streams and protecting or restoring stream ecosystems to maintain or enhance their nitrogen removal functions. Controlling loading to streams and stream nitrogen export is a proven solution to eutrophication and hypoxia problems in downstream inland and coastal waters[23]. Our findings suggest caution before implementing policies (for example, reliance on intensive agriculture for biofuels production[24]) that may yield massive land conversions and higher nitrogen loads to streams. Associated increases in streamwater $NO_3^-$ concentration may reduce the efficacy of streams as nitrogen sinks, yielding synergistic increases in downstream transport to estuaries and coastal oceans[25–27].

## METHODS SUMMARY

We added tracer $^{15}NO_3^-$ using standardized protocols to 72 streams across the contiguous United States and Puerto Rico. Within each of eight regions (Supplementary Fig. 1), three streams were bordered by agricultural lands, three by urban areas, and three by extant vegetation typical of the biome ('reference streams') providing a broad array of stream conditions and land-use intensities. We performed these tracer additions on one date in each stream, generally during the spring or summer. We measured $NO_3^-$ uptake rates for entire stream reaches from measurements of tracer $^{15}N$ in $NO_3^-$, $N_2$ and $N_2O$ downstream from the isotope addition based on the nutrient spiralling approach[2,28,29] and a model of denitrification[30].

Our model of $NO_3^-$ removal from water across a stream network accounted for network topology and downstream changes in channel geometry and discharge. We implemented the model using the topology of a fifth-order stream network, the Little Tennessee River in North Carolina, USA. Simulations included increasing $NO_3^-$ loading rates from the catchment to the network from 0.0001 to 100 kg N $km^{-2}$ $d^{-1}$ (yielding input $NO_3^-$ concentrations from 0.15 μg N $l^{-1}$ to 150 mg N $l^{-1}$). For each $NO_3^-$ loading rate, we conducted model runs using the median observed $v_f$ and allowing $v_f$ to vary with predicted in-stream $NO_3^-$ concentration according to the observed relationship between $v_f$ and $NO_3^-$ concentration (Fig. 2a). These simulations were repeated using the median observed $v_{fdep}$ and the $v_{fdep}$–$NO_3^-$ concentration relationship (Fig. 2b). Therefore, model simulations bracket the range of potential network $NO_3^-$ removal ($v_f$ and $v_{fdep}$ represent upper and lower limits, respectively). To investigate the importance of stream size on network $NO_3^-$ removal, we categorized streams as either 'small' (<100 l $s^{-1}$, typical of first- and second-order streams) or 'large' (100–6,300 l $s^{-1}$, typical of third- to fifth-order streams).

**Full Methods** and any associated references are available in the online version of the paper at www.nature.com/nature.

**Received 29 June 2007; accepted 10 January 2008.**


1. Vitousek, P. M. *et al.* Human alteration of the global nitrogen cycle: Sources and consequences. *Ecol. Appl.* **7**, 737–750 (1997).
2. Galloway, J. N. *et al.* Nitrogen cycles: past, present, and future. *Biogeochemistry* **70**, 153–226 (2004).
3. Aber, J. D. *et al.* Nitrogen saturation in temperate forest ecosystems. *Bioscience* **48**, 921–934 (1998).
4. Bouwman, A. F., Van Drecht, G., Knoop, J. M., Beusen, A. H. W. & Meinardi, C. R. Exploring changes in river nitrogen export to the world's oceans. *Glob. Biogeochem. Cycles* **19**, GB1002, doi:10.1029/2004GB002314 (2005).
5. Johnes, P. J. & Butterfield, D. Landscape, regional and global estimates of nitrogen flux from land to sea: Errors and uncertainties. *Biogeochemistry* **57**, 429–476 (2002).
6. Schlesinger, W. H., Reckhow, K. H. & Bernhardt, E. S. Global change: The nitrogen cycle and rivers. *Water Resource Res.* **42**, W03S06, doi:10.1029/2005WR004300 (2006).
7. Howarth, R. W. *et al.* Riverine inputs of nitrogen to the North Atlantic Ocean: fluxes and human influences. *Biogeochemistry* **35**, 75–139 (1996).
8. Boyer, E. W. *et al.* Riverine nitrogen export from the continents to the coasts. *Glob. Biogeochem. Cycles* **20**, GB1S91, doi:10.1029/2005GB002537 (2006).
9. Van Breemen, N. *et al.* Where did all the nitrogen go? Fate of nitrogen inputs to large watersheds in the northeastern USA. *Biogeochemistry* **57**, 267–293 (2002).
10. Seitzinger, S. P. *et al.* Denitrification across landscapes and waterscapes: a synthesis. *Ecol. Appl.* **16**, 2064–2090 (2006).
11. Hedin, L. O. *et al.* Thermodynamic constraints on nitrogen transformations and other biogeochemical processes at soil–stream interfaces. *Ecology* **79**, 684–703 (1998).
12. Stream Solute Workshop. Concepts and methods for assessing solute dynamics in stream ecosystems. *J. N. Am. Benthol. Soc.* **9**, 95–119 (1990).
13. Dodds, W. K. *et al.* N uptake as a function of concentration in streams. *J. N. Am. Benthol. Soc.* **21**, 206–220 (2002).
14. O'Brien, J. M., Dodds, W. K., Wilson, K. C., Murdock, J. N. & Eichmiller, J. The saturation of N cycling in Central Plains streams: $^{15}N$ experiments across a broad gradient of nitrate concentrations. *Biogeochemistry* doi:10.1007/s10533-007-9073-7 (2007).
15. Hall, R. O. & Tank, J. L. Ecosystem metabolism controls nitrogen uptake in streams in Grand Teton National Park, Wyoming. *Limnol. Oceanogr.* **48**, 1120–1128 (2003).
16. Mulholland, P. J. *et al.* Effects of light on $NO_3^-$ uptake in small forested streams: diurnal and day-to-day variations. *J. N. Am. Benthol. Soc.* **25**, 583–595 (2006).
17. Christensen, P. B., Nielsen, L. P., Sørensen, J. & Revsbech, N. P. Denitrification in nitrate-rich streams: Diurnal and seasonal variation related to benthic oxygen metabolism. *Limnol. Oceanogr.* **35**, 640–651 (1990).
18. Piña-Ochoa, E. & Alvarez-Cobelas, M. Denitrification in aquatic environments: A cross-system analysis. *Biogeochemistry* **81**, 111–130 (2006).
19. Alexander, R. B., Smith, R. A. & Schwarz, G. E. Effect of stream channel size on the delivery of nitrogen to the Gulf of Mexico. *Nature* **403**, 758–761 (2000).
20. Peterson, B. J. *et al.* Control of nitrogen export from watersheds by headwater streams. *Science* **292**, 86–90 (2001).
21. Seitzinger, S. P. *et al.* Nitrogen retention in rivers: Model development and application to watersheds in the northeastern USA. *Biogeochemistry* **57**, 199–237 (2002).
22. Wollheim, W. M., Vörösmarty, C. J., Peterson, B. J., Seitzinger, S. P. & Hopkinson, C. S. Relationship between river size and nutrient removal. *Geophys. Res. Lett.* **33**, L06410 (2006).
23. McIsaac, G., David, M. B., Gertner, G. Z. & Goolsby, D. A. Nitrate flux in the Mississippi River. *Nature* **414**, 166–167 (2001).
24. Hill, J., Nelson, E., Tilman, D., Polasky, S. & Tiffany, D. Environmental, economic, and energetic costs and benefits of biodiesel and ethanol biofuels. *Proc. Natl Acad. Sci. USA* **103**, 11206–11210 (2006).
25. Tilman, D., Cassman, K. G., Matson, P. A., Naylor, R. & Polasky, S. Agricultural sustainability and intensive production practices. *Nature* **418**, 671–677 (2002).
26. Foley, J. A. *et al.* Global consequences of land use. *Science* **309**, 570–574 (2005).
27. Beman, J. M., Arrigo, K. R. & Matson, P. A. Agricultural runoff fuels large phytoplankton blooms in vulnerable areas of the ocean. *Nature* **434**, 211–214 (2005).
28. Newbold, J. D., Elwood, J. W., O'Neill, R. V. & Van Winkle, W. Measuring nutrient spiraling in streams. *Can. J. Fish. Aquat. Sci.* **38**, 860–863 (1981).
29. Webster, J. W. & Valett, H. M. in *Methods in Stream Ecology* (eds Hauer, F. R. & Lamberti, G. A.) 169–186 (Elsevier, New York, 2006).
30. Mulholland, P. J. *et al.* Stream denitrification and total nitrate uptake rates measured using a field $^{15}N$ isotope tracer approach. *Limnol. Oceanogr.* **49**, 809–820 (2004).


**Supplementary Information** is linked to the online version of the paper at www.nature.com/nature.

**Acknowledgements** Funding for this research was provided by the National Science Foundation. We thank N. Ostrom for assistance with stable isotope measurements of $N_2$ and $N_2O$, and W. Wollheim for initial development of the model that we modified to estimate denitrification rates from field data. We thank M. Mitchell, B. Roberts and E. Bernhardt for their comments on earlier versions of the paper. We thank the NSF LTER network, US Forest Service, National Park Service and many private landowners for permission to conduct experiments on their lands. Partial support to P.J.M. during manuscript preparation was provided by the US Department of Energy, Office of Science, Biological and Environmental Research under contract with UT-Battelle.

**Author Contributions** P.J.M. coordinated the stream $^{15}N$ experiments and analysed the compiled experimental data sets. A.M.H. and G.C.P. conducted the stream network modelling. P.J.M., A.M.H. and G.C.P. wrote major portions of the manuscript. S.K.H. established sampling protocols and coordinated the $^{15}N$ analysis of dissolved $N_2$ samples. Except for A.M.H., all authors listed to J.R.W. were joint project Principal Investigators and contributed to the conceptual and methodological development of the project and analysis of data. Authors listed from C.P.A. to S.M.T. coordinated field experiments and analysed data from one or more biomes. All authors discussed the results and commented on the manuscript.

**Author Information** Reprints and permissions information is available at www.nature.com/reprints. Correspondence and requests for materials should be addressed to P.J.M. (mulhollandpj@ornl.gov).

LETTERS

# Influence of the Gulf Stream on the troposphere

Shoshiro Minobe[1], Akira Kuwano-Yoshida[2], Nobumasa Komori[2], Shang-Ping Xie[3,4] & Richard Justin Small[3]

**The Gulf Stream transports large amounts of heat from the tropics to middle and high latitudes, and thereby affects weather phenomena such as cyclogenesis[1,2] and low cloud formation[3]. But its climatic influence, on monthly and longer timescales, remains poorly understood. In particular, it is unclear how the warm current affects the free atmosphere above the marine atmospheric boundary layer. Here we consider the Gulf Stream's influence on the troposphere, using a combination of operational weather analyses, satellite observations and an atmospheric general circulation model[4]. Our results reveal that the Gulf Stream affects the entire troposphere. In the marine boundary layer, atmospheric pressure adjustments to sharp sea surface temperature gradients lead to surface wind convergence, which anchors a narrow band of precipitation along the Gulf Stream. In this rain band, upward motion and cloud formation extend into the upper troposphere, as corroborated by the frequent occurrence of very low cloud-top temperatures. These mechanisms provide a pathway by which the Gulf Stream can affect the atmosphere locally, and possibly also in remote regions by forcing planetary waves[5,6]. The identification of this pathway may have implications for our understanding of the processes involved in climate change, because the Gulf Stream is the upper limb of the Atlantic meridional overturning circulation, which has varied in strength in the past[7] and is predicted to weaken in response to human-induced global warming in the future[8].**

It is a challenging task to isolate the climatic influence of the Gulf Stream from energetic weather variability using conventional observations, which are spatially and temporally sporadic. Recently, high-resolution satellite observations of surface winds made it possible to map the influence of the Gulf Stream[9,10] and other major sea surface temperature (SST) fronts[11–14] on the near-surface atmosphere. The Gulf Stream affects the 10-m wind climatology as observed by the QuikSCAT satellite[15], with wind divergence and convergence on the cold and warm flanks, respectively, of the Gulf Stream front[9,10] (Fig. 1a). However, the mechanism by which the SST fronts influence surface winds is still under much debate[9,10].

The identification of the mechanism responsible has been hampered by the need to know parameters not available from satellite observations, for which we turn to high-resolution atmospheric operational analyses from the European Centre for Medium-Range Weather Forecasts (ECMWF). The operational analysis successfully captures the observed pattern of wind divergence (Fig. 1b). Interestingly, the wind convergence closely resembles the pattern of the laplacian of sea-level pressure ($\nabla^2$SLP) (Fig. 1c). This correspondence is consistent with an immediate consequence of a marine atmospheric boundary layer (MABL) model[16] (see Methods Summary). Note that it is virtually impossible to see the correspondence between the wind convergence and SLP itself without taking the laplacian. The laplacian operator acts as a high-pass filter, unveiling the SST frontal effect that is masked by large-scale atmospheric circulations.

In contrast to the free atmosphere where wind velocities are nearly non-divergent, substantial divergence occurs in the MABL in the presence of strong friction and is proportional to the SLP laplacian in the MABL model described in the Methods Summary. Such a linear relation approximately holds in observations (Fig. 1f), with a correlation coefficient as high as 0.70 for a region where wind

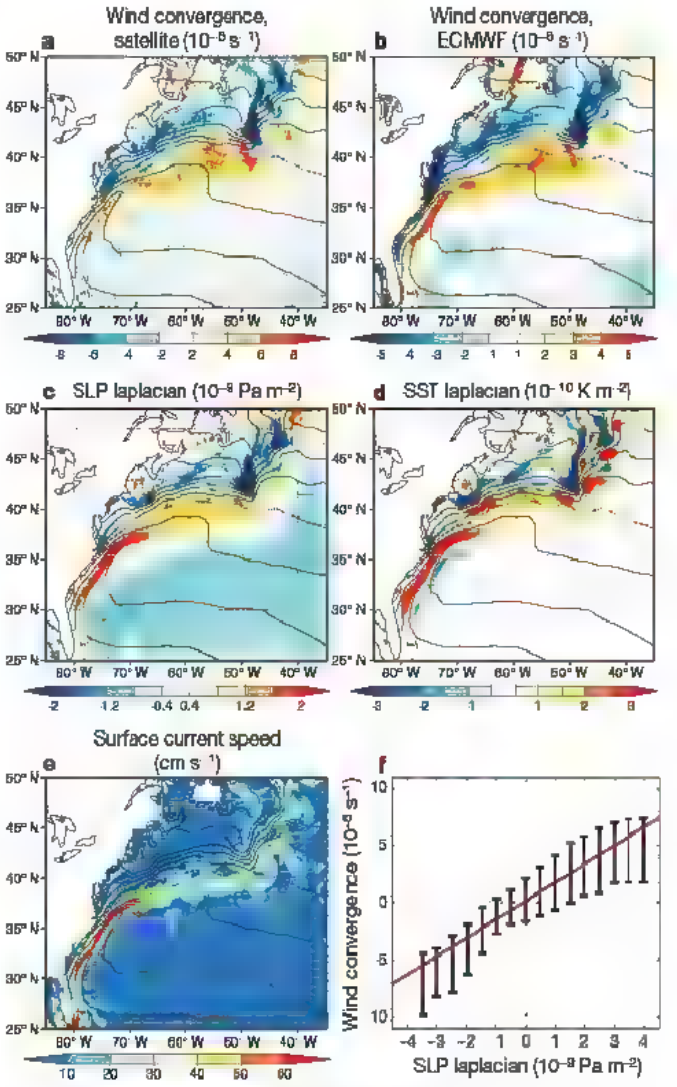


**Figure 1 | Annual climatology of surface parameters.** **a**, **b**, 10-m wind convergence (colour) in QuikSCAT satellite observations (**a**) and in the ECMWF analysis (**b**). **c**, **d**, SLP laplacian (**c**) and sign-reversed SST laplacian (**d**) in the ECMWF analysis. **e**, Surface geostrophic current speed. In **a**–**e**, SST contours (2 °C interval and dashed contours for 10 °C and 20 °C) are shown. **f**, Relationship between the SLP laplacian and wind convergence based on monthly climatology in the red-dashed box in **c**; the regression line is shown red. Error bars, ±1 s.d. of wind convergence for each bin of SLP

[1]Department of Natural History Sciences, Graduate School of Science, Hokkaido University, Sapporo 060-0810, Japan. [2]Earth Simulator Center, Japan Agency for Marine-Earth Science and Technology, Yokohama 236-0001, Japan. [3]International Pacific Research Center, [4]Department of Meteorology, University of Hawaii at Manoa, Honolulu, Hawaii 96822, USA.

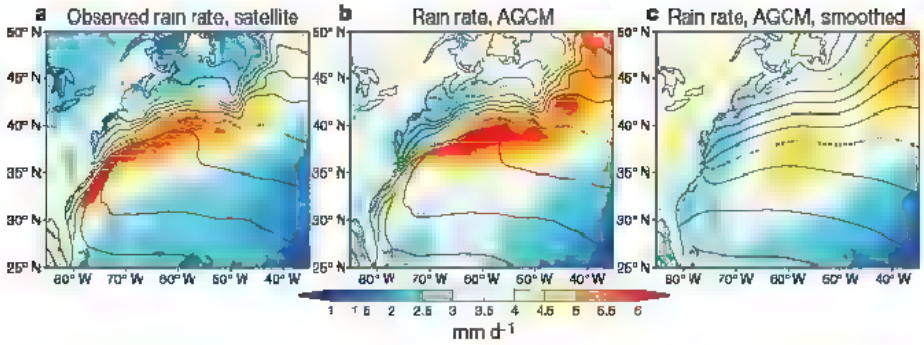


**Figure 2 | Annual climatology of rain rate.** **a**, Observed by satellites. **b**, **c**, In the AGCM with observed (**b**) and smoothed (**c**) SSTs. Contours are for SST, as in Fig. 1.

convergence and divergence are strong (80°–40° W, 30°–48° N, red-dashed box in Fig. 1c). Furthermore, consistent with the MABL model[16] where SST variations force pressure adjustments, the pattern of laplacian SST with sign reversed ($-\nabla^2$SST) exhibits some similarities to laplacian SLP and wind convergences (Fig. 1d). These results indicate that MABL pressure adjustments to SST gradients near the Gulf Stream are important for surface wind divergence. Relatively high pressures on the colder flank and relatively low pressures on the warmer flank induce cross-frontal components of near-surface winds, leading to divergence and convergence (Supplementary Fig. 1).

Previous studies suggested that warmer SSTs induce stronger vertical momentum mixing, and the enhanced mixing is responsible for mesoscale features in the surface wind convergence field[9,10], consistent with a numerical model experiment focusing on near-surface adjustments[17]. Our observational result indicates the importance of the overlooked pressure adjustment mechanism, consistent with both a recent short (a few days) regional model experiment for the Gulf Stream[18] and a numerical study of tropical instability waves[19]. Note that the observed surface wind convergence is roughly collocated with the axis of the Gulf Stream (Fig. 1e, Supplementary Fig. 1).

Satellite observations further reveal that the Gulf Stream anchors a narrow rain band roughly collocated with the surface wind convergence (Fig. 2a). Although there was evidence that the Gulf Stream affects precipitation[20], our high-resolution analysis reveals that the narrow rain band meanders with the Gulf Stream front and is confined to its warmer flank with SSTs greater than 16 °C. This close covariation in space is strongly indicative of an active role of the Gulf Stream. The precipitation pattern is well reproduced in the operational analysis (Supplementary Fig. 2), with a bias of excessive rain rates compared to satellite observations.

The causality is further examined using an atmospheric general circulation model (AGCM)[4]. It successfully captures the rain band following the meandering Gulf Stream, although the rain rate near the coast is somewhat too weak compared with satellite observations (Fig. 2b). When the SST is smoothed (see Methods for details), however, the narrow precipitation band disappears in the AGCM (Fig. 2c). Compared to the smoothed SST run, rain-bearing low-pressure systems tend to develop along the Gulf Stream front in the control simulation (Supplementary Fig. 3). These results indicate that the narrow precipitation band in the western North Atlantic results from the forcing by the sharp SST front of the Gulf Stream.

Similar to precipitation, surface evaporation also exhibits a narrow banded structure on the offshore side of the SST front (Supplementary Fig. 2). This evaporation band is consistent with a short-term field observation[21]. The amount of evaporation is slightly larger than that of precipitation, indicating that local evaporation supplies much of the water vapour for precipitation. The local enhancement of evaporation on the warmer flank of the Gulf Stream is due to enhanced wind speed and the large disequilibrium of air temperature from SST[9,13].

As precipitation off the US east coast is often associated with deep weather systems, the rainfall pattern described above suggests that the Gulf Stream's influence may penetrate to the free atmosphere. Indeed, the upward motion across the Gulf Stream displays a deep structure extending to the upper troposphere (Fig. 3a). The upward motion is anchored by wind convergence in the MABL (Fig. 3a). The latter peaks at the sea surface, and is strongly affected by SST (Fig. 1). It is interesting to note that although surface convergence and divergence are similar in magnitude (Fig. 1), the upward motion over surface wind convergence is much stronger and deeper than the downward motion over the wind divergence (Fig. 3a). This is suggestive of the importance of condensational heating above the MABL in developing the asymmetry between the upward and downward motion.

The upward wind velocity is strongest just above the MABL between the 850 and 700 hPa levels (Fig. 3a). The horizontal distribution at these levels is quite similar to the distribution of the surface convergence. The structure trapped by the Gulf Stream is clearly visible at 500 hPa and remains discernible at the 300 hPa level (Supplementary Fig. 4). Remarkably, the divergence in the upper troposphere is also dominated by a meandering band following the Gulf Stream front (Fig. 3b)—such a pattern is required by mass conservation, with the tropopause acting virtually as a lid for the mean circulation.

Next we examine the occurrence of high clouds, and infer cloud-top temperature using three-hourly outgoing long-wave radiation (OLR) derived from satellite observations. Lower OLR levels indicate lower temperatures and higher altitudes of cloud tops. Figure 3c shows the occurrence rate of OLR lower than 160 W m$^{-2}$, which roughly corresponds to a cloud-top height of about 300 hPa. A narrow band of high occurrence hugs the SST front of the Gulf Stream in

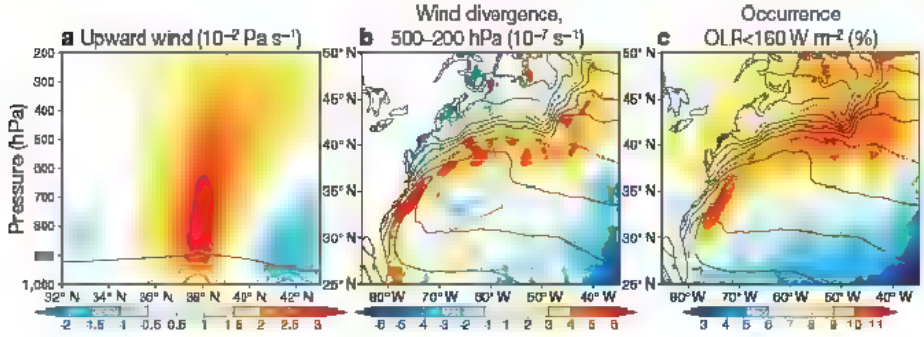


**Figure 3 | Annual climatology of parameters connecting MABL and free atmosphere.** **a**, Vertical wind velocity (upward positive; colour), boundary layer height (black curve) and wind convergence (contours for $\pm 1, 2, 3 \times 10^{-6}$ s$^{-1}$) averaged in the along-front direction in the green box in **b**, based on the ECMWF analysis. **b**, Upper-tropospheric wind divergence averaged between 200 and 500 hPa (colour). **c**, Occurrence frequency of daytime satellite-derived OLR levels lower than 160 W m$^{-2}$ (colour). Contours in **b** and **c** are for SST, as in Fig. 1.

daytime. This high-occurrence band is slightly shifted to the north compared with the bands of surface wind convergence and precipitation, consistent with the northward tilt of positive vertical velocity towards higher altitudes (Fig. 3a). At night time, the Gulf Stream-related signature is less prominent, suggesting a diurnal cycle of atmospheric convection. Our OLR result is consistent with fragmental evidence reported previously. Satellite observations showed a high frequency of lightning occurrence along the Gulf Stream, indicative of cold ice clouds[22]. With a limited offshore coverage, coastal radars showed an echo height distribution suggestive of deep convection over the Gulf Stream[23]. The Gulf Stream's signature in high cloud as reported here is strong evidence that the influence of the Gulf Stream on the atmosphere is not limited to the MABL, as reported previously[9,10], but penetrates deeply into the upper troposphere.

In summary, the present study shows that the Gulf Stream affects the entire troposphere, from the surface to the tropopause, in a systematic manner (Supplementary Fig. 1). In the MABL, the Gulf Stream directly influences air temperature and pressure fields. The resultant relatively low (high) pressures on the warm (cold) flank of the Gulf Stream front cause wind convergence (divergence). The Gulf Stream-induced convergence anchors the upward motion where precipitation is locally enhanced providing diabatic heating to the atmosphere. Remarkably, upper-tropospheric divergence shows a banded structure similar to the surface convergence and precipitation patterns, all meandering with the Gulf Stream. The deep influence of the Gulf Stream is further corroborated by frequent occurrence of high-level clouds along it. We thus suggest that on the warmer flank of the Gulf Stream front, roughly corresponding to the current axis, high instability of the atmosphere as manifested in enhanced latent and sensible heat flux leads to deep convection, enabling the influence of this warm ocean current to reach the entire troposphere.

Diabatic heating originating from surface heat fluxes over the North Atlantic Ocean is important for maintaining climatological circulations of the atmosphere, both over the ocean basin and in downwind regions, including Europe[5,6]. Deep condensational heating by the Gulf Stream and the resultant upper-tropospheric divergence revealed by this study may be important for generating stationary Rossby waves that produce remote responses (Supplementary Fig. 5). Indeed, several recent studies suggested that SST anomalies near the Gulf Stream induce atmospheric circulation changes[24–26], with significant feedback from changes in synoptic eddies[27].

The Gulf Stream is the upper limb of Atlantic meridional overturning circulation (AMOC). Both the AMOC and the Gulf Stream display large variability in palaeoclimate observations[28]. How the effects of AMOC changes in the middle-to-high latitudes are transmitted throughout the Northern Hemisphere has been a long-standing problem[7]. Whereas recent coarse-resolution model simulations pointed to the tropical Atlantic as an important conduit[29], our results suggest an additional, more direct pathway via the Gulf Stream's deep heating of the atmosphere. The AMOC is projected to slow down in response to increasing greenhouse-gas concentrations[8], giving rise to changes in the Gulf Stream[30]. It is conceivable that such Gulf Stream changes would cause precipitation anomalies along the warm current, and induce atmospheric circulation changes by way of adjustments in planetary waves and storm tracks.

## METHODS SUMMARY

We used the following satellite products: QuikSCAT wind velocity on a 0.25° grid from Remote Sensing Systems, the TRMM 3B43 precipitation product derived from the Tropical Rainfall Measuring Mission (TRMM) and other satellite data on a 0.25° grid; three-hourly OLR data on a 1° grid from the NASA Langley Atmospheric Science Data Center; and monthly sea surface geostrophic current velocity on a 1/3° Mercator grid distributed by Aviso. The monthly operational analysis was provided by the European Centre for Medium-Range Weather Forecasts with an original model resolution of 38 km and re-gridded on a 1/2° grid. The AGCM has T239 horizontal resolution (~50 km) and 48 levels[4]. The analysis period is from January 2002 to February 2006, except for the OLR data that end in June 2005. More detailed information can be found in Methods.

To understand the relation between wind convergence and SLP laplacian, we use an MABL model[16]. Its momentum equations may be cast as $\varepsilon u - fv = -p_x/\rho_0$, $\varepsilon v + fu = -p_y/\rho_0$, where $x$ and $y$ are the eastward and northward coordinates, respectively, $u$ and $v$ are the surface wind velocities in the respective directions, $\rho_0$ is the MABL density, $p$ is the pressure, $\varepsilon$ is the constant damping coefficient, and $f$ is the Coriolis parameter. It can be shown that the wind speed convergence is proportional to the laplacian of pressure: $-(u_x + v_y)\rho_0 = (p_{xx} + p_{yy})\varepsilon/(\varepsilon^2 + f^2)$. In the model, SLP is forced by SST[16]: $\varepsilon p + H(u_x + v_y) = -\gamma T$, where $T$ is the SST, $\gamma$ is a constant, and $H$ is the equivalent depth. Thus, a relation between the SST laplacian and wind convergence is also expected, albeit one weaker than that for the SLP laplacian.

**Full Methods** and any associated references are available in the online version of the paper at www.nature.com/nature.

**Received 1 August 2007; accepted 16 January 2008.**


1. Sanders, F. Explosive cyclogenesis in the west-central North Atlantic Ocean 1981–84. Part I: Composite structure and mean behavior. *Mon. Weath. Rev.* 114, 1781–1794 (1986).
2. Kuo, Y. H., Shapiro, M. A. & Donall, E. G. The interaction between baroclinic and diabatic processes in a numerical simulation of a rapidly intensifying extratropical marine cyclone. *Mon. Weath. Rev.* 119, 368–384 (1991).
3. Young, G. S. & Sikora, T. D. Mesoscale stratocumulus bands caused by Gulf Stream meanders. *Mon. Weath. Rev.* 131, 2177–2191 (2003).
4. Enomoto, T., Kuwano-Yoshida, A., Komori, N. & Ohfuchi, W. in *High Resolution Numerical Modeling of the Atmosphere and Ocean* (eds Hamilton, K. & Ohfuchi, W.) Ch. 5, 77–97 (Springer, New York, 2008).
5. Hoskins, B. J. & Valdes, P. J. On the existence of storm-tracks. *J. Atmos. Sci.* 47, 1854–1864 (1990).
6. Held, I. M., Ting, M. & Wang, H. Northern winter stationary waves: Theory and modeling. *J. Clim.* 15, 2125–2144 (2002).
7. Broecker, W. S. Does the trigger for abrupt climate change reside in the ocean or in the atmosphere? *Science* 300, 1519–1522 (2003).
8. Meehl, G. A. *et al.* in *Climate Change 2007: The Physical Scientific Basis* (eds Solomon, S. *et al.*) Ch. 10 (Cambridge Univ. Press, Cambridge, UK, 2007).
9. Xie, S.-P. Satellite observations of cool ocean-atmosphere interaction. *Bull. Am. Meteorol. Soc.* 85, 195–208 (2004).
10. Chelton, D. B., Schlax, M. G., Freilich, M. H. & Milliff, R. F. Satellite measurements reveal persistent small-scale features in ocean winds. *Science* 303, 978–983 (2004).
11. Xie, S.-P. *et al.* Bathymetric effect on the winter sea surface temperature and climate of the Yellow and East China Seas. *Geophys. Res. Lett.* 29, 2228, doi:10.1029/2002GL015884 (2002).
12. Chelton, D. B. & Wentz, F. J. Global microwave satellite observations of sea surface temperature for numerical weather prediction and climate research. *Bull. Am. Meteorol. Soc.* 86, 1097–1115 (2005).
13. Tokinaga, H., Tanimoto, Y. & Xie, S.-P. SST-induced surface wind variations over the Brazil-Malvinas confluence: Satellite and in situ observations. *J. Clim.* 18, 3470–3482 (2005).
14. O'Neill, L. W., Chelton, D. B., Esbensen, S. K. & Wentz, F. J. High-resolution satellite measurements of the atmospheric boundary layer response to SST variations along the Agulhas Return Current. *J. Clim.* 18, 2706–2723 (2005).
15. Liu, W. T. Progress in scatterometer applications. *J. Oceanogr.* 58, 121–136 (2002).
16. Lindzen, R. S. & Nigam, R. S. On the role of sea surface temperature gradients in forcing low level winds and convergence in the tropics. *J. Atmos. Sci.* 44, 2418–2436 (1987).
17. Skyllingstad, E. D., Vickers, D., Mahrt, L. & Samelson, R. Effects of mesoscale sea-surface temperature fronts on the marine atmospheric boundary layer. *Boundary-Layer Meteorol.* 123, 219–237 (2007).
18. Song, Q., Cornillon, P. & Hara, T. Surface wind response to oceanic fronts. *J. Geophys. Res.* 111, C12006, doi:10.1029/2006JC003680 (2006).
19. Small, R. J., Xie, S.-P. & Wang, Y. Q. Numerical simulation of atmospheric response to Pacific tropical instability waves. *J. Clim.* 16, 3723–3741 (2003).
20. Pan, J., Yan, X.-H., Zheng, Q. & Liu, W. T. Observation of western boundary current atmospheric convergence zones using scatterometer winds. *Geophys. Res. Lett.* 29, 1832, doi:10.1029/2002GL015015 (2002).
21. Neiman, P. J. & Shapiro, M. A. The life cycle of an extratropical marine cyclone. Part I: Frontal-cyclone evolution and thermodynamic air-sea interaction. *Mon. Weath. Rev.* 121, 2153–2176 (1993).
22. Christian, H. J. *et al.* Global frequency and distribution of lightning as observed from space by the Optical Transient Detector. *J. Geophys. Res.* 108 (D1), 4005, doi:10.1029/2002JD002347 (2003).
23. Trunk, T. J. & Bosart, L. F. Mean radar echo characteristics during project GALE. *Mon. Weath. Rev.* 118, 459–469 (1990).
24. Czaja, A. & Frankignoul, C. Observed impact of Atlantic SST anomalies on the North Atlantic Oscillation. *J. Clim.* 15, 606–623 (2002).

25. Ciasto, L. M. & Thompson, D. W. J. North Atlantic atmosphere-ocean interaction on intraseasonal time scales. *J. Clim.* 17, 1617–1621 (2004)
26. Watanabe, M., Jin, F. F. & Pan, L. Accelerated iterative method for solving steady problems of linearized atmospheric models. *J. Atmos. Sci.* 63, 3366–3382 (2006)
27. Peng, S. & Robinson, W. A. Relationships between atmospheric internal variability and the responses to an extratropical SST anomaly. *J. Clim.* 14, 2943–2959 (2001).
28. Lund, D. C., Lynch-Stieglitz, J. & Curry, W. B. Gulf Stream density structure and transport during the last millennium. *Nature* **444**, 601–604 (2006)
29. Timmermann, A. *et al.* The influence of a weakening of the Atlantic meridional overturning circulation on ENSO. *J. Clim.* 20, 4899–4919 (2007)
30. Dai, A., Hu, A., Meehl, G. A., Washington, W. M. & Strand, W. G. Atlantic thermohaline circulation in a coupled general circulation model: Unforced variations versus forced changes. *J. Clim.* 18, 3270–3293 (2005)

**Supplementary Information** is linked to the online version of the paper at www.nature.com/nature.

**Acknowledgements** We thank M. Watanabe and K. Yamazaki for discussions. S.M., N.K. and A.K.-Y. were supported by a Grant-in-aid for Scientific Research (*kaken-hi*) and S.M. was supported by the 21st Century Center of Excellence programme 'Neo-Science of Natural History' led by H. Okada, both from the Ministry of Education, Culture, Sports, Science and Technology, Japan. S.-P.X. was supported by NASA, NOAA, NSF and JAMSTEC. The numerical calculation was carried out on the Earth Simulator supported by JAMSTEC.

**Author Contributions** S.M. analysed satellite and operational data, N.K. and A.K.-Y. conducted and analysed AGCM experiments, R.J.S. conducted experiments using a linear baroclinic model and analysed the results, and S.M. and S.-P.X. wrote the paper. All authors discussed the results and commented on the manuscript.

**Author Information** Reprints and permissions information is available at www.nature.com/reprints. Correspondence and requests for materials should be addressed to S.M. (minobe@sci.hokudai.ac.jp).

LETTERS

# Diversity and productivity peak at intermediate dispersal rate in evolving metacommunities

P. A. Venail[1]*, R. C. MacLean[3]*†, T. Bouvier[2], M. A. Brockhurst[4], M. E. Hochberg[1] & N. Mouquet[1]*

**Positive relationships between species diversity and productivity have been reported for a number of ecosystems[1,2]. Theoretical and experimental studies have attempted to determine the mechanisms that generate this pattern over short timescales[1,2], but little attention has been given to the problem of understanding how diversity and productivity are linked over evolutionary timescales. Here, we investigate the role of dispersal in determining both diversity and productivity over evolutionary timescales, using experimental metacommunities of the bacterium *Pseudomonas fluorescens* assembled by divergent natural selection. We show that both regional diversity and productivity peak at an intermediate dispersal rate. Moreover, we demonstrate that these two patterns are linked: selection at intermediate rates of dispersal leads to high niche differentiation between genotypes, allowing greater coverage of the heterogeneous environment and a higher regional productivity. We argue that processes that operate over both ecological and evolutionary timescales should be jointly considered when attempting to understand the emergence of ecosystem-level properties such as diversity–function relationships.**

Our current understanding of the relationship between diversity and productivity is based on the ecological effects of 'complementarity' and 'sampling'[1]. 'Complementarity' suggests that species richness enhances productivity because of niche differentiation (for example, complementarity) or positive interactions (for example, facilitation) between species and therefore more of the available resources can be exploited. 'Sampling' means that more-diverse communities are, by chance, more likely to contain species with a higher average productivity than are communities with low diversity. Disentangling these two effects has been a major challenge in biodiversity research because both lead to a positive relationship between diversity and productivity, but differ considerably in their implications for understanding the consequences of diversity loss[1]. It is less clear, however, how the ecological mechanisms driving species coexistence (for example, environmental heterogeneity, dispersal) are responsible for the shape of this relationship[3,4] and the underlying evolutionary mechanisms remain largely unexplored.

Population genetic[5] and ecological models[6] consider environmental heterogeneity and intermediate dispersal to be central both to the emergence and the maintenance of genetic polymorphism within metapopulations and to species diversity within metacommunities[7–10]. Given that diversity and productivity are likely to be correlated[1], dispersal rate should also play a key role in determining community structure and function (for example, productivity) over both ecological and evolutionary timescales. Some experimental studies support the idea that dispersal in heterogeneous environments is important in the emergence and maintenance of diversity[11,12], but the simultaneous consideration of ecological and evolutionary mechanisms controlling diversity has yet to be considered. Here we report the results of a long-term experiment in heterogeneous metacommunities in which the level of dispersal between patches was manipulated. This experimental design enabled us to investigate the effect of dispersal on both biodiversity and productivity.

Bacteria afford us the opportunity to obtain rapid ecological and evolutionary responses using experimental designs that fulfil the assumptions of theoretical models[13]. We allowed a single clone of *Pseudomonas fluorescens* SBW25 to evolve for ~500 generations in a highly spatially heterogeneous environment (that is, Biolog GN2 microplates containing 95 unique sources of carbon) under four levels of dispersal. All the genetic and metabolic variability that appeared during the experiment evolved *de novo* by mutation so that each emerging genotype with its own functional properties can be considered to be equivalent to an ecological 'species' and the contents of a Biolog microplate can therefore represent a metapopulation of genotypes or a metacommunity of species[14,15]. Performance on each carbon source was estimated every 24 h (±20 min) by measuring optical density with a spectrophotometer. The sum of absorbances over a Biolog microplate therefore reflects the resource-use capacity of each metacommunity, considered as a proxy for its productivity (for further details, see Methods)

Metacommunity productivity significantly increased during the selection period in all treatments (Fig. 1a) and this increase was greatest at an intermediate dispersal rate, as determined by quadratic regression and multiple means comparison tests (Fig. 1b). Frequency distributions of productivity on individual substrates help to link this result to the pattern of resource use. The distributions were initially bimodal (Fig. 1c–f), revealing high inequality in resource exploitation by the ancestral genotype and a source–sink-like structure of the metacommunity. The distribution of productivity on individual substrates remained bimodal in the non-dispersal treatment (Fig. 1c), revealing that selection could not generate local adaptation on 'poor' substrates in the absence of dispersal. The increase in productivity in metacommunities with dispersal (Fig. 1b) was primarily driven by an increase in productivity on substrates that were initially poorly exploited, as revealed by the switch to unimodality in the distribution of productivity on individual substrates (Fig. 1d–f).

To investigate the mechanisms underlying the hump-shaped dispersal–productivity relationship (Fig. 1b), we estimated the functional composition of evolved metacommunities at the end of the selection period by assaying the productivity of 16 randomly chosen genotypes from each metacommunity on each substrate. One potential explanation for this hump-shaped pattern is that highly

[1]Université Montpellier 2, CNRS, UMR 5554 Institut des Sciences de l'Evolution, CC065 Place Eugène Bataillon, [2]Université Montpellier 2, CNRS, Ifremer, UMR 5119 Ecosystemes Lagunaires, CC093 Place Eugène Bataillon, 34095 Montpellier cedex 05, France. [3]NERC Center for Population Biology Imperial College London, Silwood Park Campus, Ascot SL5 7PY UK. [4]School of Biological Sciences, Biosciences Building, University of Liverpool, Crown Street, Liverpool, L69 7ZB, UK. †Present address: Department of Zoology, University of Oxford, South Parks Road, Oxford, OX1 3PS, UK.
*These authors contributed equally to this study

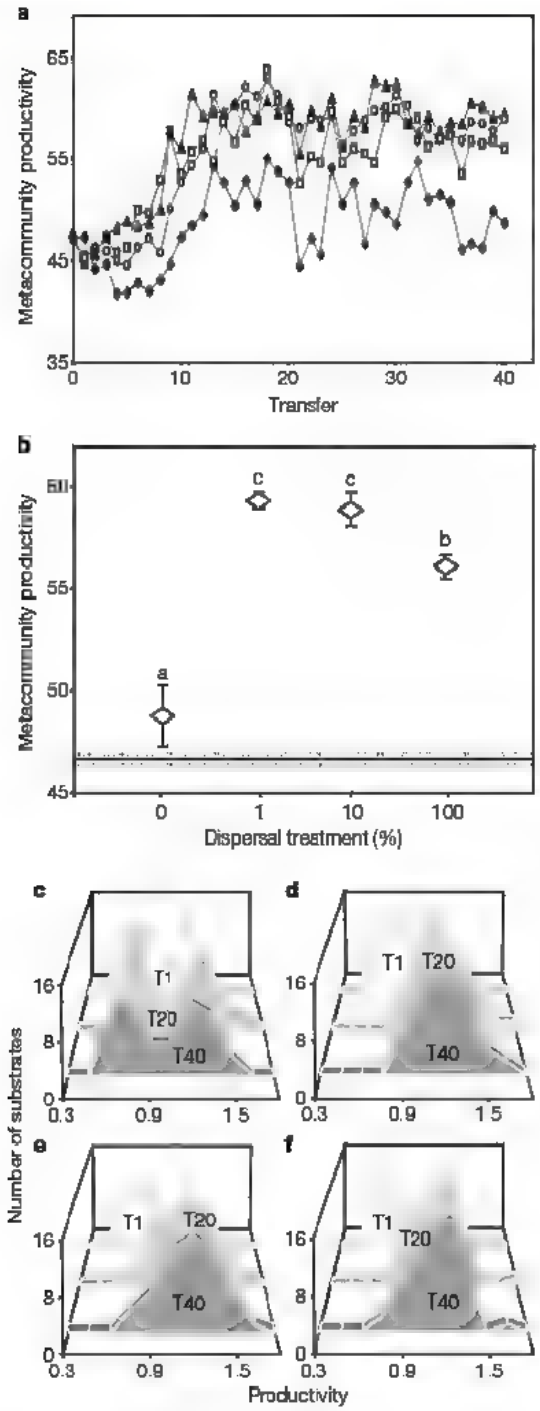


**Figure 1 | Metacommunity productivity as a function of dispersal rate.** **a**, Plotted points show the temporal variation in mean productivity of metacommunities ($n = 3$) with 0% dispersal (diamonds), 1% dispersal (triangles), 10% dispersal (circles), and 100% dispersal (squares). In all cases, a plateau in productivity was observed in the second half of the selection period, suggesting that maximal metacommunity productivity was attained. **b**, Mean metacommunity productivity (±s.e.m; $n = 3$) as a function of dispersal rate at the end of the selection period (transfer 40). Productivity peaks at intermediate dispersal rates, as judged by quadratic regression (transfer 40; quadratic test: $F_{2,9} = 47.8$, $P < 0.0001$, quadratic parameter $t = -7.98$, $P < 0.0001$) and multiple means comparison (Tukey's test: $q = 3.2$, $\alpha = 0.05$, grouped means are labelled 'a' for 0%, 'b' for 100% and 'c' for 1% and 10%). The solid line represents the mean productivity of the replicate measures of the ancestral clone (dotted lines indicate ±s.e.m; $n = 12$). This pattern is consistent over the plateau period (summed metacommunity productivity values over the last twenty transfers; quadratic test: $F_{2,9} = 34.337$, $P < 0.0001$, quadratic parameter $t = 6.52$, $P = 0.0001$; Tukey's test: $q = 3.202$; $\alpha = 0.05$). **c–f**, Frequency distributions of mean productivity on individual substrates of the three replicates of each dispersal treatment at the beginning (T1), middle (T20) and at the end of the selection period (T40) for no dispersal (**c**), 1% dispersal (**d**), 10% dispersal (**e**) and 100% dispersal (**f**) treatments.

productive genotypes are selected at intermediate dispersal rates. To test this hypothesis, we estimated the genotypic productivity for each clone as the sum of productivity scores from each individual substrate. Across all dispersal treatments, the average genotypic productivity was lower than that of the ancestral clone (Fig. 2) and there were no significant differences in mean genotypic performances between dispersal treatments or between replicates within treatments.

Alternatively, it is possible that productivity peaks at intermediate dispersal rate because of increased diversity at the scale of the metacommunity. To test this hypothesis, we partitioned the total within-metacommunity variance of individual performances into effects of genotype ($G$), environment ($E$), and genotype-by-environment interaction ($G \times E$). The $E$ component measures variation in growth between substrates (that is, environmental heterogeneity) and the $G$ component measures variation in mean individual productivity among genotypes[16,17]. The $G \times E$ component reflects differences in the response of different genotypes to different environmental conditions; this is a measure of the amount of niche variation within metacommunities. $G \times E$ variance can be further broken down into inconsistency ($I$), which measures niche differentiation (that is, complementarity) or functional diversity within the metacommunity[17], and responsiveness ($R$), which measures diversity of niche breadth within the metacommunity (see Box 1).

The absolute quantities of $G$, $E$ and $G \times E$ do not differ between dispersal treatments (Fig. 3a). However, the proportion of total variance attributable to inconsistency varies among dispersal treatments, with maximal functional diversity (that is, inconsistency) at an intermediate dispersal rate (Fig. 3b). The proportion of total variance attributable to responsiveness declines with increasing dispersal (see Supplementary Figure) but represents only 2 to 3% of total phenotypic variance. Given that both functional diversity and productivity peak at an intermediate dispersal rate, this analysis supports the idea that differences between metacommunities in productivity stem from differences in diversity. Further support for this comes from the observation that the rank-order diversity and productivity of individual metacommunities are reasonably well correlated (Fig. 4; $n = 12$, $P = 0.04$, $r^2 = 0.34$).

In the absence of dispersal, the community present on each substrate behaves as a closed system, where *in situ* mutation is the only source of variation. Under such conditions, adaptation to poorly exploited habitats is obstructed by low effective population size, which reduces the rate of supply of beneficial mutations and increases

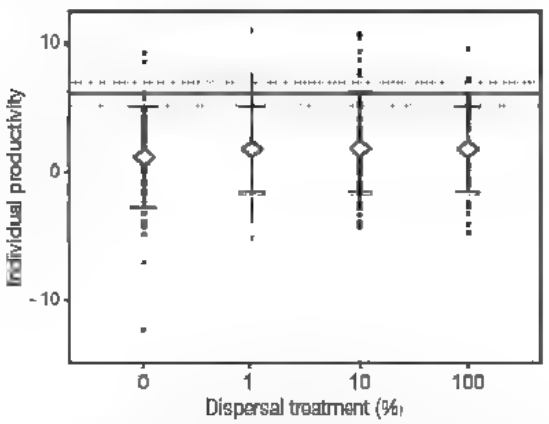


**Figure 2 | Individual genotypic productivity for each dispersal level.** Plotted points represent the productivity of individual genotypes at the end of the selection period for each dispersal treatment ($n = 48$); diamond symbols show the mean genotypic productivity for each dispersal treatment (±s.e.m; $n = 3$) and the solid line represents the mean productivity of replicate measures of the ancestral clone (dotted lines indicate ±s.e.m; $n = 12$). We observed no differences in mean individual genotypic performances between dispersal treatments or between replicates within treatments (nested analysis of variance, ANOVA. $F_{3,180} = 0.46$, $P = 0.46$ and $F_{8,180} = 1.75$, $P = 0.09$, $n = 192$)

**Box 1 | Responsiveness and inconsistency**

Responsiveness and inconsistency are relative measures of the diversity of resource exploitation strategies and niche differentiation (functional diversity). In our 'common garden' assays, the performances of different genotypes over different environments ($V_P$) can be decomposed into genotypic ($V_G$), environmental ($V_E$) and genotype-by-environment interaction ($V_{GE}$) components as follows:

$$V_P = V_G + V_E + V_{GE} \quad (1)$$

The genotypic variance is the variance of average performances of a given genotype across all environments, and the environmental variance is the variance of environmental deviations (deviation of each phenotypic value from the mean performance of the genotype across all environments). The covariance term arises if genotypic values and environmental deviations are correlated and the interaction component arises as genotypes react differently to different environments[27]. Furthermore, the interaction component ($G \times E$) can be partitioned into responsiveness and inconsistency[16,27]: $V_{GE} = R + I$. The responsiveness component $R$ indicates differences in environmental variances and thus measures diversity of resource exploitation strategies (specialists and generalists):

$$R = \sum \frac{(\sigma_{Ei} - \sigma_{Ej})^2}{2G(G-1)} \quad (2)$$

The inconsistency component $I$ indicates non-correlations between genotypes over environments.

$$I = \sum \frac{\sigma_{Ei}\,\sigma_{Ej}\,(1-\rho_{Ei,Ej})}{G(G-1)} \quad (3)$$

where $G$ is the number of genotypes tested, $\sigma_{Ei}$ and $\sigma_{Ej}$ are the standard deviations of environmental responses for each genotype, and $\rho_{Ei,Ej}$ is the environmental correlation among each pair of genotypes tested. The lack of correlation implies that each genotype is fittest in a different environment or, more generally, that reaction norms are negatively correlated over the different environments. $I$ is a measure of niche differentiation or functional diversity[17] because it reflects specialization on different resources. Measures of functional diversity based on trait diversity are probably more informative than simple measures of diversity itself[28].

The Box 1 Figure shows various possible outcomes of selection in the simplest metacommunity constituted of two wells (with different resources) and no dispersal. Depending on the reaction norms obtained after evolution, one can differentiate between situations with no responsiveness and/or no inconsistency, leading to contrasted ecological interpretations.

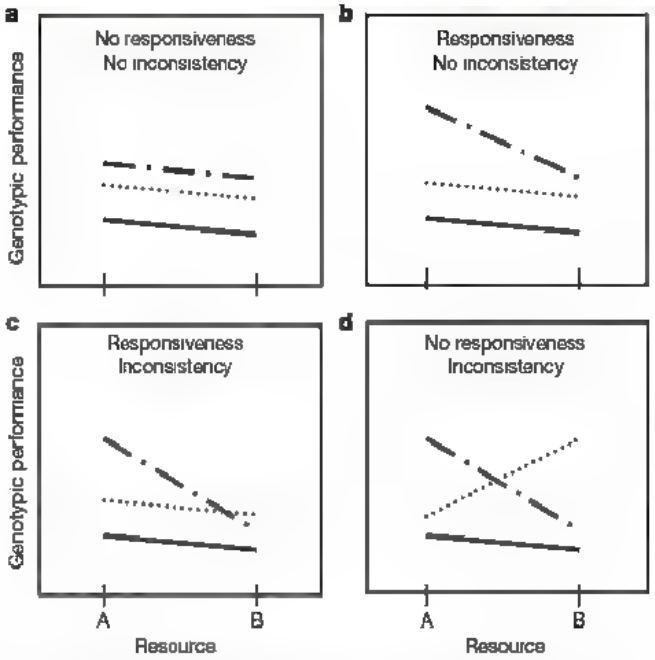


**Box 1 Figure Four scenarios of responsiveness and inconsistency.** Each dashed line represents the reaction norm over resources A and B of two genotypes that have evolved in A and B respectively from the same isogenic population (solid line). In **a** the evolved genotypes have parallel reaction norms and there is no $G \times E$ interaction. The environmental variances of two genotypes are equal (no $R$) and reaction norms are parallel (no $I$). In **b** genotypes do not respond equally to different environments, they have different environmental variances ($R$) but their responses are highly correlated (no $I$). In both cases regional functional diversity is low because genotypes are regionally redundant in their resource utilization. In **c** the reaction norms intersect ($I$) and environmental variances differ ($R$). In this case, $R$ and $I$ account for the interaction component of total phenotypic variance. Finally, in **d** the ranking of genotypes changes over resources ($I$), but in this case they have the same environmental variation (no $R$). In **c** and **d** regional functional diversity is high because genotypes exploit different resources.

the effect of genetic drift. Evidence for this constraint can be seen by the observation that adaptation to 'poor' substrates was impossible without dispersal (Fig. 1c). At the metacommunity scale, this results in low productivity (because only a minority of substrates make substantial contributions to total production) and low diversity (because the metacommunity is dominated by genotypes that are specialized on a narrow range of productive resources). With dispersal, beneficial mutations generated *ex situ* are constantly introduced by migration, allowing adaptation to 'poor' quality habitats[18] (see Supplementary Discussion). We argue that the consequences of adaptation to poor substrates, in terms of both diversity and productivity, depend on the strength of selection for specialists with high productivity on a narrow range of substrates, and generalists with intermediate productivity on a wide range of substrates.

At low and intermediate dispersal rates, selection favours resource specialization[15]. At the scale of the metacommunity this results in high diversity because of substrate specialists, and high productivity because each substrate is exploited efficiently. Consistent with this argument, functional diversity (that is, inconsistency) is high in the 10% migration treatment (Fig. 3b) and average niche breadth is low, reflecting resource specialization (Fig. 3c). At high dispersal rates, selection favours generalists across multiple substrates instead of resource specialists[15], resulting in intermediate diversity and productivity at the scale of the metacommunity. In support of this argument, inconsistency is low in the 100% dispersal treatment (Fig. 3b), reflecting lower functional diversity, and average niche breadth is high (Fig. 3c), demonstrating the presence of generalists.

In summary, we have shown that both functional diversity and productivity peak at an intermediate dispersal rate in bacterial communities assembled by natural selection, resulting in a positive correlation between diversity and productivity (Fig. 4). The productivity of individual genotypes did not differ between dispersal treatments (Fig. 2), implying that a 'sampling' effect cannot account for this pattern. Instead, our results indicate that communities with higher functional diversity evolve at an intermediate dispersal rate (Fig. 3b), demonstrating that niche differentiation (that is, 'complementarity') contributes to the observed differences in productivity between dispersal treatments (Fig. 4).

We point out, however, that the correlation between diversity and productivity is not perfect: we estimate that 34% of the variation in productivity among communities can be accounted for by variation in functional diversity. An intriguing possibility is that facilitative interactions between genotypes[19,20] play an important role in determining productivity. Distinguishing the effects of niche

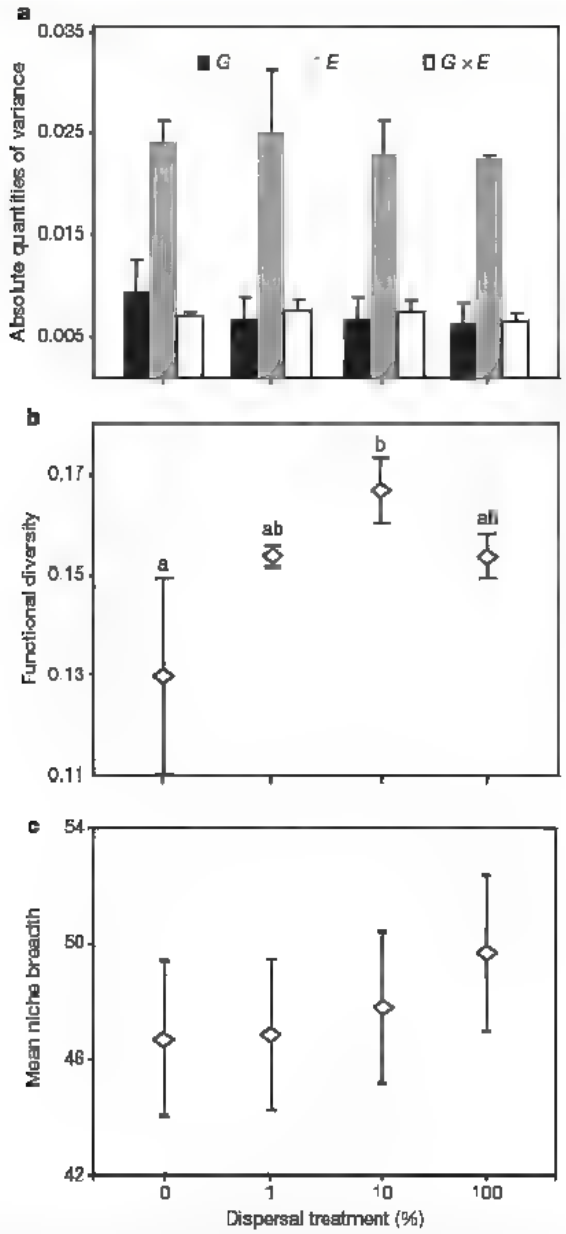


**Figure 3 | Phenotypic variance partitioning and niche breadth for each dispersal treatment.** **a**, Bars show the mean quantity of phenotypic variance (±s.e.m; $n = 3$) attributable to effects of $G$, $E$ and $G \times E$. The absolute quantities of $G$, $E$ and $G \times E$ do not differ between dispersal treatments (one-way ANOVA, $n = 12$, $P > 0.05$). **b**, Diamond symbols show functional diversity measured as a percentage of total phenotypic variance attributable to inconsistency. Functional diversity peaks at an intermediate dispersal level as judged by quadratic regression (quadratic test $F_{2,9} = 9.84$, $P = 0.05$, $n = 12$; quadratic parameter $t = -3.16$, $P = 0.012$) and multiple means comparison (Tukey's test: $q = 3.2$, $\alpha = 0.05$, grouped means are labelled 'a' for 0%, 1% and 100%; and 'b' for 1%, 10% and 100%). **c**, Diamond symbols show the average genotypic niche breadth for each dispersal treatment (±s.e.m; $n = 48$), calculated as the number of substrates giving positive growth scores for each genotype. Average niche breadth increases exponentially with dispersal rate ($F_{1,3} = 420$, $P = 0.0024$, $r^2 = 0.99$) and there are no differences in mean niche breadth among replicate lines nested within treatments ($F_{3,8} = 1.43$, $P = 0.19$).

differentiation (that is, functional diversity) and facilitation is difficult in practice, and they are usually referred to collectively as complementarity[21]. Disentangling these two effects may be an interesting prospect for future research. It is important to note, however, that facilitation via biochemical mechanisms such as cross-feeding[22] requires niche differentiation into different metabolic phenotypes, suggesting that the potential for facilitation was also greatest at an intermediate dispersal rate.

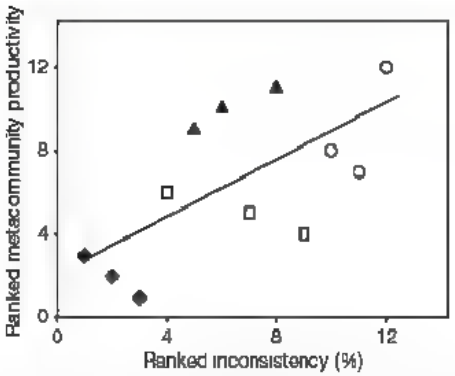


**Figure 4 | Metacommunity diversity and productivity.** Plotted points show the rank-order productivity and functional diversity of metacommunities with 0% dispersal (diamonds), 1% dispersal (triangles), 10% dispersal (circle), and 100% dispersal (squares). Diversity and productivity are positively correlated (Spearman's test: $F_{1,10} = 5.26$, $P = 0.04$, $r^2 = 0.34$, $n = 12$).

Most of our understanding of biodiversity and ecosystem function comes from models of niche differentiation driven by exploitative competition[23,24] and experiments on ecological timescales (reviewed in refs 1 and 2). This work differs from previous studies in two important respects. First, previous empirical studies have manipulated either diversity or productivity as the independent variable and then measured the response of the dependent variable (again, either diversity or productivity)[1,2]. Here, we have manipulated an independent variable (dispersal) that is predicted to play an important part in the emergence and maintenance of diversity, and we have independently measured the response of both diversity and productivity. Second, previous experimental studies of the relationship between diversity and productivity have focused on communities that are artificially assembled by choosing species from pre-existing pools (see, for example, the BIODEPTH experiment[25]), whereas we have studied the properties of communities that are naturally assembled by *in situ* evolutionary diversification. Although it is not entirely clear whether the results of microbial experiments can be extrapolated to understand patterns in communities of multicellular eukaryotes[13], the controlled nature of microbial experiments has allowed us to gain insights into some of the most complex interactions in natural systems: how ecological and evolutionary mechanisms combine to determine community structure and function[26].

## METHODS SUMMARY

We selected populations derived from a single clone of *Pseudomonas fluorescens* SBW25 on Biolog GN2 microplates under four different dispersal treatments (three replicate lines per treatment). Every 24 h (±20 min) we measured the absorbance at 590 nm on each line on every substrate, which provides an accurate measure of both cell density and productivity on each substrate. After the assay, migration was allowed to occur between substrates in each line such that 0%, 1%, 10% or 100% of the population on each substrate was derived from a pool of immigrants derived from all substrates (further details in Methods). Finally, we transferred 1 μl from each substrate to a fresh Biolog plate. Microplates were incubated at 28 °C in a humidified incubator.

We measured the growth of 16 randomly sampled genotypes from each selection line at transfer 40 across all 95 Biolog substrates in two large assays (eight clones per line per assay). As a control, we also assayed six colonies of the ancestral clone in each assay. The ancestral clone gave equivalent growth scores in both assays across all substrates.

**Full Methods** and any associated references are available in the online version of the paper at www.nature.com/nature.

**Received 13 November; accepted 20 December 2007.**

1. Loreau, M. *et al.* Biodiversity and ecosystem functioning: current knowledge and future challenges. *Science* 294, 804–808 (2001).
2. Hooper, D. U. *et al.* Effects of biodiversity on ecosystem functioning: a consensus of current knowledge. *Ecol. Monogr.* 75, 3–35 (2005).

3 Cardinale, B. J., Nelson, K. & Palmer, M. A. Linking species diversity to the functioning of ecosystems: on the importance of environmental context. *Oikos* 91, 175–183 (2000)
4 Mouquet, N., Moore, J. L. & Loreau, M. Plant species richness and community productivity: why the mechanism that promotes coexistence matters. *Ecol. Lett.* 5, 56–65 (2002).
5 Hanski, I. A. & Gaggiotti, O. E. *Ecology, Genetics and Evolution of Metapopulations* (Elsevier Academic, Burlington, 2004).
6 Holyoak, M., Leibold, M. A. & Holt, R. D. *Metacommunities. Spatial Dynamics and Ecological Communities* (Chicago Univ. Press, Chicago, 2005)
7 Levene, H. Genetic equilibrium when more than one ecological niche is available. *Am. Nat.* 87, 331–333 (1953)
8 Day, T. Competition and the effect of spatial resource heterogeneity on evolutionary diversification. *Am. Nat.* 155, 790–803 (2000)
9 Amarasekare, P. & Nisbet, R. Spatial heterogeneity, source-sink dynamics, and the local coexistence of competing species. *Am. Nat.* 158, 572–584 (2001)
10. Mouquet, N. & Loreau, M. Coexistence in metacommunities: the regional similarity hypothesis. *Am. Nat.* 159, 420–426 (2002)
11 Cadotte, M. W. & Fukami, T. Dispersal, spatial scale, and species diversity in a hierarchically structured experimental landscape. *Ecol. Lett.* 8, 548–557 (2005)
12 Habets, M., Rozen, D. E., Hoekstra, R. F. & de Visser, J. The effect of population structure on the adaptive radiation of microbial populations evolving in spatially structured environments. *Ecol. Lett.* 9, 1041–1048 (2006)
13. Prosser, J. I. *et al.* The role of ecological theory in microbial ecology. *Nature Rev. Microbiol.* 5, 384–392 (2007).
14. Cohan, F. M. What are bacterial species? *Annu. Rev. Microbiol.* 56, 457–487 (2002).
15. Kassen, R. The experimental evolution of specialists, generalists, and the maintenance of diversity. *J. Evol. Biol.* 15, 173–190 (2002)
16. Barrett, R. D. H., MacLean, R. C. & Bell, G. Experimental evolution of *Pseudomonas fluorescens* in simple and complex environments. *Am. Nat.* 166, 470–480 (2005)
17 Hall, A. R. & Colegrave, N. How does resource supply affect evolutionary diversification? *Proc. R. Soc. Lond. B* 274, 73–78 (2007).
18. Lenormand, T. Gene flow and the limits to natural selection. *Trends Ecol. Evol.* 17, 183–189 (2002)
19 Bruno, J. F., Stachowicz, J. J. & Bertness, M. D. Inclusion of facilitation into ecological theory. *Trends Ecol. Evol.* 18, 119–125 (2003).
20 Cardinale, B. J., Palmer, M. A. & Collins, S. L. Species diversity enhances ecosytem functioning through interspecific facilitation. *Nature* 415, 426–429 (2002)
21 Loreau, M. & Hector, A. Partitioning selection and complementarity in biodiversity experiments. *Nature* 412, 72–76 (2001)
22. Treves, D. S., Manning, S. & Adams, J. Repeated evolution of an acetate-crossfeeding polymorphism in long-term populations of *Escherichia coli*. *Mol. Biol. Evol.* 15, 789–797 (1998).
23. Loreau, M. Biodiversity and ecosystem functioning: A mechanistic model. *Proc. Natl Acad. Sci. USA* 95, 5632–5636 (1998)
24 Tilman, D., Lehman, C. L. & Thomson, K. T. Plant diversity and ecosystem productivity: Theoretical considerations. *Proc. Natl Acad. Sci. USA* 94, 1857–1861 (1997)
25. Hector, A. *et al.* Plant diversity and productivity experiments in European grasslands. *Science* 286, 1123–1127 (1999).
26. Fussmann, G. F., Loreau, M. & Abrams, P. A. Eco-evolutionary dynamics of communities and ecosystems. *Function. Ecol.* 21, 465–477 (2007)
27 Bell, G. The ecology and genetics of fitness in *Chlamydomonas*. 1. Genotype-by-environment interaction among pure strains. *Proc. R. Soc. Lond. B* 240, 295–321 (1990).
28. McGill, B. J., Enquist, B. J., Weiher, E. & Westoby, M. Rebuilding community ecology from functional traits. *Trends Ecol. Evol.* 21, 178–185 (2006)
29 Cooper, V. S. & Lenski, R. E. The population genetics of ecological specialization in evolving *Escherichia coli* populations. *Nature* 407, 736–739 (2000).

**Supplementary Information** is linked to the online version of the paper at www.nature.com/nature.

**Acknowledgements** This work was supported by research grant 'Programme National EC2CO' (to N.M. and P.A.V.), by 'Le Fond National de la Science' and 'Programme Microbiologique' (to M.E.H.) and grants from NERC UK to the Centre for Population Biology (to R.C.M.). We thank B. Bochner for advice on the Biolog microplates, C. Bouvier for methodological advices and help with the spectrophotometer, and C. de Mazancourt and I. Olivieri for discussions. R. Barrett provided the ancestral bacterial strain. T. Bell, B. Facon and V. Ravigne provided comments on an earlier version of our manuscript.

**Author Information** Reprints and permissions information is available at www.nature.com/reprints. Correspondence and requests for materials should be addressed to P.A.V. (pvenail@univ-montp2.fr) and N.M. (nmouquet@univ-montp2.fr).

LETTERS

# Shotgun bisulphite sequencing of the *Arabidopsis* genome reveals DNA methylation patterning

Shawn J. Cokus[1]*, Suhua Feng[1,2]*, Xiaoyu Zhang[1]†, Zugen Chen[3], Barry Merriman[3], Christian D. Haudenschild[4], Sriharsa Pradhan[5], Stanley F. Nelson[3], Matteo Pellegrini[1] & Steven E. Jacobsen[1,2]

**Cytosine DNA methylation is important in regulating gene expression and in silencing transposons and other repetitive sequences[1,2]. Recent genomic studies in *Arabidopsis thaliana* have revealed that many endogenous genes are methylated either within their promoters or within their transcribed regions, and that gene methylation is highly correlated with transcription levels[3–5]. However, plants have different types of methylation controlled by different genetic pathways, and detailed information on the methylation status of each cytosine in any given genome is lacking. To this end, we generated a map at single-base-pair resolution of methylated cytosines for *Arabidopsis*, by combining bisulphite treatment of genomic DNA with ultra-high-throughput sequencing using the Illumina 1G Genome Analyser and Solexa sequencing technology[6]. This approach, termed BS-Seq, unlike previous microarray-based methods, allows one to sensitively measure cytosine methylation on a genome-wide scale within specific sequence contexts. Here we describe methylation on previously inaccessible components of the genome and analyse the DNA methylation sequence composition and distribution. We also describe the effect of various DNA methylation mutants on genome-wide methylation patterns, and demonstrate that our newly developed library construction and computational methods can be applied to large genomes such as that of mouse.**

To generate a DNA methylation map at one-nucleotide resolution across the genome, we adapted the Illumina 1G Genome Analyser using Solexa sequencing technology (Illumina GA) for shotgun sequencing of bisulphite-treated *Arabidopsis* genomic DNA. Sodium bisulphite converts unmethylated cytosines to uracils, but 5-methylcytosines remain unconverted. Hence, after amplification by polymerase chain reaction (PCR), unmethylated cytosines appear as thymines and methylated cytosines appear as cytosines[7]. We created genomic DNA libraries after bisulphite conversion and produced ~3.8 billion nucleotides of high-quality sequence that successfully mapped to the genome. We subsequently used several filters to ensure accuracy, including only retaining reads mapping to sequences that are unique in the genome after bisulphite conversion from every possible methylation pattern (see Supplementary Methods and Supplementary Table 1). This resulted in a conservative data set of ~2.6 billion nucleotides mapping to unique genomic locations with very high confidence, covering ~93% of all cytosines that could theoretically be covered (~92% of the ~43 million cytosines in the ~120-megabase (Mb) *Arabidopsis* genome can be covered uniquely with 31 nucleotide sequences). This represents ~20-fold average coverage, similar to typical coverage in a traditional bisulphite-sequencing experiment for a single locus.

Methylation in *Arabidopsis* exists in three sequence contexts: CG, CHG (where H is A, C or T) and asymmetric CHH[1]. We observed overall genome-wide levels of 24% CG, 6.7% CHG and 1.7% CHH methylation (Supplementary Fig. 1a). Most CGs were either unmethylated or highly methylated (80–100%), whereas CHH sites were either unmethylated or methylated at ~10%. CHG sites showed a more uniform distribution of between 20% and 100% (Supplementary Fig. 1b–d). These differences underscore the fact that each type of methylation is under distinct genetic control[1]. Our reads also contained 504-fold average coverage of 99.97% of theoretically coverable cytosines in the unmethylated chloroplast genome[3,8], giving false-positive rates of 0.29% (CG), 0.29% (CHG) and 0.25% (CHH) (Supplementary Figs 1a and 2). The BS-Seq data were highly consistent with traditional bisulphite sequencing data from individual methylated or unmethylated loci[3] (Supplementary Table 2, Supplementary Fig. 3, and below).

Although CG, CHG and CHH methylation were highly correlated, showing enrichment in repeat-rich pericentromeric regions (Fig. 1a), a marked deviation was found within gene bodies, which contained almost exclusively CG methylation (Fig. 1b). This is consistent with previous studies[3,4,9] and with a depletion of short interfering RNAs (siRNAs) in the bodies of genes (Fig. 1b). Conversely, genomic regions corresponding to siRNAs were highly correlated with CG, CHG and CHH methylation, consistent with the known molecular nature of RNA-directed DNA methylation (Fig. 1c)[1]. For methylation of all types there was a strong positive correlation with the length of the methylated sequence (Fig. 1d).

BS-Seq seems to be more sensitive than previously used microarray-based methods[3–5]. For example, we found a cluster of five methylated CG sites in a 34-base-pair region and a lone methylated CG site, both within the *FWA* locus, that were not detected by previous methods (Supplementary Fig. 4). We also found CG methylation within genes previously classified as unmethylated[3,4] (Supplementary Fig. 5). Finally, in analysing genes for which expression is de-repressed in DNA methyltransferase mutants, BS-Seq was more accurate in identifying genes with promoter methylation that was otherwise variably detected in previous microarray studies (Supplementary Fig. 6).

BS-Seq can be used to analyse repetitive sequences that are difficult to study with microarrays as they may exceed the dynamic detection range or cross-hybridize. For example, we mapped methylation across the highly repetitive *Arabidopsis* ribosomal DNA loci and found high levels of CG, CHG and CHH methylation, including on the minimal promoter and upstream *SAL1* repeats (Supplementary Fig. 7). Further, we detected methylation in telomeric repeat sequences $(CCCTAAA)_n$ that have not been previously shown to

[1]Department of Molecular Cell and Developmental Biology, [2]Howard Hughes Medical Institute, [3]Department of Human Genetics, David Geffen School of Medicine, University of California at Los Angeles, Los Angeles, California 90095, USA. [4]Illumina Inc., Hayward, California 94545, USA. [5]New England BioLabs, Ipswich, Massachusetts 01938, USA. †Present address, Department of Plant Biology, University of Georgia, Athens, Georgia 30602, USA.
*These authors contributed equally to this work

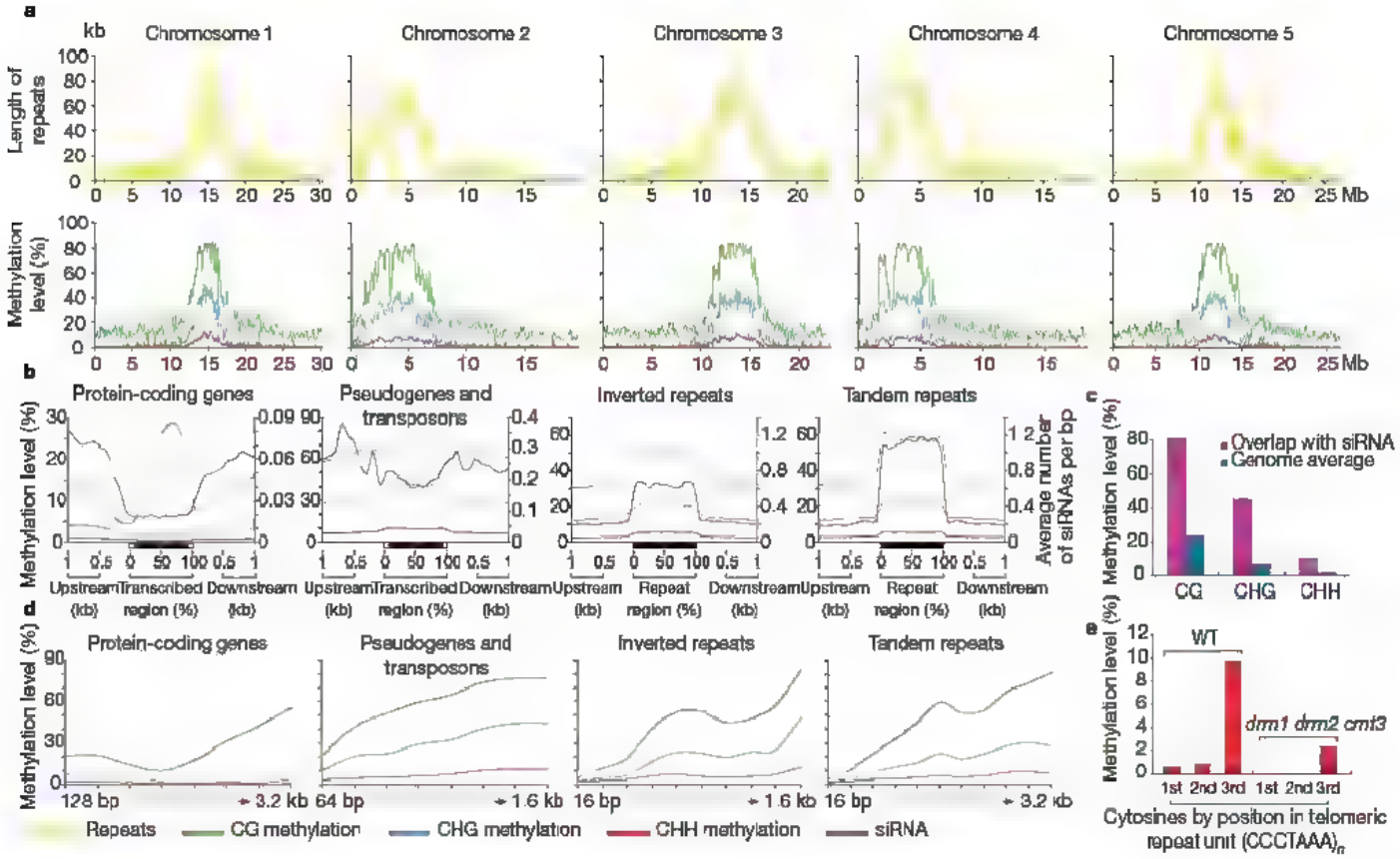


**Figure 1 | Methylation of different fractions of the *Arabidopsis* genome.** **a**, Chromosome-wide distribution of methylation and correlation with repeats in sliding 100-kb windows. **b**, Methylation levels and siRNA abundance[26] are plotted across different types of repeats and genes. **c**, High levels of methylation are detected at loci corresponding to siRNAs. **d**, Relationship between methylation levels and the length of different types of repeats and genes. **e**, From left to right, methylation levels of the three consecutive cytosines in the $(CCCTAAA)_n$ telomeric repeat unit are calculated in wild type (WT) and the *drm1 drm2 cmt3* mutant, respectively

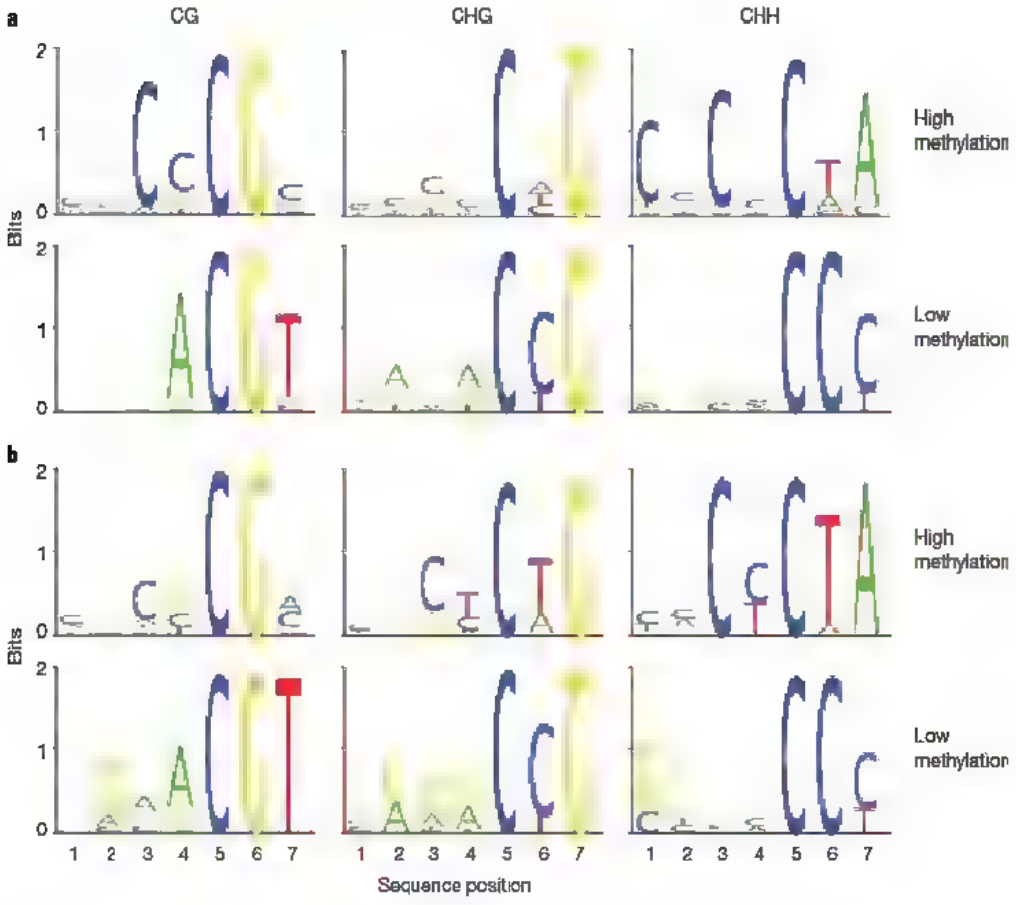


**Figure 2 | Sequence preferences for methylation in CG, CHG and CHH contexts.** Logos of sequence contexts that are preferentially methylated at the highest or lowest levels for 7-mer sequences in which the methylated cytosine is in the fifth position. In **a**, all genomic 7-mers in chromosome 1 were analysed, whereas, in **b**, sequences were restricted to previously defined methylated sequences[3]. The logo graphically displays the sequence enrichment at a particular position in the alignment of 7-mers in each class, measured in bits. The maximum sequence conservation per site is 2 bits (that is, 1 base) when a site is perfectly conserved, and 0 if there is no preference for a nucleotide.

be methylated (Fig. 1e). Interestingly, most methylation occurred at the cytosine in the third position (Fig. 1e).

The single-base resolution of BS-Seq allows determination of the precise boundaries between methylated and unmethylated regions.

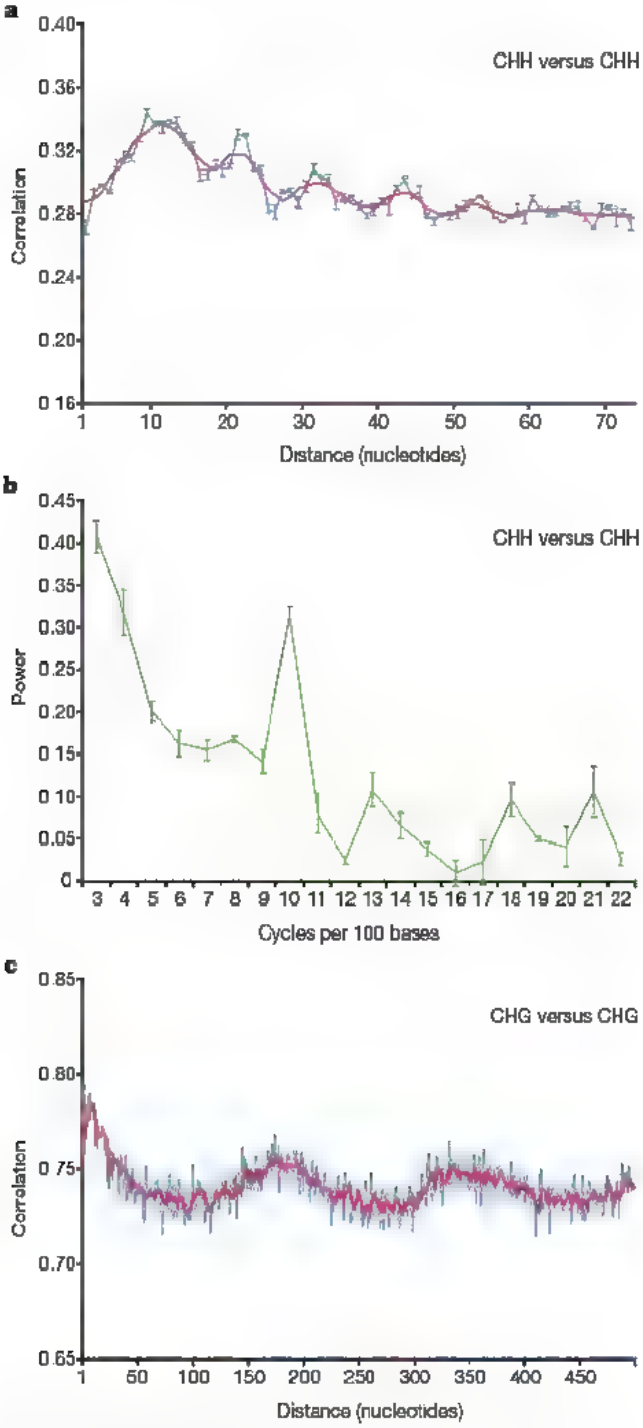


**Figure 3 | Methylation shows periodic patterns.** **a**, **c**, Correlation of the methylation status of cytosines in a CHH (**a**) and CHG (**c**) context. The *x* axis indicates the distance between the two cytosines. The *y* axis indicates the level of autocorrelation in methylation. The red line shows a running average of windows that are ±2 bases around a single base. **b**, Fourier transform analysis of CHH methylation correlation. The *x* axis indicates the number of cycles per 100 bases. The *y* axis is the amplitude of the corresponding frequency. The peak at position 10 represents a periodicity of ten nucleotides, with a *P*-value smaller than $10^{-108}$ for observing this periodicity value by chance in random permutations of the genome. In **a**–**c**, Monte Carlo sampling of three data sets, each consisting of half the data, was used to compute the mean and standard deviations of the autocorrelations and Fourier transforms. Mean values are shown, and error bars (**a** and **b**) represent standard deviations. In **a** and **b**, methylation from the whole genome was analysed, whereas, in **c**, the analysis was restricted to previously defined methylated sequences[3] (see Supplementary Fig. 15 for details).

For example, we found that the boundary between tandem repeats and flanking DNA showed a sharp drop in methylation, but DNA methylation extended from inverted repeats into flanking DNA, showing a more gradual reduction (Fig. 1b). This apparent 'spreading' of methylation was not correlated with siRNA spreading, because siRNA-abundance levels drop sharply at the flanks of both tandem and inverted repeats (Fig. 1b).

We analysed the relationship between sequence context and preference of methylation. We calculated the percentage methylation of all possible 7-mer sequences in which the methylated cytosine was either in the fifth position (allowing an analysis of four nucleotides upstream of CG, CHG and CHH methylation; Fig. 2 and Supplementary Table 3) or in the first position (allowing analysis of six nucleotides following the methylated cytosine; Supplementary Fig. 8 and Supplementary Table 4). To ensure that sequence preferences were not simply 7-mers enriched in particular components of the genome, we analysed all of chromosome 1, only sequences previously defined to be methylated by methyl-DNA immunoprecipitation, or a group of 9,507 body-methylated genes containing mostly CG methylation[3] (Fig. 2 and Supplementary Figs 8 and 9). We observed a surprisingly high level of sequence context specificity. The 7-mers with the highest and lowest levels of methylation showed a 13-fold difference for CG-methylation, an 11-fold difference for CHG methylation, and >900-fold difference for CHH methylation (Supplementary Table 3).

Sequences with the lowest CG methylation were highly enriched for the sequence ACGT (Fig. 2 and Supplementary Fig. 9). Poorly methylated CHG sites were depleted of upstream cytosines but tended to contain cytosine after the methylated cytosine. This trend is consistent with a nearest-neighbour analysis of wheat germ DNA that found CAG and CTG sites methylated at a higher level than CCG sites[10]. Highly methylated CHH sequences had a very specific configuration, with a tendency for cytosines and CG dinucleotides to be present upstream (Supplementary Table 3) and the sequence TA following the methylated cytosine. In contrast, poorly methylated CHH sequences always contained a cytosine after the methylated cytosine, and frequently contained a cytosine but always lacked an adenine two nucleotides downstream (Fig. 2 and Supplementary Fig. 8). These results are consistent with data from individual plant genes showing that cytosines preceding a cytosine are undermethylated whereas those following a cytosine are more heavily methylated[11–13], and with asymmetric methylation in mammalian genomes that is found at CT and CA sequences more frequently than CC sequences[14]. It is also of interest that *Arabidopsis* telomere sequences $(CCCTAAA)_n$ are composed of nearly optimal asymmetric target units, possibly explaining the high methylation of the third cytosines (Fig. 1e). Although the molecular basis for these trends is unknown, the results suggest that DNA methyltransferases show strong sequence preferences beyond the CG, CHG and CHH contexts. Finally, we found that regions with higher concentrations of CG dinucleotides were more heavily methylated at CG sites (Supplementary Fig. 10). Interestingly, this is different from observations in mammalian genomes, which show the opposite trend: CGs are depleted in methylated regions and at a higher density in unmethylated CpG islands.

We used autocorrelation analysis to examine the correlation between methylation in different sequence contexts and methylation at adjacent residues. We observed significant correlation between methylated cytosines for distances up to 5,000 nucleotides or more—probably a reflection of regional foci of methylation throughout the genome and of large blocks of pericentromeric heterochromatin (Supplementary Fig. 11 and Supplementary Table 5). We also found a high correlation of CHG and CHH methylation within several nucleotides downstream of methylated CG sites, and a tendency for CHH methylation four nucleotides downstream of methylation at CHG sites (Supplementary Fig. 12 and Supplementary Table 5).

These data suggest complex interactions between the different types of methylation.

We analysed the propensity for full methylation of the strand-symmetrical CG and partially symmetrical CHG sequences. As expected, CG methylation on one strand was highly correlated with CG methylation on the opposing strand. We also saw a high correlation for CHG methylation of the two strands, showing that, as for CG methylation, CHG sites show a strong tendency for symmetrical methylation (Supplementary Fig. 12). Unexpectedly, we observed a correlation between CHH methylation on one strand, and methylation at the cytosine three nucleotides downstream and on the opposite strand (Supplementary Fig. 12 and Supplementary Table 5). Because the sequence of such sites is CHHG, this shows that 'asymmetric' methylation shows a propensity for symmetrical methylation at these sites, even though methylation on CHHG sites is not particularly prominent in the genome (Supplementary Fig. 8 and Supplementary Table 4).

Autocorrelation analysis also revealed a marked periodicity of ten nucleotides (the length of one helical DNA turn) for CHH methylation (Fig. 3a, b). We confirmed this period using data from the whole genome and from regions previously defined to be methylated, and confirmed that the periodicity was not caused by our computational filtering of the data (Supplementary Fig. 13). We observed this period both when looking at the average methylation of cytosines in the genome (Fig. 3a, b and Supplementary Fig. 13) and when individual reads are examined directly (Supplementary Fig. 14). Mammalian DNA methyltransferase 3a (Dnmt3a) was recently shown to act as a tetramer with DNA methyltransferase 3-like protein (Dnmt3L), and two active sites methylate two CG sequences spaced ~8–10 nucleotides apart[15]. Because DOMAINS REARRANGED METHYLASE 2 (DRM2) is the main enzyme controlling asymmetric methylation in *Arabidopsis* and is a homologue of Dnmt3[16], these data suggest that the mechanism of action of these enzymes may be conserved between plants and mammals.

Autocorrelation also showed a period of 167 nucleotides (Fig. 3c and Supplementary Fig. 15), which is similar to, but slightly shorter than, estimates of the average spacing of nucleosomes in plant chromatin[17–19]. One explanation for this period is that nucleosomes or particular histone modifications might dictate access to the DNA by methyltransferase proteins. Furthermore, the slightly shorter length of 167 nucleotides relative to most estimates of plant nucleosome repeat length (175–185 nucleotides)[17–19] suggests that DNA-methylated chromatin may be more compact because of shorter linker regions or depletion in linker histones[20].

We used BS-Seq to study the genome-wide effects of a variety of *Arabidopsis* methyltransferase mutants on DNA methylation (Fig. 4). The MET1, CMT3 and DRM1/DRM2 DNA methyltransferase enzymes are mostly responsible for CG, CHG and CHH methylation, respectively, although at many loci CHG and CHH methylation is redundantly controlled by CMT3 and DRM1/DRM2 (refs 1 and 12). We sequenced and mapped ~90 million nucleotides of BS-Seq data from each of several combinations of DNA methyltransferase mutants (Supplementary Table 1) including *met1* single mutants, *cmt3* single mutants, *drm1 drm2* double mutants, *met1 cmt3* double mutants, *met1 drm1 drm2* triple mutants and *drm1 drm2 cmt3* triple mutants[21]. We then analysed the effect of these mutants on global methylation, on methylation in genes and chromosomes, and on methylation in rDNA and telomeres (Supplementary Table 6, Figs 1e and 4, and Supplementary Figs 7 and 16). The *met1* single mutant, or any mutant combination containing *met1*, essentially eliminated CG methylation throughout the genome. For instance, gene-body methylation, which is almost exclusively CG, was eliminated in all *met1*-containing strains (Fig. 4a). Surprisingly, in the *met1 drm1 drm2* triple mutant, we observed a marked hypermethylation of CHG sites in the bodies of genes (Fig. 4a). This methylation was skewed towards the 3′ end and in this way assumed a pattern of methylation similar to the missing CG methylation. Although previous studies have suggested that the *drm1 drm2 cmt3* triple mutant eliminates CHG and CHH methylation[12], BS-Seq data shows residual methylation (Supplementary Table 6), particularly in pericentromeric heterochromatin (Fig. 4b), suggesting that another enzyme is involved[22]. Furthermore, the *met1 cmt3* double mutant was equally effective in reducing CHH methylation, as was *drm1 drm2 cmt3* (Supplementary Table 6), suggesting that CHH methylation depends in part on the presence of CG and CHG methylation. These compensating behaviours suggest that the different DNA methyltransferases act redundantly, and help to explain the viability of these mutant combinations, whereas the *met1 cmt3 drm1 drm2* quadruple mutant causes embryonic lethality[21].

The BS-Seq procedure described here should be generally useful in other organisms. For example, we applied BS-Seq to quantify the

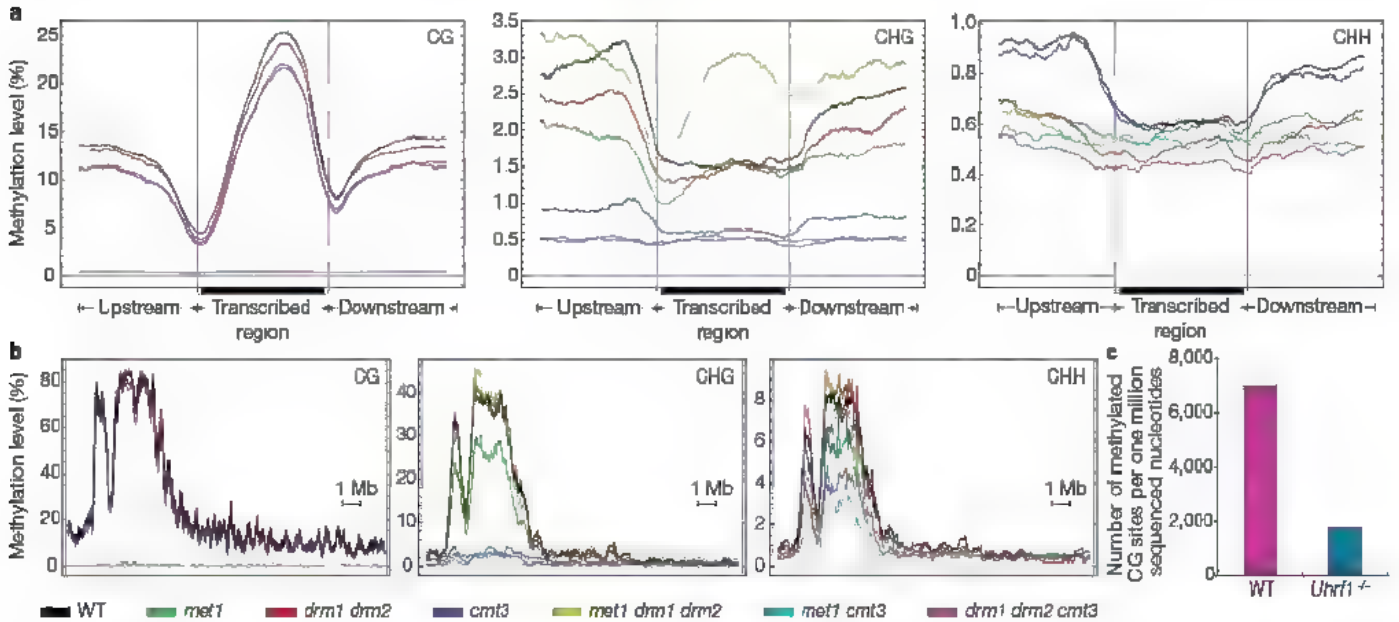


**Figure 4 | BS-Seq profiling of methylation mutants in *Arabidopsis* and mouse.** **a**, BS-Seq data mapping to protein-coding genes was plotted in 500-nucleotide sliding windows. Two vertical blue lines mark the boundaries between upstream regions and gene bodies (left) and between gene bodies and downstream regions (right). **b**, Distribution of methylation along chromosome 4 in 25-nucleotide sliding windows. In **a** and **b**, a horizontal blue line indicates zero per cent methylation. **c**, Comparison of the amount of CG methylation in wild type and mouse *Uhrf1*$^{-/-}$ embryonic stem cells, represented as the average number of CGs appearing per million sequenced nucleotides.

overall genomic methylation difference between wild-type mouse embryonic stem cells and cells carrying a mutation in the *Uhrf1* gene recently shown to control maintenance of CG methylation[23,24]. By analysing ~60 million nucleotides of shotgun sequencing data from each, we found that *Uhrf1*$^{-/-}$ cells contained only 25% of the CpG methylation level of the wild type (Fig. 4c). Furthermore, to demonstrate that the complete analysis pipeline used for *Arabidopsis* is applicable to larger genomes, we produced a library from mouse germ-cell tissue and generated ~46 million nucleotides of high quality mapped BS-Seq data. Approximately 66% of the reads mapped uniquely—a level only slightly lower than that of *Arabidopsis* (Supplementary Table 1), suggesting that it is practical to apply BS-Seq to entire mammalian genomes.

In summary, BS-Seq analysis of wild type and methyltransferase mutants has allowed a more detailed characterization of the *Arabidopsis* methylome. In addition, the computational approaches developed in this study should be generally useful for other short-read sequencing genomics approaches. An installation of the UCSC browser allowing community access to detailed methylation patterns of individual genes and a source code distribution of the computational methods are available at http://epigenomics.mcdb.ucla.edu/BS-Seq/.

## METHODS SUMMARY

**Construction and sequencing of DNA libraries.** Bisulphite treatment of DNA was performed as described previously[25], except that adaptor sequences and PCR conditions were modified and optimized for this study. Library generation and ultra-high-throughput sequencing were carried out according to manufacturer instructions (Illumina).

**Processing of sequence data and mapping of reads.** Raw data from Illumina GA were processed using the initial stages of the Solexa software pipeline (Illumina) into short reads, except that per-lane per-cycle multidimensional gaussian mixture models (GMMs) were developed to optimize base call A-versus-C-versus-G-versus-T probability distribution accuracies at each sequenced base compared to the Solexa software pipeline's '.prb' files. Sequenced reads were mapped to reference genomes fully using per-base probabilities from the GMMs using highly optimized novel C++ tools. Sequences that mapped to more than one position with similar scores (within 1% of the maximum likelihood mapping) were removed to retain only reads that mapped uniquely. To eliminate unconverted bisulphite reads, a filter discarded reads with three or more consecutive methylated cytosines when each of these was in a CHH context, resulting in a loss of ~0.23% of reads. This filter was effective and gave only minimal loss of true CHH methylation (Supplementary Table 1 and Supplementary Figs 13, 17 and 18).

**Validation of BS-Seq results.** Traditional bisulphite sequencing was used to validate BS-Seq results at select loci (Supplementary Table 2 and Supplementary Figs 4, 6 and 17). The PCR primers used in the validation are listed in Supplementary Table 7.

**Received 28 November 2007; accepted 30 January 2008.**
**Published online 17 February 2008.**

1. Henderson, I. R. & Jacobsen, S. E. Epigenetic inheritance in plants. *Nature* 447, 418–424 (2007).
2. Goll, M. G. & Bestor, T. H. Eukaryotic cytosine methyltransferases. *Annu. Rev. Biochem.* 74, 481–514 (2005).
3. Zhang, X. *et al.* Genome-wide high-resolution mapping and functional analysis of DNA methylation in *Arabidopsis*. *Cell* 126, 1189–1201 (2006).
4. Zilberman, D., Gehring, M., Tran, R. K., Ballinger, T. & Henikoff, S. Genome-wide analysis of *Arabidopsis thaliana* DNA methylation uncovers an interdependence between methylation and transcription. *Nature Genet.* 39, 61–69 (2007).
5. Vaughn, M. W. *et al.* Epigenetic natural variation in *Arabidopsis thaliana*. *PLoS Biol.* 5, e174 (2007).
6. Bentley, D. R. Whole-genome re-sequencing. *Curr. Opin. Genet. Dev.* 16, 545–552 (2006).
7. Frommer, M. *et al.* A genomic sequencing protocol that yields a positive display of 5-methylcytosine residues in individual DNA strands. *Proc. Natl Acad. Sci. USA* 89, 1827–1831 (1992).
8. Ngernprasirtsiri, J., Kobayashi, H. & Akazawa, T. DNA methylation as a mechanism of transcriptional regulation in nonphotosynthetic plastids in plant cells. *Proc. Natl Acad. Sci. USA* 85, 4750–4754 (1988).
9. Tran, R. K. *et al.* DNA methylation profiling identifies CG methylation clusters in *Arabidopsis* genes. *Curr. Biol.* 15, 154–159 (2005).
10. Gruenbaum, Y., Naveh-Many, T., Cedar, H. & Razin, A. Sequence specificity of methylation in higher plant DNA. *Nature* 292, 860–862 (1981).
11. Meyer, P., Niedenhof, I. & ten Lohuis, M. Evidence for cytosine methylation of non-symmetrical sequences in transgenic *Petunia hybrida*. *EMBO J.* 13, 2084–2088 (1994).
12. Cao, X. & Jacobsen, S. E. Locus-specific control of asymmetric and CpNpG methylation by the DRM and CMT3 methyltransferase genes. *Proc. Natl Acad. Sci. USA* 99 (Suppl 4), 16491–16498 (2002).
13. Dieguez, M. J., Vaucheret, H., Paszkowski, J. & Mittelsten Scheid, O. Cytosine methylation at CG and CNG sites is not a prerequisite for the initiation of transcriptional gene silencing in plants, but it is required for its maintenance. *Mol. Gen. Genet.* 259, 207–215 (1998).
14. Ramsahoye, B. H. *et al.* Non-CpG methylation is prevalent in embryonic stem cells and may be mediated by DNA methyltransferase 3a. *Proc. Natl Acad. Sci. USA* 97, 5237–5242 (2000).
15. Jia, D., Jurkowska, R. Z., Zhang, X., Jeltsch, A. & Cheng, X. Structure of Dnmt3a bound to Dnmt3L suggests a model for *de novo* DNA methylation. *Nature* 449, 248–251 (2007).
16. Cao, X. *et al.* Conserved plant genes with similarity to mammalian de novo DNA methyltransferases. *Proc. Natl Acad. Sci. USA* 97, 4979–4984 (2000).
17. Bers, E. P., Singh, N. P., Pardonen, V. A., Lutova, L. A. & Zalensky, A. O. Nucleosomal structure and histone H1 subfractional composition of pea (Pisum sativum) root nodules, radicles and callus chromatin. *Plant Mol. Biol.* 20, 1089–1096 (1992).
18. Vershinin, A. V. & Heslop-Harrison, J. S. Comparative analysis of the nucleosomal structure of rye, wheat and their relatives. *Plant Mol. Biol.* 36, 149–161 (1998).
19. Fulnecek, J., Matyasek, R., Kovarik, A. & Bezdek, M. Mapping of 5-methylcytosine residues in *Nicotiana tabacum* 5S rRNA genes by genomic sequencing. *Mol. Gen. Genet.* 259, 133–141 (1998).
20. Fan, Y. *et al.* Histone H1 depletion in mammals alters global chromatin structure but causes specific changes in gene regulation. *Cell* 123, 1199–1212 (2005).
21. Zhang, X. & Jacobsen, S. E. Genetic analyses of DNA methyltransferases in *Arabidopsis thaliana*. *Cold Spring Harb. Symp. Quant. Biol.* 71, 439–447 (2006).
22. Henderson, I. R. *et al.* Dissecting *Arabidopsis thaliana* DICER function in small RNA processing, gene silencing and DNA methylation patterning. *Nature Genet.* 38, 721–725 (2006).
23. Bostick, M. *et al.* UHRF1 plays a role in maintaining DNA methylation in mammalian cells. *Science* 317, 1760–1764 (2007).
24. Sharif, J. *et al.* The SRA protein Np95 mediates epigenetic inheritance by recruiting Dnmt1 to methylated DNA. *Nature* 450, 908–912 (2007).
25. Meissner, A. *et al.* Reduced representation bisulfite sequencing for comparative high-resolution DNA methylation analysis. *Nucleic Acids Res.* 33, 5868–5877 (2005).
26. Rajagopalan, R., Vaucheret, H., Trejo, J. & Bartel, D. P. A diverse and evolutionarily fluid set of microRNAs in *Arabidopsis thaliana*. *Genes Dev.* 20, 3407–3425 (2006).

**Supplementary Information** is linked to the online version of the paper at www.nature.com/nature.

**Acknowledgements** We thank Y. Bernatavichute for nuclear DNA isolation protocols, A. Clarke for providing embryonic stem cell DNA, A. Girard and G. Hannon for providing mouse germ cell DNA, J. Hetzel for technical assistance, and C. F. Li for assistance with rDNA annotation. S.F. is a Howard Hughes Medical Institute Fellow of the Life Science Research Foundation. X.Z. was supported by a fellowship from the Jonsson Cancer Center Foundation. S.E.J. is an investigator of the Howard Hughes Medical Institute. This work was supported in part by grants from the NSF Plant Genome Research Program and the NIH, and some aspects of the work were performed in the UCLA DNA Microarray Facility.

**Author Contributions** S.J.C. developed computational methods for mapping and base-calling. S.F. designed and created DNA libraries and performed all molecular biology experiments. S.F., Z.C., B.M. and S.F.N. sequenced the libraries. M.P., S.J.C., S.F. and S.E.J. analysed data. S.E.J. and M.P. designed and directed the study. X.Z., C.D.H. and S.P. assisted in the design of experiments. S.F. and S.J.C. wrote the manuscript.

**Author Information** The authors declare competing financial interests, details accompany the full-text HTML version of the paper at www.nature.com/nature. Reprints and permissions information is available at www.nature.com/reprints. Correspondence and requests for materials should be addressed to S.E.J. (jacobsen@ucla.edu) or M.P. (matteop@mcdb.ucla.edu).

LETTERS

# Adaptive coding of visual information in neural populations

Diego A. Gutnisky[1] & Valentin Dragoi[1]

**Our perception of the environment relies on the capacity of neural networks to adapt rapidly to changes in incoming stimuli[1–4]. It is increasingly being realized that the neural code is adaptive[5], that is, sensory neurons change their responses and selectivity in a dynamic manner to match the changes in input stimuli[1,2,5]. Understanding how rapid exposure, or adaptation, to a stimulus of fixed structure changes information processing by cortical networks is essential for understanding the relationship between sensory coding and behaviour[5–8]. Physiological investigations of adaptation have contributed greatly to our understanding of how individual sensory neurons change their responses to influence stimulus coding[2,9–12], yet whether and how adaptation affects information coding in neural populations is unknown. Here we examine how brief adaptation (on the timescale of visual fixation)[2,9,10] influences the structure of interneuronal correlations and the accuracy of population coding in the macaque (*Macaca mulatta*) primary visual cortex (V1). We find that brief adaptation to a stimulus of fixed structure reorganizes the distribution of correlations across the entire network by selectively reducing their mean and variability. The post-adaptation changes in neuronal correlations are associated with specific, stimulus-dependent changes in the efficiency of the population code, and are consistent with changes in perceptual performance after adaptation[2,13,14]. Our results have implications beyond the predictions of current theories of sensory coding, suggesting that brief adaptation improves the accuracy of population coding to optimize neuronal performance during natural viewing.**

Understanding how adaptation influences population coding requires an understanding of how adaptation changes the structure of interneuronal correlations across the network. Indeed, during the past decade, it has become increasingly understood that the trial-by-trial variability in neuronal responses, or 'noise', is not independent, but that it exhibits correlations[15,16]. This implies that the accuracy of the population code must depend on the distribution of noise correlations across the network[17–19]. Theoretically, it has been proposed that adaptation would reduce neuronal correlations, and hence redundancy[20,21], to improve stimulus coding[1]. In reality, exactly how the structure of correlations across a population of neurons is affected by adaptation, and how it influences the efficiency of coding, is unknown.

We address this issue in the context of the macaque primary visual cortex (V1), in which adaptation has been shown previously to induce changes in the response magnitude and selectivity of individual neurons[2,5,9–11]. We focus on a particular, rapid form of adaptation that is believed to occur spontaneously during visual fixation when cortical cells are exposed to redundant information for hundreds of milliseconds[2,9]. Our hypothesis is that rapid adaptation changes the structure of noise correlations in V1 and increases the amount of information in a population code in a way that is consistent with perceptual performance.

Responses to dynamic test stimuli in area V1 of a fixating monkey were recorded before and after brief (400-ms) adaptation to a sine-wave grating of fixed orientation (Fig. 1a). We used a movie sequence as the test stimulus (see Methods), in which each frame was a sine-wave grating of pseudorandom orientation flashed at 60 Hz. The stimulus was fixed across trials and covered multiple neuronal receptive fields (Supplementary Fig. 1). We measured noise correlations (trial-to-trial covariation of spike counts of a cell pair) between pairs of nearby neurons ($n = 423$ pairs). We confirmed previous findings[16] that noise correlations are independent of stimulus orientation; only 5% of the pairs exhibited a significant relationship between the correlation coefficient and stimulus orientation (see Methods).

Figure 1b shows an example of a pair of cells preferring nearby orientations that exhibit a strong reduction in correlations after adaptation (the pre-adaptation condition is labeled 'control'). Across the population, we found an overall post-adaptation decrease in the absolute correlation coefficients that was significant both for positive (mean reduction 22%, $P < 10^{-8}$, Wilcoxon signed rank test) and for negative (mean reduction 74%, $P < 10^{-5}$) coefficients (Fig. 1c; the post-adaptation reduction in correlations is significant in each monkey, Supplementary Fig. 2). This reduction in correlation strength is also found in cells that exhibit positive correlations before adaptation and negative correlations after adaptation (mean reduction 73%, $P < 10^{-6}$) and negative correlations before adaptation and positive correlations after adaptation (mean reduction 42%, $P < 0.005$). Overall, correlation coefficients decayed exponentially with the difference ($\Delta\theta$) in the cells' preferred orientation[22]; Supplementary Fig. 3a shows that adaptation reduces the peak and slope of the exponential decay of correlation coefficients. We further examined whether the decrease in correlations after adaptation could be due to the small (5.8%), but significant ($P < 10^{-6}$), reduction in mean firing rates (Supplementary Fig. 1). However, we found no relationship between the mean changes in firing rates after adaptation and the changes in correlation coefficients[23] (Fig. 1d, $P > 0.3$, Pearson correlation).

Because adaptation is an orientation-specific phenomenon[2,3,10,11], we reasoned that the degree of decorrelation would depend on the relationship between the adapting stimulus and the preferred orientation of the cells in a pair. We therefore selected the cell pairs that preferred nearby orientations ($\Delta\theta < 30°$), and compared the mean correlation coefficients before and after adaptation to stimuli of different orientation; we defined $\Delta\phi$ as the minimum difference between the adapting stimulus and the preferred orientation of each cell in a pair (Fig. 1e; see Methods and Supplementary Fig. 4). There is a strong reduction in correlations (Fig. 1f) for adapting stimuli near ($\Delta\phi \leq 30°$, 31%, $P < 0.005$; Wilcoxon rank sum test) and far ($\Delta\phi > 60°$), 43%, $P < 0.0005$) relative to the orientation of the cell pair, but intermediate adaptation ($30° < \Delta\phi \leq 60°$) was ineffective at reducing correlations (19%; $P > 0.1$).

[1]Department of Neurobiology and Anatomy, University of Texas-Houston Medical School, Houston, Texas 77030, USA

These results indicate that brief adaptation reduces the strength of correlations in an orientation-asymmetric manner. We quantified the orientation dependency of this decorrelation by estimating the probability density function (pdf) of correlations, before and after adaptation, as a function of $\Delta\theta$ and $\Delta\phi$ using the kernel density estimation technique (see Supplementary Information). Contrary to the common belief that adaptation would only influence the responses of cells of similar preferred orientation (but consistent with Fig. 1f), we found a non-monotonic decorrelation profile (Fig. 2a)—that is, cells of similar ($\Delta\theta < 30°$) and largely dissimilar ($\Delta\theta > 60°$) orientation preference exhibit significant decorrelation, whereas cells with $\Delta\theta$ between 30° and 60° show only a weak decrease in correlations, both for near and far adaptation. This is shown in Fig. 2b, in which an adaptation decorrelation index is used to represent the magnitude of post-adaptation changes in absolute correlations; Supplementary Fig. 5 demonstrates the temporal stability of the decorrelation.

The changes in correlation structure after adaptation are described not only by changes in mean correlation coefficients but also by changes in the variability of correlations. Although it has been theoretically suggested that a small variability of correlations could increase coding efficiency[24], exactly how the variability of correlations influences population coding is unknown. Figure 3 shows that adaptation reduces not only the strength but also the variability of correlations (see also Supplementary Fig. 3b), both for near and for far adaptation. We explored this issue by estimating the pdf of correlations for pairs of cells with $\Delta\theta$ between 0° and 30° (small $\Delta\theta$), between 30° and 60° (intermediate $\Delta\theta$), and between 60° and 90° (large $\Delta\theta$). Figure 3d–f illustrates representative examples in which the adapting stimulus is near the preferred orientation of at least one of the cells in the pair ($\Delta\phi \leq 30°$) or far from both cells ($\Delta\phi > 30°$). For small $\Delta\theta$ (Fig. 3d), the post-adaptation pdf is sharper and shifted to the left relative to the pdf before adaptation. That is, there is both a significant decorrelation ($P < 0.0001$) and a reduction in correlation variability after adaptation. For intermediate $\Delta\theta$ (Fig. 3e), only far adaptation ($\Delta\phi > 30°$) induces a significant decorrelation ($P < 0.001$). Contrary to expectation, for large $\Delta\theta$ (Fig. 3f), the adaptation-induced reduction in the mean and variability of correlations is even larger than that observed in cells preferring nearby orientations.

Together, these results raise the issue of whether the changes in the strength and variability of noise correlations after adaptation would affect the efficiency of the population code. We therefore computed network efficiency by estimating the Fisher information as the upper limit with which any decoding mechanism can extract information about stimulus orientation[17,18]. Consistent with the fact that second-order statistics are able to capture most of the variability of the population response[25], we assumed that the joint neuronal responses to stimulus orientation can be described by a multivariate gaussian defined by the mean firing rate and covariance matrix[17,18]. Fisher information was computed by assuming, first, that adaptation changes only the mean correlations, and second, both the mean

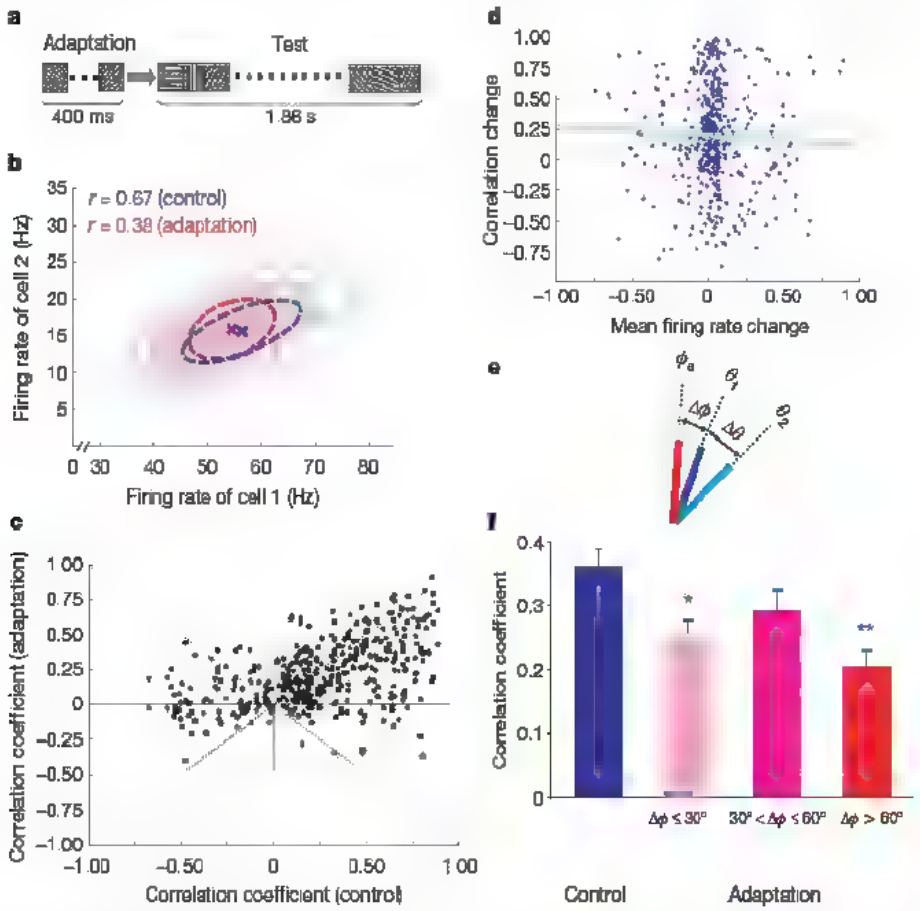


**Figure 1 | Adaptation-induced response decorrelation in V1.** **a**, Schematic representation of the stimulus sequence: an adapting stimulus of fixed orientation was presented for 400 ms and was followed by a 60-Hz test stimulus of random orientation presented for 1.86 s. **b**, Scatter plot showing the trial-by-trial responses of two cells recorded simultaneously. Each dot represents the firing rates of both cells in a given trial. The dotted ellipses represent the two-dimensional gaussian fits of the firing rate distributions during control and adaptation (crosses represent the means). '*r*' represents the correlation coefficient. **c**, Correlation coefficients for the population of cell pairs. Each dot represents the correlation coefficient for a pair of cells during control and adaptation (irrespective of the difference in preferred orientation). **d**, The post-adaptation changes in correlations cannot be attributed to the changes in the geometric mean firing rates of the cells in a pair ($P > 0.3$). The light blue line represents the linear regression fit. **e**, Schematic representing the preferred orientations of the cells in a pair ($\theta_1$ and $\theta_2$) and the adapting orientation ($\phi_a$). $\Delta\theta$ and $\Delta\phi$ are defined in the text. **f**, The reduction in the mean correlation coefficients after adaptation depends on the adapting orientation (for pairs for which $\Delta\phi < 30°$). All panels are based on the correlation analysis of $n = 423$ cell pairs ($\Delta\theta < 30°$, 223 pairs; $\Delta\theta > 30°$, 200 pairs). Error bars represent s.e.m. (*$P < 0.005$; **$P < 0.0005$)

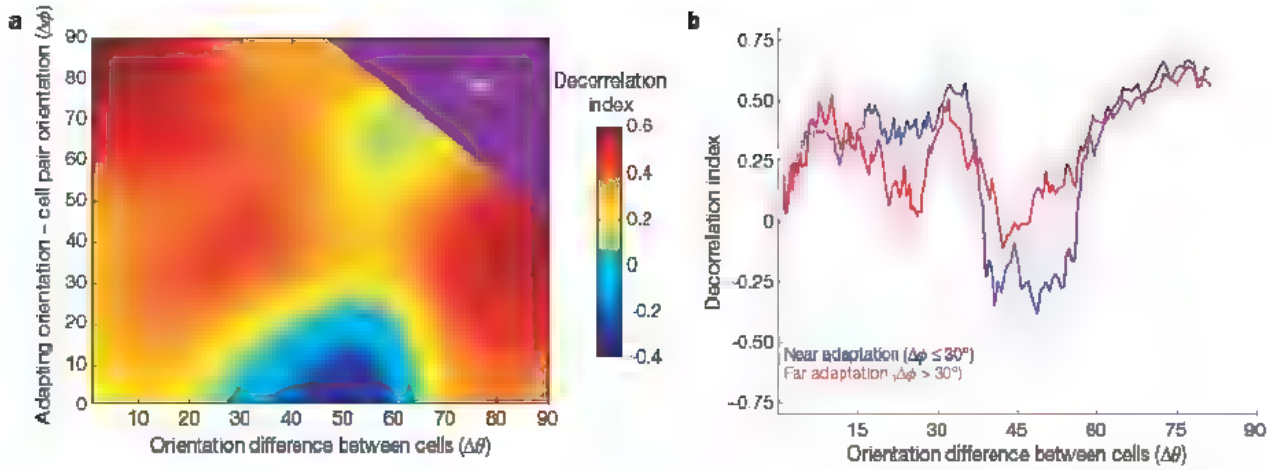


**Figure 2 | Rapid adaptation changes the structure of interneuronal correlations.** **a**, Decorrelation index as a function of the difference between the preferred orientations of the cells in a pair ($\Delta\theta$) and the minimum difference between the adapting orientation and that of each cell ($\Delta\phi$). The region of possible ($\Delta\theta$, $\Delta\phi$) pairs is described by $\Delta\phi + \Delta\theta \leq 135°$ (although $\Delta\phi$ varies between 0° and 90°, $\Delta\theta$ is not completely independent of $\Delta\phi$). **b**, Adaptation decorrelates V1 responses in an orientation-asymmetric manner. Pairs were grouped depending on whether $\Delta\phi$ is smaller (near adaptation) or greater (far adaptation) than 30°; this ensures that the number of pairs in each category is approximately the same (46% of pairs had $\Delta\phi < 30°$ and 54% of pairs had $\Delta\phi > 30°$). The decorrelation index was calculated using the experimentally measured pairwise correlations in a sliding window of 20 points on the *x*-axis. Error bars represent s.e.m.

and variability of correlations (using the pdfs in Fig. 3a–c). Figure 4a shows that whereas the post-adaptation reduction in mean correlations caused a 25% improvement in the network orientation discriminability threshold, if both the changes in the mean and variability of correlations are taken into account the post-adaptation discrimination threshold is improved by 40%. Interestingly, for small populations, the post-adaptation network performance is slightly better than that of uncorrelated (independent) neurons, possibly due to a reduction in correlation variability[24].

The fact that adaptation changes interneuronal correlations in an orientation-asymmetric manner (Fig. 2) could cause the network efficiency to depend on the relationship between the adapting and test orientations. Indeed, we found that test stimuli similar or largely dissimilar with respect to the adapting orientation cause the largest improvement in coding efficiency. As shown in Fig. 4b, brief adaptation caused an almost fourfold increase in Fisher information when the network discriminated stimuli of similar and largely dissimilar orientation relative to the adapting stimulus, and a threefold increase

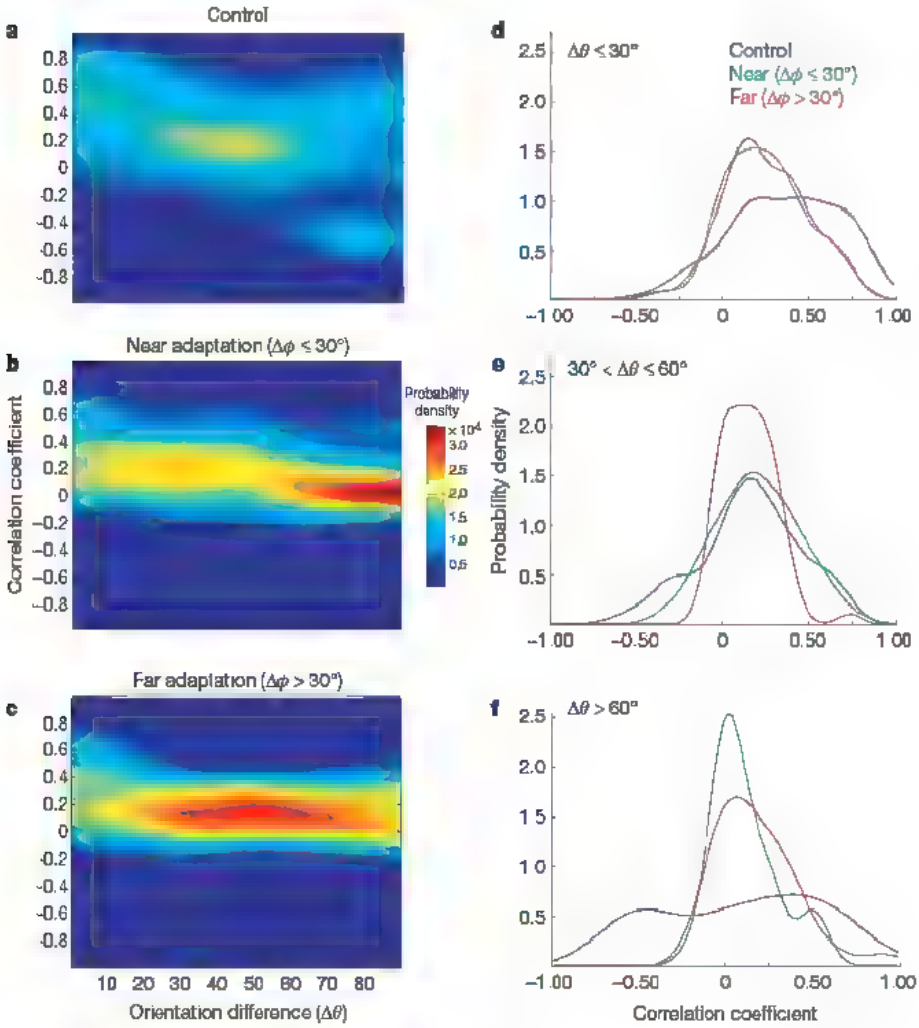


**Figure 3 | Rapid adaptation changes the mean and variability of correlations.** **a–c**, Probability density functions of correlations in control and adaptation (near, $\Delta\phi \leq 30°$; far, $\Delta\phi > 30°$) as a function of $\Delta\theta$. Both near and far adaptation reduces the variability of correlations. **d–f**, Probability density functions of correlation coefficients in control and adaptation in different $\Delta\theta$ bins (<30°, 30°–60°, and >60°). Adaptation decreases the mean and variability of correlations for small and large $\Delta\theta$ values.

in Fisher information for the discrimination of intermediate orientations. This is consistent with the larger reduction in the mean and variability of correlations for small and large $\Delta\theta$ (<30° and >60°) relative to intermediate orientations ($\Delta\theta$ between 30° and 60°; Fig. 3d–f). Although these results may seem surprising, they are in agreement with human psychophysical data reporting that brief adaptation improves orientation discrimination near and far from the adapting orientation[2,13]. Importantly, we also found that the increase in population coding efficiency through decorrelation would be equivalent to an overall post-adaptation increase in firing rates of approximately 55%.

In addition to noise correlations, the population code is also characterized by signal correlations[26]—correlations in the neurons' average responses to a stimulus set. Rapid adaptation causes repulsive shifts in the neurons' orientation tuning curves and changes in firing rates[2,11] (Supplementary Fig. 6) to influence signal correlations. By examining the affect of the adaptation-induced changes in noise and signal correlations on coding efficiency (Fig. 4b), we found that, in agreement with psychophysical studies[2,13,14], the enhancement in network performance after adaptation is orientation-specific. Although these results have been obtained by computing correlations throughout the stimulus presentation, they also hold when noise correlations are measured on the timescale of visual fixation, during the first 400 ms of stimulus presentation (Supplementary Fig. 7). Thus, the post-adaptation improvement in network performance may influence sensory coding during natural viewing.

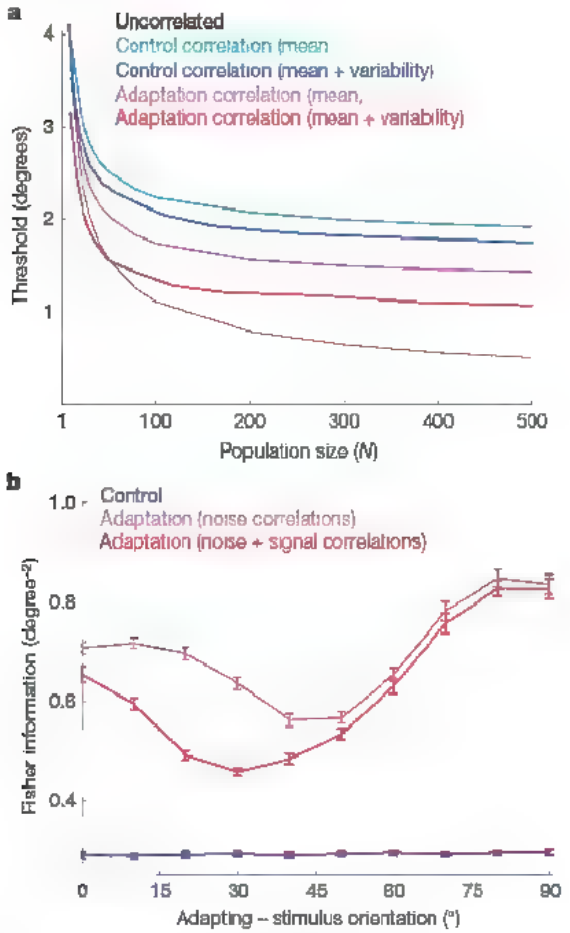


**Figure 4 | Rapid adaptation enhances the efficiency of population coding.** **a**, Adaptation increases the orientation discrimination performance of a neural population of variable size. Light blue and light red curves, adaptation changes only the mean correlation coefficients; dark blue and dark red curves, adaptation changes both the mean and variability of correlations. **b**, The efficiency of population coding (Fisher information) depends on $\Delta\theta$ and the adapting orientation (fixed at 0°; abscissa represents the test orientation). In control trials, Fisher information is independent of the test orientation. Post-adaptation changes in noise correlations cause the largest improvement in network performance when test stimuli are similar or largely dissimilar with respect to the adapting orientation. Combining the effects of noise and signal correlations yields a more pronounced U-shape profile of Fisher information. The error bars represent s.e.m.

We have demonstrated the functional significance of rapid adaptation by V1 networks for the coding of image features. Theoretically, adaptation has been proposed to reduce redundancy in sensory neurons, possibly by decorrelating responses, to improve coding efficiency[1,4]. However, in addition to the lack of experimental support, theories proposing the decorrelation hypothesis were unable to predict the changes in correlations across the entire network engaged in sensory computations. We provide empirical evidence that adaptation causes both a selective reduction in the strength and variability of correlations and an improvement in the efficiency of population coding. These results are consistent with the 'efficient coding hypothesis'[1,4]—that is, sensory neurons are adapted to the statistical properties of the stimuli that they are exposed to (Supplementary Fig. 8a, b)—and with psychophysical changes in human discrimination performance after adaptation (Supplementary Fig. 8c). We further propose that adaptation takes advantage of the rapid sequence of fixations during natural viewing to optimize image-discrimination performance in real time[2,27].

Our results argue that the visual system uses a metabolically inexpensive solution (selective decorrelation) to adapt neural responses to the statistics of the input stimuli and to improve coding efficiency. This raises the issue of whether decorrelation is an advantageous coding strategy in the visual cortex. Whereas selective decorrelation improves sensory discriminations by increasing network efficiency and possibly the organization of cell ensembles (Supplementary Fig. 9), it could be detrimental for other types of information processing. For instance, theoretical studies have suggested that temporally decorrelated inputs are transmitted less efficiently than correlated inputs[28]. Indeed, it is well known that in addition to sensory discriminations, the visual system is often required to perform other complex computations, such as contour grouping[29] or figure-ground segregation[30], which may require strong correlations between neurons. Hence, the fact that we did not observe a complete, homogeneous, decorrelation of responses in V1 could constitute a trade-off between distinct optimization goals during sensory processing[6].

## METHODS SUMMARY

All experiments were performed in accordance with protocols approved by NIH. Multiple single-unit recordings were performed from V1 of two fixating monkeys (*Macaca mulatta*). Stimuli were presented so that they covered the centre of the neurons' receptive fields. In control trials, movie strips[2] were presented for ~1.86 s (16 orientations × 7 repeats at 60 Hz; random spatial phase). In adaptation trials, movies were preceded by a 400-ms grating of fixed orientation. The Pearson correlation coefficient of spike counts, $R_{sc}$, of two cells is defined as

$$R_{sc} = \frac{\sum_{i=1}^{N} (r_1^i - \bar{r}_1)\cdot(r_2^i - \bar{r}_2)}{\sigma_1\,\sigma_2}$$

where $N$ is the number of trials, $r_j^i$ is the firing rate of cell '$j$' in trial '$i$' averaged over the entire stimulus sequence, and $\sigma$ is standard deviation of the responses. Correlation coefficients after adaptation depend on three variables: the adapting orientation, $\phi_a$, and the preferred orientation of the cells in a pair, $\theta_1$ and $\theta_2$. To ensure that the parameter space is adequately sampled, the distance between the adapting orientation and the preferred orientation of one of the cells was held constant while varying the relative difference between the two cells' preferred orientations ($\Delta\theta$). We defined $\Delta\phi$ as the minimum difference between the adapting stimulus and the preferred orientation of each cell in a pair, that is, $\Delta\phi = \min(|\phi_a - \theta_1|, |\phi_a - \theta_2|)$. We define an adapting stimulus 'near' to a cell pair when the adapting orientation is <30° relative to at least one of the cells in the pair. Similarly, a 'far' adapting stimulus is oriented at least 30° away from both cells.

We calculated a decorrelation index as the percentage change in absolute correlation coefficient:

$$DI = \frac{|R_{control}| - |R_{adaptation}|}{|R_{control}|}$$

where $R_i$ represents the correlation coefficients measured in condition '$i$'. The

Monte Carlo simulations, kernel density estimation and Fisher information calculations are explained in the Methods and Supplementary Information.

**Full Methods** and any associated references are available in the online version of the paper at www.nature.com/nature.

**Received 7 May 2007; accepted 9 January 2008.**


1. Barlow, H. B. in *Sensory Communication* (ed. Rosenblith, W. A.) 217–234 (MIT, Cambridge, Massachusetts, 1961)
2. Dragoi, V., Sharma, J., Miller, E. K. & Sur, M. Dynamics of neuronal sensitivity in visual cortex and local feature discrimination. *Nature Neurosci.* 5, 883–891 (2002)
3. Dragoi, V., Turcu, C. M. & Sur, M. Stability of cortical responses and the statistics of natural scenes. *Neuron* 32, 1181–1192 (2001)
4. Simoncelli, E. P. Vision and the statistics of the visual environment. *Curr. Opin. Neurobiol.* 13, 144–149 (2003)
5. Sharpee, T. O. *et al.* Adaptive filtering enhances information transmission in visual cortex. *Nature* 439, 936–942 (2006).
6. Schwabe, L. & Obermayer, K. Rapid adaptation and efficient coding. *Biosystems* 67, 239–244 (2002).
7. Wainwright, M. J. Visual adaptation as optimal information transmission. *Vision Res.* 39, 3960–3974 (1999)
8. Vinje, W. E. & Gallant, J. L. Sparse coding and decorrelation in primary visual cortex during natural vision. *Science* 287, 1273–1276 (2000).
9. Muller, J. R., Metha, A. B., Krauskopf, J. & Lennie, P. Rapid adaptation in visual cortex to the structure of images. *Science* 285, 1405–1408 (1999)
10. Felsen, G. *et al.* Dynamic modification of cortical orientation tuning mediated by recurrent connections. *Neuron* 36, 945–954 (2002)
11. Dragoi, V., Sharma, J. & Sur, M. Adaptation-induced plasticity of orientation tuning in adult visual cortex. *Neuron* 28, 287–298 (2000)
12. Kohn, A. & Movshon, J. A. Neuronal adaptation to visual motion in area MT of the macaque. *Neuron* 39, 681–691 (2003)
13. Clifford, C. W., Wyatt, A. M., Arnold, D. H., Smith, S. T. & Wenderoth, P. Orthogonal adaptation improves orientation discrimination. *Vision Res.* 41, 151–159 (2001)
14. Regan, D. & Beverley, K. I. Postadaptation orientation discrimination. *J. Opt. Soc. Am.* 2, 147–155 (1985)
15. Zohary, E., Shadlen, M. N. & Newsome, W. T. Correlated neuronal discharge rate and its implications for psychophysical performance. *Nature* 370, 140–143 (1994)
16. Kohn, A. & Smith, M. A. Stimulus dependence of neuronal correlation in primary visual cortex of the macaque. *J. Neurosci.* 25, 3661–3673 (2005)
17. Abbott, L. F. & Dayan, P. The effect of correlated variability on the accuracy of a population code. *Neural Comput.* 11, 91–101 (1999)
18. Sompolinsky, H., Yoon, H., Kang, K. J. & Shamir, M. Population coding in neuronal systems with correlated noise. *Phys. Rev. E* 64, 051904 (2001)
19. Pouget, A., Dayan, P. & Zemel, R. Information processing with population codes. *Nature Rev. Neurosci.* 1, 125–132 (2000)
20. Reich, D. S., Mechler, F. & Victor, J. D. Independent and redundant information in nearby cortical neurons. *Science* 294, 2566–2568 (2001)
21. Schneidman, E., Bialek, W. & Berry, M. J. II. Synergy, redundancy, and independence in population codes. *J. Neurosci.* 23, 11539–11553 (2003)
22. Tso, D. Y., Gilbert, C. D. & Wiesel, T. N. Relationships between horizontal interactions and functional architecture in cat striate cortex as revealed by cross-correlation analysis. *J. Neurosci.* 6, 1160–1170 (1986)
23. de la Rocha, J., Doiron, B., Shea-Brown, E., Josić, K. & Reyes, A. Correlation between neural spike trains increases with firing rate. *Nature* 448, 802 (2007)
24. Wilke, S. D. & Eurich, C. W. On the functional role of noise correlations in the nervous system. *Neurocomputing* 44–46, 1023–1028 (2002)
25. Schneidman, E., Berry, M. J. II, Segev, R. & Bialek, W. Weak pairwise correlations imply strongly correlated network states in a neural population. *Nature* 440, 1007–1012 (2006).
26. Averbeck, B. B. & Lee, D. Coding and transmission of information by neural ensembles. *Trends Neurosci.* 27, 225–230 (2004)
27. Dragoi, V. & Sur, M. Image structure at the center of gaze during free viewing. *J. Cogn. Neurosci.* 18, 737–748 (2006)
28. Salinas, E. & Sejnowski, T. J. Impact of correlated synaptic input on output firing rate and variability in simple neuronal models. *J. Neurosci.* 20, 6193–6209 (2000)
29. Roelfsema, P. R., Lamme, V. A. & Spekreijse, H. Synchrony and covariation of firing rates in the primary visual cortex during contour grouping. *Nature Neurosci.* 7, 982–991 (2004).
30. van der Togt, C., Kalitzin, S., Spekreijse, H., Lamme, V. A. & Super, H. Synchrony dynamics in monkey V1 predict success in visual detection. *Cereb. Cortex* 16, 136–148 (2006).


**Supplementary Information** is linked to the online version of the paper at www.nature.com/nature.

**Acknowledgements** We thank K. Josić for comments on the manuscript. This work was supported by the Pew Scholars Program, the James S. McDonnell Foundation and the National Eye Institute (V.D.)

**Author Information** Reprints and permissions information is available at www.nature.com/reprints. Correspondence and requests for materials should be addressed to V.D. (v.dragoi@uth.tmc.edu).

LETTERS

# A skin microRNA promotes differentiation by repressing 'stemness'

Rui Yi[1,2], Matthew N. Poy[3], Markus Stoffel[3] & Elaine Fuchs[1,2]

**In stratified epithelial tissues, homeostasis relies on the self-renewing capacity of stem cells located within the innermost basal layer[1]. As basal cells become suprabasal, they lose proliferative potential and embark on a terminal differentiation programme[2,3]. Here, we show that microRNA-203 is induced in the skin concomitantly with stratification and differentiation. By altering miR-203's spatiotemporal expression *in vivo*, we show that miR-203 promotes epidermal differentiation by restricting proliferative potential and inducing cell-cycle exit. We identify *p63* as one of the conserved targets of miR-203 across vertebrates. Notably, p63 is an essential regulator of stem-cell maintenance in stratified epithelial tissues[4–9]. We show that miR-203 directly represses the expression of *p63*: it fails to switch off suprabasally when either Dicer1 or miR-203 is absent and it becomes repressed basally when miR-203 is prematurely expressed. Our findings suggest that miR-203 defines a molecular boundary between proliferative basal progenitors and terminally differentiating suprabasal cells, ensuring proper identity of neighbouring layers.**

MicroRNAs are small, non-coding RNAs that regulate gene expression post-transcriptionally by directly targeting RNA-induced silencing complex (RISC) to cognate messenger RNA targets[10]. When miRNAs are globally ablated in skin epithelium by conditionally targeting the gene that encodes the miRNA-processing enzyme Dicer1, hair follicles fail to invaginate. This distorts epidermal morphology, compromising the barrier and underscoring the functional importance of these small RNAs in skin development[11,12]. To gain further insight into the possible significance of different skin miRNAs, we constructed epidermal miRNA libraries using total RNAs isolated from pure epidermis starting from embryonic day 13.5 (E13.5), when it is still a single-layered epithelium, to postnatal day 4.5 (P4.5), when it is fully stratified. Among more than 100 epidermal miRNAs cloned, miR-203 barely surfaced in the pool of E13.5 clones but emerged as one of the most abundant epidermal miRNAs from E15.5 onwards (Fig. 1a).

The significant upregulation of miR-203 between E13.5 and E15.5 was suggestive that this miRNA may be absent in multipotent progenitors of single-layered epidermis, but is induced upon stratification and differentiation. By *in situ* hybridization[13], miR-203 was largely confined to suprabasal cells of epithelial tissues, and was especially prominent in skin (Fig. 1b, d, e and Supplementary Fig. 1). The specificity of hybridization was confirmed by analysing conditionally ablated *Dicer1* skin, in which expression of miR-203 and other mature miRNAs was abolished[11] (Supplementary Fig. 1a). Quantification of its differential expression by quantitative PCR with reverse transcription (qRT–PCR) revealed ~25-fold more miR-203 in E15.5 suprabasal cells than in their basal counterparts (Fig. 1c). Similarly, miR-203 was rapidly upregulated when primary mouse keratinocytes were induced by calcium to differentiate *in vitro* (Supplementary Fig. 1b).

Epidermal development precedes that of its appendages. However, at early stages of hair follicle development, miR-203 was not detected. By E17.5, faint miR-203 hybridization was detected within the

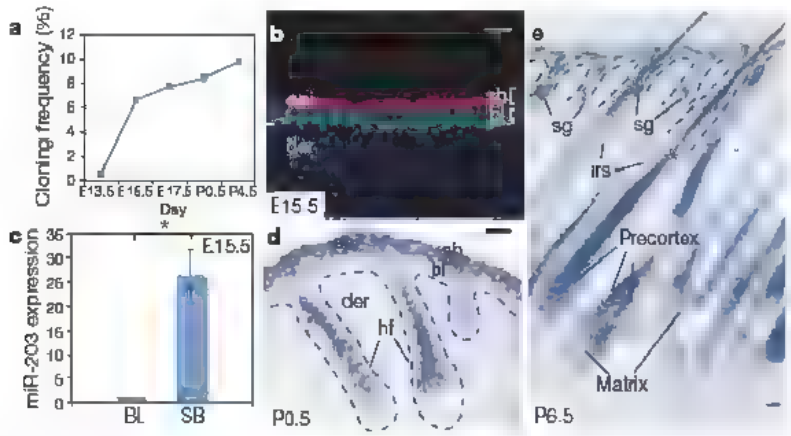


**Figure 1 | Spatiotemporal expression of miR-203 during skin development.** **a**, Temporal induction of miR-203 as measured by cloning frequency. **b**, **d**, **e**, *In situ* hybridization reveals restriction of miR-203 to suprabasal, differentiating layers of skin. sb, suprabasal; bl, basal layer; epi, epidermis; der, dermis; sg, sebaceous gland; irs, inner root sheath; hf, hair follicle. Asterisks in **e** represent brown melanin pigment that is not a hybridization signal. In **b**, anti-β4-integrin co-labelling is in green and miR-203 *in situ* pseudocoloured signal is in red. **c**, qRT–PCR of FACS-purified cells from E15.5 epidermis reveals 25-fold more miR-203 in suprabasal (SB) versus basal layer (BL) cells (*$P < 0.002$). Error bars (s.d.) are derived from three experiments with basal layer level set as 1. Scale bars are 30 μm.

[1]Howard Hughes Medical Institute, and [2]Laboratory of Mammalian Cell Biology and Development, The Rockefeller University, New York City, New York 10065, USA. [3]Swiss Federal Institute of Technology ETH Zurich, Institute of Molecular Systems Biology, CH-8093 Zürich, Switzerland.

emerging suprabasal cells of developing hair follicles and expression was also seen in stratified layers of developing tongue epithelia (Supplementary Fig. 1f, g). As development advanced, miR-203 expression intensified in differentiating cells of epidermis, hair follicles and sebaceous glands (Fig. 1d, e). Present throughout transcriptionally active, terminally differentiating cells of skin epithelium, miR-203 was conspicuously absent in its proliferating progenitor compartments. Interestingly, miR-203's sequence and expression pattern seemed to be conserved among vertebrates, in which the epidermis is stratified, but not in eukaryotes that have a single-layered epidermis (Supplementary Fig. 2a, b)

If miR-203 functions in the switch between proliferative and terminally differentiating compartments in vertebrate skin, it may be expected to repress its basal targets once basal cells become suprabasal and enter the terminal differentiation programme. To test this hypothesis, we generated transgenic mice expressing miR-203 under the control of the *keratin 14 (K14)* promoter, active by E15 in basal progenitors of stratified epithelia[14]. Most *K14-miR-203* mice died shortly after birth owing to apparent dehydration and/or malnutrition. By E18.5, the level of transgenic basal miR-203 was comparable to endogenous suprabasal miR-203 (Fig. 2a). Moreover, transgenic miR-203 expression did not interfere with endogenous miRNA processing[15] (Supplementary Fig. 3).

At E18.5, *K14-miR-203* back skin epidermis was noticeably thinner than that of its wild-type littermates (Supplementary Fig. 4a). By the time of birth (P0), transgenic epidermis consisted of a layer of flattened basal cells and one layer of suprabasal cells (Fig. 2b). Hence, a thin epidermis can reflect either defective differentiation, as in mice conditionally targeted by *K14-Cre* for Notch effector protein RBPJ[16], or impaired stem cells, as in *p63* null epidermis[4,6,9]. To distinguish between these possibilities, we first examined keratin 10, an early differentiation marker downstream of canonical Notch signalling[16]. At E18.5, many keratin-10-positive cells within *K14-miR-203* epidermis were aberrantly juxtaposed to the basement membrane (Fig. 2c). As development progressed, basal progenitor/stem cells marked by keratin 5 were missing over increasingly larger epidermal stretches that were replaced by flat cells expressing keratin 10 (Fig. 2d). No discernible apoptotic cells were detected as judged by TdT-mediated dUTP nick end labelling (TUNEL) assay and active caspase-3 (data not shown).

The depletion of basal stem cells in *K14-miR-203* epidermis bore a resemblance to *p63* null epidermis[6,9]. Interestingly, anti-p63 immunolocalization revealed only sporadic, weak expression in E18.5 *K14-miR-203* basal cells (Fig. 2e). Quantification of 5-bromodeoxyuridine (BrdU)-positive cells after a 2-h pulse-labelling revealed a significant reduction in the proliferative pool of E18.5 transgenic progenitors (Fig. 2f).

To address whether miR-203 restricts the proliferative potential of epidermal stem cells, we compared the clonogenic capacity of primary mouse keratinocytes cultured from E18.5 transgenic with wild-type littermates. As expected, wild-type keratinocytes formed typical holoclones composed of small, undifferentiated cells capable of long-term passage[17,18]. By contrast, transgenic keratinocytes produced mostly paraclones, composed of large, flattened cells[17,18] (Supplementary Fig. 4b). Moreover, approximately fourfold fewer, and significantly smaller, colonies formed from transgenic compared with wild-type keratinocytes (Fig. 2g and Supplementary Fig. 4c). On passage, only wild-type clones gave rise to colonies. Consistent with a requirement for p63 in maintaining proliferative potential of epidermal stem cells[9], p63 was markedly diminished in transgenic keratinocytes

To test whether these dramatic effects of transgene expression are specific to miR-203, we transduced primary mouse keratinocytes with retroviral vectors expressing either miR-203 or miR-203M, a miR-203 mutant harbouring mutations within the 5′ seed (Supplementary Fig. 4d), or empty vector alone. Only miR-203 impaired keratinocyte proliferation and colony formation (Fig. 2h and Supplementary Fig. 4e).

To identify early consequences of losing miR-203 expression, we first examined p63 and cell-cycle status in E18.5 *Dicer1* null epidermis. In contrast to the wild type[3,5,9], *Dicer1* null epidermis showed frequent p63-positive, BrdU-positive and phospho-histone-H3-positive mitotic suprabasal cells (Supplementary Fig. 5a–c). Fluorescence-activated cell sorting (FACS) quantification revealed an approximately threefold increase in the number of G2/M phase suprabasal cells (Supplementary Fig. 5d).

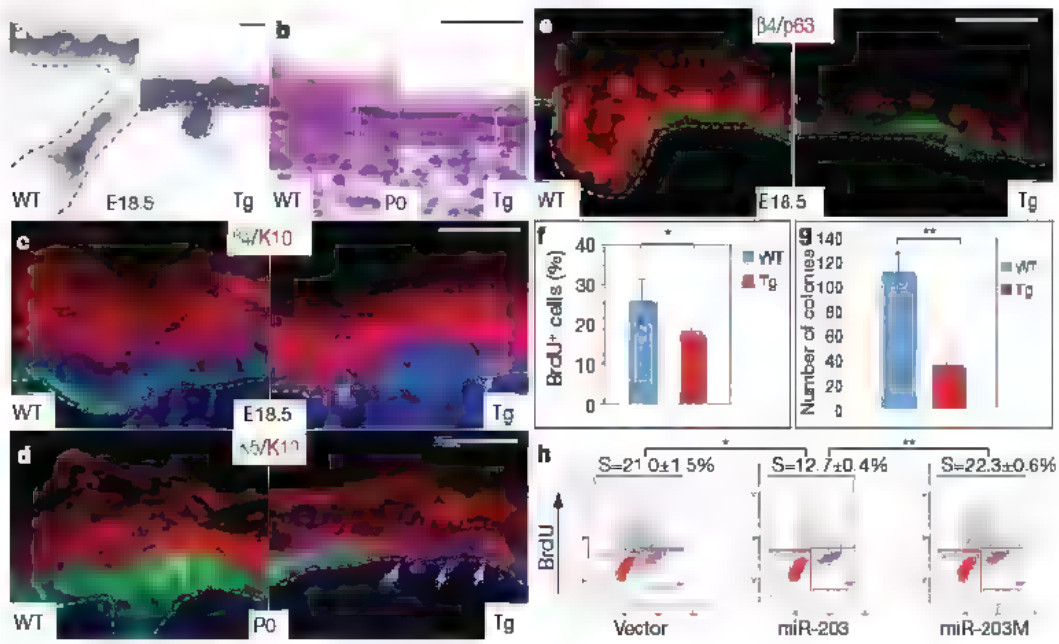


**Figure 2 | Premature activation of miR-203 in epidermis restricts its proliferative potential. a**, *In situ* hybridization detects precociously expressed miR-203 in basal epidermis and hair germs of *K14-miR-203* Tg skin. WT, wild type. **b**, By P0, Tg epidermis is thinner than the wild type. **c–f**, Signs of basal cell depletion in Tg skin. Arrows denote keratin-10 (K10)-positive, keratin-5 (K5)-negative, β4-integrin-low cells aberrantly juxtaposed to basement membrane. Note marked reduction of p63 in **e**. In **f**, quantifications reflect $^{*}P < 0.003$, $n = 8$. **g**, Marked reduction in Tg versus wild-type colony-forming efficiency *in vitro* ($^{**}P < 0.0001$, $n = 3$) In **f** and **g**, error bars (s.d.) are derived from eight or three experiments as indicated. **h**, Transduction of primary mouse keratinocytes with miR-203, but not empty vector or mutant miR-203M, results in a marked decline in S-phase cells that incorporate BrdU ($^{*}P < 0.001$, $^{**}P < 0.0001$) Values represent mean ± s.d. from three experiments. Scale bars are 30 μm.

To test specifically whether miR-203 represses proliferative potential of suprabasal cells *in vivo*, we adapted the antagomir method[19] to repress miR-203 expression in dorsal skin of neonatal mice, in which basal-layer proliferation is still high. We first used a dye-conjugated antagomir to document efficient incorporation in epidermis within 24 h following a single subcutaneous injection (Supplementary Fig. 6a). One day after three dorsal injections, antagomir-203, but not mm-antagomir-203 (a 4-nucleotide mismatched control) or PBS markedly and specifically repressed miR-203 expression in surrounding skin (Fig. 3a and Supplementary Fig. 6b, c).

Similar to E18.5 *Dicer1* null skin, antagomir-treated P4 epidermis showed atypical expansion of p63 expression and BrdU-positive suprabasal cells (Fig. 3b, c). This was further substantiated by the presence of suprabasal cells positive for p63 and the mitotic marker phospho-histone H3 (Fig. 3d). Finally, quantification of epidermal cells harvested 4 h after BrdU injections revealed that proliferative cells were more numerous in antagomir-203-treated dorsal epidermis than either PBS- or mm-antagomir-203-treated skin (Fig. 3e).

Because these abnormalities occurred early after miR-203 repression, it was unlikely that they arose secondarily from physical perturbations to the skin or mouse. Moreover, the alterations were recapitulated *in vitro* with an antisense oligonucleotide[20] that specifically blocked calcium-induced expression of endogenous miR-203 (Supplementary Fig. 6d). BrdU labelling and FACS analysis revealed that anti-miR-203 *in vitro* partially blocked the ability of keratinocytes to exit the cell cycle during calcium-induced differentiation (Fig. 3f).

Having established early consequences of inhibiting miR-203 expression, we examined longer-term effects *in vivo*. Although tail-vein injections of antagomirs afford efficient delivery for some adult tissues[19], it was only partially effective in targeting miR-203 knockdown to skin (Supplementary Fig. 7). Similarly, sustained subcutaneous antagomir injections were not effective once skin matured. To ablate miR-203 efficiently in adult skin, we engineered *K14-Cre*$^{Tm}$/*Dicer1* inducible conditional knockout (iKO) mice and examined long-term consequences of conditionally inducing *Dicer1* ablation. By 30 days, the epidermis had thickened markedly and suprabasal cells were more numerous (Fig. 3g). Atypical p63-positive suprabasal cells were now prevalent in iKO epidermis (Fig. 3h). These results suggested that miR-203 may be required to effectively repress suprabasal p63 and in turn restrict cell proliferation in differentiating epidermis. Importantly, by targeting *Dicer1* after follicles had matured and anchored within the dermis, we could attribute these defects specifically to alterations originating in the epidermis rather than secondarily arising from perturbed hair follicle morphogenesis.

Whereas miR-203 markedly impaired proliferative potential, it had minimal effects on the induction of terminal differentiation markers whether *in vivo* (Fig. 2c, d) or *in vitro* (Supplementary Fig. 8). Thus, of the two key features involved in terminal differentiation, suprabasal miR-203 seemed to act predominantly by restricting proliferative potential of progenitors as they transitioned from basal to suprabasal layers. Although loss of miR-203 resulted in increased suprabasal proliferation, neither *p63* overexpression nor miR-203 reduction are associated with psoriasis[21,22], suggesting that neither p63 nor the miRNA are obligatory features of the hyperproliferative state.

Bioinformatics suggest that miRNAs and their predicted targets tend to be mutually exclusive in neighbouring tissues[23,24]. On the basis of the inverse correlation that we observed between miR-203 and p63 in expression and function, *p63* mRNA surfaced as a possible miR-203 target. Consistent with *in vivo* results (Fig. 2e), p63 was markedly diminished in *K14-miR-203* transgenic primary mouse keratinocytes that were cultured in low calcium (Fig. 4a). Conversely, knocking down endogenous miR-203 in calcium-treated wild-type primary mouse keratinocyte cultures strongly impaired the rapid down-regulation of p63 protein upon terminal differentiation (Fig. 4b), even though *p63* mRNA levels remained appreciable (Supplementary Fig. 9). Conversely, transduction of miR-203 in wild-type primary mouse keratinocytes cultured in low calcium strongly inhibited p63 protein expression (Fig. 4b), while only slightly decreasing *p63* mRNA (Fig. 4b right-hand graph). Thus, miR-203 seemed to regulate p63 primarily through translational repression.

To further define the parallels, we examined the status of p21, a well-established p63 target that functions to restrict proliferative

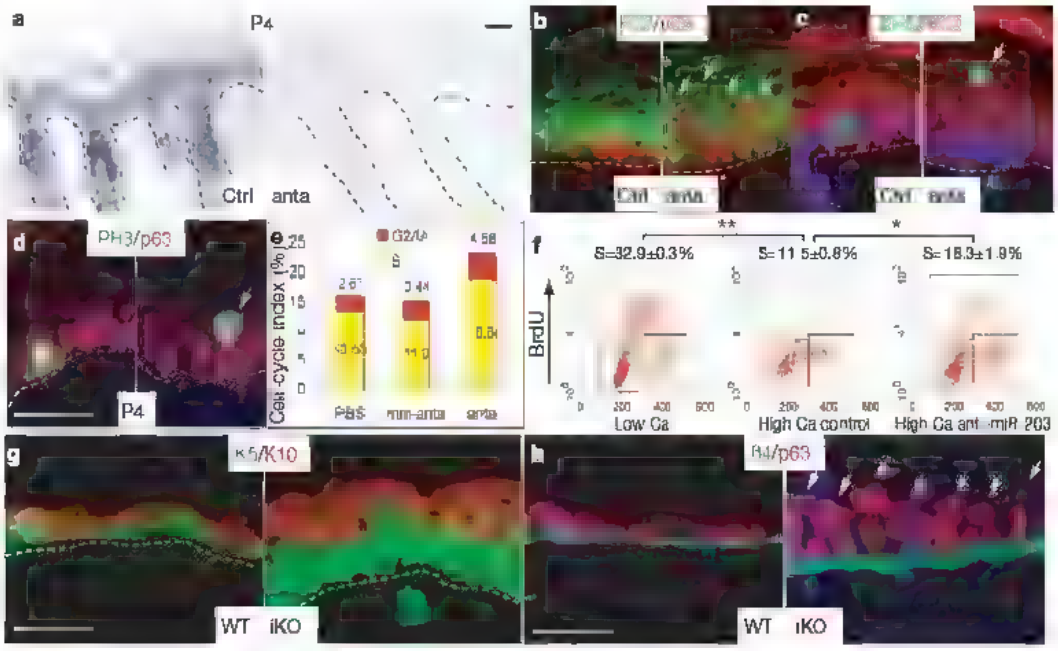


**Figure 3 | Inhibition of miR-203 results in increased epidermal proliferation.** **a–d**, P4 skins analysed after treatment of mice with mm-antagomir-203 (Ctrl) or antagomir-203 (anta). **a**, miR-203 *in situ* hybridizations. **b–d**, Immunofluorescence microscopy. Arrows denote basal-like features in suprabasal cells of antagomir-203-treated epidermis PH3, phospho-histone H3. **e**, Elevated epidermal proliferation determined by BrdU injections at 4-h intervals and FACS quantification. **f**, The reduction in cycling cells that typically occurs upon calcium-induced differentiation of primary mouse keratinocytes *in vitro* is partially abrogated by anti-miR-203 oligonucleotides. Values represent mean ± s.d. from three experiments (*$P < 0.005$, **$P < 0.0001$). **g**, **h**, Epidermal defects that arise 30 days after tamoxifen-induced *Dicer1* ablation (iKO). Arrows denote suprabasal p63. Scale bars are 30 μm

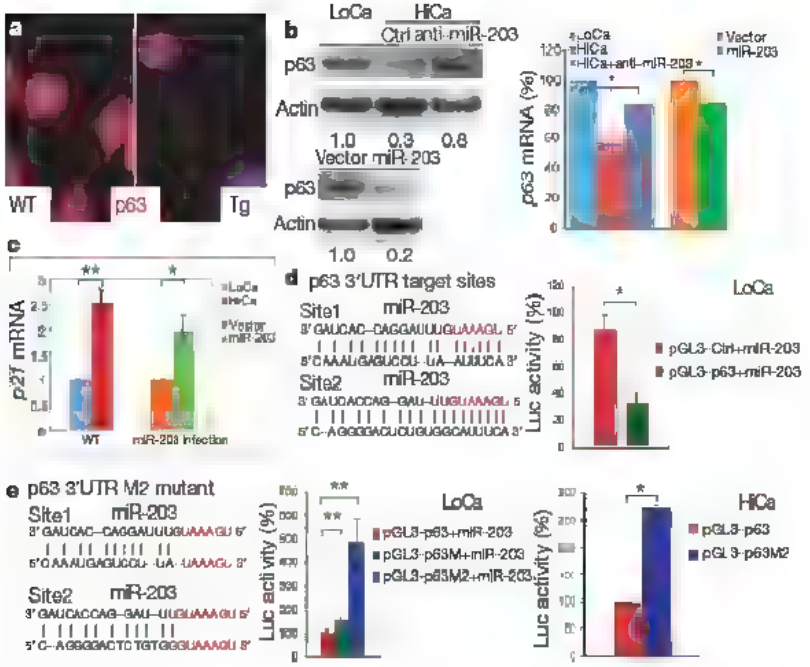


**Figure 4 | MiR-203 targets *p63* mRNA at 3′UTR. a**, p63 protein is markedly diminished in Tg versus wild-type primary mouse keratinocytes **b**, Immunoblot and qRT–PCR quantification of p63 expression. Top panel, calcium-induced (HiCa) p63 downregulation is largely relieved by anti-miR-203 oligonucleotides. Bottom panel, miR-203 transduction is sufficient to repress p63 protein expression in low calcium (LoCa). Right-hand graph, anti-miR-203 treatment slightly recovers *p63* mRNA whereas miR-203 transduction marginally reduces *p63* mRNA ($*P < 0.01$, $n = 3$). **c**, miR-203 transduction in LoCa primary mouse keratinocytes elevates *p21* mRNA level ($**P < 0.005$, $*P < 0.002$, $n = 3$) **d**, Insertion of two miR-203 target sequences within mouse *p63* 3′UTR leads to diminished luciferase (Luc) reporter activity in the presence of miR-203 ($*P < 0.002$, $n = 3$). pGL3 is a luciferase-expressing plasmid from Promega. **e**, Mutation of both target sites (p63M2) abolishes miR-203-mediated repression of luciferase activity; a single-site mutation (p63M) has marginal effects ($**P < 0.0001$, $n = 6$). In HiCa, wild-type but not mutant *p63* 3′UTR represses luciferase activity ($*P < 0.002$, $n = 3$). For all graphs, error bars (s.d.) are derived from the number of experiments as indicated.

potential of basal epidermal cells[25] and is normally repressed in proliferative keratinocytes[26–28]. Upon miR-203 transduction, however, p21 was upregulated in undifferentiated wild-type primary mouse keratinocytes to an extent that was nearly comparable to its levels in differentiated primary mouse keratinocytes (Fig. 4c). This finding extends the correlation between miR-203 and p63 to p63's downstream targets, and provides mechanistic insight into how miR-203 may inhibit proliferative potential of epidermal stem cells.

DeltaNp63α is the main isoform expressed in epidermis. Within the 3′UTR of Δ*Np63α* mRNA, a hexamer and heptamer match perfectly to miR-203's 5′ seed sequence (Fig. 4d). When introduced into the 3′UTR of a luciferase reporter gene, a 599-base-pair mouse Δ*Np63α* 3′UTR fragment encompassing these two putative target sites caused a threefold reduction in activity in *K14-miR-203*-expressing keratinocytes cultured in low calcium (Fig. 4d). Mutations within these two sites together abolished miR-203-mediated repression under the same conditions (Fig. 4e, LoCa). When these assays were performed in high-calcium primary mouse keratinocytes in which endogenous miR-203 was induced (Supplementary Fig. 1b), exogenous miR-203 was not needed to elicit the wild-type *p63* 3′UTR-specific reduction in luciferase activity (Fig. 4e, HiCa). Together, these results indicate that miR-203's effect on p63 is direct and is mediated through these 3′UTR target sites.

MiR-203 and its suprabasal expression seem to have emerged in vertebrate evolution concomitant with a stratified epidermis. Similarly, the basal expression and function of p63 in stratified epithelia also seems to be conserved[4–7,9]. Interestingly, the putative miR-203 recognition sequence exists four times in the *p63* 3′UTR of zebrafish and twice in mouse and human. Moreover, when similarly tested, the *p63* 3′UTR fragments flanking the hexamer motifs from either zebrafish or human reduced luciferase reporter activity comparably to that from mouse (Supplementary Fig. 10). These data suggest that this mechanism for regulating *p63* by miR-203 may be conserved across vertebrates.

Strictly on the basis of bioinformatic studies, the mRNA encoding a zinc-finger protein, Zfp281, is the top candidate of miR-203 targets, as it harbours four perfectly conserved miR-203 consensus sites in its 3′UTR[29] (Supplementary Fig. 11a). Similarly to p63, Zfp281 is also enriched in basal epidermal stem cells (Supplementary Fig. 11b). In both *K14-miR-203* transgenic mice and miR-203-transduced primary mouse keratinocytes, *Zfp281* mRNA was markedly reduced (Supplementary Fig. 11c). Using a luciferase reporter assay, we showed that the *Zfp281* 3′UTR, but not the mutant form with mutations at four target sites, was specifically regulated by co-transfected and endogenous miR-203 (Supplementary Fig. 11a). Intriguingly, even though Zfp281 has not been previously studied in skin development, it has been implicated in maintaining the proliferative potential of embryonic stem cells[30], and in this regard its function resembles that ascribed to p63 in keratinocytes.

Taken together, our studies provide evidence that miR-203 acts at least in part by targeting and negatively regulating suprabasal expression of basal genes, thereby acting as a switch between proliferation and differentiation. Although the mechanisms underlying this balance are complex and likely to be dominated by transcriptional controls, the mutually exclusive expression patterns, opposite functions and evolutionarily conserved regulation offer strong support for the intimate relation between miR-203 and its targets in refining the boundary between these two stages in epidermis.

## METHODS SUMMARY

**Antagomir synthesis and injection.** Antagomir-203 and mm-antagomir-203 were designed and synthesized (Dharmacon) as described[19]. The antagomir-203 sequence was 5′-UpsCps UAGUGGUCCUAAACAUUpsUpsCpsAps-Chol-3′ and mm-antagomir-203 was 5′-UpsCpsUcGUGuUCaUAAACAcUpsUpsCpsAps-Chol-3′. Lower-case letters indicate the mismatched nucleotide. Subcutaneous injection was performed on newborn CD-1 mice at a dosage of 80 mg kg$^{-1}$, according to an established protocol approved by LARC animal facility at the Rockefeller University. Tail-vein injections were performed as described[19]. After three initial injections, a booster injection was performed every 4 days. Total treatment was 15 days.

**Full Methods** and any associated references are available in the online version of the paper at www.nature.com/nature.

**Received 9 August 2007; accepted 8 January 2008.**
**Published online 2 March 2008.**

1. Fuchs, E. Scratching the surface of skin development. *Nature* 445, 834–842 (2007)
2. Lechler, T. & Fuchs, E. Asymmetric cell divisions promote stratification and differentiation of mammalian skin. *Nature* 437, 275–280 (2005).
3. Clayton, E. *et al.* A single type of progenitor cell maintains normal epidermis. *Nature* 446, 185–189 (2007).
4. Mills, A. A. *et al.* p63 is a p53 homologue required for limb and epidermal morphogenesis. *Nature* 398, 708–713 (1999)
5. Parsa, R., Yang, A., McKeon, F. & Green, H. Association of p63 with proliferative potential in normal and neoplastic human keratinocytes. *J. Invest. Dermatol.* 113, 1099–1105 (1999)
6. Yang, A. *et al.* p63 is essential for regenerative proliferation in limb, craniofacial and epithelial development. *Nature* 398, 714–718 (1999)
7. Lee, H. & Kimelman, D. A dominant-negative form of p63 is required for epidermal proliferation in zebrafish. *Dev. Cell* 2, 607–616 (2002).
8. Truong, A. B., Kretz, M., Ridky, T. W., Kimmel, R. & Khavari, P. A. p63 regulates proliferation and differentiation of developmentally mature keratinocytes. *Genes Dev.* 20, 3185–3197 (2006).
9. Senoo, M., Pinto, F., Crum, C. P. & McKeon, F. p63 is essential for the proliferative potential of stem cells in stratified epithelia. *Cell* 129, 523–536 (2007)
10. Bartel, D. P. MicroRNAs: genomics, biogenesis, mechanism, and function. *Cell* 116, 281–297 (2004)
11. Yi, R. *et al.* Morphogenesis in skin is governed by discrete sets of differentially expressed microRNAs. *Nature Genet.* 38, 356–362 (2006)
12. Andl, T. *et al.* The miRNA-processing enzyme dicer is essential for the morphogenesis and maintenance of hair follicles. *Curr. Biol.* 16, 1041–1049 (2006)
13. Wienholds, E. *et al.* MicroRNA expression in zebrafish embryonic development. *Science* 309, 310–311 (2005).
14. Vasioukhin, V., Degenstein, L., Wise, B. & Fuchs, E. The magical touch: genome targeting in epidermal stem cells induced by tamoxifen application to mouse skin. *Proc. Natl Acad. Sci. USA* 96, 8551–8556 (1999)
15. Grimm, D. *et al.* Fatality in mice due to oversaturation of cellular microRNA/short hairpin RNA pathways. *Nature* 441, 537–541 (2006).
16. Blanpain, C., Lowry, W. E., Pasolli, H. A. & Fuchs, E. Canonical notch signaling functions as a commitment switch in the epidermal lineage. *Genes Dev.* 20, 3022–3035 (2006)
17. Barrandon, Y. & Green, H. Three clonal types of keratinocyte with different capacities for multiplication. *Proc. Natl Acad. Sci. USA* 84, 2302–2306 (1987)
18. Blanpain, C., Lowry, W. E., Geoghegan, A., Polak, L. & Fuchs, E. Self-renewal, multipotency, and the existence of two cell populations within an epithelial stem cell niche. *Cell* 118, 635–648 (2004)
19. Krutzfeldt, J. *et al.* Silencing of microRNAs *in vivo* with 'antagomirs'. *Nature* 438, 685–689 (2005)
20. Davis, S., Lollo, B., Freier, S. & Esau, C. Improved targeting of miRNA with antisense oligonucleotides. *Nucleic Acids Res.* 34, 2294–2304 (2006).
21. Haider, A. S. *et al.* Genomic analysis defines a cancer-specific gene expression signature for human squamous cell carcinoma and distinguishes malignant hyperproliferation from benign hyperplasia. *J. Invest. Dermatol.* 126, 869–881 (2006).
22. Sonkoly, E. *et al.* MicroRNAs: novel regulators involved in the pathogenesis of psoriasis? *PLoS ONE* 2, e610 (2007).
23. Farh, K. K. *et al.* The widespread impact of mammalian MicroRNAs on mRNA repression and evolution. *Science* 310, 1817–1821 (2005)
24. Stark, A., Brennecke, J., Bushati, N., Russell, R. B. & Cohen, S. M. Animal MicroRNAs confer robustness to gene expression and have a significant impact on 3′UTR evolution. *Cell* 123, 1133–1146 (2005).
25. Topley, G. I., Okuyama, R., Gonzales, J. G., Conti, C. & Dotto, G. P. p21(WAF1/Cip1) functions as a suppressor of malignant skin tumor formation and a determinant of keratinocyte stem-cell potential. *Proc. Natl Acad. Sci. USA* 96, 9089–9094 (1999)
26. Okuyama, R. *et al.* p53 homologue, p51/p63, maintains the immaturity of keratinocyte stem cells by inhibiting Notch1 activity. *Oncogene* 26, 4478–4488 (2007)
27. Nguyen, B. C. *et al.* Cross-regulation between Notch and p63 in keratinocyte commitment to differentiation. *Genes Dev.* 20, 1028–1042 (2006).
28. Westfall, M. D., Mays, D. J., Sniezek, J. C. & Pietenpol, J. A. The Delta Np63 alpha phosphoprotein binds the p21 and 14-3-3 sigma promoters *in vivo* and has transcriptional repressor activity that is reduced by Hay-Wells syndrome-derived mutations. *Mol. Cell. Biol.* 23, 2264–2276 (2003).
29. Grimson, A. *et al.* MicroRNA targeting specificity in mammals: determinants beyond seed pairing. *Mol. Cell* 27, 91–105 (2007)
30. Wang, J. *et al.* A protein interaction network for pluripotency of embryonic stem cells. *Nature* 444, 364–368 (2006).

**Supplementary Information** is linked to the online version of the paper at www.nature.com/nature.

**Acknowledgements** We thank D. O'Carroll and A. Tarakhovsky for *Dicer1*$^{fl/fl}$ mice; A. Schaefer and P. Greengard for dye-conjugated antagomir-124; Z. Zhang and F. Dietrich for miRNA library sequencing; B. Liu for bioinformatics assistance; A. Giraldez for zebrafish cDNA; N. Stokes and L. Polak for assistance with animals; S. Maze and X. Fan for assistance in the flow cytometry core facility; J. Racelis for assistance with *in situ* hybridization; and D. Wang and E. Fuchs laboratory members for discussions. R.Y. is supported by the Pathway to Independence Award from the NIH. M.N.P. is supported by the Ruth L. Kirschstein NRSA Fellowship from the NIH. E.F. is an investigator of the Howard Hughes Medical Institute. This work was supported by the HHMI and the NIH.

**Author Contributions** R.Y. and E.F. designed the research. R.Y. performed the experiments. M.N.P. and M.S. designed and contributed to the antagomir experiments. R.Y. and E.F. analysed the data and wrote the paper.

**Author Information** Reprints and permissions information is available at www.nature.com/reprints. The authors declare competing financial interests: details accompany the full-text HTML version of the paper at www.nature.com/nature. Correspondence and requests for materials should be addressed to E.F. (fuchslb@rockefeller.edu).

LETTERS

# The M2 splice isoform of pyruvate kinase is important for cancer metabolism and tumour growth

Heather R. Christofk[1], Matthew G. Vander Heiden[1,2], Marian H. Harris[3], Arvind Ramanathan[4], Robert E. Gerszten[4,5,6], Ru Wei[4], Mark D. Fleming[3], Stuart L. Schreiber[4,7] & Lewis C. Cantley[1,8]

**Many tumour cells have elevated rates of glucose uptake but reduced rates of oxidative phosphorylation. This persistence of high lactate production by tumours in the presence of oxygen, known as aerobic glycolysis, was first noted by Otto Warburg more than 75 yr ago[1]. How tumour cells establish this altered metabolic phenotype and whether it is essential for tumorigenesis is as yet unknown. Here we show that a single switch in a splice isoform of the glycolytic enzyme pyruvate kinase is necessary for the shift in cellular metabolism to aerobic glycolysis and that this promotes tumorigenesis. Tumour cells have been shown to express exclusively the embryonic M2 isoform of pyruvate kinase[2]. Here we use short hairpin RNA to knockdown pyruvate kinase M2 expression in human cancer cell lines and replace it with pyruvate kinase M1. Switching pyruvate kinase expression to the M1 (adult) isoform leads to reversal of the Warburg effect, as judged by reduced lactate production and increased oxygen consumption, and this correlates with a reduced ability to form tumours in nude mouse xenografts. These results demonstrate that M2 expression is necessary for aerobic glycolysis and that this metabolic phenotype provides a selective growth advantage for tumour cells *in vivo*.**

Otto Warburg noted that tumour cells, unlike their normal counterparts, use aerobic glycolysis with reduced mitochondrial oxidative phosphorylation for glucose metabolism, and proposed that this was an early and essentially irreversible step that ultimately led to tumorigenesis[1]. A recent study showed that aerobic glycolysis and the enhanced production of lactate in tumour cells, despite long-held beliefs, is not usually due to mitochondrial defects in oxidative phosphorylation[3]. These findings are consistent with the idea that tumour cells preferentially use glucose for purposes other than oxidative phosphorylation, and that this metabolic switch may be required to support cell growth. Microarray studies have shown that glycolytic genes comprise one of the most upregulated gene sets in cancer[4,5]. Among those genes significantly upregulated in tumours is pyruvate kinase, which regulates the rate-limiting final step of glycolysis[4,5]. Four pyruvate kinase isoforms exist in mammals: the L and R isoforms are expressed in liver and red blood cells; the M1 isoform is expressed in most adult tissues, and the M2 isoform is a splice variant of M1 expressed during embryonic development[6]. Notably, it has been reported that tumour tissues exclusively express the embryonic M2 isoform of pyruvate kinase[2,7].

To confirm that tumour tissues switch pyruvate kinase expression from an adult isoform to the embryonic M2 isoform, antibodies that distinguish pyruvate kinase M1 from pyruvate kinase M2 (PKM1 and PKM2, respectively) were generated (Supplementary Fig. 1). Mammary gland tissues from MMTV-NeuNT mice, a breast cancer tumour model, were analysed before and after tumour development for pyruvate kinase isoform expression[2]. As shown in Fig. 1a, the primary pyruvate kinase isoform before tumour development is PKM1; however, the primary isoform from four independent tumours is PKM2. All cell lines examined, including multiple cancer lines derived from different tissues, also exclusively express the M2 isoform of pyruvate kinase (Fig. 1b). Immunohistochemistry of human colon cancer using the PKM1- and PKM2-specific antibodies shows selective expression of PKM1 in the stromal cells and PKM2 in the cancer cells (Fig. 1c).

Given that PKM2 is selectively expressed in proliferating cells, we assessed its importance for cell proliferation via short hairpin

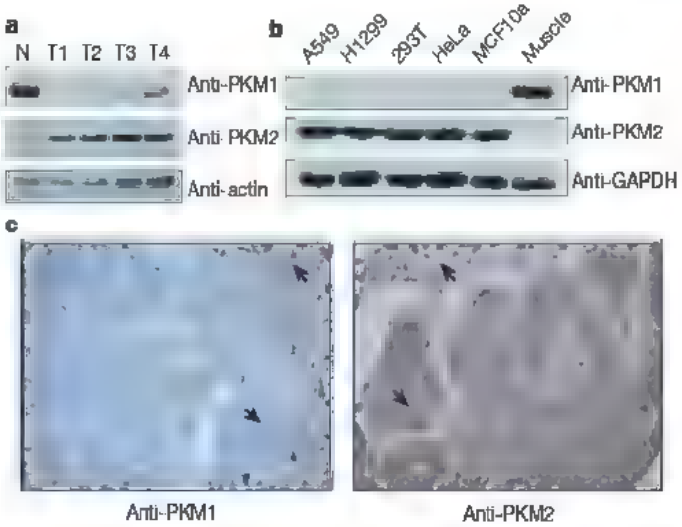


**Figure 1 | Tumour tissues and cell lines express the M2 isoform of pyruvate kinase. a,** Immunoblotting of mammary gland protein lysates from MMTV-NeuNT mice before (N) and after (T) tumour development. T1–T4 represent lysates from tumours that developed in four different mice. Proteins from total cell extracts were immunoblotted for PKM1, PKM2 and actin. **b,** Immunoblotting of protein lysates from cell lines. A549 and H1299 are lung carcinoma cell lines; 293T is a transformed embryonic kidney cell line; HeLa is a cervical carcinoma cell line; and MCF10a is an immortalized breast epithelial cell line. Mouse muscle lysate was included as a control for M1 antibody staining. Total cell extracts were probed with antibodies towards PKM1, PKM2 and GAPDH. **c,** Immunohistochemistry of human colorectal cancer with antibodies towards PKM1 and PKM2. Stromal cells (arrows pointing upward) stain positive for PKM1; cancer cells (arrows pointing downward) stain positive for PKM2. Images are shown at ×400 magnification.

[1]Department of Systems Biology, Harvard Medical School, Boston, Massachusetts 02115, USA. [2]Dana Farber Cancer Institute, Boston, Massachusetts 02115, USA. [3]Department of Pathology, Children's Hospital, Boston, Massachusetts 02115 USA. [4]Chemical Biology Program, Broad Institute of Harvard and MIT, Cambridge, Massachusetts 02142, USA. [5]Cardiology Division and Center for Immunology and Inflammatory Diseases, Massachusetts General Hospital, Boston, Massachusetts 02129, USA. [6]Donald W. Reynolds Cardiovascular Clinical Research Center on Atherosclerosis, Harvard Medical School, Boston, Massachusetts 02115 USA. [7]Department of Chemistry and Chemical Biology, Harvard University, Cambridge, Massachusetts 02138, USA. [8]Division of Signal Transduction, Beth Israel Deaconess Medical Center, Boston, Massachusetts 02115, USA.

(sh)RNA knockdown (Fig. 2a). Stable knockdown of *PKM2* in the human lung cancer cell line H1299 results in decreased rates of glucose metabolism and reduced cell proliferation (Fig. 2b, c). Glucose metabolism was monitored by following the conversion of 5-$^3$H-glucose to $^3H_2O$, which occurs at the enolase step immediately preceding pyruvate kinase. To address whether it is the M2 isoform that is specifically critical for cell proliferation, we made stable cell lines expressing Flag-tagged mouse PKM1 (mM1) or PKM2 (mM2) and then induced stable knockdown of endogenous *PKM2* using shRNA expression (Fig. 2a). Both mM1 and mM2 were able to rescue the glucose metabolism and proliferation defects of the knockdown cells when grown in the artificially high glucose and oxygen conditions of cell culture (Fig. 2b, c). Similar results were obtained using A549 cells, and no changes in cell size were observed in either cell line (data not shown).

To examine whether PKM2 expression enhances tumour cell growth under lowered oxygen and glucose conditions, proliferation rates of the M1 and M2 rescue cells (M2 knockdown cells expressing mM1 or mM2) were measured in physiological glucose levels and hypoxic oxygen. Proliferation of neither the M1 nor the M2 cells was affected by growth in normal (5 mM) glucose (data not shown); however, proliferation of the M1 cells was significantly decreased compared to the M2 cells in 0.5% oxygen (Fig. 3a). The per cent decrease in oxygen consumption after addition of subsaturating amounts of oligomycin, a specific inhibitor of mitochondrial ATP synthase, was the same in both the M1 and M2 cells (data not shown). However, oligomycin treatment at the same dose affected the proliferation rate of the M1 cells significantly more than the M2 cells (Fig. 3a). These data suggest that the M1 cells are more dependent on oxidative phosphorylation for cell proliferation.

Consistent with published findings that PKM1 is a more active enzyme than PKM2, we found that the M1 rescue cells had 60% higher pyruvate kinase activity than the M2 rescue cells (Supplementary Fig. 2a). However, the adenine nucleotide levels in the M1 and M2 cells were comparable in normal culture conditions as well as

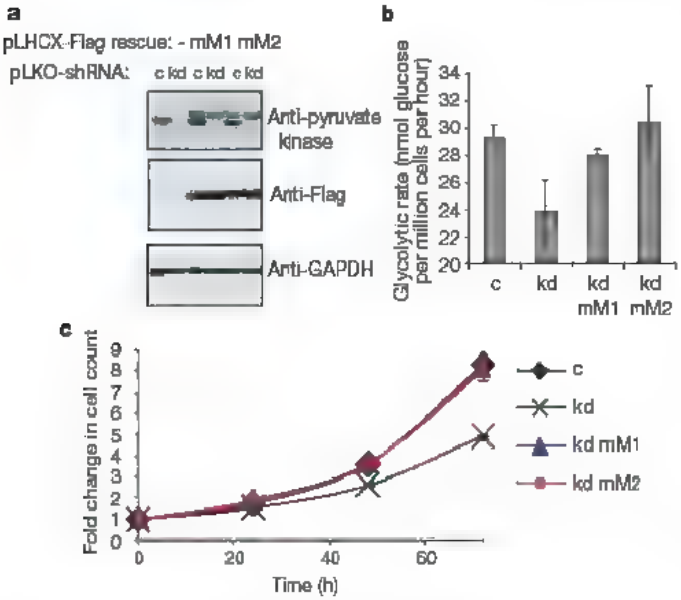


**Figure 2 | PKM2 knockdown is rescued by expression of PKM1 *in vitro*.** **a**, Immunoblotting of H1299 cells stably expressing shRNA constructs and rescue constructs. Cells were infected with retrovirus containing the empty vector, pLHCX, or pLHCX with Flag-tagged mouse M1 (mM1) or mouse M2 (mM2). After 2 weeks selection in hygromycin, the cells were infected with lentivirus containing the pLKO vector with control shRNA (c) or shRNA that knocks down PKM2 expression (kd). The cells were then selected in puromycin for 1 week. Total cell extracts were immunoblotted with antibodies for pyruvate kinase (recognizes both M1 and M2), Flag and GAPDH. **b**, **c**, c, cells with empty rescue vector and control shRNA; kd, cells with empty rescue vector and knockdown shRNA; kd mM1, cells with Flag–mM1 rescue and knockdown shRNA; kd mM2, cells with Flag–mM2 rescue and knockdown shRNA. **b**, Glycolytic rates of the knockdown and rescue cells. **c**, Proliferation curves of the knockdown and rescue cells. Error bars in **b** and **c** denote s.e.m. ($n = 3$).

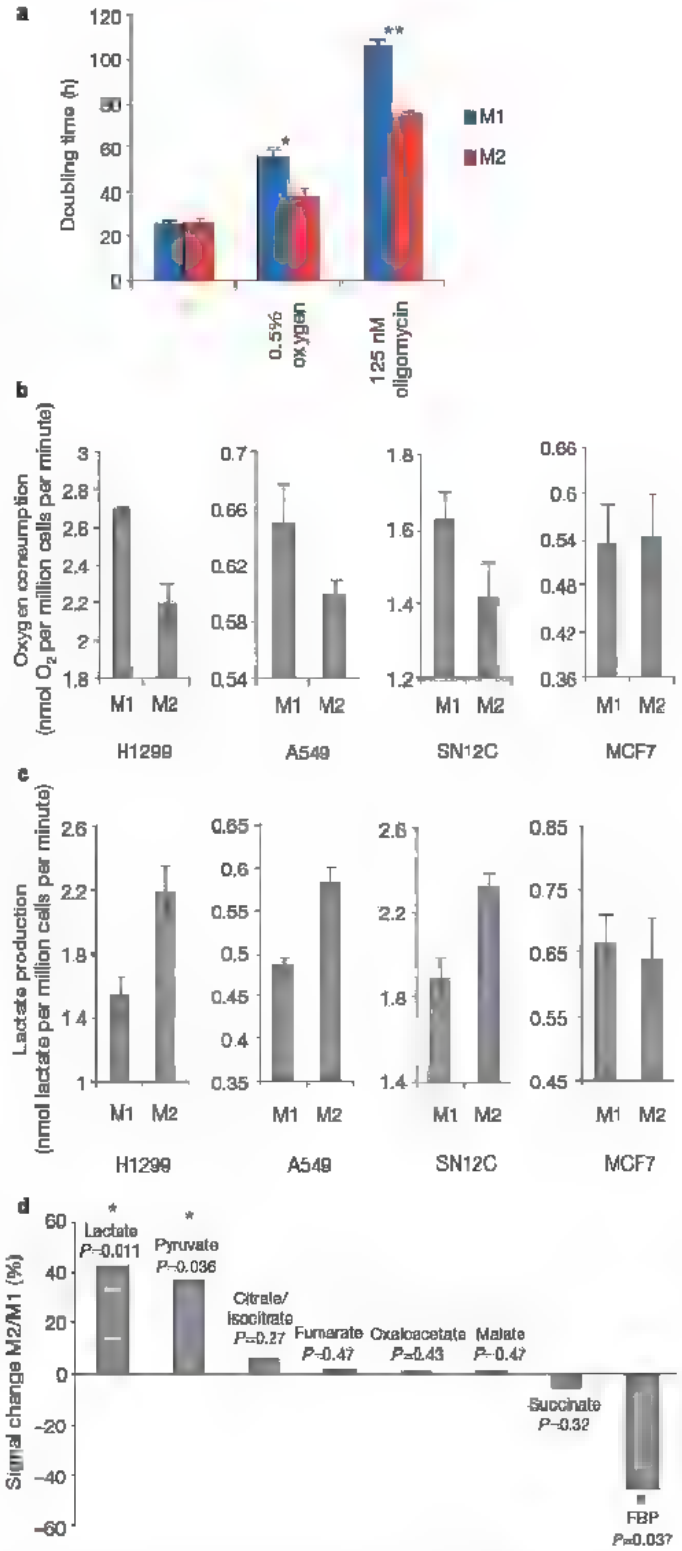


**Figure 3 | M1 expression results in increased oxidative phosphorylation.** **a**, Doubling times of the M1 and M2 H1299 rescue cells grown in normal oxygen conditions (–), 0.5% oxygen, and in the presence of 125 nM oligomycin. Asterisk, $P = 0.016941$, double asterisk, $P = 0.000048$. **b**, **c**, Data from four different cell lines (H1299, A549, SN12C and MCF7) are indicated. **b**, Oxygen consumption of the M1 and M2 rescue cells. **c**, Lactate production of the M1 and M2 rescue cells. **d**, Metabolite levels in the M1 and M2 H1299 rescue cells as determined by LC-MS. Detected metabolites are represented as the percentage signal change in the M2 versus M1 cells. FBP represents both fructose-1,6-bisphosphate and fructose-2,6-bisphosphate, as the two are undistinguishable by LC-MS. Values were obtained by analysis of six samples. Error bars in **a**, **b** denote s.e.m. ($n = 3$); error bars in **c** denote s.e.m. ($n = 6$).

on treatment with saturating or subsaturating amounts of oligomycin (Supplementary Fig. 2b, c, and data not shown). These data suggest that changes in ATP levels or mitochondrial coupling do not account for the observed changes in proliferation rates in the M1 and M2 cells.

Given the reduced proliferation of the M1 cells in response to both hypoxic conditions and oligomycin treatment, we hypothesized that the M1 rescue cells may preferentially metabolize glucose by oxidative phosphorylation rather than rely on aerobic glycolysis. To test this hypothesis, we compared oxygen consumption, lactate production and metabolite levels in the M1 and M2 rescue H1299 cells. We found that the M1 cells consume more oxygen and produce less lactate than the M2 cells (Fig. 3b c). These differences in oxygen consumption and lactate production were statistically significant ($P < 0.02$) Similar results were observed when endogenous PKM2 was replaced with mouse PKM1 or mouse PKM2 in two other invasive cancer cell lines, A549 and SN12C (Fig. 3b, c). However, switching pyruvate kinase isoform expression from M2 to M1 in a non-invasive breast cancer cell line known to have low aerobic glucose consumption rates, MCF7[9], had no significant affect on lactate production and oxygen consumption (Fig. 3b, c).

An increase in lactate levels in the H1299 M2 rescue cells was also found by liquid-chromatography-mass-spectrometry-based (LC-MS) measurement of metabolites (Fig. 3d). Additional metabolite levels were also different in the M2 cells as compared with the M1 cells. Pyruvate levels were increased and fructose-bisphosphate levels were decreased in the M2 cells (Fig. 3d). Together, these data show that the ratio of lactate production to oxygen consumption is higher in the M2 cells than in the M1 cells and that other glycolytic intermediates are affected by differential expression of these pyruvate kinase isoforms.

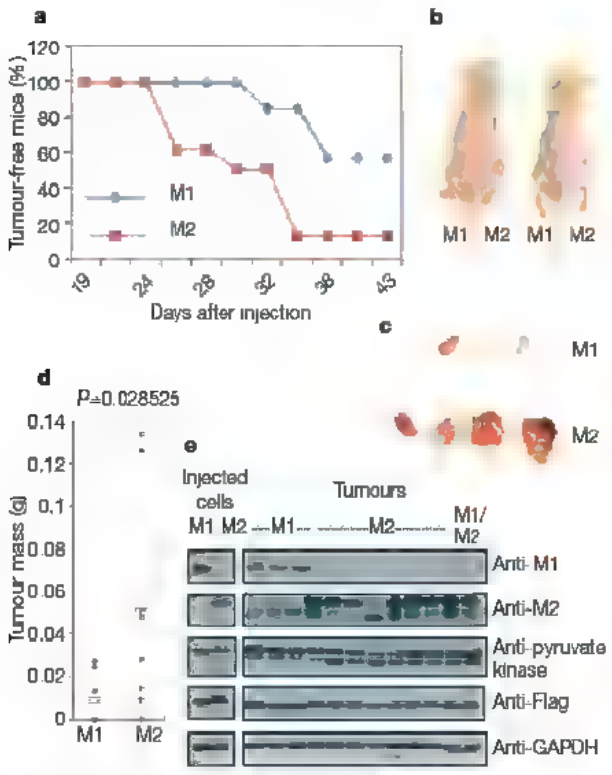


**Figure 4 | M1 expression reduces the tumorigenicity of lung cancer cells.** **a**, Tumour formation over time in nude mice injected with M1 and M2 rescue H1299 cells. After 43 days, 3 out of 7 mice injected with M1 cells and 7 out of 8 mice injected with M2 cells formed tumours **b**, Mice injected with M1 cells on the left flank and M2 cells on the right flank. The mouse on the left only formed a tumour from the M2 cells The mouse on the right formed a bigger tumour from the M2 cells than from the M1 cells. **c**, Dissected tumours from the nude mice. The only three tumours derived from M1 cells are shown (top row), and these tumours were smaller than four of the tumours from the M2 cells (bottom row) **d**, Mass of the dissected tumours. Each dot represents the tumour mass from one mouse. The blue line indicates the mean tumour mass originating from M1 cells and M2 cells. **e**, Immunoblotting of tumour lysates originating from M1 cells, M2 cells, or a 50/50 mixture of M1 and M2 cells (M1/M2) The left panel shows lysates from the injected cells. The right panel shows lysates from the dissected tumours. Lysates were immunoblotted with antibodies towards M1, M2, pyruvate kinase (recognizes both M1 and M2), Flag and GAPDH

To determine whether M2 isoform expression is important for tumour cell growth *in vivo*, we performed xenograft studies using the M1 and M2 rescue cells. Nude mice were injected with 5 million M1 or M2 rescue H1299 cells, and tumour growth was monitored over a 7-week period. As shown in Fig. 4a, mice injected with the M1 cells showed a delay in tumour development as compared with those injected with the M2 cells. Fewer tumours developed from the M1 cells, and those that did were smaller in size (Fig. 4b, c). As judged by total tumour mass, the M2 cells gave rise to significantly larger tumours than the M1 cells (Fig. 4d). Western blot analysis of the developed tumours shows that the Flag-tagged rescue mM1 and mM2 proteins are retained in the tumours; however, endogenous expression of PKM2 returned in both cases (Fig. 4e). No tumours were recovered that solely expressed mM1. To determine whether this was the result of loss of shRNA-mediated knockdown of endogenous PKM2 or whether it represented a selective growth advantage for cells expressing M2, a 50/50 mixture of the M1 and M2 cells was injected into nude mice. Tumours that arose from the mixture of M1 and M2 cells only retained expression of the Flag–mM2 rescue protein, demonstrating that most of the tumour, if not the entire tumour, was derived from the M2-expressing cells (Fig. 4e). These data show that PKM2 expression provides a selective growth advantage for tumour cells *in vivo*.

We show that the switch to the M2 isoform of pyruvate kinase in tumour cells is necessary to cause the metabolic phenotype known as the Warburg effect; however, the mechanism by which this occurs is as yet unknown. Given that PKM2 is expressed during embryonic development and in many non-transformed cell lines, M2 expression alone is unlikely to be a transforming event. Rather, the presence of PKM2 may contribute to a metabolic environment that is amenable to cell proliferation. An attractive hypothesis is that PKM2, which undergoes complex regulation by both fructose-1,6-bisphosphate and protein-tyrosine kinase signalling, provides the flexibility to distribute glucose metabolites into anabolic versus catabolic processes, depending on the demands of rapidly growing cells[10]. It remains unclear, however, why more of the pyruvate made in PKM2-expressing cells is converted to lactate whereas more of the pyruvate generated in PKM1 cells is metabolized in the mitochondria. One explanation is that M2 expression results in higher expression of lactate dehydrogenase. Alternatively, M2 expression might lead to reduced mitochondrial density and decreased expression of proteins involved in oxidative phosphorylation. To test these hypotheses, we analysed the expression of the lactate dehydrogenase and $F_1F_0$-ATPase proteins in the M1 and M2 cells. No differences in the protein levels were detected (data not shown); however, differential activities of lactate dehydrogenase, pyruvate dehydrogenase and/or pyruvate dehydrogenase kinase, or proteins involved in oxidative phosphorylation in the M1 and M2 cells, could account for the observed shift to aerobic glycolysis in the M2-expressing cells.

It is also possible that the M2 isoform of pyruvate kinase has functions independent of its role in glycolysis. GAPDH has been identified to be part of a transcription factor complex[11], and a recent study (ref. 12) suggested that the M2 isoform of pyruvate kinase has a role in caspase-independent cell death. In addition, we have recently found that PKM2 has the unique ability among pyruvate kinase isoforms to interact with tyrosine-phosphorylated proteins[10]. It is therefore possible that such an alternative function of PKM2 independent of its enzymatic activity promotes aerobic glycolysis and tumour growth.

Dependence on PKM2-mediated aerobic glycolysis for tumour growth is probably variable in cancer cells given the reliance of some tumours on alternative energy sources such as fatty acid oxidation. This idea is supported by our finding that replacement of PKM2 with mouse PKM1 in the MCF7 cancer cell line had no effect on glucose metabolism as measured by lactate production and oxygen consumption. Glutamine metabolism has also recently been identified as an important source of mitochondrial fuel in cancer cells[13]. It is possible that differences in glutamine metabolism may contribute to the metabolic phenotypes of PKM1 and PKM2 cells.

A well known difference between the M1 and M2 isoforms of pyruvate kinase is that M2 is a low activity enzyme that relies on allosteric activation by the upstream metabolite fructose-1,6-bisphosphate, whereas M1 is a constitutively active enzyme. Additionally, we have recently found that the activity of the M2 isoform (but not the M1 isoform) can be inhibited by tyrosine kinase signalling in tumour cells[10]. Decreased M2 activity as a result of growth-factor-stimulated kinase signalling pathways would be predicted to build up phosphoenolpyruvate levels, which would result in inhibition of the isoform of phosphofructokinase-2 expressed in tumour cells, PFKFB3[14,15]. This would result in reduced fructose-2,6-bisphosphate levels, which would in turn reduce fructose-1,6-bisphosphate levels. This type of regulation is consistent with our results showing a significant reduction in fructose-bisphosphate levels in the M2 cells as compared with the M1 cells. It is therefore possible that differential levels of fructose-bisphosphate, or other upstream metabolites in the glycolytic pathway, mediate the switch to aerobic glycolysis from oxidative phosphorylation in M2-expressing cells by an as yet unexplained mechanism. An alternative explanation is that M1 preferentially shuttles pyruvate to the mitochondria or M2 preferentially shuttles pyruvate to lactate dehydrogenase. For example, tyrosine phosphorylation of lactate dehydrogenase might facilitate its binding to PKM2[10], thereby channelling the product of pyruvate kinase to lactate. Regardless of the mechanism by which PKM2 promotes the Warburg effect, the finding that expression of the M2 isoform is advantageous for tumour cell growth *in vivo* demonstrates that the unique metabolism of tumour cells is critical for tumorigenesis.

## METHODS SUMMARY

Cells were lysed in Nonidet P-40 lysis buffer, and western blot analysis was carried out according to standard protocols. Paraffin-embedded colon cancer and control tissues were stained with polyclonal PKM1 and PKM2 antibodies using an automated immunostainer and analysed using immunohistochemistry kits and EDTA-based antigen retrieval (Ventana Medical Systems). For cell line construction, Flag-tagged mouse pyruvate kinase isoforms were cloned into pLHCX and used to make retrovirus to infect H1299, A549, SN12C and MCF7 cells. After 2 weeks of selection in 350 μg ml$^{-1}$ hygromycin (150 μg ml$^{-1}$ hygromycin for MCF7), the stable cells expressing Flag-tagged mouse pyruvate kinase were infected with lentivirus containing knockdown or control shRNA towards human *PKM2*. These cells were selected for 1 week in 2 μg ml$^{-1}$ puromycin before experimentation. Cellular glucose metabolism rates were measured by following the conversion of 5-$^3$H-glucose to $^3H_2O$, as described previously[16]. Cellular proliferation rates were determined by seeding $5 \times 10^4$ cells in triplicate in 6-well plates and taking cell counts every 24 h using a Coulter particle analyser for a 3–5-day period. Pyruvate kinase activity was assessed using a continuous assay coupled to lactate dehydrogenase. Adenine nucleotide levels were measured using an ATP bioluminescence assay kit (Roche) as well as by high-performance liquid chromatography (HPLC), as described previously[17]. Lactate production was measured using a fluorescence-based assay kit (BioVision). Oxygen consumption rates were measured using an anaerobic chamber fitted with a polarographic oxygen electrode, as described previously[16]. Metabolite extracts were prepared from $2 \times 10^7$ cells using cold 80% ethanol, 0.1% formic acid. After centrifugation, the metabolite extracts were dried under nitrogen, reconstituted in water and analysed by LC-MS as described previously[18]. Nude mice were injected subcutaneously with $5 \times 10^6$ H1299 cells as described previously[19]. Tumour formation was assessed every 2–3 days, and the tumours were dissected and weighed at 7 weeks after injection.

**Full Methods** and any associated references are available in the online version of the paper at www.nature.com/nature.

**Received 18 October 2007; accepted 19 January 2008.**

1. Warburg, O. On the origin of cancer cells. *Science* 123, 309–314 (1956).
2. Mazurek, S., Boschek, C. B., Hugo, F. & Eigenbrodt, E. Pyruvate kinase type M2 and its role in tumor growth and spreading. *Semin. Cancer Biol.* 15, 300–308 (2005).
3. Fantin, V. R., St-Pierre, J. & Leder, P. Attenuation of LDH-A expression uncovers a link between glycolysis, mitochondrial physiology, and tumor maintenance. *Cancer Cell* 9, 425–434 (2006).
4. Majumder, P. K. *et al.* mTOR inhibition reverses Akt-dependent prostate intraepithelial neoplasia through regulation of apoptotic and HIF-1-dependent pathways. *Nature Med.* 10, 594–601 (2004).
5. Altenberg, B. & Greulich, K. O. Genes of glycolysis are ubiquitously overexpressed in 24 cancer classes. *Genomics* 84, 1014–1020 (2004).
6. Jurica, M. S. *et al.* The allosteric regulation of pyruvate kinase by fructose-1,6-bisphosphate. *Structure* 6, 195–210 (1998).
7. Dombrauckas, J. D., Santarsiero, B. D. & Mesecar, A. D. Structural basis for tumor pyruvate kinase M2 allosteric regulation and catalysis. *Biochemistry* 44, 9417–9429 (2005).
8. Muller, W. J., Sinn, E., Pattengale, P. K., Wallace, R. & Leder, P. Single-step induction of mammary adenocarcinoma in transgenic mice bearing the activated c-neu oncogene. *Cell* 54, 105–115 (1988).
9. Gatenby, R. A. & Gillies, R. J. Why do cancers have high aerobic glycolysis? *Nature Rev. Cancer* 4, 891–899 (2004).
10. Christofk, H. R., Vander Heiden, M. G., Wu, N., Asara, J. M. & Cantley, L. C. Pyruvate kinase M2 is a phosphotyrosine binding protein. *Nature* doi:10.1038/nature06667 (this issue).
11. Zheng, L., Roeder, R. G. & Luo, Y. S phase activation of the histone H2B promoter by OCA-S, a coactivator complex that contains GAPDH as a key component. *Cell* 114, 255–266 (2003).
12. Stetak, A. *et al.* Nuclear translocation of the tumor marker pyruvate kinase M2 induces programmed cell death. *Cancer Res.* 67, 1602–1608 (2007).
13. DeBerardinis, R. J. *et al.* Beyond aerobic glycolysis: transformed cells can engage in glutamine metabolism that exceeds the requirement for protein and nucleotide synthesis. *Proc. Natl Acad. Sci. USA* 104, 19345–19350 (2007).
14. Manes, N. P. & El-Maghrabi, M. R. The kinase activity of human brain 6-phosphofructo-2-kinase/fructose-2,6-bisphosphatase is regulated via inhibition by phosphoenolpyruvate. *Arch. Biochem. Biophys.* 438, 125–136 (2005).
15. Telang, S. *et al.* Ras transformation requires metabolic control by 6-phosphofructo-2-kinase. *Oncogene* 25, 7225–7234 (2006).
16. Vander Heiden, M. G. *et al.* Growth factors can influence cell growth and survival through effects on glucose metabolism. *Mol. Cell. Biol.* 21, 5899–5912 (2001).
17. Budinger, G. R. *et al.* Cellular energy utilization and supply during hypoxia in embryonic cardiac myocytes. *Am. J. Physiol.* 270, L44–L53 (1996).
18. Sabatine, M. S. *et al.* Metabolomic identification of novel biomarkers of myocardial ischemia. *Circulation* 112, 3868–3875 (2005).
19. Engelman, J. A. *et al.* Allelic dilution obscures detection of a biologically significant resistance mutation in EGFR-amplified lung cancer. *J. Clin. Invest.* 116, 2695–2706 (2006).

**Supplementary Information** is linked to the online version of the paper at www.nature.com/nature.

**Acknowledgements** We thank M. Bentires-Alj for the MMTV-NeuNT tissue lysates and W. Hahn for the lentiviral shRNA constructs. We thank S. Soltoff for use of the anaerobic chamber and oxygen electrode, and Q. Song for use of the hypoxia chamber. We thank I. Rhee and T. Yuan for help with the nude mouse injections. We thank M. Liu for technical assistance. R.E.G. is supported by funding from the National Institutes of Health, the Donald W. Reynolds Foundation, the Fondation Leducq, and the Broad Institute Scientific Planning and Allocation of Resources Committee. M.G.V.H. is a Damon Runyon Fellow supported by the Damon Runyon Cancer Research Foundation. This research was supported by funding to L.C.C. from the National Institutes of Health. S.L.S. is an Investigator with the Howard Hughes Medical Institute.

**Author Contributions** M.H.H. and M.D.F. contributed the immunohistochemistry data (Fig. 1c). A.R., R.E.G., R.W. and S.L.S. contributed the metabolite measurement data (Fig. 3d). H.R.C. and M.G.V.H. performed all other experiments. H.R.C., M.G.V.H. and L.C.C. designed the study and wrote the paper.

**Author Information** Reprints and permissions information is available at www.nature.com/reprints. The authors declare competing financial interests: details accompany the full-text HTML version of the paper at www.nature.com/nature. Correspondence and requests for materials should be addressed to L.C.C. (lcantley@hms.harvard.edu).

LETTERS

# UNC93B1 delivers nucleotide-sensing toll-like receptors to endolysosomes

You-Me Kim[1], Melanie M. Brinkmann[1], Marie-Eve Paquet[1] & Hidde L. Ploegh[1]

**Signalling by means of toll-like receptors (TLRs) is essential for the development of innate and adaptive immune responses[1–3]. UNC93B1, essential for signalling of TLR3, TLR7 and TLR9 in both humans and mice, physically interacts with these TLRs in the endoplasmic reticulum (ER)[4–6]. Here we show that the function of the polytopic membrane protein UNC93B1 is to deliver the nucleotide-sensing receptors TLR7 and TLR9 from the ER to endolysosomes. In dendritic cells of 3d mice, which express an UNC93B1 missense mutant (H412R) incapable of TLR binding, neither TLR7 nor TLR9 exits the ER. Furthermore, the trafficking and signalling defects of the nucleotide-sensing TLRs in 3d dendritic cells are corrected by expression of wild-type UNC93B1. However, UNC93B1 is dispensable for ligand recognition and signal initiation by TLRs. To our knowledge, UNC93B1 is the first protein to be identified as a molecule specifically involved in trafficking of nucleotide-sensing TLRs. By inhibiting the interaction between UNC93B1 and TLRs it should be possible to achieve specific regulation of the nucleotide-sensing TLRs without compromising signalling via the cell-surface-disposed TLRs.**

Toll-like receptors (TLRs) control host immune responses against pathogens through recognition of molecular patterns uniquely present in microorganisms[1–3]. Certain members of the TLR family, including TLR1, TLR2, TLR4 and TLR6, sense the presence of protein or lipid components of bacteria and fungi and are found on the plasma membrane[7–9]. On the other hand, TLR3, TLR7/8 and TLR9, which engage double-stranded RNA, single-stranded RNA and unmethylated CpG DNA, respectively, are found inside cells[8–13]. Intracellular localization of these nucleotide-sensing TLRs is important for recognition of viral DNAs and RNAs while preventing activation by host-derived nucleic acids[14]. TLR9 resides in the ER before stimulation and is rapidly recruited to lysosomes on activation[12]. In lysosomes, TLR9 co-localizes with internalized CpG DNA and transmits signals in a MyD88-adaptor-dependent fashion[8,12]. However, the molecular mechanisms underlying the unusual intracellular trafficking of TLR9 are not known.

UNC93B1, a poorly characterized multi-transmembrane-domain-containing protein, has an essential role in signalling by the nucleotide-sensing TLRs[4,5,15]. In mice, a missense mutation in the *Unc93b1* gene (encoding UNC93B1 with a H412R mutation) abrogates signalling via TLR3, TLR7 and TLR9 without compromising other TLRs[4]. These mutant mice (termed '3d' or 'triple D' for the combined signalling defects of TLR3, TLR7 and TLR9) show increased susceptibility to infection by a variety of pathogens[4]. Functional null mutations of *UNC93B1* are responsible for herpes simplex encephalitis

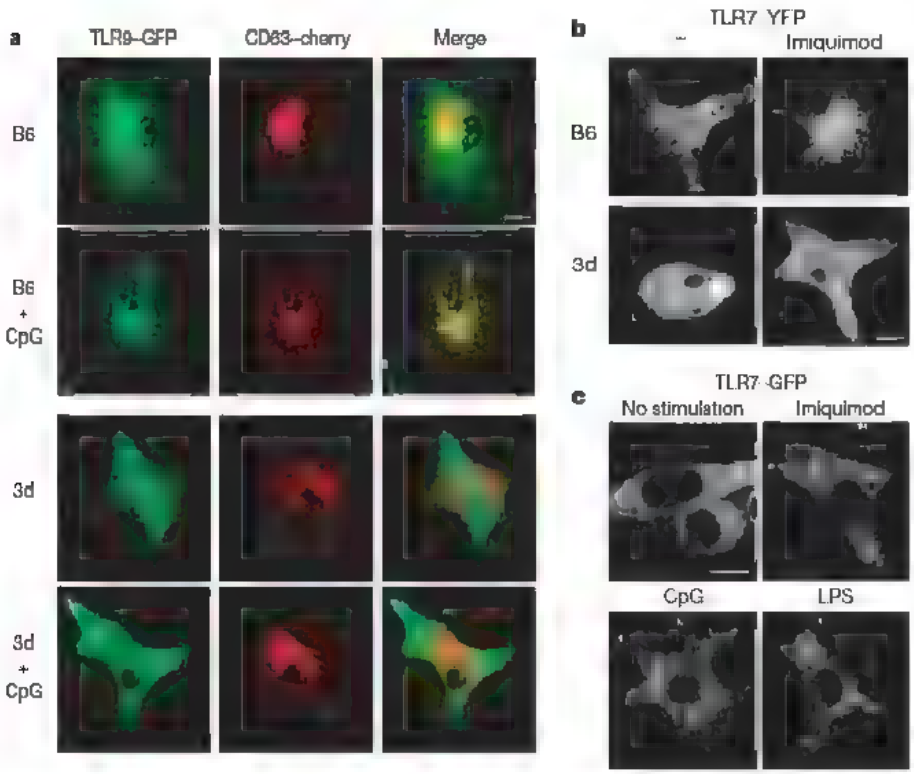


**Figure 1 | TLR7 and TLR9 fail to translocate to endolysosomes in 3d cells. a, b,** TLR9–GFP and CD63–cherry (**a**) or TLR7–YFP (**b**) were expressed in either wild-type (C57BL/6, B6) or 3d BM-DCs and live cells were imaged before and after stimulation with 1 μM CpG (**a**) or 1 μM imiquimod (**b**) for 2 h. **c,** RAW macrophages stably expressing TLR7–GFP were stimulated with 1 μM imiquimod, 1 μM CpG or 1 μg ml$^{-1}$ LPS or left unstimulated. Live cells were imaged after 4 h of agonist stimulation. Scale bar, 10 μm.

[1]Whitehead Institute for Biomedical Research, 9 Cambridge Center, Cambridge, Massachusetts 02142, USA.

in children[5]. As in 3d mice, cells from UNC93B1-deficient patients are defective in signalling via the nucleotide-sensing TLRs 3, 7, 8 and 9 (ref. 5). We have shown that UNC93B1 specifically binds to TLRs 3, 7, 9 and 13 via the transmembrane domains of the TLRs. The point mutation H412R of UNC93B1 in 3d mice abolishes these interactions[6]. The physical interactions between UNC93B1 and its client TLRs thus somehow control proper TLR signalling[6].

The interactions between UNC93B1 and the nucleotide-sensing TLRs are stably maintained even after stimulation of various TLRs[6] (Supplementary Fig. 1a). Neither UNC93B1 nor its client TLRs ever acquire endoglycosidase H (endo H) resistance[6,12,14], even though they do so when cells are treated with brefeldin A (Supplementary Fig. 1b). Therefore, we postulated that the UNC93B1–TLR complex may reach lysosomes without passing through the Golgi, and that the interaction between UNC93B1 and TLR9 controls TLR9 trafficking. To test this hypothesis, we expressed TLR9–green fluorescent protein (GFP) fusion protein in bone-marrow-derived dendritic cells (BM-DCs) from wild-type (C57BL/6) and UNC93B1 mutant (3d) mice and compared localization of TLR9 before and after stimulation with CpG DNA (ODN 1826). The majority of TLR9 is expressed in the ER of wild-type cells[12,13] (Fig. 1a and Supplementary Fig. 2b). In a small fraction of unstimulated wild-type cells we also found TLR9 in endosomes as well as in the ER (data not shown). On activation of wild-type cells with CpG, TLR9 changed its localization from mostly ER to endosomes and tubular lysosomes, as inferred from co-localization with the late endosome/lysosomal marker proteins CD63 and Lamp1 (Fig. 1a and Supplementary Figs 2c and 3a). In contrast, in dendritic cells of 3d mice TLR9 remained in the ER and failed to translocate to endolysosomes, even after stimulation with CpG.

Like TLR9, TLR7 resides intracellularly[9,11]. To analyse subcellular localization of TLR7 we expressed TLR7–yellow fluorescent protein (YFP) fusion protein in BM-DCs. We found that TLR7, like TLR9, is localized in the ER of unstimulated dendritic cells (Fig. 1b and Supplementary Fig. 2a). Moreover, we also observed trafficking of TLR7 from the ER to endolysosomes when wild-type cells were stimulated with the synthetic TLR7 agonist imiquimod (Fig. 1b and Supplementary Fig. 4). TLR7 is also transported to endosomes in response to stimulation with agonists that do not target TLR7 directly (Fig. 1c). However, in BM-DCs of 3d mice TLR7 failed to exit the ER, similarly to what we observed for TLR9. In contrast to TLR7 and TLR9, the localization of TLR4 at the cell surface is not affected by the 3d mutation, consistent with the ability of 3d cells to respond to lipopolysaccharide (LPS)[4] (Supplementary Fig. 5). Therefore, UNC93B1 specifically interacts with intracellular nucleotide-sensing TLRs and regulates their trafficking to endolysosomes, from where the receptors transmit signals via MyD88/TRIF-dependent pathways[8,12].

Although 3d mice also have defects in cross-presentation and major histocompatibility complex (MHC) class-II-mediated antigen presentation[4,15], we observed no significant differences in the localization of class I and class II MHC molecules in 3d cells when compared to wild-type cells (Supplementary Fig. 6).

To confirm that the failure of mutant UNC93B1 to interact with TLRs causes the TLR trafficking defects in 3d cells, we co-expressed TLR9–GFP with wild-type UNC93B1 fused to a red fluorescent protein (UNC93B1–cherry) in 3d cells[17]. Indeed, in 3d cells that express wild-type UNC93B1–cherry, TLR9 trafficking was normal on CpG stimulation, TLR9–GFP translocated properly into endolysosomes (Fig. 2a). Expression of mutant UNC93B1–cherry did not rescue the TLR9 trafficking defect in 3d cells. Wild-type UNC93B1–cherry co-localized with TLR9 in endolysosomes (Fig. 2a). Thus, UNC93B1 travels to endolysosomes along with TLR9 when cells are stimulated.

TLR9 was also recruited to phagosomal membranes when BM-DCs from wild-type mice were incubated with polystyrene beads (Fig. 2b). However, in 3d cells, TLR9 failed to translocate to phagosomes and remained in the ER, although 3d dendritic cells efficiently phagocytosed the beads[4]. Expression of wild-type but not mutant UNC93B1 in 3d cells restored trafficking of TLR9 to phagosomes (Fig. 2c). Wild-type UNC93B1–cherry co-localized with TLR9 in phagosomes. Therefore, UNC93B1 is required for proper trafficking of TLR9 to phagosomes as well as to endolysosomes. This trait may provide a link between the 3d mutation and the reported defect in cross-presentation[4], a process favoured by phagocytosis of antigen-positive materials[18].

Next we investigated whether expression of wild-type UNC93B1 in BM-DCs of 3d mice not only restores TLR trafficking but also corrects the signalling defects. BM-DCs from 3d mice failed to produce tumour-necrosis factor (TNF) when stimulated with imiquimod or CpG[4,6] (Fig. 2d). However, on stimulation with TLR agonists, 3d cells that express wild-type UNC93B1 produced as much TNF as did wild-type cells[4] (Fig. 2d). Expression of additional mutant UNC93B1 (H412R) in 3d cells did not restore cytokine production in response to TLR7 or TLR9 activation. Expression of wild-type or mutant UNC93B1 did not affect LPS-induced TNF production (Fig. 2d).

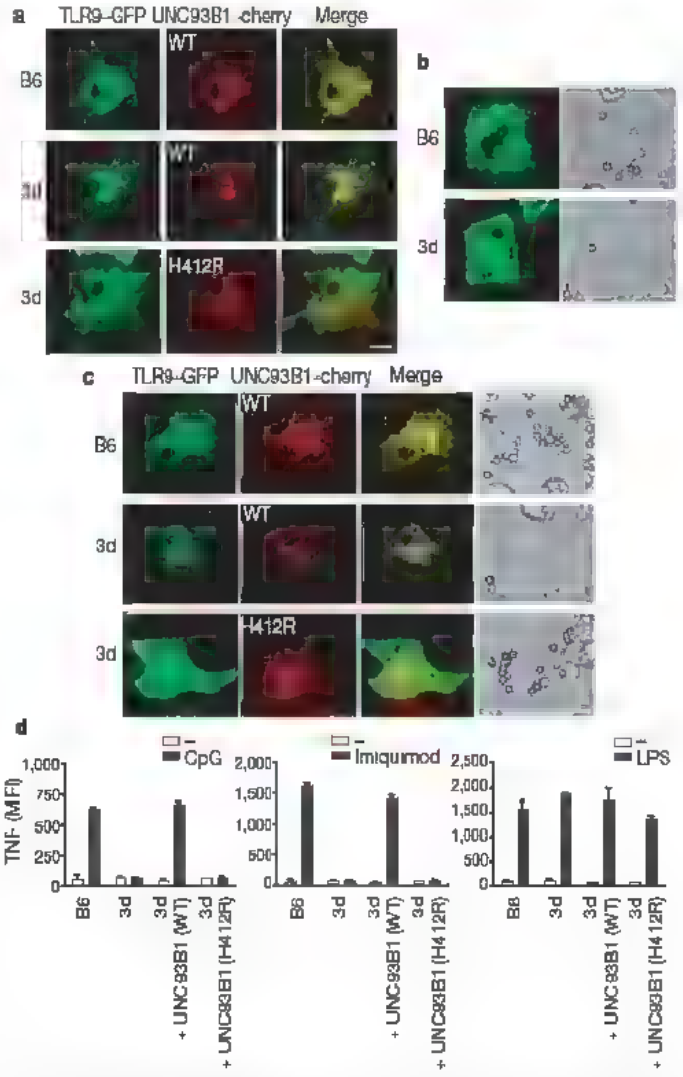


**Figure 2 | Expression of wild-type UNC93B1 in 3d cells rescues defects of TLR trafficking and signalling.** **a**, TLR9–GFP and UNC93B1–cherry (wild type or H412R mutant) were co-expressed in wild-type (B6) or 3d BM-DCs. After stimulation with 1 μM CpG for 2 h, live cells were imaged. **b, c**, TLR9–GFP alone (**b**) or TLR9–GFP and UNC93B1–cherry (wild type or H412R mutant) together (**c**) were expressed in wild-type or 3d BM-DCs. Cells were incubated with 3 μm polystyrene beads for 1 h and imaged. **d**, BM-DCs (wild type or 3d) expressing GFP alone without exogenous UNC93B1 expression or 3d BM-DCs expressing either wild-type or mutant UNC93B1–GFP were stimulated with 1 μM CpG (left panel), 100 nM imiquimod (middle panel) or 1 μg ml$^{-1}$ LPS (right panel) for 4 h in the presence of 10 μg ml$^{-1}$ brefeldin A. Cells were fixed and stained for intracellular TNF. TNF levels in GFP-positive cells were measured by flow cytometry. MFI, mean fluorescence intensity. Scale bars, 10 μm.

Unlike wild-type UNC93B1–cherry, mutant UNC93B1–cherry showed a weak and diffuse labelling pattern in stimulated cells (Fig. 2a). To determine more accurately the localization of mutant UNC93B1, we expressed wild-type and mutant UNC93B1–GFP fusion proteins in wild-type and 3d BM-DCs. Before stimulation, both wild-type and mutant UNC93B1 were found in the ER[4] (Fig. 3a and Supplementary Fig. 7). When cells were stimulated with a dye-labelled CpG (TAMRA–CpG), wild-type UNC93B1–GFP co-localized with TAMRA–CpG in endolysosomes. Wild-type UNC93B1 also co-localized with class II MHC and CD63 in CpG-stimulated cells (Supplementary Figs 3b and 7). Furthermore, endogenous wild-type UNC93B1 co-localized with Lamp1 when BM-DCs were stimulated with CpG (Supplementary Fig. 7c). In contrast, mutant UNC93B1–GFP did not translocate to endolysosomes on stimulation with CpG (Fig. 3a and Supplementary Figs 3b and 7). Therefore, mutant UNC93B1 not only fails to interact with TLRs to deliver the receptors to endolysosomes, but it is also defective in its own trafficking. It is likely that an as yet unidentified ER protein interacts with wild-type UNC93B1 and facilitates trafficking of UNC93B1–TLR complexes to endolysosomes. The H412R mutation, localized within a transmembrane segment of UNC93B1, may cause disruption of such interaction(s) and result in mislocalization of both UNC93B1 and its client TLRs.

The 3d mutation in UNC93B1 is a loss of function mutation. To provide positive evidence for the role of UNC93B1 in trafficking of TLRs, we enforced an aberrant localization of UNC93B1 and determined where TLRs would now localize to. We delivered wild-type UNC93B1 to the cell surface by engraftment of a dominant plasma-membrane-sorting sequence—derived from the yeast membrane protein Ist2p—onto the cytosolic tail of UNC93B1–GFP[19,20]. When co-expressed, both TLR9–cherry and UNC93B1–GFP–Ist2p are targeted to the plasma membrane (Fig. 3b). In contrast, TLR9–cherry remained in the ER when co-expressed with the H412R mutant UNC93B1–GFP–Ist2p, even though the mutant UNC93B1–GFP–Ist2p was detectable at the cell surface. These data establish that UNC93B1 is necessary and sufficient to determine intracellular localization of TLR9 through physical interaction.

Does UNC93B1 have a role in ligand recognition and recruitment of signalling adaptors to TLRs, in addition to its role of determining intracellular localization of the nucleotide-sensing TLRs? We expressed a chimaeric TLR with the TLR9 ectodomain fused to the transmembrane and cytosolic domain of TLR4 (TLR9/4) in BM-DCs. TLR9/4 no longer interacts with UNC93B1 because it lacks the TLR9 transmembrane domain (ref. 6 and data not shown). As reported, TLR9/4 resides at the cell surface[14] (Fig. 4a). When we expressed TLR9/4 in BM-DCs of 3d mice, the mutant cells regained their responsiveness to CpG stimulation and produced TNF (Fig. 4b). UNC93B1 is therefore dispensable for CpG recognition and for initiation of TLR signalling via adaptor recruitment. We conclude that the signalling defects seen in the cells of 3d mice are solely due to the

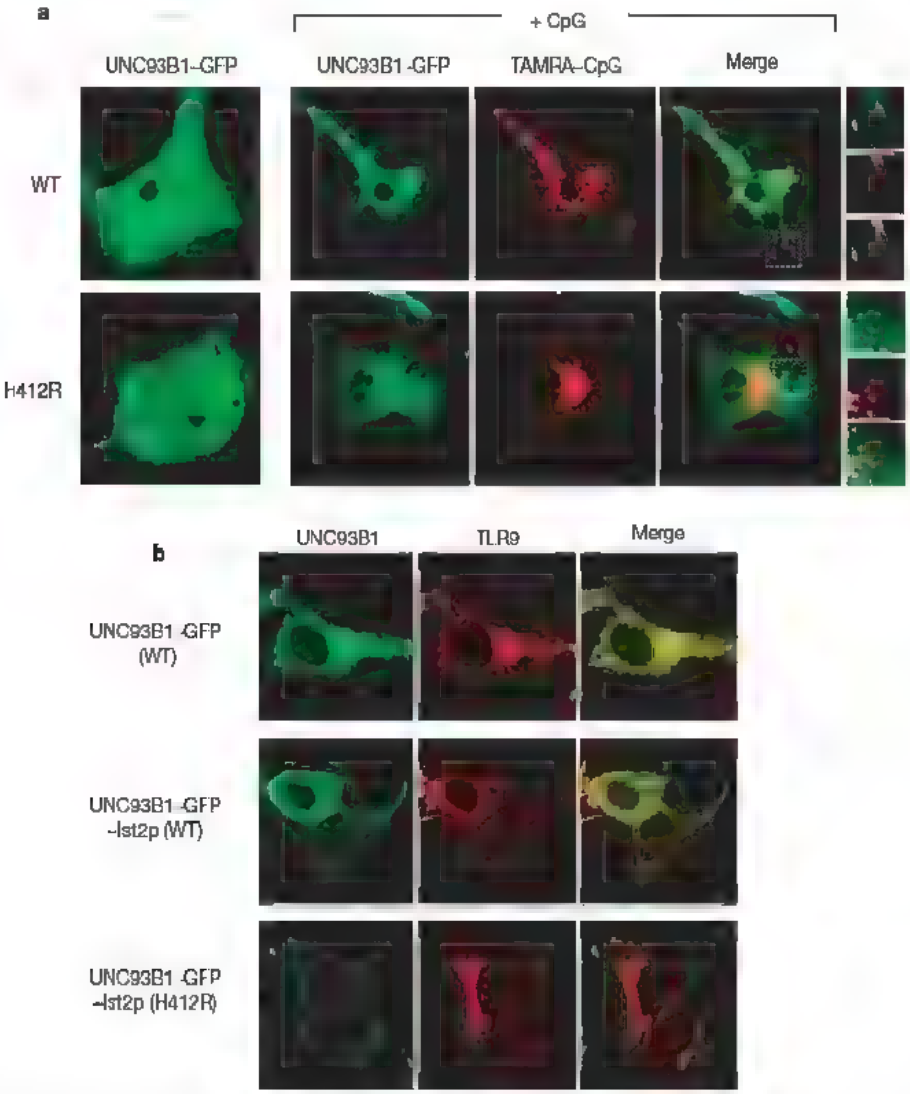


**Figure 3 | Wild-type UNC93B1 delivers the nucleotide-sensing TLRs to endolysosomes. a**, Wild-type or H412R mutant UNC93B1–GFP was expressed in wild-type and 3d BM-DCs, respectively. Cells were either left untreated ( ) or incubated with 1 μM TAMRA-labelled CpG for 15 min, washed and imaged after an additional 2 h of incubation ( + CpG). **b**, UNC93B1–GFP or UNC93B1–GFP–Ist2p (wild type or H412R mutant) was co-expressed with TLR9–cherry in HEK-293T cells. Cells were imaged 24 h after transfection.

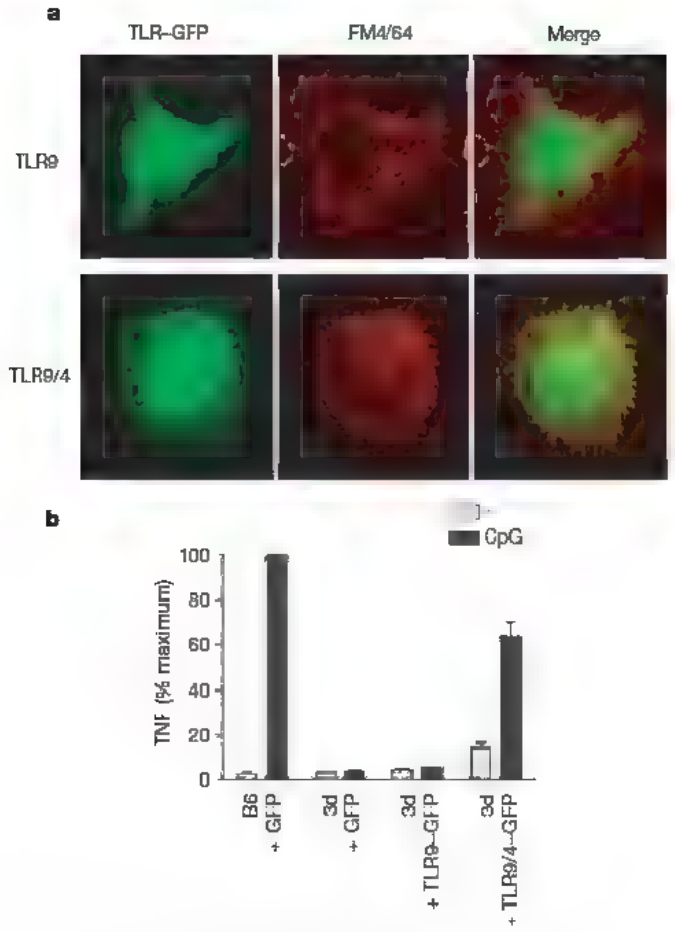


**Figure 4 | UNC93B1 is dispensable for ligand recognition and signal initiation by TLR. a**, TLR9–GFP or TLR9/4–GFP was expressed in BM DCs of 3d mice. Live cells were imaged after the plasma membrane was stained with the lipophilic dye FM4/64. **b**, BM-DCs (wild type (B6) or 3d) expressing GFP alone without exogenous TLR expression or 3d BM-DCs expressing either TLR9–GFP or TLR9/4–GFP were stimulated with 1 μM CpG for 4 h in the presence of 10 μg ml$^{-1}$ brefeldin A. Cells were fixed and stained for intracellular TNF. TNF levels in GFP-positive cells were measured by flow cytometry. The data (mean ± s.e.m.) are generated from four independent experiments and the levels of TNF are represented as the percentage of TNF level detected in wild-type cells.

failure of the nucleotide-sensing TLRs to reach the endolysosomes, where they initiate MyD88/TRIF-dependent signalling pathways[21–23].

UNC93B1 specifically controls trafficking of nucleotide-sensing TLRs. In 3d cells that express mutant UNC93B1 which is unable to interact with its client TLRs, the nucleotide-sensing TLRs cannot leave the ER and fail to signal (Supplementary Fig. 8). In contrast, trafficking and signalling of plasma-membrane-localized TLRs are not affected by the UNC93B1 mutation. Manipulation of the UNC93B1–TLR interaction should thus allow specific regulation of signalling via nucleotide-sensing TLRs without compromising the function of the other TLRs. New challenges lie in defining the molecular nature of signals that promote intracellular TLR trafficking (Supplementary Fig. 8). In addition, the unconventional means of delivery of TLR7 and TLR9 from the ER to endolysosomes by UNC93B1 constitutes a new pathway in need of further probing to understand the mechanisms of TLR trafficking and signal transduction.

## METHODS SUMMARY

Murine UNC93B1 was carboxy-terminally fused with GFP or cherry tag[17] and cloned into the pMSCVneo vector (Clontech). C-terminally GFP- or cherry-tagged murine TLR7 and TLR9 were cloned into the pMSCVpuro vector (Clontech). UNC93B1–GFP–Ist2p was generated by fusing the last 69 amino acids of yeast Ist2p (ref. 24) to the C terminus of UNC93B1–GFP and cloned into pcDNA3.1 (Clontech). The cherry–KDEL construct was generated by substituting the GFP sequence in pCMV/Myc/ER/GFP (Clontech) with the cherry sequence by PCR. For retroviral gene transduction, viruses produced in HEK 293T cells were added to RAW macrophages or BM-DCs at day 1 of BM DC culture. The following day, cells were fed with fresh media. Pulse–chase, immunoprecipitation and endo H assays of UNC93B1 and TLRs were performed as described[6]. For TNF assay, BM-DCs were stimulated with TLR agonists for 4 h in the presence of 10 μg ml$^{-1}$ brefeldin A. The cells were fixed, permeabilized and stained with phycoerythrin (PE)-conjugated anti-CD11c (clone HL3) and Alexa-Fluor-647-conjugated anti-TNF (clone MP6-XT22) antibodies. Fluorescence intensity was measured with an LSR I flow cytometer (BD biosciences). Data were collected with CellQuest (BD Biosciences) and analysed with FlowJo (TriStar). For immunofluorescence staining of MHC class I and II, BM-DCs grown on coverglasses were fixed, permeabilized and stained with a rabbit polyclonal anti-MHC class I (p8), a hamster monoclonal anti-MHC class II (clone N22) or a rat monoclonal anti-lamp1 (clone 1D4B) antibody followed by Alexa Fluor-conjugated secondary antibodies (Invitrogen). After washes, coverglasses were mounted on a slideglass using Fluoromount G (Southern Biotech). For live cell imaging, cells were grown in 8-well-chambered coverglasses (LAB-TEK). Images were acquired using a spinning disk confocal microscope. Metamorph (Molecular Devices) was used for image acquisition and figures were constructed using Adobe Photoshop and Illustrator. Quantitative co-localization analyses were performed using applications 'Measure Colocalization' and 'Correlation Plot' in MetaMorph software (Molecular Devices).

**Full Methods** and any associated references are available in the online version of the paper at www.nature.com/nature.

**Received 5 September 2007; accepted 3 January 2008.**
**Published online 27 February 2008.**

1. Janeway, C. A. Jr & Medzhitov, R. Innate immune recognition. *Annu. Rev. Immunol.* 20, 197–216 (2002).
2. Takeda, K., Kaisho, T. & Akira, S. Toll-like receptors. *Annu. Rev. Immunol.* 21, 335–376 (2003).
3. Kawai, T. & Akira, S. TLR signaling. *Cell Death Differ.* 13, 816–825 (2006).
4. Tabeta, K. *et al.* The Unc93b1 mutation 3d disrupts exogenous antigen presentation and signaling via Toll-like receptors 3, 7 and 9. *Nature Immunol.* 7, 156–164 (2006).
5. Casrouge, A. *et al.* Herpes simplex virus encephalitis in human UNC-93B deficiency. *Science* 314, 308–312 (2006).
6. Brinkmann, M. M. *et al.* The interaction between the ER membrane protein UNC93B and TLR3, 7, and 9 is crucial for TLR signaling. *J. Cell Biol.* 177, 265–275 (2007).
7. Latz, E. *et al.* Lipopolysaccharide rapidly traffics to and from the Golgi apparatus with the toll-like receptor 4-MD-2-CD14 complex in a process that is distinct from the initiation of signal transduction. *J. Biol. Chem.* 277, 47834–47843 (2002).
8. Ahmad-Nejad, P. *et al.* Bacterial CpG-DNA and lipopolysaccharides activate Toll-like receptors at distinct cellular compartments. *Eur. J. Immunol.* 32, 1958–1968 (2002).
9. Nishiya, T. & DeFranco, A. L. Ligand-regulated chimeric receptor approach reveals distinctive subcellular localization and signaling properties of the Toll-like receptors. *J. Biol. Chem.* 279, 19008–19017 (2004).
10. Matsumoto, M. *et al.* Subcellular localization of Toll-like receptor 3 in human dendritic cells. *J. Immunol.* 171, 3154–3162 (2003).
11. Nishiya, T., Kajita, E., Miwa, S. & Defranco A. L. TLR3 and TLR7 are targeted to the same intracellular compartments by distinct regulatory elements. *J. Biol. Chem.* 280, 37107–37117 (2005).
12. Latz, E. *et al.* TLR9 signals after translocating from the ER to CpG DNA in the lysosome. *Nature Immunol.* 5, 190–198 (2004).
13. Leifer, C. A. *et al.* TLR9 is localized in the endoplasmic reticulum prior to stimulation. *J. Immunol.* 173, 1179–1183 (2004).
14. Barton, G. M., Kagan, J. C. & Medzhitov, R. Intracellular localization of Toll-like receptor 9 prevents recognition of self DNA but facilitates access to viral DNA. *Nature Immunol.* 7, 49–56 (2006).
15. Conley, M. E. Immunodeficiency: UNC-93B gets a tol call. *Trends Immunol.* 28, 99–101 (2007).
16. Janssen, E. *et al.* Efficient T cell activation via a Toll-Interleukin 1 Receptor-independent pathway. *Immunity* 24, 787–799 (2006).
17. Shaner, N. C. *et al.* Improved monomeric red, orange and yellow fluorescent proteins derived from *Discosoma* sp. red fluorescent protein. *Nature Biotechnol.* 22, 1567–1572 (2004).
18. Kovacsovics-Bankowski, M., Clark, K., Benacerraf, B. & Rock, K. L. Efficient major histocompatibility complex class I presentation of exogenous antigen upon phagocytosis by macrophages. *Proc. Natl Acad. Sci. USA* 90, 4942–4946 (1993).
19. Juschke, C., Ferring, D., Jansen, R. P. & Seedorf, M. A novel transport pathway for a yeast plasma membrane protein encoded by a localized mRNA. *Curr. Biol.* 14, 406–411 (2004).

20. Franz, A., Maass, K. & Seedorf, M. A complex peptide-sorting signal, but no mRNA signal, is required for the Sec-independent transport of Ist2 from the yeast ER to the plasma membrane. *FEBS Lett.* 581, 401–405 (2007)
21. Schnare, M., Holt, A. C., Takeda, K., Akira, S. & Medzhitov, R. Recognition of CpG DNA is mediated by signaling pathways dependent on the adaptor protein MyD88. *Curr. Biol.* 10, 1139–1142 (2000)
22. Hoebe, K. *et al.* Identification of *Lps2* as a key transducer of MyD88-independent TIR signalling. *Nature* 424, 743–748 (2003)
23. Yamamoto, M. *et al.* Role of adaptor TRIF in the MyD88-independent toll-like receptor signaling pathway. *Science* 301, 640–643 (2003)
24. Juschke, C., Wachter, A., Schwappach, B. & Seedorf, M. SEC18/N5F-independent, protein-sorting pathway from the yeast cortical ER to the plasma membrane. *J. Cell Biol.* 169, 613–622 (2005).

**Supplementary Information** is linked to the online version of the paper at www.nature.com/nature.

**Acknowledgements** We are grateful to J. Vyas for CD63–cherry-expressing lentivirus, B. Beutler for 3d mice, and T. Nishiya for TLR–YFP constructs. We also thank M. Seedorf for sharing his insights on the Ist2p sequence tag and for providing us with Ist2p tag constructs. We thank B. Mueller and J. Loureiro for discussions and critical reading of the manuscript. This study was supported by grants from the NIH (to H.L.P.), the German Research Council (to M.M.B.) and fonds de recherche en sante du Quebec (to M.-E.P.).

**Author Information** Reprints and permissions information is available at www.nature.com/reprints. Correspondence and requests for materials should be addressed to Y.-M.K. (ykim@wi.mit.edu) or H.L.P. (ploegh@wi.mit.edu)

LETTERS

# An allylic ketyl radical intermediate in clostridial amino-acid fermentation

Jihoe Kim[1], Daniel J. Darley[1]†, Wolfgang Buckel[1] & Antonio J. Pierik[1]

**The human pathogenic bacterium *Clostridium difficile* thrives by the fermentation of L-leucine to ammonia, $CO_2$, 3-methylbutanoate and 4-methylpentanoate under anaerobic conditions[1]. The reductive branch to 4-methylpentanoate proceeds by means of the dehydration of (*R*)-2-hydroxy-4-methylpentanoyl-CoA to 4-methylpent-2-enoyl-CoA, which is chemically the most demanding step. Ketyl radicals have been proposed[2] to mediate this reaction catalysed by an iron–sulphur-cluster-containing dehydratase, which requires activation by ATP-dependent electron transfer from a second iron–sulphur protein functionally similar to the iron protein of nitrogenase. Here we identify a kinetically competent product-related allylic ketyl radical bound to the enzyme by electron paramagnetic resonance spectroscopy employing isotope-labelled (*R*)-2-hydroxy-4-methylpentanoyl-CoA species. We also found that the enzyme generated the stabilized pentadienoyl ketyl radical from the substrate analogue 2-hydroxypent-4-enoyl-CoA, supporting the proposed mechanism. Our results imply that also other 2-hydroxyacyl-CoA dehydratases[3] and the related benzoyl-CoA reductases[4]—present in anaerobically living bacteria—employ ketyl radical intermediates. The absence of radical generators such as coenzyme $B_{12}$, *S*-adenosylmethionine or oxygen makes these enzymes unprecedented in biochemistry.**

Radical anions are versatile intermediates in enzymatic reactions because they combine reactivity 'Umpolung'[5], which is polarity inversion, with acid–base catalysis. Thus, the transfer of one electron can reduce an electrophilic carbonyl to a nucleophilic ketyl radical, which is stabilized by the negative charge of the oxygen interacting with the half-filled $2p_z$ orbital at the carbon[6] Ketyl radicals eliminate adjacent leaving groups or are protonated to form neutral radicals. In organic chemistry, the reduction of α-hydroxyketones to unsubstituted ketones by inorganic one-electron donors ($Zn^0$, $Cr^{2+}$ or $Sm^{2+}$) initially converts the ketone to a ketyl capable of expelling the adjacent hydroxyl group. The resulting enoxy radical is reduced to the enolate by a second electron and protonated to the ketone[2]. Similarly, the mechanism of several radical enzymes can be formulated to proceed through ketyl radical intermediates, but experimental evidence for this is lacking[2,7].

Ketyl radicals have also been proposed as intermediates for 2-hydroxyacyl-CoA dehydratases, which are a class of enzymes involved in the fermentation of 12 of the 20 proteinogenic amino acids used by certain anaerobic bacteria[1,3]. The required elimination of the β-hydrogen as a proton ($pK \approx 40$) and removal of the hydroxyl group adjacent to a thioester carbonyl is, in terms of chemistry, a very challenging reaction. It was proposed that the partial positive charge of the carbonyl is reversed by one-electron reduction of the substrate (**1**; Fig. 1) to a substrate-derived ketyl radical (**2**), which expels the α-hydroxyl group. The resulting enoxy radical (**3**), with a much more acidic β-hydrogen ($pK \approx 14$)[8], is deprotonated by a base within the enzyme, yielding the resonance-stabilized, product-related allylic ketyl radical (**4**). A final oxidation leads to the product 2-enoyl-CoA (**5**) with the electron returning to the dehydratase for the next turnover[3].

The anaerobic human pathogenic bacterium *Clostridium difficile* causes hospital-acquired diarrhoea, pseudomembranous colitis and occasionally death[9] by overgrowth in the gastrointestinal tract. Pathogenicity involves the synthesis of virulent toxins[10], the production of noxious *p*-cresol from tyrosine[11] and a large repertoire of amino-acid fermentations[12]. Leucine, which is indispensable for growth, serves as both oxidant and reductant (Stickland reaction[13]); 1 mol is oxidized to ammonia, 3-methylbutanoate and $CO_2$, and 2 mol are reduced to 4-methylpentanoate and ammonia[14]. In the reductive branch, leucine is transaminated to 2-oxo-4-methylpentanoate, which is reduced by NADH and esterified by CoA transfer to (*R*)-2-hydroxy-4-methylpentanoyl-CoA[15]. The subsequent difficult dehydration is catalysed by two oxygen-sensitive proteins: a homodimeric activator and a heterodimeric dehydratase. Activation occurs by ATP-hydrolysis-driven electron transfer from the readily reducible $[4Fe–4S]^{+}/[4Fe–4S]^{2+}$ cluster of the activator to the [Fe–S] cluster of the dehydratase. After such a single activation step, the dehydratase can recycle the electron for about $10^4$ turnovers[16]. After the dehydration to 4-methylpent-2-enoyl-CoA reduction to 4-methylpentanoyl-CoA and CoA transfer lead to liberation of the final product, 4-methylpentanoate[16]

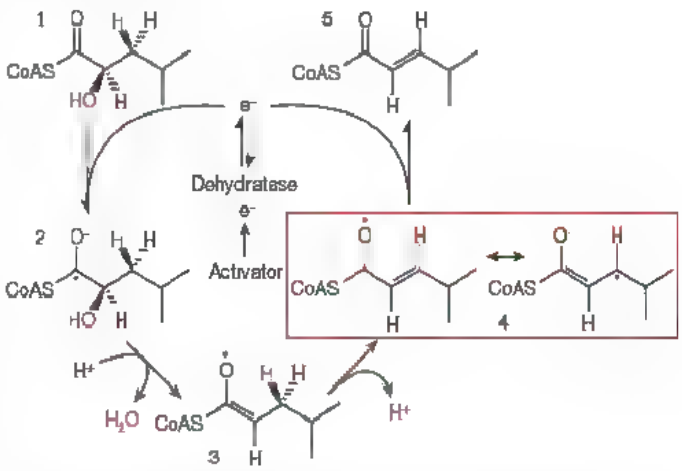


**Figure 1 | Proposed mechanism for the enzymatic dehydration of (*R*)-2-hydroxy-4-methylpentanoyl-CoA.** Substrate (**1**) is converted to 4-methylpent-2-enoyl-CoA (**5**) by 2-hydroxy-4-methylpentanoyl-CoA dehydratase and its activator from *Clostridium difficile* through a substrate-derived ketyl radical (**2**), an enoxy radical (**3**) and a product-related allylic ketyl radical (**4**), the subject of this article, shown in two mesomeric forms. The activator is reduced by ferredoxin or flavodoxin *in vivo*, and by sodium dithionite *in vitro*.

[1]Laboratorium für Mikrobiologie, Fachbereich Biologie, Philipps-Universität, D35032 Marburg, Germany †Present address: Department of Pharmacy and Pharmacology, University of Bath, Claverton Down, Bath BA2 7AY, UK

In the presence of activator, ADP and dithionite as *in vitro* reductant, 2-hydroxy-4-methylpentanoyl-CoA dehydratase did not show a signal by electron paramagnetic resonance (EPR) spectroscopy in the $S = 1/2$ region ($g \approx 2$; Fig. 2a, spectrum 1). The sample exhibited only the $S = 3/2$ signals at $g = 4$–6 (Fig. 2b, spectrum 1) of the $[4Fe–4S]^{+}$ cluster of the activator[17]. Replacement of ADP by ATP reductively activated the dehydratase, which showed a broad $S = 1/2$ EPR signal (Fig. 2a, spectrum 2) with minor changes of the activator signals (Fig. 2b, spectrum 2). Because of the excess of dithionite, the activator remained reduced. The $g$ values (2.03 and 1.92), line width and broadening beyond detection above 20 K are all characteristic features of other $[4Fe–4S]^{+}$ cluster-containing proteins. On addition of the substrate (*R*)-2-hydroxy-4-methylpentanoyl-CoA to the activated dehydratase, the line shape and $g$ values in the EPR spectrum of its $[4Fe–4S]^{+}$ cluster changed substantially. We attribute the change in the $[4Fe–4S]^{+}$ signal to the binding of substrate **1** or product **5** in the non-radical form (Fig. 1). In parallel, a sharp EPR signal with an average $g$ value, $g_{av}$, of 2.0038 ± 0.0002 (mean ± s.e.m.) was formed (Fig. 2a, spectrum 3), which is reminiscent of signals observed with organic radicals[18]. This signal has a microwave power of half-saturation at 10 K of 0.12 ± 0.03 mW and broadened beyond detection at temperatures above 60 K. Magnetic coupling of the radical with a paramagnetic state of the dehydratase (that is, $[4Fe–4S]^{+}$) can be excluded by the minor effect on relaxation and the narrow line width. In contrast, the paramagnetic excited state(s) of the $[4Fe–4S]^{2+}$ cluster at 5–8 Å distance from organic radicals in lysine 2,3-aminomutase[19,20] and coproporphyrinogen III oxidase[21] cause enhanced dipolar relaxation similar to that observed here.

Close inspection of the radical species in the $g = 2$ region revealed two dominating hyperfine splittings from distinct $I = 1/2$ nuclei with coupling constants of 1.45 and 1.15 mT (Fig. 2c, non-labelled), which are values typical for protons[18]. To determine the origin of these two protons, a series of $^{2}H$-labelled substrates were prepared (Supplementary Methods, Supplementary Fig. 1 and Supplementary Table 1) and the effect of labeling on the hyperfine couplings of the EPR signal was determined (Fig. 2c). On $^{2}H$-labelling of the C-2 position (for numbering see Fig. 2d), the magnitude of the two hyperfine couplings remained unchanged and, with the exception of a minor change of the line shape on the high-field side, the overall line width of the EPR signal was also comparable. In contrast, $^{2}H$ at the C-3 or C-4 position led to pronounced changes. In the case of $^{2}H$ at C-3, the proton hyperfine coupling of 1.15 mT disappeared and a single hyperfine coupling of 1.45 mT remained. On $^{2}H$-labelling of the C-4 position, exactly the opposite occurred: the 1.45-mT proton hyperfine coupling was lost and the second splitting was unaffected. Labelling at both the C-3 and C-4 positions abolished both the 1.45-mT and 1.15-mT proton hyperfine couplings. Numeric simulation of the EPR spectra was performed with appropriate downscaling of proton hyperfine couplings by a factor of 6.514 (the $^{1}H/^{2}H$ gyromagnetic ratio[18]). With the same parameters used for the non-labelled substrate, simulations of the EPR spectra of radical species obtained from substrates deuterated at C-3 and C-4 as well as at both of these positions matched the experimental spectra (Fig. 2c, red traces). Washout of $^{2}H$ from both the C-3 and C-4 positions into a protein or organic cofactor-derived radical species could in principle explain our observations. Compelling evidence against such a 'secondary' labelling situation was provided by the marked effect of (*R*)-2-hydroxy-4-methyl[1-$^{13}$C]pentanoyl-CoA, obtained from 2-oxo-4-methyl[1-$^{13}$C]pentanoate, on the EPR signal (Fig. 2c, [1-$^{13}$C]). Successful simulation of the asymmetric EPR signal required a slightly rhombic $g$-tensor ($g_{xyz}$ = 2.0049, 2.0038, 2.0027) and substantial anisotropy of the $^{13}$C hyperfine tensor ($A_{xy}$ = 0.4 mT, $A_z$ = 3.7 mT, $A_{iso}$ = 1.5 mT).

The observed hyperfine couplings define a delocalized spin density minimally residing on carbon atoms 1 and 3. This notion eliminates both the substrate-derived ketyl radical (**2**, Fig. 1) and the enoxy radical (**3**, Fig. 1) as potential candidates, because neither of these radicals can give rise to the experimentally observed 1.45-mT coupling with the proton at C-4. In contrast, the experimentally observed $^{1}H$ and $^{13}C$ hyperfine couplings can be accounted for by the spin densities of the delocalized allylic ketyl radical species (**4**, Figs 1 and 2d). In agreement with this assignment, the experimental $g_{av}$ (2.0038 ± 0.0002) is higher than those of all-carbon (hydroxy)allylic radicals (2.0025–2.0034) and closer to those of allylic *O*/*S*-substituted ketyl radicals in non-biological systems (2.0032–2.0044; Supplementary Table 2). Hyperfine coupling constants of the proton attached to the nodal central carbon atom range from 0.38 to 0.44 mT for all-carbon, or 0.05 to 0.36 mT for *O*/*S*-substituted planar allylic radicals

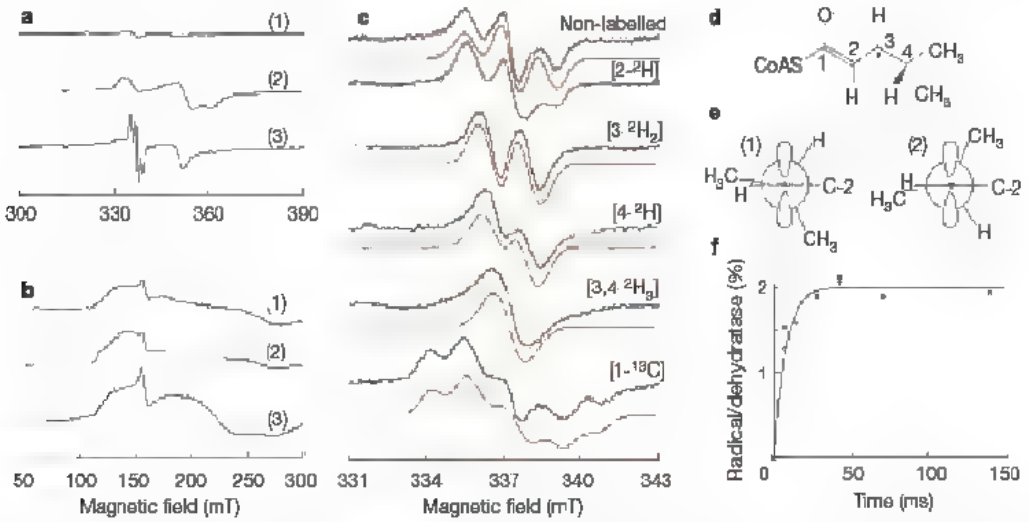


**Figure 2 | EPR spectroscopy of the product-related allylic ketyl radical intermediate in 2-hydroxy-4-methylpentanoyl-CoA dehydratase. a, b,** Low-spin (**a**) and high-spin (**b**) EPR signals of [Fe–S] clusters and organic radical. 2-hydroxy-4-methylpentanoyl-CoA dehydratase and its activator were mixed in the presence of ADP (spectra 1), ATP (spectra 2) or ATP and (*R*)-2-hydroxy-4-methylpentanoyl-CoA (spectra 3). **c,** EPR signals (black) of the organic radical in activated dehydratase in the presence of ATP and (*R*)-2-hydroxy-4-methylpentanoyl-CoA isotopically labelled in the indicated positions (numbering as in **d**). Red traces are simulations of the experimental spectra. **d,** Derived structure of the product-related allylic ketyl radical. **e,** Newman projections along the C-3–C-4 bond of possible conformers 1 and 2. **f,** Formation of the product-related allylic ketyl radical, as determined by rapid freeze-quench EPR spectroscopy. The solid line is a nonlinear least-squared fit of the signal intensity (black circles) as a function of time to a first-order rate equation (for spectra see Supplementary Fig. 3). For synthesis of substrates, sample preparation, EPR conditions and simulation see Methods, Supplementary Text and Supplementary Fig. 1.

(Supplementary Table 2). Thus, the observed lack of a resolved coupling of the proton at C-2 in our system is in perfect agreement with the existence of an allylic ketyl radical. Support is also found in the magnitude of the $^{13}C$ hyperfine coupling constant and absence of coupling with the $CH_2$ moiety of CoA (see Supplementary Discussion and Supplementary Tables 3 and 4).

The conformation of the isopropyl moiety in the product-related radical bound to the dehydratase could be determined from the angular dependence of the hyperfine coupling of the $^1H$ attached to C-4. From the McConnell equation, $A^1_H = \rho(0.092 + 4.2\cos^2\theta)$ (where $\theta$ is the dihedral angle and $\rho$ is the spin density, assumed to be $0.5 \pm 0.1$)[19], and the 1.45-mT proton hyperfine coupling constant, four possible dihedral angles between the $\pi$ orbital at C-3 and C4-H can be calculated: +35, −35, +145 and −145° (all ±10°). If we restrict $\theta$ to values for which energetically unfavourable steric repulsion of the methyl groups with C2-H of the allyl group is avoided, two conformers are possible: +35 and +145° (Fig. 2e, conformers 1 and 2, respectively).

For samples prepared under a broad variety of experimental conditions, a maximal allylic ketyl radical content of (2.1 ± 0.4)% was calculated from double integration and calibration with a $Cu^{2+}$ EPR standard. At time scales from 20 to 250 s, the intermediate slowly decayed, probably because of side reactions of the radical (Supplementary Fig. 2, about 0.004 $s^{-1}$). To assess the mechanistic relevance of this observation, the rate of formation of this partly populated intermediate was measured after mixing the activated dehydratase with its natural substrate (*R*)-2-hydroxy-4-methylpentanoyl-CoA (Fig. 2f). The intermediate was trapped by rapid freeze-quenching of the reaction mixture in liquid-nitrogen-cooled isopentane (about 130 K). Even at the shortest reaction time point accessible (7 ms), the characteristic EPR signal of the allylic ketyl radical with spectral properties indistinguishable from manually mixed samples (at least 15 s) was detected (Supplementary Fig. 3). The same fractional population of the allylic ketyl radical was seen for all time points longer than 40 ms. From the observed time dependence for the development of the radical (7–40 ms), a formation rate of 140 ± 30 $s^{-1}$ was estimated (Fig. 2f). This rate is as high as steady-state enzymatic turnover (150 $s^{-1}$) and therefore shows kinetic competence of the radical intermediate. Radical 4 is therefore a genuine intermediate but has a low population under turnover conditions. Apparently the electron is mainly located at the [4Fe–4S] cluster.

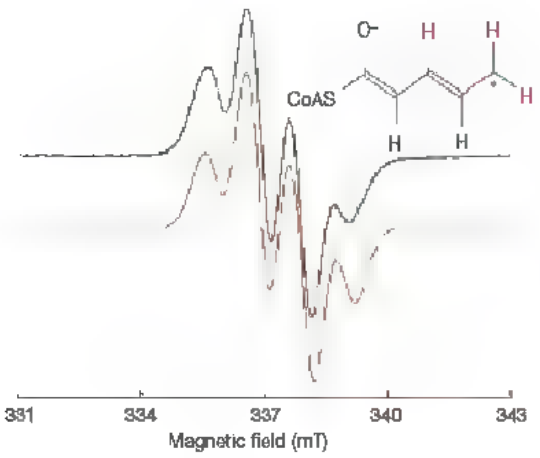


**Figure 3 | EPR spectrum of the pentadienyl ketyl radical formed from the 2-hydroxypent-4-enoyl-CoA substrate analogue.** On incubation of activated 2-hydroxy-4-methylpentanoyl-CoA dehydratase with 2-hydroxypent-4-enoyl-CoA, an intense radical EPR signal is generated (black trace). The spectrum can be simulated (red trace) with hyperfine splitting parameters appropriate for the pentadienyl ketyl radical structure (inset). For experimental details and simulation see Methods.

Support for the catalytic competence of the allylic ketyl radical intermediate was gained by the effect of the substrate analogue 2-hydroxypent-4-enoyl-CoA on the dehydratase. The molecule was predicted to arrest catalysis because the resonance-stabilized pentadienyl ketyl radical intermediate (Fig. 3, inset) would be too stable to undergo reoxidation to the product. Steady-state kinetics did indeed reveal that 2-hydroxypent-4-enoyl-CoA acted as a potent inhibitor, competitive with the natural substrate ($K_i = 62$ μM). Incubation with the dehydratase gave rise to an EPR signal (Fig. 3) that, also on rapid freeze-quenching, amounted to (12 ± 1)% of the enzyme concentration. The value of $g_{av}$ (2.0030 ± 0.0002) and estimated isotropic proton hyperfine couplings (1.11, 0.96 and 0.88 mT) match those expected for the pentadienyl ketyl radical (Supplementary Table 5). In particular, the intermediacy of the 5′-deoxyadenosyl radical in adenosylcobalamin-dependent and *S*-adenosylmethionine-dependent radical enzymes was demonstrated by a similar methodology with anhydroadenosyl derivatives[20]. In such systems, the stability of a crucial but undetectable intermediate was increased as a result of resonance-stabilization of an allylic radical species.

Most of the radical enzymes described previously[22] require either preformed biradical oxygen or homolysis of covalent bonds in the special cofactors coenzyme $B_{12}$ or *S*-adenosylmethionine for radical generation. Here we have shown experimentally that under anaerobic conditions an enzyme can generate a radical intermediate with an iron–sulphur cluster as a prosthetic group and a single electron as a cofactor. This mechanism could represent an ancient way of radical formation preceding the evolution of other, more recent, types of radical generator. The consumption of valuable proteinogenic amino acids and the production of short-chain fatty acids seem to be an unlikely evolutionary driver of the 2-hydroxyacyl-CoA dehydratases. Rather, because dehydration of 2-hydroxyacyl-CoA is a reversible reaction[23], involvement in primordial amino acid biosynthesis from 2-enoates seems a more likely possibility.

## METHODS SUMMARY

All manipulations were performed under strictly anaerobic conditions in an anaerobic glove box (Coy Laboratories). For handling outside the glove box, the samples were protected from air by anaerobic manipulation by using syringes with Teflon plunger tips and employing glass vials tightly stoppered with rubber bungs. 2-Hydroxy-4-methylpentanoyl-CoA dehydratase was purified[16] from *C. difficile* (DSMZ 1296T) and its activator was obtained[16] from *Escherichia coli* by overexpression of the gene. After activation of dehydratase (66 μM) for 5 min at 23 °C with an equimolar concentration of activator, the CoA ester (final concentration 1 mM) was added and the sample was frozen in a quartz tube. EPR spectra were recorded on a Bruker EMX 6/1 spectrometer with a standard TE102 rectangular cavity, cooled by an Oxford Instruments ER-4112HV helium-flow cryostat and simulated with the program SAE07 supplied by S. P. J. Albracht[24]. For rapid freeze-quenching, activated dehydratase was mixed with an equal volume of CoA ester in an SFM-20 instrument interfaced with MPS32 software (BioLogic) and frozen in liquid-nitrogen-cooled isopentane. All reported errors are s.e.m.

**Full Methods** and any associated references are available in the online version of the paper at www.nature.com/nature.

**Received 6 August 2007; accepted 10 January 2008.**

1. Buckel, W. in *Biology of the Prokaryotes* (eds Lengeler, J. W., Drews, G. & Schlegel, H. G.) 278–326 (Thieme, Stuttgart, 1999)
2. Buckel, W. & Keese, R. One electron redox reactions of CoASH esters in anaerobic bacteria. A mechanistic proposal. *Angew. Chem. Int. Edn Engl.* 34, 1502–1506 (1995)
3. Buckel, W., Hetzel, M. & Kim, J. ATP-driven electron transfer in enzymatic radical reactions. *Curr. Opin. Chem. Biol.* 8, 462–467 (2004)
4. Boll, M. & Fuchs, G. Unusual reactions involved in anaerobic metabolism of phenolic compounds. *Biol. Chem.* 386, 989–997 (2005)
5. Seebach, D. Methods of reactivity umpolung. *Angew. Chem. Int. Edn Engl.* 18, 239–258 (1979)
6. Brückner, R. *Reaktionsmechanismen* (Spektrum Akademischer, Heidelberg, 2003).
7. Buckel, W. & Golding, B. T. Radical enzymes in anaerobes. *Annu. Rev. Microbiol.* 60, 27–49 (2006).

8 Smith, D. M., Buckel, W. & Zipse, H. Deprotonation of enoxy radicals: theoretical validation of a 50-year-old mechanistic proposal. *Angew. Chem. Int. Edn Engl.* **42**, 1867–1870 (2003)
9 Sebaihia, M. & Thomson, N. R. Colonic irritation. *Nature Rev. Microbiol.* **4**, 882–883 (2006).
10. Reineke, J. *et al.* Autocatalytic cleavage of *Clostridium difficile* toxin B. *Nature* **446**, 415–419 (2007)
11 Selmer, T. & Andrei, P. I. *p*-Hydroxyphenylacetate decarboxylase from *Clostridium difficile*. A novel glycyl radical enzyme catalysing the formation of *p*-cresol. *Eur. J. Biochem.* **268**, 1363–1372 (2001)
12. Sebaihia, M. *et al.* The multidrug-resistant human pathogen *Clostridium difficile* has a highly mobile, mosaic genome. *Nature Genet.* **38**, 779–786 (2006).
13. Barker, H. A. Amino acid degradation by anaerobic bacteria. *Annu. Rev. Biochem.* **50**, 23–40 (1981)
14. Elsden, S. R. & Hilton, M. G. Volatile acid production from threonine, valine, leucine and isoleucine by clostridia. *Arch. Microbiol.* **117**, 165–172 (1978).
15. Kim, J., Darley, D., Selmer, T. & Buckel, W. Characterization of (*R*)-2-hydroxyisocaproate dehydrogenase and a family III coenzyme A transferase involved in reduction of L-leucine to isocaproate by *Clostridium difficile*. *Appl. Environ. Microbiol.* **72**, 6062–6069 (2006)
16. Kim, J., Darley, D. & Buckel, W. 2-Hydroxyisocaproyl-CoA dehydratase and its activator from *Clostridium difficile*. *FEBS J.* **272**, 550–561 (2005).
17 Hans, M., Buckel, W. & Bill, E. The iron–sulfur clusters in 2-hydroxyglutaryl-CoA dehydratase from *Acidaminococcus fermentans*. Biochemical and spectroscopic investigations. *Eur. J. Biochem.* **267**, 7082–7093 (2000).
18. Weil, J. A. & Bolton, J. R. *Electron Paramagnetic Resonance: Elementary Theory and Practical Applications* 2nd edn (Wiley, Bognor Regis, 2007)
19. Wu, W. *et al.* Lysine 2,3-aminomutase and trans-4,5-dehydrolysine: characterization of an allylic analogue of a substrate-based radical in the catalytic mechanism. *Biochemistry* **39**, 9561–9570 (2000)
20. Magnusson, O. T., Reed, G. H. & Frey, P. A. Characterization of an allylic analogue of the 5′-deoxyadenosyl radical: an intermediate in the reaction of lysine 2,3-aminomutase. *Biochemistry* **40**, 7773–7782 (2001)
21. Layer, G. *et al.* The substrate radical of *Escherichia coli* oxygen-independent coproporphyrinogen III oxidase HemN. *J. Biol. Chem.* **281**, 15727–15734 (2006)
22 Stubbe, J. & Van der Donk, W. A. Protein radicals in enzyme catalysis. *Chem. Rev.* **98**, 705–762 (1998)
23 Buckel, W. The reversible dehydration of (*R*)-2-hydroxyglutarate to (*E*)-glutaconate. *Eur. J. Biochem.* **106**, 439–447 (1980).
24. Beinert, H. & Albracht, S. P. J. New insights, ideas and unanswered questions concerning iron–sulfur clusters in mitochondria. *Biochim. Biophys. Acta* **683**, 245–277 (1982)

**Supplementary Information** is linked to the online version of the paper at www.nature.com/nature.

**Acknowledgements** We thank R. K. Thauer for the use of his EPR spectrometer, and V. Schünemann and M. Bennati for the use of their freeze-quench instruments.

**Author Information** Reprints and permissions information is available at www.nature.com/reprints. Correspondence and requests for materials should be addressed to A.J.P. (perik@staff.uni-marburg.de)

LETTERS

# Transcriptional repression mediated by repositioning of genes to the nuclear lamina

K. L. Reddy[1,2], J. M. Zullo[1,2], E. Bertolino[2] & H. Singh[1,2]

**Nuclear compartmentalization seems to have an important role in regulating metazoan genes[1,2]. Although studies on immunoglobulin and other loci have shown a correlation between positioning at the nuclear lamina and gene repression, the functional consequences of this compartmentalization remain untested[2,3]. We devised an approach for inducible tethering of genes to the inner nuclear membrane (INM), and tested the consequences of such repositioning on gene activity in mouse fibroblasts. Here, using three-dimensional DNA-immunoFISH, we demonstrate repositioning of chromosomal regions to the nuclear lamina that is dependent on breakdown and reformation of the nuclear envelope during mitosis. Moreover, tethering leads to the accumulation of lamin and INM proteins, but not to association with pericentromeric heterochromatin or nuclear pore complexes. Recruitment of genes to the INM can result in their transcriptional repression. Finally, we use targeted adenine methylation (DamID) to show that, as is the case for our model system, inactive immunoglobulin loci at the nuclear periphery are contacted by INM and lamina proteins. We propose that these molecular interactions may be used to compartmentalize and to limit the accessibility of immunoglobulin loci to transcription and recombination factors.**

In mammalian nuclei, chromatin is organized into structural domains by association with distinct nuclear compartments[2]. Several studies have shown a correlation between the transcriptional repression of mammalian genes and their positioning at the nuclear periphery[3–7]. In yeast, the nuclear periphery is comprised of at least two sub-compartments: a repressive compartment consisting of foci of silencing factors, and a permissive compartment involving nuclear pore complexes (NPCs) that facilitates gene expression[8–10]. However, metazoan systems exhibit a greater complexity of nuclear compartments and chromosome organization. The nuclear periphery in mammalian cells is constituted by a distinct set of INM proteins, such as LBR, LAP2 and emerin (EMD), as well as an underlying nuclear lamina, which have been proposed to interact with transcriptional repressors[11–14]. The ability of this nuclear compartment to regulate gene activity has not been functionally tested in metazoan cells[2].

We designed a two-component inducible system that would relocalize an integrated reporter gene from the interior of a mammalian nucleus to the INM (Fig. 1a). The reporter construct is comprised of the herpes simplex virus thymidine kinase promoter and the hygromycin resistance gene (*Tk-hyg*) as well as a nearby array of Lac operators (*lacO*) that constitute binding sites for the *Escherichia coli* Lac repressor (LacI) (Fig. 1 and Supplementary Fig. 1a)[4,5]. The second component is either a nucleoplasmic green fluorescent protein (GFP)–LacI that binds *lacO* sites and enables visualization of the reporter gene or a tethering protein GFP–LacI–ΔEMD that is targeted to the INM by means of a carboxy-terminal segment of EMD[16]. The GFP fusion proteins were stably expressed in NIH3T3 fibroblast clones harbouring the reporter gene(s) integrated at single (S) or multiple (M) chromosomal sites. Reporter gene visualization and/or repositioning were controlled using the allosteric inhibitor IPTG (isopropyl β-D-1-thiogalactopyranoside), which regulates LacI binding to *lacO* sites. The initial disposition of the integrated reporter genes was analysed in cells stably expressing GFP–LacI. Up to four bright GFP foci were visible in clone-M nuclei because these cells have four integration sites, each containing multiple copies of the reporter gene (Supplementary Fig. 1d, e). In contrast, clone-S nuclei exhibited dimmer single GFP foci owing to a single site of insertion with fewer copies (1–2) of the reporter (Supplementary Fig. 1c, d). We next generated clone-M and clone-S derivatives stably expressing GFP–LacI–ΔEMD. As anticipated, this tethering protein localized to the INM. On removal of IPTG, large GFP foci were observed at the nuclear periphery in clone-M but not in clone-S cells expressing GFP–LacI–ΔEMD (Supplementary Fig. 1e). This suggested that the reporter genes were being repositioned to the nuclear membrane in clone-M cells.

Not all tethered reporter genes were expected to accumulate the fusion protein at levels that are discernable as fluorescent signals above the distribution in the INM. This was probably the case for clone-S cells. Therefore, we undertook fluorescent DNA *in situ* hybridization on three-dimensional preserved nuclei (3D DNA-immunoFISH) to assess quantitatively the disposition of all *Tk-hyg* integrations (Fig. 1b, c and Supplementary Fig. 2). Under control conditions, the integrated reporter genes were distributed throughout the nucleoplasm, with approximately 25–30% being positioned near the nuclear periphery (Fig. 1d). This frequency represents the initial sub-nuclear distribution and is similar to that observed for endogenous genes that are not associated with the nuclear periphery[17]. On withdrawal of IPTG, most *Tk-hyg* insertions were found to be associated with the nuclear lamina in clone-M (70%) and clone-S (90%) cells expressing GFP–LacI–ΔEMD. Moreover, in clone-M cells, reporter genes residing on different chromosomes were repositioned to distinct regions of the INM in a single nucleus (Fig. 1b). In clone-S cells, repositioning was mediated by fewer copies of the *lacO* segments (1–2) compared with in clone-M cells (~25 copies per integration site, Supplementary Fig. 1d). We note that repositioning requires breakdown and reformation of the nuclear envelope during mitosis (Supplementary Fig. 3 and Supplementary Discussion). These data provide the first demonstration of directed repositioning of chromosomal segments to the INM–lamina compartment, and suggest that an intervening cell cycle may be necessary for such re-configuration.

We next analysed the consequences of accumulating GFP–LacI–ΔEMD at sites of tethering on the disposition of other proteins at the INM. Lamin A and B1, key components of the lamina, and the INM protein LAP2 accumulated at sites of tethering (Fig. 2a and Supplementary Fig. 4). No such interactions were observed on non-tethered

[1]Howard Hughes Medical Institute, [2]Department of Molecular Genetics and Cell Biology, The University of Chicago, GCIS W522, 929 East 57th Street, Chicago, Illinois 60637, USA

chromosomal segments bearing *lacO* sites. Interestingly, NPCs did not accumulate around the tethered chromatin domains and, in approximately half of the nuclei, NPCs were diminished at these regions (Fig. 2b). Furthermore, the tethered loci were not preferentially associated with pericentromeric heterochromatin in either clone-M or clone-S cells (Supplementary Fig. 5). Our results suggest that local accumulation of EMD by means of an association with chromatin can nucleate the assembly of specific INM and lamin components.

The accumulation of INM–lamina components at sites of tethering may not necessarily reflect molecular interactions with the underlying chromosomal DNA. Furthermore, in clone-S cells, the accumulation of INM and lamin proteins could not be monitored by means of immunofluorescence. Therefore, we used the DamID methodology to detect INM–lamina protein interactions with the test gene upon tethering[18]. EMD and lamin B1 (LMNB1) fusion proteins containing the *E. coli* DNA adenine methyltransferase

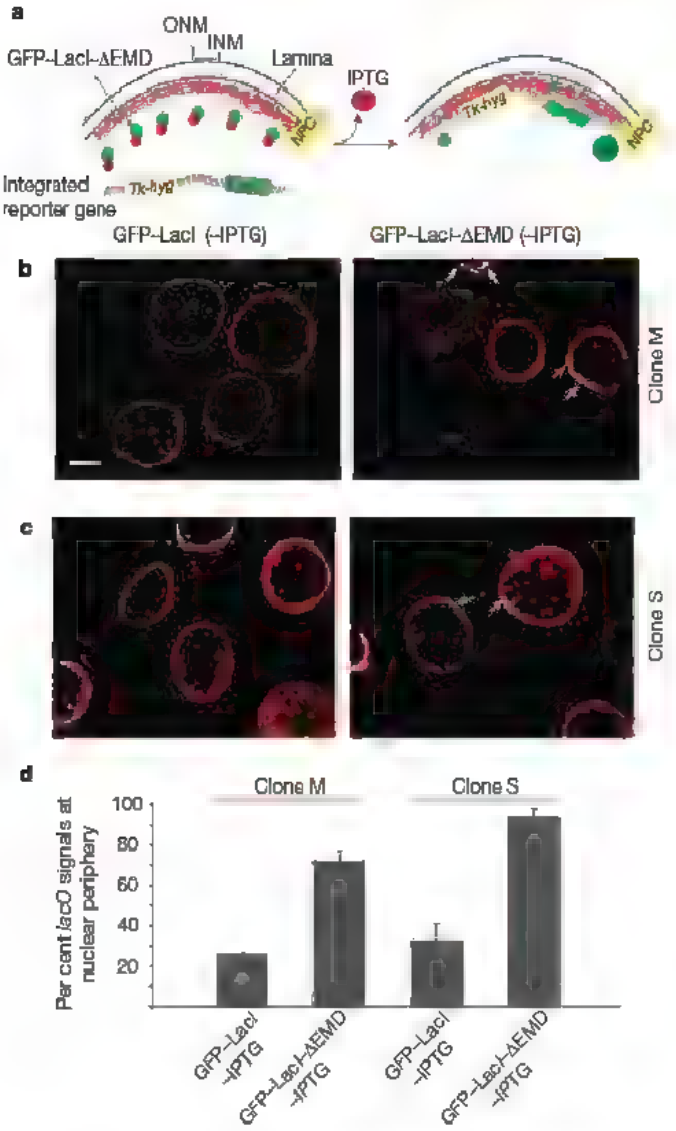


**Figure 1 | Quantitative analysis of tethered loci by 3D DNA-immunoFISH.** **a**, The stably integrated reporter gene contains an array of *lac* operators. The GFP–LacI–ΔEMD tethering protein is targeted to the INM and is unable to bind *lacO* sites in the presence of IPTG (red circles with cross in the centre). Upon withdrawal of IPTG, the tethering protein can bind to *lacO* sites in the integrated reporter gene construct. This interaction is anticipated to result in tight association of the reporter gene with the INM. (see also Supplementary Fig. 1e). ONM, outer nuclear membrane. **b**, Positioning of integrated reporter genes in clone-M nuclei detected by 3D DNA-immunoFISH. Shown is the nuclear distribution of *lacO*-bearing reporter genes in clone-M cells expressing GFP–LacI (left), and the repositioning of reporter genes in clone-M cells expressing GFP–LacI–ΔEMD upon IPTG withdrawal (24 h, right). Two confocal image planes of the same sets of nuclei are shown. In **a** and **b**, arrows mark co-localization of the *lacO* FISH signals with the nuclear lamina. Scale bar, 5 μm. **c**, Positioning of integrated reporter genes in clone-S nuclei. Single confocal planes of clone S cells expressing either GFP–LacI (–IPTG) or GFP–LacI–ΔEMD (–IPTG) are shown. **d**, The percentage of *lacO* signals at the nuclear periphery was determined by co-localization with LMNB1. In a given nuclear volume, *lacO* and LMNB1 signal intensities were converted to histograms. *lacO* signals were scored as peripheral if their peak intensity overlapped with LMNB1 (see Supplementary Fig. 2). The standard error bars indicate the deviation between two experiments under the indicated conditions. In a given experiment, either 50 (clone M) or 30 (clone S) nuclei were analysed for each condition.

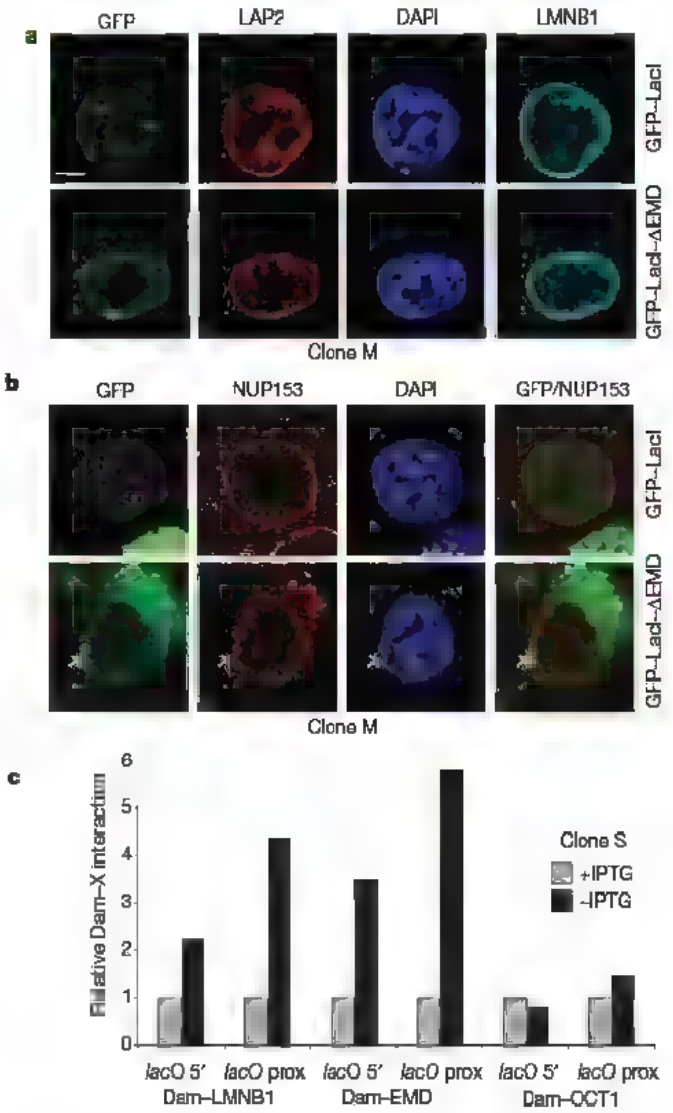


**Figure 2 | Lamin B, EMD and LAP2, but not NPCs, accumulate at sites of tethered foci.** **a**, **b**, Shown are *lacO* insertions detected by GFP fluorescence in clone-M cells expressing either GFP–LacI or GFP–LacI–ΔEMD upon IPTG withdrawal (24 h). Antibodies directed against LMNB1 (**a**, cyan), LAP2 (**a**, red) or NUP153 (**b**, red) were used to analyse accumulation of these components at sites of tethered *lacO* foci (arrows). The DNA-specific dye, DAPI (4′,6-diamidino-2-phenylindole), was used to stain the nuclei. All images shown are single confocal sections. Arrows mark tethered loci. Scale bar, 5 μm. **c**, Molecular interactions of LMNB1, EMD and OCT1 with the reporter gene, detected by DamID-mediated methylation, in clone-S nuclei. All interactions were normalized to the signal from cells tranduced with Dam alone. Untethered test genes (+IPTG) were set to one after normalization, the *y*-axis indicates the fold change in the Dam–X signal (where X is LMNB1, EMD or OCT1) upon tethering (−IPTG). A representative experiment is shown. *lacO 5′* and *lacO* prox are PCR primer pairs that are positioned upstream or downstream of the *lacO* arrays, respectively.

(Dam) were expressed in clone-M and close-S cells. We detected an increase in Dam–EMD- and Dam–LMNB1-mediated methylation of the reporter genes upon tethering (Fig. 2c and Supplementary Fig. 4b). Collectively, these data show that tethering of a chromosomal segment to the INM facilitates the localized recruitment of lamin and INM proteins to the DNA.

To test the consequence of repositioning of reporter genes to the INM, we analysed transcript levels of *hyg* (Fig. 3a and Supplementary Fig. 6). Upon tethering, *hyg* gene activity was repressed in clone-M and clone-S cells. Importantly, binding of nucleoplasmic GFP–LacI molecules to *lacO* sites in the reporter construct did not impair *hyg* expression (Supplementary Fig. 6). The EMD segment (Δ1–64) used in tethering lacks a domain required for interaction with transcriptional repressors[19]. Nevertheless, to rule out the possibility that this segment was mediating repression in the absence of repositioning to the nuclear lamina, we generated a nucleoplasmic version that lacks the C-terminal transmembrane domain necessary for targeting to the INM (GFP–LacI–ΔEMD*). Importantly, GFP–LacI–ΔEMD* did not repress the *hyg* gene (Supplementary Fig. 6). We next performed single-cell analysis using 3D RNA-immunoFISH. This enabled direct comparison of the transcriptional activity of untethered versus tethered loci. Most of the GFP–LacI foci (70%) were associated with *hyg* RNA signals (Fig. 3b). In contrast, most of the tethered, GFP–LacI–ΔEMD-bound loci (80%) showed no or reduced *hyg* RNA signals. We note that in GFP–LacI–ΔEMD-expressing cells, not all loci are tethered (Fig. 1d), and consequently *hyg* signals were observed emanating from them (Fig. 3b). Collectively, these results demonstrate that the test gene undergoes transcriptional repression as a consequence of repositioning to the INM.

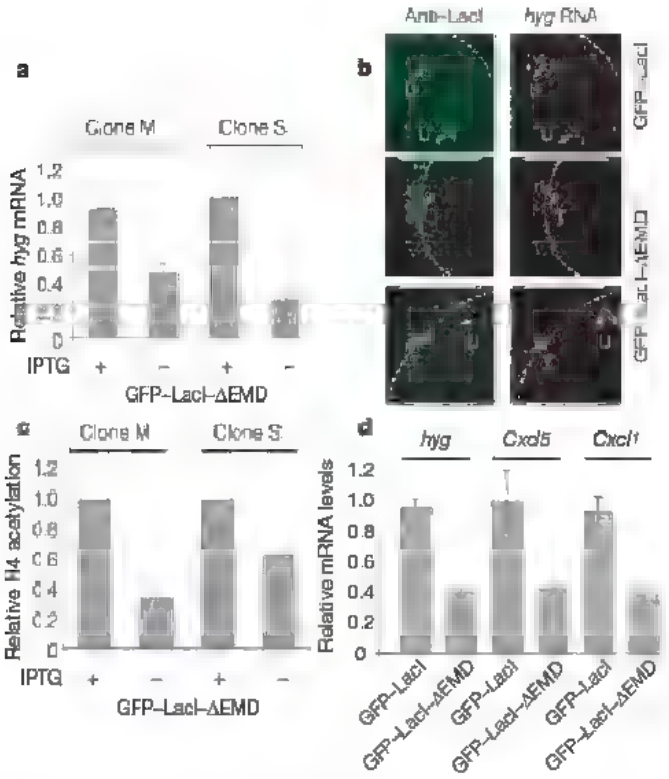


**Figure 3 | Tethering leads to transcriptional repression and histone deacetylation of genes at site of attachment to the INM.** **a**, Relative transcript levels of the *hyg* reporter gene were measured in clone-M and clone-S cells by Q-PCR under non-tethering (+IPTG) versus tethering (−IPTG) conditions. Transcript levels were normalized to endogenous mouse *Hprt1* messenger RNA. **b**, Three-dimensional RNA-immunoFISH was performed on clone-M cells under non-tethering (GFP–LacI, −IPTG) versus tethering (GFP–LacI–ΔEMD, −IPTG) conditions. Foci detected by a LacI antibody (green) were scored for association with nascent *hyg* transcripts (red). Upper panels show untethered loci bound by GFP–LacI. The middle and lower panels show tethered (T) and untethered (U) foci in nuclei under tethering conditions. The dashed line indicates the edge of the nuclei, as determined by DAPI staining. **c**, Cross-linked chromatin from the indicated cells was immunoprecipitated using an antibody to acetylated histone H4. The histogram shows relative H4 acetylation levels of the HSV-TK promoter region of the test gene under the indicated conditions after normalization to the β-actin promoter. **d**, Q-PCR analysis of *hyg*, *Cxcl1* and *Cxcl5* mRNA in clone-M cells under the indicated conditions. Transcript levels were normalized to *Hprt1* mRNA. Error bars indicate the standard deviation between three experiments.

Given the evidence that genes associated with the nuclear lamina are hypo-acetylated and that LAP2β interacts with HDAC3, we determined the consequences of tethering on the H4 acetylation status of our reporter gene (Fig. 3c)[12,20]. The untethered promoter region displayed a high degree of acetylation. Upon tethering, a decrease in histone H4 acetylation was observed. Thus, the transcriptional repression caused by tethering of a gene to the INM is accompanied by histone H4 hypo-acetylation.

We next explored if endogenous genes flanking a *lacO* insertion site might also be repressed on relocalization to the INM; we did this by surveying clone-M cells using genome-wide expression analysis. We identified 51 genes that were repressed under tethering conditions including a pair on chromosome 5 (*Cxcl1* and *Cxcl5*, Supplementary Fig. 7a). Transcriptional repression of the *Cxcl1* and *Cxcl5* genes was verified by quantitative PCR (Q-PCR, Fig. 3d). Importantly, a bacterial artificial chromosome (BAC) probe covering this region co-localized with a *lacO* integration site (Supplementary Fig. 7b). In clone-S cells, the test gene is inserted 227 kb away from the nearest gene whose activity was unaffected by tethering (data not shown). These results show that endogenous flanking genes can be repressed by tethering to the INM, and suggest that a delimited inactive chromosomal domain may be generated around a site of attachment.

As is the case for our tethered test gene, transcriptionally inactive and hypo-acetylated immunoglobulin heavy chain (*Igh*) loci in NIH3T3 fibroblasts and in T cells are positioned at the nuclear lamina (Fig. 4a and data not shown)[3]. Therefore, we used the aforementioned Dam-fusion proteins to test if the *Igh* loci in NIH3T3 cells were in molecular contact with the INM–lamina. We note that the Dam–OCT1 (also known as POU2F1) fusion protein monitors the accessibility of immunoglobulin loci at the nuclear periphery because OCT1 is a transcription factor that binds to *VH* gene promoters and regulates their activity[21]. For DamID, we used primers spanning a domain of the *Igh* locus containing the *VHJ558* gene family, implicated in mediating association with the nuclear periphery[17,21]. Both LMNB1 and EMD were seen to interact with peripherally positioned *VH* genes in NIH3T3 nuclei (Fig. 4a). These interactions were not limited to the *Igh* gene promoters (*VHJ558* and *VHJ558a*), but were also detected in an intergenic region (*VHI–C*) of this *VH* gene family, suggesting multiple contacts with the INM and lamina over a genomic region spanning at least 400 kb (ref. 22). Importantly, no interaction was detected at a region upstream (HS1, 42 kb) of the *VHJ558* gene family[23]. Thus, the observed contacts of the *Igh* locus with the INM are not simply caused by cytological proximity, but probably reflect specific molecular interactions. Importantly, such INM–lamina contacts were not seen in pro-B nuclei (Fig. 4b). At this developmental stage, the *Igh* loci are transcriptionally active and positioned away from the nuclear periphery. As expected, OCT1 was seen to interact with the U7 small nuclear RNA gene promoter in both cell types. In contrast, OCT1 could access the *VH* gene promoters in pro-B but not in NIH3T3 nuclei. These findings demonstrate cell-type-specific molecular interactions of EMD and LMNB1 with an endogenous locus. We suggest that, similar to our test gene, such interactions with the INM–lamina may establish an inactive state that inhibits access of transcriptional activators and the recombination machinery to *Igh* loci.

How does attachment of a mammalian gene to the INM promote its repression? Two possibilities include, first, sequestration from the RNA Pol II apparatus and, second, assembly of a repressive

chromatin structure. In support of the former, the β-globin locus moves away from the nuclear periphery and engages with centrally positioned RNA Pol II factories to enable high levels of transcription[24]. Initial activation of this locus at the periphery may involve an association with NPC, as has been observed for yeast and *Drosophila* genes[9,10,25]. This mode of gene activation could also account for the behaviour of other mammalian genes that have been reported to be active while positioned at the nuclear periphery[4,26]. In support of the second possibility, we note that INM proteins interact with transcriptional co-repressors and chromatin-modifying enzymes[12–14]. Because tethering of a chromosomal region to the nuclear membrane by interactions with EMD can result in the accumulation of lamin A, lamin B and LAP2, we suggest that such self-reinforcing protein–DNA and protein–protein interactions could result in the establishment of a distinct repressive chromatin structure. We note the *lacO* arrays used in our test gene may poise it to undergo repression on association with the INM. Nevertheless, our results suggest the existence of DNA elements that function to repress gene activity by tethering chromosomal regions to the INM–lamina. Consistent with this possibility, genome-wide analysis in *Drosophila* cells has revealed clusters of transcriptionally silent and hypo-acetylated genes that interact with LMNB1 and are positioned at the nuclear periphery[20]. We propose that the INM–lamina compartment, which is a distinctive structural feature of metazoan nuclei, can be used to assemble repressive peripheral chromatin domains.

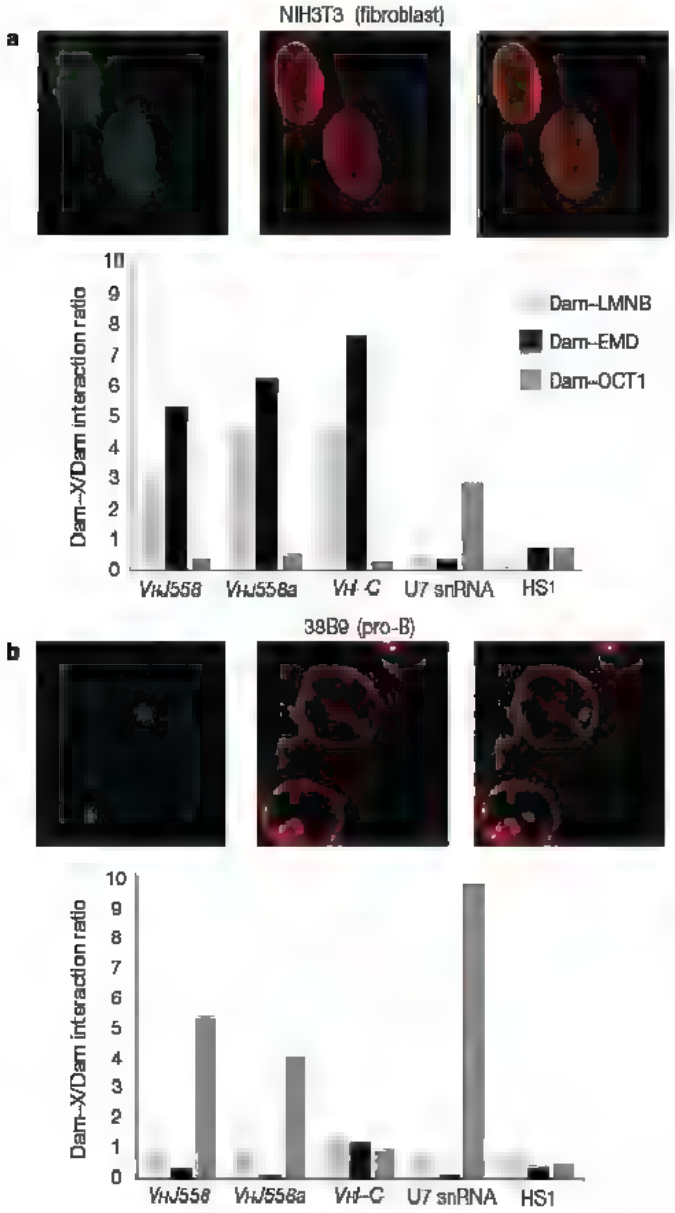


**Figure 4 | Inactive immunoglobulin heavy chain loci that are positioned at the nuclear periphery contact the nuclear lamina. a,** Interaction of *Igh* loci with the INM detected by 3D DNA-immunoFISH and DamID in NIH3T3 nuclei. The upper panel shows that a BAC probe hybridizing to the distal region of the *Igh* locus (green) colocalizes with the nuclear lamina (LMNB1, red). The lower panel shows the molecular interactions of LMNB1 and EMD with the *Igh* loci in NIH3T3 nuclei detected by DamID-mediated methylation. Signals were normalized to a Dam-only control, and therefore the *y*-axis indicates the ratio of Dam–X (where X is LMNB1, EMD or OCT1) divided by the Dam-only signal. *VHJ558* and *VHJ558a* correspond to promoter regions in the *Igh VH* region, whereas the *VH* intergenic region (*VHI–C*) is positioned 400 kb away from *J558a*. HS1 is a hypersensitive site immediately upstream of the most distal *VHJ558* gene. The U7 snRNA genes are ubiquitously expressed and are regulated by OCT1. A representative experiment is shown. **b,** Interaction of the *Igh* loci with the INM detected by 3D DNA-immunoFISH and DamID in 38B9 pro-B-cell nuclei. In the upper panel, *Igh* loci and the nuclear lamina were detected by 3D DNA-immunoFISH as in **a**. The lower panel shows molecular interactions of OCT1, LMNB1 and EMD at *Igh* loci in 38B9 pro-B cells detected by DamID (normalized as above). In pro-B cells, *VH* promoters are activated by OCT1

## METHODS SUMMARY

*Tk hyg lacO* was constructed by modifying pSV2-DHFR 8.32 from A. Belmont[25]. The pMSCV(puro)eGFP–LacI retroviral vector was constructed using GFP LacI from p3′ssEGFP–LacI. EGFP LacI ΔEMD and EGFP LacI ΔEMD* were generated by in-frame fusion with EGFP–LacI.

Immunofluorescence was performed using standard laboratory protocols[27]. Immunofluorescence coupled with 3D DNA-immunoFISH was performed as described previously[21]. Two-dimensional FISH procedures were performed as described previously[5]. Probes to the *lacO* sites and the *Cxd5* genomic region (RP23-307P18) were generated by nick translation (Roche) with Alexafluor-568 (Molecular Probes) or biotin-labelled nucleotides. For RNA FISH, cells were plated, fixed and permeabilized as described previously[28]. All reagents were treated with DEPC to ensure RNase-free conditions. All DNA probes were labelled by nick translation (Roche) with Alexafluor-568 (Invitrogen), biotin or digoxigenin (Roche) nucleotides. Protein-antigen detection was performed as described for immunofluorescence. Images were obtained by laser scanning confocal microscopy using a Leica SP2 AOBS (University of Chicago, Digital Light Microscopy Facility) and an Olympus Fluoview 1000. For quantitative image analysis, 3D DNA-immunoFISH samples were imaged at ×100 using a ×2 optical zoom, with a *z*-step of 0.2 μm between optical slices.

RNA was prepared using TRIzol reagent (Invitrogen), and complementary DNA was generated using SuperScriptII reverse transcriptase (Invitrogen). Q-PCR experiments were performed on a Stratagene Mx4000 machine using SYBR green dye master mix (Stratagene). All reactions were compared to a standard curve to enable determination of the relative copy number.

For microarray analysis, RNA was prepared using TRIzol reagent. Probe preparation, hybridization and initial analyses were carried out by the Functional Genomics Facility at the University of Chicago. Two or more genes within 500 kb were scored as a cluster.

DamID was performed as described previously using self-inactivating retroviral vectors for transduction[21].

**Received 7 November 2007; accepted 23 January 2008.**
**Published online 13 February 2008.**

1. Lanctot, C., Cheutin, T., Cremer, M., Cavalli, G. & Cremer, T. Dynamic genome architecture in the nuclear space: regulation of gene expression in three dimensions. *Nature Rev. Genet.* 8, 104–115 (2007).
2. Misteli, T. Beyond the sequence: cellular organization of genome function. *Cell* 128, 787–800 (2007).
3. Kosak, S. T. *et al.* Subnuclear compartmentalization of immunoglobulin loci during lymphocyte development. *Science* 296, 158–162 (2002).
4. Hewitt, S. L., High, F. A., Reiner, S. L., Fisher, A. G. & Merkenschlager, M. Nuclear repositioning marks the selective exclusion of lineage-inappropriate transcription factor loci during T helper cell differentiation. *Eur. J. Immunol.* 34, 3604–3613 (2004).
5. Zink, D. *et al.* Transcription-dependent spatial arrangements of CFTR and adjacent genes in human cell nuclei. *J. Cell Biol.* 166, 815–825 (2004).
6. Chuang, C.-H. *et al.* Long-range directional movement of an interphase chromosome site. *Curr. Biol.* 16, 825–831 (2006).
7. Williams, R. R. *et al.* Neural induction promotes large-scale chromatin reorganisation of the *Mash1* locus. *J. Cell Sci.* 119, 132–140 (2006).
8. Andrulis, E. D., Neiman, A. M., Zappulla, D. C. & Sternglanz, R. Perinuclear localization of chromatin facilitates transcriptional silencing. *Nature* 394, 592–595 (1998).

9 Taddei, A. *et al.* Nuclear pore association confers optimal expression levels for an inducible yeast gene. *Nature* 441, 774–778 (2006).
10. Schmid, M. *et al.* Nup-PI: The nucleopore–promoter interaction of genes in yeast. *Mol. Cell* 21, 379–391 (2006).
11 Shaklai, S., Amariglio, N., Rechavi, G. & Simon, A. J. Gene silencing at the nuclear periphery. *FEBS J.* 274, 1383–1392 (2007).
12. Somech, R. *et al.* The nuclear-envelope protein and transcriptional repressor LAP2β interacts with HDAC3 at the nuclear periphery, and induces histone H4 deacetylation. *J. Cell Sci.* 118, 4017–4025 (2005).
13. Holaska, J. M., Lee, K. K., Kowalski, A. K. & Wilson, K. L. Transcriptional repressor germ cell-less (GCL) and barrier to autointegration factor (BAF) compete for binding to emerin *in vitro*. *J. Biol. Chem.* 278, 6969–6975 (2003).
14. Polioudaki, H. *et al.* Histones H3/H4 form a tight complex with the inner nuclear membrane protein LBR and heterochromatin protein 1. *EMBO Rep.* 2, 920–925 (2001).
15. Belmont, A. S., Li, G., Sudlow, G. & Robinett, C. Visualization of large-scale chromatin structure and dynamics using the lac operator/lac repressor reporter system. *Methods Cell Biol.* 58, 203–222 (1999).
16. Tsuchiya, Y., Hase, A., Ogawa, M., Yorifuji, H. & Arahata, K. Distinct regions specify the nuclear membrane targeting of emerin, the responsible protein for Emery–Dreifuss muscular dystrophy. *Eur. J. Biochem.* 259, 859–865 (1999).
17 Yang, Q., Riblet, R. & Schildkraut, C. L. Sites that direct nuclear compartmentalization are near the 5′ end of the mouse immunoglobulin heavy-chain locus. *Mol. Cell. Biol.* 25, 6021–6030 (2005).
18. Vogel, M. J., Peric-Hupkes, D. & van Steensel, B. Detection of *in vivo* protein–DNA interactions using DamID in mammalian cells. *Nature Protocols* 2, 1467–1478 (2007).
19 Bengtsson, L. & Wilson, K. L. Multiple and surprising new functions for emerin, a nuclear membrane protein. *Curr. Opin. Cell Biol.* 16, 73–79 (2004).
20 Pickersgill, H. *et al.* Characterization of the *Drosophila melanogaster* genome at the nuclear lamina. *Nature Genet.* 38, 1005–1014 (2006).
21. Bertolino, E. *et al.* Regulation of interleukin 7-dependent immunoglobulin heavy-chain variable gene rearrangements by transcription factor STAT5. *Nature Immunol.* 6, 836–843 (2005).
22 Johnson, K., Angelin-Duclos, C., Park, S. & Calame, K. L. Changes in histone acetylation are associated with differences in accessibility of $V_H$ gene segments to V–DJ recombination during B-cell ontogeny and development. *Mol. Cell. Biol.* 23, 2438–2450 (2003).
23. Pawlitzky, I. *et al.* Identification of a candidate regulatory element within the 5′ flanking region of the mouse Igh locus defined by pro-B cell-specific hypersensitivity associated with binding of PU.1, Pax5, and E2A. *J. Immunol.* 176, 6839–6851 (2006).
24. Ragoczy, T., Bender, M. A., Telling, A., Byron, R. & Groudine, M. The locus control region is required for association of the murine beta-globin locus with engaged transcription factories during erythroid maturation. *Genes Dev.* 20, 1447–1457 (2006).
25. Mendjan, S. *et al.* Nuclear pore components are involved in the transcriptional regulation of dosage compensation in *Drosophila*. *Mol. Cell* 21, 811–823 (2006).
26. Kim, S. H. *et al.* Spatial genome organization during T-cell differentiation. *Cytogenet. Genome Res.* 105, 292–301 (2004).
27. Solovei, I. *et al.* Spatial preservation of nuclear chromatin architecture during three-dimensional fluorescence *in situ* hybridization (3D-FISH). *Exp. Cell Res.* 276, 10–23 (2002).
28. Jolly, C., Mongelard, F., Robert-Nicoud, M. & Vourc'h, V. Optimization of nuclear transcript detection by FISH and combination with fluorescence immunocytochemical detection of transcription factors. *J. Histochem. Cytochem.* 45, 1585–1592 (1997).

**Supplementary Information** is linked to the online version of the paper at www.nature.com/nature.

**Acknowledgements** We thank A. Belmont for the *lacO* and GFP-LacI plasmids and K. Van Steensel for DamID plasmids. We are grateful to members of the laboratory for critical input and support by the Howard Hughes Medical Institute. J.M.Z. is supported by an NIH training grant.

**Author Contributions** K.L.R. designed and performed most of the experiments, J.M.Z. carried out the DamID experiments with K.L.R. E.B. contributed the microarray analysis. K.L.R. and H.S. wrote the manuscript.

**Author Information** The microarray data can be found at the Gene Expression Omnibus at NCBI (http://www.ncbi.nlm.nih.gov/projects/geo/) under accession number GSE10176. Reprints and permissions information is available at www.nature.com/reprints. Correspondence and requests for materials should be addressed to H.S. (hsingh@uchicago.edu).

ERRATUM

doi:10.1038/nature06844

# The X-ray crystal structure of RNA polymerase from Archaea

Akira Hirata, Brianna J. Klein & Katsuhiko S. Murakami

*Nature* 451, 851–854 (2008)

In the PDF and print versions of this Letter, the Protein Data Bank (PDB ID) code of the *Sulfolobus solfataricus* RNA polymerase (RNAP) was wrongly listed as 2PM2. The correct code is 2PMZ. This is correct in the full-text HTML version and on the contents page.

# Eclectic Electric

## A versatile technology applied to microscopes

Piezoelectricity is a technology that brings precision and subtlety to a broad range of applications. In microscopy, piezo-technology allows for an amazing level of precision and accuracy when sensitive and exact measurements are required. Take a look at the products below for some of the newest developments in microscopy.

The **Nikon SMZ range of stereo zoom microscopes** has been further extended with the launch of the new **SMZ445** and **SMZ460** models. With fixed inclination angles of 45 and 60 degrees, these latest additions provide a new entry-point into high quality optical performance. In standard format, the SMZ445 offers a total magnification range of 8x to 35x and has a working distance of 100mm. This can be extended to 4x to 70x by changing the eyepieces and selecting an auxiliary objective. Comparable figures for the SMZ460 are 7x to 30x, extendable to 3.5x to 60x. Compact yet robust, both models feature lightweight porro prism optics and have ESD protection to prevent electrostatic damage to samples. With the addition of these two new models, the user can harness the quality of Nikon ultra-high performance optics for applications requiring anything from a 4.3:1 up to a 15:1 zoom ratio.

**Olympus introduces the updated dotSlide digital virtual microscopy system,** which scans entire slides at high resolution and fidelity, making them accessible and fully navigable anywhere on the globe. The three available models (dotSlide MD, manual version; dotSlide SL, fully automated version with slide loader; and dotSlide TMA, with tissue microarray module) enable users to examine the virtual slide as if they were viewing the original on a microscope. The dotSlide is ideal for all aspects of pathology and research, meaning that users can review cases without being near a microscope. This also enables quicker second opinions and remote consults, as well as consistent training and discussion. The unique technology also ensures that the dotSlide range provides high throughput and high content capabilities for both pathology and research applications.

With the **LSM 5 EXCITER laser scanning microscope, Zeiss** is offering users in materials research and quality analysis microscope system that also analyzes relatively soft materials such as polymers in a non-contact procedure and with high measuring accuracy and resolution. LSM 5 EXCITER increases the speed, reliability and convenience of materials analysis. Special software functions allow the quantitative surface examination and analysis of materials. With the non-contact confocal technique, 2D and 3D topographies can be visualized and measured, roughness and waviness determined, and porosity and volume content measured with a high degree of quality and reliability. The possibility of working both in reflected and fluorescent light expands the flexibility of analytical techniques. The StitchArt plus option allows extra-long line profiles or image stack arrays to be captured automatically with variable overlapping areas. Numerous other automated processes and adjusting functions are an integral part of the StitchArt plus option. These include, for example, autofocus, automatic contrast and brightness optimization as well as the precise, first-order correction of the objective's residual field curvature. LSM 5 EXCITER is offered in combination with the Axio Imager and Axio Observer microscopes – also with polarization equipment. Piezo-technology and nanometer scaling allow fast and exact measurements.

**Agilent introduces the Magnetic AC Mode III (MAC Mode III) controller,** which is particularly useful in areas that require high resolution and force sensitivity, such as biology, polymers and surface science. Built on field-proven technology, this gentle, nondestructive atomic force microscopy (AFM) technique is designed for imaging delicate samples in liquid or air. MAC Mode III offers three user-

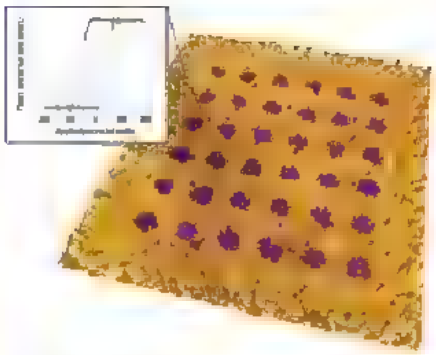

Rendered topography of a $LiNbO_3$ sample by Asylum Research

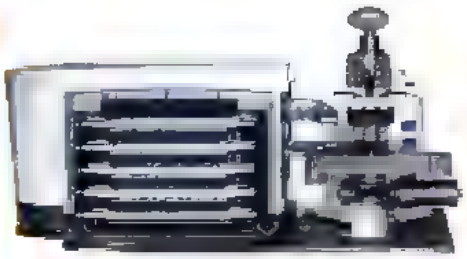

The dotSlide digital virtual microscopy system from Olympus

**"Electromechanics and PFM is a growing area of research..."**

Dr. Roger Proksch, president and Co-founder, Asylum Research

configurable lock-in amplifiers, affording researchers versatility, higher accuracy and quicker time to results. It has a wider operating frequency range – up to 6 MHz – enabling scientists to investigate higher harmonic modes. Built-in Q control further enhances the resonance peak. Higher harmonic imaging provides contrast beyond that seen with fundamental amplitude and phase signals, allowing scientists to collect additional information about the mechanical properties of the sample surface. The Agilent MAC Mode III allows one-pass multi-channel detection for Kelvin force microscopy (KFM) and electric force microscopy (EFM). Simultaneous, high-accuracy topography and surface potential measurements are facilitated by a servo-on-height cantilever approach that is not susceptible to scanner drift. KFM/EFM offers excellent utility for measuring dielectric films, metal surfaces, piezoelectrics and conductor-insulator transitions. MAC Mode III can be operated simultaneously with environmental control, temperature control, electrochemical control and controlled fluid exchange. Agilent's acoustic AC mode is included with MAC Mode III.

FEI introduces its latest and most powerful scanning electron microscope (SEM), the **Nova NanoSEM 30 series**. This high-end, versatile field emission SEM series features new low kV performance for enhanced surface characterization, high current for compositional analysis capabilities and the world's only high-resolution operation in low vacuum to characterize uncoated and even insulating samples. The advanced performance of the Nova NanoSEM 30 series enables the characterization and analysis of a large range of samples, including demanding ones such as nanoparticles, insulating substrates such as glass or polymers, porous materials, metals and composites. Beyond its new imaging and analytical performance, the NOVA NanoSEM 30 series also provides researchers with novel prototyping capabilities based on electron beam lithography, electron beam induced deposition and in-situ experimentation for manipulation and testing. The three instruments of the Nova NanoSEM 30 Series owe their superior performance to the newly introduced Schottky gun and beam deceleration technologies. The 230 and 430 systems feature 50 x 50mm and 100 x 100mm 5-axis motorized stages, respectively. The 630 system is equipped with a 5-axis high precision and stability, 150 x 150mm piezo stage.

**BTX Microslides** are designed to fit on a microscope and allow observation of the dimer formation during electrofusion. These Microslides are composed of a glass slide and two strips of stainless steel (wire or bar) and are available in 0.5mm, 1.0mm, 3.2mm and 10mm gap sizes. The Microslides are used primarily with the ECM 2001 Electro Cell Manipulator. The Microslide fits on the microscope allowing observation of the alignment and fusion process. The Microslide 450 is composed of a glass microslide and two strips of 0.5mm stainless steel tubing which functions as electrodes to provide a divergent field. These wires are set apart at different gaps to provide various field strengths and volumes. The Micrograbber is used to connect the Microslide 450 to the coaxial connection cable, which will then be hooked up to the ECM 2001 generator. Microslide 453 has two stainless steel square bars that are set apart at various gaps to provide homogeneous fields. The square post cable is used to connect the Microslide to the coaxial connection cable, which is hooked up to the ECM 2001 generator. The Microslides have been used for embryo manipulation and cell or protoplast fusion.

In response to the growing applications of electromechanical imaging and spectroscopy, **Asylum Research** has developed the new **Piezo Force Module** which enables very high sensitivity, high bias, and crosstalk-free measurements of piezoelectrics, ferroelectrics, multiferroics, and biological systems. It is exclusively available for the MFP-3D Atomic Force Microscope. "Electromechanics and PFM is a growing area of research with studies ranging from data storage devices to MEMS to electromotor proteins and electrophysiology. Our Piezo Force Module uses a special high voltage accessory and advanced imaging modes to measure piezoresponse, even for the weakest piezoelectric materials," said Dr. Roger Proksch, president and co-founder of Asylum Research. The Piezo Force Module is an MFP-3D accessory that enables high voltage PFM measurements and advanced imaging modes for characterizing the sample material. With the Piezo Force Module, a bias is applied to the AFM tip using proprietary electronics, a high voltage cantilever, and sample holder.

**Companies mentioned in this Product Focus:**

Agilent - www.agilent.com
Asylum Research - www.asylumresearch.com
BTX - www.btxonline.com
FEI - www.fei.com
Nikon - www.nikoninstruments.com
Olympus - www.olympusamerica.com
Zeiss - www.zeiss.de

# Sign up for *Nature China* table of contents e-alerts

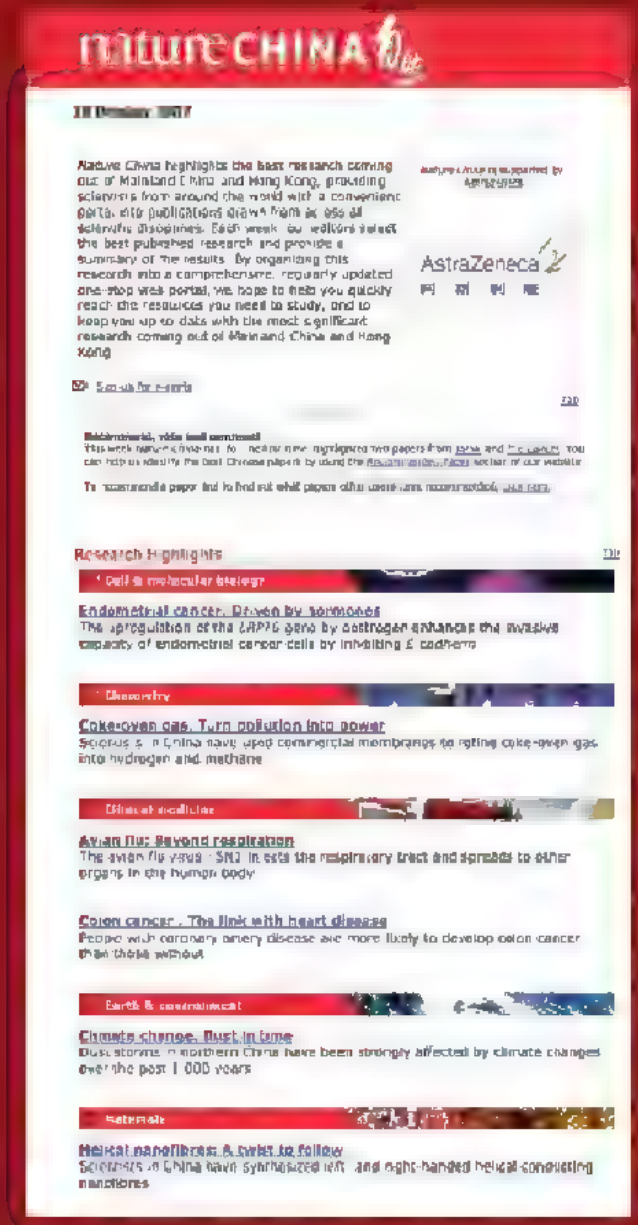


Keep up to date with the latest leading research from Mainland China and Hong Kong by registering for *Nature China* e-alerts. Providing you with weekly research highlights from the region drawn from a variety of publications covering topics including:

- biotechnology
- cell & molecular biology
- chemistry
- clinical medicine
- developmental biology
- earth & environment
- ecology & environment
- genetics
- materials
- neuroscience
- physics
- space & astronomy

Go to **www.naturechina.com** and click on the e-alert sign up button for further details

For scientists in Mainland China and Hong Kong please visit **www.naturechina.com.cn**

**E-alert sign up**

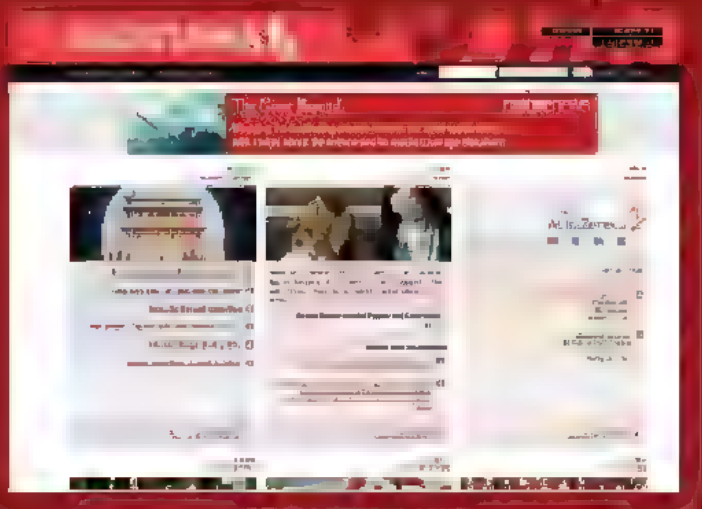

Supported by

AstraZeneca

**www.naturechina.com**

nature publishing group npg

# Cell Death & Differentiation

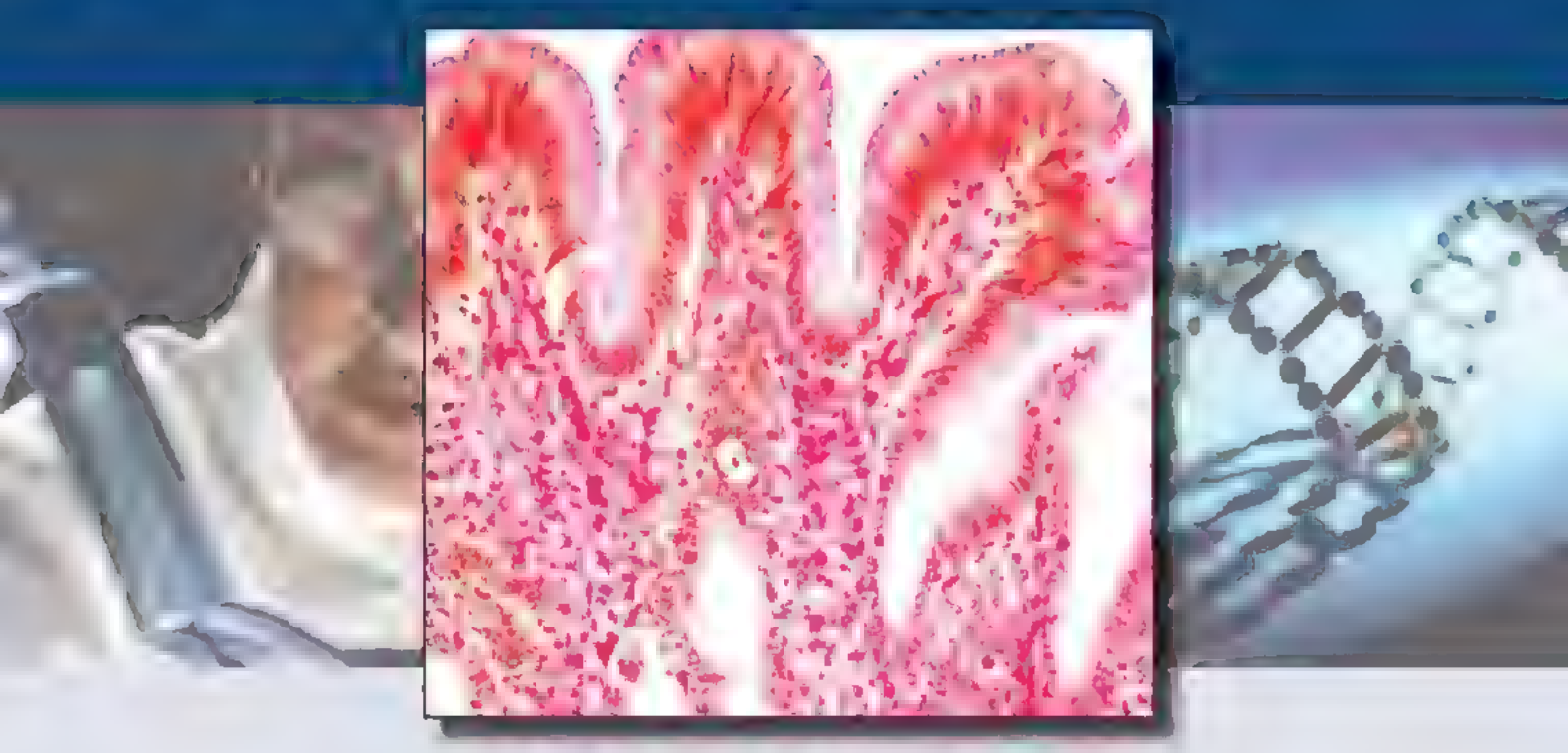

BIOCHEMISTRY

**CELL BIOLOGY**

MOLECULAR BIOLOGY

*Cell Death & Differentiation* expands coverage to all areas of cell death and disease. The journal provides a unified forum for scientists as well as clinical researchers. High-quality original papers together with topical reviews, meeting reports, editorial correspondence and commentaries keep you updated on the latest research in the field.

**Cell biology:** one of the many topics addressed by *Cell Death & Differentiation*.
Now reporting on: stem cell research; neurology; apoptosis; and immunogenicity.

www.nature.com/cdd

nature publishing group npg

NATURE|Vol 452|13 March 2008

THE CAREERS MAGAZINE FOR SCIENTISTS

- FOCUS
- SPOTLIGHT
- RECRUITMENT
- ANNOUNCEMENTS
- EVENTS

# nature jobs

**PROSPECTS**
The trials of being a young scientist

**CAREER VIEW**

**COMING SOON**
Highlight on Francophone countries (20 March)

Health disparities and minorities (20 March)

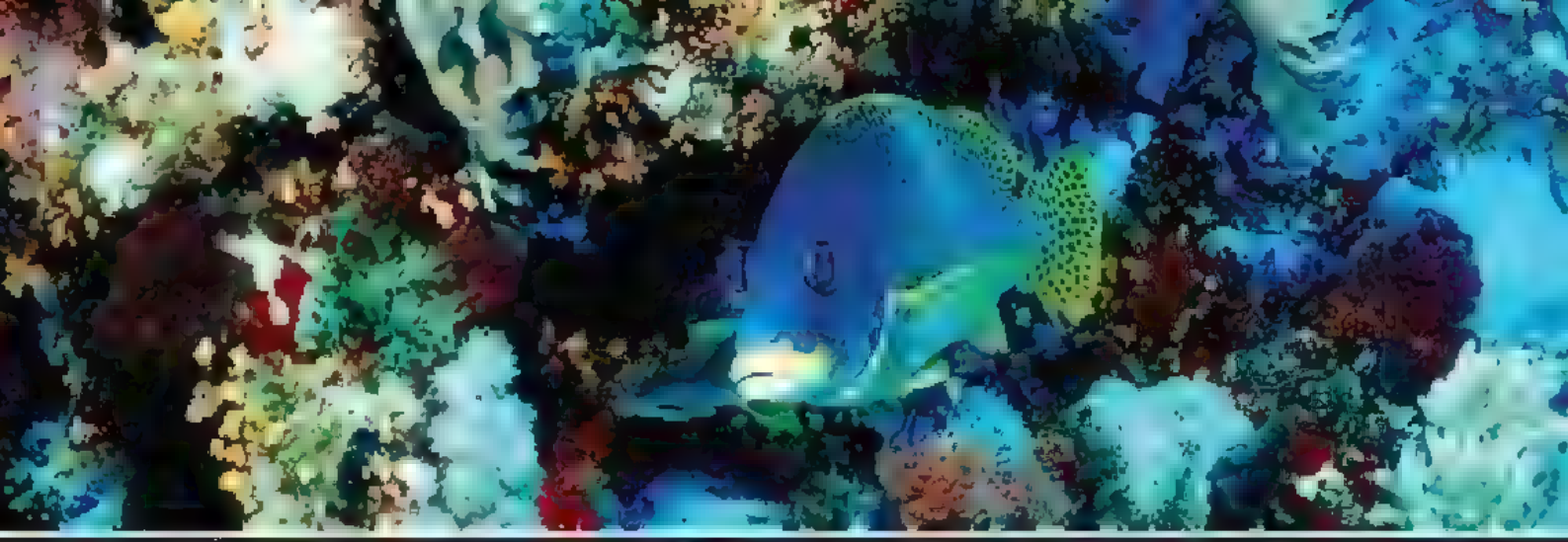

*Naturejobs* is pleased to present a

# FOCUS ON CONSERVATION BIOLOGY

**ISSUE DATE:**
**APRIL 10, 2008**

**DEADLINE FOR ADVERTISERS:**
US APRIL 03, 2008
UK/EU/ROW APRIL 04, 2008

The first ever *Naturejobs'* Focus on Conservation Biology is a unique opportunity to present your job, employer marketing, event or announcement to readers interested in this burgeoning field of study.

Human impact on the environment and the importance of conservation biology are increasingly recognized as world-wide concerns. The new issues and strategies that are rapidly being discussed fall under a broad range of scientific disciplines such as atmospheric sciences, environmental sciences, ecology, genetics, agriculture, plant sciences, marine biology, Earth sciences, and zoology.

Nature Publishing Group is dedicated to reporting the latest issues in conservation biology with key papers published in *Nature* as well as targeted publications such as *Nature Geoscience* and the online resource, *Nature Reports: Climate Change*.

The Focus on Conservation Biology will be a valuable reference for readers interested in the subject. Whether you are recruiting, creating awareness or positioning your organization, this feature will deliver targeted impact. The Focus is featured at the start of the *Naturejobs* section.

- **Book into the May issue of *Nature Geoscience* by April 15 to receive a 25% discount on the normal rate***
- **Maximize impact with a Job of the Week slot on the *Nature Geoscience* homepage**

**CALL TODAY TO ADVERTISE WITH *NATUREJOBS*!**

Europe: +44 (0)20 7843 4961 | US: +1 800 989 7718 | Japan: +81 3 3267 8765 | India: +91 124 288 1057

If you are interested in advertising events relating to conservation biology please call Claudia Paulsen Young on +44 (0)20 7014 4015 or email c.paulsenyoung@nature.com

Remember, it's FREE to post all your jobs online at www.naturejobs.com using our simple auto-post function.

*This discount is subject to the same advert running in the April 10 issue of *Nature* and is only applicable on the standard *Nature Geoscience* advertising rates when a full price advert has been placed in *Nature*.

naturejobs@nature.com www.naturejobs.com

naturejobs

nature publishing group npg

# naturejobs

Officials at the Howard Hughes Medical Institute (HHMI) in Chevy Chase, Maryland, last year went on a 'listening tour', travelling around the United States to hear first-hand about young scientists' struggles to secure funding. "People at the early stages of their career are standing in line," says Jack Dixon, the HHMI's chief scientific officer. "There are a lot of quality people in this country who are struggling to get their first grant." Dixon says words such as 'queue' and 'holding pattern' were used a lot by young scientists — especially when talking about the R01, the main grant used by the National Institutes of Health (NIH) to fund individual investigators

NIH data confirm the anecdotes. The success rates for new grants fell from 26% in 2000 to 19% in 2007. And renewals haven't fared much better, falling from 50% in 2000 to 36% in 2007. The problem is a lack of money, rather than a dearth of quality scientists, says Dixon. For the past five years, the NIH budget has been relatively flat, which means that much of the money is spoken for, given that its grants typically run for five years. This may affect young investigators most, because young first-time applicants generally have a lower success rate than their more experienced peers. As a result, the average age of first-time R01 recipients has risen from the mid-30s of 1980 to a high of 42, says Dixon.

"If that's the norm, then we're losing people during the most productive years of their research career," Dixon says. The HHMI this week announced a programme to help address this problem. It plans to fund up to 70 young scientists for six years, from a pool of some $300 million. Only researchers who have led independent labs for two to six years are eligible. And although scientists with existing R01s can compete for the grant, researchers with support from multiple foundations won't be eligible. "We want to spread the wealth around," says Dixon.

Dixon acknowledges that funding 70 scientists won't solve the problem, but he hopes that other organizations will follow suit — and that the NIH can find the money and the wherewithal to support more early-career scientists.

**Paul Smaglik is moderator of the Nature Networks Career Forum.**

CONTACTS
**Acting Editor:** Gene Russo

US Head Office
New York
75 Varick Street, 9th Floor
New York, New York 10013-1917
Tel: +1 800 989 7718
Fax: +1 800 989 7103
e-mail: naturejobs@natureny.com

**US Sales Manager/Corporations:**
Peter Bless
Tel: +1 800 989 7718

San Francisco Office
**Classified Sales Representative:**
Michaela Bjorkman
West USA/West Corp. Canada
225 Bush Street, Suite 1453
San Francisco,
California 94104
Tel: +1 415 781 3803
Fax: +1 415 781 3805
e-mail: m.bjorkman@nature.com

India
Vikas Chawla
Tel: +91 1242881057
e-mail: v.chawla@nature.com

European Head Office, London
The Macmillan Building,
4 Crinan Street,
London N1 9XW, UK
Tel: +44 (0) 20 7843 4961
Fax: +44 (0) 20 7843 4996
e-mail: naturejobs@nature.com

**European Sales Manager:**
Andy Douglas (4975)
**Advertising Production Manager:**
Stephen Russell
To send materials use London address above.
Tel: +44 (0) 20 7843 4816
Fax: +44 (0) 20 7843 4996
e-mail: naturejobs@nature.com
***Naturejobs* web development:** Tom Hancock
***Naturejobs* online production:** Dennis Chu

Japan Head Office, Tokyo
Chiyoda Building, 2-37
Ichigayatamachi,
Shinjuku-ku, Tokyo 162-0843
Tel: +81 3 3267 8751
Fax: +81 3 3267 8746

**Asia-Pacific Sales Manager:**
Ayako Watanabe
Tel: +81-3-3267-8765
e-mail: a.watanabe@natureasia.com
**Business Development Manager, Greater China/Singapore:**
Gloria To
Tel: +852 2811 7191
e-mail: g.to@natureasia.com

## JOBS OF THE WEEK

**Head, Department of Marine Biology**
**Texas A & M University at Galveston**
Galveston, Texas (USA)
**Turn to page 3**

**Biochemist**
**Leibniz Institute for Zoo and Wildlife Research**
Berlin (Germany)
**Turn to page 16**

**PhD Training Programme**
**Trinity College Dublin**
Dublin (Ireland)
**Turn to page 4**

**Career Scientist - Ophthalmology**
**Mayo Clinic**
Rochester, MN (USA)
**Turn to page 4**

**Independent Research Fellowships**
**University of Bristol**
Bristol (UK)
**Turn to page 15**

# MOVERS

**Daniel Kelly, scientific director, Burnham Institute for Medical Research, Orlando, Florida**

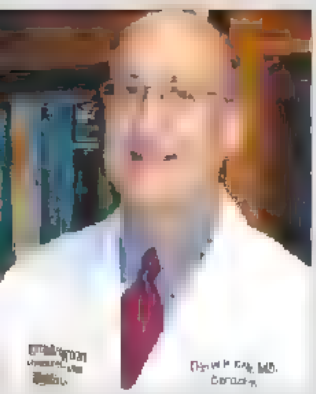

**2006-present:** Chief, Cardiovascular Division, Department of Medicine, Washington University School of Medicine, St Louis, Missouri
**1999-present:** Professor of medicine, molecular biology and pharmacology, Washington University School of Medicine, St Louis, Missouri

Daniel Kelly is a self-described late bloomer. Trained as a clinical physician, he realized several years into his schooling that he was most interested in the fundamental basis of disease. But he felt he was too far along to pursue the now common MD/PhD. So Kelly immersed himself in a research postdoctoral fellowship at Washington University School of Medicine in St Louis, Missouri, to learn the molecular biology of mitochondrial enzyme pathways and the genetic basis of diseases that cause heart failure and metabolic disorders in children.

"It was an exhilarating but disorienting time," he says, lamenting that the intensity and costs of training made it hard to deviate from a career path late in the game.

Following his fellowship, Kelly slowly began doing more basic science and less clinical medicine after setting up a lab at Washington University. In the mid-1990s, he founded the Center for Cardiovascular Research and established a cross-department network of scientists interested in various aspects of cardiovascular disease and metabolism, a rarity at the time. The centre has made great strides in linking cell metabolic disorders to disease, in part thanks to Kelly's pioneering work in mice.

In 2006, Kelly became chief of the cardiovascular division at Washington University's School of Medicine. He enjoyed the challenge, but found that his true passion lay in research discovery and building innovative research environments. When the Burnham Institute for Medical Research in San Diego contacted him about the position of scientific director at its new Florida locale — due to open in 2009 — Kelly seized the opportunity to take a cross-disciplinary approach involving research on cardiovascular diseases, obesity, diabetes and other metabolic disorders.

"Kelly's willingness to step out of his productive, mid-career position is the type of risky career move needed for the biomedical sciences to evolve," says Jeff Gordon, director of the Center for Genome Sciences at Washington University.

Over the next year, Kelly will begin recruiting the roughly 30 principal investigators to be taken on within five years. As well, he plans to build relationships with the new medical school at the University of Central Florida, the University of Florida and Scripps Florida. "I never thought my career would lead to Orlando, but that just shows how following your vision can take you to unexpected places," says Kelly. ■

**Virginia Gewin**

# Sunny view for Florida life sciences

In its bid to kindle a biotechnology boom, Florida is luring high-profile institutions to the southeastern part of the state with big bucks (see *Nature* **446,** 1112–1113; 2007). The state's 'innovation incentive' funds will devote more than $220 million to three research institutes in Jupiter, Port St Lucie and Miami.

With more than $90 million from the state and $87 million from Palm Beach County, the Max Planck Florida Institute will be housed at the Jupiter campus of Florida Atlantic University, near Scripps Florida, which was set up in 2004 as an offshoot of Scripps in La Jolla, California. Max Planck Florida — the first Max Planck institute outside Europe — expects to create 170 positions, including division directors in three main areas: bioimaging, bioactivity measures and cellular mechanisms. Herbert Jäckle, a vice-president in the Max Planck Society, admits it's a high-risk venture. "But it's worth building up because of the fantastic spirit there," he says. The presence of Scripps influenced the society's decision to head for the sunshine state. Until a new facility is built (probably by 2010), Max Planck Florida will take over the space Scripps is now using for its temporary labs.

In nearby Port St Lucie, Oregon Health and Science University's Vaccine and Gene Therapy Institute will receive $60 million in state funding and a new facility to study therapies in humans. Director Jay Nelson says it will soon begin recruiting 20 primary investigators; roughly 200 new employees will focus on the genetic basis of infection.

At the University of Miami, the Institute for Human Genomics — started last year by husband-and-wife team Margaret Pericak-Vance and Jeffery Vance — received an extra $80 million from the state last month to expand. The Vances have recruited dozens of researchers from their former base, Duke University in Durham, North Carolina. The new funds, says Pericak-Vance, will aid computational infrastructure and help lure recruits who combine clinical specialisms with an interest in genomics. Pericak-Vance expects to have some 300 staff, once technical and support staff join in the next five years. New facilities are also under construction, largely funded by the University of Miami.

"I've never seen this level of cooperation between state, universities, counties and institutes, to realize their vision of creating a San Diego or Boston," says Nelson. "And they are going to do it." ■

**Virginia Gewin**

**POSTDOC JOURNAL**

# David versus Goliath

Living in the Middle East, I often hear allusions to the biblical battle between David and Goliath, when a single stone took down the giant. As I put the finishing touches to a manuscript on the natural variation of flowering shoot systems in tomato, I realize the same allusion applies to young scientists. Biology is competitive.

There are many Goliath scientists with large grants and armies of postdocs. I've met many such giants, and some were frightening, cornering me at a poster session to tell me my data were bunk and my models were wrong. But others have been collegial, offering constructive criticism or sharing seeds from a particularly important mutant plant.

As I develop my ideas in a new field where I am keenly aware of competition, I find myself unable to avoid proverbial David-versus-Goliath battles. I've been debating whether it would be prudent to e-mail or even call a few Goliaths, in the hopes of establishing productive collaborations. But it might not go well.

I seem to recall the story ending with David cutting off Goliath's head. That suggests one way for me to go about it — publish fast and scoop the Goliath. But to be honest, I'm just not sure how fearless a David I am. And who knows? Collaborating just might help me become a Goliath one day. ■

**Zachary Lippman is a postdoctoral fellow at the Hebrew University of Jerusalem's faculty of agriculture.**

EMBL

Australian Government

National Health and Medical Research Council

*In accordance with Australia's Associate Membership of EMBL up to 2 fully funded research groups are able to be located at an EMBL site in Europe for a maximum period of 5 years. Funding from Australia's National Health and Medical Research Council (NHMRC) is available to support the placement of one group, subject to approval. To be eligible for NHMRC support applicants must be working in a field of relevance to human health.*

# Group Leaders

## 5 years in Europe and 4 years in Australia

Applications are invited from suitably qualified scientists wishing to develop their research program as a group leader within EMBL for consideration as one of the groups to be constituted under the Associate Membership agreement. The position will be continued for a further 4 years at an Australian institution.

**EMBL Site:** The group's location will be dependent on the successful applicant's preferences and the proposed research program. Options available include Heidelberg (Germany) – EMBL Headquarters – and the EMBL Outstations in Hinxton (UK) – the European Bioinformatics Institute, EBI –, Grenoble (France), Hamburg (Germany) and Monterotondo (Italy).

**Australian Site:** The group leaders' location in Australia will depend on the location of the approved Australian institution. Approved Australian institutions for the NHMRC funded position are those that are able to satisfy NHMRC and EMBL that the proposed program of research is of a standard sufficient to compete for funding from Australian research funding agencies. As such, there are research institutions meeting this requirement in every Australian State or Territory.

The European Molecular Biology Laboratory (EMBL) is an international research organisation offering a highly collaborative, uniquely international culture. It fosters top quality, interdisciplinary research by promoting a vibrant environment consisting of young independent research groups composed of outstanding graduate students and postdoctoral fellows. The Scientific Programme of EMBL emphasises experimental analysis at multiple levels of biological organisation, from the molecule to the organism, as well as Computational Biology, Bioinformatics and Systems Biology. In addition to exciting colleagues, the laboratory provides excellent shared facilities for a variety of advanced experimental approaches. High-level expertise is also available in Computational Biology, diverse aspects of experimental Molecular Biology as well as Physics, Biophysics, Chemical Biology and instrument development.

Successful candidates will lead a research group for a period of five years at the selected EMBL site in Europe and will participate in the collegial culture of EMBL. Following their term in Europe, candidates will continue as Group Leaders at an Australian institution. Successful applicants will need to select and finalise arrangements with an approved Australian institution prior to the commencement of their placement in Europe. Candidates will also participate in a program of linking activities with the Australian institution while in Europe.

**Commencing date in Europe: 2008 or early 2009**

Further information about the position can be obtained from: EMBL Director General, Iain Mattaj (dg-office@embl.de) or NHMRC Executive Director Research Investment Branch, Elim Papadakis (elim.papadakis@nhmrc.gov.au).

EMBL is an inclusive, equal opportunity employer offering attractive conditions, benefits and child care facilities appropriate to an international research organisation.

To apply please email a CV, including a summary of present and future research interests and the names of three referees, quoting ref. N/08/006 in the subject line to:
application@embl.de

**Closing date: 16 May 2008**

**www.embl.org**

W1278837FI

USDA ars Agricultural Research Service

www.ars.usda.gov

*"The Nation's premier food and agricultural research agency"*

## RESEARCH LEADER

**National Center for Genetic Resources Preservation (NCGRP)**

**Plant and Animal Genetic Resources Preservation Research Unit**

**Ft. Collins, Colorado**

**Senior Scientific Research Service (SSRS)**

**RA-0401-00/00; Starting Salary Range of $140,000 to $165,000 with full potential to $191,300**

***Applications must be received by April 17, 2008***

The USDA, Agricultural Research Service (ARS) is seeking a senior-level research scientist for a permanent full-time leadership position. This SSRS position offers a highly qualified, talented, world-class research scientist who also possesses administrative capabilities, the opportunity to conduct research in the field of plant germplasm preservation at the nation's premier plant, animal, and microbial germplasm repository.

This position affords the opportunity to:

- Direct an internationally recognized group of scientists working at the leading edge of plant and animal genetic resource preservation/conservation.
- Work collaboratively with domestic and international university, industry and government agencies.
- Oversee state-of the art facilities with unique physical capabilities and pre-eminent scientific equipment.
- Impact the conservation/preservation of plant and animal genetic resources essential for the Nation's food and agricultural security.

***Join us in enhancing the health and wealth of the Nation and its people***
***solving problems, expanding knowledge, delivering answers***

Application instructions and a full job announcement can be found at http://www.ars.usda.gov/careers (ARS-SSRS 08-07). To have a printed copy mailed or for questions about this position, call Deborah Crump at (301) 504-1448 or E-Mail: deborah.crump@ars.usda.gov and for technical questions regarding the position, please contact Larry Chandler at (970) 492-7058 or E-Mail: larry.chandler@ars.usda.gov.

To learn more about the location, visit their website at http://www.ars.usda.gov/main/site_main.htm?modecode=54-02-05-00

*USDA/ARS is an equal opportunity employer and provider*

NW127377R



## Faculty Positions

**Department of Biochemistry**
**Faculty of Medicine**
**University of Toronto**

The Department of Biochemistry, University of Toronto invites applications for two tenure-track positions at the rank of Assistant Professor commencing on July 1, 2008.

We seek candidates with a Ph.D. in biochemistry, biophysics, cell biology or a related discipline. Candidates must also have at least two years post-doctoral training and have an excellent publication record.

The Department is interested in individuals who employ modern molecular approaches in studies of macromolecular complexes, membrane protein structure, lipid-protein interactions and dynamics, single molecule visualization and dynamics in living cells, non-coding RNA, or chromatin. Successful applicants will be expected to establish an independent research program, compete effectively for external funding, and contribute actively to the undergraduate and graduate teaching programs in the Department. Salary will be commensurate with qualifications and experience.

Applicants should arrange to have three letters of reference sent directly to the mailing address below. In addition, applicants should send their curriculum vitae, copies of significant publications, and a 2-3 page description of their research plans either by e-mail to: chair.biochemistry@utoronto.ca or by mail to: Chair, Department of Biochemistry, Room 5205, Medical Sciences Building, University of Toronto, Toronto, Ontario, M5S 1A8, Canada. Closing date for applications is April 30, 2008, or until the positions are filled.

*The University of Toronto is strongly committed to diversity within its community and especially welcomes applications from visible minority group members, women, Aboriginal persons, persons with disabilities, members of sexual minority groups, and others who may contribute to the further diversification of ideas. All qualified candidates are encouraged to apply; however, Canadians and permanent residents will be given priority.*

www.biochemistry.utoronto.ca

NW127239R

100 years of **bio**chemistry at U of T
1908-2008

## Assistant Editor

### *Nature Biotechnology*

*Nature Biotechnology* seeks an Assistant Editor for its editorial team based in New York. Expertise in systems biology and/or computational biology would be desirable, but not required.

Members of the editorial team evaluate manuscripts, oversee the peer review process, commission and edit secondary materials such as Reviews, and write short pieces and editorials for the journal. The successful applicant will attend scientific meetings and visit laboratories to maintain contact with the international scientific community. The position will play a key role in consolidating *Nature Biotechnology's* presence in the fields of systems biology and computational biology.

Excellent communication skills and a willingness and ability to learn new fields are a must. Applicants should have completed a Ph.D. in the biological sciences.

To apply, an interested candidate should submit a curriculum vitae, a short (500-1000 words) News and Views-style article on an exciting and newsworthy recent development in biotechnology, and a cover letter explaining their interest in the position to Human Resources Department, Nature Publishing Group.

All applications should be sent via email to: admin@natureny.com.

Please place "Assistant Editor Nature Biotechnology" in the subject line.

All applicants will be reviewed upon receipt with a close date of March 31, 2008.

Nature Publishing Group
75 Varick Street
New York, New York 10013, USA

nature publishing group npg

N125903R

# Graduate Assistantships for the study of Complex Systems at The University of Vermont

Are you an integrative thinker who wants to develop and apply cutting edge approaches for understanding the complex natural, social, and/or engineered systems that are central to tackling todays most pressing problems? Here is an opportunity to research those problems in Burlington, Vermont – one of the most beautiful places in the country to live and work.

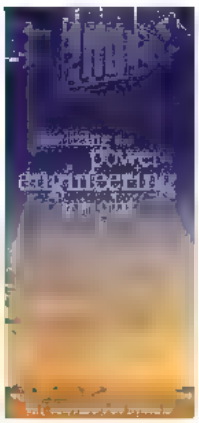

**The Complex Systems Center in the College of Engineering & Mathematical Sciences at the University of Vermont is excited to announce the availability of new graduate research assistantships in support of our interdisciplinary emphasis in complex systems analysis and engineering. These highly competitive and prestigious assistantships carry a stipend of $30,000 per year, in addition to tuition and health insurance benefits.**

We seek to support innovative and forward-thinking doctoral students who will conduct transformative, high-impact research in theory, methodology, and/or applications of complex systems science and engineering. Recipients will matriculate into doctoral programs in Computer Science, Mathematics, Materials Science, or Engineering (Civil, Environmental, Electrical, or Mechanical) and study with faculty who are at the forefront of interdisciplinary research in complex systems. Some examples of exciting ongoing projects include creating resilient autonomous robots through cognitive self-modeling, improving forecasts in chaotic weather systems, understanding the spread of ideas and influence in complex social networks, developing and applying hierarchical artificial neural networks for multi-scale environmental modeling, developing a multi-scale agent-based model of the complex transportation energy market, studying complexity and sensitivity in an agent-based transportation model coupled with a model of land use change, studying emergent evolutionary and population dynamics in spatially structured ecosystems, developing novel evolutionary computational approaches for understanding the genetic causes of complex diseases, and designing multi-agent control methods for mitigating the negative effects of cascading failures in power networks. Applicants need not restrict their proposed interests to existing projects, but are advised to identify and contact potential advisor(s) with whom they would like to work. For more information on our complex systems activities and how to apply, please visit www.uvm.edu/complexsystems.

Founded in 1791, the University of Vermont is considered a public ivy and is consistently ranked as one of the top public universities in the United States. The University is located in Burlington, Vermont, rated as one of the best small cities in America, and enjoys a panoramic setting on the shores of Lake Champlain bordered by the Adirondack and Green Mountains. Roughly 150,000 people, from increasingly diverse cultural backgrounds, live in the greater Burlington area. The University encourages applicants who can contribute to the diversity and excellence of the academic community.

**Complex Systems Center**
*Achieving insight, innovative design, and informed decision-making through systems thinking*

The University of Vermont
Founded in 1791

NW126165R

# nature chemical biology

## Locum Assistant Editor

*Nature Chemical Biology* seeks a Locum Assistant Editor to join their editorial team for a period of six months to cover a maternity leave. The journal publishes high quality articles at the interface of chemistry and biology. For more information about *Nature Chemical Biology*, see our website (http://www.nature.com/naturechemicalbiology).

Candidates should have a broad interest in science, excellent communication skills, and a willingness and ability to learn new fields. Applicants should have a Ph.D. in chemistry or biology, with demonstrable research achievements. Postdoctoral experience is preferred but not required. The journal team is particularly interested in broadly trained applicants with significant knowledge of chemical and biological systems.

Key elements of the position include the selection of manuscripts for publication, and commissioning, editing and writing other content for the journal. This is a demanding and extremely stimulating position, which requires a keen interest in the practice and communication of science. The successful candidate will therefore be dynamic, motivated and outgoing, and must possess excellent interpersonal skills.

To apply, please submit a CV, a cover letter explaining your interest in the position and possible start date, along with a 'News & Views' style article (800 words or less) on a recent paper from the chemical biology literature. Applications should be sent (attached pdf files preferred) to Human Resources Department, Nature Publishing Group by e-mail, admin@nature.com as soon as possible but not later than 17 March 2008. Position in our Boston office.

nature publishing group npg

*NPG is an Equal Opportunity Employer. Additional information about Nature Publishing Group is available at http://www.nature.com.*

N126444R

# HEAD – DEPARTMENT OF MARINE BIOLOGY

## TEXAS A & M UNIVERSITY AT GALVESTON

Texas A & M University at Galveston – the coastal campus of Texas A & M University – is seeking a new Head for the Department of Marine Biology. The department has 13 full-time faculty, 60 Doctoral and Masters graduate students, and 500 undergraduates pursuing Bachelor of Science degrees in Marine Biology, Marine Fisheries and Marine Biology with a certificate in Biomedical Science (see www.marinebiology.edu for details).

The successful applicant will be conferred the title of Professor and Head of Marine Biology with tenure and will assume responsibility for administering, promoting and enhancing the Marine Biology Department's graduate and undergraduate programs and facilities, including a new multi-institutional graduate degree program in Marine Biology and a new science building. The successful applicant will also be expected to establish an active research program or engage in other scholarly activities. Applicants must have a Ph.D. in the marine biological sciences or a related field, a record of scholarly achievement, prior administrative experience, and research credentials expected of a full Professor.

Interested persons must submit a letter of application, resume, statements on leadership and teaching philosophies, research plans and equipment requirements; and three letters of reference to: **Human Resources Department – MARB Department Head, Texas A & M University at Galveston, P.O. Box 1675, Galveston, Texas 77553-1675.** Official TAMUG applications must be completed in its entirety and submitted to the Human Resources office. Employment is contingent upon successful completion of a background check, reference check, and degree verification. Applications can be downloaded from: www.tamug.tamu.edu/hrd.

*Texas A & M University is an Affirmative Action/Equal Opportunity employer committed to excellence through diversity and particularly invites applications from minorities, women, veterans and persons with disabilities.*

NW127237R

**TRINITY COLLEGE**
The University of Dublin

# *Molecular Medicine – 'From Genes to Function'*

## A 4 year Integrated PhD Research and Training Programme in Molecular Medicine

The faculty of Health Sciences invites applications for a prestigious four-year Ph.D. programme in Molecular Medicine. Supported by the Health Research Board, this programme has been running successfully for two years and is now recruiting for a third cohort of students. The programme takes an integrated, multidisciplinary approach to the training of scientists in Molecular Medicine with an emphasis on the interaction of genetic and environmental influences in development of common diseases. One of only two schemes of its kind in Ireland, it integrates both genetic and cell biology approaches to deliver a broad based training programme of the highest standards internationally. **Successful applicants will receive an annual student stipend of €18K.**

Situated on the St. James' Hospital Campus, the Trinity College Institute of Molecular Medicine (IMM) is a state-of-the-art facility equipped to the highest standards and dedicated to research into the molecular basis of human disease, this programme will bring together world class scientists from the IMM, the Smurfit Institute of Genetics and the Department of Biochemistry, TCD in a multi-disciplinary research environment. The IMM is a component of the prestigious Dublin Molecular Medicine Centre and the Euro Life consortium of leading European Universities

For information on the principal investigators and research areas, please see our web page at http://oscar.gen.tcd.ie/molmed/phd

Applications are invited from high calibre applicants with backgrounds in biological, medical, dental, and pharmaceutical sciences, while other appropriate backgrounds may also be considered, with a minimum of 2:1 result in a primary degree or equivalent. This programme is open to both EU and NON-EU applicants. Tuition fees will be covered to the cost of the EU amount. Application forms can be obtained from http://www.tcd.ie/graduate_studies/g-admsn.htm or telephone + 353 1 8961166

Completed application forms should be sent with a C.V., personal statement, copy of degree transcripts and 2 academic references to:

Molecular Medicine Administrator
Department of Clinical Medicine
Trinity Centre for Health Sciences
St. James' Hospital, Dublin 8. , Ireland

Email: molec.medic@tcd.ie

**The closing date for applications is 5pm, Thursday 28th March 2008.** Some relevant applications may be accepted after the closing date depending on availability
**Applicants must be available for interview in the Trinity Centre for Health Sciences on the 15th to 16th April 2008 inclusive.** This programme is open to both EU and Non-EU applicants
Admission will be limited to six students per year

W127613R

MAYO CLINIC

*Heal the sick, advance the science, share the knowledge*

## Career Scientist – Ophthalmology

The Department of Ophthalmology at the Mayo Clinic in Rochester, MN, is seeking an outstanding scientist at the Associate Professor or Full Professor level to study pathogenesis of eye disease. We are seeking a highly productive individual (PhD, MD/PhD, or MD) with expertise in biochemical, developmental, or cell biological approaches toward understanding eye disease, with preference given to individuals interested in the pathogenesis of retinal related disorders. Candidates should have a track record of extramural funding, demonstrated ability to collaborate with other scientists and clinicians, and experience mentoring junior investigators.

The successful candidate will receive a generous start-up package, substantial internal funding, research space, and an opportunity to interact with exceptional basic and clinical investigators. Salary will be determined by experience. Learn more about Mayo Clinic and Rochester, MN, at: **www.mayoclinic.org**

Interested candidates should submit a curriculum vitae and letter of interest to:

**Jose Pulido, MD, MS, MPH**
**Chair, Career Scientist Search Committee**
**Department of Ophthalmology**
**Mayo Clinic**
**200 First Street SW • Rochester, MN 55905**
**E-mail: OphthalmolSciSearch@mayo.edu**

*Mayo Foundation is an affirmative action and equal opportunity employer and educator. Post-offer/pre-employment drug screening is required.*

NW127641R

MAX-PLANCK-GESELLSCHAFT

**IMPRS-MCB**
From Molecules to Biological Systems

ALBERT-LUDWIGS-UNIVERSITÄT FREIBURG

**The International Max Planck Research School for Molecular and Cellular Biology** (IMPRS-MCB) of the Max Planck Institute of Immunobiology and the Albert-Ludwigs-University in Freiburg i. Br. (Germany) invites suitable candidates to apply for a position in the preparatory program of our

## International PhD program 2008/2009

starting on **October 1, 2008** in Freiburg i. Br. (Germany).

We invite applications from all countries. Applicants must hold a Masters degree or a Diploma (or equivalent) in Biology, Biochemistry, Medicine, Chemistry, or related fields. It is not necessary to hold the degree at the point of application. However, you must have been awarded your degree prior to the start of the program in October 2008. Candidates have to be fluent in written and spoken English and should document their proficiency in English (TOEFL etc.). German is not required. All applications are reviewed and candidates are selected for personal interviews in Freiburg based on their academic qualification, motivation, CV, suitability to the program, and two confidential letters of recommendation. The closing date for online registration is May 3, 2008 and for full applications **May 10, 2008.** Online-registration and full details of the requirements for the application including the application form can be found at http://www.imprs-mcb.mpg.de. The Max Planck Society strives to offer more employment for the disabled. Disabled candidates are encouraged to apply. A childcare facility is attached to the Institute.

W127688R

UNIVERSITY OF HELSINKI

The Institute for Molecular Medicine Finland (FIMM, www.fimm.fi) was established in 2007 as a partner institution of the European Molecular Biology Laboratory (www.embl.org) together with the new Nordic nodes for molecular medicine in Norway and Sweden. FIMM was inaugurated as a joint venture of the University of Helsinki, the Hospital District of Helsinki and Uusimaa (HUS), the National Public Health Institute (KTL) with VTT Technical Research Centre of Finland joining in 2008. FIMM headquarters are located in the brand new Biomedicum Helsinki 2 research building on the Meilahti medical campus in Helsinki.
The research areas of FIMM include 1) Genetic epidemiology and genomics of cardiovascular and neuropsychiatric diseases and cancer 2) Medical systems biology and medical bioinformatics of common diseases, with a focus on cancer, diabetes and obesity 3) Leveraging the aforementioned research for translational applications, including health impact of genes, new diagnostic methods, biomarkers and therapeutics. FIMM also develops infrastructures for biobanking, medical bioinformatics, high-throughput sequencing, high-throughput screening, and other translational research platforms, including participation in the EU's ESFRI programs BBMRI and EATRIS.

FIMM is seeking outstanding international candidates for the prestigious positions of

## Group leaders in Molecular Medicine

Group leaders are expected to initiate a new research program as part of the new Nordic EMBL Partnership for Molecular Medicine. The group leaders are nominated for a 5-year term, which is renewable for up to four additional years. We expect to hire 3 - 4 new principal investigators from this call.

FIMM provides attractive sustainable support packages for new international group leaders of up to 1,2 - 1,7 M euro for the five year period. This includes salaries of the group leader, 1 - 2 postdoctoral fellows, 2 - 3 doctoral students and technician(s), consumables and modern laboratory facilities. The candidates are expected to complement this budget through other national or international grants and/or through industrial collaborations.

Qualification requirements include a MD/PhD, PhD or equivalent degree, appropriate postdoctoral training and a track-record of high-impact publications in the top journals for biology or medicine. Group leader positions are intended for early-stage independent investigators, comparable with the assistant or associate professor level, with the latter group expected to show a track record for attracting significant independent funding.

Successful candidates are expected to initiate a new independent research program at FIMM with a clear relevance to molecular medicine with significant translational opportunities.

Applications should include a covering letter summarizing the applicant's career and future plans (1 page), CV and a list of publications (past 10 years, with 5 most significant publications indicated), short research plan (max 3 pages) with a summary of expected translational, medical or public health impact, and names of three references.

Applications should be addressed to the Board of FIMM and sent electronically to the Institute for Molecular Medicine Finland (FIMM) at fimm-email@helsinki.fi to arrive no later than 8 April 2008. The first candidates may be nominated in June with an anticipated starting date in the fall of 2008, or at the latest by the end of the year.

Details of the call for group leader positions are available at www.fimm.fi. For further information please contact Director, Professor Olli Kallioniemi (olli.kallioniemi AT helsinki.fi).

Helsinki 7 March 2008
**Administration Office**

KTL HUS EMBL

W127672R

香 港 大 學
THE UNIVERSITY OF HONG KONG

Founded in 1911, The University of Hong Kong is committed to the highest international standards of excellence in teaching and research, and has been at the international forefront of academic scholarship for many years. Of a number of recent indicators of the University's performance, one is its ranking at 18 among the top 200 universities in the world by the UK's Times Higher Education Supplement. The University has a comprehensive range of study programmes and research disciplines, with 20,000 undergraduate and postgraduate students from 50 countries, and a complement of 1,200 academic members of staff, many of whom are internationally renowned.

## Research Assistant Professorships and Post-doctoral Fellowships

Applications are invited for a number of positions as Research Assistant Professor (RAP) (Ref: RF 2007 2008-570) and Post-doctoral Fellow (PDF) (Ref: RF-2007/2008-571), at the University of Hong Kong, on or before February 28, 2009. Appointments will be made for a period of 2 to 3 years.

RAP and PDF posts are created specifically to bring new impetus and vigour to the University's research enterprise. Positions are available from time to time to meet the strategic research needs identified by the University. Positions are available in the following Faculties/Departments/Schools/Centres/Institutes:

- Architecture
- School of Chinese
- School of Humanities
- School of Modern Languages and Cultures
- Centre for the Advancement of University Teaching
- Faculty of Education
- Civil Engineering
- Electrical and Electronic Engineering
- Industrial and Manufacturing Systems Engineering
- Law
- Centre for Cancer Research
- School of Chinese Medicine
- Research Centre of Heart, Brain, Hormone and Healthy Aging
- Medicine
- Microbiology
- Li Ka Shing Faculty of Medicine
- Pathology
- Physiology
- Psychiatry
- Centre for Reproduction, Development and Growth
- Surgery
- Area of Excellence (AoE) in Developmental Genomics and Skeletal Research and the Department of Biochemistry
- School of Biological Sciences
- Chemistry
- The Swire Institute of Marine Science
- Institute of Molecular Technology for Drug Discovery and Synthesis
- Physics
- Geography
- Psychology

Research Assistant Professors

The main focus of an RAP's duty is research. RAPs can however be assigned some teaching duties, up to 50% of the normal teaching load. Applicants should be research active and have a proven publication record. A highly competitive salary commensurate with qualifications and experience will be offered, with a contract-end gratuity and University contribution to a retirement benefits scheme (totalling up to 15% of basic salary). Annual leave, and medical/dental benefits will also be offered.

Post-doctoral Fellows

PDFs are expected to devote full-time to research. Applicants should be doctoral degree holders having undertaken original research that has contributed to the body of knowledge. A highly competitive salary commensurate with qualifications and experience will be offered. Annual leave, and medical/dental benefits will also be available.

Procedures

Prospective applicants are invited to visit the following webpage <https://www.hku.hk/apptunit/> to view the full list of the research areas and their home Faculties/Departments/Schools/Centres for which RAP/PDF positions are currently available. Before preparing an application they should contact the Head of the appropriate academic unit to ascertain that their research expertise matches the research area for which a vacant RAP/PDF post is available.

Applicants must submit a completed University application form, which should clearly state **which position they are applying for**; and in which **academic discipline**. They should also provide further information such as details of their research experience, publications, research proposals, etc.

**Further particulars and application forms** (272/302 amended) can be obtained at https://www.hku.hk/apptunit/, or from the Appointments Unit (Senior), Human Resource Section, Registry, The University of Hong Kong, Hong Kong (fax: (852) 2540 6735 or 2559 2058, e-mail: senrappt@hkucc.hku.hk). **Closes April 18, 2008**. Candidates who are not contacted within 3 months of the closing date may consider their applications unsuccessful.

JP1273/7/8R

*The University is an equal opportunity employer and is committed to a No-Smoking Policy*

CHARITÉ

# New Faculty Positions
## Neuroscience Berlin

The Charité, the Freie Universität Berlin, and the Humboldt-Universität zu Berlin as well as the extra-university institutions (MDC, FMP, DRFZ) invite applications for multiple faculty positions. In general, professorships will be established as tenure-track or tenured positions ranging from assistant (W1) to full professor (W3) depending on the candidate's prior achievements. In addition, we will establish several junior research groups. This is part of an ambitious recruitment effort aimed at significantly increasing the complement of interdisciplinary neuroscience investigators in Berlin.

The historical and beautiful Charité Campus Mitte is located right in the heart of Berlin. The Charité is not only one of the largest clinics in Europe, but also one of Germany's oldest hospitals, rich with clinical experience and basic research. Good child care facilities as well as support for foreigners are provided in this lively and exciting city of Berlin.

Of particular interest are neuroscientists with broad expertise in anatomy, biology, chemistry, physics, or physiology. We envisage to establish a new research unit for behavioural analysis which will be headed by a faculty position (W3-Full Professorship). Furthermore, researchers interested in mechanisms of neuronal damage, endogenous neuroprotection, regeneration, interaction of the nervous system with the immune system, neurodevelopment as well as developmental disorders and mechanisms of neuronal plasticity, will allow us to complement our interdisciplinary network.

However, demonstrated excellence in research is more important than the area of research. Thus, the primary criteria for appointment will be outstanding records of innovative research and academic performance, including landmark papers in leading journals, as well as high potential for establishing a rigorous and substantial independent research program, inspiring mentorship, and fruitful collaboration.

The positions offer the opportunity to be involved in basic research training for medical students, to mentor graduate students with a strong interest in basic science and translational research. In addition to the PhD students that are actively pursuing graduate studies, we maintain a large and highly regarded MD/PhD program. Further, state-of-the-art genomics, proteomics, and neuroimaging facilities, as well as extensive dedicated animal housing are available to all members of the neuroscience community.

The successful applicant will be expected to develop and maintain an externally-funded research program and to teach at the undergraduate and graduate level. Preference will be given to individuals whose interests are synergistic with ongoing research programs at the center.

The Center's institutions are equal opportunity employers, committed to the advancement of individuals without regard to ethnicity, religion, sex, age, disability or any other protected status.
Please send a curriculum vitae, description of achievements and research interests to:

**Dean Prof. Dr. Martin Paul**
**Charité – Universitätsmedizin Berlin**
**Charitéplatz 1 | 10117 Berlin | Germany**
**email: neurocure@charite.de**

The search will continue until the positions are filled. To ensure full consideration, applications should be received by **April 15, 2008.** The electronic submission of your documents is strongly encouraged. For additional information on research programs and facilities, see **www.neurocure.de**

The successful candidate will join an interactive group of investigators in state-of-the-art research facilities at Charité Campus Berlin Mitte. She will have joint appointments in the respective home institutions and the excellence cluster NeuroCure.

DRFZ FMP MDC

W1271/22R

## Senior Lecturer/Lecturer

**School of Biomedical Sciences (Centre for Vision Science)** Ref: 08/100335

Interviews will be held on 23 May 2008

Lecturer salary scale £30,012 - £44,074 per annum (including contribution points)

Senior Lecturer salary scale £42,791 - £54,206 per annum (including contribution points)

Closing date 4.00pm, Friday 4 April 2008

## Research Fellow

Ref: 08/100332

**School of Pharmacy**

Funded by BBSRC/EPSRC for 3 years to assist in the development of novel bacterial protease-triggered drug releasing hydrogels for medical device applications.

Interviews will be held on 17 April 2008

Salary scale £27,466 – £35,837 per annum (including contribution points)
Closing date 4.00pm, Monday 31 March 2008

## Research Fellow

Ref: 08/100336

**School of Biomedical Sciences (Centre for Vision Science)**

This post is available immediately for 36 months. Interviews will be held 28 April 2008

Salary scale £27,466 - £35,837 per annum (including contribution points)
Closing date 4.00pm, Friday 4 April 2008

Please visit our website for further information and to apply online – **www.qub.ac.uk/jobs** or alternatively contact the address below.

The University is committed to equal opportunities and to selection on merit. It therefore welcomes applications from all sections of society.

Fixed term contract posts are available for the stated period in the first instance but in particular circumstances may be renewed or made permanent subject to availability of funding.

**Personnel Department**
**Queen's University Belfast**
Belfast, BT7 1NN.
Tel (028) 90973044
or (028) 90973854
(answering machine)
Fax (028) 90971040
E-mail on personnel@qub.ac.uk

Queen's University Belfast

Rg Queen's University Belfast is a member of the Russell Group of universities. One of the United Kingdom's top 20 research-intensive universities.

U127700A

CHARITÉ

UNIVERSITÄTSMEDIZIN BERLIN
GLIEDKÖRPERSCHAFT DER FREIEN UNIVERSITÄT UND DER HUMBOLDT-UNIVERSITÄT ZU BERLIN

The Charité invites applications for

## University Professorships at the Integrated Center for Research and Treatment 'Center for Stroke Research Berlin'

6 positions according to salary levels Bes.Gr. W1, W2 W3 BBesG (tenure track) depending on prior achievements
(Ref No 333/2008)

The positions come along with postdoctoral and/or PhD student positions and with technical support.

The professorships are part of the Center for Stroke Research Berlin (CSB), funded within the Integrated Research and Treatment Center (IFB) initiative by the Bundesministerium für Bildung und Forschung (BMBF). The CSB is an interdisciplinary center aiming at visible improvements in stroke research, promotion and training of young scientists and clinician scientists as well as in the medical care of affected patients. Dedicated to bench to bedside as well as bedside to bench translation, its activities span from basic stroke research to patient care. The 'Berlin Stroke Alliance' of the CSB links such partners as health insurers, emergency service operators, the Berlin fire department, private groups running rehabilitation and care centers. The CSB will thus be able to recruit and follow up a large number of stroke patients from the hyperacute to the chronic stage. The CSB will also provide unique diagnostic and therapeutic facilities, such as magnetic resonance imaging.

According to the application of the Charité and the recommendations of the international review board the CSB welcomes applications with a focus on the following topics:

- Clinical epidemiology of stroke
- Neurology with focus on stroke
- Preclinical molecular imaging of stroke
- Interdisciplinary stroke research
- Experimental stroke research

Qualifications: as per § 100 Berlin Higher Education Act (BerlHG) for W1-positions university degree, outstanding thesis; for W2/W3-positions Junior Professorship or postdoctoral thesis (Habilitation) or equivalent scientific achievement and teaching qualifications.

The Charité is an equal opportunity employer committed to excellence through diversity. As women are under-represented in scientific work, we explicitly encourage women to send in their application.

For details on application see www.charite.de/jobs/prof.html application instructions. Please send curriculum vitae, description of achievements and research interests, and brief research concept by 10.04.2008 to:

**Charité - Universitätsmedizin Berlin**
**Prof. Dr. Martin Paul, Dean, 10098 Berlin**

The Charité is the medical school of the Humboldt-Universität zu Berlin und the Freie Universität Berlin. For more information see www.strokecenter.de and www.charite.de.

W127380A

UNIVERSITY OF OXFORD

U127851A

**University of Oxford**
**Theoretical Chemistry**
**Postdoctoral research associate**

Using a wide range of computational techniques, the aim of this 18-month project is to develop a theoretical understanding of the role of polymer structures on electronic processes that determine the performance and efficiency of optoelectronic polymer devices. A PhD in theoretical/computational chemistry/condensed matter physics is required.

**Contact**
Jane Blakeman
Tel: +44 (0)1865 275414
Email: jane.blakeman@chem.ox.ac.uk
http://www.chem.ox.ac.uk/jobs.asp

High-profile speakers discuss science careers in the engaging podcast series on **naturejobs.com**

naturejobs making science work

Have you listened to the new podcasts on **naturejobs.com**?

naturejobs making science work

MRC Medical Research Council

wellcome trust

# Research Group Leaders in fundamental stem cell biology

## Wellcome Trust Centre for Stem Cell Research

Under the leadership of Austin Smith and Fiona Watt, the Wellcome Trust Centre for Stem Cell Research is pursuing a broad programme of basic research in embryonic, foetal and adult stem cell biology.

The Centre has openings for Group Leaders to lead independent research teams. Interest is welcomed from stem cell biologists and from individuals with a background of achievement in relevant disciplines, such as development, signalling, cancer, or computational biology. We invite proposals in all aspects of vertebrate stem cell research, although areas of particular interest for the current round are quantitative analysis and modelling of cell fate decisions; haematopoietic stem cells, induced reprogramming, and endodermal stem/progenitor cells.

Candidate **Senior Group Leaders** will have an established international reputation for creative research with commensurate achievements and experience in team leadership. Candidate **Junior Group Leaders** will have post-doctoral experience with demonstrable capacity to complete substantive and innovative research.

Personal Fellowship support may be available for up to three years. During this time Group Leaders will be expected to win competitive external Fellowships offered by agencies such as The Wellcome Trust, Medical Research Council, Cancer Research-UK and British Heart Foundation.

The Centre provides newly refurbished personal office and laboratory space, core infrastructure and services, and start up support. Excellent opportunities for biomedical translation are available through interactions with clinical research groups supported by the Medical Research Council Cambridge Centre in Stem Cell Biology and Medicine.

**For further details see www.cscr.cam.ac.uk**

**If you are interested in joining CSCR as an independent Group Leader please send a 1-2 page outline research proposal and CV by email to cscr-gls@cscr.cam.ac.uk by 11th April 2008. Shortlisted candidates will be asked to attend interviews on both 30th April and 1st May 2008.**

**The University is committed to Equality of Opportunity.**

**www.cam.ac.uk/jobs/**

**A world of opportunities**

UNIVERSITY OF CAMBRIDGE

U127704R

---

CRG

The Center for Genomic Regulation (CRG, http://www.crg.es/) is a leading genomics research institute, associated with the University Pompeu Fabra (UPF) and located at the Parc de Recerca Biomèdica de Barcelona (PRBB, http://www.prbb.org/). The CRG contains six research programmes: Gene Regulation, Differentiation and Cancer, Cell Biology and Development, Systems Biology, Genes and Disease and Genomic Bioinformatics, and has a partnership with the EMBL through the Systems Biology programme. The PRBB includes three other institutions devoted to biomedical research: the Department of Life and Health Sciences of the UPF (CEXS/UPF, http://www.upf.edu/cexs/), the Municipal Institute of Medical Research (IMIM, http://www.imim.es/) and the Centre for Regenerative Medicine of Barcelona (CMRB, http://www.cmrbarcelona.org/). To give support to this scientific community the CRG has built state of the art Genomics and Light microscopy facilities as well as Screening and FACS facilities. New developments contemplate a top of the art proteomics facility.

**Bioinformatician for an Epigenetic Project - ref. BIOINFO-0308-1**

The CRG is looking for a Bioinformatician for an Epigenetic Project. The Project "Epigenetics: Mechanisms and Disease" involves 9 Spanish groups and is coordinated by M. Beato from the CRG, where 2 other groups, T. Graf and L. Di Croce, participate in the project. The successful candidate will work at the Genomic Facility of the CRG that includes Genotyping, Sequencing, Microarray and next generation sequencing (Genome Analyzer 1G [Illumina-Solexa] and GS-FLX 454 Roche), and will be responsible for advising and evaluating results obtained with expression profiling, ChIP-on-chip, tiling arrays, Chip-seq, genotyping and high-throughput array-based DNA methylation experiments. Experience in dealing with any of these techniques will be an advantage. The successful candidate is expected to provide expertise to all members of the Project, including the groups of M. Esteller, F. Azorín, M. A. Peinado, M. Martínez-Balbas, J. C. Reyes and G. López-Rivas, and to collaborate with other colleagues within the CRG Genomic Facility and the Bioinformatics and Genomics programme.

The position involves a competitive salary initially for 3 years and financed by the Epigenetic Project, but could be extended to an open-ended contract with the CRG.

Candidates should send a CV with list of publications and description of their experience as well as the addresses of 3 potential references to:

**Reyes Perza**
**Centre de Regulació Genòmica**
**Dr. Aiguader 88, 08003-Barcelona, Spain**
reyes.perza@crg.es

*Applications Deadline: 8 weeks after the publication of this add.*

W127710R

---

MAX PLANCK INSTITUTE FOR HUMAN COGNITIVE AND BRAIN SCIENCES LEIPZIG

The Max Planck Institute for Human Cognitive and Brain Sciences in Leipzig, Germany, Department of Cognitive Neurology (Head of Department: Prof. Dr. Arno Villringer) invites you to apply for

## PostDoctoral and PhD positions

The focus of our multi-disciplinary research group is on stroke rehabilitation in humans. We are aiming to merge stimulation protocols (e. g. TMS, tDCS), cognitive tasks and drug administration to induce neuroplasticity as observed by electrophysiological methods and functional magnetic resonance imaging (alone AND in combination, e. g. fMRI-EEG). Candidates interested in clinical neuroscience, neuroplasticity, as well as in higher cognitive function and brain imaging are invited to apply. The successful candidates should be enthusiastic and will have a strong interest in this exciting research area.

A background in EEG, TMS or fMRI acquisition and analysis techniques (SPM, FSL, Matlab, BESA etc.) would be of advantage. The Max Planck Institute in Leipzig offers an excellent multi-disciplinary and interactive research environment with access to excellent research facilities (3T and 7T research MRI scanners, MEG, EEG and TMS devices). The positions are funded for maximally 3 years from now and will be held open until suitable candidates have been found.

For further details please contact Dr. Burkhard Pleger by email bpleger@cbs.mpg.de or phone: +49 (0) 341-9940-135.

In order to increase the proportion of female staff members, female scientists are particularly encouraged. Disabled applicants are preferred if qualification is equal.

Please send your application including the name of referees by email (preferred) or post, citing the **code number "D 1/08"** to:

**Max-Planck-Institut für**
**Kognitions- und Neurowissenschaften**
**- Verwaltung -**
**Stephanstraße 1a, D-04103 Leipzig**
**www.cbs.mpg.de**

W127686R

---

# Max-Planck-Institut für Molekulare Pflanzenphysiologie

The Max Planck Institute of Molecular Plant Physiology in Potsdam invites applications for a

## Postdoctoral Position

**(code 11/08)**

in Quantitative Genetics, to work on projects related to the analysis of variation in growth and metabolism in Arabidopsis and crop plants. The position offers the possibility to apply quantitative genetics in an interdisciplinary environment. We are investigating phenotypic variations in metabolism in large populations of inbreds and accessions/cultivars, using robotised methods to analyse enzyme activities and metabolites. The institute has a large number of bioinformaticians and modellers, and is one of the BMBF-funded Systems Biology Centres in Germany.

The candidate should have a PhD in Plant Biology, Genetics or Mathematics. The position requires experience in the creation and genotyping of plant populations, in experimental design, and in statistical analysis. Experience in the analysis of population structure and association mapping is desirable. The position is funded initially for 30 months.

For further information contact Prof. Mark Stitt (Phone: +49-(0)331 567 8100, mail: mstitt@mpimp-golm.mpg.de or visit http://www.mpimp-golm.mpg.de).

Applications including CV, list of publications and letters of recommendation from two referees should be sent by the 3. April 2008 to:

Max-Planck-Institut
für Molekulare Pflanzenphysiologie
-Personalverwaltung-
Wissenschaftspark Golm
Am Mühlenberg 1, 14476 Potsdam

MAX PLANCK GESELLSCHAFT

W127658R

## UNIVERSITY OF BASEL, DEPARTMENT OF PHYSICS

# Three Faculty Positions in Experimental Physics

## (a) Nano Technology / Quantum Optics
## (b) Nano Physics / Atomic, Molecular and Optical Physics
## (c) Condensed Matter Physics

The Department of Physics at the University of Basel invites applications for two tenure-track assistant professorship positions and one associate or full faculty position. We seek interactive and creative scientists conducting outstanding experimental research that complements, strengthens and expands our activities in condensed matter physics and in particular nanophysics (http://physik.unibas.ch). Possible research directions include (but are not limited to): quantum optics, atomic, molecular and optical physics, soft and hard condensed matter physics, nano materials or scanning probe physics. For all positions, strong synergies with at least some of the Departments existing groups and activities in nano physics would be advantageous.

The successful applicants are expected to establish strong, independent research programs participating actively in the Swiss Nanoscience Institute (SNI) hosted at our Department as well as the Basel QC2 Center for Quantum Computation and Quantum Coherence. The ideal candidates will play an active role in our physics degree program as well as our recently established nano science curriculum teaching at all levels.

Applicants should provide a curriculum vitae, a publication list indicating five outstanding papers, a statement of research interests, a statement of teaching interests and experience, together with the names and addresses of five potential referees to: **Prof. Dr. Hans-Peter Hauri, Dean, Faculty of Science, University of Basel, Klingelbergstrasse 50, 4056 Basel, Switzerland,** and electronically (pdf or zip) to Marianne.Hess@unibas.ch.

**The deadline for receipt of the application is May 31, 2008,** but applications will continue to be considered until the positions are filled. The University of Basel is an equal opportunity employer and would like to particularly encourage applications from highly qualified female candidates. For additional information please contact any of the faculty members in condensed matter physics, http://physik.unibas.ch

UNI BASEL

W127411R

HOWARD HUGHES MEDICAL INSTITUTE

# Independent Fellow Positions at the Janelia Farm Research Campus

We invite applications for independent fellow positions from biochemists, biologists, chemists, computer scientists, engineers, mathematicians, neurobiologists, and physicists who are passionate in their pursuit of important problems in basic scientific and technical research.

Fellows are independent scientists with labs of up to two additional members. Appointments are for five years.

**Application deadline: July 15, 2008**

**For more information and to submit an application:**

**www.hhmi.org/ref/janelia/nat**

HHMI
janelia farm
research campus

The Janelia Farm Research Campus of the Howard Hughes Medical Institute pursues challenging basic biomedical problems for which future progress requires technological innovation.

Janelia Farm focuses on two research areas: the identification of general principles that govern how information is processed by neuronal circuits, using genetic model systems in conjunction with imaging, electrophysiological, and computational methods· and the development of imaging technologies and computational methods for image analysis.

Janelia Farm is now home to a growing and multidisciplinary community of 27 research groups, supported by outstanding shared resources within a unique campus less than an hour from Washington, D.C. We value research collaboration between groups as a mechanism to enable long-range innovative science and encourage the self-assembly of interdisciplinary teams of scientists. We welcome coordinated applications from groups of individuals Applications from individuals at all career stages are invited.

All laboratories are internally funded, without extramural grants. Lab heads have no formal teaching duties and minimal administrative responsibilities. They are expected to engage in the direct conduct of research and in intellectual interaction with their colleagues. Individual research groups are limited in size, comprising postdoctoral associates, graduate students, and technicians. Janelia Farm hosts conferences, and group leaders are encouraged to organize meetings in their areas of interest.

Janelia Farm offers a supportive working environment with on-site child care, fitness center, and dining facilities on a 689-acre campus along the Potomac River in Northern Virginia.

The Howard Hughes Medical Institute is an equal opportunity employer

NW127141R

science foundation ireland
fondúireacht eolaíochta éireann

# Ireland

## funds great research...

## ...maybe it's your turn!

Science Foundation Ireland, (SFI)
**the national foundation for excellence in scientific research is investing in academic researchers and research teams who are most likely to generate new knowledge, leading edge technologies, and competitive enterprises.**

SFI has a flexible grants and awards portfolio and several times a year issues calls for proposals from scientists and engineers. SFI also accepts unsolicited proposals throughout the year. SFI's award programmes include:

**Principal Investigator Programme**
for outstanding researchers, normally ranging between €50,000 - €1 million per year and may be up to five years in duration.

**Research Professor Recruitment Awards**
for outstanding researchers, with particularly distinguished international reputations, awards normally ranging up to €500,000 per annum for up to two years.

**E.T.S. Walton Visitor Awards**
supporting leading international scientists who visit Ireland to undertake research for up to one year, normally ranging up to €200,000.

**President of Ireland Young Researcher Awards (PIYRA)**
attracting to Ireland and supporting Irish researchers within five years of completing their PhD, normally up to €1 million over five years.

## Positions with SFI

**SFI Scientific Programme Officers**
As a Scientific Programme Officer you will be a key decision maker within the Foundation and will have responsibility for managing a portfolio of scientific investments made by SFI. In managing the peer-review process you will be required to interact with international researchers at the highest level. Candidates must possess a relevant PhD together with five years experience beyond the PhD in academia or industry.

To discuss the career opportunities as a Programme Officer and see how you can have an impact on Irish science e-mail your c.v. to hr@sfi.ie

## Current employment opportunities on SFI funded research projects

**Trinity College Dublin**
*Further Details:*
**www.tcd.ie/vacancies**

Professorship and Lectureship in Microbial Molecular Pathogenesis (School of Genetics and Microbiology)

**University of Limerick**
*Further Details:*
**www.ul.ie/hrvacancies**

Postdoctoral positions in Software Engineering, Lero, Department of Computer Science and Information Systems

PhD Studentship in Mathematical Modelling of Dynamics on Complex Networks

Postgraduate (PhD) Studentship in Mathematical Modelling

## National University of Ireland, Galway

*Further Details*
**www.nuigalway.ie/vacancies**

Stokes Professorship of Immunology, School of Medicine

Stokes Professorship of Biophotonics

Stokes Professorship of Bioinformatics

Postdoctoral Researcher with experience in gene targeting to work on modeling the DNA damage response in DT40 cells.

PhD Studentships 2 positions to study the role of DNA damage-dependent checkpoint proteins and in the cellular responses to DNA damage.

## National Centre for Biomedical Engineering Sciences (NCBES)

Postdoctoral Researcher in particle image velocimetry for biomedical fluid dynamics

Technical Officer – Network of Excellence for Functional Biomaterials (NFB).

PhD Studentships Network of Excellence for Functional Biomaterials (NFB) developing the next generation of biomaterials at a nanoscale level

## Dublin City University

*Further Details*
**www.dcu.ie/vacancies/current.shtml**

Stokes Professor of Financial Mathematics- School of Mathematical Sciences

## Centre for Next Generation Localisation (NGL)

***This is a multi-university collaborative initiative led by DCU.***

Language Technology

Postdoctoral Positions in Machine Translation

Postdoctoral Position in Natural Language Processing

PhD Scholarships in machine Translation

## Athlone Institute of Technology

*Further Details:*
**http://www.ait.ie/vacancies/**

PhD in Biomedical Microbiology.

## Royal College of Surgeons in Ireland

*Further Details:*
**http://www.rcsi.ie/index.jsp?1nID=93&pID=96&nID=130**

One Lecturer and 2 PhD posts at RCSI as part of the Irish Drug Delivery Research Network Cluster.

## National University of Ireland Maynooth

*Further Details*
**http://personnel.nuim.ie/vacancies**

## National Centre for Geocomputation (NCG)

*Further Details:*
**http://ncg.nuim.ie/ncg/funding/positions/**

**PhD Fellowships in Advanced Geotechnologies**

Sensor Integration - 4 positions. Research topics: sensor integration and data fusion, real-time dynamic geospatial monitoring, adaptive and smart geosensor networks.

Spatial Algorithms - 3 positions. Research topics: structuring LiDAR data, spatial anomaly analysis, wayfinding, spatial modelling and data integration, change detection

Spatial Visualisation - 2 positions. Research topics: knowledge discovery from spatio-temporal data, 3D Virtual Environments, 3D computer vision and visual sation of temporal data.

Location-Based Services - 1 position. Research topics: data capture, exploration and visualisations for application driven LBS for scientific and technical applications.

**Post-doctoral Research Fellowships in Advanced Geotechnologies**

Sensor Integration – 3 positions. Research topics include sensor integration and data fusion, rea - time dynamic geospatial monitoring, adaptive and smart geosensor networks.

Spatial Algorithms – 1 position. Research topics: structuring LiDAR data, spatial anomaly analysis, wayfinding, spatial modelling and data integrat on, change detection.

Spatial Visualisation – 2 positions. Research topics: knowledge discovery from spatio-temporal data, 3D Virtual Environments, 3D computer vision and visual sation of temporal data.

Location-Based Services - 1 position. Research topics: data capture, exploration and visualisations for application driven LBS for scientific and technical applications.

sfi
science foundation ireland
fondúireacht eolaíochta éireann

NDP
National Development Plan 2007 – 2013

**Science Foundation Ireland**
Wilton Park House, Wilton Place, Dublin 2, Ireland. **tel** +353 1 607 3200 **fax** +353 1 607 3201 **email** info@sfi.ie

MANCHESTER 1824

The University of Manchester

**Faculty of Life Sciences**

## Post Doctoral Research Associate - Investigating Specificity of Yeast Protein Complexes Using Bioinformatics Methods (Ref LS/80100)

## Post Doctoral Research Associate - Investigating Specificity of Yeast Protein Complexes Using Experimental Methods (Ref LS/80101)

## Post Doctoral Research Associate – A Rational in silico approach to mapping interactomes, applied to Candida Glabrata (Ref LS/80102)

**£26,666 - £32,796 per annum**

**LS/80100** Based in the bioinformatics laboratories of Drs Simon Lovell and David Robertson, we seek a capable and enthusiastic computational biologist to study protein-protein interactions, specifically to investigate determinants of binding specificity in protein complexes. This will involve the use of evolutionary and structural information to gain insight into the nature of protein interactions in the cellular interactome. The post forms part of an interdisciplinary project with Dr Daniela Delneri and a complementary molecular biology post is advertised (see LS/80101).

You should have (or expect to hold shortly) a relevant PhD. Experience of computer-based research is required and experience in protein structure analysis and/or molecular evolution an advantage

**Informal enquiries may be addressed to: Dr. Simon Lovell, Tel.: +44 (0)161 275 5748, E-mail: simon.lovell@manchester.ac.uk**

**LS/80101.** Based in the laboratory of Dr Daniela Delneri, we seek a capable and enthusiastic molecular biologist to study protein-protein interactions, specifically to understand the efficiency with which homologous proteins from different species are able to interact to form complexes. The position will involve the use of substantial molecular biology and biochemistry including classical genetic tools, gene targeting protein purification and analytical techniques. The post forms part of an interdisciplinary project with Drs Simon Lovell and David Robertson and a complementary computational biology bioinformatics post is also advertised.

You should have (or expect to hold shortly) a PhD in Genetics, Molecular Biology or Biochemistry with associated relevant research experience Experience in yeast manipulation techniques will be an advantage

**Informal enquiries may be addressed to: Dr. Daniela Delneri, Tel.: +44 (0)161 275 5686, E-mail: d.delneri@manchester.ac.uk**

**LS/80102:** Based in the bioinformatics laboratories of Drs Simon Lovell and David Robertson, we seek a capable and enthusiastic computational biologist to study protein-protein interactions networks, specifically to develop evolutionary and structure-based methods to infer interaction networks between species. The post forms part of an interdisciplinary project in collaboration with Imperial College London. Our combined aim is to develop a rational and integrated approach to reliably and comprehensively predict protein interactions using sophisticated bioinformatics, statistical and comparative approaches.

You should have (or expect to hold shortly) a relevant PhD. Experience of computer-based research is required and experience in protein structure analysis, network analysis and/or molecular evolution an advantage

**Informal enquiries may be addressed to: Dr Simon Lovell, Tel: +44 (0)161 275 5748, E-mail: simon.lovell@manchester.ac.uk**

All posts are funded by the BBSRC and are tenable immediately for up to 3 years.

Further information can be found at www.manchester.ac.uk/bioinformatics.

**Application forms and further particulars can be obtained at www.manchester.ac.uk/aboutus/jobs/ Or from;**

**The Directorate of Human Resources**
**Tel: ++44 (0) 161 275 8836**
**Email: Lifesciences-hr@manchester.ac.uk**

**The closing date for applications is 28 March 2008.**
**Please quote appropriate reference.**

*The University will actively foster a culture of inclusion and diversity and will seek to achieve true equality of opportunity for all members of its community.*

U127697R

www.manchester.ac.uk/jobs

## *Director*

**ADVANCED MATERIALS PROCESSING AND ANALYSIS CENTER and NANOSCIENCE TECHNOLOGY CENTER**

The University of Central Florida, with over 48,000 students, is searching for a Director of its Advanced Materials Processing and Analysis Center (AMPAC) and NanoScience Technology Center (NSTC). The successful candidate is expected to lead both centers and develop plans for the merger of the two centers with a recurring annual budget approaching $5 million. The candidate must have a Ph.D. in an appropriate discipline from an accredited institution and must be eligible for appointment with tenure at the full professor rank. NSTC has grown to 14 faculty with over 75 Ph.D. students and staff in less than 3 years. It has 20,000 sq ft of state-of-the-art laboratory space with approximately $8M in external funding to date. AMPAC, with 19 MS and 53 PhD students, currently has 9 tenured/tenure-earning faculty, 17 affiliated faculty, & 5 full-time staff who support two major multi-user facilities, the 7,000 sq ft Materials Characterization Facility (MCF) and the 2,600 sq ft class 100/1000 clean room Advanced Microfabrication Facility (AMF).

**For more information see http://www.creol.ucf.edu/TheCollege/Positions/AmpacDirector.aspx. (also see http://www.ampac.ucf.edu/ & http://www.nanoscience.ucf.edu/.**

Review of candidates will begin on March 31, 2008 and continue until the position is filled.

*UCF is an EO/AA employer*

NW127664R

University of BRISTOL

www.bristol.ac.uk

# Independent Research Fellowships

The RAE Grade 5 School of Biological Sciences, is seeking to recruit highly motivated independent Research Fellows. The School works on a diverse range of taxa at all levels (genes, cells, whole organisms, ecosystems) and has strong research links with other world-leading groups in the University (Biochemistry, Computer Science, Earth Sciences, Experimental Psychology, Geography, Mathematics, Physics). In 2011, we will move to a new state-of-the-art building.

Our Fellowship programme (see www.bio.bris.ac.uk/independentresearchfellowships) outlines our commitment to supporting the career development of Fellows through to permanent positions.

**If you are interested in applying for a Fellowship based at Bristol, please contact the Head of School, Professor Paul Hayes, e-mail paul.hayes@bristol.ac.uk to discuss your plans.**

EXCELLENCE THROUGH DIVERSITY

U127879A

LEARNING • DISCOVERY • ENTERPRISE

---

CHARITÉ

UNIVERSITÄTSMEDIZIN BERLIN

GLIEDKÖRPERSCHAFT DER FREIEN UNIVERSITÄT UND DER HUMBOLDT-UNIVERSITÄT ZU BERLIN

The recently established Berlin-Brandenburg School for Regenerative Therapies is a facility of the Charité – Universitätsmedizin Berlin and is closely linked to the Berlin-Brandenburg Center for Regenerative Therapies. The highly interactive research program of the center comprises work in four medical research fields (musculoskeletal, immunological, cardiovascular and nervous system), each of which is linked to the overlapping platforms of basic research, bioengineering, and translational research. Based on the collaboration of a range of partner research institutions and, with the support of the regional development agencies and local industry partners, the Berlin-Brandenburg region offers optimal conditions for the education of young scientists eager to develop and successfully transfer research findings into clinical applications.

The DFG Graduate School "Berlin-Brandenburg School for Regenerative Therapies" invites applications for the following position (Salary Group W2 BBesG):

## University Professorship "Engineering Basis of Regeneration"

(Ref. No. 334/2008)

The initial appointment is for five years with the possibility of further extension following successful evaluation. For further detailed information about this announcement please visit: http://www.bsrt.de; http://www.b-crt.de and http://www.charite.de

W127868A

---

nature physics

## Locum Associate Editor

*Nature Physics* seeks a Locum Associate Editor to join its editorial team for a period of nine months, to cover maternity leave.

*Nature Physics* is a prestigious journal covering all areas of research in physics. For more information about the journal, see our website (http://www.nature.com/nphys).

The ideal candidate will have completed a Ph.D. in a physics discipline, and postdoctoral experience is preferred (but not required). Key elements of the position include the selection of manuscripts for publication, as well as commissioning, editing and writing for the journal.

This is a demanding and intellectually stimulating role that calls for a keen interest in the practice and communication of science. The successful candidate will therefore be highly motivated and must possess excellent interpersonal skills.

The position will be based in our London office.

Applicants should send a CV (including a brief account of their research and other relevant experience); a research highlight in *Nature Physics* style (200 words or less) on a recent relevant paper in the literature; and a brief cover letter explaining their interest in the post and their salary expectations.

Applications should be sent to Denise Pitter, Personnel Assistant at londonrecruitment@macmillan.co.uk. Applicants should clearly mark on their submissions the reference number NPG/LON/829. Incomplete applications will not be considered.

All candidates must demonstrate the right to live and work in the UK to be considered for the vacancy.

Closing Date: Monday 31st March 2008

nature publishing group npg

N125344A

---

The University of Nottingham

School of Biology - Institute of Genetics

## Director of the Frozen Ark Project & Professor of Genetics & Conservation

Applications are invited for the above post in the Institute of Genetics and School of Biology at the University of Nottingham. The successful candidate will be expected to conduct an international quality programme of research, direct this major conservation genetics initiative and contribute to teaching within the School of Biology. Direction of the Frozen Ark Project will be the main administrative task and the person appointed will be spared other such duties within the School and Institute.

Applications will be considered from candidates who work in the area of genetics and conservation and whose research strengthens existing areas within the Institute and School.

Information about research in the Institute of Genetics is available at: http://www.nottingham.ac.uk/genetics and further information about the School of Biology is available at: http://www.nottingham.ac.uk/biology.

Salary will be within the professorial scale, minimum £51,095 per annum.

Informal enquiries may be addressed to Professor J D Brook, tel: 0115 823 0345 or Email: David.Brook@Nottingham.ac.uk. Further information about the Frozen Ark project is available at http://www.frozenark.org or by contacting Professor Emeritus B Clarke, Email: Bryan.Clarke@Nottingham.ac.uk.

For more details and/or to apply on-line please access http://jobs.nottingham.ac.uk/JK25526. If you are unable to apply on-line please contact the Human Resources Department, tel: 0115 951 3262 or fax: 0115 951 5205. **Please quote ref: JK/25526. Closing date: 18 April 2008.**

**This post is open until filled - review of applications from 18 April 2008.**

U127707AM

**http://jobs.nottingham.ac.uk**

Durham University

**BIOPHYSICAL SCIENCES INSTITUTE**

## THREE CHAIRS IN BIOPHYSICAL SCIENCES

**(OF WHOM ONE MAY BECOME THE INSTITUTE DIRECTOR)**

*Salaries will be by negotiation within the Professorial Range*

Three Chair positions are available in the School of Biological & Biomedical Sciences, the Department of Chemistry and the Department of Physics which are aligned to the newly created Institute of Biophysical Sciences (BSI) at Durham. The applicants will conduct research within the broad field of the physical sciences applied to questions of biological importance. They will develop and deliver teaching programmes in this area and provide academic leadership within the BSI. The applicants' research must be of the highest quality and relevant to the plans of the BSI

The post of first Director of the Institute is also vacant; suitable applicants for these chairs may be considered for that post also.

Informal enquiries may be made to the Heads of each School or Department or to the Chair of the BSI Steering Committee They are: Professor C.J. Hutchison, biosci headofschool@durham.ac.uk; (for Biological & Biomedical Sciences), Professor J.A.K. Howard CBE FRS, j.a.k.howard@durham.ac.uk (for Chemistry), and Professor R.A.Abram, physics.head@durham.ac.uk (for Physics); and Professor J.M Chamberlain, martyn.chamberlain@durham.ac.uk (for BSI)

**Closing date: 18th April 2008**

**Please quote the following Reference Numbers:**

**2325/NAT (Physics)**
**2326/NAT (Chemistry)**
**2327/NAT (Biological & Biomedical Sciences)**

**Further details of the post and an application form are available on our website (https://jobs.dur.ac.uk) or Tel: 0191 334 6499; Fax: 0191 334 6495.**

U127705R

## Postdoctoral opportunities at Karolinska Institutet

The Division of Metabolic Diseases at the Department of Laboratory Medicine is located at the Huddinge campus of Karolinska Institutet and offers an outstanding research environment. Applications are invited from individuals of the highest calibre with Ph.D. and/or M.D. degrees. A strong background in molecular biology or mouse genetics is required

**Project I:** Mouse models to study mitochondrial dysfunction and regulation of mitochondrial DNA expression (supervisor Nils-Göran Larsson)

**Project II:** Mitochondrial dysfunction in ageing (supervisor Aleksandra Trifunovic)

**Recent publications:** [Nature 2004.429 417-423] [PNAS 2005.102 17993-17998] [Cell 2007 27,130(2).273-85]

**Application:** Candidates should e-mail a letter of interest, CV, publication list and names of three references in one file (pdf format preferred) to lene.sorensen@ki.se

A working knowledge of the English language is required.

**Deadline April 30, 2008.**

www.ki.se
www.mitomed.se

W127134RM

**Leibniz Institute for Zoo and Wildlife Research**

The Leibniz Institute for Zoo and Wildlife Research (IZW) in Berlin is Germany's premier wildlife research institute (www.izw-berlin.de) To continue and develop its revised and expanded research program in the fields of evolutionary adaptations, wildlife diseases, reproductive biology and biological conservation the institute seeks to appoint

## 1 biochemist

within its research group Reproduction Biology She/He will conduct research projects in the field of wildlife reproduction biology with emphasis on feto-maternal interaction and contraception in wildlife animals, participate in ongoing research projects of the IZW, and develop a rigorous, externally funded research concept based on interdisciplinary co-operation with the other research groups at the IZW

A degree and PhD in biochemistry/biotechnology or similar subjects, postdoctoral experience and knowledge in reproduction biology particularly in protein biochemistry and molecular biology, and a track record in the acquisition of external project funding will be advantageous, a knowledge of standard biochemical and molecular biological methods is particularly appreciated The successful candidate will have a strong interest in interacting with scientists from a wide variety of fields, be confident and fluent in written and spoken English and show a keen interest to work with wildlife even if she/he has no prior experience in doing so.

The position is initially limited to three years starting after **1 January 2009.** The IZW is determined to increase the proportion of women in successful scientific careers and particularly encourages female scientists to apply Applications preferably reach us by **15 April 2008 (reference. KZ 08/2008).** Please direct informal enquiries to Dr Katarina Jewgenow (Tel. +(49)-30-5168611, jewgenow@izw-berlin.de) and submit your CV list of publications and externally funded projects, a letter indicating your research interests and experience, and the names and contact details of three referees to

**Eva-Maria Wagner, Leibniz Institute for Zoo and Wildlife Research**
**P.O. Box 601103, D-10252 Berlin, Germany**
**Fax +(49)-30-5126104, e-mail: wagner@izw-berlin.de**

W127516R

**www.cam.ac.uk/jobs/**
A world of opportunities

UNIVERSITY OF CAMBRIDGE

## Research Associate

Department of Veterinary Medicine
£25,134 - £32,796 pa
Limit of tenure: 3 years

Applications are sought for a post-doctoral research associate position in CNS regeneration biology The project will involve using genetic strategies to enhance remyelination by adult stem cells in animal models and contribute to the elucidation of the mechanisms of this important repair process in the ageing adult mammalian CNS

Applicants must have a PhD in neuroscience and extensive experience/skills in immunohistochemistry, in situ hybridisation and basic molecular biology skills.

For informal enquiries please contact Professor Robin Franklin by email rjf1000@cam.ac.uk

**Further particulars are available at: http://www.vet.cam.ac.uk/news/**

**Applicants should supply the following documents:**

- **A letter of application stating areas of interest**
- **A full CV, with names and contact details of three referees**
- **A completed application form PD18, (parts 1 and 3 only) available from Miss Melissa Large, 01223 337055 or www.admin.cam.ac.uk/offices/personnel/forms/pd18/**

**Applications should be sent for the attention of Miss Melissa Large, Department of Veterinary Medicine, Madingley Road, Cambridge CB3 0ES Applications can be made via email to recruit@vet.cam.ac.uk with the above documents as word attachments.**

**Please quote reference: PN03125. Closing date: 28 March 2008. Interview date: 17 April 2008.**

**The University is committed to Equality of Opportunity.**

U127702R

**Project Eng. Air Emissions**
Engineering
Responsibilities/Attributes: Manage and conduct CofA projects for industrial and commercial facilities; Quantification of process emissions; Analyze and assess sound and vibration generation from industrial and commercial facilities; Develop pollution abatement strategies; Train technical staff in support of the above functions.

Contact
http://www.kellyscientific.com
NW127543RL

**Regulatory Affairs Consultant**
Pharmaceuticals
**Tasks:** Evaluation of data, Review of documentation and preparation of regulatory and associated dossiers, Peer review/QA of documents prepared within the Company, Liason with Clients and Regulatory Authorities, Keeping the Project Manager informed of progress. **Qualifications Required:** A degree and ten years' experience in Regulatory Affairs.

Contact
http://www.kellyscientific.com
NW127544RL

**Documentation Coordinator**
Dublin based pharma company
Responsibility will be to play a key role in developing and maintaining the quality of our documentation system in the Production Depts. The successful candidate will ensure that an efficient and effective system is maintained in compliance with Company and External Regulatory requirements.

Contact
http://www.kellyscientific.com
NW127545RL

**Quality Control Supervisor**
Manufacturing
Develops, implements and maintains the activities of QC systems. Oversees development and implementation of standards, methods and procedures for inspecting, testing and evaluating the precision, accuracy and reliability of company products. Makes recommendations for corrective action necessary to ensure conformity with quality specifications.

Contact
http://www.kellyscientific.com
NW127546RL

**Chemistry Technician**
Support developing adhesives
Responsible for Chemical Formulation and Mechanical testing of assembled components, dispatching compliant samples to customers or contacts aboard in a professional manner, and timely ordering of chemicals. Required: Honours Degree in Chemistry, minimum of NCEA Laboratory Technicans certificate and have relevant industrial experience.

Contact
http://www.kellyscientific.com
NW127547RL

**Microbiologistes**
Pharmaceuticals
2 postes de microbiologiste à combler au sein d'une entreprise d'envergure en pharmaceutique. L'entreprise est située à Montréal, les postes sont permanents et de bonnes conditions de travail sont offertes. Les tâches peuvent inclure: Tests de stérilité sur les produits, matières premières et intermédiaires, Détection d'endotoxines bactériennes

Contact
http://www.kellyscientific.com
NW127548RL

**Technicien(ne) de production**
Pharmaceuticals
Notre client, une importante entreprise du domaine pharmaceutique, est à la recherche de technicien(ne)s à la production, de nuit. Le titulaire du poste aura à manipuler, diluer et mélanger diverses substances en respectant les procédures, l'intégrité et la stérilité lors des opérations, Faire la stérilisation du matériel

Contact
http://www.kellyscientific.com
NW127549RL

**Packaging Technician**
Technician, Packaging Development
Responsibilities: to carry out laboratory activities, to attend and participate in work discussions, to perform testing on packaging materials and products, to carry out evaluation of new packs and moulded components, to perform testing of new packaging technologies. Degree in Chemistry or related discipline desirable but not essential.

Contact
http://www.kellyscientific.com
NW127553RL

**Organic Section Head**
Environmental Testing
An exciting opportunity has arisen for a competent analyst to make their next step in an environmental testing company. Requires excellent knowledge and competency in gas chromatography. Full management training will be provided. Must have a thorough understanding of GC analysis and instrumentation with the ability to move into a supervisory role.

Contact
http://www.kellyscientific.com
NW127554RL

**Formulation Scientist**
Pharmaceuticals
Pharmaceutical company located in León, Spain
**Key responsibilities:** Coordinate the formulation and analytical activities for assigned projects; Coordinate and supervise the implementation of quality systems within team members, Supervise and evaluate the documentation for Regulatory purposes.

Contact
http://www.kellyscientific.com
NW127555RL

**Research Chemists**
Adhesives, Sealants, & Surface
**Responsibilities:** Plan and implement programmes of work, as agreed with the Group Manager Support and motivate assigned staff in product development project work, ensure that projects comply with the requirements of our design control system, participate in the overall product development for the RD&E department. **Required:** PHD in Chemistry.

Contact
http://www.kellyscientific.com
NW127556RL

**Project Associate**
Manufacturing
**Key responsibilities:** Ensure information flow between third party manufacturers, regional services and markets; Administrative data collection, data compiling and data maintenance (artwork status, regulatory timings, phase-in/phase-out dates); Create relevant data's and provide third party manufacturers, regional services and markets with them

Contact
http://www.kellyscientific.com
NW127557RL

**Senior Project Engineer**
Sealants and adhesives
**Responsibilities:** Generate concepts/ ideas that revolve around equipment/ fixture type solutions, design equipment/fixtures with deliverables that are aligned with the requirements of the manufacturing process stakeholders, to validate & commission new equipment liaising with other departments and work closely with our in-house Engineering Workshop.

Contact
http://www.kellyscientific.com
NW127558RL

**Senior CRA**
Clinical Research
Hong Kong - Our Client is the global contract service provider in drug developments. They offer full range GCP compliant clinical services for Phase I to IV trial across a wide range of therapeutic areas. They are currently looking for a Senior Clinical Research Associate to cope with their business expansion BS in Pharmacy or Biomedical Science.

Contact
http://www.kellyscientific.com
NW127560RL

**Chemical Engineer**
Sealants and adhesives
**Responsibilities:** To effectively and efficiently plan, organize and control process development projects and problem solving for Manufacturing plants. **Requires:** Honours degree in Chemical engineering with > 1 years relevant work experience.

Contact
http://www.kellyscientific.com
NW127561RL

**Quality Control Supervisor**
Manufacturing
Develops, implements and maintains the activities of QC systems. Oversees development and implementation of standards, methods and procedures for inspecting, testing and evaluating the precision, accuracy and reliability of company products. Makes recommendations for corrective action necessary to ensure conformity with quality specifications.

Contact
http://www.kellyscientific.com
NW127562RL

**Biokinetics Experimentalist**
6 months, Full Time
This is a laboratory-based position, supporting fungicide development projects by carrying out routine experiments and assays. Candidate must be reliable, able to follow instructions, have an eye for detail, A Level qualified and have some laboratory experience in a scientific field. A degree is not necessary and not suitable for PhD level.

Contact
http://www.kellyscientific.com
NW127563RL

**Analytical Chemist**
An environmental contract lab
Responsibilities: Analysis, as directed by the Scientists/ Team Leaders in either the wet chemistry (BOD, COD TP, SS etc.), analytical (GC-FID, GC-MS, IC) or microbiological (TVC, Coliforms) laboratories, carry out laboratory analysis in accordance with in-house standard operating procedures (SOP's). Must hold a degree in analytical chemistry.

Contact
http://www.kellyscientific.com
NW127564RL

**Validation Engineer**
Pharmaceuticals
Our client requires an experienced Validation Engineer to work at various sites in Ireland. The job requirements include (but are not limited to) an understanding of basic GMP skills, Working knowledge of the principles of Validation as associated with performance of work for the Pharmaceutical and other Health related industries.

Contact
http://www.kellyscientific.com
NW127565RL

**Formulations Scientist**
Drug Development
This role involves working within the Research lab, formulating and developing anti-microbial agents in a variety of forms, and working to apply these agents into a number of applications. The candidate will have formulations experience within the medical devices or healthcare industry ideally with working knowledge of anti-microbial development.

Contact
http://www.kellyscientific.com
NW127567RL

## Models of Disease

*Calls for Proposals*

The Medical Research Council aims to commit up to £10m for research grants on the evaluation and validation of human and animal models of disease, *in vivo, in vitro and in silico*. This call is one of our strategic initiatives to target 'bottlenecks' in translation, an element of the joint translational research strategy with NIHR.

Models are seen as valuable tools for developing new health interventions, both where they help identify pathways of disease and potential treatable targets, as well as suitable platforms for testing effects of interventions, for example in predictive toxicology.

The MRC invites applications to evaluate and qualify the potential of existing human or animal models of disease in identifying disease mechanisms or interventions that hold promise for the detection, prevention or treatment of disease. The call includes *in vitro* and *in vivo* disease models, and also the development of *in silico* models based on experimental data from animal and human studies.

Research studies should focus on further developing and validating existing models using available tests to demonstrate the similarity of symptoms, treatment response, and disease mechanism between the model and the clinical disease state. Comparisons between models would also be welcome.

**For more information please see: http://www.mrc.ac.uk/ApplyingforaGrant/CallsForProposals/Modelsofdisease/index.htm**

*The deadline for applications is 4pm, Wednesday 16th April 2008*

U127571A

## EAGLES Health Lecturer Tour Grants

European Action on Global Life Sciences (EAGLES) Health Programme funded by the European Commission will award grants of up to 5.000€ to leading biomedical scientists and other health specialists, including commentators and journalists, from the developing countries (DEC) to undertake Lecture Tours around Europe. Such tours may involve scientists from both DEC and Europe. The objective is to influence public and political opinion in Europe about the role of European biomedical research policies in meeting the health challenges faced by the DEC.

The EAGLES Lecturers will be chosen for their experience and knowledge of the health challenges in the DEC and their ability to communicate the needs of the DEC to the European public and European institutions. Their remit will be to communicate from their own personal experiences how European health research programmes and policies affect and might affect their own countries and regions. Each EAGLES Lecturer Tour is planned to have a duration of between 1 to 2 weeks. For more details please see the EAGLES website: http://www.efb-central.org/eagles/site

*Applications should be sent by to EAGLES-grant@efb-central.org by 9 April, 2008.*

EAGLES

BIOTECHNOLOGY

W127708A

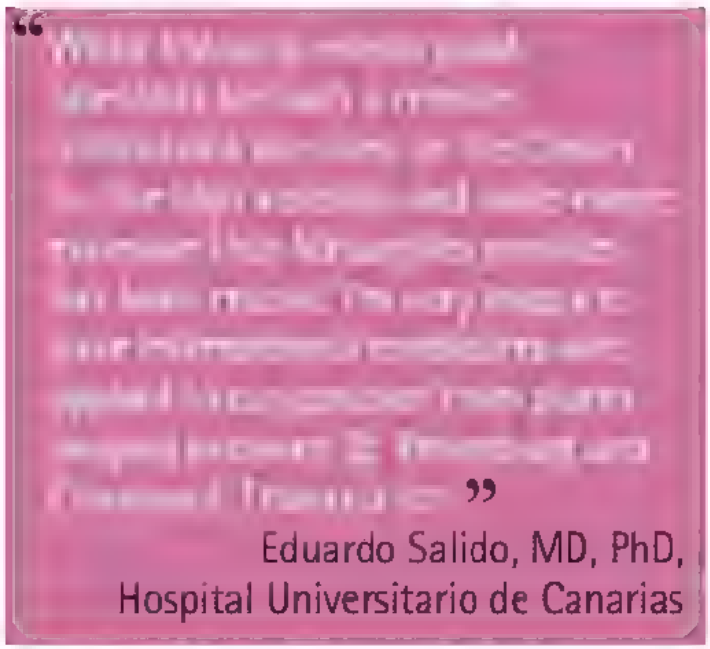

HOWARD HUGHES MEDICAL INSTITUTE

# HHMI Seeks Early Career Scientists

The Howard Hughes Medical Institute invites applications from highly promising scientists from the full range of disciplines relevant to biological and medical inquiry who have led independent laboratories for two to six years. HHMI will provide flexible research support to as many as 70 individuals.

**Eligibility**

- Tenure-track or equivalent position at an eligible U.S. institution with a rank of assistant professor or higher
- Two to six years of experience since first appointment as an assistant professor or equivalent

**Candidates must indicate their intent to apply before submitting an application.**

**Deadline for intent to apply:**
**April 30, 2008, at 2:00 p.m. ET**

**Application deadline:**
**June 10, 2008, at 2:00 p.m. ET**

**Intent to apply and application:**
**www.hhmi.org/earlycareer2009/nat**

The HHMI Early Career Scientist Program comes at a critical time for the nation and the long-term health of its research infrastructure. The initiative reflects HHMI's view that the constrained funding environment has inhibited the ability of highly creative academic scientists to establish and develop their research programs.

HHMI will select up to 70 early career scientists who have led laboratories for two to six years at one of the approximately 200 U.S. medical schools, universities, and research institutes that are eligible for this competition. Early career scientists will receive nonrenewable six-year appointments to HHMI and substantial research support while remaining affiliated with their home institutions. Candidates must apply directly to HHMI.

HHMI, a nonprofit medical research organization, plays a powerful role in advancing biomedical research and education in the United States. HHMI's flagship program in biomedical research rests on the conviction that scientists of exceptional talent, commitment, and imagination will make fundamental biological discoveries for the betterment of human health if they receive the resources, time, and freedom to pursue challenging questions.

*The Howard Hughes Medical Institute is an equal opportunity employer.*

HHMI
HOWARD HUGHES MEDICAL INSTITUTE

NW125718A

# CAPITA FOUNDATION

*Funding Innovative Research*

## Funding for *creative* hearing research

**Deadline: June 1, 2008**

Annual grants up to $40,000(US) for cutting edge auditory research projects

### Acknowledgement of 2006 awards

- *Optical stimulation a novel principle for neural interfaces*
  **Claus-Peter Richter, M.D., Ph.D.,** Northwestern University Feinberg School of Medicine, Department of Otolaryngology
- *Testing the perceptual limits of acoustic and electric hearing in children using cochlear implants*
  **Kevin Franck, Ph. D.,** The Children's Hospital of Philadelphia
- *Thin Sheet Laser Imaging Illuminator*
  **Peter A. Santi, Ph.D.,** University of Minnesota, Dept. of Otolaryngology

Applicants with a Ph D , pursuing independent research. Thinking outside the box is most welcome. University affiliation is required. The closing date for receipt of applications is June 1, 2008. Candidates are requested to submit no more than one page, detailing future plans, plus CV to: Capita Foundation, 4082 Nabal Drive, La Mesa, CA 91941.

Visit us at http://www.capitafoundation.com

NW126836A

---

UNIVERSITY OF COPENHAGEN

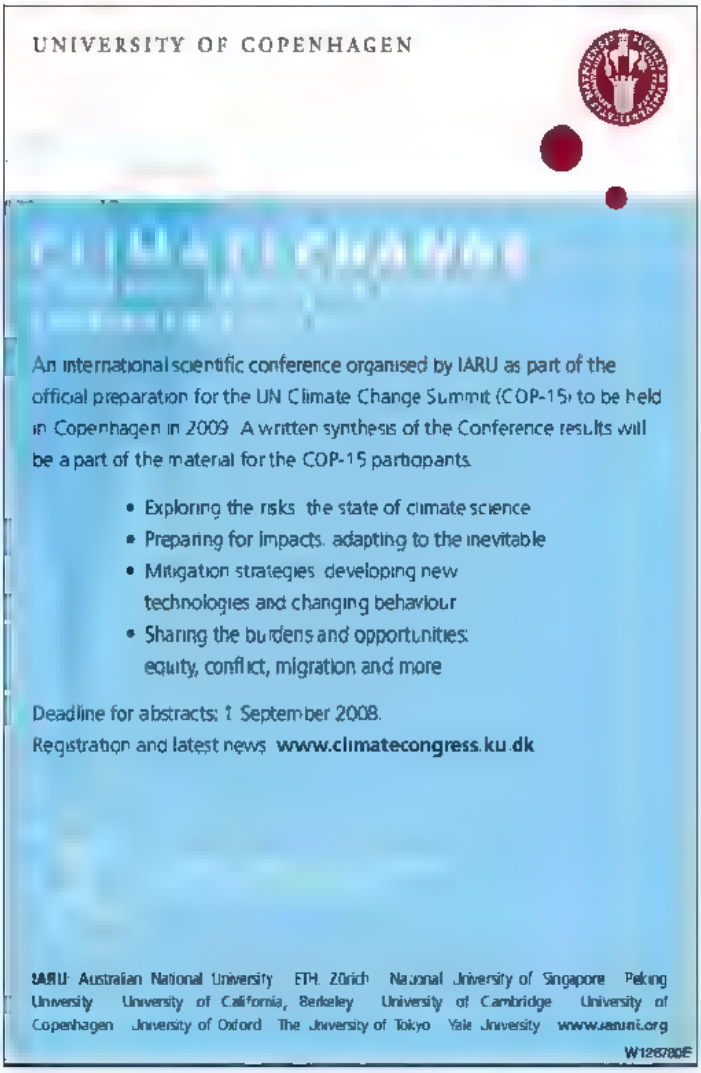

An international scientific conference organised by IARU as part of the official preparation for the UN Climate Change Summit (COP-15) to be held in Copenhagen in 2009. A written synthesis of the Conference results will be a part of the material for the COP-15 participants.

- Exploring the risks: the state of climate science
- Preparing for impacts: adapting to the inevitable
- Mitigation strategies: developing new technologies and changing behaviour
- Sharing the burdens and opportunities: equity, conflict, migration and more

Deadline for abstracts: 1 September 2008.
Registration and latest news: **www.climatecongress.ku.dk**

IARU: Australian National University · ETH Zürich · National University of Singapore · Peking University · University of California, Berkeley · University of Cambridge · University of Copenhagen · University of Oxford · The University of Tokyo · Yale University · www.iaruni.org

W126780E

---

## Europe's most important interdisciplinary forum

**Learn** about new trends and directions in research, business, science policy and funding
**Network** with the leaders of the world science community
**Communicate** your leading research and ideas to an international audience
**Participate** in the debate, the discussion and the excitement of European science and technology
**Meet** and **talk** to scientific journalists from Europe and around the world
**Develop** your career, your future projects, your horizons and your contacts

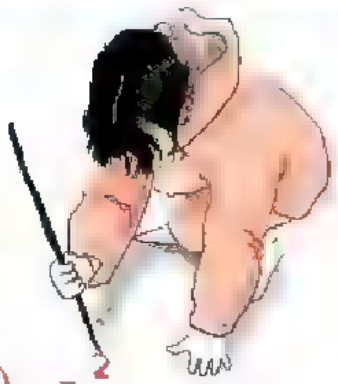

### Scientific themes

The human mind and behaviour
The very big and the very small
Open society, open science
Engineering the body
What should we eat and how should we look like?
Enhancing energy security, fighting global warming
Science and innovation policy
Science and art
Screening: burdens and benefits
Communicating science


A FORUM FOR LEADING SCIENTISTS, YOUNG RESEARCHERS, POLICY MAKERS, BUSINESS PEOPLE AND JOURNALISTS

# EUROSCIENCE OPEN FORUM
# ESOF 2008
## SCIENCE FOR A BETTER LIFE
## BARCELONA, JULY 18-22

www.esof2008.org

W127698E

---

**REPROGRAPHICS:** CTT, London E17 6BU UK and **Alden Multimedia**, Northampton UK
**PRINTED BY:** St. Ives Plymouth Ltd. UK; **Publishers Press**, Lebanon Junction, Ky, USA and **Obun Printing Co. Inc**, Tokyo, Japan

# nature events

## Directory 2008
## get your free digital edition!

**Events are essential for every scientist. From delegates discussing hot issues and opinion, through to networking and collaboration. Events provide a platform for learning and advancement.**

With a burgeoning number of events across the globe, where can you find a complete resource to ensure you attend the right events in 2008?

The *Natureevents* Directory is published once a year and covers a complete range of scientific events, conferences and courses around the world.

Plan your year ahead, go to **www.natureevents.com** and download the digital edition of the 2008 *Natureevents* Directory for free.

If you are interested in advertising an event please call +44 (0)20 7014 4015
for US please call +1 800 989 7718 or email natureevents@nature.com

**www.natureevents.com**

---

nature events

nature publishing group npg

Images courtesy of "SOHO (ESA & NASA)"

# The protocol

Your children deserve the best.

Ralph Greco

"First time?" Mrs Samulsen asked.

"No, ah ..." Mrs McVane replied, poking her index finger into her magazine, "... ah, we ... we're old patients."

"Can't be too old," Mrs Samulsen chuckled. "I'd have seen ya ... I'm Samantha."

"Ah," Mrs McVane coughed. "Julia. Julia McVane."

"I hope you don't think I'm too forward," Mrs Samulsen said, leaning forward in the hard-backed chair.

Mrs McVane leaned back in hers.

"I mean, I don't usually get to talk to any of the other moms; everybody's in and out so fast," the taller lady explained. Flicking her fiery red ponytail to the quiet nurses' 'station' at their left, she continued: "Forget talking to them, you fill out the monthly report and bam ..." at this Mrs McVane jumped "... they just slide that window shut."

"Yes," Mrs McVane said, attempting to light her eyes on the magazine tented on her leg.

"Doctor Reilly is the best though ..." Mrs Samulsen continued. "... I never felt he was pushing it on us, you know? He really worked to get Billy, that's my boy, he's five, the right one for our needs ..."

The verbose woman suddenly stopped, sat back, smiled and said: "... ADHD."

"Oh, yes?" Julia asked.

Her magazine flopped into her lap.

"Well he is expensive, but, well ... I don't see why you have to necessarily hide your wealth," Mrs Samulsen continued. "I'm not saying flaunt it, but ... I hope I'm not talking out of turn here?" and here Mrs Samulsen finally took a breath. "Shouldn't parents want the best for their children?"

"Yes. Yes of course."

"I, well ... maybe I'm letting my mouth run a little too much."

"No, no, I ..."

"I mean, Billy was getting to the age where we couldn't not have him on something," Mrs Samulsen continued to the pretty dark face facing her. "I didn't want him missing school, having to repeat a course ... not make a team he wanted to be on."

"Of course."

"God knows we weren't going to be one of those couples."

"It's so sad that that still happens."

"It breaks my heart! I mean, who suffers? Keeping them off ... well, they just never fit in and you know how cruel kids can be."

"It really is a quality-of-life decision," Julia said.

"I mean, Billy is in an accelerated track, took him no time at all to be right in step with the rest of his class."

"Yes, everyone benefits."

"Sorry," Mrs Samulsen said, sitting back in her chair then sighing. "Like I said, there's never anybody here to talk to."

JACEY

"How old is your son?" she added a minute later, her eyes still closed.

"He's ten. Ten," Julia heard herself say.

"You must have started him years ago?" Mrs Samulsen said, opening her eyes. "I really am preaching to the converted."

"Two thousand," Julia offered, turning to Mrs Samulsen to continue. "My husband's very active in the private science sector. He understood the protocol concept even before it went mainstream."

"Damned if I can understand it," Mrs Samulsen said and both women laughed. "But I know it works."

"Jack says ..."

"... like allergy treatments, building an immunity, right?" Mrs Samulsen finished then chuckled. "That's about as much as I understand it."

"You understand it fine," Julia smiled.

"Going to keep me in suspense, or you gonna tell me what you gave him?" Mrs Samulsen said after another ten seconds of silence.

Julia inhaled and regarded the magazine in her lap one last aching time.

"Well there really were very few things available mail-order at the time," she said looking up again. "A little dyslexia, maybe some hyperactivity, but you couldn't get much. There's no Doctor Reilly in Greenpoint, I can tell you that."

Mrs Samulsen smiled wide, opened her mouth, but Julia continued.

"When we moved we finally decided on a low-grade reading problem — for Jacob, that's my son — but we've since matriculated him into full-blown dyslexia."

"Well, they have whole tracts for that nowadays," Mrs Samulsen said, beaming.

"Yes, he's fit in perfectly."

"Do you have any other children?" Mrs Samulsen asked. "I mean, we only have little Billy but I always wonder if we'd give a second child the same protocol."

"Well, we might adopt, I don't kn ..."

"They say it's harder with them when they're not your own," Mrs Samulsen continued. "But they can still make pretty good progress inhibiting if they get them early."

"So how often do you have to come?" she added.

"Dyslexia takes a while to stick. We gave him three shots a week when he was younger, but now it's mostly maintenance," she said, the voice coming out of pretty lips obviously not her own.

"We're still in the early stages. I mean, the ADHD we chose is pretty extensive," Mrs Samulsen countered. "But like we said, you have to do what's best no matter the cost."

"Don't let anyone else tell you different ... Samantha."

Mrs Samulsen — Samantha — beamed and placed her soft pale hand over the dark forearm of her new friend.

"Jacob you bring Billy outside now, okay?" the nurse said from behind the partition.

The single white wooden door that led from the waiting room into the doctor's examination room opened to the two women. Standing in the doorway was a bright-eyed little boy of no more then five, a mess of red curls surrounding his bobbing head. He was smiling, holding the hand of the bigger boy standing next to him, a handsome child with skin the colour of muted chocolate and eyes the same deep rich green as his mother's.

"Isn't that darling?" Mrs Samantha Samulsen said.

"We are blessed," Mrs Julia McVane agreed. ■

**Ralph Greco is a freelance writer and ASCAP licensed musician, living in the wilds of New Jersey.**

# 25,000 Tagged ORF Clones

## including the ones you want


## TrueORF™

### for tagged protein expression

TrueORF enables the expression of the encoded transcript as a C-terminally tagged protein with Myc and FLAG® epitopes, facilitating multiple applications that utilize an anti-tag antibody, such as protein detection, protein purification, subcellular localization, etc.

- Genome-wide coverage
- Sequence verified and guaranteed
- The C-terminal dual tag of Myc and FLAG®
- Transfection-ready: Provided as 10 ug of purified plasmid
- Easy shuttling into 20 tagged vectors using PrecisionShuttle™ system

FLAG® is a registered trade mark of Sigma-Aldrich

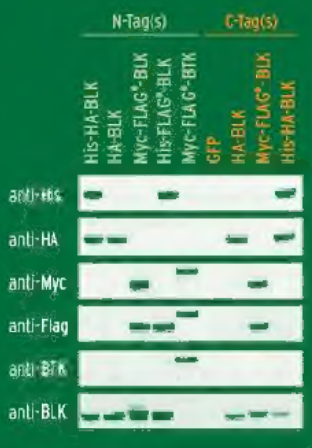


The Western blot analysis of HEK293 cell lysate over-expressing BLK or BTK tagged with indicated epitopes.

ORIGENE
Your Gene Company

1-888-267-4436 • origene.com

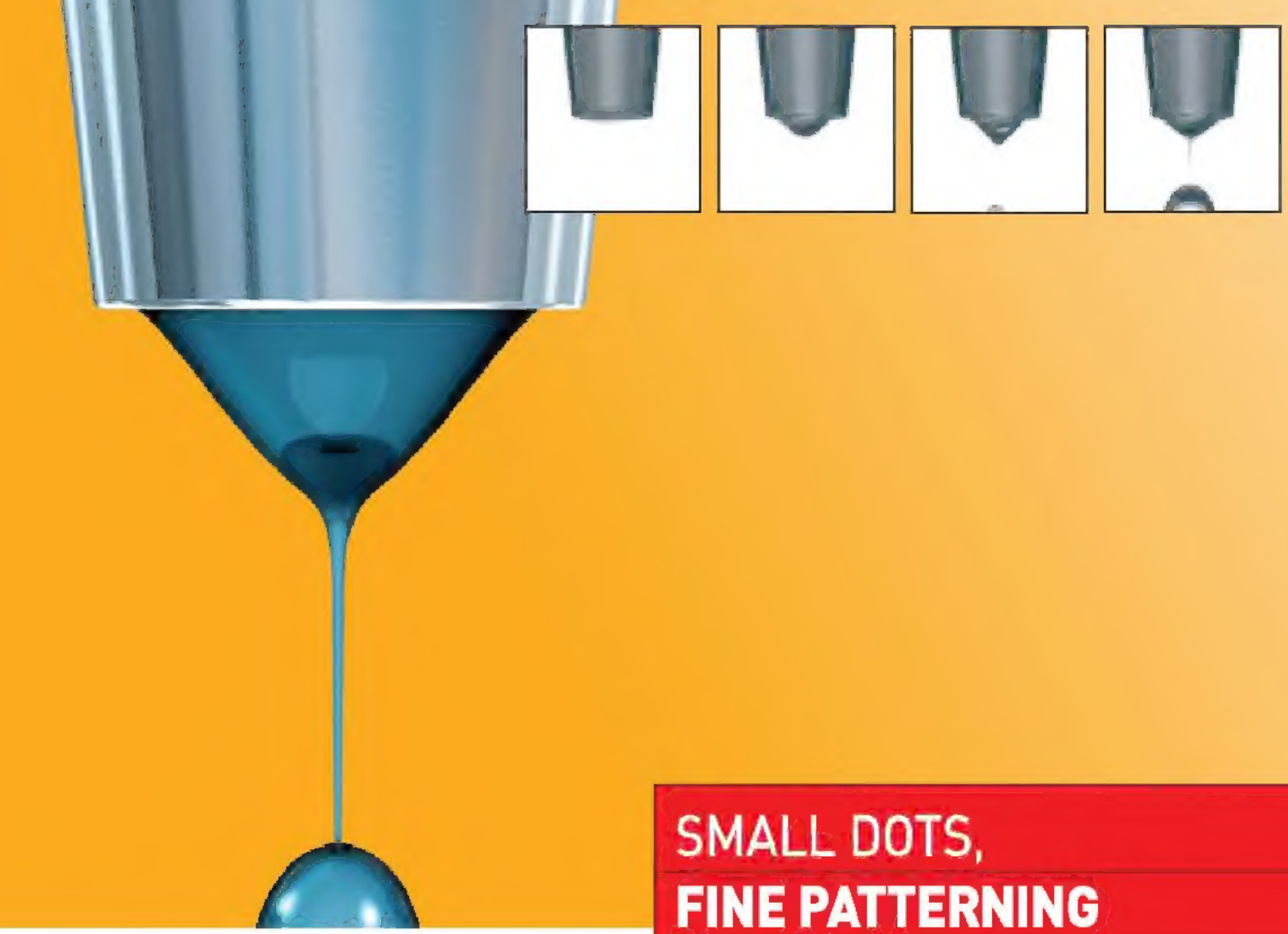

# SMALL DOTS, FINE PATTERNING

## Hamamatsu Photonics Micro-Droplet technology brings a new era of microfabrication.

DNA microarray applications have expanded rapidly with increasing capacity, accomplished through smaller spot size. Hamamatsu Photonics has now made it possible to cut the spot size of current arrays to a mere 1μm in diameter.

This is just one application of the Hamamatsu Photonics micro-droplet technology, a method that uses electrostatic force to guide samples with tremendous accuracy onto substrates. An electric pulse creates the charge that transports the samples, and the "on-demand" sample size is readily adjusted by varying the length of the pulse. Samples can be 10 femtoliters or smaller in volume.

Unlike conventional spotting technologies, like the ink jet printer, Hamamatsu Photonics micro-droplet technology can even handle viscous samples such as glycerin and UV cured resins. The resins can be patterned in lines less than 5μm in width. The micro-droplet technology thus has a wide range of applications in microfabrication: printing gold nanosuspensions that can be used for fabricating circuits, spotting the ink on unpainted pixels of the red-green-blue filters used in flat panel displays, or the creation or repair of photomasks used in fabricating semiconductors.

Hamamatsu Photonics researchers came across the idea of the micro-droplet technology when working on the optical properties of single molecules—another example of Hamamatsu Photonics "following the light" to far reaching technological applications.

Basic principle of the Micro-Droplet technology

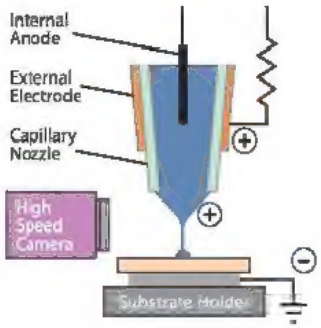


**Hamamatsu Photonics' expertise with light has revealed an elegant solution to a complex problem.**

HAMAMATSU

Photon is Our Business

For more information, visit our site at: http://jp.hamamatsu.com/en/rd/publication

**HAMAMATSU PHOTONICS K. K.**
325-6, Sunayama-cho, Naka-ku, Hamamatsu City, 430-8587 Japan Telephone: (81)53-452-2141, Fax: (81)53-456-7889 URL http://www.hamamatsu.com